



Joint Research Programme
BTO 2021.062 | November 2021

CHalk AquifeR Management (CHARM): Analysing the capacity of the Cretaceous Aquifer in Brabant, Belgium

Joint Research Programme

Report

CHalk AquifeR Management (CHARM): Analysing the capacity of the Cretaceous Aquifer in Vlaams-Brabant, Belgium

BTO 2021.062 | November 2021

This research is part of the Joint Research Programme of KWR, the water utilities and Vewin.

Project number

402045.068

Project manager

Dr. Gerard van den Berg

Client

BTO - Bedrijfsonderzoek

Authors

- Dr. Gert Ghysels (Vrije Universiteit Brussel)
- Dr. Syed MT Mustafa (Vrije Universiteit Brussel)

Supervision

- Dr. Simon Six (De Watergroep)
- Dr. Alexander Vandenbohede (De Watergroep)
- Bo Van Limbergen (De Watergroep)
- Tom Diez (De Watergroep)

Quality Assurance

- Prof. dr. ir. Marijke Huysmans (Vrije Universiteit Brussel)
- Dr. ir. Gijsbert Cirkel (KWR)

Sent to

This report is distributed to BTO-participants. A year after publication it is public.

Keywords

Cretaceous aquifer, groundwater modelling, uncertainty analysis

Year of publishing
2021

PO Box 1072
3430 BB Nieuwegein
The Netherlands



November 2021 ©

More information
Dr. ir. Gijsbert Cirkel
T 06-20614497
E Gijsbert.cirkel@kwrwater.nl

T +31 (0)30 60 69 511
E info@kwrwater.nl
I www.kwrwater.nl

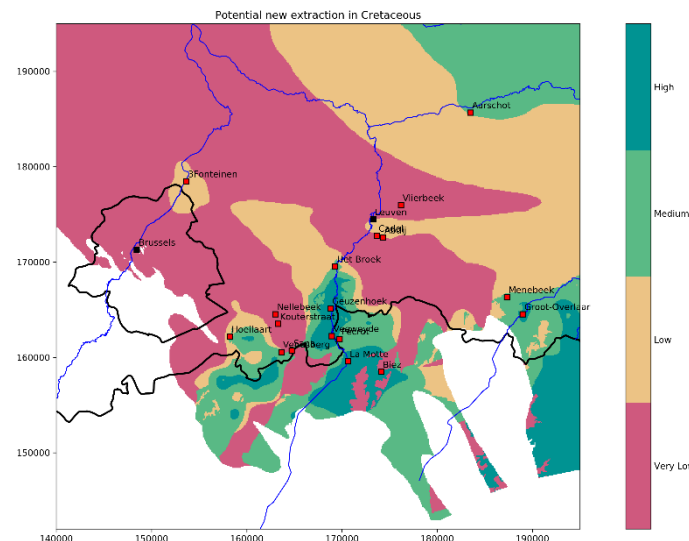
All rights reserved by KWR. No part of this publication may be reproduced, stored in an automatic database, or transmitted in any form or by any means, be it electronic, mechanical, by photocopying, recording, or otherwise, without the prior written permission of KWR.

Managementsamenvatting

Analyse van de draagkracht van de Krijt aquifer in Brabant (België) door de combinatie van grondwatermodellering met een onzekerheidsanalyse

Auteurs Gert Ghysels, Syed MT Mustafa, Marijke Huysmans, Simon Six, Alexander Vandenbohede, Bo Van Limbergen, Tom Diez & Gijsbert Cirkel.

Het grondwater in de Krijt aquifer is een strategisch belangrijke grondstof voor de productie van drinkwater in de regio Brabant en Limburg (België). Deze gespannen waterlaag is gekarakteriseerd door een sterke ruimtelijke variabiliteit in hydraulische eigenschappen die gelinkt kan worden aan bepaalde goed-doorlaatbare intervallen in het Krijt en aan de aanwezigheid van gespleten zones. In het verleden werden op lokale schaal grondwatermodellen gemaakt om de impact van de waterwinning op het grondwatersysteem in kaart te brengen. Met deze modellen kon de interactie tussen de verschillende winningen en een meer globale waterbalans echter niet opgesteld worden. Een grootschalig regionaal model (MODFLOW) van het Krijt en Paleocean aquifer systeem, dat tijdsafhankelijk werd gekalibreerd, is opgesteld om hieraan tegemoet te komen. Dit model is gebruikt om de huidige toestand van deze grondwaterlaag te analyseren en om toekomstige exploitatiestrategieën te verkennen. De resultaten tonen aan dat de exploitatie van het Krijt met de huidige volumes in het algemeen duurzaam is en op lange termijn volgehouden kan worden. Het potentieel voor extra onttrekking in deze grondwaterlaag is gevisualiseerd aan de hand van een potentieelkaart (zie figuur). Extra aandacht is besteed aan alle bronnen van onzekerheid in het model. De onzekerheid op de modelvoorspellingen is gekwantificeerd aan de hand van het IBMUEF framework.



Kaart die het potentieel voor extra onttrekking in de Krijt aquifer visualiseert.

Belang: De Krijt aquifer is een belangrijke bron van drinkwater van goede kwaliteit

De Krijt aquifer is één van de belangrijkste grondwaterlagen die gebruikt wordt voor de productie van drinkwater door De Watergroep. Deze overwegend gespannen grondwaterlaag is van maatschappelijk groot belang enerzijds omwille van

de goede waterkwaliteit en anderzijds omwille van de grote volumes water die erin aanwezig zijn. Om verschillende redenen is de onzekerheid over de eigenschappen van deze grondwaterlaag groot. Door zijn grote diepte zijn boringen en observatiedata beperkt. Een sterke ruimtelijke variabiliteit is aanwezig in de hydraulische eigenschappen van deze

laag, en ze reageert traag op veranderingen in het systeem. De verschillende waterwinningen die aanwezig zijn in dit systeem interageren met elkaar wat een regionale aanpak vereist.

Aanpak: Analyse van (hydro)geologische data, grondwatermodelering en onzekerheidsanalyse

De beschikbare (hydro)geologische data is geanalyseerd om de kennis over de aanwezigheid en de doorlatendheid van sterk watervoerende intervallen in het Krijt te verbeteren. Een regionaal grondwatermodel is opgesteld om het effect van de huidige onttrekkingen van De Watergroep te analyseren. Verschillende onttrekkingssenarios voor de toekomst zijn opgesteld om de duurzaamheid van deze strategieën voor de toekomst te bepalen. In het basisscenario wordt de duurzaamheid van de huidige onttrekking geanalyseerd (voor de periode 2021-2040). Verder is een maximaal scenario gedefinieerd waarin aan de maximaal vergunde debieten gepompt wordt. Om de grenzen van de huidige exploitatie af te toetsen is nagegaan wat het effect is van een stijging van 10% van de huidige debieten. Voor de winning van Venusberg is de geplande verhoging van de debieten (+100% en +300%) uitgerekend. Ten slotte is er nagegaan in welke mate en hoe snel de Krijt aquifer herstelt als alle onttrekking stilgelegd wordt. Een belangrijke bemerking is dat deze scenario's zijn uitgerekend met de huidige grondwatervoeding. Het effect van een daling in voeding is in dit project niet geanalyseerd. Een onzekerheidsanalyse is uitgevoerd op het grondwatermodel om de onzekerheid op de voorspelde grondwaterpeilen en afdelingen te kwantificeren.

Resultaten: Grondwatermodelering toont dat huidige exploitatie duurzaam is

De doorlatendheden van het Krijt bekomen via pompproeven variëren over een groot bereik (van 0.1 tot >100 m/d) en tonen een sterke ruimtelijke variabiliteit. Ten eerste is er een verschil tussen de afzettingen van het Krijt op Formatie niveau: de primaire permeabiliteit van het fijnkorrelige Gulpen krijt is significant lager dan die van de grofkorreligere kalkarenieten van Maastricht. Ten tweede speelt een hardground aan de top van het Zeven Wegen krijt (Formatie van Gulpen), die geassocieerd kan worden met een sterke piek in het gamma-ray signaal, een

belangrijke rol voor de putopbrengsten in het noordelijke deel van het studiegebied. Deze hardground is geassocieerd met een fosfaatgrind dat in dikte en permeabiliteit toeneemt naar het zuiden. De hydrogeologische eigenschappen van dit grind zijn ruimtelijk sterk variabel, zoals aangegeven voor de winning van Korbeek-Dijle Het Broek waar op korte afstand de doorlatendheden variëren tussen 1 en 23 m/d. De lage opbrengsten van het Krijt in Overijse Nellebeek kunnen verklaard worden door de afwezigheid van dit hardground interval richting de as van het Brabant Massief naar het westen toe. In het zuiden van het studiegebied, waar het Krijt dicht tegen het oppervlak zit, zorgt de aanwezigheid van gespleten zones voor een sterke stijging van de permeabiliteit. Dit zorgt voor een duidelijk verschil in permeabiliteit tussen de riviervalleien (hoog) en de heuvelruggen (laag).

Een tijdsafhankelijk grondwatermodel is opgesteld voor de complexe Krijt aquifer. Degelijke modelprestaties worden bekomen over een groot bereik aan stijghoogtes. Een scenario analyse van toekomstige onttrekkingsstrategieën toont aan dat voor het overgrote deel van de sites de huidige onttrekking duurzaam is. Onttrekking aan maximaal vergunde debieten zorgt voor een sterke afdeling voor de noordelijke winningen (regio Leuven). Voor de winning van Korbeek-Dijle Het Broek zorgt het hoge vergunde debiet voor sterke peildalingen. De huidige debieten zijn echter wel duurzaam, maar de onttrekking in de meest noordelijke winningen kan best verminderd worden om het effect op de stijghoogtes te minimaliseren. Voor de winningen Overijse Kouterstraat en Nellebeek zakken de peilen tot dichtbij of zelfs tot onder het dak van het Krijt bij de vergunde debieten. Aangezien het hier om beperkte volumes gaat, is het beter om deze af te bouwen in de toekomst. Voor de winning Overijse Venusberg is een stijging van +100% van de huidige vergunde debieten mogelijk, maar zorgt een stijging van +300% voor een daling van het peil tot onder het dak van het Krijt. Continue onttrekking aan deze debieten is dus niet aan te raden, en moet beperkt blijven tot korte periodes om piekverbruiken op te vangen. De onttrekkingen in het zuidelijke deel van de Dijle vallei hebben een beperkte invloed op de stijghoogtes in vergelijking met de grote volumes die

More information

XXXXX

T 06-20614497

E Gijsbert.cirkel@kwrwater.nl

PO Box 1072
3430 BB Nieuwegein
The Netherlands



hier geproduceerd worden. Belangrijk hier is om het effect van een daling van de grondwatervoeding op te volgen, aangezien het effect hiervan in dit freatische deel van de aquifer snel zichtbaar is. In de huidige modelopzet was het niet mogelijk om scenario's van dalende grondwatervoeding uit te rekenen. Het is aan te raden om een tijdsreeksanalyse toe te passen op de grondwaterpeilen in het voedingsgebied om het effect van dalende voeding op deze peilen te voorspellen.

De onzekerheid op de modelvoorspellingen is in het algemeen van dezelfde orde van grootte als de invloed van de onttrekking. Dit duidt het belang aan van het in rekening brengen van deze onzekerheid bij beslissingen over het management van de onttrekkingen. Op basis van de modelresultaten is een potentieelkaart opgesteld die het potentieel voor aanvullende onttrekking in het Krijt visualiseert. De zone met het meeste potentieel is de zuidelijke Dijle vallei (van Het Broek tot Pécrot). Ook de regio Tienen kan interessant zijn voor toekomstige onttrekking. De huidige kennis over het Krijt in die regio is echter beperkt. Tenslotte is er ook potentieel voor de noordoostelijke hoek van het studiegebied, waar de meer permeabele kalkarenieten van de Formatie van

Maastricht aanwezig zijn boven op de minder permeabele afzettingen van de Formatie van Gulpen.

Implementatie:

Deze studie toont het belang aan van het combineren van pompproeven, flowmetingen en geofysische metingen om de ruimtelijke variabiliteit in de putopbrengsten te verklaren. De regionale modeleringsaanpak verschafft belangrijke inzichten in de capaciteit en de huidige toestand van de grondwaterlaag. Het model kan gebruikt worden om verschillende strategieën voor de exploitatie van de grondwaterwinningen te verkennen. De onzekerheidsanalyse geeft inzicht in de betrouwbaarheid van de modelresultaten zodat gefundeerde beslissingen kunnen genomen worden met betrekking tot het management van de grondwaterlaag voor drinkwater doeleinden. De potentieelkaart die is opgesteld, kan gebruikt worden om na te gaan welke gebieden het meest geschikt zijn voor nieuwe onttrekking of voor het ruimtelijk optimaliseren van huidige onttrekkingen.

Het Rapport

Dit onderzoek is beschreven in het rapport 402045.068 (BTO-2021.062).

More information

XXXXX
T 06-20614497
E Gijsbert.cirkel@kwrwater.nl

PO Box 1072
3430 BB Nieuwegein
The Netherlands



Contents

Report	iii
<i>Managementsamenvatting</i>	iv
Contents	vii
1 Introduction	1
1.1 Problem statement	1
1.2 Goal of the project	2
1.3 Outline	3
2 Geology and Hydrogeology	4
2.1 Geology of the Cretaceous deposits in Flanders	4
2.2 Hydrogeology of the Paleocene and Cretaceous aquifer systems in Brabant	7
2.3 Hydrogeological properties of the Cretaceous	14
2.3.1 Pumping tests	14
2.3.2 Correlation with flow and geophysical measurements	17
2.3.3 Spatial variability of the hydraulic conductivity of the Cretaceous	25
3 Extraction and Hydraulic Heads	30
3.1 Extraction De Watergroep	30
3.2 Extraction DOV	50
3.3 Evolution of hydraulic heads in the Brabant area	53
4 Groundwater Modelling: Brabant Model	61
4.1 Model Area	61
4.2 Discretization	62
4.3 Boundary conditions	65
4.4 Observation Data	69
4.5 Hydraulic conductivity	70
4.6 Steady-state modelling	72
4.6.1 Steady-state model 2018	72
4.6.2 Steady-state model 2000-2004	80
4.7 Transient modelling	86
4.7.1 Initial heads	86
4.7.2 Boundary conditions	87
4.7.3 Observations	91
4.7.4 Hydrogeological parameters	91

4.7.5	Solver	92
4.7.6	Results	92
4.7.7	Water Budget	105
4.8	Discussion	107
5	Scenario Analysis	109
5.1	Overview of scenarios	109
5.2	Scenario 1: Current/normal situation	112
5.3	Scenario 2: Maximal permitted situation	116
5.4	Scenario 3: Current/normal situation +10%	123
5.5	Scenario 4: Venusberg +100%/+300%	127
5.6	Scenario 5: no extraction De Watergroep in the Cretaceous	130
6	Uncertainty Analysis	135
6.1	Integrated Bayesian Multi-model Uncertainty Estimation Framework (IBMUEF)	135
6.2	Parameter and boundary condition uncertainty analysis	135
6.3	Threshold levels	136
6.4	Results	137
6.4.1	Parameter uncertainty	137
6.4.2	Prediction uncertainty in simulated heads for different scenarios	137
6.4.3	Prediction uncertainty in simulated heads for selected extraction sites	140
6.4.4	Prediction uncertainty in simulated heads for all extraction sites	148
7	Potential Maps	152
7.1	Drawdown	152
7.2	Difference with top of the Cretaceous	155
7.3	Depth of the Cretaceous	157
7.4	Potential for additional extraction in the Cretaceous	158
8	Conclusions	160
8.1	Extractions and hydraulic heads	160
8.2	Geology and hydrogeology	161
8.3	Groundwater modelling: the Brabant Model	163
8.4	Scenario analysis	164
8.5	Uncertainty analysis	165
8.6	Potential maps	166
8.7	Limitations and directions for future research	166
8.8	Management conclusions	168
9	References	170
I	Appendix	172

1 Introduction

De Watergroep is the largest public drinking water company of Flanders. It is responsible for the provision of drinking water in the provinces of Limburg, Vlaams-Brabant and large parts of East and West Flanders (De Watergroep, 2017). Annually, De Watergroep produces around 140 million m³ of drinking water. Most of this drinking water is produced from local groundwater and surface water. For the provinces of Vlaams-Brabant and Limburg, groundwater is the source of 100% of drinking water as they have highly permeable aquifers that can be used for the production of water. In Vlaams- and Waals Brabant and the southern part of Limburg, the Chalk or Cretaceous Aquifer¹ (HCOV 1100) is one of the most important aquifers for the provision of drinking water.

In the evaluation of the state of the Cretaceous Aquifer, as defined in the European Framework Directive Water (2000/60/EG) and the directive Groundwater (2006/118/EG), the aquifer passed all tests on the quantitative criteria (CIW, 2016). This aquifer is therefore currently in a favorable quantitative state, both for the phreatic and confined part of the aquifer. However, in the report an area was delineated around Leuven that needs to be closely monitored, due to a limited depression in the hydraulic head. Furthermore, in the vicinity of the extraction sites of De Watergroep the observation is made that the groundwater levels are strongly dependent on the extracted volumes. The state of the aquifer is therefore closely monitored through measurements of groundwater levels and extraction rates.

The provision of water forms one of the basic elements of the economy and society in general. About 75% of the licensed extraction rate in the Cretaceous Aquifer has been granted to the drinking water companies. The other 25% is important for industry, agri- and horticulture, energy, and trade and services (CIW, 2016). The Cretaceous Aquifer is of great societal importance, mainly in its confined part, because it is well protected against potential negative influences on the quality of the water. The confined part of the aquifer is in a favourable qualitative state (CIW, 2016) and it forms a strategic aquifer with clean groundwater. This in contrast with shallow, phreatic aquifers where the influence by NO₃⁻ and pesticides is omni-present.

1.1 Problem statement

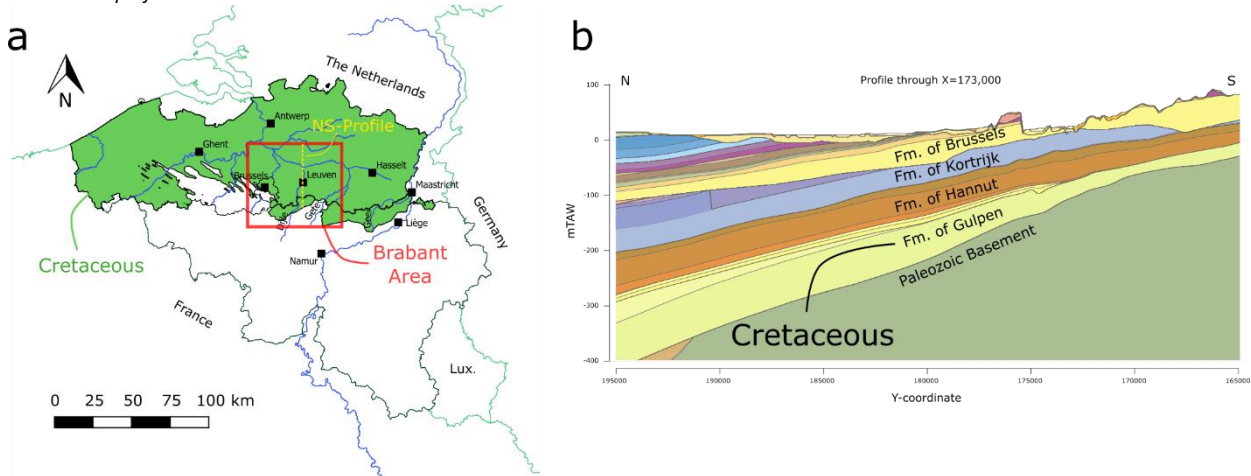
In this project, we focus on the part of the Cretaceous Aquifer in the provinces of Vlaams- and Waals-Brabant, which we call the Brabant area (Figure 1a). De Watergroep annually extracts 12 to 14 million m³ in Waals- and Vlaams-Brabant at 18 extraction sites. The Cretaceous Aquifer outcrops in the northern part of Wallonia around the axis Waver, Waremme and the Jeker valley in the east. In this area, the aquifer is fed by precipitation and thus has a phreatic character. Towards the north, the aquifer dips into the subsurface, and it is covered by younger Tertiary layers: mainly the Formations of Heers, Hannut and Kortrijk (Figure 1b). These layers give the aquifer a confined character.

Due to several reasons, the uncertainty regarding this aquifer is large in the Brabant area. Due to its relatively large depth in its confined part, only scarce boreholes and head observation wells are available, resulting in limited information on the hydrogeological properties of the aquifer. Furthermore, these hydrogeological properties are strongly spatially variable, both horizontally as vertically. Due to the lack of information, this spatial variability is very difficult to map. This heterogeneity is a result of the presence of a double porosity system in the aquifer and the presence of different Formations and Members with varying lithology. Next, we also see that the aquifer reacts slowly to changes in the system and that extractions can lead to large drawdowns, mainly in its northern part. Due to the regional effect of extraction in the Brabant area, large-scale models need to be set-up as smaller-scale models cannot

¹ The Dutch name for this aquifer is the 'Krijt Aquifer'. 'Krijt' is used both for the geological period (Cretaceous in English) and the lithology (Chalk in English). As the aquifer does not solely consist of chalk deposits, we prefer the English translation 'Cretaceous Aquifer' instead of 'Chalk Aquifer'.

accurately capture the effect of the extractions. However, such regional models are complex and time-consuming to set-up. Most of these factors are less of an issue in the province of Limburg, where the Cretaceous is largely unconfined to semi-unconfined. Moreover, hydrogeological properties vary less strongly in this area. Therefore, we focused on the Brabant area in this project, as the effect of these uncertainties play an important role in the management strategies of the extraction sites in this area.

Figure 1: (a) Map of the extent of the Cretaceous, the delineation of the Brabant area and location of north-south geological profile; (b) Geological north-south profile.



1.2 Goal of the project

The goal of the CHARM project is to analyse the capacity² of the Cretaceous Aquifer on a regional scale and to deliver a management instrument so that decisions can be made with regards to the quantitative use of this aquifer for drinking water purposes. This project provides insights in the current state of the aquifer and the sustainability of the current extraction practices. The results of this project enable De Watergroep to optimize the distribution of extraction rates over the aquifer so that groundwater can be produced in a sustainable way in the future.

Due to the lack of information, our knowledge on the geology and hydrogeological properties of the Cretaceous Aquifer is limited. This project aims to improve the knowledge on the (hydro)geology of the Cretaceous by combining borehole descriptions, geophysical measurement and flow measurements with pumping tests performed on the extraction wells. This way, the spatial variation of well yields can be explained.

A regional groundwater model is set-up for the Brabant area so that the regional effect of the extraction can be captured. This groundwater model can then be used as a management tool to better optimize the extraction in the Cretaceous. Extra attention will be given to all sources on uncertainty and their effect on the model results. Due to the model scale and the large uncertainty and sensitivity of the model parameters, an approach with only one groundwater model can only provide limited insights on the capacity of the aquifer. An alternative methodology is established in which a possible range of values for each model parameter is assessed. This way, a more substantiated assessment of the state of the aquifer and the effect of extraction can be performed.

Furthermore, the aim is to explore different extraction scenarios with the groundwater model and to assess the potential for additional extraction. The results of this provide a clear view of the capacity of the aquifer and the ways

² The capacity of an aquifer can be interpreted as the amount of water that can be extracted without exceeding the critical extraction rate, which is the extraction rate at which the aquifer is emptied on the long term. Another interpretation is that the capacity of an aquifer is a situation where the extraction has no negative effects on other extraction sites or sectors. In the situation where the groundwater levels are continuously decreasing, the term groundwater mining is used, with lack of water resulting in economical damage (Foster & MacDonald, 2014).

to optimize the distribution of the extraction rates. Extra attention is given to visualizing the potential for extraction in a clear way.

1.3 Outline

In Chapter 3, the extraction by De Watergroep and other companies or organisations is analysed in detail. Furthermore, the effect of these extractions on the evolution of hydraulic heads in the aquifer is analysed.

In Chapter 2, the geology and hydrogeology of the Cretaceous is discussed. First, an overview is given of the geology of the Cretaceous deposits in Flanders. Next, the hydrogeology of the two aquifer systems modelled in the Brabant area, the Paleocene and Cretaceous Aquifer systems, is discussed. During the last few decades, De Watergroep has collected a large quantity of (hydro)geological data, including borehole descriptions, geophysical measurements and flow measurements, and hydraulic conductivities based on pumping tests. The results of pumping tests are correlated with the flow and geophysical measurements as to explain the strong variation in well yields in the Brabant area.

In Chapter 4, groundwater models (MODFLOW) are set-up for the Brabant area. These models include the deposits confined by the Ieperian Aquitard: the Paleocene and Cretaceous aquifer systems. The conceptual model and model set-up are discussed in detail. First, a steady-state modelling approach is adapted to provide insights in the important parameters in the model area. Steady-state models are set-up for the year 2018 and for the period 2000-2004. The results of the latter are used as a start for a transient model for the period 2004-2020. The results of these models are discussed in detail.

In Chapter 5, a scenario analysis is performed based on the transient model. The transient model is extended to 2040, and different extraction scenarios are calculated. The effects of an increase in extraction on the state of the aquifer are simulated and the sustainability of these extraction scenarios are analysed.

In Chapter 7, the potential for extraction in the Cretaceous is visualized by combining different factors, including the drawdown of a synthetic well, the difference between the head in the Cretaceous and the top of the Cretaceous, and the depth of the Cretaceous. By weighting these different factors and classifying the results in different potential classes, a clear view of the potential for additional extraction in the Cretaceous is obtained. These results can be used to optimize the distribution of the extraction rates in this aquifer.

In Chapter 6, an uncertainty analysis is performed on the groundwater model, quantifying the parameter and total uncertainty. The Integrated Bayesian Multi-model Uncertainty Estimation Framework (IBMUEF) of Mustafa et al. (2020) is applied, in which the DREAM algorithm for uncertainty analysis (Vrugt, 2016) is coupled with MODFLOW. This uncertainty analysis is applied on the scenarios defined in Chapter 5, resulting in uncertainty estimates on the predictions in these scenarios. Based on the results of this uncertainty analysis, well-founded decisions regarding the sustainable use of the Cretaceous for drinking water purposes can be made.

2 Geology and Hydrogeology

2.1 Geology of the Cretaceous deposits in Flanders

The Cretaceous deposits in Flanders have been discussed in detail by Lagrou et al. (2005, 2011). The following summary of the geology of the Cretaceous is largely based on these studies, combined with the works of Vandenbergh et al. (2004), Dusar & Lagrou (2007) and Slimani et al. (2014).

Deposits from the Cretaceous occur almost everywhere in Flanders, with the exception of the paleotopographical highs along the WNW-ESE running axis of the Brabant Massif (Figure 2). The largest Cretaceous sequences are found in the Campine Basin, which was a basin between the two topographical highs of the Brabant Massif and the inverted Ruhr Valley Graben. The Cretaceous deposits are mostly covered by a northward thickening Cenozoic sequence (Dusar & Lagrou, 2007). Outcrops are limited to the area between Maastricht and Visé and surroundings (southern Limburg, Pays de Herve and eastern Hesbaye), the area around Mons and to some small erosion windows on the Hesbaye-Hainaut loess plateau. In the rest of Flanders, the Cretaceous is only known from boreholes and reflection seismics, mainly in the Campine Basin (Dusar & Lagrou, 2007). The Cretaceous has rarely been a target for drilling. Drilling through the Cretaceous is difficult due to the extreme difference in rock mechanical properties of flint nodules or silicified beds versus soft chalks and calcarenites.

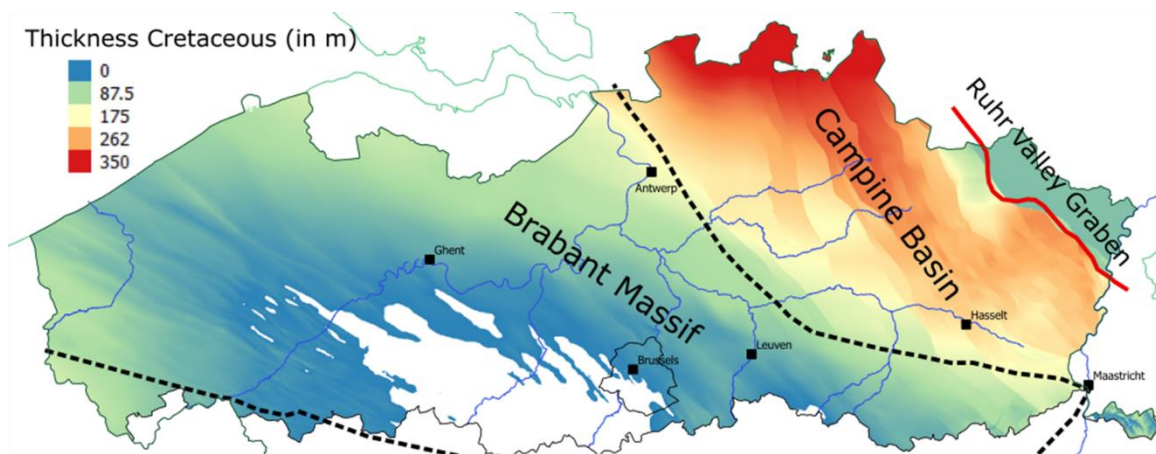


Figure 2: Thickness of the Cretaceous deposits in Flanders. Dotted line indicates boundary of the Brabant Massif. Red line indicates edge of the Ruhr Valley Graben.

A lithostratigraphic correlation scheme of the Cretaceous is shown in Figure 3. Note that this framework includes the lowermost Paleocene, i.e., carbonates from the Danian, as these are often undistinguishable from the underlying Maastrichtian deposits. The Cretaceous deposits overlay the Cambrian to Silurian deposits of the Brabant Massif. Before the Cretaceous onlap, a long phase of weathering has affected the Palaeozoic bedrock. The sedimentary succession of the Upper Cretaceous to Paleocene deposits in northern Belgium is controlled by both stepwise marine transgressions to final flooding, and tectonic relaxation pulses of the Brabant Massif and inverted Ruhr Valley Graben (Figure 2). Cenomanian to Turonian deposits (mainly the Vert Galant, Esplechin and Maisières Formations; Figure 4a) are only present south of the Brabant Massif axis. The transgression during the Santonian-Campanian passed over the paleotopographic high of the Brabant Massif, resulting in deposits in the Campine Basin. Late Santonian sediments comprise glauconite-bearing chalk on the west-central Brabant Massif (Nevele Formation), glauconitic sands on the eastern Brabant Massif and coastal to estuarine sands and clays with lignite towards the Ruhr Valley Graben (Aachen Formation) (Figure 4a).

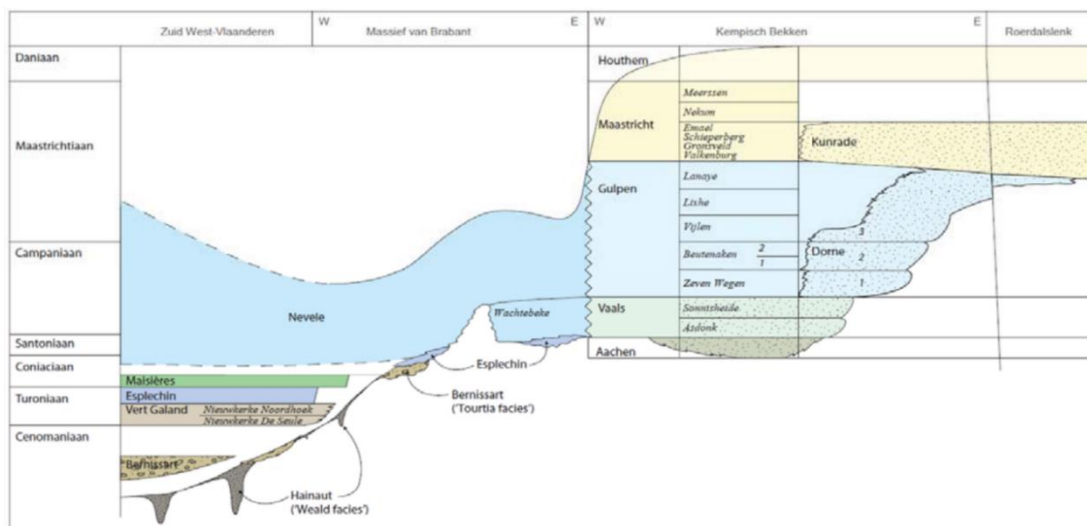


Figure 3: Lithostratigraphic correlation scheme of the Cretaceous deposits in Flanders (Lagrou et al. 2011).

In the Lower Campanian widespread deposition of chalk occurred on the western and northern Brabant massif (Nevele Formation). In the Campine Basin and the eastern Brabant Massif green sands and clays were deposited (Vaals Formation; Figure 4a), including the Herve smectite facies. Maximal flooding occurred during the Upper Campanian transgressive phase, with the deposition of white chalks of the Zeven Wegen Member of the Gulpen Formation. The Nevele Formation groups the chalk deposits on the western and central parts of the Brabant Massif, west of the line Antwerp-Brussels (Figure 4a-b). Towards the Campine basin, the chalks of the Nevele Formation laterally grade into more diverse sedimentary units which make up the lower part of the Gulpen Formation, i.e., the Member of Zeven Wegen and the Vaals Formation. The Zeven Wegen chalk consists of white, fine-grained chalk, the typical “writing chalk”, and is present in the entire area east of the Antwerp-Brussels line (Figure 4b). The top of the white Zeven Wegen chalk is marked by the Froidmont Hardground, which is the most pronounced hardground in the entire Campine Basin (Slimani et al. 2014).

In the Campine Basin, the Beutenaken, Vijlen, Lixhe and Lanaye Members are found on top of the Zeven Wegen chalk (Figure 4c). The Beutenaken Member consists of marly chalk to marls, Late Campanian in age, and indicates a transgression after tectonic uplift. The Vijlen Member, silty chalk with fine silex, is Early Maastrichtian in age and is deposited in a time of major flooding. The Beutenaken and Vijlen Members are only present in the Campine basin. The Lixhe and Lanaye Members are respectively deeper and shallower facies compared to the Vijlen chalk. The Lixhe Member consists of white fine-grained chalk with extensive silex intervals. The Lanaye Member consists of very fine calcarenites with extensive silex intervals. The Lanaye and Lixhe Members can also be found on the eastern flank of the Brabant Massif, in e.g., the Leuven area. In the northeast of the Campine basin, near the faults related to the Ruhr Valley Graben, the Gulpen deposits have a sandier character (Figure 4b and Figure 4c). A new formation is defined for these more proximal deposits: the Formation of Dorne.

Capping the Lanaye chalk is the Lichtenberg Horizon which separates the underlying fine chalks of the Gulpen Formation from overlying porous calcarenites of the Maastricht Formation. The calcarenite lithology of the Maastricht Formation points to shallower facies. The deposits of the Maastricht Formation are only present east of the Brabant Massif, in the Campine basin (Figure 4d). In the northeast of the Campine basin, a typical banded calcarenite is identified which is characterized by the alteration of hard and soft calcarenites. These deposits correspond with the Kunrade Formation, a more coastal equivalent of the Maastricht Formation (Figure 4d). The Cretaceous/Paleocene boundary is represented by local impact and storm-related sediments. To the north of the Brabant Massif, the Houthem Formation is the oldest Danian chalk deposit, while to the south, the oldest Danian units are represented by the Ciply chalk and Mons limestone.

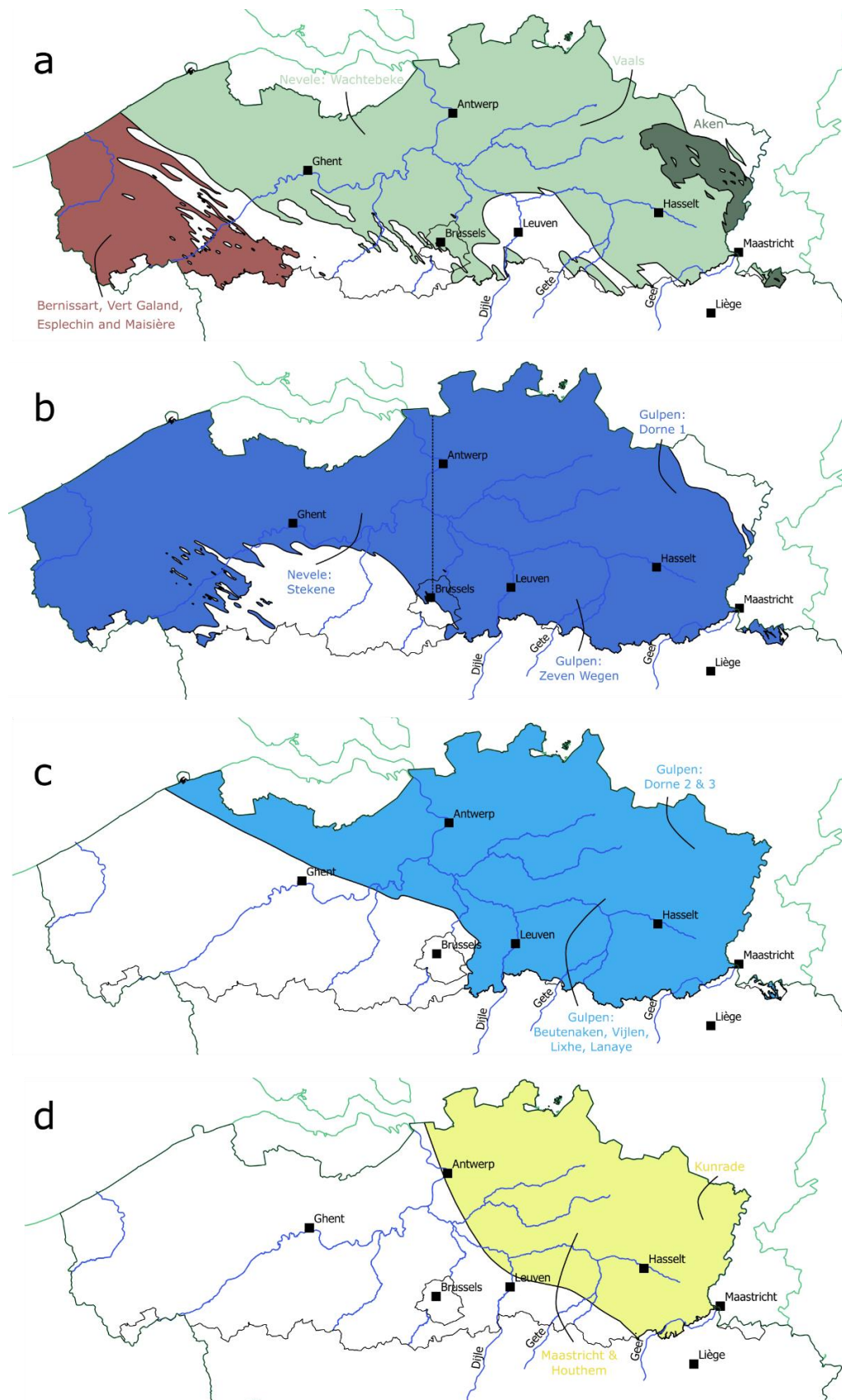


Figure 4: Extent of the Cretaceous deposits in Flanders: (a) Bernissart, Vert Galand, Esplechin and Maisière; Nevele: Wachtebeke; Vaals; Aken; (b) Nevele: Stekene; Gulpen: Zeven Wegen and Dorne 1; (c) Gulpen: Beutenaaken, Vijlen, Lixhe, Lanaye and Dorne 2 & 3; (d) Maastricht, Kunrade & Houthem (source: G3Dv3, Deckers et al. 2019).

The stratigraphic subdivision of the Cretaceous deposits in the Campine and at the northern side of the Brabant Massif is summarized in Table 1.

Table 1: Stratigraphic subdivision for the Campine and northern side of the Brabant Massif (Lagrou et al. 2011).

Chronostratigraphy	Formation	Member	Lithological description
Danian	Houthem		Pale beige, soft, fine to coarse calcarenite
Maastrichtian	Maastricht	Meerssen	Pale, soft, coarse calcarenite ("tuffeau")
		Nekum	Pale, soft, fine calcarenite with silex at base
		Emael	Pale beige, fine, hard calcarenite with silex
		Schiepersberg	
		Gronsveld	
		Valkenburg	
Campanian	Gulpen	Lanaye	Pale grey very fine calcarenite with thick silex intervals
		Lixhe	White, fine-grained chalk with ample black silex intervals
		Vijlen	Pale grey silty chalk with fine silex
	Beutenaken	Beutenaken	Grey marls
		Beutenaken	Grey marly chalk
		Zeven Wegen	White, fine-grained chalk ("writing chalk")
Santonian	Vaals	Sonnisseide	Glauconitic fine sand and silt (east) and marls (west)
		Asdonk	Green clayey glauconitic sandy marls
Santonian	Aken		Quartz sands with lignite

2.2 Hydrogeology of the Paleocene and Cretaceous aquifer systems in Brabant

The main focus of the CHARM project is on the Cretaceous and Paleocene aquifer systems in the Brabant region for which a groundwater model (the Brabant Model) will be set up (see Chapter 4). In this section, we focus on the geology and hydrogeology of the layers that are important for this modelling approach. In Figure 5 the Brabant Model area is indicated on a map showing the extent of the Cretaceous deposits in Flanders. The study area extends from X=140,000-195,000 and Y=142,000-195,000 m (Lambert-72 coordinates) and comprises the province of Vlaams-Brabant as well as the northern part of the province of Waals-Brabant.

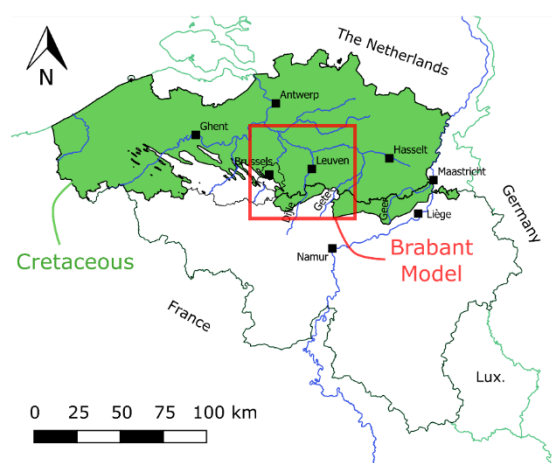


Figure 5: Map of the extent of the Cretaceous deposits in Flanders and the location of the study area of the Brabant Model.

The main confining units in Flanders are shown in Figure 6. In the Brabant area, the Ieperian Aquitard is the main unit that confines the aquifer systems of the Cretaceous and the Paleocene. Note that in the largest part of the area, these aquifer systems are confined, with exception for the southern part (in Wallonia) and in the south-east in the Tienen area. In these areas, the aquifer systems are either overlain by the Quaternary deposits (mainly in the river valleys and in the south-east) or by the Brussels sands, a highly permeable sand deposit.

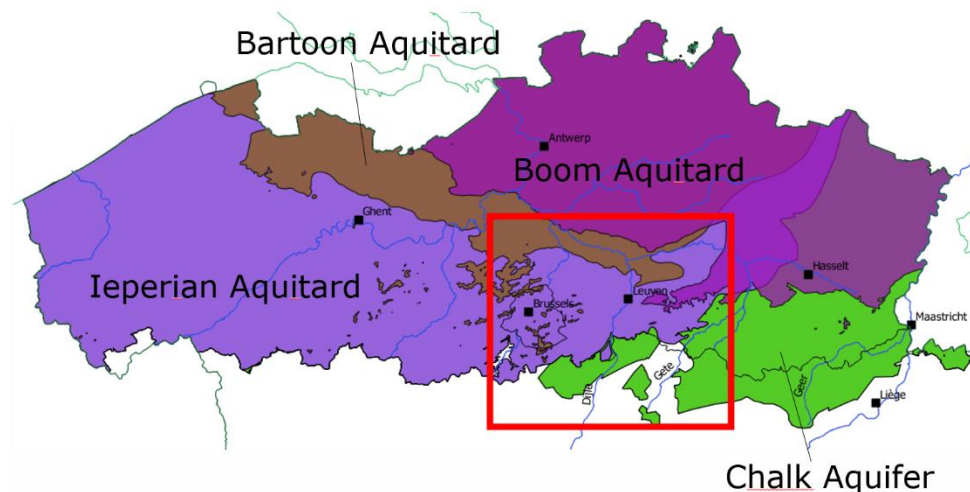


Figure 6: Map of the main confining units overlying the Chalk aquifer: the Ieperian, Bartoon and Boom Aquitards.

In Figure 9 geological profiles through the study area are shown. Note that the Cretaceous deposits are close to the surface in the southern part, near the Flanders-Wallonia boundary³. The Cretaceous deposits dip into the subsurface towards the north and quickly reach depths of several hundreds of meters. On top of the Cretaceous, deposits from the Paleocene aquifer system are present: the Formation of Heers and the Formation of Hannut. On top of the Paleocene aquifer system, the Ieperian aquitard system forms the confining unit at the top of the model. Below the Cretaceous, the Palaeozoic basement is present, which is the impermeable boundary at the bottom. The geological units that are present in the study area are discussed below. The link is made with the hydrogeological units defined in the framework of HCOV (Hydrogeological coding of the subsurface of Flanders). An overview of the HCOV units in the Paleocene and Cretaceous aquifer systems are shown in Table 2 and their extent and thickness are shown in Figure 7 and Figure 8. The geological and hydrogeological classifications used in this section are based on the 3D geologic (G3Dv3) and hydrogeologic (H3D) model of Flanders (Deckers et al., 2019).

³ Note that the geological profiles are limited to Flanders. A N-S profile that extends to the Walloon region is shown in Figure I. 1, showing that the Cretaceous deposits can be unconfined in the south, and that they wedge out against the Palaeozoic bedrock.

Table 2: Overview of the HCOV coding of the hydrogeological units comprising the Cretaceous and Paleocene aquifer systems.

Main Unit		Sub Unit		Base Unit				
A1000	Paleocene Aquifersysteem	A1010	Landeniaan Aquifersysteem	A1011	Zand van Knokke	A1012	Zandige afzettingen van Loksbergen en Dormal	
				A1013	Zand van Grandglise			
		A1020	Landeniaan en Heersiaan Aquitard	A1021	Siltige afzettingen van Halen en Tufsteen van Lincet			
		A1030	Heersiaan en Opglabbeek Aquifersysteem	A1022	Kleien van Waterschei en Beselare			
				A1031	Kleiige mergels van Maaseik			
				A1032	Mergels van Gelinden			
				A1033	Zand van Orp			
				A1034	Zand van Eisden			
				A1035	Klei van Opoeteren			
A1100	Krijt Aquifersysteem	/		A1101	Kalkareniet van Houthem			
				A1102	Kalkarenieten van Maastricht en Kunrade			
				A1103	Krijtafzettingen van Gulpen en Nevele, zanden en mergels			
				A1104	Zand van Aken			

Palaeozoic basement

The basement, the Brabant Massif, are deposits from the Palaeozoic, mainly Cambrian to Silurian in age. Towards the Campine basin, also Devonian and Carbonian deposits are present. Before the Cretaceous onlap, a long phase of weathering has affected the Palaeozoic bedrock, resulting in a paleo-relief at the top with cliffs of up to 20m in height in the western part of the study area (Matthijs et al. 2005). The Palaeozoic basement is present over the entirety of the study area.

Formation of Vaals

The Formation of Vaals is present on top of the basement in parts of the study area (Figure 4a). These are deposits from the Early Campanian consisting of glauconite-bearing sands at the top with a transition to grey-green clayey marls at the bottom. The latter are often called the "Smectite of Hervé". Due to the presence of this clayey-marly layer, the Formation of Vaals is often assumed as an impermeable boundary limiting the Cretaceous aquifer at its bottom. Often, only a couple of meters of Vaals Formation is present. In the hydrogeological coding (HCOV), the Formation of Vaals is part of A1103, a base unit of the Cretaceous aquifer system (A1100).

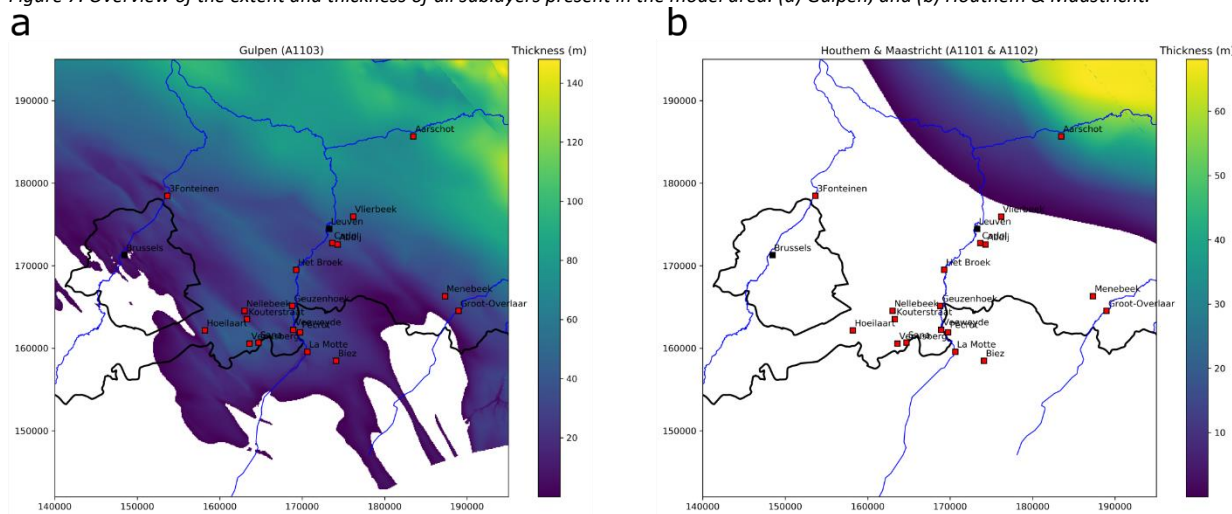
Formation of Gulpen

The Formation of Gulpen is an extensive chalk deposit of Campanian to Maastrichtian age. The majority of the extraction wells of De Watergroep produce drinking water from these deposits. The Formation of Gulpen is close to the surface in the southern part of the area, but dips downwards towards the north where it quickly reaches depths of several 100s of meters (Figure 9). It has a thickness of a couple of meters in the southwest to more than 100m in the north-east. In the northeast, thickness increase up to 100m (Figure 7a). Different members are present in the study area. The Member of Zeven Wegen at the bottom forms the largest part of the Cretaceous deposits in the area (Figure 4b). The Member of Zeven Wegen consists of white, fine-grained chalk, the typical "writing chalk". On top of the Zeven Wegen Chalk, the Members of Lanaye and Lixhe are found in most of the study area, with exception of the westernmost part of the study area, starting from the area around the extraction site of Nellebeek (Figure 4c). The Lixhe Member consists of white fine-grained chalk with extensive silex intervals. The Lanaye Member consists of very fine calcarenites with extensive silex intervals. Often, only a couple of meters of Lanaye and/or Lixhe are found on top of the Zeven Wegen chalk in the study area. The other members of Gulpen are not identified in this area. Possibly, these are present in the north-eastern most part of the area, but they are not explicitly described in the available borehole data. In the Vilvoorde area, the Formation of Nevele is described, which is the lateral equivalent of the Formation of Gulpen. In the hydrogeological coding (HCOV), the Formations of Gulpen and Nevele are part of A1103, a base unit of the Cretaceous aquifer system (A1100).

Formation of Maastricht and Houthem

The Formations of Maastricht and Houthem are found on top of the Gulpen Formation. These are coarser-grained calcarenites of Maastrichtian to Danian age. The calcareous of Houthem and Maastricht are only present in the north-eastern most corner of the area. These deposits dip strongly towards the north east, with thickness ranging from a couple of meters in the northeast of Leuven to approx. 80m in the north-eastern most corner (Figure 7b). The extraction site of Aarschot extracts water from the Formation of Maastricht. In the hydrogeological coding (HCOV), the Formation of Maastricht comprises A1103 and the Formation of Houthem A1101, both base units of the Cretaceous aquifer system (A1100).

Figure 7: Overview of the extent and thickness of all sublayers present in the model area. (a) Gulpen; and (b) Houthem & Maastricht.



Formation of Heers

The Formation of Heers is a deposit from the Middle-Paleocene (Selandian), consisting mainly of marls and sands. These deposits are only present in the east and north-east part of the study area (Figure 9c and Figure 9d). These deposits are part of the Heersian and Opgrabbeek Aquifersystem (A1030). At the bottom, the Sands of Orp (A1033) are present with a limited thickness of a couple of meters to a maximum of about 15m (Figure 8a). On top of Orp, the marls of Gelinden (A1032) and the clayey marls of Maaseik (A1031) are present. These units also have a limited thickness of a couple of meters to maximum about 15m (Figure 8b).

Formation of Hannut

The Formation of Hannut is a deposit from the Late-Paleocene (Thanetian). These deposits dip towards the north and have a thickness of 50 to 100m. They are part of the Landenian and Heersian Aquitard (A1020). At the bottom, the clays of Waterschei en Beselare (A1022) are present. These deposits are only present in the north-eastern half of the studied area, with thickness ranging from a couple of meters in the Leuven area to approx. 25m in the north-east (Figure 8c). Next, the Member of Halen and Lincent is present (A1022), which consist of silty deposits of Halen and the “tuffeau” of Lincent in the Tienen area. The Halen and Lincent Member consists of clayey sand to silt, often lithified to silt or fine-grained sandstone, with intercalations of sandy clay (Diez and Van Limbergen, 2014). In the tuffeau area, these deposits are more chalky to marly and often silicified. Due to the dissolution of spicula, these deposits have a strongly increased porosity. In the Tienen area, where these deposits are close to the surface (Figure 9b), they are fractured, resulting in high permeabilities (Vandenbergh and Gullentops, 2001). The Member of Halen and Lincent is present over more or less the entire area and dips towards the north-east where a maximum thickness of >50m is reached (Figure 8d). The Member of Grandglise at the top of the Formation of Hannut consists of fine sands and is part of the Landenian Aquifersystem (A1010). The sands of Grandglise (A1013) are present throughout

the entire model area, with an average thickness of approx. 20m and maximum thickness of 40m in the east (Figure 8e).

Formation of Tienen

Locally, the sandy deposits of Loksbergen and Dormaal (A1012) are present on top of the sands of Grandglise, with whom they form the Landenian Aquifersystem (A1010). These are deposited in a continental environment in a 20km wide north-east oriented erosional channel. Locally, a thickness of up to 30m is observed.

Formation of Kortrijk

The Formation of Kortrijk is a clay deposit from the Ieperian (early Eocene). In general, it consists of clay but internally there is a certain alteration of clay with more silty or sandy intercalations. Hydrogeologically, it is classified as the Ieperian Aquitard (A0900) which is the main confining unit on top of the Paleocene and Cretaceous aquifer systems. It is present in most of the study area, with the exception for the southern part (in Wallonia) and in the south-east in the Tienen area (Figure 9a-b). In general, it has a thickness of several tens of meters with a maximum thickness of approx. 100m in the northwest (Figure 8f).

Formation of Brussels

The Formation of Brussels is a heterogeneous sandy deposit from the Eocene (Lutetian). In some areas in the south where the Formation of Kortrijk is absent, the Brussel Sands (A0600) are present directly on top of the Paleocene aquifer system (Figure 9a). In these areas, it forms one unconfined aquifer with the sands of Grandglise. To the west of the extraction site of De Watergroep in Hoeilaart (with filters in Grandglise) the Formation of Kortrijk is locally eroded and deposits from the Formation of Brussels are present directly on top of the sands of Grandglise. This channel is only partially present in the map of the Ieperian aquitard in Figure 8f which is based on the latest version of the geological 3D model (G3Dv3). This local, steep channel is described in Houthuys (2011) and is part of the Basin of Brussels, an elongated valley which was connected to the North Sea Basin in the Eocene. The channel present near Hoeilaart is one of five NE-SW oriented channels, which have a steep eastern flank. An east-west geological profile through the extraction site of Hoeilaart, indicating the local erosion of the Formation of Kortrijk by a channel filled with Brussel sands, is added in the Appendix in Figure I. 2.

Quaternary

Locally, Quaternary deposits are present directly on top of the Paleocene and Cretaceous deposits. This is mainly the case in the river valleys in the south, and in the south-east in the Tienen region, where the Paleocene deposits are close to the surface and only covered by a Quaternary cover (Figure 9b). A distinction can be made between permeable fluvial deposits of the Pleistocene at the bottom and the less permeable loamy cover at the top. The fluvial deposits consist of fine to coarse sand and are strongly heterogeneous.

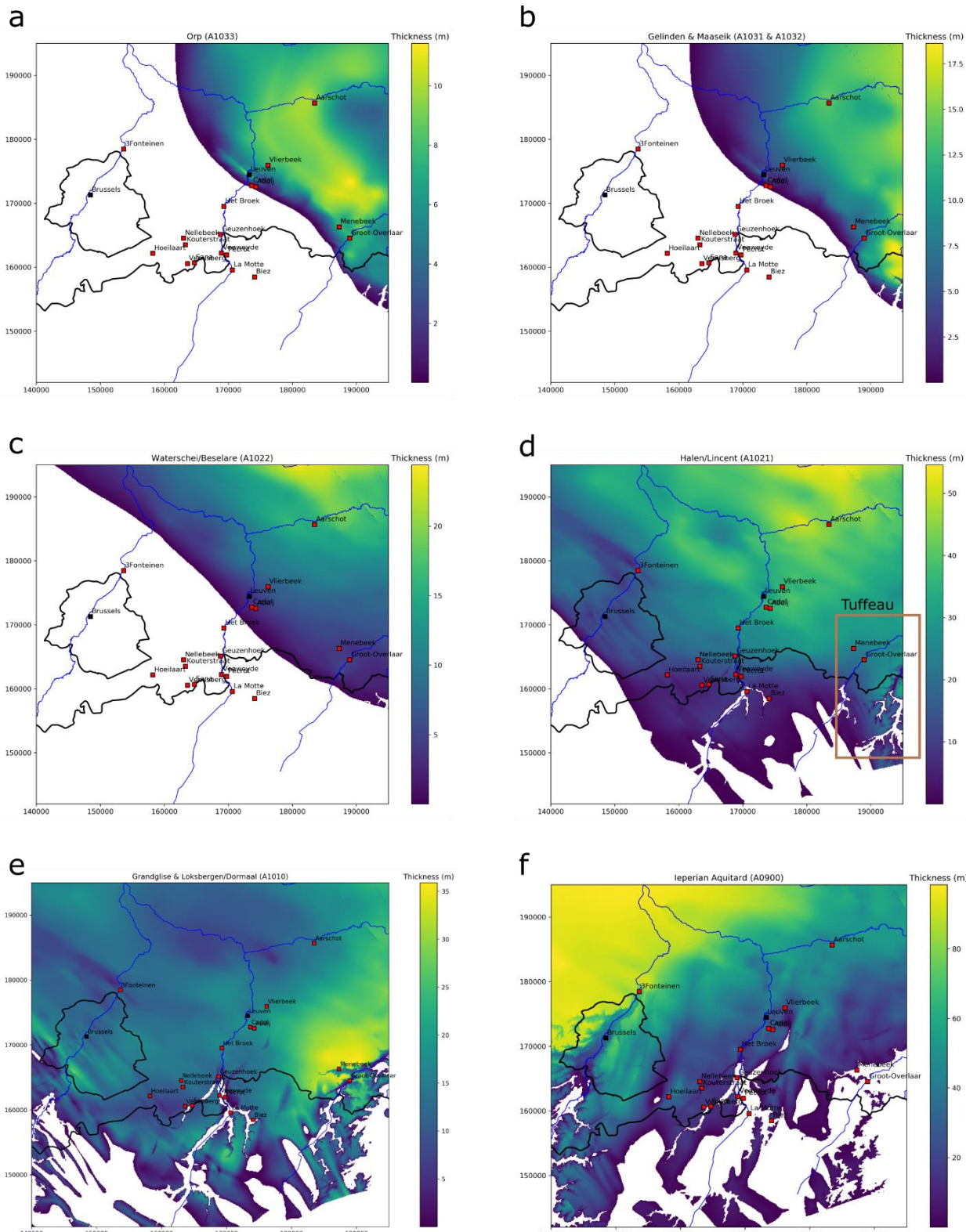


Figure 8: Overview of the extent thickness of all sublayers present in the model area. (a) Orp; (b) Gelinden & Maaseik; (c) Waterschei & Beselare; (d) Halen & Lincent, with indication of the "tuffeau" zone; (e) Grandgise & Loksbergen/Dormaal; and (f) the confining Ieperian Aquitard.

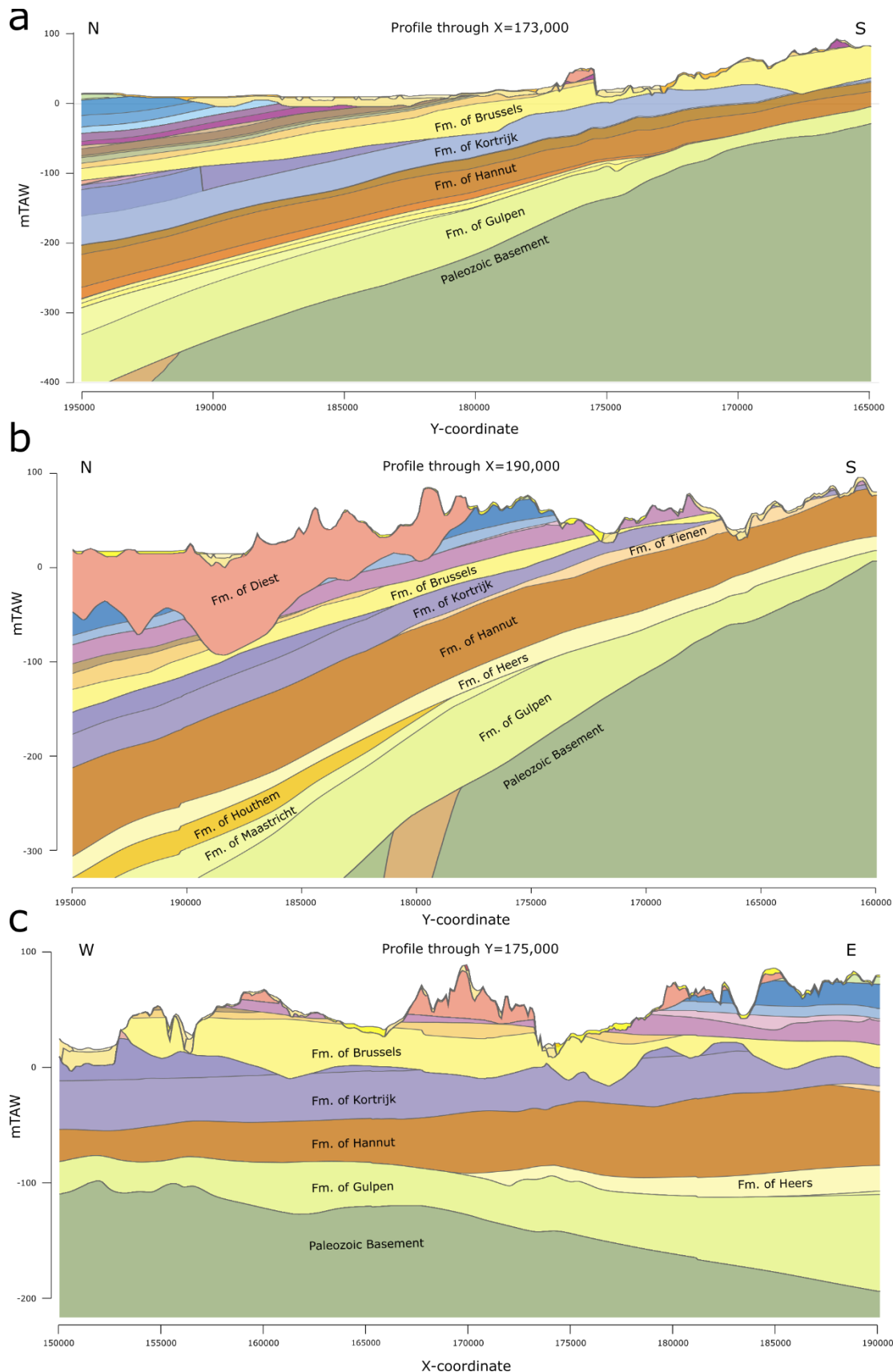


Figure 9: Geological profiles: (a) north-south profile through Leuven area ($X=173,000$); (b) north-south profile through Tienen area ($X=190,000$); (c) west-east profile through Leuven area ($Y=175,000$) (adapted from DOV).

2.3 Hydrogeological properties of the Cretaceous

Throughout the last few decades, De Watergroep has performed several pumping tests on their extraction wells in the Cretaceous. Often also geophysical measurements and flow measurements are performed. These measurements can provide valuable insights in the hydrogeological properties of the Cretaceous and can help explain the different well yields observed in the extraction sites.

2.3.1 Pumping tests

In Table 3, an overview is shown of all pumping test data for the extraction sites in the Cretaceous. For some wells, multiple pumping tests have been performed or multiple methods of analysis have been used. In this case, an average of estimated horizontal hydraulic conductivity (HK), transmissivity (T) and/or storage (S) is calculated. In total, pumping test data is available for 30 different wells. The Formations and Members present at the filter intervals are shown in the table. Note that for 3010-006, 3010-017 and 3010-018, two separate filters are present: one in the Member of Lincent in the Formation of Hannut and the second in the Formation of Gulpen.

In Figure 10, the estimated HK for all pumping tests on wells in the Cretaceous is visualized on a map of the depth of the top of the Cretaceous. Note that there is a strong spatial variability in the estimated HK values that seems to be correlated with the depth of the top of the Cretaceous, with higher HK in the south and low HK in the north. In the southern part of the Dijle valley (Geuzenhoek, Veeweyde, Sana & Venusberg) conductivities are very high, ranging between 20 to 110 m/d. In Nellebeek and Kouterstraat, HK is significantly lower. At the site of Het Broek, there is a strong variability between the different extraction wells. Estimated HK is significantly higher in the southern wells (10-20 m/d), compared to the more northern wells (1-2 m/d). The sites near Leuven all have very low conductivities, ranging between 0.1 to 0.2 m/d. At the Aarschot site, HK is around 2 m/d. At the Vilvoorde site, estimated HK is around 13 m/d. All these pumping tests have been analysed with a variety of methods. There is a certain degree of uncertainty related to the resulting HK estimates due to the choice of method, the aquifer thickness used, etc.

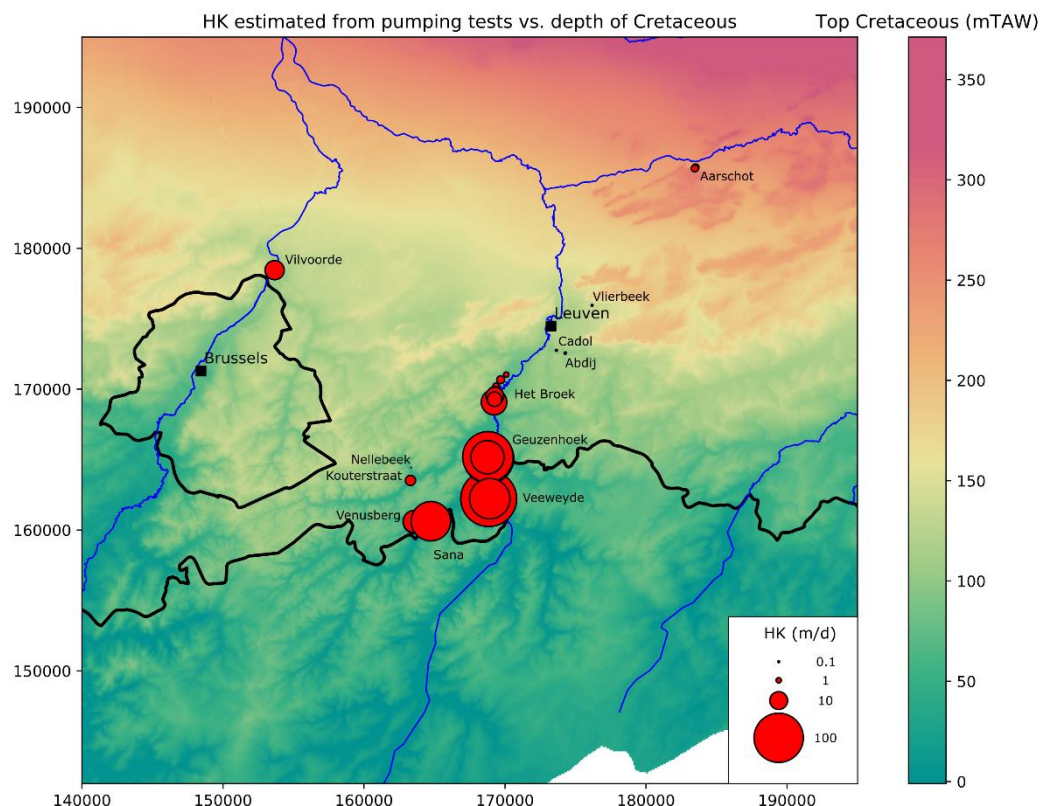


Figure 10: HK estimates from pumping tests on extraction wells in the Cretaceous. Background map shows the depth of the top of the Cretaceous.

Table 3: Overview of all pumping test data for extraction sites in the Cretaceous. ^apart of filter in Member of Lincent; ^bpart of filter in Gulpen; ZW: Zeven Wegen; *only partial data available.

Well	X	Y	Site	Formation	Members Filter (m-topo)	HK (m/d)	T (m ² /d)	S (m ⁻¹)	Topo. (mTAW)	Pumping test	Year	Flow	Geophys.
3001-107	183511	185746	Aarschot	Maastricht/ Gulpen	Maastricht (238-246m); Gulpen (246-253m)	1.73	69.17	1.00E-04	13.8	Theis	2014	No	No
3001-108	183464	185677	Aarschot	Maastricht /Gulpen	Maastricht (236-246m); Gulpen (246-277m)	1.76	70.50	1.00E-04	18.63	Theis	2014	Yes	Yes*
3006-001	173644	172757	Cadol	Gulpen	Lixhe (96-111m); ZW (111-127m)	0.14	4.28	1.00E-04	24.66	Theis	1993	Yes	Yes
3006-116	174276	172561	Abdij	Gulpen	Lixhe (101-114m); ZW (114-131m)	0.21	6.55	1.00E-04	28.5	Theis	1993	Yes	Yes
3007-001	176177	175954	Vlierbeek	Gulpen	Lixhe (142-152m); ZW (152-178m)	0.13	4.59	1.00E-04	25.64	Theis	1993	Yes	Yes
3008-001	169223	169076	Het Broek	Gulpen	Lixhe + ZW (71-108m)	23.30	945.00		27.77	Theis	1988	No	No
3008-002	169373	170207	Het Broek	Gulpen	Lixhe + ZW (74-111m)	1.50	71.00		26.72	Theis	1987	No	No
3008-003	169696	170670	Het Broek	Gulpen	Lixhe (75-86m); ZW (86-113m)	2.20	75.00		25.74	Theis	1987	Yes	Yes
3008-004	170091	171033	Het Broek	Gulpen	Lixhe (75-89) + ZW (89-115m)	1.00	37.00		24.87	Theis	1988	No	Yes
3008-005	169298	169638	Het Broek	Gulpen	Lixhe (68-80m); ZW (80-112m)	8.60	435.40		27.11	Theis	1988	No	No
3008-006	169280	169513	Het Broek	Gulpen	Lixhe (69-76m); ZW (76-108m); Vaals (108-111m)	11.20	598.30		27.15	Theis	1988	No	No
3008-064	169259	169286	Het Broek	Gulpen	Lanaye (66.5-68m); Lixhe (70-78m); ZW (78-103m)	7.50	255.00	1.20E-06	25.68	MLU	2017	Yes	Yes
3010-001	163297	163520	Kouterstraat	Gulpen	Gulpen (52-66m)	3.71	52.27		51.48	Theis-Jacob	1978	No	No
3010-006 ^a	162999	164519	Nellebeek	Hannut	Lincent (49-67m)	7.30	131.40	1.00E-04	62.00	Theis	1990	No	No
3010-006 ^b	162999	164519	Nellebeek	Gulpen	ZW (67-81m)	0.00	0.00		62.00	Theis	1990	No	No
3010-017 ^a	162999	164519	Nellebeek	Hannut	Lincent (51-66.5m)	1.65	23.25		60.00	Theis	2013	Yes	No
3010-017 ^b	162999	164519	Nellebeek	Gulpen	Gulpen (66.5-81m)	0.00	0.00		60.00	Theis	2013	Yes	No
3010-018 ^a	163340	164438	Nellebeek	Hannut	Lincent (53-64m)	4.21	42.09	2.17E-08	61.61	MLU	2016	Yes	Yes
3010-018 ^b	163340	164438	Nellebeek	Gulpen	Gulpen (69-83m)	0.01	0.23	1.30E-04	61.61	MLU	2016	Yes	Yes
3011-005	163610	160562	Venusberg	Gulpen	ZW (32-66m); Vaals (66-68m)	18.90	682.00		49.3	Theis/Jacob/ Hantush	2000	Yes	Yes
3011-006	163583	160581	Venusberg	Gulpen	ZW (32-66m); Vaals (66-68m)	18.60	670.78	6.64E-04	50.30	Theis/Jacob/ Hantush	2000	No	No
3011-007	163555	160607	Venusberg	Gulpen	ZW (32-66m); Vaals (66-68m)	17.10	613.67	2.93E-04	52.23	Theis/Jacob/ Hantush	2000	No	No
3011-008	164745	160598	Sana	Gulpen	ZW (23.9-51.5m)	36.79	1214.07	2.50E-02	39.54	Hyparyden	1978	No	No

3011-009	164746	160626	Sana	Gulpen	ZW (25.5-48m)	55.55	1833.15	2.40E-02	39.49	Hyparyden	1994	No	No
3012-001	168889	162233	Veeweyde	Gulpen	ZW (21-52m)	98.83	3390.00	2.10E-04	33.86	Theis/Cooper-Jacob	1977/1984	No	No
3012-002	168936	162225	Veeweyde	Gulpen	ZW (17.90-48.40m)	101.84	3503.33	2.38E-04	33.58	Theis/Cooper-Jacob	1977/1984	No	No
3012-003	168845	162230	Veeweyde	Gulpen	ZW (23.6-46.4m)	111.70	3686.25	1.61E-04	37.73	Theis/Cooper-Jacob	1996	Yes	Yes
3012-007	168841	165088	Geuzenhoek	Gulpen	Lixhe (37-44m); ZW (44-72.3m)	90.41	3345.00		30.27	Theis/Cooper-Jacob/Theis-recovery	1984/1991	No	No
3012-008	168789	165194	Geuzenhoek	Gulpen	Lixhe (41.3-44m); ZW (44-72m)	91.04	2795.00		29.35	Theis/Cooper-Jacob/Theis-recovery	1984	No	No
3012-009	168758	165170	Geuzenhoek	Gulpen	ZW (48-77m)	39.48	1145.00		29.02	Theis/Cooper-Jacob/Theis-recovery	1997	Yes*	No
3012-059	168917	162226	Veeweyde	Gulpen	ZW (18.3-48.5m)	58.40	2160.80		34.53	MLU	2017	Yes	Yes
3014-004	153662	178449	Vilvoorde	Gulpen	Nevele (115-145m)	13.08	392.42	5.41E-04	13.31	MLU	2016	Yes	Yes

2.3.2 Correlation with flow and geophysical measurements

At several extraction wells, both geophysical and flow measurements are performed (Table 3). These can give additional insights in which intervals of the Cretaceous deposits provide the highest well yields. This way, the local geology can be correlated with the well yields. Note that the flow measurements are visualized in different ways depending on the availability of the data: sometimes actual well yields per meter of filter are available in m/h/m, other times only the cumulative well yield in m/h, and sometimes well yields are expressed as a percentage. Often, the source data was not available, making it difficult to derive the actual well yields per meter of filter.

The flow measurement and stratigraphy of the extraction well 3001-108 at the **Aarschot** site is visualised in Figure 11. In both 3001-107 and 3001-108, the top part of the filter (8-10m) is situated in the Formation of Maastricht, while the rest of the filter consists of the Formation of Gulpen (10m at 3001-107, 30m at 3001-108). Only the gamma-ray signal of the top part of the Cretaceous in 3001-107 is available. The flow measurement (Figure 11) shows that the largest part of the flow originates from the top 6m of the filter (50%) in the Formation of Maastricht. About 34% of flow comes from the top of the Formation of Gulpen (251-259m), while only 15% comes from the bottom 15m of the filter. Without the gamma-ray signal, it is difficult to identify the different Members in the Formation of Gulpen. However, the available geological data indicates that the part of the Formation of Gulpen that is present here consists of the Members of Lixhe and Lanaye. The Member of Zeven Wegen is estimated to be at approx. 300m below ground level. This is supported by the flow in this bottom part of the filter, as in general the Member of Zeven Wegen has a very low primary permeability and thus low flow.

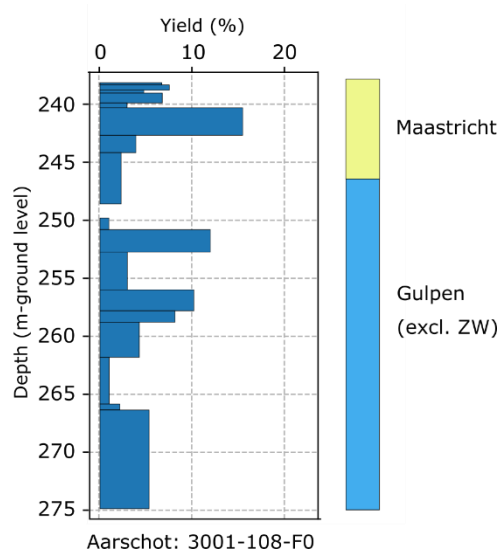


Figure 11: Stratigraphy and flow measurement results for 3001-108-F0 (Aarschot site).

The flow and gamma-ray measurements for the sites of **Vlierbeek**, **Cadol** and **Abdij** are shown in Figure 12. These three extraction wells have a filter which consists of the Member of Lixhe at the top and the Member of Zeven Wegen at the bottom, both part of the Formation of Gulpen. The Formation of Maastricht is absent in this area. The boundary between the Members of Lixhe and Zeven Wegen is characterized by a hardground interval below a phosphite horizon. This hardground is clearly visible as a peak in the gamma-ray signal of Cadol and Abdij (Figure 12b-c). This hardground interval corresponds with an interval of 2 to 3m that provides most of the flow for these wells. For Vlierbeek, no gamma-ray measurements are available but a similar peak in the yield is visible (Figure 12a) indicating the presence of this hardground.

For **Vlierbeek**, the top 10m of the filter interval consists of Lixhe (142-152m from the ground level) and the bottom 26m of Zeven Wegen (152-178m from the ground level) (Figure 12a). About 80% of the flow comes from an interval

between 150-152m, corresponding with the hardground. The rest of the flow (20%) comes from the top part of the filter (Lixhe; 142-150m). The bottom part of the filter (Zeven Wegen) does not contribute to the flow at all. In 1993, a pumping test was performed on the extraction well of Vlierbeek (De Watergroep, 1993), resulting in a HK estimate of 0.13 m/d for the entire filter. Recalculating for the different parts of the filter, this results in a HK of 1.9 m/d for the hardground interval (2m), and a HK of 0.1 m/d for the top 10m of the filter (Lixhe).

For **Cadol**, the top 15m of the filter consists of Lixhe (96-111m) and the bottom 16m of Zeven Wegen (111-127m) (Figure 12b). About 70% of the flow is provided by a 2m interval corresponding to the hardground. The top 6m (Lixhe) provides the rest of the flow. In 1993, a pumping test was performed on the extraction well of Cadol (De Watergroep, 1993), resulting in an HK estimate of 0.14 m/d for the entire filter. Recalculating for the HK of the hardground interval (2m), an HK of 1.5 m/d is obtained. For the top 6m of Lixhe, an HK of 0.2 m/d is obtained.

For **Abdij** the top 13m of the filter consists of Lixhe (101-114m) and the bottom 17m of Zeven Wegen (114-131m) (Figure 12c). About 70% of the flow is provided by a 2m interval corresponding to the hardground (De Watergroep, 2010). A 4m interval between 106-110m (Lixhe) provides the rest of the flow. In 1993, a pumping test was performed on the extraction well of Abdij (De Watergroep, 1993), resulting in an HK estimate of 0.21 m/d for the entire filter. Recalculating for the HK of the hardground interval (2m), an HK of 2.2 m/d is obtained. For the part of Lixhe (4m) contributing the remainder of the flow, an HK of 0.5 m/d is obtained.

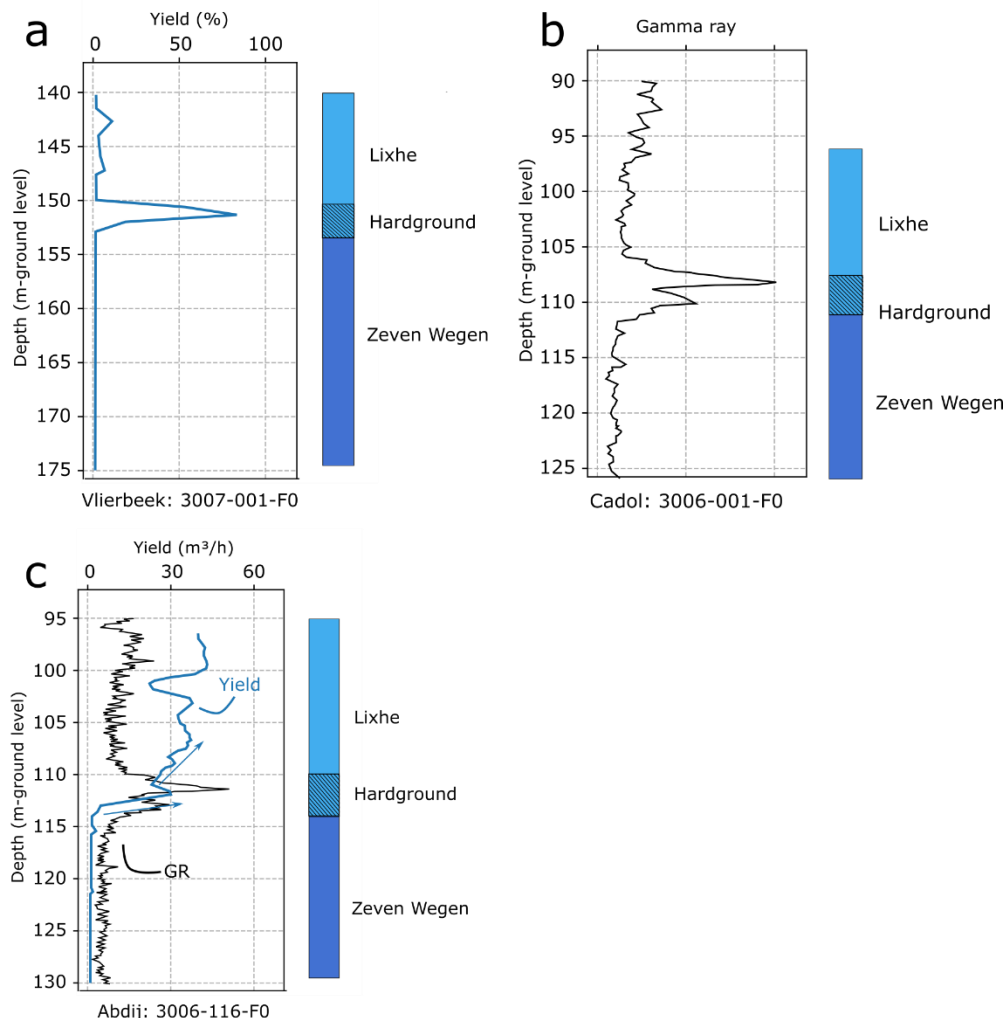


Figure 12: Stratigraphy, flow and gamma-ray measurements for the sites around Leuven: (a) Vlierbeek; (b) Cadol; (c) Abdij.

The extraction site of **Het Broek** consists of multiple production wells. As discussed before, there is a strong spatial variation in the estimated HK for these wells, with lower HK for the northern wells (3008-002, -003 and -004) compared to the southern wells (3008-001, -005, -006, 063 and -064) (Figure 10). For all wells, the top 10-15m consists of Lixhe, while the bottom part (20-30m) consists of Zeven Wegen.

For the **northern part of Het Broek**, flow measurements and gamma-ray logs⁴ are available for wells 3008-003 and 3008-004 (Figure 13). At both wells, a clear peak in the gamma-ray signal is visible around 85m from the surface. This peak is similar to peaks in the sites near Leuven and corresponds with the hardground interval. The flow measurement on 3008-003 indicates that most of the flow comes from the interval near this hardground, while the bottom part of the filter (Zeven Wegen) contributes no flow at all (Figure 13a). About 60% of the flow comes from the interval between 81-83m, and the remaining 40% from the interval between 85-87m. In 1987, a pumping test was performed on the extraction well 3008-003, resulting in an HK estimate of 2.2 m/d for the entire filter (De Watergroep, 1988). Recalculating for the HK of the hardground interval (6m), an HK of 13.9 m/d is obtained. For 3008-004, based on a pumping test in 1988, an HK estimate of 1.0 m/d was obtained (De Watergroep, 1988). Assuming that all the flow originates from a hardground interval with a similar thickness as in -003, this would correspond with an HK of 6.7 m/d. For well 3008-002, no gamma-ray or flow measurements are available. The pumping test in 1988 resulted in an HK estimate of 1.5 m/d, which would correspond with a HK of the hardground interval of approx. 9 m/d. Note that the hardground interval is larger in thickness (6m) compared to the wells around Leuven (2m) and has a significantly larger HK.

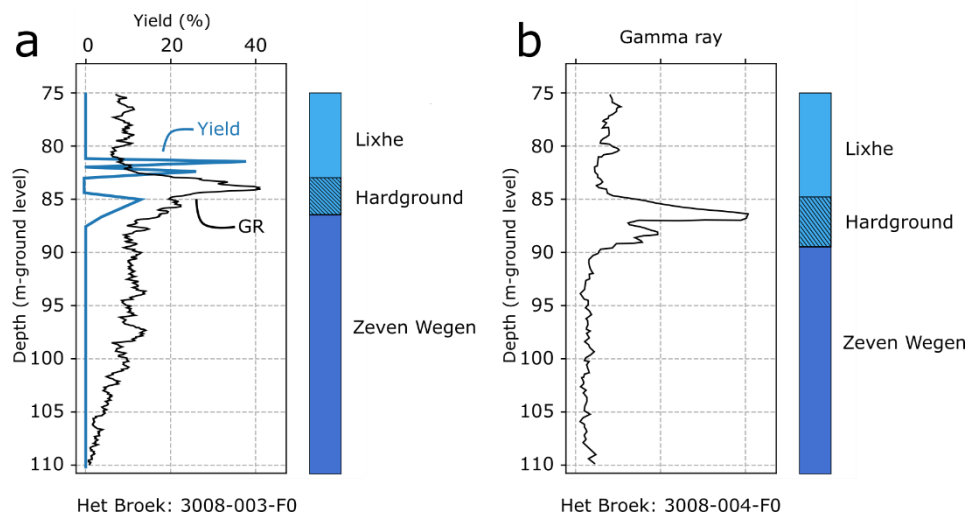


Figure 13: Stratigraphy, flow and gamma-ray measurements for the northern wells of Het Broek: (a) 3008-003; and (b) 3008-004.

For the **southern part of Het Broek**, flow measurements and gamma-ray logs are available for the wells 3008-063 and 3008-064 (Figure 14). The top 1.5m of the filter consists of the Member of Lanaye, then about 7m of Lixhe is present and the rest of the filter consists of Zeven Wegen. For both wells, flow and gamma-ray measurements are available. The gamma-ray peak corresponding to the hardground is clearly visible. The increase in gamma-ray at the bottom in 3008-063 might indicate the presence of the Smectite of Hervé (Formation of Vaals). Like the previous wells, most of the flow comes from the hardground interval which is approx. 6m in thickness. A pumping test was performed on 3008-064 in 2017 which was analysed with MLU (Hemker & Randall, 2013), resulting in an HK of 7.5 m/d (De Watergroep, 2017b). Recalculating for the 6m thick hardground interval results in a HK of 45.6 m/d. In 1988, pumping tests were performed on 3008-001, -005 and -006, resulting in HK estimates of 23.3, 8.6 and 11.2 m/d (De Watergroep, 1988). Assuming that all flow comes from a similar 6m interval, respectively HK estimates of 143.7; 63.1

⁴ Available on paper in the archive of De Watergroep.

and 78.4 m/d are obtained for the hardground interval. These HK estimates for the hardground interval are high compared to those for the more northern wells. In the borehole description of 3008-064, performed by Michiel Dusar, the hardground interval is described as a phosphatic gravel, consisting of beige balls of up to 1 cm in size of hard fine-grained phosphatic chalk. This phosphatic gravel might be the result of reworking or erosion and redeposition of chalk material. This interval associated with the hardground clearly has higher permeabilities than in the Leuven area and the northern wells of Het Broek, indicating a stronger reworking or even karstification of this interval. There is a clear trend of increasing permeability of this interval from the north towards the south.

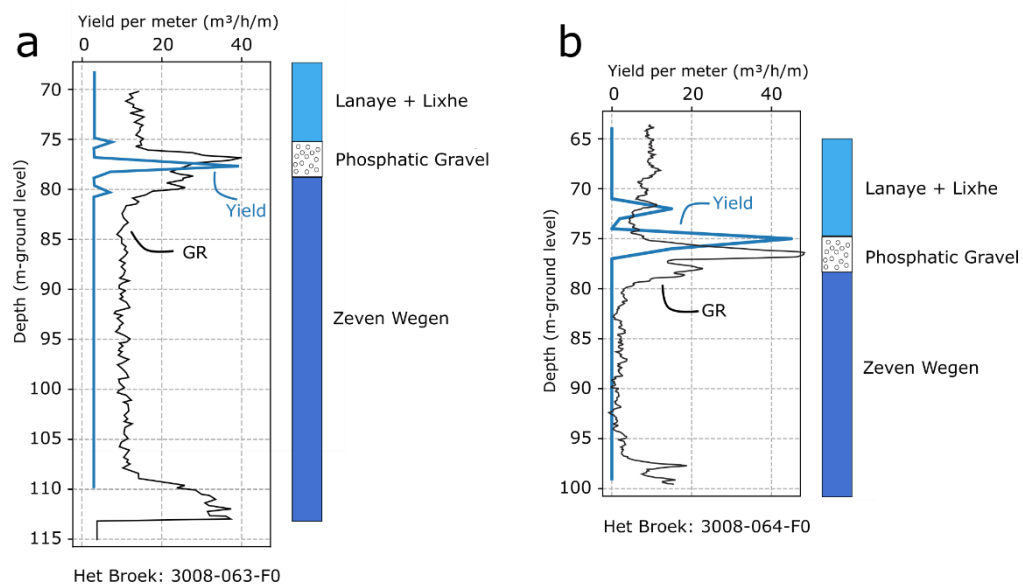


Figure 14: Stratigraphy, flow and gamma-ray measurements for the southern wells of Het Broek: (a) 3008-063; and (b) 3008-064.

For the site of **Nellebeek**, a flow measurement is available for 3010-017 and a flow measurement and gamma-ray log for 3010-018 (Figure 15). The wells at this site are a special case as the wells have a filter both in Lincent (Formation of Hannut) and the Formation of Gulpen. The boundary between these two Formations is clearly visible in the gamma-ray log for 3010-018 (Figure 15b). The part of the filter consisting of the Cretaceous has a very low gamma-ray signal and contributes nothing to the flow in the well, indicating that this interval consists solely of Zeven Wegen. This means that Lixhe and the hardground at the top of Zeven Wegen are not present here. This explains the absence of flow in the bottom part of the filter, also in 3010-017 (Figure 15a). Most of the flow in both wells comes from an interval around 55m in Lincent, with some small contributions around 60m. The deposits of Lincent are described as silty clay with claystone and occasional fractures. At 53m in Lincent, there were water losses during the drilling of the well, indicating a water-bearing character. This might be related to either fracturing of the claystone or a more permeable (sandy) interval. A pumping test was performed on 3010-006 in 1990, which was analysed with the Theis method (De Watergroep, 2015). The resulting HK estimate for the entire filter is 4.1 m/d. Recalculation for only Lincent results in an HK of 7.3 m/d. As all the flow comes from an interval of approx. 5m in Lincent, recalculation results in an HK of 26.2 m/d for this interval. Well 3010-006 was later renewed to well 3010-017, on which a pumping test was performed in 1990. Analysis with the Theis method resulted in an HK for the entire filter of 0.85 m/d (De Watergroep, 2013). Recalculating for the entire Lincent section results in an HK of 1.65 m/d. Recalculating for the permeable part of Lincent (5m) contributing all the flow, an HK of 6.8 m/d is obtained. At 3010-018, a pumping test was performed in 2016. Analysis with MLU resulted in an HK of Lincent of 4.2 m/d and 0.0135 m/d for the Cretaceous (De Watergroep, 2016). Recalculating for only the 5m interval of Lincent contributing to the flow, an HK of 9.2 m/d is obtained.

The absence of the hardground and the Members of Lixhe and Lanaye results in a very low permeable Cretaceous interval. Only the tight chalk of Zeven Wegen is present in this area (Figure 4b-c). The Cretaceous is thus not suitable for the extraction of drinking water in this area. The presence of a fractured zone in Lincent results locally in a highly permeable interval. However, the extent of this fractured zone is not clearly known.

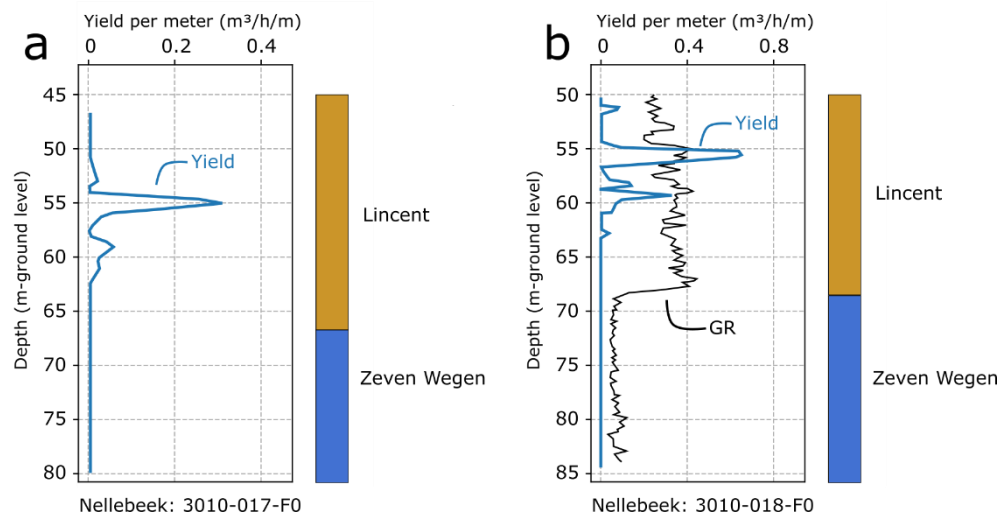


Figure 15: Stratigraphy, flow and gamma-ray measurements for the site of Nellebeek: (a) 3010-017; and (b) 3010-018.

For the site of **Kouterstraat**, no gamma-ray or flow measurements are available. The filter of extraction well 3010-001 is situated in the Formation of Gulpen. However, from the description it is not clear if Lixhe is present at the top or if the entire interval consists solely of Zeven Wegen chalk. A pumping test was performed in 1978 and was analysed with Theis-Jacob, resulting in an HK estimate of 3.7 m/d (De Watergroep, 1978). This relatively high HK is either an indication of the presence of the hardground interval and/or the more permeable deposits of Lixhe at the top, or of the presence of fractures. However, without gamma-ray log or flow measurement, it is difficult to conclude what the exact reason is.

For the site of **Venusberg**, a flow measurement is available for well 3011-005 (Figure 16). A gamma-ray log was also obtained but only after the well casing was installed, resulting in a strongly weakened gamma-ray signal. The filter in this well is situated in Zeven Wegen at the top (32-66m) and the Smectite of Hervé (Vaals) at the bottom (66-68m). The gamma-ray log shows a small, strong peak around 27m, which might correspond with the boundary between Zeven Wegen and Lixhe. However, this part is not included in the filter. This indicates that the filter consists only of Zeven Wegen. The flow measurement shows that flow is more or less distributed along the entire filter, with three main zones of flow: 35% coming from 39-42m, 45% from 47-56m and 20% from 56-65m. The first zone has an important permeability and/or fracture network because the gradient of the flow reduction is stronger than the other zones. The permeability seems to be caused by the presence of fractures in these zones. A pumping test has been performed on this well in 2000 which was analysed with the Theis, Jacob and Hantush methods, resulting in an average HK estimate of 18.9 m/d (De Watergroep, 2001). This high HK indicates the presence of secondary permeability, probably related to fractures, in the zones with high flow, as the initial permeability of Zeven Wegen is normally very low. In the lithological description of this well by Michiel Dusar, the presence of fractures is mentioned for the part of the Cretaceous up to 50m below the surface. Furthermore, around a depth of 30m an interval with phosphatic concretions is described, which are badly rounded and up to 2 cm in diameter. This might correspond with the phosphatic gravel described around Het Broek. However, this phosphatic gravel interval is not part of the filter at this well. Furthermore, the presence of Tertiary deposits in the top of the Cretaceous is described, which could be related to the filling up of the eroded and karstified top of the Cretaceous.

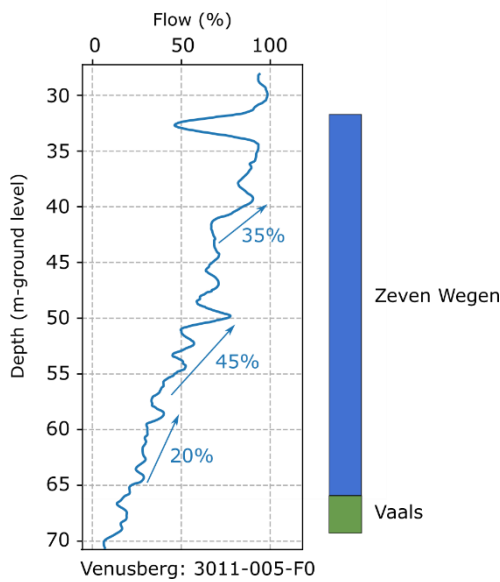


Figure 16: Stratigraphy and flow measurement for well 3011-005 (Venusberg).

For the site of **Sana**, no gamma-ray or flow measurements are available. The extraction wells have a filter in Zeven Wegen of about 25-30m in length. On both 3011-008 and -009 a pumping test has been performed, in respectively 1978 and 1994. These tests are analysed with Hyparyden (Hydraulic Parameter Identification, Lebbe 1999). The resulting HK estimates are 36.8 m/d for -008 and 55.6 m/d for -009 (De Watergroep, 2004). These high HK values indicate the presence of fractures in the otherwise low permeable Zeven Wegen chalk. The difference in estimated HK between the two wells is explained by the presence of a complex fracture network.

For the site of **Veeweyde**, gamma-ray and flow measurements are available for 3012-003 and -059 (Figure 17). In the gamma-ray log of -003, a peak is visible around 20m, which probably corresponds with the hardground/phosphatic gravel interval (Figure 17a). The first few meters of the Cretaceous are described as Lixhe and/or Lanaye, while the majority of the Cretaceous (22-45m) corresponds to the Zeven Wegen chalk, characterized by a low gamma-ray signal. At the bottom, there is an increase in gamma-ray, which might indicate the presence of the Smectite of Hervé (Vaals). The filter at -003 is located from 23.6-46.4m, and thus does not include the hardground interval or the overlying Lixhe/Lanaye deposits but only the Zeven Wegen chalk and a couple meters of the smectite. The flow measurement shows several short intervals which contribute most of the flow: 20% from 40-45m, 20% from 36-37m, 40% from 30-32m and 20% from 25-26m. A pumping test has been performed on -003 in 1996, and using the Theis and Cooper-Jacob methods, an HK of 111.7 m/d is estimated (De Watergroep, 2004). Considering this very high HK, the high flow in the different intervals is probably related to secondary fracture related permeability. Pumping tests on the nearby wells -001 and -002, performed in 1977 and 1984, result in similarly high HK estimates of 98.8 and 101.8 m/d (using the Theis and Cooper-Jacob methods) (De Watergroep, 2004). This indicates a similar presence of fracture related secondary permeability. For well -059 both gamma-ray and flow measurements are available (Figure 17). No peak in the gamma-ray at the top is observed, indicating that the boundary Zeven Wegen/Lixhe-Lanaye is located higher up but is not present in the filter interval. The low gamma-ray signal from 20-44m indicates the presence of the Zeven Wegen chalk. The increase in gamma-ray at the bottom of the Cretaceous interval might indicate the presence of the Smectite of Hervé (Vaals). The flow measurement shows that the flow is relatively well-spread over the entire filter, but that again most of the flow comes from a couple of short intervals: 15% of the flow from 30-31m and 15% of flow from 38-39m. These intervals most probably correspond with strongly fractured zones. However, the rest of the filter also contributes to the flow, indicating a wide-spread presence of secondary permeability in the Zeven Wegen chalk. The pumping test on -059, performed in 2017 and analysed with MLU, results

in an estimated HK of 58.4 m/d (De Watergroep, 2017c). This is lower than the estimates for the other three wells, which can be due to a lesser degree of fracturation or due to a difference in the methods applied to estimate the HK.

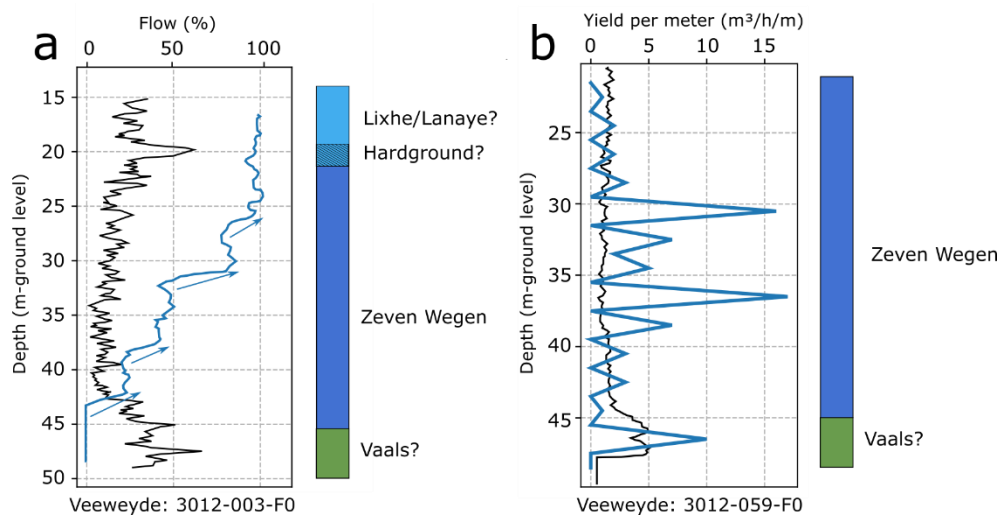


Figure 17: Stratigraphy, flow and gamma-ray measurements for the site of Veeweyde: (a) 3012-003; and (b) 3012-059.

For the site of **Geuzenhoek** a gamma-ray log is available for the top of the Cretaceous for the observation well 3012-058 (Figure 18). For the extraction wells, no gamma-ray logs are available. A clear peak in the gamma-ray signal is visible around 42-45m, which indicates the presence of the hardground corresponding to the boundary between Lixhe and Zeven Wegen. In the lithological description of 3012-007, rolled phosphatic concretions and gravel-like deposits are described, confirming the hypothesis of a phosphatic gravel deposit near the hardground interval. The filter of well -007 is partially located in Lixhe (top 7m), while the rest of the filter is part of Zeven Wegen (approx. 30m). For well -008 only the top 3m is located in Lixhe, the bottom 30m in Zeven Wegen. For well -009, the filter is only situated in the Zeven Wegen deposits. The Lixhe part is not present in the filter interval. Pumping tests have been performed on -007 (1984 and 1991), -008 (1984) and -009 (1997) and analysed with different methods (Theis, Cooper-Jacob and Theis-recovery) (De Watergroep, 2021). This resulted in HK estimates of respectively 90.4, 91.0 and 39.5 m/d.

A flow measurement has been performed on extraction well 3012-009. However, only a description of the results is available. The flow measurement indicates that 70% of the flow comes from the top 6m of the filter. However, this part is in connection with the hardground/phosphatic gravel interval through the gravel pack. The high flow might thus be largely coming from this highly permeable interval. The other 30% of the flow comes from the lowest 12m of the filter, while there is an interval of 12m in the middle of the filter that doesn't contribute to the flow at all. The flow in the bottom part of the filter is probably related to the presence of a fracture network. It is difficult to assess if the flow in the top part of the filter is solely due to the connection with the hardground interval or if the top part is also fractured. In general, there seems to be a combination of a large contribution from the hardground interval (like Het Broek) and a more limited contribution due to the presence of fractures (like Veeweyde). The larger HK estimates for -007 and -008 compared to -009 can be explained by the location of the filter: at -007 the filter completely comprises the hardground interval and at -008 partially, while at -009 the filter is only connected with this interval through the gravel pack.

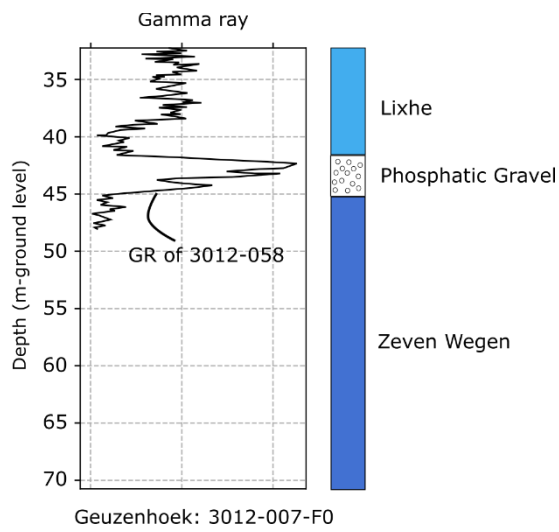


Figure 18: Stratigraphy and gamma-ray measurement for well 3012-007 (Geuzenhoek).

For the site of **Vilvoorde** flow and gamma-ray measurements are available for well 3014-004 (Figure 19). The filter is situated in the Formation of Nevele (approx. 30m in thickness), which is a lateral equivalent of the Formation of Gulpen. The gamma-ray signal shows a larger variation than seen at the other sites, with two main peaks at around 124m and 140-144m. In the borehole description, these intervals correspond with the presence of more clayey chalk deposits. Another possibility is that the first gamma-ray peak at 124m corresponds with the peak associated with the hardground at the sites more towards the west. It consists of one main peak and a smaller second peak, which is similar to the peak associated with the hardground. A pumping test has been performed on 3014-004 in 2016. Analysis with MLU resulted in an HK estimate of 13.1 m/d (De Watergroep, 2017d). The flow measurement shows that flow is equally distributed over the entire filter, with more flow near the top and the base. This indicates the presence of a fracture network, as the deposits are in general described as white chalk which has a low primary permeability.

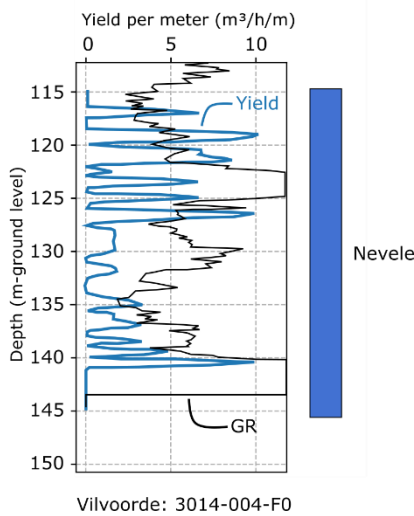


Figure 19: Stratigraphy, flow and gamma-ray measurement for well 3014-004 (Vilvoorde).

For the wells of **Pécrot**, **La Motte** and **Biez**, limited data is available. No gamma-ray, flow measurements or pumping tests are found. Due to the proximity of Pécrot and La Motte to Veeweyde, we expect a similar situation with a strong presence of a fracture network resulting in high permeabilities. This is confirmed by the high extraction rates at these

sites which have limited effects on the hydraulic heads. A similar situation is expected for Biez. At this site, there is a drainage gallery at which the presence of fractures in the gallery wall is clearly visible. In these southernmost areas the Cretaceous deposits seem to be strongly fractured and karstified.

Interpretation

The presence of the interval associated with the hardground plays a crucial role for the well yields at the extraction wells in the Cretaceous. In the Leuven area, the permeability of this interval is relatively limited (around 2 m/d), but the permeability significantly increases towards the south, with around 9 m/d for the northern wells of Het Broek and 60-140 m/d for the southern wells of Het Broek. The thickness also increases from north (2-3m) to south (5-6m). This hardground interval also plays an important role for the sites of Venusberg and Geuzenhoek. The hardground at the top of the Zeven Wegen chalk is also described by Vandenberghe & Gullentops (2001) as characterized by branched glauconite-bearing bioturbations, at least partially cemented with phosphate cement. On top of the hardground, a phosphite horizon is observed, which indicates an important time hiatus between the Zeven Wegen chalk and the coarser deposits of Lixhe and Lanaye. The hardground probably corresponds with two hardgrounds more to the east in Limburg: Bovenste Bos (Froidmont) and Wahlwiller (Lixhe). The lithological descriptions at Het Broek, Venusberg and Geuzenhoek indicate the presence of a phosphatic gravel, consisting of well-rounded (Het Broek) to badly rounded (Geuzenhoek) balls of 1-2cm in diameter of hard fine-grained phosphatic chalk. This phosphatic gravel might be the result of reworking or erosion and redeposition of chalk material. This interval associated with the hardground clearly has higher permeabilities in the south (Het Broek S, Venusberg, Geuzenhoek) than in the north (Het Broek N, Leuven area) indicating a stronger reworking or even karstification of this interval. In Biez, a similar interval with eroded coarse chalk with flint and a phosphate layer is identified, associated with a hardground (Vandenberghe & Gullentops, 2001).

The Zeven Wegen chalk is characterized by little to no flow contribution for the wells in the north (Leuven area, Het Broek, Nellebeek). This fine-grained chalk has a very low primary permeability, resulting in low well yields in the north. However, towards the south, we see at multiple sites (Venusberg, Sana, Veeweyde, the wells in the Walloon region) that there is a significant contribution of flow all throughout the Zeven Wegen chalk. In some of the borehole descriptions, fracture zones in the Zeven Wegen chalk are observed. This corresponds well with the very high flows identified over the entire chalk interval at these sites. Most of the flow is concentrated at several relatively thin fracture zones. Due to these fracture zones, the well yields in these southern wells are very high. The site of Geuzenhoek is a bit of a transition between the area with fracture zones in the south, and the northern wells where the hardground interval plays the largest role.

The Members of Lixhe and Lanaye are present on top of the Zeven Wegen chalk at most of the sites (with exception of Nellebeek). In the northern site, these Members contribute a little to the total flow, more than the Zeven Wegen chalk, but all in all still a quite low contribution. At Aarschot, the coarser-grained and more permeable calcarenites of Maastricht are present on top of the Formation of Gulpen. Most of the flow comes from these Maastrichtian deposits, with a limited contribution from the top of Gulpen (Lixhe/Lanaye).

2.3.3 Spatial variability of the hydraulic conductivity of the Cretaceous

The map of the pumping test estimates (Figure 10) shows that there is a trend of increasing HK from the north towards the south in the Cretaceous. This corresponds with the depth of the Cretaceous deposits, which are near surface in the south, but dip strongly towards the north (see e.g., Figure 9a-b). When plotting the depth of the top of the Cretaceous versus the horizontal conductivity estimated based on the pumping tests, a clear trend of decreasing HK with depth is observed (Figure 20). Note that the x-axis is in a logarithmic scale. However, two wells clearly deviate from this trend: the wells of Nellebeek and Vilvoorde. When these two outliers are not considered, the following correlation between depth d (in m) and hydraulic conductivity K (in m/d) is obtained:

$$K = e^{\frac{d-84.704}{-14.17}}$$

This correlation between HK and depth of the Cretaceous includes both the effect of fractures and the presence and permeability of the hardground/phosphatic gravel interval. In the southern part of the area, where the Cretaceous deposits are close to the surface, the chalk is fractured, resulting in a strong increase of hydraulic conductivity. More towards the north, where the Cretaceous is deeper in the subsurface, these fractures are not observed, resulting in a much lower hydraulic conductivity. These fractures are probably related to the decrease in pressure due to the exhumation of overlying layers. Superimposed on this, is the effect of an increase in permeability of the hardground/phosphatic gravel interval from the north towards the south. The combination of these two factors results in the correlation shown in *Figure 20*. Note that this correlation is only valid for the Formation of Gulpen. In the north-eastern part of the area the Formation of Maastricht is present. These deposits consist of coarser grained calcarenites with a higher primary permeability. Even when these deposits are present very deep in the subsurface, decent permeabilities are observed. For the Aarschot site, an HK of 5.9 m/d is estimated for the top of Maastricht, which is situated at a depth of more than 230m.

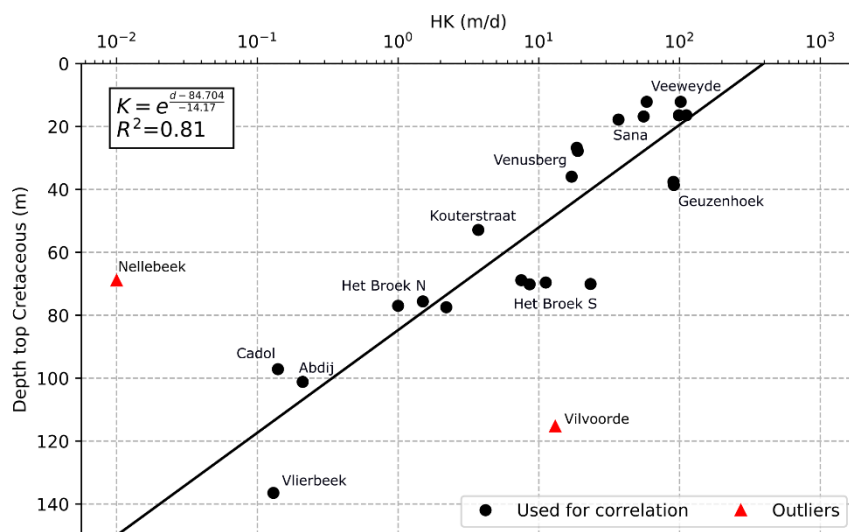


Figure 20: Correlation between depth of the top of the Cretaceous sediments and the estimated HK based on pumping tests.

The site of Nellebeek is an exception to the general trend, as a very low HK (0.01 m/d) is estimated for the Cretaceous. Looking at the correlation depth-HK, an HK of 2-3 orders of magnitude larger is to be expected. This can be explained by the absence of the hardground interval in this area, which is the reason for the larger HK in areas at a similar depth as e.g., Het Broek. At the site of Nellebeek, the Cretaceous deposits only consist of the Zeven Wegen chalk, while the Lixhe and Lanaye deposits are absent. For the Vilvoorde site, the opposite is observed, with an HK estimate (13.1 m/d) being approx. two orders of magnitude higher than expected based on the large depth of the Cretaceous. Combined with the fact that the flow is spread over the entire filter (Nevele Formation), this indicates the presence of fractures in the Cretaceous in this area. This is the only area where fractures are observed at such a deep depth. A possible explanation for this is the fact that these deposits are closer to the axis of the Brabant Massif. The fractures might possibly be related to earlier phases of fracturing related to the upheaval of the Brabant Massif.

Using the correlation between depth and HK, a spatially distributed map of HK can be generated (Figure 21). This map clearly demonstrates the very high hydraulic conductivities in the river valleys in the south, where the Cretaceous deposits are close to the surface. The HK decreases over several orders of magnitude towards the north.

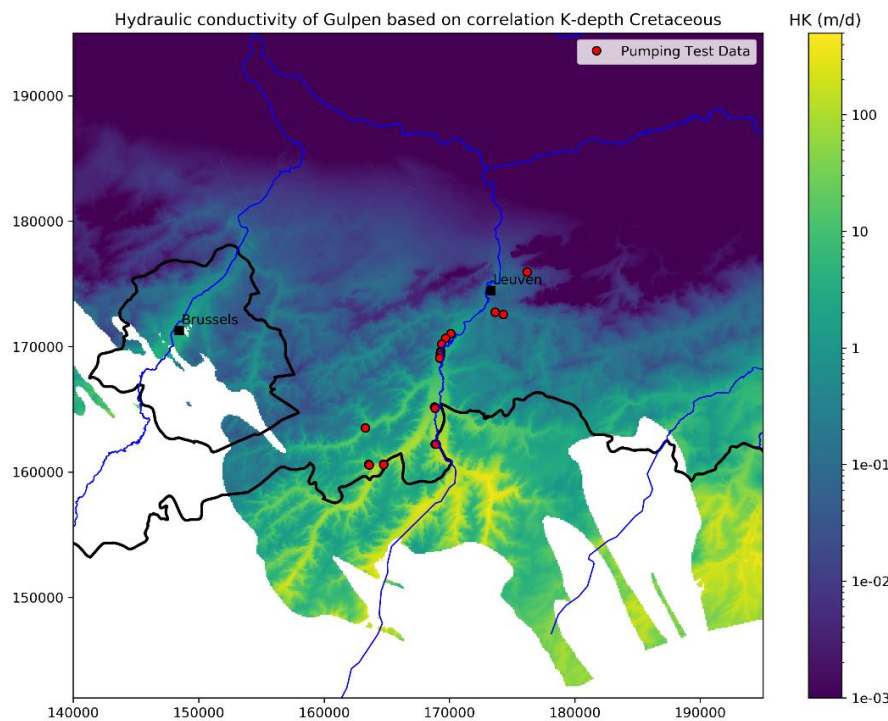


Figure 21: Map of the spatial variability of HK of the Cretaceous based on the correlation between the depth of the top of the Cretaceous and HK estimates from pumping tests.

The correlation gives a rough estimation of the trend in HK. However, for some locations, the difference between the HK based on the pumping tests and the HK based on the correlation is still quite high (Figure 20). A small deviation from the regression line can already result in a significant under- or overestimation of HK due to the use of the logarithmic scale. This is the case for the wells of Het Broek, which show a quite strong variation in HK (1 to 23 m/d) even though they are all situated at a similar depth. Therefore, we tried to improve the HK map by combining this correlation with the kriging interpolation technique. Kriging was applied on the residuals of the depth-HK correlation. The resulting spatially variable field of the residuals was then re-added to the correlation. This way, the actual pumping test data is used as primary data, strongly affecting the HK field close to these pumping tests, while in areas far away from pumping test data, the HK field is purely based on the correlation depth-HK. This way, a much better match is obtained between the HK obtained by the pumping tests and the HK simulated using kriging with the correlation depth-HK as secondary data (Figure 22).

The improved HK field is visualized in Figure 23. The difference between the initial and improved HK field is shown in Figure 24. This clearly shows that only in the area around the pumping test wells the HK field is changed.

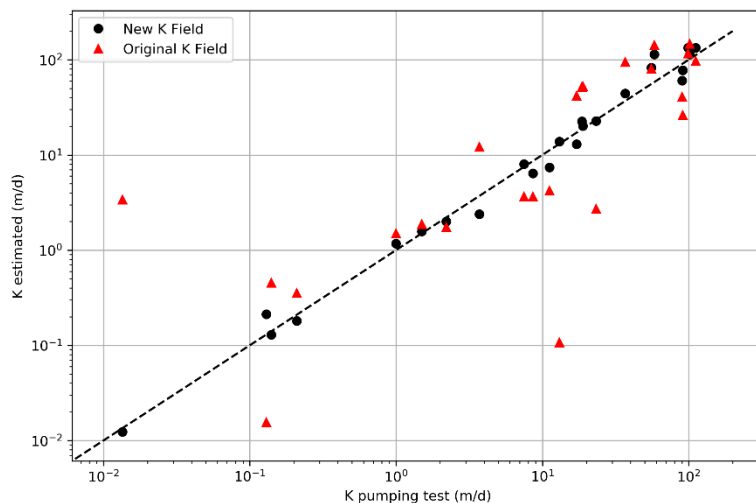


Figure 22: Comparison between HK derived from the pumping tests (x-axis) and HK estimated based on: (1) only the correlation depth-HK (red triangles); and (2) the use of kriging with the correlation depth-HK as secondary data (black dots).

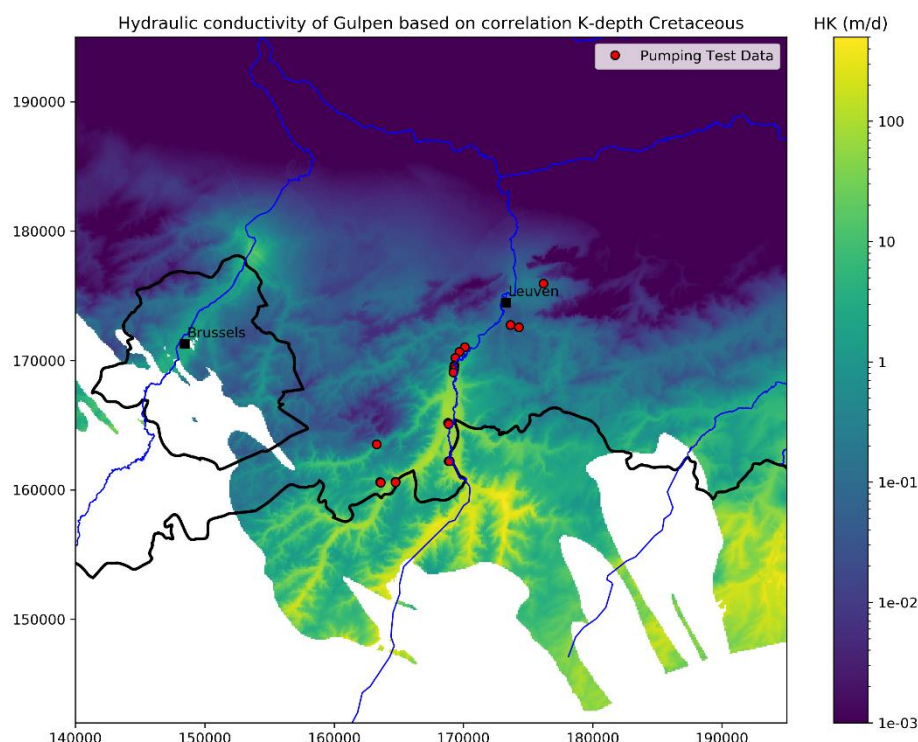


Figure 23: Map of the spatial variability of HK of the Cretaceous based kriging using the correlation between the depth of the top of the Cretaceous and HK estimates from pumping tests as secondary information.

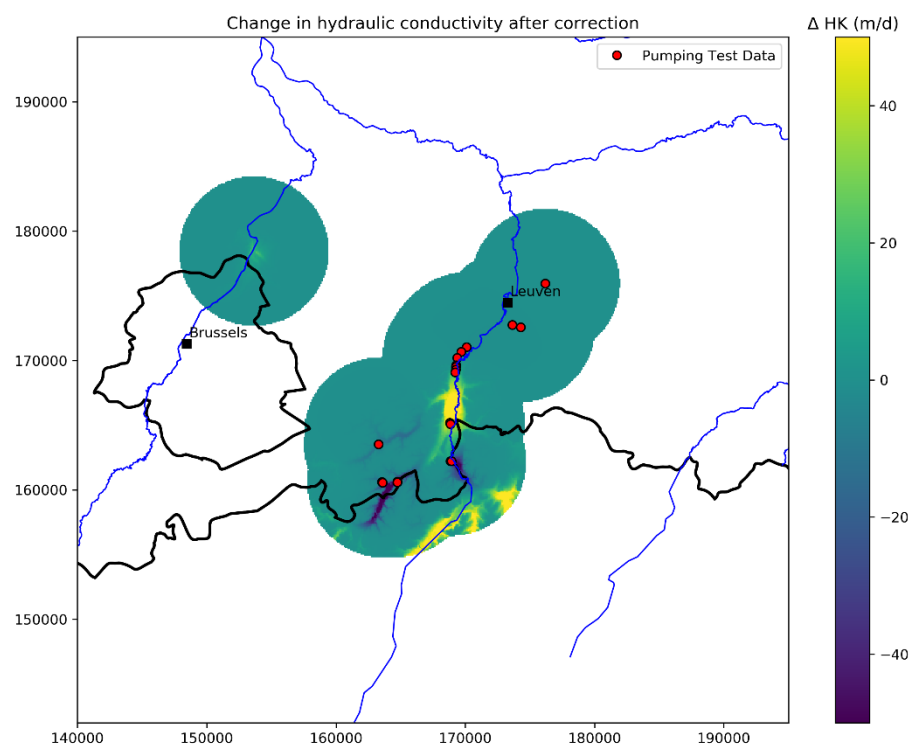


Figure 24: Map showing the difference between the initial HK field based on the correlation HK-depth (Figure 21) and the improved HK field based on kriging used the HK-depth correlation as secondary information (Figure 23).

3 Extraction and Hydraulic Heads

In this chapter, the extractions in the Cretaceous and Paleocene aquifer systems are discussed. First, the extraction by De Watergroep is analysed, including the effect of this extraction on the hydraulic heads around the extraction sites. Secondly, extractions by other companies or organisations in the area are discussed. Finally, an overview is given of the evolution of hydraulic head in different parts of the Brabant area.

3.1 Extraction De Watergroep

In the Brabant area, De Watergroep produces drinking water from 18 different extraction sites, 15 of which are in the Cretaceous, two in Lincent and one in Grandglise. The extracted rates for the last 30 years are shown in Figure 25 and, Table I. 1 and Table I. 2. The total extraction rates increased throughout this period, from about 3.5M m³/year in the early nineties, to approx. 15M m³/year around the year 2000, from which point on the rates stayed more or less stable. Note that most of the drinking water is produced from the Cretaceous aquifer (around 12-14M m³/year), a bit less than 2M m³/year from Lincent and around 400k m³/year from Grandglise. The total permitted rate for all these extraction sites is approx. 20.5 m³/year, which means that only 75% of the permitted rates are used.

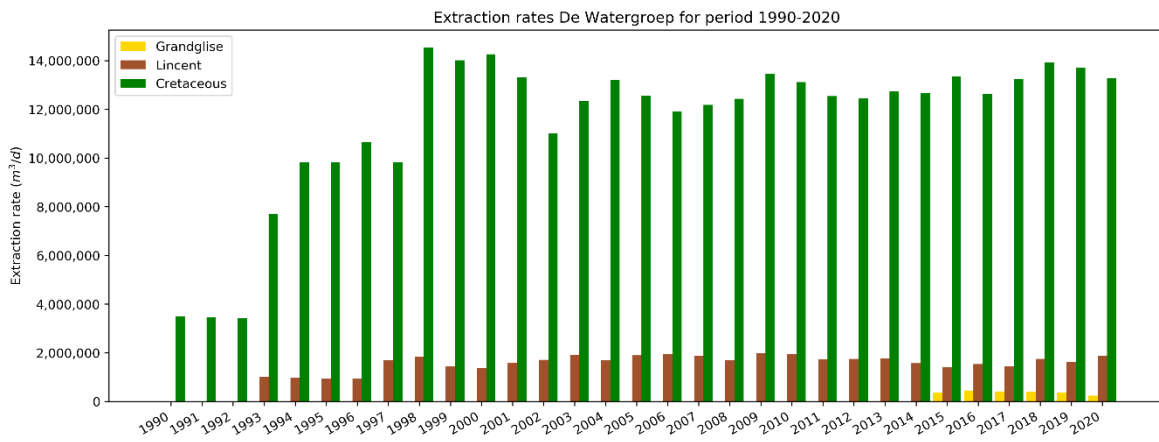


Figure 25: Overview of the evolution of the extraction rates at the sites of De Watergroep in Grandglise, Lincent and the Cretaceous.

The spatial distribution of the extraction is visualized in Figure 26. Note that the extraction sites in the Cretaceous are mainly located in the Dijle valley (and valleys of its tributaries) to the south of Leuven, with also three sites in the Walloon region. The site of Het Broek has the largest permitted rate (4.38M m³/year), followed by the sites of Pécrot (3.285M m³/year), La Motte (2.92M m³/year), Veeweyde and Geuzenhoek (both 2.372M m³/year). Some smaller sites are located around the city of Leuven, in Vilvoorde and Aarschot. The two extraction sites in Lincent are situated in the SE of the area, in the region around Tienen. These produce water from the “tuffeau” of Lincent (see section 1). Finally, the site of Hoeilaart is the only one producing drinking water from the sands of Grandglise.

In the following sections, the extraction sites of De Watergroep are discussed in more detail, including plots of the evolution of extraction rates and hydraulic heads through time.

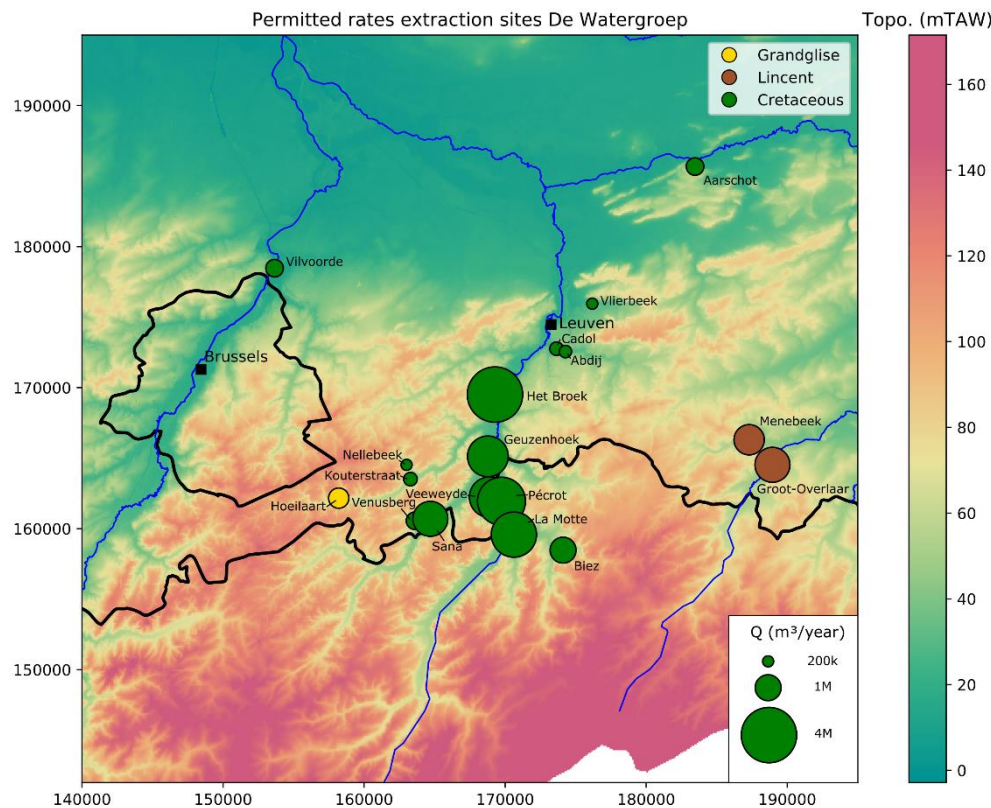


Figure 26: Map of the permitted rates for the extraction sites of De Watergroep.

Aarschot Schoonhoven

The site of Aarschot Schoonhoven consists of one production well (3001-108-F0) with a filter in the Cretaceous deposits of the Formation of Maastricht and Gulpen. The permitted rate for this site is 438k m³/year. Production started in the year 2016, and yearly 200-300k m³/year is effectively extracted (Figure 27). Next to the production well, an observation well in the Cretaceous (3001-107-F1) and in Grandgliste (3001-109-F3) are present (Table 4). The evolution of the observed hydraulic heads is visualized in Figure 27. Note the decrease in head of approx. 30m in the production well after start of extraction in 2016. The drawdown in the observation well in the Cretaceous is up to 10m, while no significant effect on the heads in Grandgliste is observed.

Table 4: Overview of the characteristics of the wells at Aarschot Schoonhoven.

Well	X	Y	Layer	HCOV	Z (mTAW)	Filter top	Filter bot	Type
3001-107-F1	183511	185746	Maastricht/Gulpen	1111/1112	13.80	-224.20	-239.20	observation
3001-108-F0	183464	185677	Maastricht/Gulpen	1111/1112	18.63	-218.60	-257.77	production
3001-109-F3	183520	185738	Grandgliste	1013	14.29	-118.71	-123.71	observation

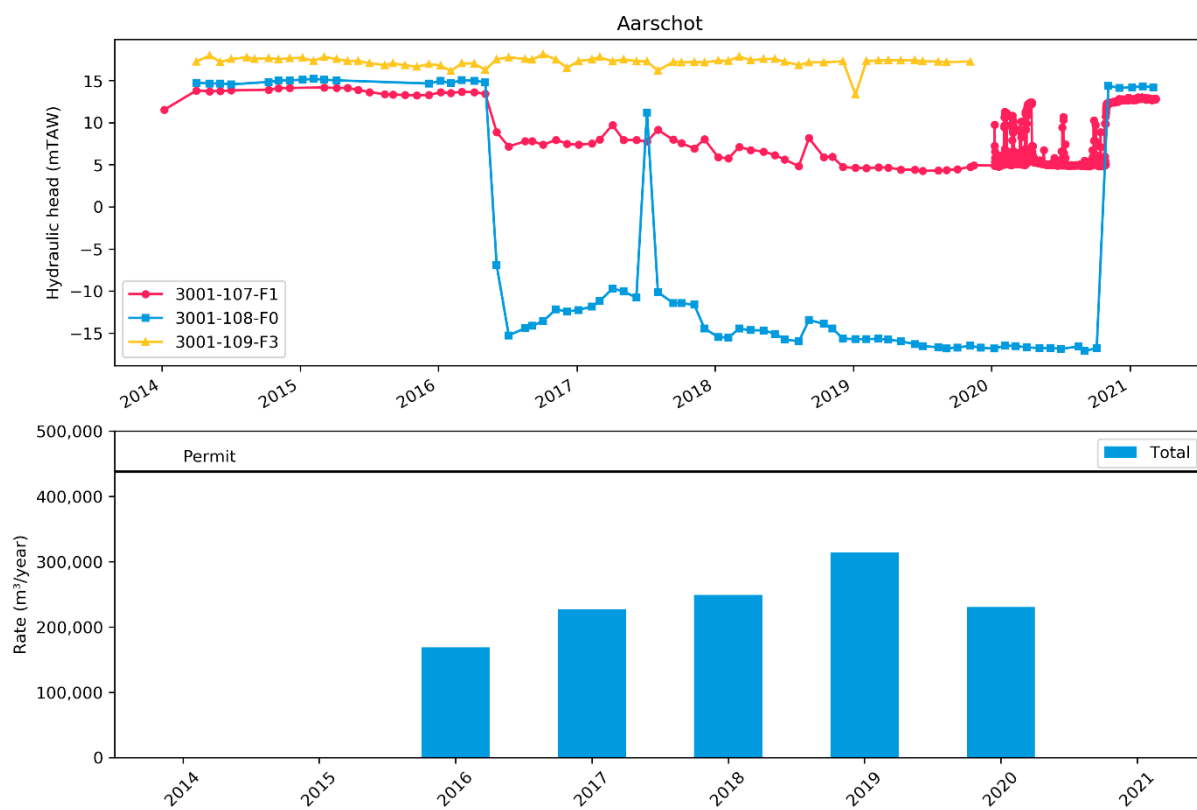


Figure 27: Evolution of the hydraulic heads (top) and extraction rates (bottom) for the site of Aarschot Schoonhoven.

Kessel-lo Vlierbeek

The site of Kessel-lo Vlierbeek consists of one production well (3007-001-F0) with a filter in the Cretaceous deposits of the Formation of Gulpen. The permitted rate for this site is 175.2k m³/year. On average, about 100-150k m³/year is effectively extracted (Figure 28Figure 27). Next to the production well, a multi-level observation well with filter in the Cretaceous (3007-038-F3) and in Lincent (3007-038-F2) is present (Table 5). The evolution of the observed hydraulic heads is visualized in Figure 28. Note the decrease in head of approx. 50m in the production well after start of extraction. The recovery of the head at times of no extraction is relatively slow. The hydraulic heads follow the pattern of changes in the extraction rates. The drawdown in the observation well in the Cretaceous is in the order of 10m, while no significant effect on the heads in Grandglise is observed.

Table 5: Overview of the characteristics of the wells at Kessel-lo Vlierbeek.

Well	X	Y	Layer	HCOV	Z (mTAW)	Filter top	Filter bot	Type
3007-001-F0	176177	175954	Gulpen	1113	25.64	-116.36	-152.36	production
3007-038-F2	176189	175999	Lincent	1014	25.44	-39.57	-44.57	observation
3007-038-F3	176189	175999	Gulpen	1113	25.44	-111.50	-115.50	observation

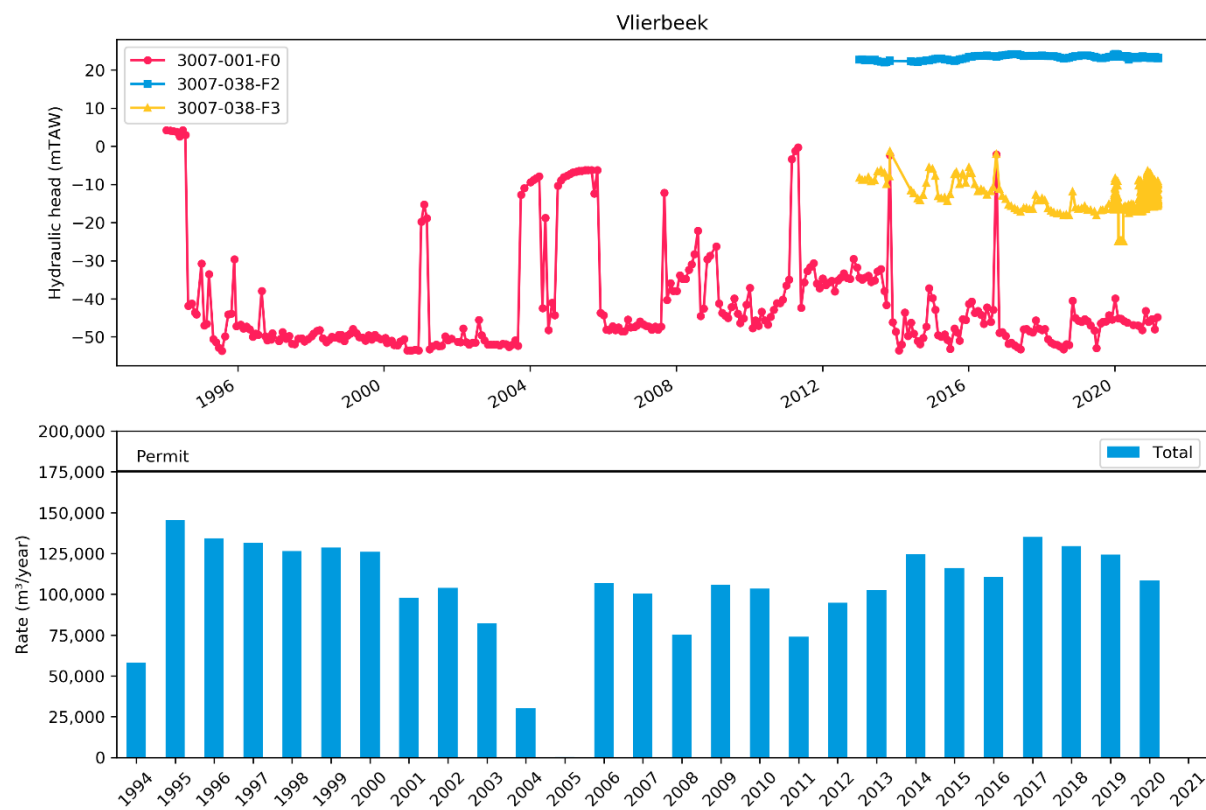


Figure 28: Evolution of the hydraulic heads (top) and extraction rates (bottom) for the site of Kessel-lo Vlierbeek.

Heverlee Cadol & Abdij

The sites of Heverlee Cadol and Abdij consist of one production well each (3006-001-F0 and 3006-116-F0), both with a filter in the Cretaceous deposits of the Formation of Gulpen. The permitted rate for these sites is respectively 262.8k and 219k m³/year. The site of Cadol is in production since the early nineties, with effective extraction rates varying around 200k m³/year (Figure 29). The site of Abdij started production in 2015, with an effective extraction rate of approx. 175k m³/year. Next to the production wells, one multi-level observation well with filter in the Cretaceous (3006-159-F2) and in Grandglise (3006-159-F1) is present (Table 6), located between the two production wells. The evolution of the observed hydraulic heads is visualized in Figure 28. Note the decrease in head of approx. 50m in the production well of Cadol after start of extraction. The effect on the production well of Abdij, acting as an observation well, was approx. 10m. Note the slight increase in heads from 2005 onward, which might be related to the termination of extraction at the Inbev site in Leuven (see section 3.2.). The start of production in Abdij resulted in a drawdown of approx. 40m in the production well. Note the slight decrease in heads at the production well in Cadol in this period. The drawdown due to the start of production in Abdij is approx. 15m in the observation well in the Cretaceous. No significant effect on the heads in Grandglise are observed.

Table 6: Overview of the characteristics of the wells at Heverlee Cadol and Abdij.

Well	X	Y	Layer	HCOV	Z (mTAW)	Filter top	Filter bot	Type
3006-001-F0	173644	172757	Gulpen	1113	24.84	-73.71	-100.76	production
3006-116-F0	174276	172561	Gulpen	1113	28.50	-72.50	-101.50	production
3006-159-F1	173862	172721	Grandglise	1013	24.89	-15.11	-20.11	observation
3006-159-F2	173862	172721	Gulpen	1113	24.89	-74.11	-79.11	observation

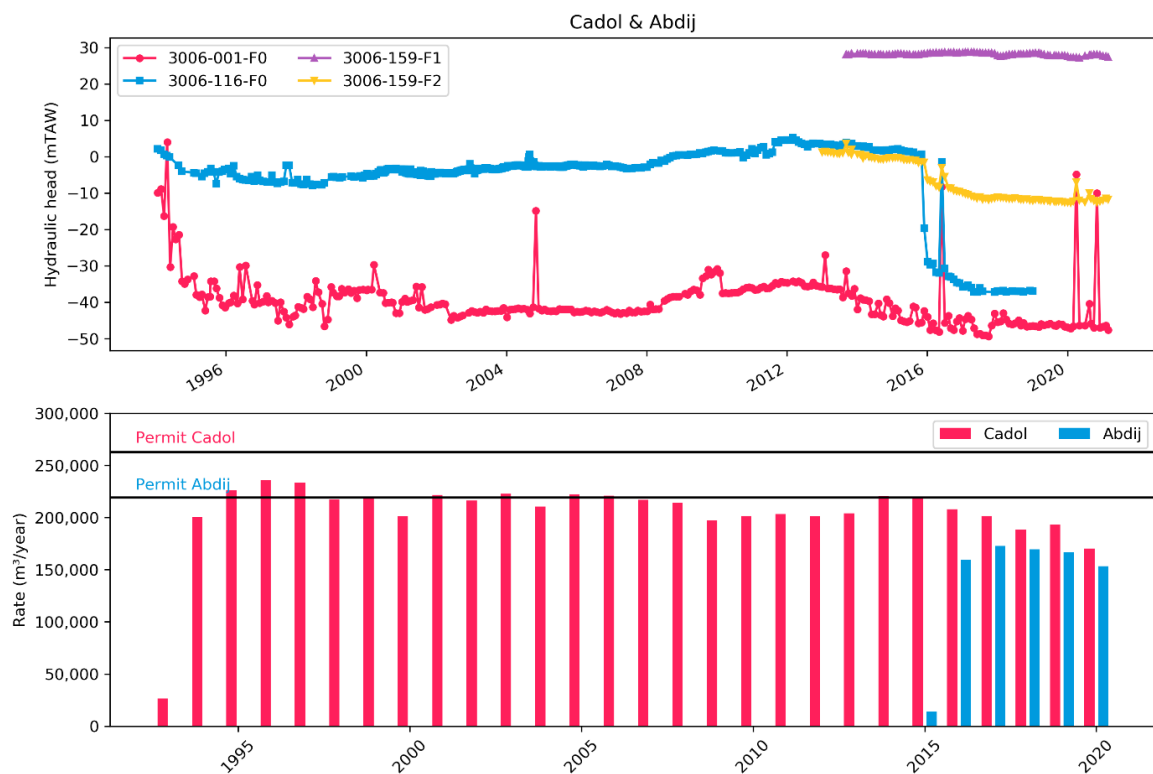


Figure 29: Evolution of the hydraulic heads (top) and extraction rates (bottom) for the sites of Heverlee Cadol and Abdij.

Korbeek-Dijle Het Broek

The site of Korbeek-Dijle Het Broek consists of seven production wells, all with filter in the deposits of the Formation of Gulpen. The permitted rate for this site is 4.38M m³/year. However, actual rates are significantly lower and vary from 2 to 3M m³/year (Figure 30). A normal extraction rate for the recent years is around 2.5M m³/year. The site of Het Broek is in production since the early nineties. In the first twenty years, almost all extraction was from the wells 3008-001-F0, 3008-005-F0 and 3008-006-F0, all three of them situated in the southern part of the site. As discussed in section 2.3, these wells are characterized by significant higher hydraulic conductivities than the northern wells. Around 2010, the more northern wells 3008-002-F0 and 3008-003-F0 were also used for production. In 2020, well 3008-005-F0 was replaced by two newer production wells: 3008-063-F0 and 3008-064-F0. In 2020, the extraction rates were higher than usual (3M m³/year) to compensate for the temporary shutdown of the site of Geuzenhoek.

Table 7: Overview of the characteristics of the wells at Korbeek-Dijle Het Broek.

Well	X	Y	Layer	HCOV	Z (mTAW)	Filter top	Filter bot	Type
3008-001-F0	169223	169076	Gulpen	1113	27.77	-39.68	-79.68	observation
3008-002-F0	169373	170207	Gulpen	1113	26.72	-47.78	-82.78	production
3008-003-F0	169696	170670	Gulpen	1113	25.74	-49.26	-84.26	production
3008-004-F0	170091	171033	Gulpen	1113	24.01	-51.99	-84.99	production
3008-005-F0	169298	169638	Gulpen	1113	27.14	-40.36	-90.83	production
3008-006-F0	169280	169513	Gulpen	1113	27.13	-37.87	-83.67	production
3008-063-F0	169298	169655	Gulpen	1113	27.07	-44.23	-85.23	production
3008-064-F0	169259	169286	Gulpen	1113	25.68	-42.32	-76.32	production
3008-065-F3	169282	169688	Grandglise	1013	27.35	-1.65	-5.65	observation
3008-066-F3	170086	171028	Grandglise	1013	23.86	-9.14	-14.14	observation
3008-058-F2	171911	172554	Grandglise	1013	23.72	-13.28	-18.28	observation
3008-058-F3	171911	172554	Gulpen	1113	23.72	-67.28	-72.28	observation

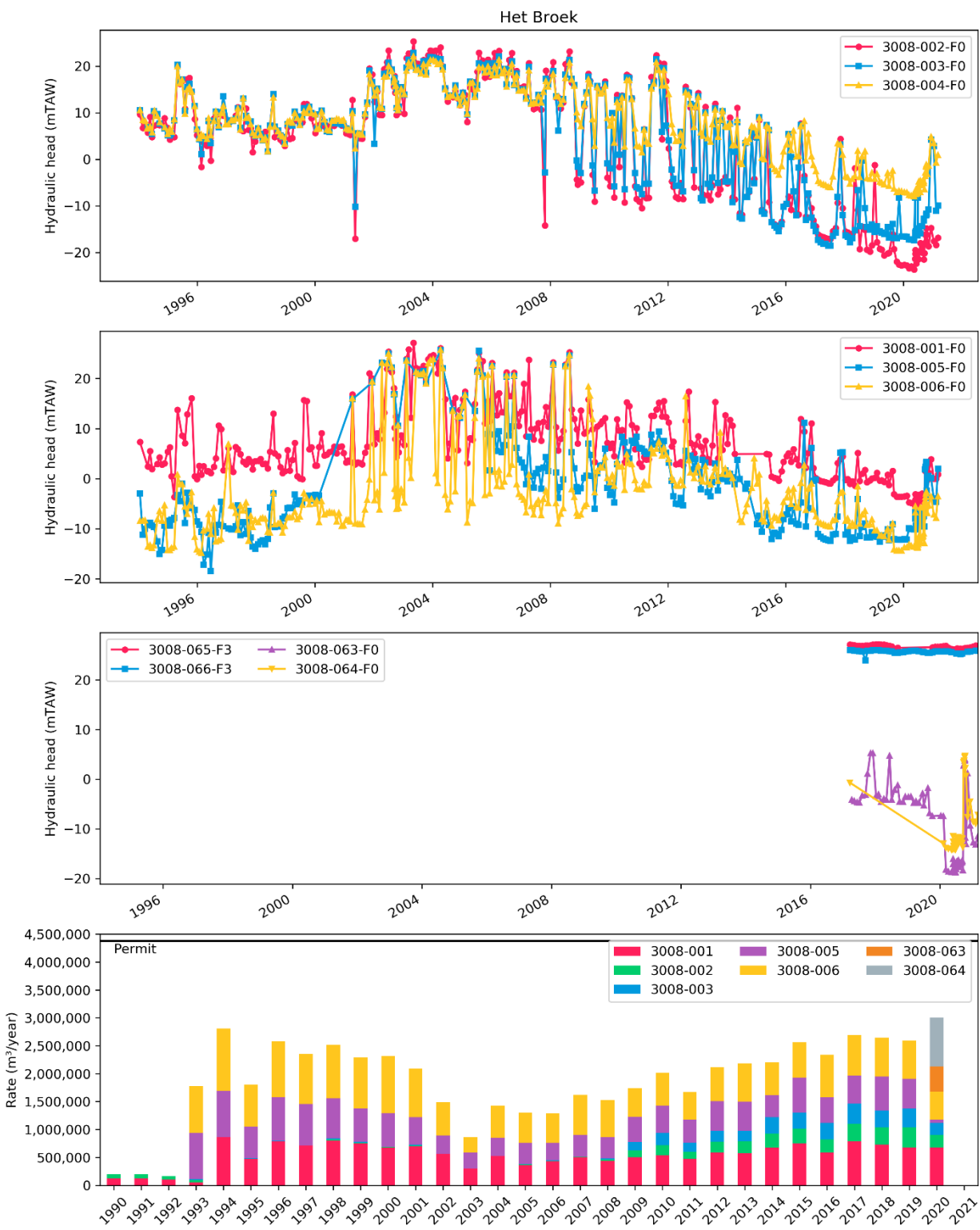


Figure 30: Evolution of the hydraulic heads (top three plots) and extraction rates (bottom plot) for the site of Korbeek-Dijle Het Broek.

Next to the seven production wells, five wells are used as observation wells. Well 3008-004-F0 was initially meant as a production well but due to too low well yields, it is only used as an observation well (with filter in Gulpen). Wells 3008-065-F3 and 3008-065-F3 are observation wells with filter in the sands of Grandglise. Finally, a multi-level well with filter in Gulpen (3008-053-F3) and Grandglise (3008-058-F2) is present. The evolution of the observed hydraulic

heads in the observation and extraction wells is visualized in Figure 30. In the first plot, the heads in the northern production wells are visualized. Note the significant downwards trend from 2010 onwards related to the increased production from these wells, with a decrease of 20-40m for production wells 3008-002-F0 and 3008-003-F0, and a decrease of up to 20m in the observation well 3008-004-F0. The variations in head seem to be mostly related to changes in the extraction rates in these extraction wells. There is no clear indication of an influence of the start of production in Heverlee Abdij in 2015, more towards the north. In the second plot, the heads in the southern production wells are visualized. Note the clear correlation with the extraction rates in these wells, with higher heads in the earlier 2000s (up to +20-30m compared to the nineties) that can be linked with the significant lower extraction rates. The last ten years, there is a slight decreasing trend due to increasing extraction rates. In the third plot, the heads of the two new production wells 3008-063-F0 and 3008-064-F0 is visualized, together with the heads in the observation wells with filter in Grandglise. Start of production in these new production wells lead to a decrease in heads of 10-20m. No clear effect on the heads in Grandglise is identified, indicating a strong resistance of the less permeable Lincent layer in between Grandglise and the Cretaceous.

Overijse Venusberg

The site of Overijse Venusberg consists of one production well (3011-005-F0) with a filter in the Cretaceous deposits of the Formation of Gulpen. The permitted rate for this site is 438k m³/year. On average, about 400k m³/year is effectively extracted (Figure 31^{Figure 27}). Next to the production well, two observation wells with filter in the Cretaceous (3011-006-F2 and 3011-024-F2) and a multi-level observation well with filter in the Cretaceous (3011-007-F3) and in Lincent (3011-007-F3) are present (Table 8). The evolution of the observed hydraulic heads is visualized in Figure 31. Note the limited decrease in head of approx. 2m in the production well after start of extraction. The variation of head in the production well and in the observation wells in the Cretaceous close by can be linked to variations in extraction rates. There is no clear effect of the extraction on the head in Lincent. The variations in this observation well are related to seasonal changes in recharge.

Table 8: Overview of the characteristics of the wells at Overijse Venusberg.

Well	X	Y	Layer	HCOV	Z (mTAW)	Filter top	Filter bot	Type
3011-005-F0	163610	160562	Gulpen	1113	49.29	17.50	-18.50	production
3011-006-F2	163584	160581	Gulpen	1113	50.42	18.42	10.42	observation
3011-007-F2	163555	160607	Lincent	1014	52.25	27.25	26.25	observation
3011-007-F3	163555	160607	Gulpen	1113	52.25	17.25	7.25	observation
3011-024-F2	164171	160305	Gulpen	1113	42.34	22.34	17.34	observation

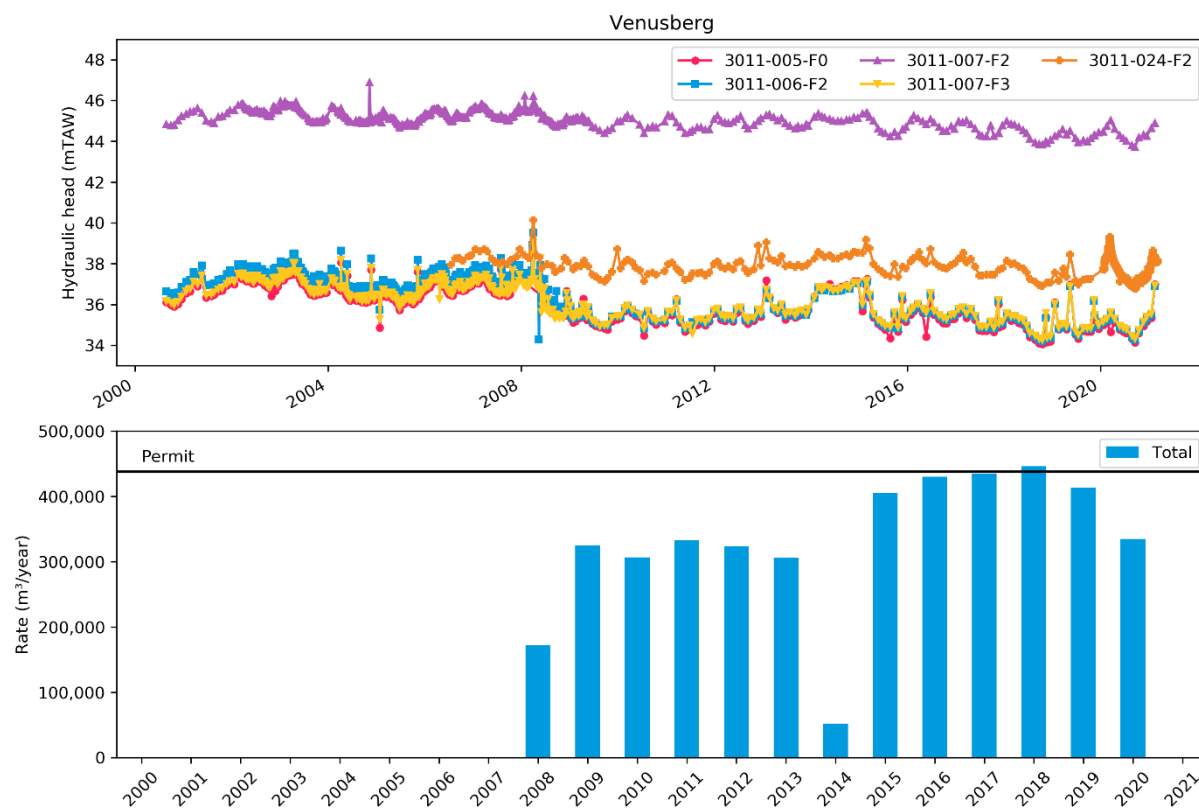


Figure 31: Evolution of the hydraulic heads (top) and extraction rates (bottom) for the site of Overijse Venusberg.

Overijse Sana

The site of Overijse Sana consists of two production wells (3011-008-F0 and 3011-009-F0) with a filter in the Cretaceous deposits of the Formation of Gulpen. The permitted rate for this site is 1.752M m³/year. Well 3011-008-F0 is used as the main production well, while 3011-009-F0 is used as a back-up well. On average, about 1.5M m³/year is effectively extracted (Figure 32Figure 27). Next to the production wells, three observation wells with filter in the Cretaceous (3011-010-F1, 3011-014-F1 and 3011-023-F2) are present (Table 9). The evolution of the observed hydraulic heads is visualized in Figure 32. Note the decrease in head of approx. 4-5m in the production well after start of extraction in 1986. The variation of head in the production well and in the observation wells in the Cretaceous nearby can be linked to variations in extraction rates. However, there seems to be a decrease in head of around 2m since 2014 which can't be correlated to an increase in extraction. This is possibly linked to increased extraction in Venusberg or to a decrease in recharge during the last few dry years. The decrease is more limited in the nearby observation wells, which might indicate that well clogging of the production well could also be a possibility. Note that the hydraulic heads show a limited seasonal variability.

Table 9: Overview of the characteristics of the wells at Overijse Sana.

Well	X	Y	Layer	HCOV	Z (mTAW)	Filter top	Filter bot	Type
3011-008-F0	164745	160598	Gulpen	1113	39.47	15.57	-12.03	production
3011-009-F0	164746	160626	Gulpen	1113	38.87	13.36	-9.14	production
3011-010-F1	164754	160614	Gulpen	1113	39.23	13.41	-0.59	observation
3011-014-F1	164742	160610	Gulpen	1113	39.15	16.15	-8.85	observation
3011-023-F2	164979	160933	Gulpen	1113	39.09	19.09	14.09	observation

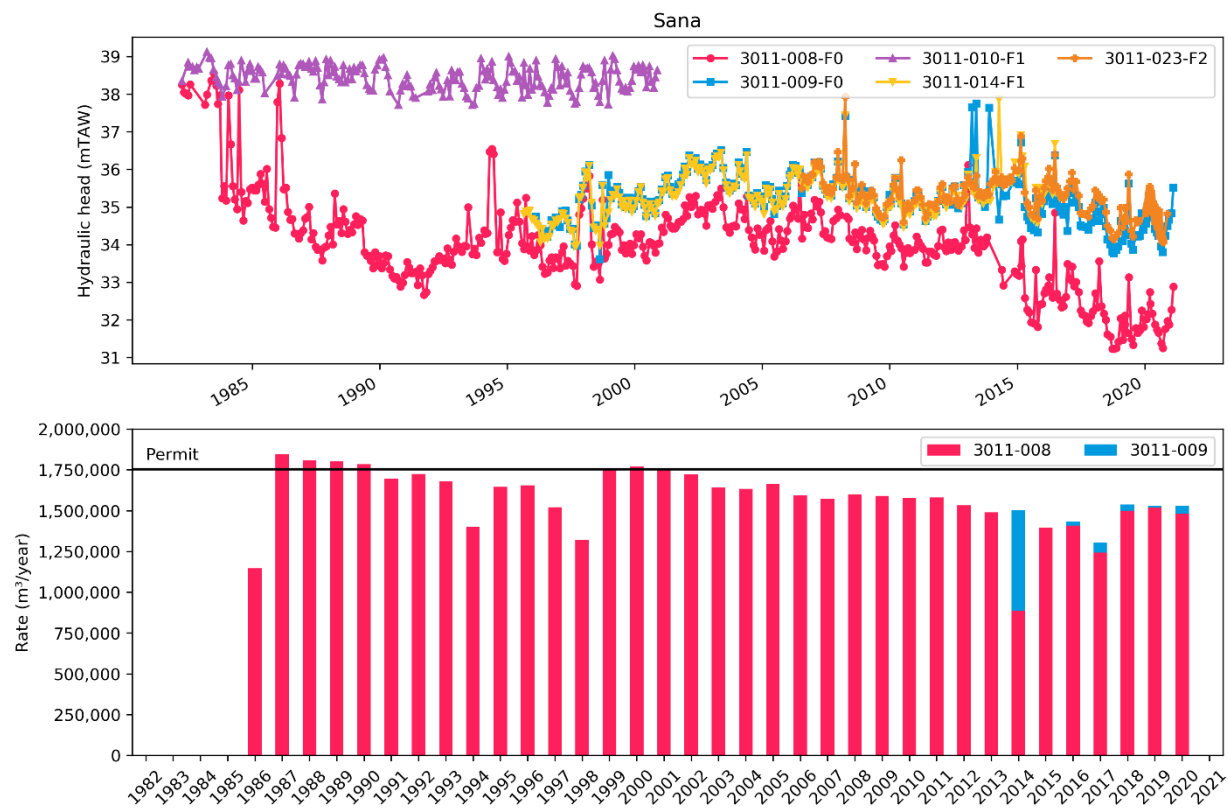


Figure 32: Evolution of the hydraulic heads (top) and extraction rates (bottom) for the site of Overijse Sana.

Overijse Nellebeek

The site of Overijse Nellebeek consists of three production wells (3010-006-F0, 3010-017-F0 and 3010-018-F0) with a filter in both the Member of Lincent and the Cretaceous Formation of Gulpen. The permitted rate for this site is 175.2k m³/year. Effective extraction rates varied between 100-150k m³/year in the period 1990-2010. From 2013 onwards, there is a significant decrease in effective extraction rates. Well 3010-006-F0 was used as a production well from the early nineties up to 2013. This well was renewed after collapsing, as well 3010-017-F0, which has been producing from 2014 to 2019. Well 3010-018-F0 was taken into production in 2019. Next to the production wells, a multi-level well with filter in the Cretaceous (3010-016-F2) and the sands of Grandglise (3010-016-F3) is present (Table 10).

The evolution of the observed hydraulic heads is visualized in Figure 33. The decrease in head of about 5m in 3010-006-F0 from the nineties to around 2010 can be explained by an increase in extraction rates. After shutdown of the well in 2013, heads swiftly recovered about 20m. From 2014 onwards, 3010-017-F0 was used as a production well. Note the significantly lower heads than for 3010-006-F0, even though extracted rates were only a third of those in 3010-006-F0. This is probably related to the presence of fractures in the claystone of Lincent in this area. As discussed in section 2.3, estimated hydraulic conductivity based on pumping tests resulted in a significantly higher HK for 3010-006-F0 than for 3010-017-F0, even though they are very close together. The filter in 3010-006-F0 might be connected to a more fractured zone in Lincent than in 3010-017-F0. Drawdown in extraction well 3010-018-F0, in production since 2019, seems to be less than in 3010-017-F0. The HK derived from a pumping test at this well is also higher, indicating the presence of the fracture zone. The fact that the filters are connected to both Lincent and the Cretaceous, makes the interpretation of the hydraulic head evolution more complex. The multi-level well (3010-016) with filter in Grandglise and the Cretaceous, shows that heads in the Cretaceous are up to 20m lower in the Cretaceous. This indicates that there is a strong resistance of the Lincent layer.

Table 10: Overview of the characteristics of the wells at Overijse Nellebeek.

Well	X	Y	Layer	HCOV	Z (mTAW)	Filter top	Filter bot	Type
3010-006-F0	162999	164519	Lincent/Gulpen	1014/1113	59.90	10.50	-21.11	production
3010-016-F2	163028	164542	Grandglise	1013	59.28	19.28	14.28	observation
3010-016-F3	163028	164542	Gulpen	1113	59.28	-8.72	-13.72	observation
3010-017-F0	163013	164525	Lincent/Gulpen	1014/1113	59.42	6.91	-23.09	production
3010-018-F0	163340	164438	Lincent/Gulpen	1014/1113	61.61	8.61	-21.39	production

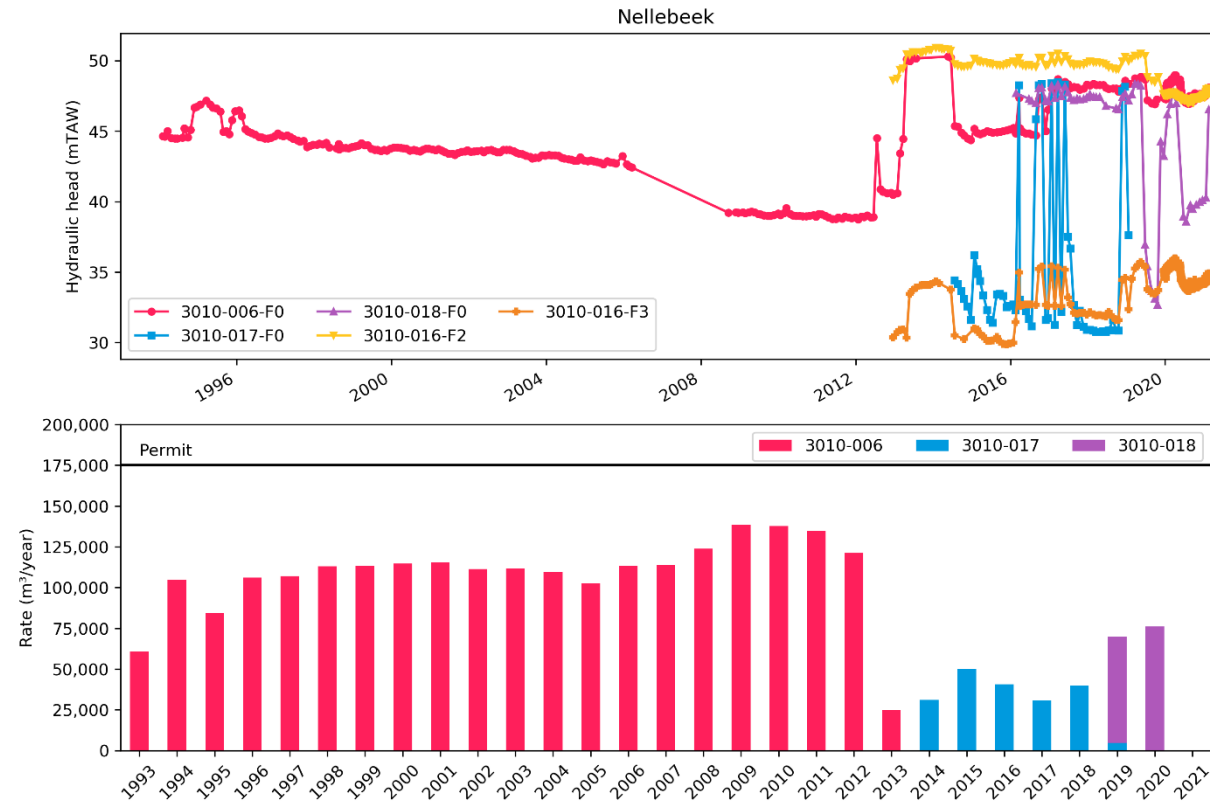


Figure 33: Evolution of the hydraulic heads (top) and extraction rates (bottom) for the site of Overijse Nellebeek.

Overijse Kouterstraat

The site of Overijse Kouterstraat consists of two production wells (3010-001-F0 and 3010-002-F0) with a filter in the Cretaceous deposits of the Formation of Gulpen. The permitted rate for this site is 262.8k m³/year. Well 3010-001-F0 is used as the main production well, while 3010-002-F0 is used as a back-up well. Effective extraction rates vary between 60 to 160k m³/year (Figure 34). Next to the production wells, one observation well with filter in the Cretaceous (3010-003-F1) and one with filter in the sands of Grandglise (3010-011-F1) is present (Table 11). The evolution of the observed hydraulic heads is visualized in Figure 34. The variation of heads in the production wells can be linked to variations in extraction rates. The effect on the heads on the observation well in the Cretaceous is limited. No clear effect on the observation well in Grandglise is visible.

Table 11: Overview of the characteristics of the wells at Overijse Kouterstraat.

Well	X	Y	Layer	HCOV	Z (mTAW)	Filter top	Filter bot	Type
3010-001-F0	163296	163523	Gulpen	1113	51.74	-2.10	-15.10	production
3010-002-F0	163288	163514	Gulpen	1113	51.56	-0.24	-14.24	production
3010-003-F1	163285	163497	Gulpen	1113	51.79	2.89	-15.61	observation
3010-011-F1	163290	163508	Grandglise	1013	51.50	29.85	20.85	observation

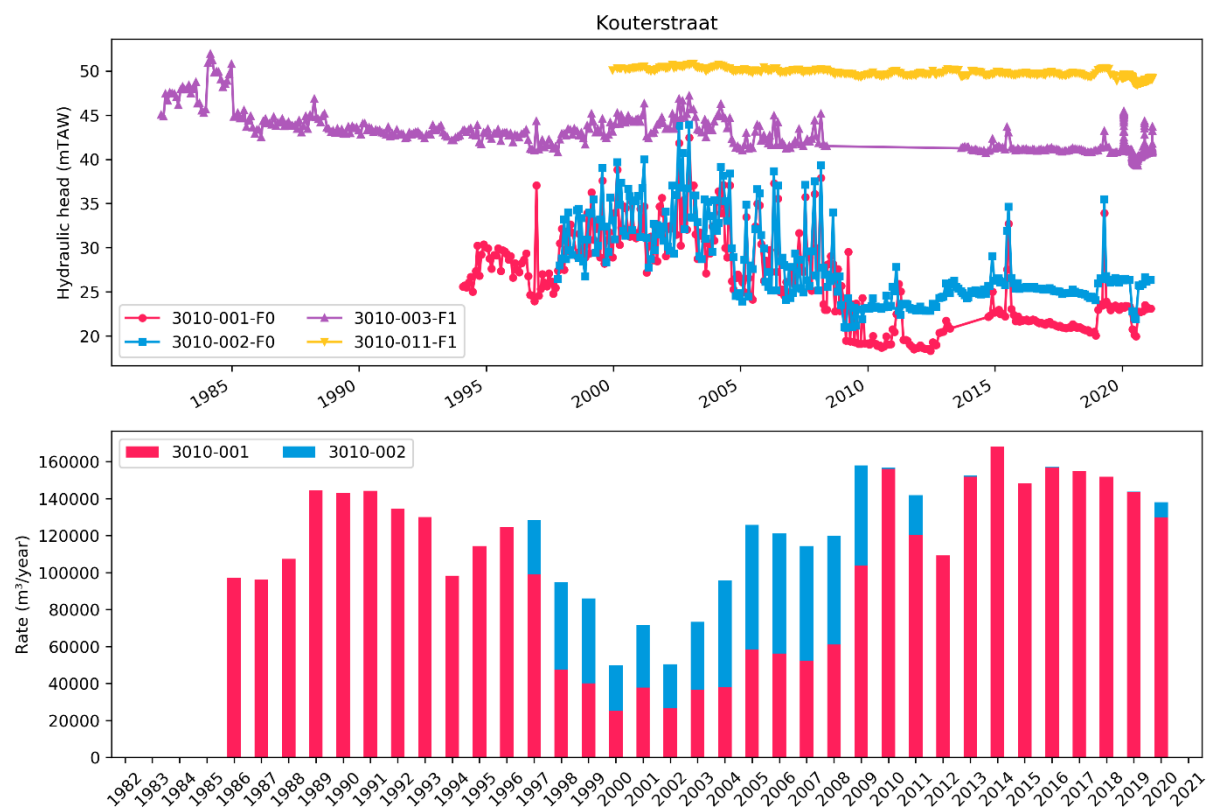


Figure 34: Evolution of the hydraulic heads (top) and extraction rates (bottom) for the site of Overijse Kouterstraat.

Sint-Agatha-Rode Veeweyde

The site of Sint-Agatha-Rode Veeweyde consists of four production wells (3012-001-F0, 3012-002-F0, 3012-003-F0 and 3012-059-F0) with a filter in the Cretaceous deposits of the Formation of Gulpen. The permitted rate for this site is 2.373M m³/year. Effective extraction rates vary between 1.5 to 2.5M m³/year (Figure 35). Wells 3012-001-F0 and 3012-002-F0 are used as the main production wells. From 2019 onwards, 3012-002-F0 is replaced by 3012-059-F0. Well 3012-003-F0 acts as a back-up well. Note the high extraction rate in 2020 (2.5M m³/year) which is to compensate for the temporary shutdown of the Geuzenhoek site. Next to the production wells, one observation well with filter in the Cretaceous (3012-004-F1) is present (Table 12). The evolution of the observed hydraulic heads is visualized in Figure 35. The variations of head in the production wells and in the observation well in the Cretaceous close by can be linked to variations in extraction rates. Note that the head in 3012-002-F0 decreases more than the one for 3012-001-F0, even though higher volumes are extracted from the latter. The head in 3012-002-F0 recovered approx. 6m after termination of production in this well.

Table 12: Overview of the characteristics of the wells at Sint-Agatha-Rode Veeweyde.

Well	X	Y	Layer	HCOV	Z (mTAW)	Filter top	Filter bot	Type
3012-001-F0	168889	162233	Gulpen	1113	33.86	12.86	-18.14	production
3012-002-F0	168936	162225	Gulpen	1113	33.58	15.68	-14.82	production
3012-003-F0	168845	162230	Gulpen	1113	37.73	14.13	-8.67	production
3012-004-F1	169109	162050	Gulpen	1113	32.79	8.75	-1.25	observation
3012-059-F0	168918	162218	Gulpen	1113	33.81	15.51	-13.69	production

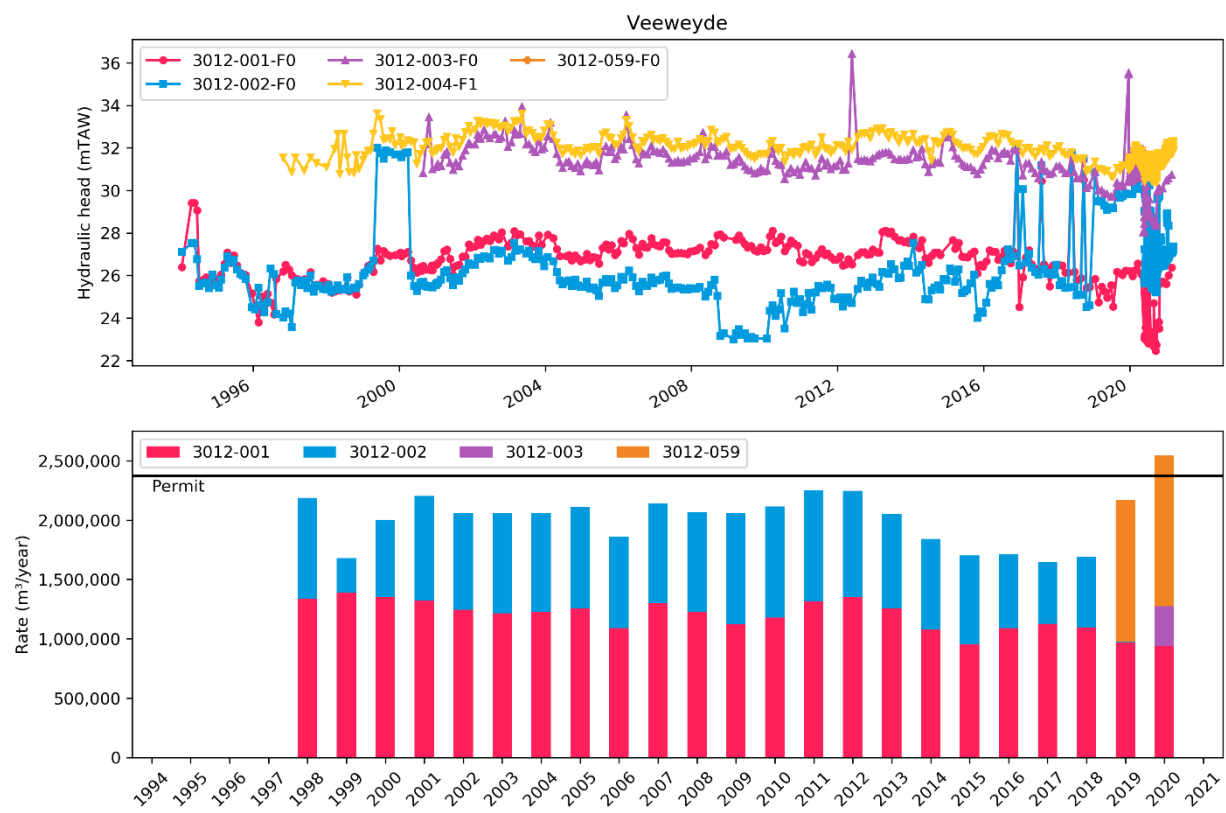


Figure 35: Evolution of the hydraulic heads (top) and extraction rates (bottom) for the site of Sint-Agatha-Rode Veeweyde.

Sint-Agatha-Rode Geuzenhoek

The site of Sint-Agatha-Rode Geuzenhoek consists of three production wells (3012-007-F0, 3012-008-F0 and 3012-009-F0) with a filter in the Cretaceous deposits of the Formation of Gulpen. The permitted rate for this site is 2.373M m³/year. Effective extraction rates are around 2M m³/year (Figure 36). Wells 3012-007-F0 and 3012-008-F0 are used as the main production wells. Well 3012-009-F0 acts as a back-up well. Since 2019, the extraction at this site was temporary shutdown due to maintenance. Next to the production wells, one multi-level observation well with filter in the Cretaceous (3012-058-F2) and Lincent (3012-058-F3) is present (Table 13). The evolution of the observed hydraulic heads is visualized in Figure 36. The variations of head in the production wells and in the observation well in the Cretaceous nearby can be linked to variations in extraction rates. Note that the head in 3012-008-F0 decreases more than the one for 3012-007-F0. Since around 2010, the heads in this well started dropping. This might be related to clogging of the well. After the halting of extraction, the hydraulic heads in wells 3012-007-F0 and 3012-009-F0 increased with 4-5m. Note the seasonal variations in both filter of observation well 3012-058. The heads in both Lincent and the Cretaceous are more or less similar in this well.

Table 13: Overview of the characteristics of the wells at Sint-Agatha-Rode Geuzenhoek.

Well	X	Y	Layer	HCOV	Z (mTAW)	Filter top	Filter bot	Type
3012-007-F0	168840	165086	Gulpen	1113	30.27	-5.03	-42.03	production
3012-008-F0	168789	165194	Gulpen	1113	29.35	-11.95	-42.65	production
3012-009-F0	168758	165170	Gulpen	1113	29.02	-18.98	-47.98	production
3012-058-F2	168496	165012	Lincent	1015	31.76	0.26	-1.74	observation
3012-058-F3	168496	165012	Gulpen	1113	31.76	-11.74	-16.74	observation

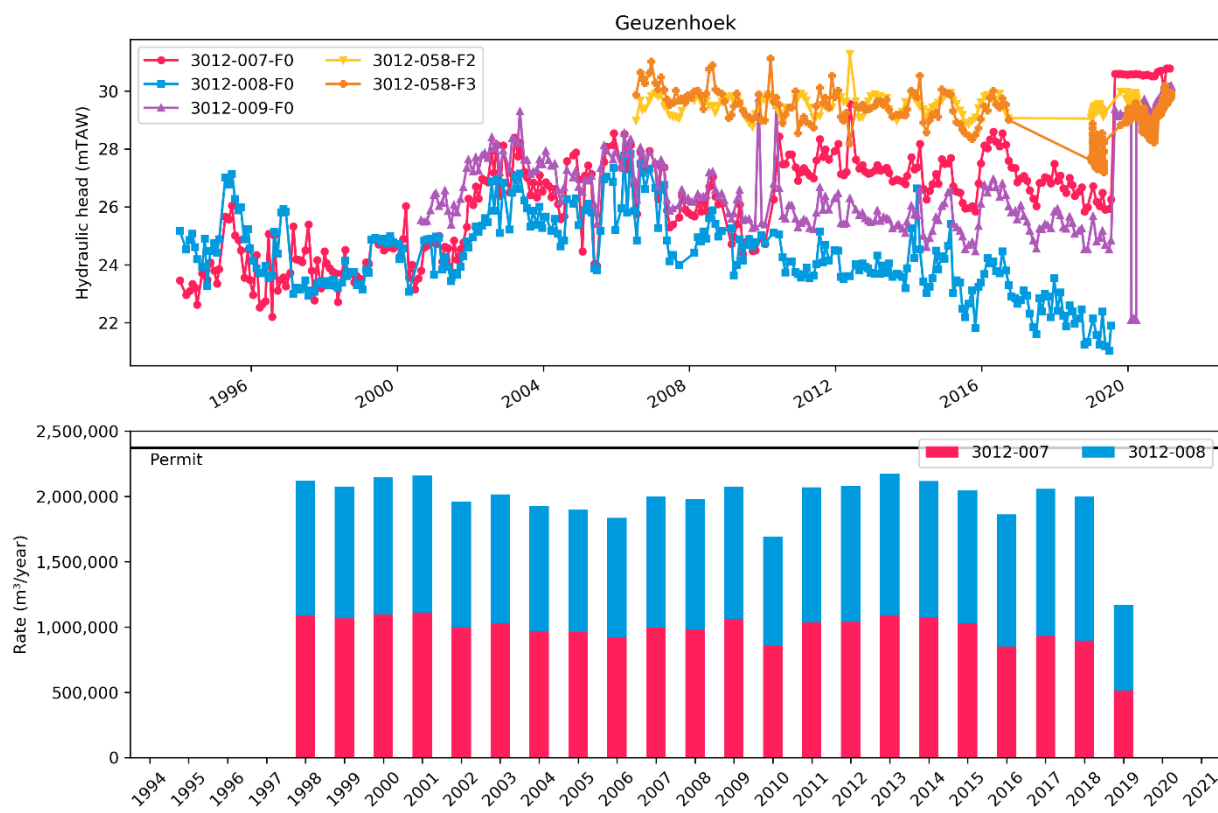


Figure 36: Evolution of the hydraulic heads (top) and extraction rates (bottom) for the site of Sint-Agatha-Rode Geuzenhoek.

Pécrot

The site of Pécrot consists of four production wells (3012-013-F0, 3012-014-F0, 3012-015-F0 and 3012-016-F0) with a filter in the Cretaceous deposits of the Formation of Gulpen. The permitted rate for this site is 3.285M m³/year. Effective extraction rates vary between 1 to 2.5M m³/year (Figure 37). Well 3012-013-F0 was only used until 1995. From then on, wells 3012-014-F0, 3012-015-F0 and 3012-016-F0 are the main production wells. Next to the production wells, two observation well with filter in the Cretaceous (3012-017-F2 and 3012-019-F1) are present (Table 14). The evolution of the observed hydraulic heads is visualized in Figure 37. The variations in head in the production wells and in the observation well in the Cretaceous nearby are in the order of magnitude of a couple of meters and can be linked to variations in extraction rates. Note that the heads in the production wells are slightly decreasing in the last few years. This decrease is a bit larger than expected based on the variation in extraction rates and might be related to a decrease in recharge in the last few dry years.

Table 14: Overview of the characteristics of the wells at Pécrot.

Well	X	Y	Layer	HCOV	Z (mTAW)	Filter top	Filter bot	Type
3012-013-F0	169674	161619	Gulpen	1113	33.23	16.98	-3.02	production
3012-014-F0	169638	162007	Gulpen	1113	32.69	20.70	-6.30	production
3012-015-F0	169627	161898	Gulpen	1113	32.21	11.22	-10.78	production
3012-016-F0	169676	161752	Gulpen	1113	32.65	17.06	-8.84	production
3012-017-F2	169628	162184	Gulpen	1113	33.37	15.87	14.87	observation
3012-019-F1	169607	161869	Gulpen	1113	32.03	20.00	-5.00	observation

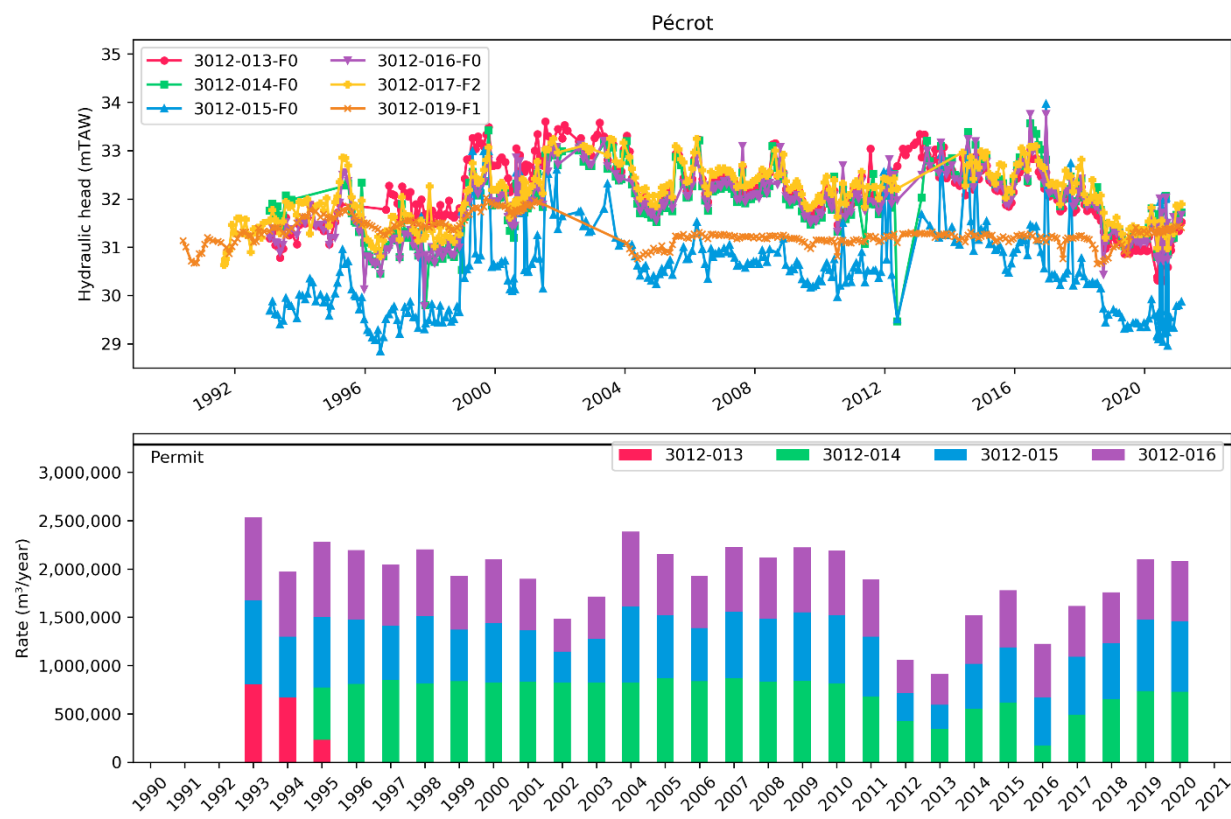


Figure 37: Evolution of the hydraulic heads (top) and extraction rates (bottom) for the site of Pécrot.

La Motte

The site of La Motte consists of two production wells (3012-020-F0 and 3012-021-F0) with a filter in the Cretaceous deposits of the Formation of Gulpen. The permitted rate for this site is 2.92M m³/year. Effective extraction rates vary between 1.5 to 2.8M m³/year (Figure 38). Next to the production wells, two observation well with filter in the Cretaceous (3012-022-F1 and 3023-019-F1) are present (Table 15). The evolution of the observed hydraulic heads is visualized in Figure 38. The variations of head in the production wells and in the observation well in the Cretaceous nearby are in the order of magnitude of a couple of meters and can be linked to variations in extraction rates. A seasonal variation is visible in all wells. Note that the heads in the production wells are decreasing (approx. 2m) in the last few years. This decrease is a larger than for e.g., Pécrot and is probably related to a decrease in recharge in the last few dry years. The clear seasonal variations indicate that the heads in this area are strongly influenced by recharge from the surface.

Table 15: Overview of the characteristics of the wells at La Motte.

Well	X	Y	Layer	HCOV	Z (mTAW)	Filter top	Filter bot	Type
3012-020-F0	170744	159698	Gulpen	1113	38.01	19.51	-0.64	production
3012-021-F0	170679	159623	Gulpen	1113	37.1	20.80	6.80	production
3012-022-F1	170691	159619	Gulpen	1113	36.95	25.00	2.50	observation
3012-023-F1	170501	159530	Gulpen	1113	35.91	25.00	2.50	observation

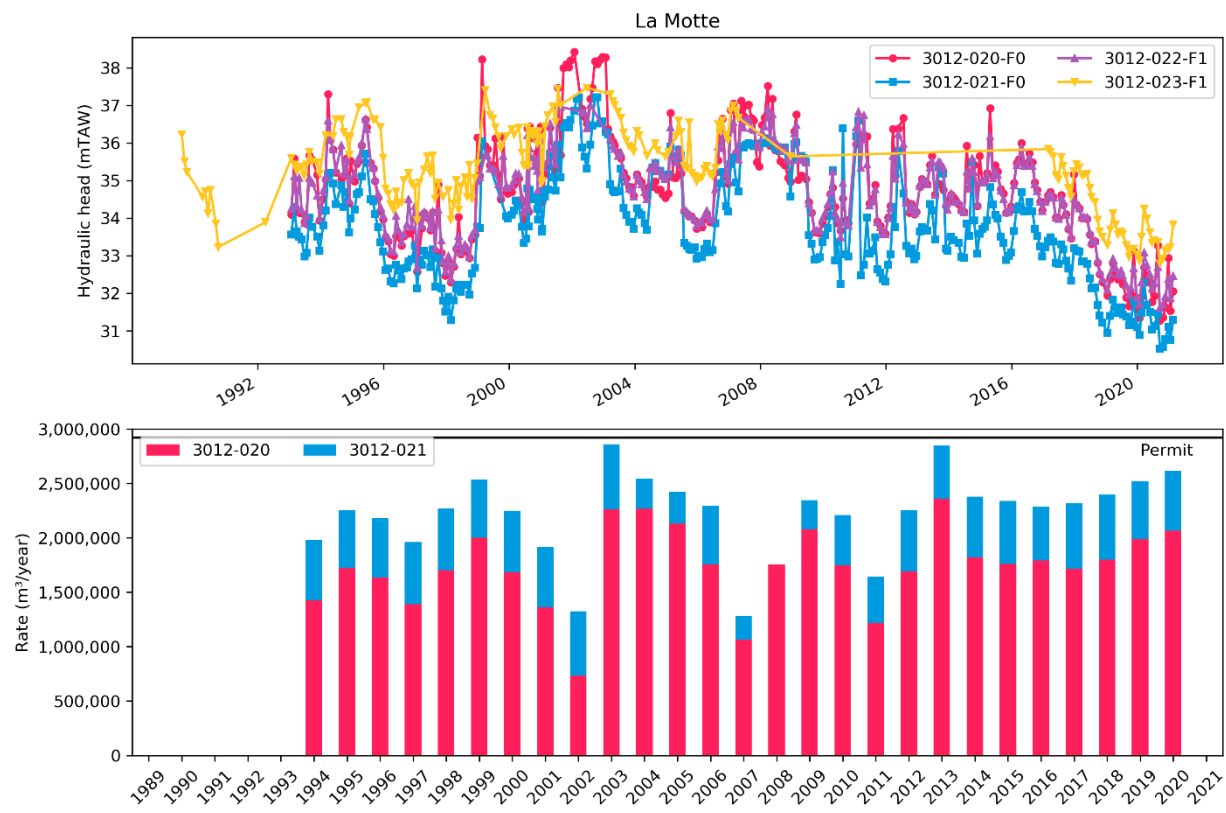


Figure 38: Evolution of the hydraulic heads (top) and extraction rates (bottom) for the site of La Motte

Biez

The site of Biez consists of one production well (3020-001-F0) with a filter in the Cretaceous deposits of the Formation of Gulpen. The permitted rate for this site 963k m³/year. Effective extraction rates are decreasing and vary between 900k m³/year in the nineties to 200-400k m³/year in recent years (Figure 39). Next to the production well, one observation well with filter in the Cretaceous (3020-002-F1)⁵ is present (Table 16). The evolution of the observed hydraulic heads is visualized in Figure 39. The heads at the production well fluctuate in a range of 6-7m and indicate that this well is not producing continuously. The heads in the observation well are very stable and do not react on changes in extraction rates.

Table 16: Overview of the characteristics of the wells at Biez.

Well	X	Y	Layer	HCOV	Z (mTAW)	Filter top	Filter bot	Type
3020-001-F0	174072	158452	Gulpen	1113	62.60	11.16	0.16	production
3020-002-F1	174109	158551	Gulpen	1113	-	-	-	observation

⁵ The exact location of the filter top and bottom could not be found. However, descriptions indicate that the filter is present in the Cretaceous.

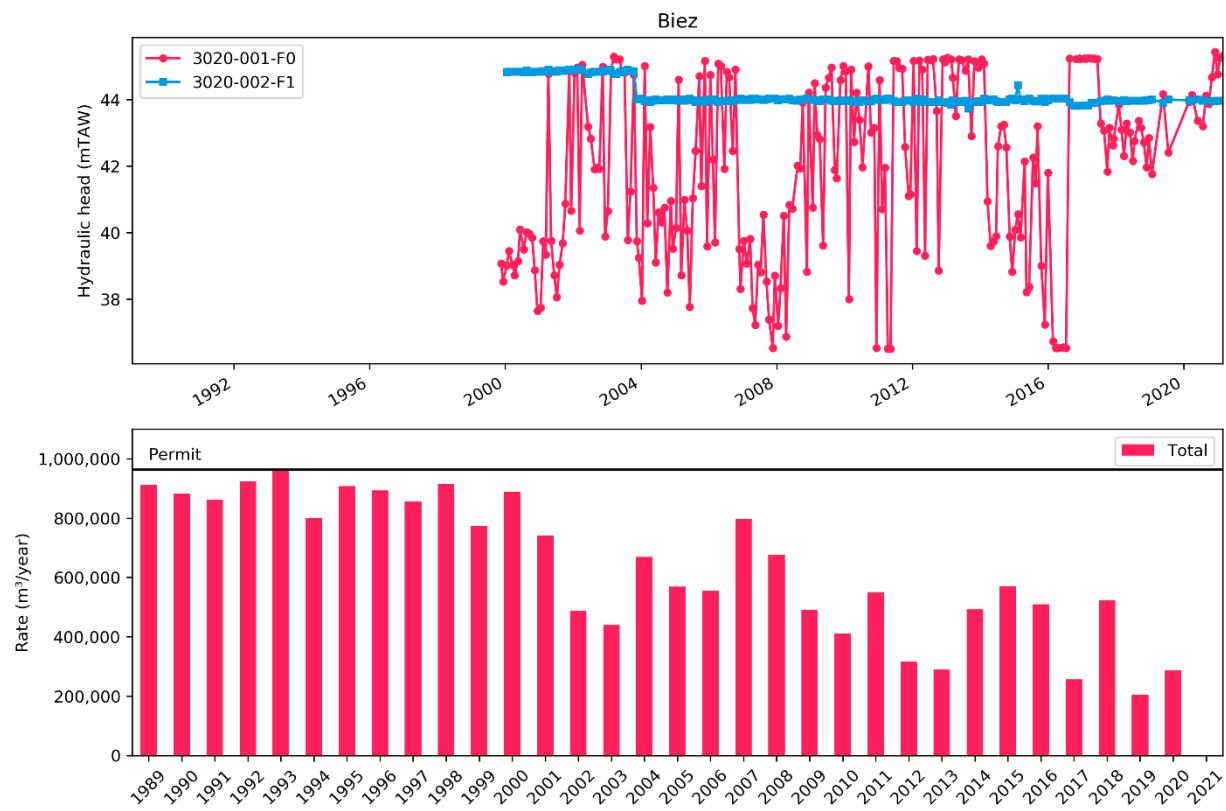


Figure 39: Evolution of the hydraulic heads (top) and extraction rates (bottom) for the site of Biez.

Vilvoorde Drie Fonteinen

The site of Vilvoorde Drie Fonteinen consists of four production wells (3014-001-F0, 3014-002-F0, 3014-003-F0 and 3012-021-F0) with a filter in the Cretaceous deposits of the Formation of Nevele (a lateral equivalent of the Formation of Gulpen). The permitted rate for this site is 438k m³/year. Since 2004, no drinking water has been produced from this site. In the nineties, effective extraction rates were approx. 500k m³/year (Figure 40). Next to the production wells, one observation well with filter in the sands of Grandglise (3014-005-F2) is present (Table 17). The evolution of the observed hydraulic heads is visualized in Figure 40. Note the very large drawdown in these wells from the beginning of the measurements around 1996. Heads recovered from around -40 to -60m up until around 10m, which is a recovery of 50-70m. This recovery is slow, and it took about 20 years to (almost) reach equilibrium. These large drawdowns might not only be related to extraction at this site, but also to a larger-scale historical extraction in this area (see section 3.3).

Table 17: Overview of the characteristics of the wells at Vilvoorde Drie Fonteinen.

Well	X	Y	Layer	HCOV	Z (mTAW)	Filter top	Filter bot	Type
3014-001-F0	153656	178455	Nevele	1113	12.08	-105.92	-128.62	production
3014-002-F0	153442	178089	Nevele	1113	13.91	-83.62	-114.29	production
3014-003-F0	153147	177510	Nevele	1113	13.86	-70.67	-114.64	production
3014-004-F0	153662	178449	Nevele	1113	13.31	-102.49	-131.69	production
3014-005-F2	153647	178466	Grandglise	1013	13.27	-73.73	-78.73	observation

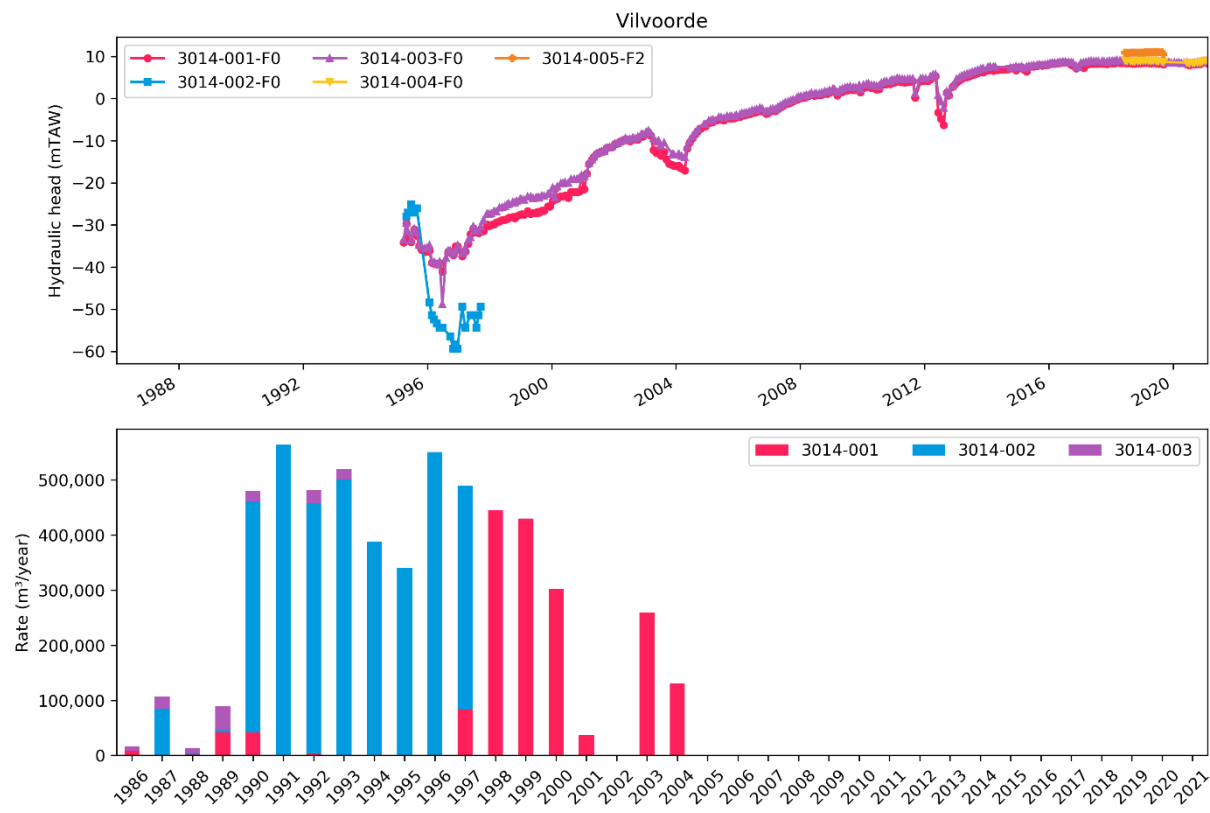


Figure 40: Evolution of the hydraulic heads (top) and extraction rates (bottom) for the site of Vilvoorde.

Hoeilaart (Hannut)

The site of Hoeilaart consists of four production wells (3023-005-F0, 3023-006-F0, 3023-007-F0 and 3023-008-F0) with a filter in the sands of Grandglise (Formation of Hannut). This site is part of De Watergroep since 2015. Before that, the Gemeentelijke Waterdienst Hoeilaart exploited this site. This is the reason for the limited hydraulic head data and no extraction rates before 2015 (Figure 41). The permitted rate for this site is 585.6k m³/year. Effective extraction rates vary between 300k and 500k m³/year (Figure 41). Next to the production wells, three observation wells with filter in Grandglise (3023-012-F1, 3023-013-F1 and 3023-014-F1) are present (Table 18). The evolution of the observed hydraulic heads is visualized in Figure 41. Note the increase in heads of 5 to 10m in all extraction wells since 2016. In the observation wells there is also an increase of 2-3m in this period.

Table 18: Overview of the characteristics of the wells at Hoeilaart in the Formation of Hannut.

Well	X	Y	Layer	HCOV	Z (mTAW)	Filter top	Filter bot	Type
3023-005-F0	158161	162137	Grandglise	1013	66.43	20.50	12.50	production
3023-006-F0	158269	162109	Grandglise	1013	65.67	20.50	12.50	production
3023-007-F0	158312	162159	Grandglise	1013	66.4	20.50	12.50	production
3023-008-F0	158263	162200	Grandglise	1013	69.5	20.50	12.50	production
3023-012-F1	158160	162154	Grandglise	1013	67.79	30.79	28.79	observation
3023-013-F1	158337	162091	Grandglise	1013	64.87	34.75	32.75	observation
3023-014-F1	158264	162164	Grandglise	1013	68.55	30.55	28.55	observation
3023-024-F0	158312	162153	Grandglise	1013	65.13	20.50	12.50	production

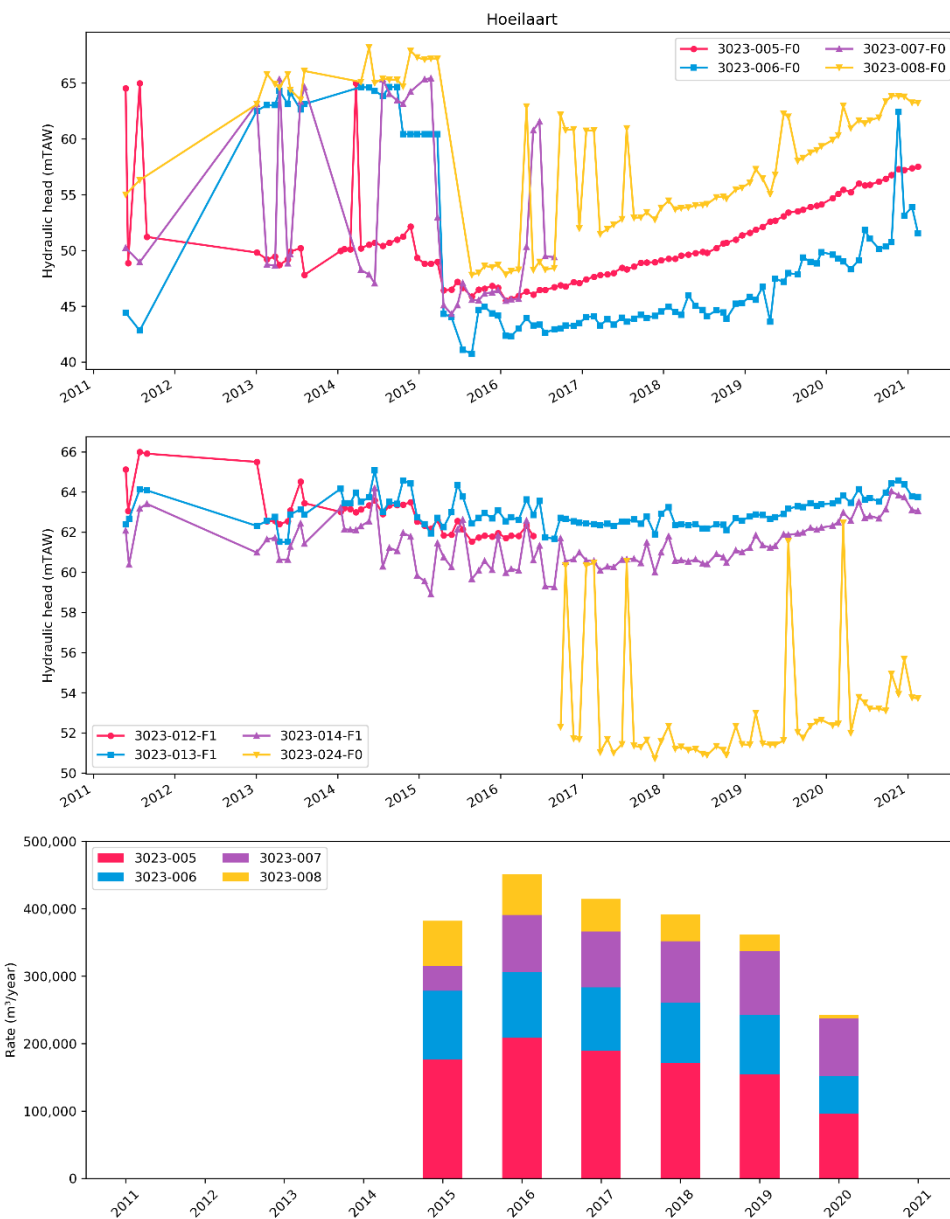


Figure 41: Evolution of the hydraulic heads (top two) and extraction rates (bottom) for the site of Hoeilaart (Formation of Hannut).

Tienen Groot-Overlaar

The site of Tienen Groot-Overlaar consists of five production wells (3003-016-F0, 3003-017-F0, 3003-018-F0, 3003-028-F0 and 3003-041-F0) with a filter in the “tuffeau” of Lincent (Formation of Hannut). The permitted rate for this site is 1.752M m³/year. Effective extraction rates vary between 600k and 1M m³/year (Figure 42). Wells 3003-016-F0 and 3003-017-F0 are the main production wells, with smaller contributions from 3003-018-F0 and 3003-028-F0. Since 2014, 3003-041-F0 is in production. This well compensates for the decrease in rates of 3003-016-F0 in recent years. Next to the production wells, three observation wells with filter in Lincent (3003-015-F1, 3003-021-F2 and 3003-022-F2) are present (Table 19). The evolution of the observed hydraulic heads is visualized in Figure 42. The hydraulic heads in the extraction wells follow more or less the fluctuations in extraction rates. Note the strong decrease in heads in 3003-028-F0, which is not only due to increased rates in this well. This drop in head might be related to clogging of this well, as this decrease is not visible in the other wells. Note the seasonal variations in the heads of the observation wells. The head in 3003-022-F2 is increasing since 2008.

Table 19: Overview of the characteristics of the wells at Tienen Groot-Overlaar

Well	X	Y	Layer	HCOV	Z (mTAW)	Filter top	Filter bot	Type
3003-016-F0	188502	164399	Lincent	1015	46.89	23.79	7.79	production
3003-017-F0	189094	164694	Lincent	1015	45.02	23.02	7.02	production
3003-018-F0	189358	164835	Lincent	1015	44.90	22.65	4.65	production
3003-028-F0	188821	164404	Lincent	1015	45.22	24.46	7.56	production
3003-041-F0	188397	164498	Lincent	1015	47.71	21.71	8.71	production
3003-015-F1	188825	164405	Lincent	1015	45.86	25.37	-0.13	observation
3003-021-F2	188121	163861	Lincent	1015	47.18	33.43	29.43	observation
3003-022-F2	189678	165613	Lincent	1015	44.23	26.83	21.83	observation

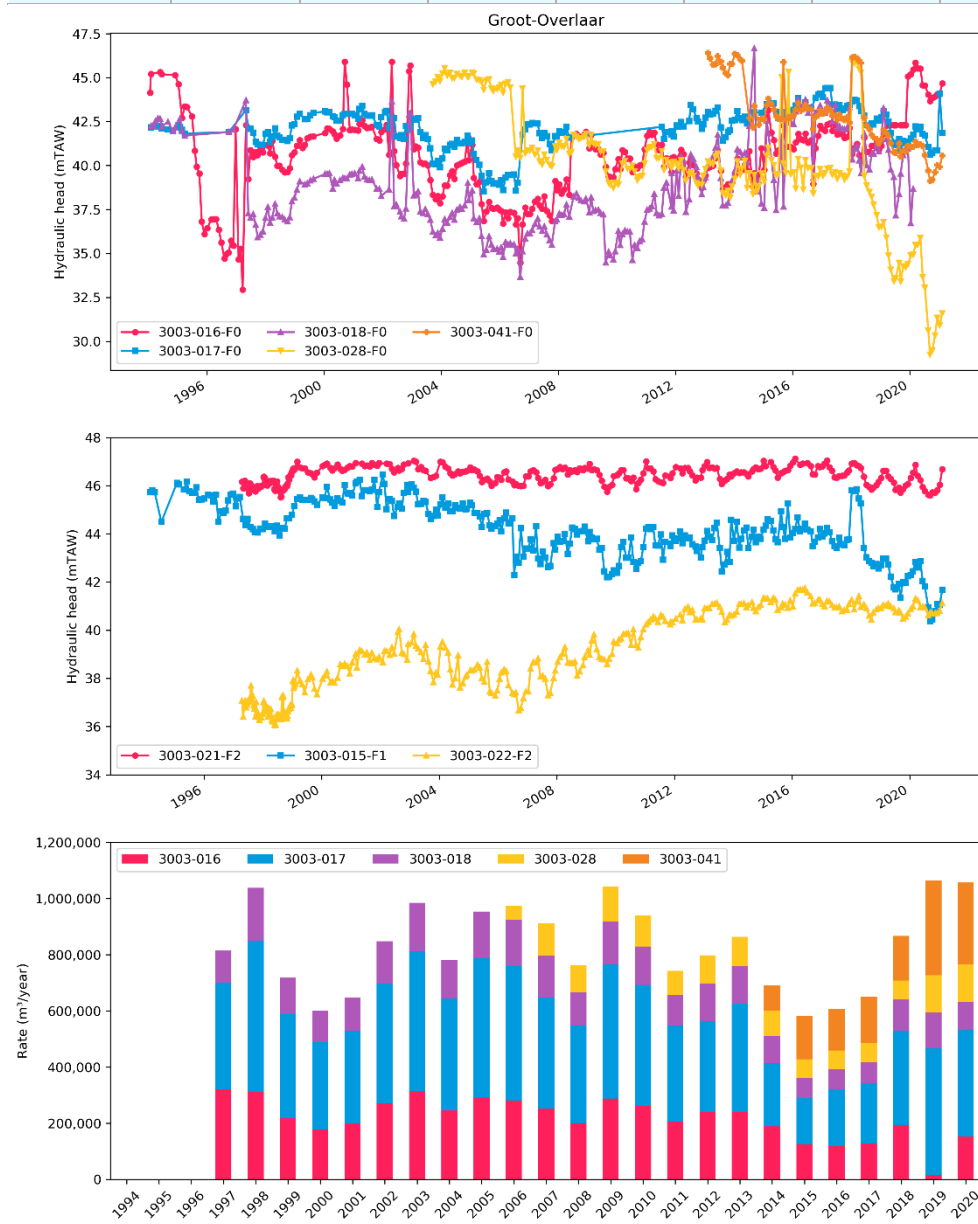


Figure 42: Evolution of the hydraulic heads (top two) and extraction rates (bottom) for the site of Tienen Groot-Overlaar.

Kumtich Menebeek

The site of Kumtich Menebeek consists of four production wells (3003-002-F0, 3003-003-F0, 3003-004-F0 and 3003-029-F0) with a filter in the “tuffeau” of Lincent (Formation of Hannut). The permitted rate for this site is 1.314M m³/year. Effective extraction rates vary between 600k and 1M m³/year (Figure 43). Wells 3003-002-F0, 3003-003-F0 and 3003-004-F0 are the main production wells. Since 2003, 3003-029-F0 is in use. Next to the production wells, six observation wells with filter in Lincent and one with filter in the Cretaceous are present (Table 20). The evolution of the observed hydraulic heads is visualized in Figure 43. The hydraulic heads in the extraction wells follow more or less the fluctuations in extraction rates. The extraction results in a decrease of about 5 to 15m in the extraction wells. Note the seasonal variations in the heads of the observation wells. The head in the well with filter in the Cretaceous is very similar to the one in wells with filter in Lincent, indicating a connection between the two.

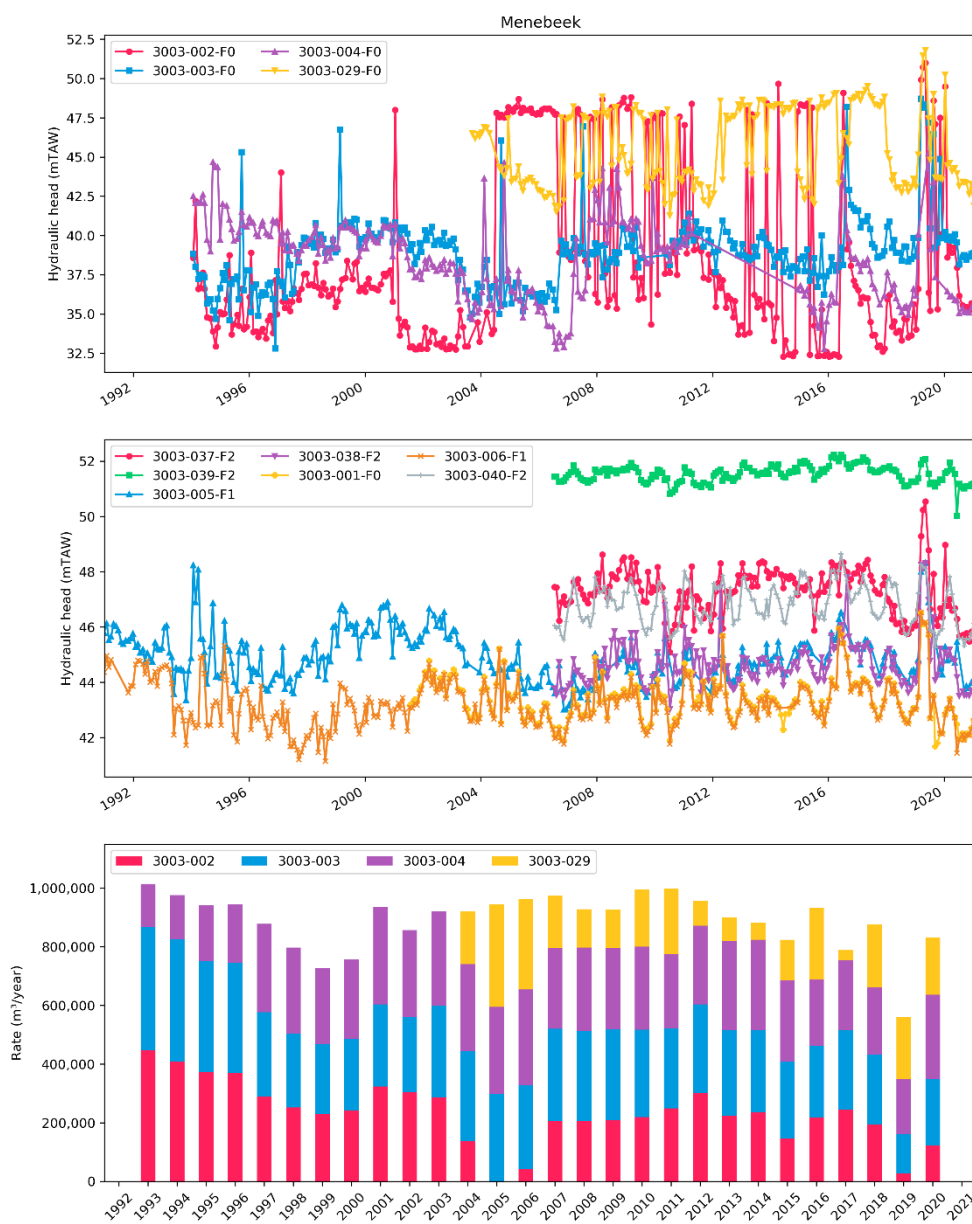


Figure 43: Evolution of the hydraulic heads (top two) and extraction rates (bottom) for the site of Kumtich Menebeek

Table 20: Overview of the characteristics of the wells at Kumtich Menebeek.

Well	X	Y	Layer	HCOV	Z (mTAW)	Filter top	Filter bot	Type
3003-002-F0	186897	166310	Lincent	1015	50.32	45.77	-22.48	production
3003-003-F0	187318	166293	Lincent	1015	48.76	24.96	-16.84	production
3003-004-F0	187636	166181	Lincent	1015	46.25	18.18	-15.82	production
3003-029-F0	186893	166240	Lincent	1015	47.76	27.76	-2.24	production
3003-001-F0	187630	166169	Lincent	1015	46.02	23.02	-18.48	observation
3003-005-F1	187412	166283	Gulpen	1113	49.25	-1.25	-67.52	observation
3003-006-F1	187621	166190	Lincent	1015	46.13	23.19	-21.81	observation
3003-037-F2	186902	1662801	Lincent	1015	48.58	28.58	23.58	observation
3003-038-F2	187335	166300	Lincent	1015	48.83	28.83	23.83	observation
3003-039-F2	186541	166265	Lincent	1015	54.98	34.48	29.48	observation
3003-040-F2	187391	165811	Lincent	1015	50.71	30.71	25.71	observation

3.2 Extraction DOV

Next to the extraction sites of De Watergroep, water is extracted from Grandglise, Lincent and the Cretaceous by other companies and organisations. For most of these extractions, only information on the permitted rates is available through Databank Ondergrond Vlaanderen (DOV; Database Subsurface Flanders⁶). For most of the largest extraction sites, effective extraction rates are provided by the VMM. An overview of all the permits in the study area with a rate higher than 3,650 m³/year is shown in Table I. 3 and Table I. 4. The extraction rates for the largest extractions based on the data of VMM is shown in Table I. 6 and Table I. 7.

The extracted rates for the DOV extraction for the period 2004-2020 are shown in Figure 44 and Table I. 5. The total extraction rates decreased throughout this period, from about 6M m³/year in the early 2000s, to approx. 2.5M m³/year in the period 2015-2020. In all three layers, there is a trend of decreasing rates. Most of the water is extracted from Lincent but extracted rates declined from 3M m³/year around 2005 to 1M m³/year in recent years. In Grandglise, rates declined from 1.5-2M m³/year to 1M m³/year. However, the permit of Gemeentelijke Waterdienst Hoeilaart (650k m³/year) is still included, even though this site is in hands of De Watergroep since 2015. The extraction from the Cretaceous decreased from 1.5M to around 300k m³/year in this period.

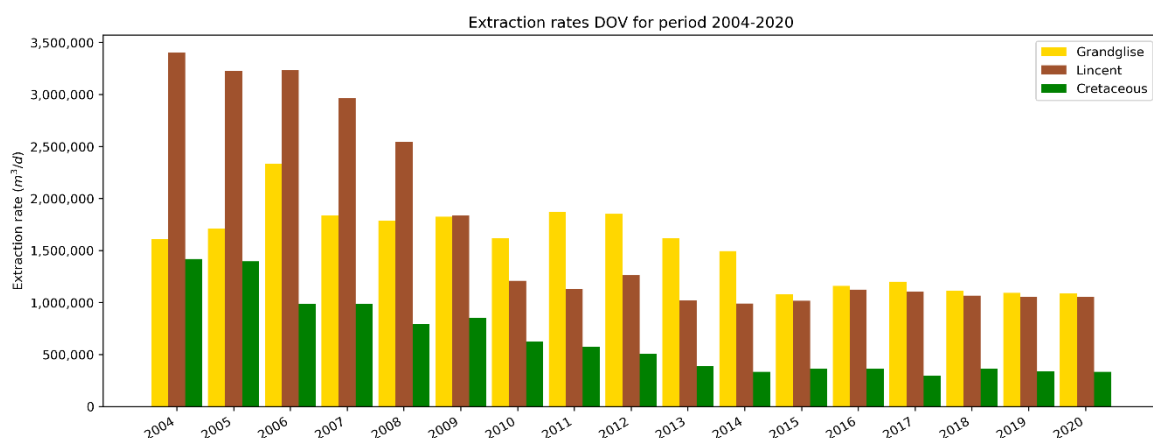


Figure 44: Overview of the evolution of the extraction rates from the wells extracted from DOV in Grandglise, Lincent and the Cretaceous.

⁶ Available online at dov.vlaanderen.be

The spatial distribution of the current and historical permits in the Paleocene aquifer system (Grandglise and Lincent) is visualized in *Figure 45*. The current permits in Grandglise are mainly situated around Leuven: Beneo Remy (554k m³/year), Inbev Leuven (500k m³/year), Cargill France (320k m³/year) and KWONET (350k m³/year). In Hoeilaart, the Gemeentelijke Waterdienst Hoeilaart has a permit for 650k m³/year, but this site has been acquired by De Watergroep. In Hoegaarden, Inbev has another permit voor 350k m³/year). In the past, there was also a permit of 351k m³/year for Tiense Suiker, but that permit expired in 2019. Most of the permits in Lincent are situated in the Tienen area: Citrique (800k m³/year), Affilips (220k m³/year and Inbev Hoegaarden (125k m³/year).

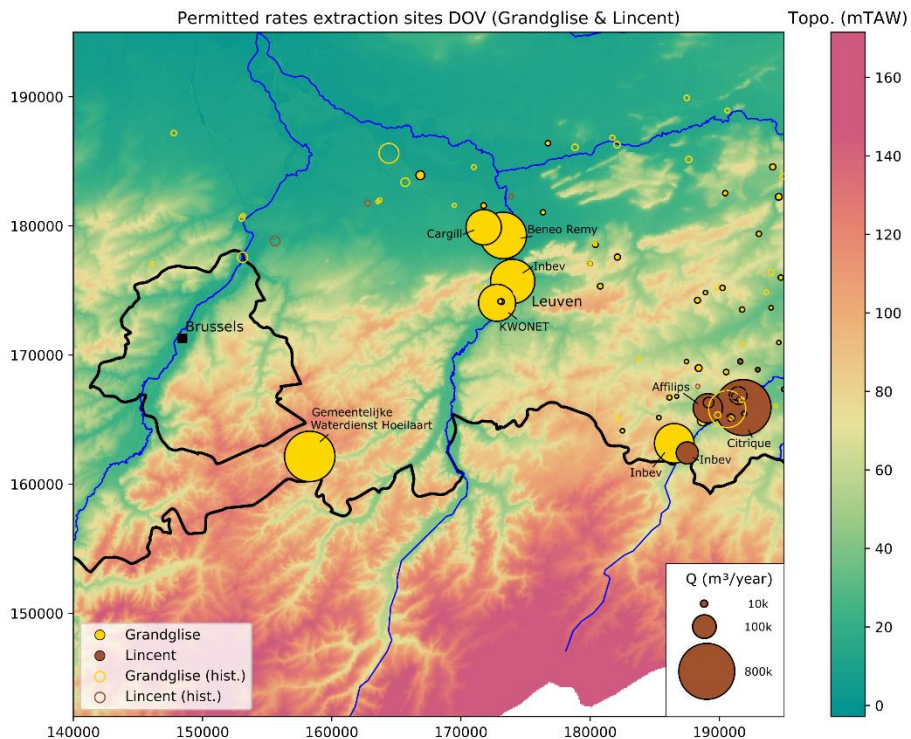


Figure 45: Map of the permitted current and historical permits from DOV for the Paleocene aquifer system (Grandglise and Hannut).

The spatial distribution of the current and historical permits in the Cretaceous for the is visualized in Figure 46. Note that the current permits are very limited, with only Abdij Averbode (62k m³/year) having a rate higher than 20k m³/year. However, there are some larger historical extractions, with Cargill France (410k m³/year) to the north of Leuven having a permit until 2013, Stad Tienen (365k m³/year) until 2005, Tiense suiker (181k m³/year) until 2019 and Inbev Leuven (100k m³/year) until 2013.

An overview of the actual reported rates (obtained from the VMM) for the largest extraction sites is shown in Table I. 6. Some of the larger wells in the Leuven area are discussed in more detail as they have a significant effect on the hydraulic heads (as discussed in section 3.3). The site of Inbev in Leuven has historically extracted water from Grandglise and the Cretaceous (Figure 47, left). For Grandglise, the permit is for 500k m³/year for the period 1995-2033. In the early 2000s, effective rates were around 400-500k m³/year, but these decreased to 100-200k m³/year in recent years (Figure 47). For the Cretaceous, the permit was for 100k m³/year for the period 1993-2013. However, since 2008 no water has been extracted from the Cretaceous. In AB Inbev (2012), the effective rates for 2006 and 2007 were reported, but it is unclear how much has been extracted in the years before. However, a decrease in the hydraulic heads of approx. 10m in the Cretaceous in the Leuven area is observed in the period 1994-2004 (see section 3.3, well 3008-044-F1) which might be (partially) caused by larger extractions of Inbev in this area.

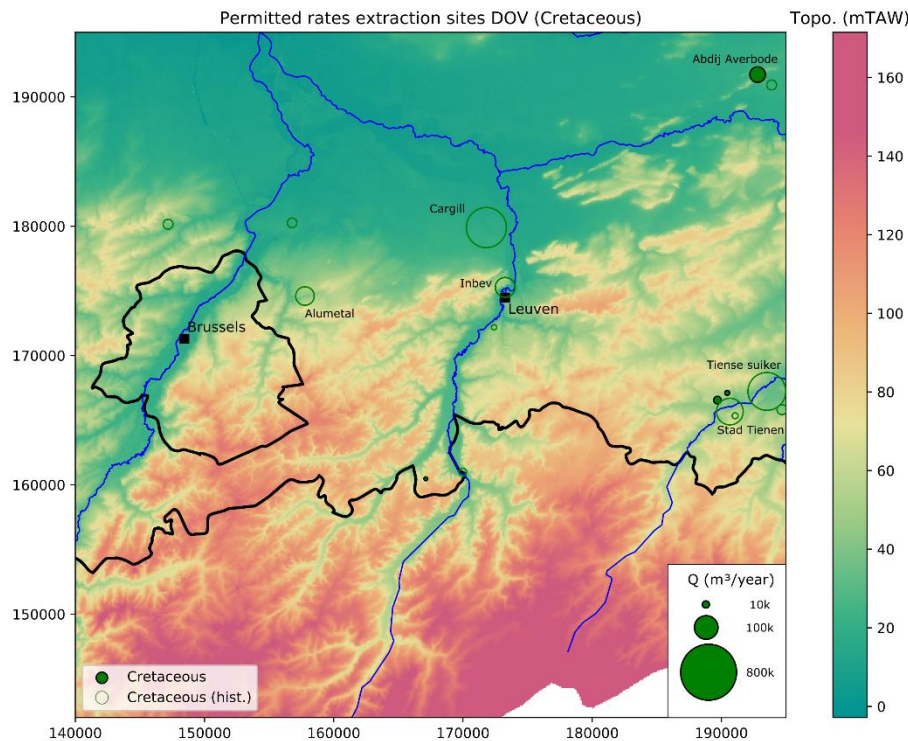


Figure 46: Map of the permitted current and historical permits from DOV for the Cretaceous.

The site of Cargill France has historically extracted water from Grandglise and the Cretaceous (Figure 47, right). For Grandglise, the permit is for 320k m³/year for the period 1999-2038. In the early 2000s, effective rates were around 200k m³/year with an outlier of 500k m³/year in 2006. In recent years, rates strongly decreased to approx. 50k m³/year (Figure 47). For the Cretaceous, the permit was for 410k m³/year for the period 1993-2013. Effective rates were around 200-300k m³/year in the 2000s and extraction stopped in 2010. The effect of this extraction is visible in a nearby well (2-0441a-F1, see section 3.3), with an increase in heads of approx. 5m after extraction was discontinued.

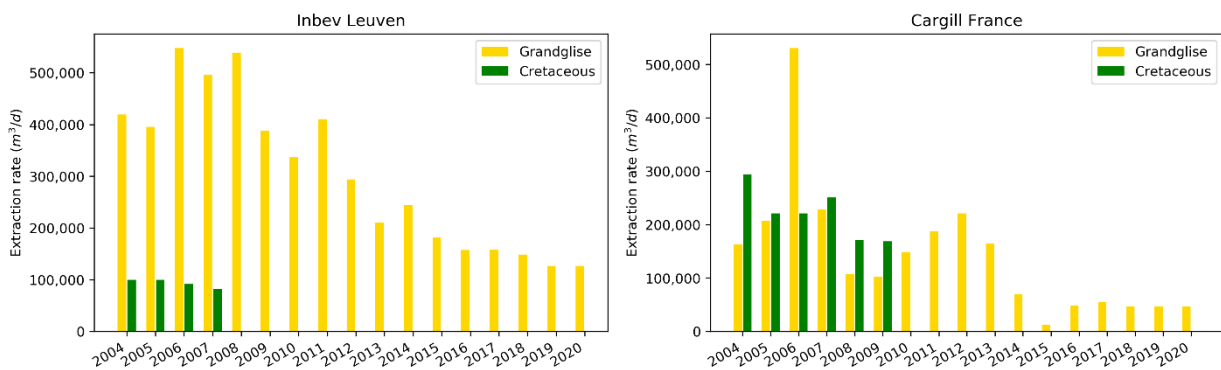


Figure 47: Overview of extraction rates for Inbev Leuven (left) and Cargill France (right) in Grandglise and the Cretaceous.

The site of Beneo Remy only extracts from Grandglise, with a permit of 554k m³/year for the period 1991-2023. Effective rates increased from around 200k m³/year in the early 2000s to approx. 300k m³/year in recent years (Figure 48).

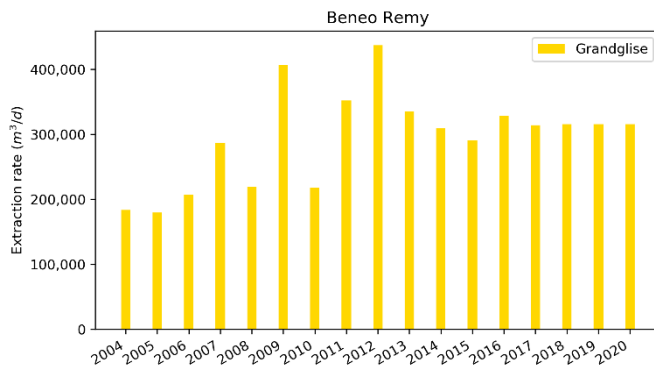


Figure 48: Overview of extraction rates for Beno Remy in Grandglise.

3.3 Evolution of hydraulic heads in the Brabant area

In this section, the evolution of the hydraulic heads in the Paleocene deposits of Grandglise and Lincent, and in the Cretaceous are discussed. The observation wells used in the following discussion are shown on a map in Figure I. 3.

The evolution of the hydraulic heads **near the western boundary, northwest of the Brussels region**, is shown in Figure 49. Note the very low heads in wells 4-0067-F1 with filter in Grandglise, which have recovered approx. 30m since the 2000s. The hydraulic head evolution is clearly indicative of extraction in this area. However, it is not clear what the origin is of this extraction. Also, the wells in Grandglise in the northwest corner (1-110a-F1) and to the east of Brussels (2-0417b-F3 and 2-0432b-F1) show a recovery in heads of several meters in the last 10-15 years. In the Cretaceous, similar trends are visible of recovery of the heads of 5-10m in the last 10-15 years. These observations indicate that both Grandglise and the Cretaceous are recovering from historical extractions in this area, with drawdowns in the Cretaceous being larger than those for Grandglise.

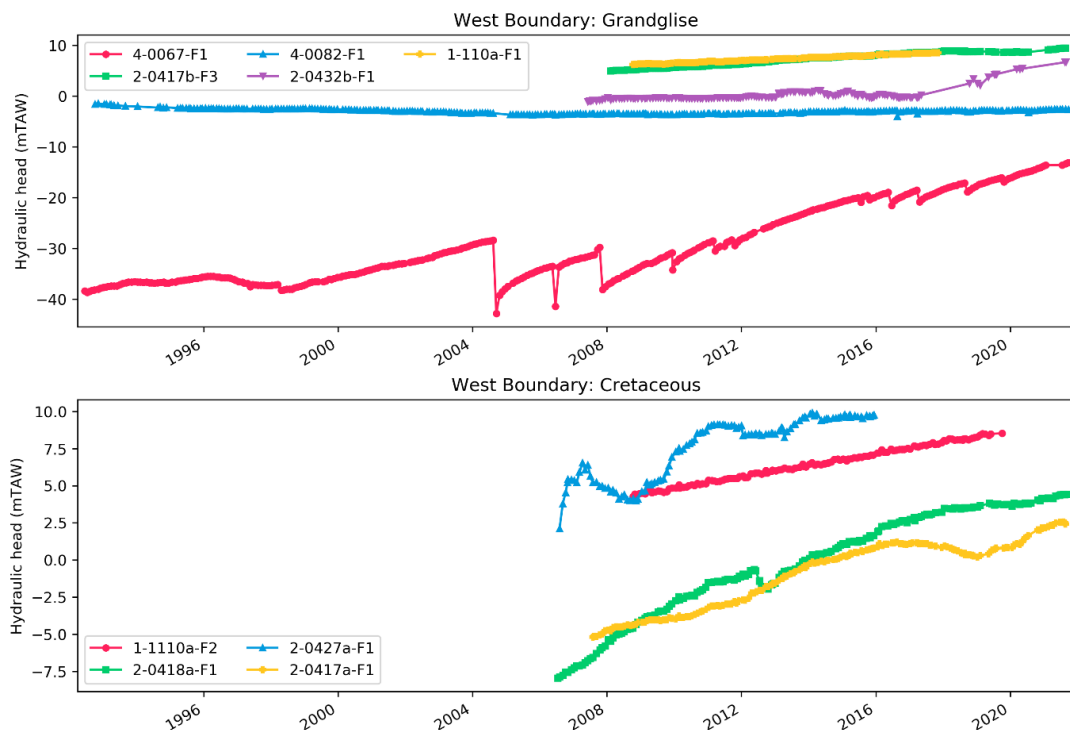


Figure 49: Evolution of hydraulic heads near the western boundary of the study area (northwest of Brussels) for Grandglise (top) and the Cretaceous (bottom).

More **towards the south, to the southwest of Brussels**, this effect of historical extraction is not visible (Figure 50). A clear trend of increasing heads towards the south is observed, following the topography. All observations show a seasonal pattern indicating the influence from recharge from the surface.

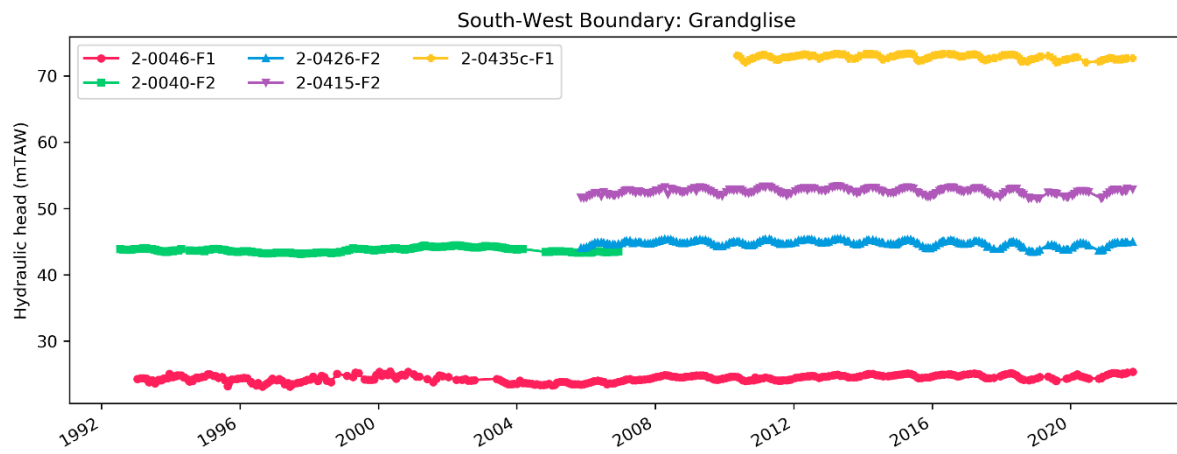


Figure 50: Evolution of hydraulic heads near the southwestern boundary of the study area (southwest of Brussels) for Grandglise.

In **the area around Vilvoorde**, heads are increasing since the start of the measurements in 2006 (Figure 51). In Grandglise, recovery is the largest (up to 4m) for the wells more towards the west (1-1110a-F1 and 2-0417b-F3) than those closer to Vilvoorde (1-2m), indicating that the source of the lower heads is situated more towards the west. In the Cretaceous, a similar trend is observed, with lower heads and larger drawdowns more towards the west (2-0418a-F1 and 2-0417a-F1), but also near Vilvoorde (2-0419a-F1) with recoveries of up to 10m. The wells more towards the northwest and northeast have smaller recoveries of approx. 5m. The drawdown near Vilvoorde might be the result of extraction at the site of Vilvoorde Drie Fonteinen (Figure 40) or other extractions in this industrial area in either the Cretaceous or the underlying Paleocene Basement. In this area, historical permits are found for Renault Industrie Belgique (Basement, 360k m³/year, period 1994-1996; and 30k m³/year, period 2000-2006), New Biolux (Basement, 90k m³/year, period 1993-1998) and Chimac (Cretaceous, 43.8k m³/year, period 1976-1997). The observed decreased head in the Cretaceous in this area is probably related to the combined effect of these extractions with the one from the site of Vilvoorde Drie Fonteinen, and extractions more towards the west.

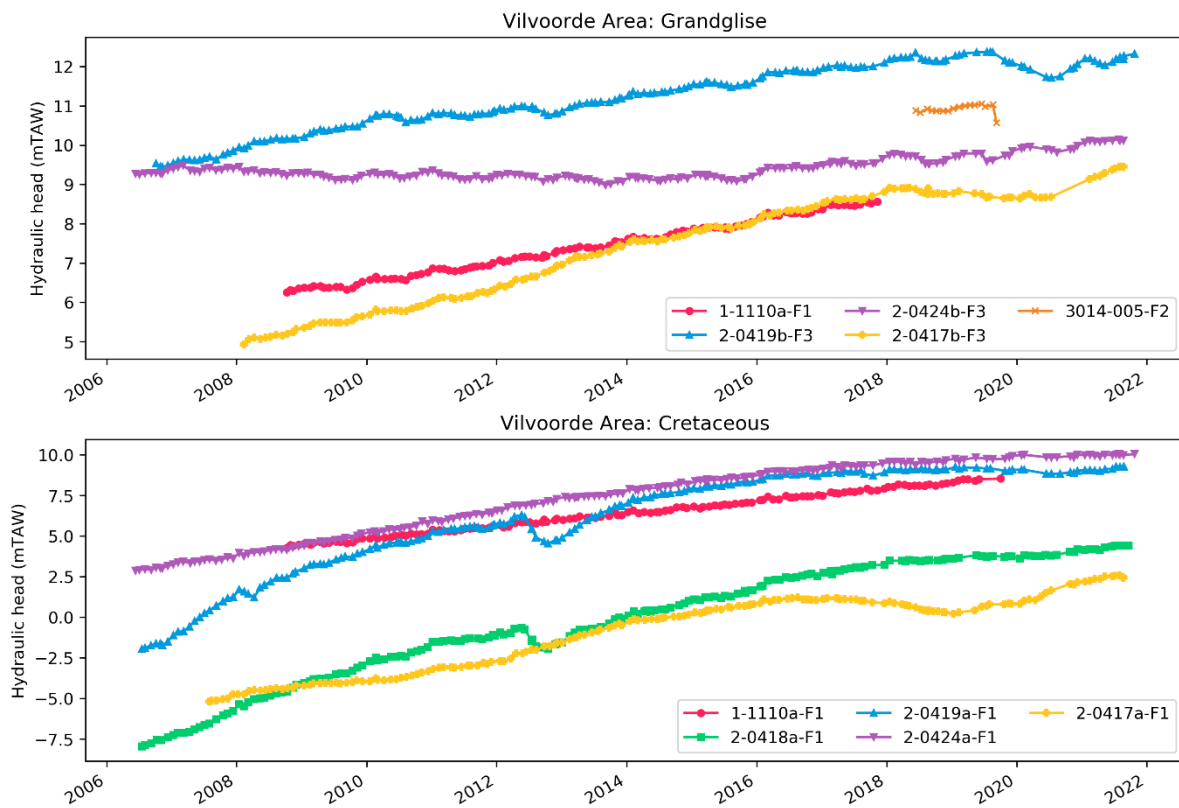


Figure 51: Evolution of hydraulic heads in the Vilvoorde area for Grandglise (top) and the Cretaceous (bottom).

The hydraulic heads in **the northeast of the study area, between Leuven and Aarschot**, are shown in Figure 52. In Grandglise, no clear trends in time are observed. The head in well 3007-038-F2 (near the Vlierbeek site) shows a slight increase since 2015, which might be linked to a decrease in extraction rates of the Inbev Leuven site (Figure 47). In the Cretaceous, there is a clear increasing trend in 2-0441a-F1 since 2009, which is probably linked with the termination of extraction from the Cretaceous by Cargill France a bit more towards the west. The extraction site of De Watergroep started production from the Cretaceous in 2016, leading to a decrease of about 10m in the observation well 3001-107-F1 nearby. The smaller decrease in head in 2-0436a-F1 might also be related to this. Similar decreases in the wells more towards the east of Leuven in recent years might also be related either to the production in Aarschot or to lower recharge of the Cretaceous in the last few dry years. The latter is unlikely due to the relatively long travel times of the groundwater in the Cretaceous. We do not expect to see such a rapid response on changes in recharge at the surface.

The hydraulic heads evolution **near the eastern boundary** of the study area, to the east of Diest, is shown in Figure 53. In the northernmost well in Grandglise, there is a slight decreasing trend. The wells more towards the south show a clear seasonal variability, with no clear increasing or decreasing trend. However, note the effect of the dry summer of 2018. In the Cretaceous, there is a slight increasing trend for the northernmost wells, with the largest increase all the way in the north for 7-0557a-F2. The lower heads in this area might be related to dewatering of the mining areas more towards the east. Also note the strong vertical gradient between the Cretaceous and Grandglise of 10-15m, indicating a strong resistance of the deposits in between. In the wells more towards the south, a seasonal pattern emerges. This is related to the fact that the Cretaceous is semi-confined to unconfined more towards the southeast.

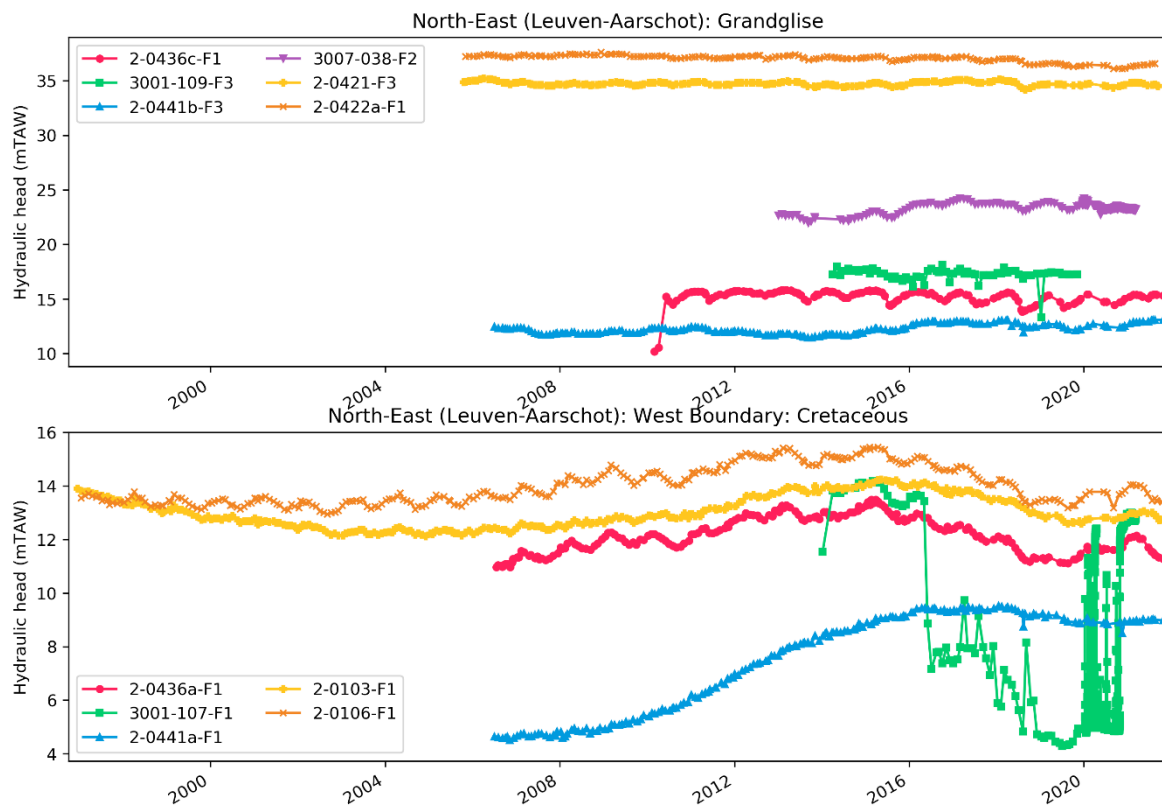


Figure 52: Evolution of hydraulic heads in the northeast part of the study area (between Leuven and Aarschot) for Grandgliste (top) and the Cretaceous (bottom).

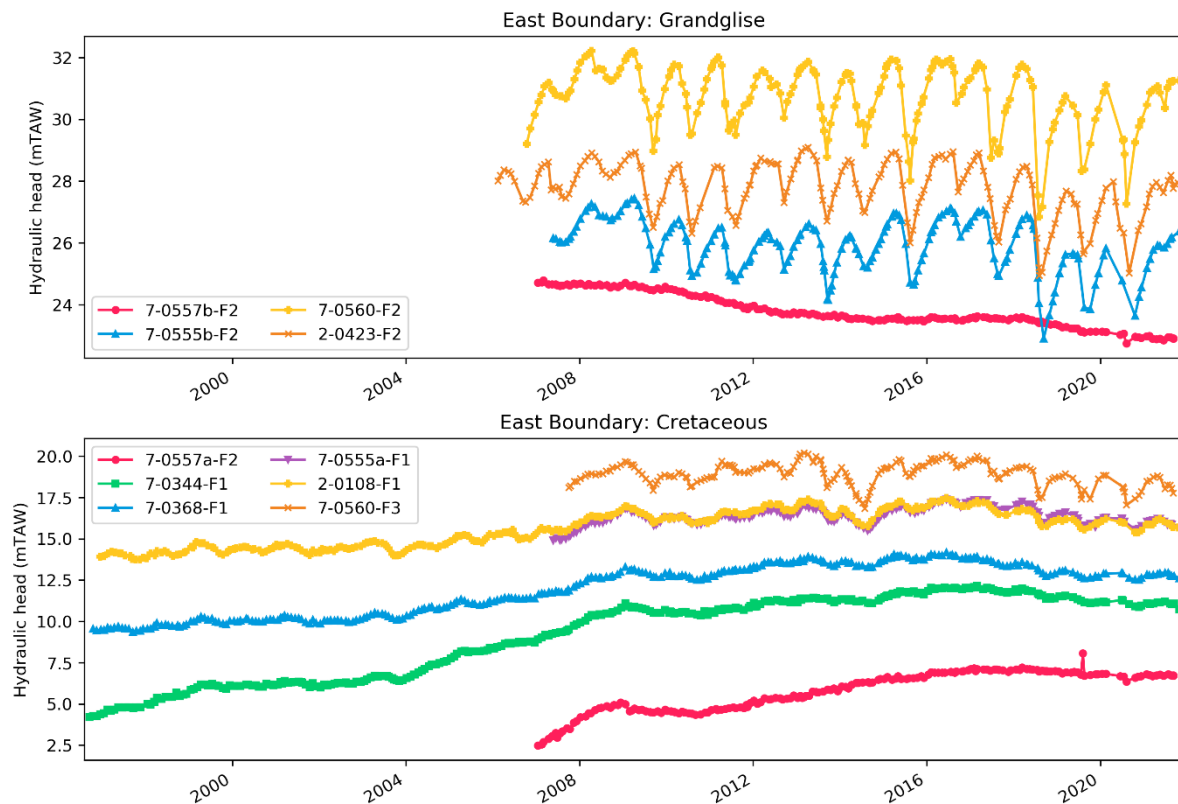


Figure 53: Evolution of hydraulic heads in the northeast part of the study area (between Leuven and Aarschot) for Grandgliste (top) and the Cretaceous (bottom).

The hydraulic heads for the wells in the area to the east of Leuven, between Leuven and Tienen, are shown in Figure 54. The wells in Grandglise show more seasonal variability towards the east, due to the unconfined character of the Paleocene deposits in the Tienen area. The wells in the Cretaceous do not show a clear seasonal variability. There is, however, a trend of decreasing heads in the period 1996-2004, followed by an increase until 2016 and finally another decrease in recent years. The decrease in the period 1996-2004 might be related to the extractions of the Inbev Leuven site in the Cretaceous, which were terminated in 2007. The decrease since 2016 might be related to the start of production in the site of Heverlee Abdij in 2015.

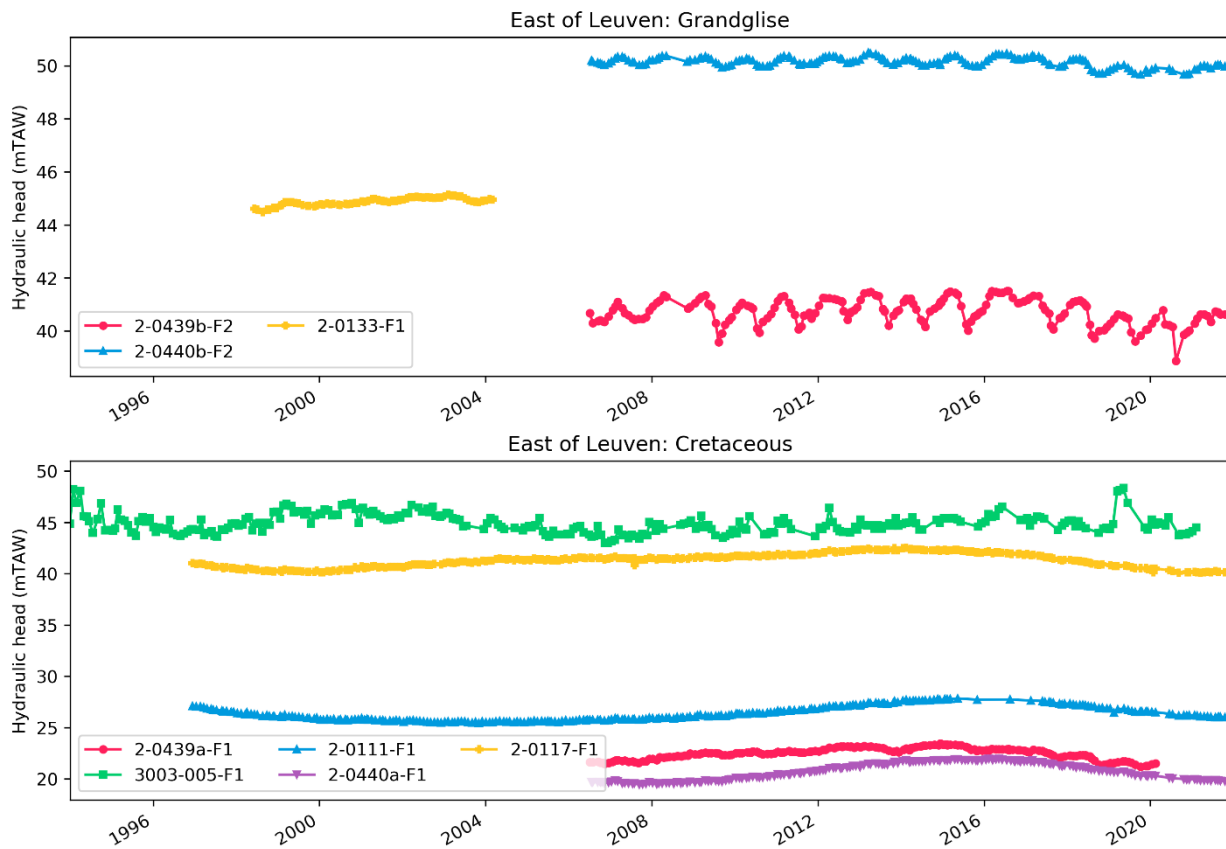


Figure 54: Evolution of hydraulic heads in the area to the east of Leuven (between Leuven and Tienen) for Grandglise (top) and the Cretaceous (bottom).

The heads in the **Leuven area** are shown in Figure 55. In Grandglise, for the wells in the north of Leuven (2-0072-F1 and 3007-038-F2), there was a slight decrease in heads in the period 1996-2008, after which heads recovered approx. 2m. This might be related to the decrease in extraction of the Inbev Leuven well extracting from Grandglise. For the Cretaceous, a long time-series is available for an observation well near Heverlee Campus (2-0005-F1/3008-044-F1 up to 2010, 2-0777-F2/3008-058-F3 from 2010 onwards). In the period 1994-2000, heads decreased about 10m, after which a recovery started until 2012, after which the heads decreased again. These trends are probably related to the combination of extraction at the Inbev site in Leuven and the extraction at Korbeek-Dijle Het Broek. The initial decrease in heads corresponds to an increase in extraction rates in Het Broek since 1993 (Figure 30), which were subsequently lower in the period 2002-2008, and then increased again from 2009 onwards. The higher extraction rates in the last few years are probably the reason for the drop in head in this period. The effect of the extraction of Het Broek is probably combined with the effect of the extraction site of Inbev Leuven, which extracted until 2007, with indications of larger extraction rates in the period 1994-2000. The start of production at Heverlee Abdij might also contribute to the drop in heads in recent years. The drop in head of approx. 10m in 3006-159-F2, an observation

well between the sites of Cadol and Abdij, is a result of the initiation of production in Abdij. The slight decrease in heads near Vlierbeek (3007-038-F3) are probably also related to this.

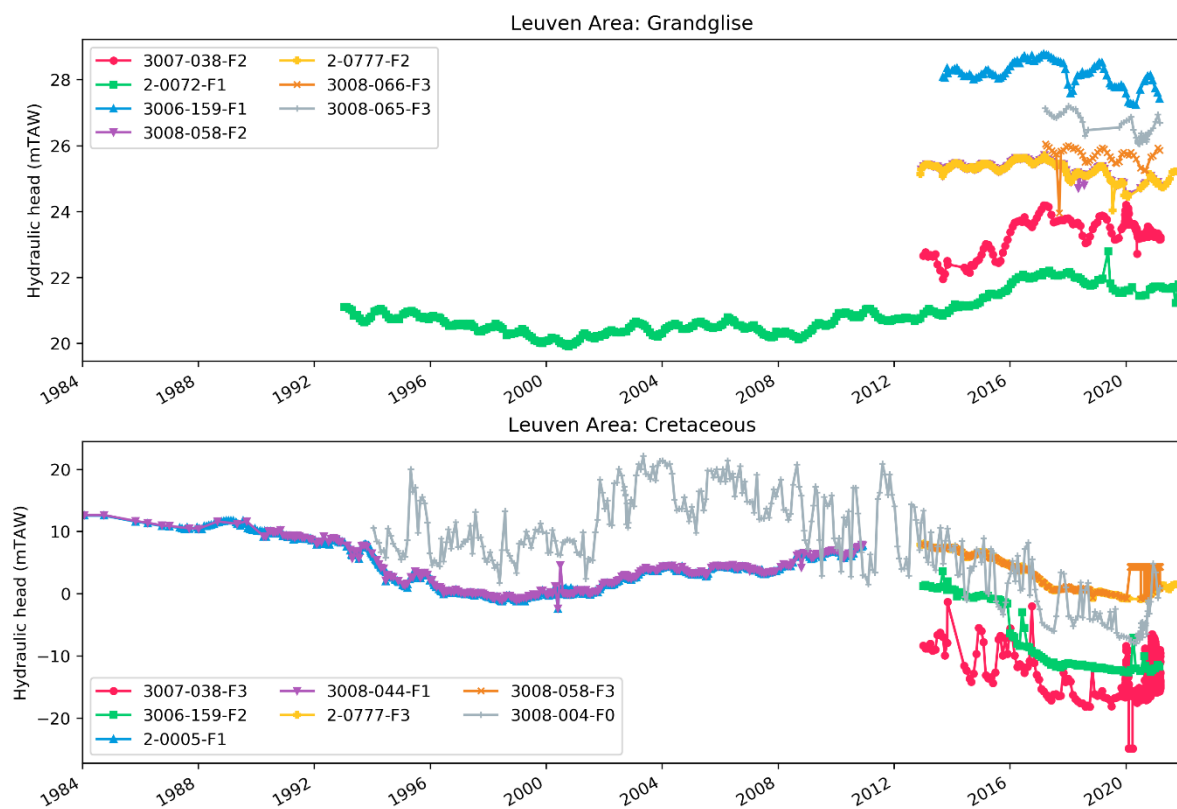


Figure 55: Evolution of hydraulic heads in the Leuven area for Grandglise (top) and the Cretaceous (bottom).

The heads in the Dijle valley to the south of Leuven are shown in Figure 56. No clear trends are visible for the observation wells in Grandglise. Note that for most of the wells a seasonal pattern is visible, indicating an influence from the recharge from the top. The heads in the Cretaceous for the wells in the Dijle valley (south of Het Broek, Veeweyde, Geuzenhoek and Pécrot) are shown in the second plot in Figure 56. Well 3012-025-F1 is situated between Het Broek and Geuzenhoek. Note the presence of a seasonal variation, indicating the influence of recharge on the heads in this area. The heads in well 3012-058-F2 also show a seasonal pattern, although this is less clear due to the influence of changes in the extraction rates of Geuzenhoek. The drop in 2019-2020 is related in an increased extraction at this site due to the temporary shutdown of Veeweyde. A similar pattern is visible for 3012-024-F1, which is located to the south of Geuzenhoek. The observation wells close to Pécrot (3012-019-F2 and 3012-056-F2) show a decrease in heads of a couple of meters in the last few years. This is probably related to a decrease in recharge in these dry years. In the third plot in Figure 56 the heads in the observation wells near Sana, Venusberg, Kouterstraat and Nellebeek are shown. The decrease in well 3011-007-F3 is related to the start of production at the site of Venusberg in 2008. For the rest, no significant trends are observed, except for a slight decrease in the last few dry years. Note the seasonal pattern present in the heads, indicating that there is an influence from recharge from the surface.

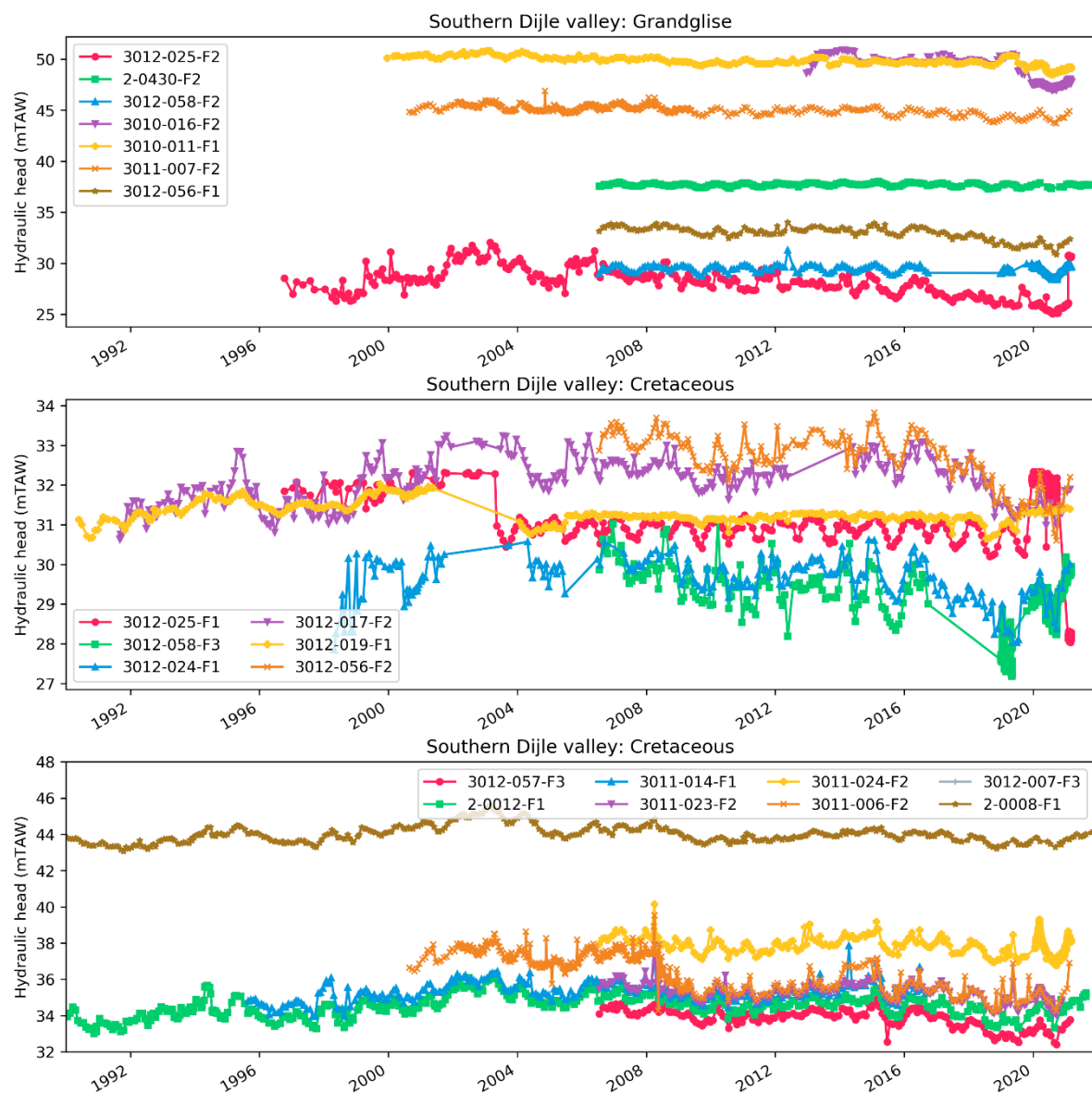


Figure 56: Evolution of hydraulic heads in the Dijle valley to the south of Leuven for Grandglise (top) and the Cretaceous (bottom two).

4 Groundwater Modelling: Brabant Model

The province of Vlaams-Brabant is an important area to produce drinking water from the Cretaceous for De Watergroep. Drinking water is produced from 14 extraction sites, most of which are situated in the southern part of the Dijle valley and in the Leuven area. Furthermore, three sites are located in Wallonia, in the province of Waals-Brabant.

However, the knowledge we have of the Cretaceous in this area is limited. This is mainly due to the relatively large depths of the aquifer in its confined part. Due to these large depths, borehole and hydrogeological data is limited. Furthermore, the hydrogeological properties of the Cretaceous in this area are strongly spatially variable (see section 2.3) and we see that the aquifer recovers slowly from historical extractions in e.g., the Vilvoorde and Leuven areas. All these factors make it difficult to set up high-quality groundwater models. Due to the regional effect of extraction, it is difficult to set-up local models for the different extraction sites. There is a need for a regional modelling approach to be able to adequately model the groundwater flow in the Cretaceous in this area. The groundwater model set-up for this area, which we call the Brabant Model, builds from earlier iterations of modelling studies in the area, mainly the model of Hoedemaekers (2016) and Van der Linden (2020). In this chapter, we describe the conceptualization and results of the Brabant Model, a complex transient regional model of the Brabant area.

4.1 Model Area

In Figure 57 the Brabant Model area is indicated on a map showing the extent of the Cretaceous deposits in Flanders. The Brabant Model extends from X=140,000-195,000m and Y=142,000-195,000m (Lambert-72 coordinates) and comprises the province of Vlaams-Brabant as well as the northern part of the province of Waals-Brabant. The total area of the model area is 55km x 53km, 2,915km². The boundaries correspond with those of Hoedemaekers (2016), except for an extension of the west boundary 5km more towards to west and an extension of the north boundary 3km more towards the north. The boundaries are chosen so that they are not too close to the influence of other extraction sites (e.g., extraction sites in the province of Limburg in the east) and are chosen far enough from the focus area (Leuven area and Dijle valley) so that the regional aspect of the extraction can be captured.

The main focus of this model is on the Cretaceous and Paleocene Aquifer systems. In the Brabant area, the Ieperian Aquitard is the main unit that confines the modelled aquifer systems. Note that in most of the area, these aquifer systems are confined by the Ieperian aquitard, with exception for the southern part (in Wallonia) and in the south-east in the Tienen area. In these areas, the aquifer systems are either overlain by the Quaternary deposits (mainly in the river valleys and in the south-east) or by the Brussels sands, a highly permeable sand deposit.

The Brabant Model includes all layers between the Formation of Kortrijk and the Palaeozoic basement, i.e., the Paleocene and Cretaceous aquifer systems. A detailed discussion of the geology of the Brabant area is done in Section 1, including the extent and thickness of all sublayers modelled in the Brabant model (Figure 7 and Figure 8) and several geological profiles (Figure 9).

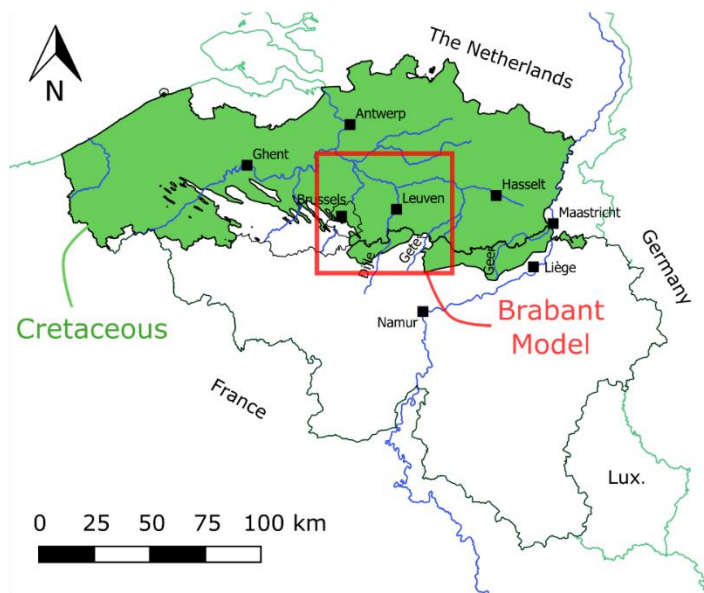


Figure 57: Map of the extent of the Cretaceous deposits and the location of the model area of the Brabant Model.

4.2 Discretization

The model area is subdivided into cells of 100x100m, resulting in a grid of 530 x 550 cells (291,500 cells in total). Vertically, the model discretised into three model layers which consist of several sublayers (Table 21). In total, the model comprises $3 \times 530 \times 550$ cells = 874,500 cells.

Layer 1 is the first aquifer in the model consisting mainly of the fine sands of Grandglise (A1013) with locally in the east the sandy deposits of Loksbergen & Dormaal (A1013). The extent and thickness of layer 1 is shown in Figure 58a. Layer 1 has an average thickness of approx. 20m, with a maximum thickness of 35m in the east.

Layer 2 is a collection of layers with low permeabilities and thus represents an aquitard in the model. It mainly consists of the silty deposits of Halen and the 'tuffeau' (porous silicified limestone) of Lincent (A1021). The latter is only present in the east of the model area. Layer 2 also includes the clay deposits of Waterschei & Beselare (A1022), the marly clays of Maaseik (A1031), the marls of Gelinden (A1032) and the sands of Orp (A1033), all of which are only present in the NE part of the model area. The extent and thickness of layer 2 is shown in Figure 58b. The thickness of this layer increases from <10m in the south to >80m in the northeast.

Finally, layer 3 is the main aquifer of interest, consisting of deposits from the Cretaceous. In the northeast, the coarse calcarenites of Houthem (A1101) and Maastricht (A1102) are present. Below that, the deposits of Gulpen are present, with at the bottom the chalk of the Member of Zeven Wegen and at the top the Members of Lanaye/Lixhe which consists of chalky marls to fine calcarenites. The extent and thickness of layer 3 is shown in Figure 58c. Layer 3 is the second aquifer in the model. However, as discussed in section 2.3.3, the permeability in this aquifer is strongly spatially variable, with very low permeabilities in the north and high permeabilities in the south. Note in Figure 7 and Figure 8 that in some areas deposits are present that are not connected with other modelled deposits. To prevent numerical issues, these disconnected areas are removed Figure 58. For simplicity, the three layers will be often described as Grandglise for layer 1, Lincent for Layer 2, and the Cretaceous for Layer 3.

Table 21: Overview of the three model layers, the sub layers and the type of lithology.

Layer	Unit	HCOV	Lithology
Layer 1	Loksbergen/Dormaal	A1012	sands
	Grandglise	A1013	fine sands
Layer 2	Halen/Lincent	A1021	silt to clayey silt, silicified limestone
	Waterschei/Beselare	A1022	clay to sandy clay
	Maaseik	A1031	marly clay
	Gelinden	A1032	marls
	Orp	A1033	clayey to marly fine sands
Layer 3	Houthem	A1101	coarse calcarenites
	Maastricht	A1102	coarse calcarenites
	Gulpen	A1103	chalk, marls and fine calcarenites

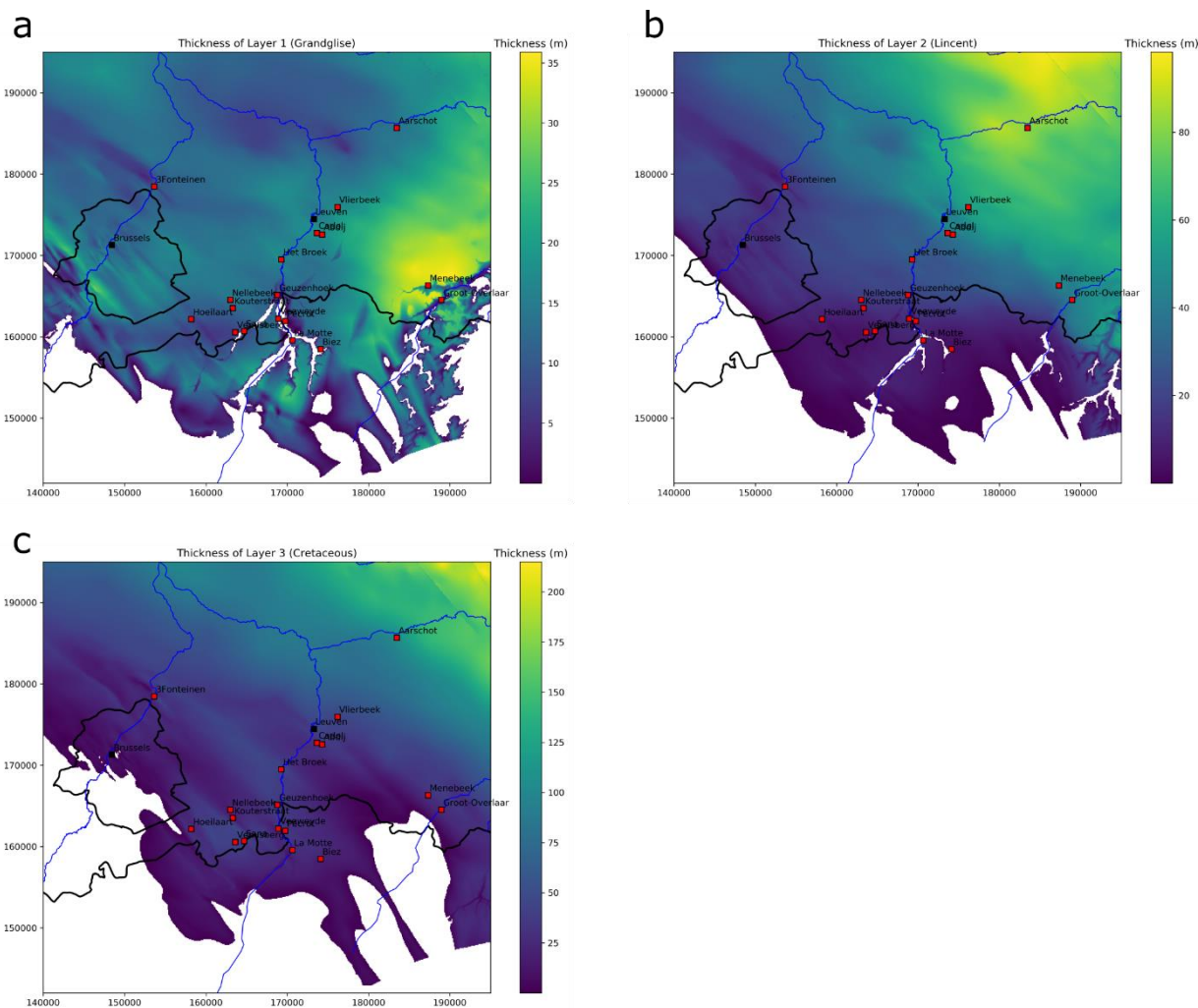


Figure 58: Thickness of the model layers: (a) Layer 1: Grandglise; (2) Layer 2: Lincent; (3) Layer 3: Cretaceous.

We chose not to discretise the model into more model layers due to several reasons. Firstly, due to computational efficiency: more model layers would make the already large and complex model slower. This would especially cause problems for the very computationally expensive uncertainty analysis (Chapter 6). Secondly, some of the sublayers

are present only in a part of the model area. Layers that are wedging out are difficult to model in MODFLOW as layers need to be defined over the entire model area. Thirdly, subdividing layer 3 in two layers consisting of the low permeable chalk at the bottom (Member of Zeven Wegen) and the coarser units at the top (other Members of Zeven Wegen, Maastricht and Houthem) was considered. However, the exact location of the boundary between these two units is not known for large parts of the model area as the available geological data does not include such a detailed subdivision of the Cretaceous deposits.

The hydrogeological properties of all subunits are taken into account in the calculation of equivalent properties for the model layers. This way, the effect of these subunits on e.g., the spatial variability of the hydraulic conductivity is modelled.

In Figure 60 and Figure 59, respectively an east-west and north-south profile through the model layers through approx. the centre of the model are shown. Note the strong variation in the base of the Cretaceous which is due to the relief in the Palaeozoic basement. Also note the presence of river valleys at the top which can incise the layers up to the Cretaceous.

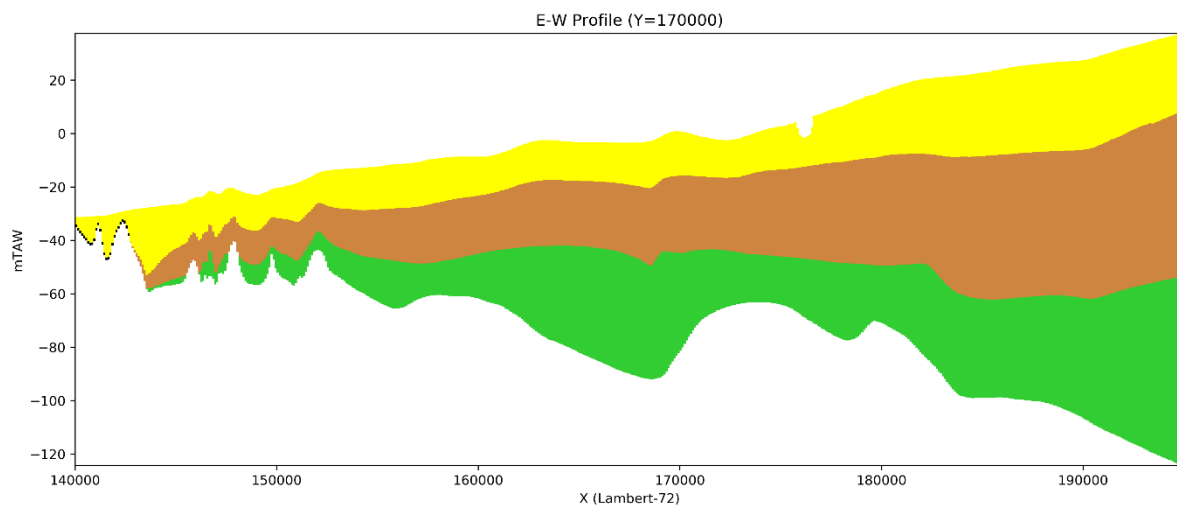


Figure 59: Cross-sections through the model layers: a N-S profile through $X=170,000$ (yellow = Grandglise; brown = Lincent; green = Cretaceous).

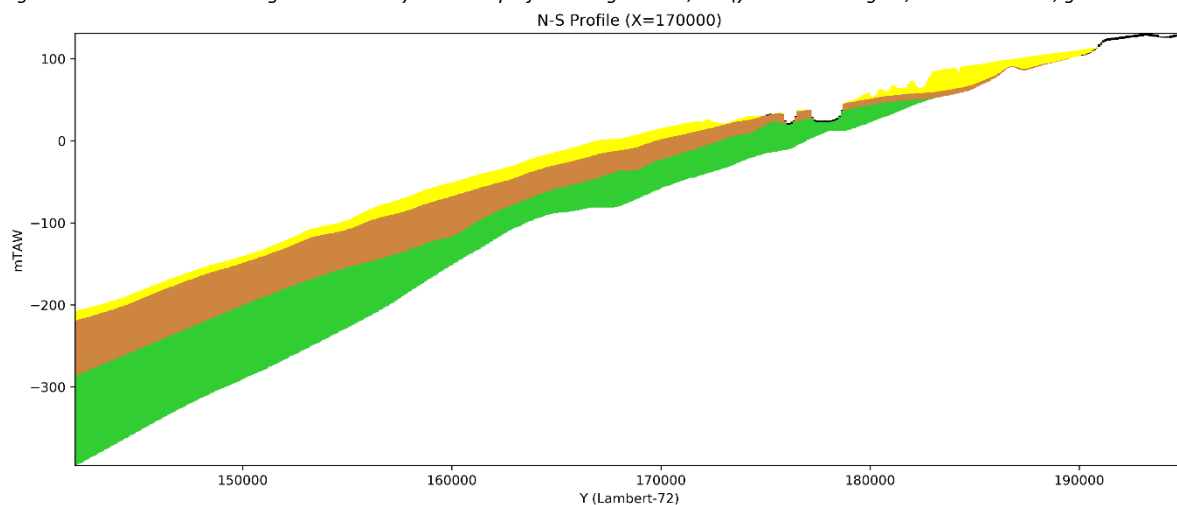


Figure 60: Cross-section through the model layers: E-W profile through $Y=170,000$ (yellow = Grandglise; brown = Lincent; green = Cretaceous).

4.3 Boundary conditions

The main boundary conditions are visualized in Figure 61.

Bottom boundary: The bottom boundary is a no-flow boundary due to the presence of the impermeable Palaeozoic basement.

Southern boundary: The modelled deposits of the Cretaceous and Paleocene wedge out against the impermeable Palaeozoic basement in the south. The purple area in Figure 61 are inactive cells, and thus the southern boundary is a no-flow boundary.

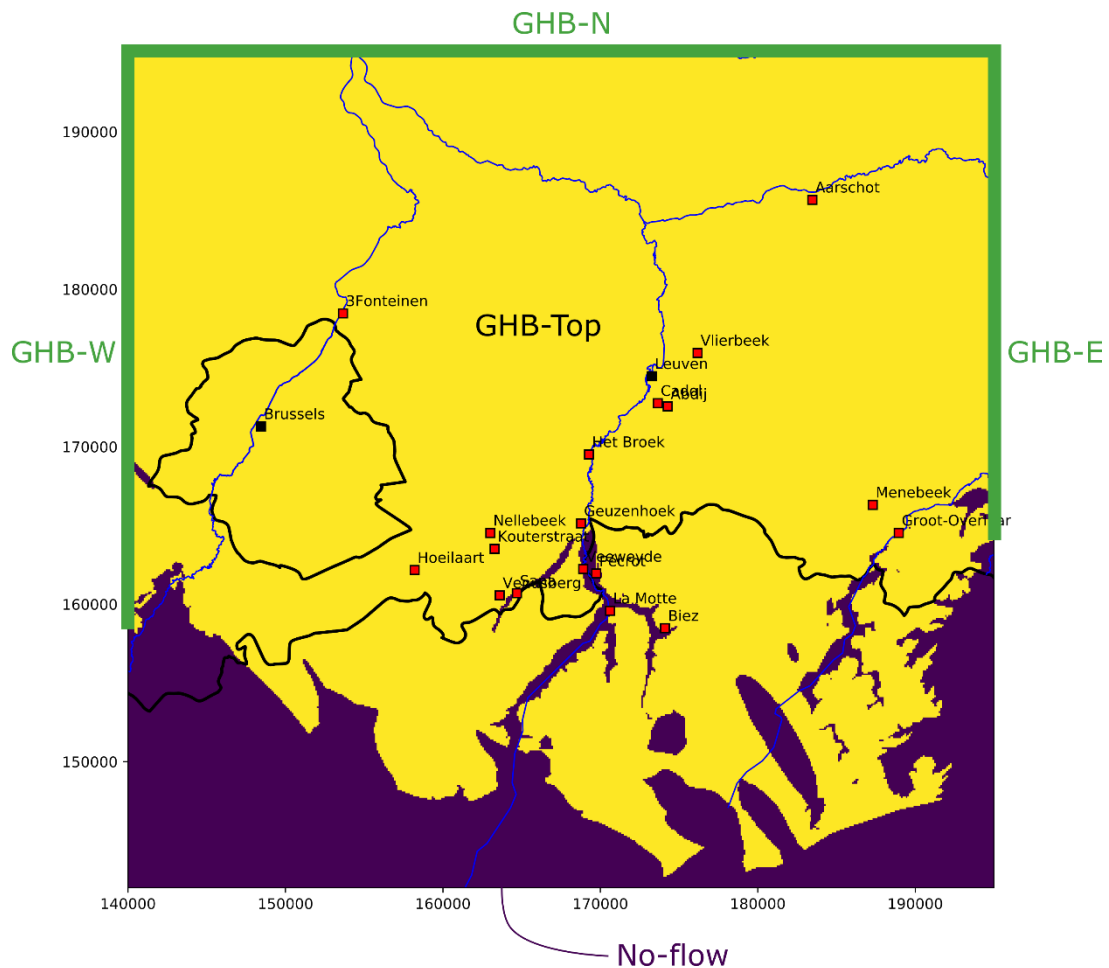


Figure 61: Overview of the different model boundary conditions: general-head boundaries in the W, N and E; general-head boundary at the top; and no-flow boundary in the south and bottom.

Western, northern and eastern boundary: The boundaries at the west, north and east in all three layers are modelled as general-head boundaries (GHB). This is a head-dependent flux boundary in which the flux going in/out of the model is proportional to the difference between the head in the boundary cells and a specified head at a certain distance D from this boundary (Figure 62). A conductance term [L^2/T] is calculated using

$$C = \frac{(K \cdot W \cdot L)}{D}$$

with K the average hydraulic conductivity of the subsurface material [L/T], W the thickness of the saturated aquifer perpendicular to the flow direction [L], L the boundary length perpendicular to the flow direction [L] and D the distance from the general-head boundary to the model boundary [L].

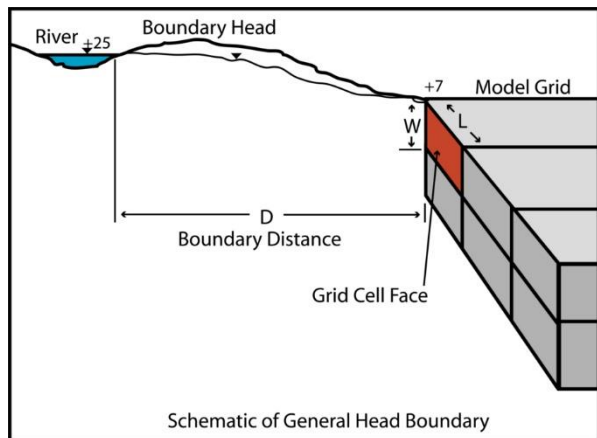


Figure 62: Illustration of the different parameters in the general-head boundary (GHB) package (Aquaveo).

The assigned heads are based on interpolation of observed head data. The western and northern GHB boundaries are assigned at a distance of 5km outside of the model area, while for the eastern GHB boundary this distance is 2 km. By assigning the GHB at a certain distance from the model boundary, we can avoid unnecessarily extending the model domain outwards but still having boundaries far enough from the focus area of the model. For the eastern boundary, the distance is limited to 2 km to avoid influence of other extraction sites more towards the east that affect the hydraulic heads at this boundary. Furthermore, a GHB is less restrictive than a conventional constant-head boundary. In the latter, the heads at the boundary cells are fixed, while with the GHB the heads can change and are dependent on the flux in/out of the model. By using the GHB, the regional effect of the extraction can be simulated more accurately.

Top boundary:

For the top boundary another GHB boundary is defined. We define different GHB zones for the top boundary, based on which deposits are present on the topmost modelled layer (Figure 63). In much of the model area, the modelled layers are confined by the Ieperian Aquitard, mainly consisting of the Formation of Kortrijk, a thick marine clay deposit (purple zone in Figure 63). However, in the southern part of the model area this clay layer can be absent and other deposits are present on top of the modelled layers: the Formation of Brussels, sandy permeable deposits (yellow in Figure 63) and Quaternary deposits in river valleys and in the SE of the model area (green).

Confined: In the confined area of the model, the GHB boundary is used to simulate the leakage through the clay deposits of the Formation of Kortrijk. Hydraulic head observations in the layers above this clay layer are analysed and a correlation between the hydraulic head and topography is derived. Based on this correlation, a spatially distributed hydraulic head map is generated, and these heads are used as a specified head in the GHB. The hydraulic conductivity used for the calculation of the GHB conductance is the vertical hydraulic conductivity of the clays of the Kortrijk Formation. The distance to the GHB is the distance between the bottom of the clay layer and half of the distance between the top of the clay layer and the topography.

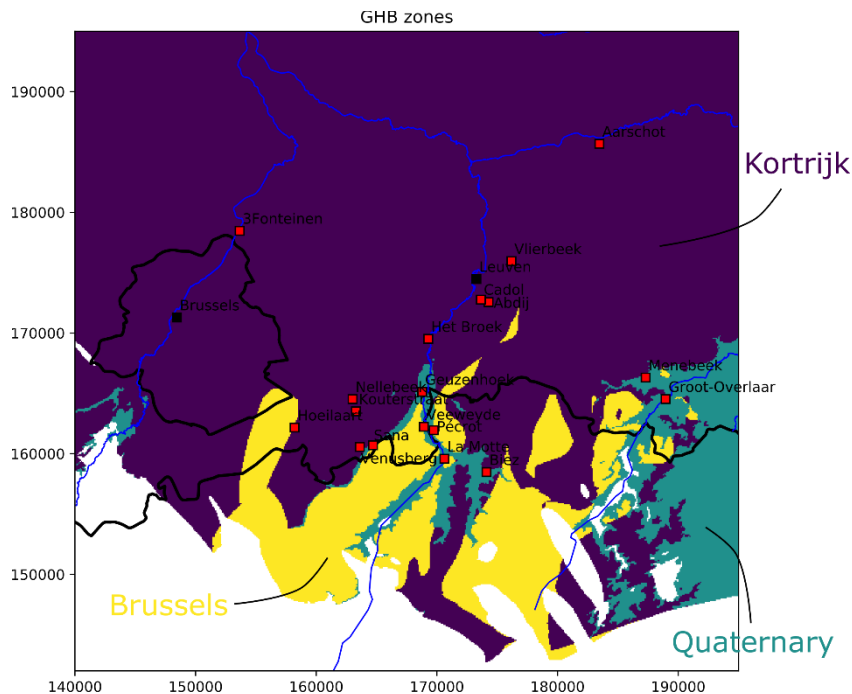


Figure 63: Overview of the three different GHB zones: Kortrijk, Brussels and Quaternary.

Unconfined: In the unconfined area of the model, the clay layer is absent and other deposits (e.g., Brussels Sands or Quaternary deposits) are present. The flow from these overlying deposits to/from the modelled layers is simulated using the GHB package. Two different zones are identified based on the type of deposits: the Brussels zone consisting of permeable sands and the Quaternary zone consisting of heterogeneous deposits. Similar to the confined zone, the specified head is based on a correlation between hydraulic heads and topography for head observations in the Brussels and Quaternary zones. Due to the difference in hydraulic properties of the two zones, two different hydraulic conductivity values are used in the calculation of the conductance. The distance used is the distance between the top of the modelled layers and the centre of the overlying layers. Note in Figure 63 that there is an extension of the Brussels zone to the southeast of Brussels, near Hoeilaart. In this area, a channel incised the Ieperian aquitard, resulting in local absence of this confining unit (as discussed in section 1).

Note that the way the flow from the overlying layers is simulated with the GHB package is an indirect way of simulating this flow. Another alternative that was explored initially was to use a combination of the Recharge and the Drain package to respectively simulate the groundwater recharge from the surface and the groundwater discharge through rivers and drains. However, as in the unconfined part deposits are present that are not explicitly modelled in the model, the flow from these overlying layers is not equal to the groundwater recharge. Furthermore, the drain elevation would then be higher than the top of the modelled layer, which is conceptually ambiguous. By using the GHB boundary, both the recharge from the overlying layers but also the discharge from the modelled layers towards rivers and drains is modelled together with one package, without the need to model these complex deposits and rivers/drains in the overlying layers. This has advantages but also some disadvantages: one cannot easily define future recharge scenarios, the hydraulic heads in the overlying layers need to be estimated and there is an infinite supply of water available from the top as lowering of the hydraulic head in overlying layers cannot be simulated.

Extraction wells:

The extraction wells in the model area can be subdivided into two groups: the extraction wells of De Watergroep used to produce drinking water and extraction wells from other companies or organisations. For the latter, the

permits are available online on DOV. The wells of De Watergroep are modelled with the Multi-Node Well 2 (MNW2) package, while the other wells are modelled with the WEL package.

Extraction wells De Watergroep: In the model area, De Watergroep produces water from the Cretaceous Aquifer from 14 extraction sites, mainly in the Dijle valley and the Leuven area (Figure 64). Furthermore, two extraction sites produce water from the 'tuffeau' of Lincent in the SE and one from the sands of Grandglise near Hoeilaart (Figure 64).

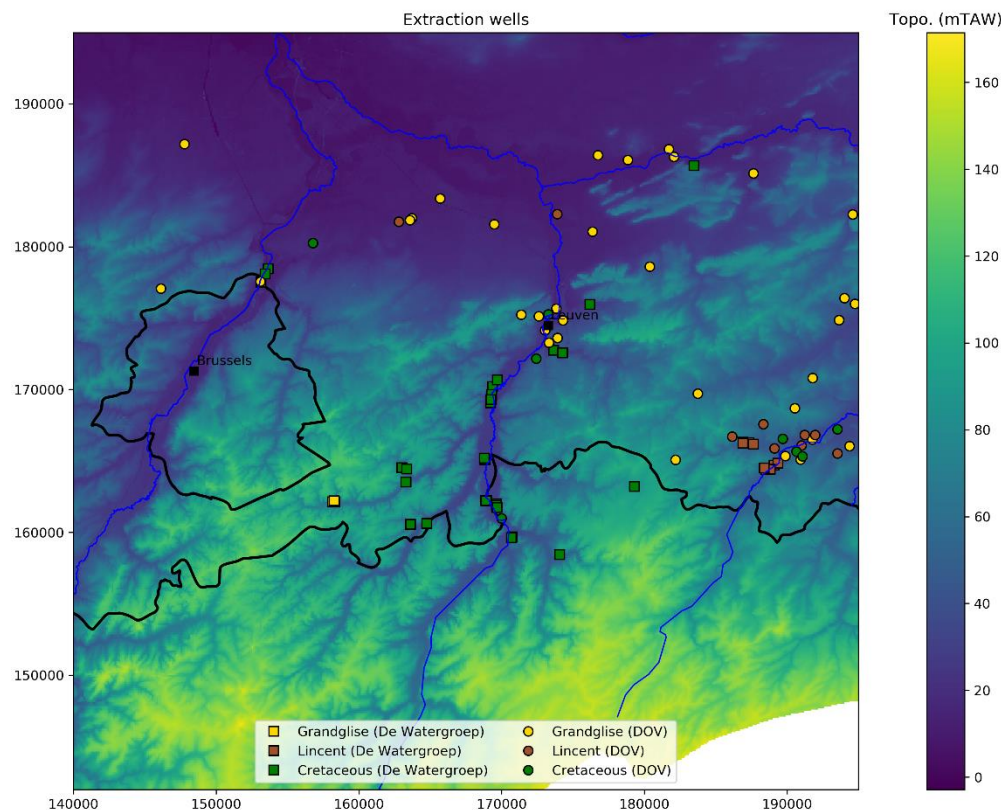


Figure 64: Overview of extraction wells of De Watergroep (squares) and DOV (circles) in the study area (period 2004-2020).

The wells of De Watergroep are modelled with the Multi-Node Well 2 (MNW2) package. This package allows wells to have a filter spanning multiple layers. However, the main advantage of this package is that also hydraulic heads in the extraction wells themselves are simulated. This is important as most hydraulic head data in the Cretaceous is coming from extraction wells. When the regular WEL package is used, only the head in the cell is simulated, which is the average head in the cell (Figure 65). However, the head in the extraction well itself can be significantly lower than the head in the cell, especially for large cell sizes and/or low hydraulic conductivities. For some extraction wells in the low permeable part of the Cretaceous around Leuven, this difference between head in the cell and head in the well can be up to several tens of meters. For the parameters of the MNW2 package, the loss-type 'Thiem' is used, the heads in the wells are corrected for partial penetration of the aquifer, and a well radius of 0.15m is assumed.

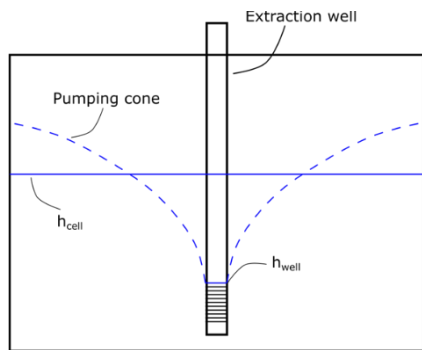


Figure 65: Illustration of the difference between the simulated head in the cell compared to head in the well.

Extraction wells DOV: The DOV wells are simulated using the WEL package. These wells are primarily located in the 'tuffeau' de Lincent area in the SE and in the Grandglise layer in e.g., the Leuven area (Figure 64). Only a couple of permits are present in the Cretaceous aquifer.

The DOV wells and the details on their permits are extracted from DOV by using the *pydov*⁷ library. In general, only permitted extraction rates are available from DOV. However, for most of the largest extraction wells actual reported rates are made available by the VMM. For the other wells, due to lack of information on the actual rates, initially the assumption is made that they extract at 80% of the total permitted rates.

4.4 Observation Data

Hydraulic head observations are used to assess the performance of the model. Both head observations from the wells of De Watergroep as head observations from other wells available through DOV are used (Figure 66). The latter are extracted from DOV using the *pydov* library. All observations are added to the model using the Head-Observation (HOB) package. This allows simulation of the head at the exact location of the observation well (interpolated based on heads in surrounding cells). For wells with filters that span multiple layers, the HOB package calculates an equivalent hydraulic head in the well.

Note that most of the observations in the Cretaceous are situated in the Dijle valley and the area around Leuven, close to the extraction sites. In other parts of the area, observations in the Cretaceous are limited. Observations in Lincent are mainly present in the 'tuffeau' zone in the east. Observations in Grandglise are also mainly available in the east. However, there are also some multi-level wells in the Dijle valley with filters in Grandglise, but these are not visible on Figure 66.

⁷ See <https://pydov.readthedocs.io/>

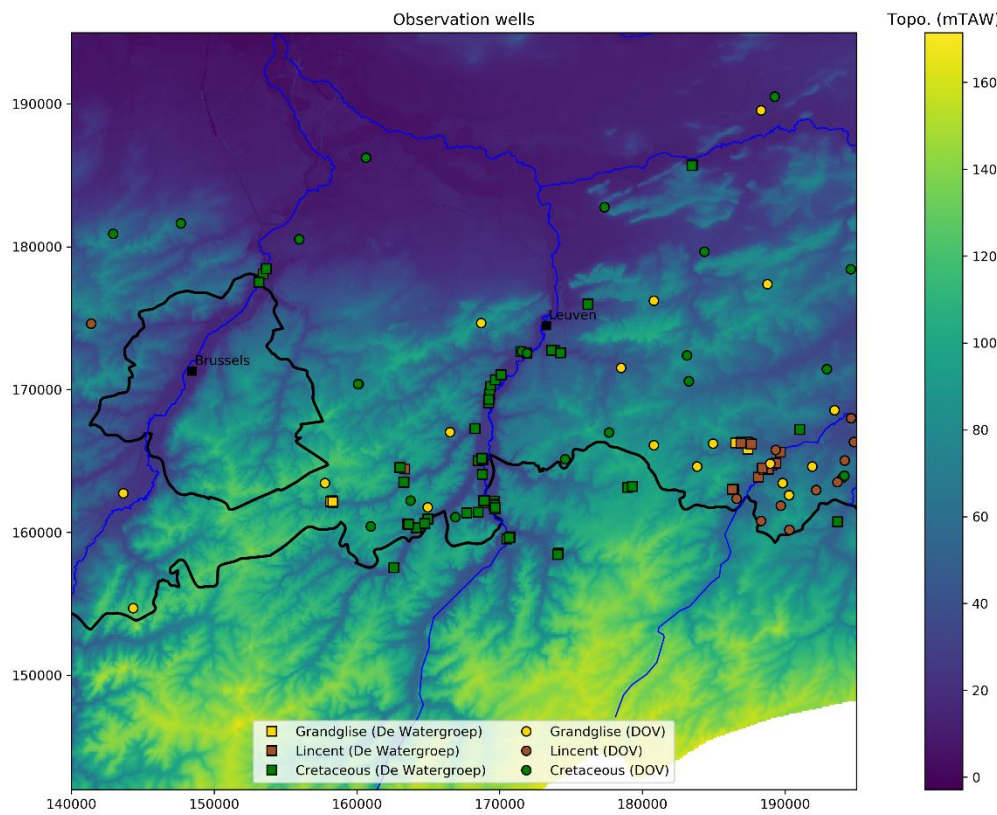


Figure 66: Overview of observation wells of De Watergroep (squares) and DOV (circles) in the study area (period 2004-2020).

4.5 Hydraulic conductivity

Initial hydraulic conductivity

In Table 22 an overview of the model layers, the sublayers, lithology and an initial estimate of horizontal conductivity (HK) is shown. These initial estimates are used as starting values in the groundwater model. The model is calibrated on these HK values.

Table 22: Overview of the three model layers, the sublayers, the type of lithology and an initial estimate of HK.

Layer	Unit	Lithology	Init. HK
Layer 1	Loksbergen/Dormaal	sands	3 m/d
	Grandgliste	fine sands	3 m/d
Layer 2	Halen	silt to clayey silt,	0.1 m/d
	Lincent	silicified limestone, fractured	Spatially variable
	Waterschei/Beselare	clay to sandy clay	0.001 m/d
	Maaseik/Gelinden	marls to marly clay	0.001 m/d
	Orp	clayey to marly fine sands	0.01 m/d
Layer 3	Houthem/Maastricht	coarse calcarenites	3 m/d
	Gulpen	chalk, marls and fine calcarenites	Spatially variable

Layer 1: Initial horizontal hydraulic conductivity (HK) for this layer is 3 m/d. This layer consists mainly of the fine sands of Grandglise. Estimated HK for Grandglise ranges from 1.1 to 3 m/d. The deposits of Loksbergen/Dormaal are only present in the east and consist of similar sandy deposits. Therefore, we opted for a homogeneous HK for this entire layer.

Layer 2: This layer consists of multiple sublayers of which several are only present in the north-eastern part of the model area. For the sands of Orp, consisting of very fine marly to clayey sands, a HK of 0.1 m/d is used. The sublayers of Gelinden & Maaseik are taken together due to the similar lithology (marls to marly clay). These deposits are characterized by very low to low permeability, and initially a HK of 0.001 m/d is used. The clay of Waterschei & Beselare is characterized by very low K. An initial estimate for HK of 0.001 m/d is used. The sublayer of Halen & Lincent can be subdivided into two zones: the 'tuffeau' of Lincent zone, consisting of porous and fractured silicified limestone in the SE (Tienen area) and the Halen zone consisting of silty to clayey silt deposits in the rest of the study area. For the latter, an initial HK of 0.1 m/d is estimated. For the Lincent zone, HK is dependent on the presence and degree of fracturing. Pumping tests performed on extraction wells in this area indicate an inverse correlation between depth and HK. A logarithmic regression is used to estimate HK based on depth (Figure 67). A cut-off depth of 50m is used: for all areas in the Lincent zone that are shallower than a depth of 50m the above correlation is used. For the deeper areas, the HK of Halen is used.

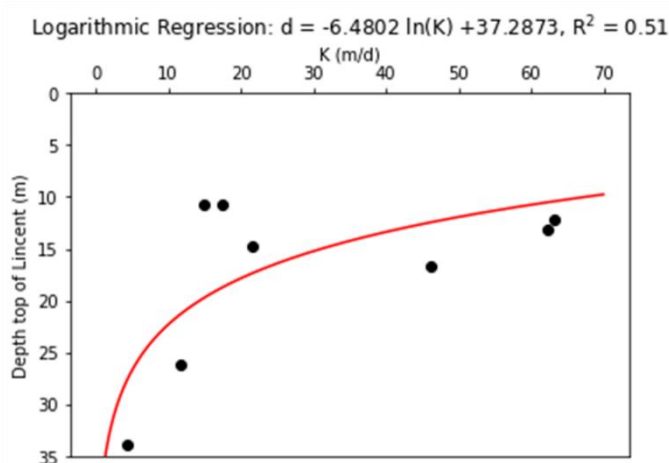


Figure 67: Logarithmic regression of the depth of the top of Lincent versus the horizontal hydraulic conductivity.

Layer 3: This layer mainly consists of the deposits of the Formation of Gulpen. In the northeast of the model, deposits of the Formations of Houthem and Maastricht are present on top of the Formation of Gulpen. The Houthem and Maastricht Formations consist of coarse-grained calcarenites. Based on pumping tests on extraction wells in these Formations more to the east in Limburg an initial HK of 3 m/d is used. As discussed in Section 2.3.3, the Formation of Gulpen is characterized by a strong spatial variability in hydraulic conductivity which is related to both differences in primary lithology of the different Members but also to the development of secondary permeability due to fractures. For the Formation of Gulpen, a correlation between depth and estimated hydraulic conductivity based on pumping tests (see Section 2.3.3) is used as a first estimate (Figure 21).

Equivalent hydraulic conductivity

For the hydraulic conductivity of the model layers, a thickness-weighted average of the hydraulic conductivity of the sublayers (Table 22) is calculated. For the equivalent horizontal hydraulic conductivity HK_{eq} (L/T), this becomes

$$HK_{eq} = \frac{\sum_{i=1}^n d_i HK_i}{d_{tot}}$$

with d_i the thickness of layer i [L], HK_i the horizontal hydraulic conductivity of layer i [L/T] and d_{tot} the total thickness of the model layer [L]. For a layer with two sublayers (Figure 68), this becomes

$$HK_{eq} = \frac{d_1 HK_1 + d_2 HK_2}{d_{tot}}$$



Figure 68: Example for the calculation of equivalent hydraulic conductivity for a model layer consisting of two sublayers.

For the vertical hydraulic conductivity initially a ratio of HK/VK of 10 is used. Similar to the horizontal hydraulic conductivity, an equivalent vertical hydraulic conductivity VK_{eq} [L/T] is calculated, but in this case a thickness-weighted harmonic mean is calculated

$$VK_{eq} = \frac{d_{tot}}{\sum_{i=1}^n \frac{d_i}{VK_i}}$$

with VK_i the vertical hydraulic conductivity of layer i [L/T]. As the harmonic mean strongly tends to the lowest value, the presence of low K sublayers will strongly affect the equivalent vertical conductivity. This is especially important for layer 2, in which the very low permeable sublayers have a strong effect on the equivalent conductivity.

4.6 Steady-state modelling

As a first step, a steady-state model is set-up which is representative for the year 2018. The year 2018 is chosen because this is the period with the most data available. This first steady-state model is set-up to improve our understanding of the hydrogeological system and to get a first estimate of the hydrogeological properties of the different layers. Based on this first steady-state model for the year 2018, a second steady-state model representative for the average condition in the period 2000 to 2004 is set-up. This model is set-up to generate initial hydraulic heads for the transient model that is set-up for the period 2004-2020. As not much data is available for the period 2000-2004, the resulting parameter values after calibration of the 2018 model are used.

4.6.1 Steady-state model 2018

Initial heads

Initial heads are based on interpolation of yearly average head observations for 2018 from wells in and surrounding the study area. As there are limited observations available for layer 2 (Lincent), the observations of layer 1 and layer 2 are merged, and one interpolation of heads is used for both layers. The initial head maps used in the model are shown in Figure 69. Note that the interpolation in the southern part (Walloon Region) is less reliable due to limited head observations in that area.

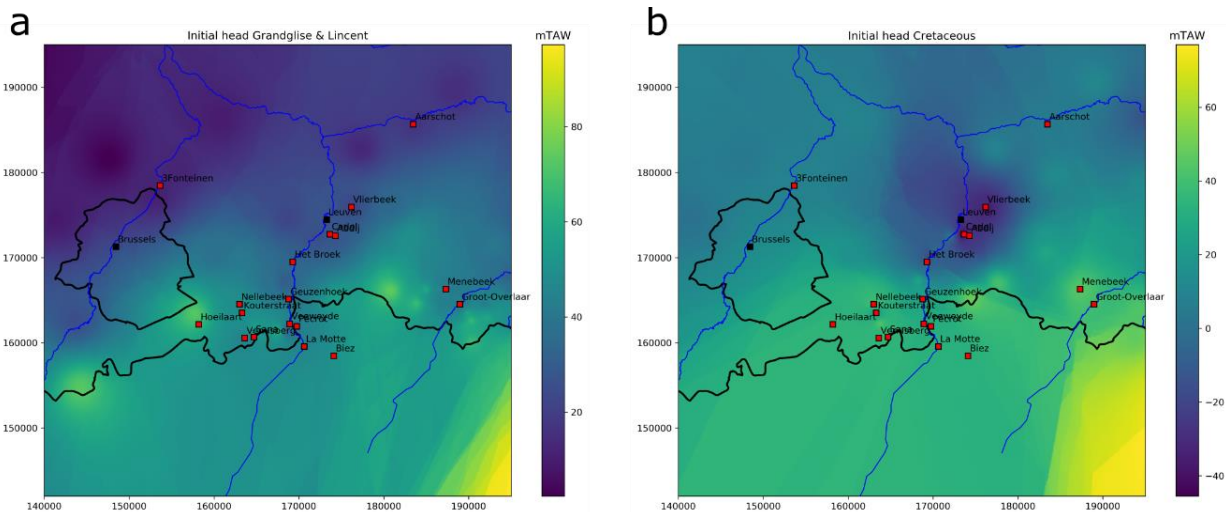


Figure 69: Maps of the initial heads based on interpolation of observed heads for the 2018 SS model for: (a) Grandglise and Lincent; and (b) the Cretaceous.

General-head boundary

West, north and east boundary

The GHB is used to simulate the flux in/out of the model through the west, north and east boundaries in all three layers. The west and north boundaries are located at 5km outside of the respective model boundaries, while the east boundary is located 2km outside of the east model boundary. The hydraulic conductivity of the respective layers is used in the calculation of the conductance. The heads assigned to these boundaries are based on interpolation of nearby head observations. As only limited observations are available near these boundaries, the heads at different points along the boundaries are estimated based on nearby observations and observed trends in the hydraulic gradient. The heads along the west, north and east boundaries are plotted in Figure 70. For the west and north boundary, heads are estimated at a couple of points along the boundary, and linear interpolation is performed to estimate the heads between these points. For the east boundary, the same thing is done for the northern part, but for the southern part also interpolation of observed heads is used (as enough measurements were available), and for the part in the Walloon region a correlation between head and topography is used. Note the effect of the topography in Figure 70c, which clearly shows the location of river valleys.

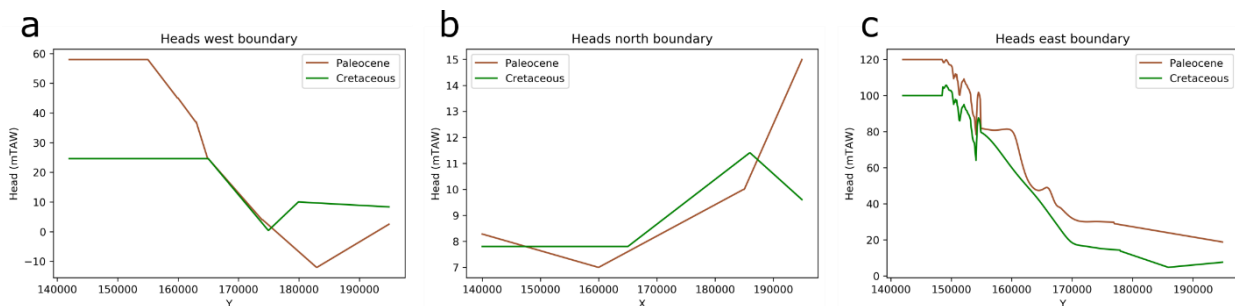


Figure 70: Specified heads used in the GHB package for the 2018 SS model for: (a) the west boundary; (b) the north boundary; and (c) the east boundary.

Top boundary

As previously explained in Boundary conditions 4.3, the general-head boundary is used to simulate both the leakage through the confining clay layer overlying most of the model area as well as the flow from the overlying layers in the unconfined part of the model area which are not explicitly modelled. The different zones defined for the GHB package are shown in Figure 63.

For the confined zone, the Kortrijk zone, yearly average head observations from 848 wells in the layers above the Formation of Kortrijk are analysed. These observation wells mainly have filters in the Brussel Sands and the Quaternary deposits. Based on a linear regression of observed hydraulic head versus topography (Figure 71a), the hydraulic head is estimated in each cell of the Kortrijk zone.

In the unconfined part of the model area, two zones are identified in which respectively the Brussels Sands and the Quaternary deposits are overlying the modelled layers. For the Brussels zone only a limited number of observations was available (17 observation wells), while for the Quaternary zone data from 61 observation wells is used. One regression of observed hydraulic head versus topography is derived for both the Brussels and Quaternary zone together (Figure 71b).

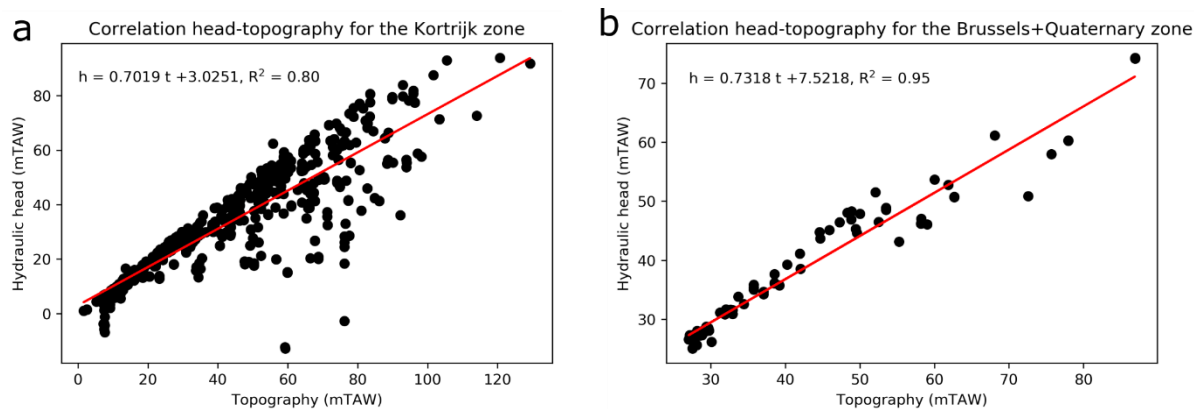


Figure 71: Correlation between observed hydraulic head and topography for the 2018 SS model for: (a) the Kortrijk zone; and (b) the Brussels and Quaternary zone.

Based on these two regressions of hydraulic head versus topography, the hydraulic head in each cell of the model area is estimated (Figure 72). This head is used as a specified head in the general-head boundary package.

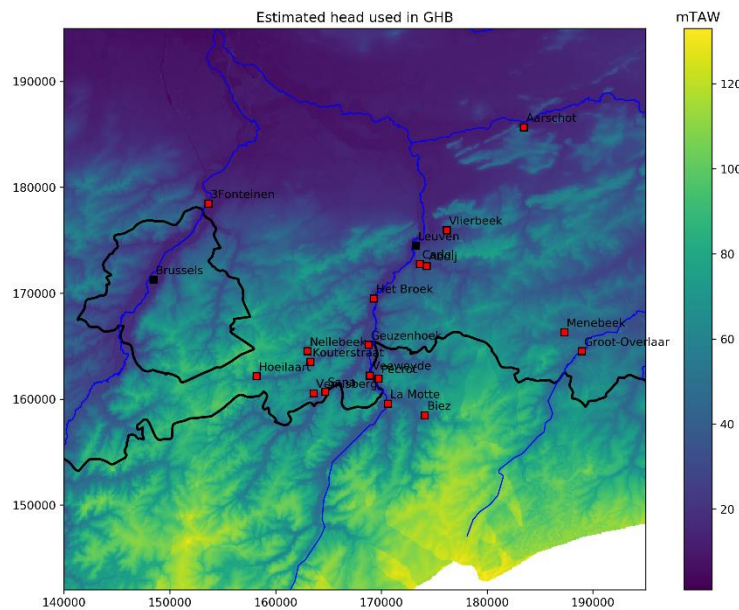


Figure 72: Estimated hydraulic head map based on correlations for the Kortrijk and Brussels & Quaternary zones which is used as specified head in the GHB package for the 2018 SS model.

Extraction wells

Extraction wells De Watergroep

The extraction wells of De Watergroep are modelled using the MNW2 package. The actual extraction rates for the year 2018 are used. An overview of all extraction wells and their extraction rates for 2018 is shown in Table I. 8. In total, 38 extraction wells are modelled, 25 of which have a filter in the Cretaceous aquifer, 9 in the 'tuffeau' of Lincent and 4 in the Grandglise aquifer. Note that there are a couple of wells with a filter spanning multiple layers. The total extraction rate of these wells in 2018 is 43,984 m³/d, of which 38,140 m³/d (87%) in the Cretaceous aquifer, 4,773 m³/d (11%) in the 'tuffeau' of Lincent and 1,071 m³/d (2%) in the Grandglise aquifer (Figure 73).

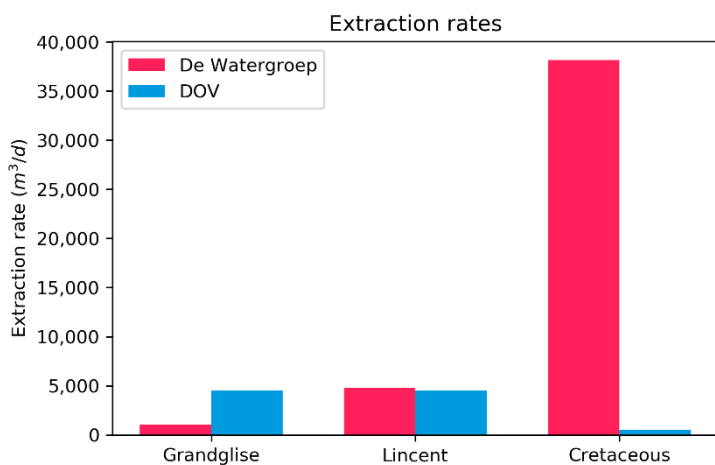


Figure 73: Overview of the extraction rates for the wells of De Watergroep and the DOV wells for the three model layers for the 2018 SS model.

The extraction wells in the Cretaceous are mainly situated in the Dijle valley (and valleys of its tributaries) and the Leuven area (Figure 74). The extraction wells in the 'tuffeau' of Lincent are situated in the Tienen area. There is only one extraction site in the Grandglise layer, the site of Hoeilaart.

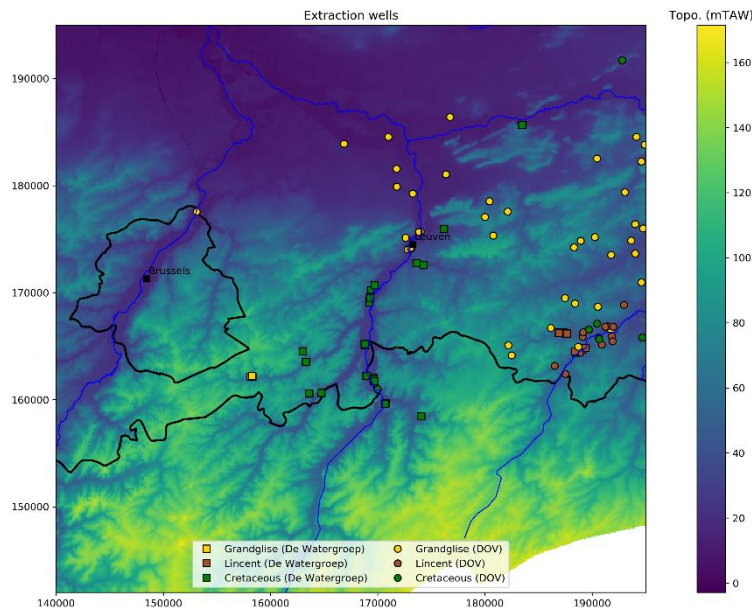


Figure 74: Overview of extraction wells of De Watergroep (squares) and DOV (circles) in the study area (year 2018).

Extraction wells DOV

The extraction wells of DOV are modelled with the Well package. For most of the large extractions, reported extraction rates are made available by the VMM. For the other extractions, only information on the permits is available. In this case, initially 80% of the permitted rates are used as extraction rates in the model. Only wells with a permit $>10 \text{ m}^3/\text{d}$ are inserted in the model. An overview of all extraction wells and their extraction rates for 2018 is shown in Table I. 9 and Table I. 10.

In total, 66 extraction wells are modelled, 44 of which have a filter in Grandglise, 15 in Lincent and 7 in the Cretaceous. The total extraction rate of these wells for 2018 is $7,142 \text{ m}^3/\text{d}$, of which $2,493 \text{ m}^3/\text{d}$ (35%) in Grandglise, $4,098 \text{ m}^3/\text{d}$ (57%) in the 'tuffeau' of Lincent and $550 \text{ m}^3/\text{d}$ (8%) in the Cretaceous aquifer (Figure 73). For 15 of the largest wells actual extracted rates are available, for a total of $6,154 \text{ m}^3/\text{d}$. Most of the extraction is from the Lincent layer ($3,904 \text{ m}^3/\text{d}$), mainly in the Tienen area (Figure 74). The extraction in Grandglise accounts for $1800 \text{ m}^3/\text{d}$, mainly in the Leuven area. The extraction in the Cretaceous is limited, and accounts for $450 \text{ m}^3/\text{d}$. The wells for which only permits are available only account for $988 \text{ m}^3/\text{d}$, of which $693 \text{ m}^3/\text{d}$ in Grandglise, $195 \text{ m}^3/\text{d}$ in Lincent and $100 \text{ m}^3/\text{d}$ in the Cretaceous.

Observation wells

The observation wells are modelled with the HOB package. The annual average hydraulic head for 2018 is used as observed head. In total, 168 observation wells are implemented of which 44 are extraction wells from De Watergroep, 51 are observation wells of De Watergroep and 73 are observation wells from DOV (Table I. 11). The distribution of the wells over the layers is as follows: 61 wells in Grandglise, 35 in Lincent and 72 in the Cretaceous. Note that several wells have filters spanning over multiple layers (Table I. 11). For these wells, an equivalent head is calculated based on a thickness-weighted average of simulated head in those layers. Most of the observations in the

Cretaceous are from extraction sites and observations wells close by (Figure 75). The observations in Lincent are mostly situated in the Tienen area, in the 'tuffeau' zone.

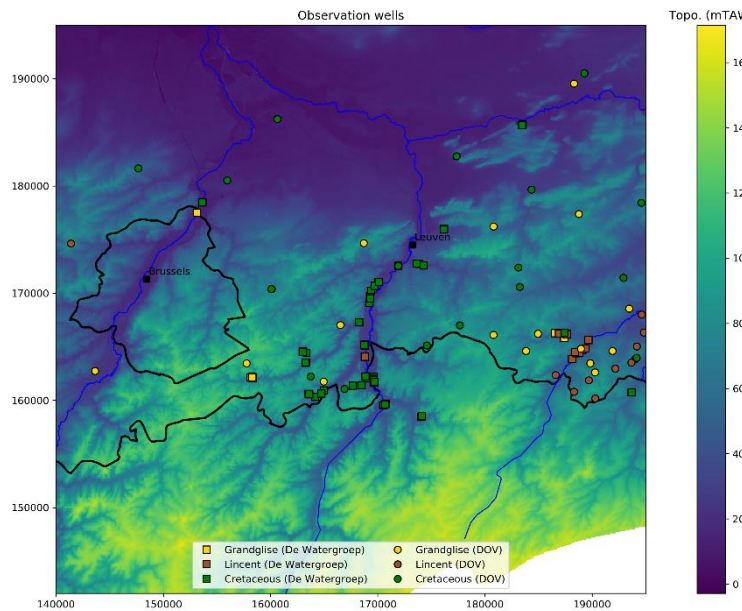


Figure 75: Overview of observation wells of De Watergroep and from DOV for the 2018 SS model⁸.

Solver

Initially, the PCG solver was used with a maximum of 100 outer and 50 inner iterations, and a head change and residual criterion for convergence of $1E^{-2}$. This resulted in a converging model that took approx. 1 minute to run. Different solvers (PCG, PCGN and GMG) were explored and their parameters (relaxation and dampening) were varied to optimize runtime. Finally, the GMG solver is used with a maximum of 50 outer and 50 inner iterations, a head change and residual criterion for convergence of $1E-2$, a relaxation parameter of 1 and a dampening parameter of 0.95. This resulted in a significant decrease of runtime from 1 minute to approx. 10 seconds.

Calibration

First, a sensitivity analysis of the parameters was performed by varying the parameters over a certain range and looking at the effect on the model results. This showed that the main parameters that influence the results are the HK of the Cretaceous, the resistance of the Lincent layer, the HK of the 'tuffeau' of Lincent zone and the conductance used in the GHB in the unconfined part of the model area. Based on these results, a first manual calibration of the model was performed. We opted for a manual calibration so that we would get improved insights in the important parameters and areas in the model. During this calibration, errors and incompleteness in the input data were identified. Furthermore, during the calibration the conceptualization of the model was continuously improved.

The simulated heads are visualized in Figure 76. Note the effect of the general-head boundary in the south in all layers. The simulated heads are strongly dependent on the specified heads in the GHB, which correlate with the topography. Also note the effect of the Brusselian channel which locally eroded the Formation of Kortrijk to the SE of Brussels. This results in a significantly higher head in all three layers. In the Cretaceous, the effect of the extraction is clearly visible in the Leuven area and in the area of het Broek. The effect of the extraction wells more towards the

⁸ Note that for multi-level piezometers, only the marker of the last layer is plotted. This is the reason that there don't seem to be many wells with filter in Grandgilde. However, there are quite some multi-level piezometers with filter in both Grandgilde and the Cretaceous in the Dijle valley.

southern part of the Dijle valley is less clearly visible. Also note the effect of the extraction of Het Broek on the heads in the overlying layers of Lincent and Grandglise⁹.

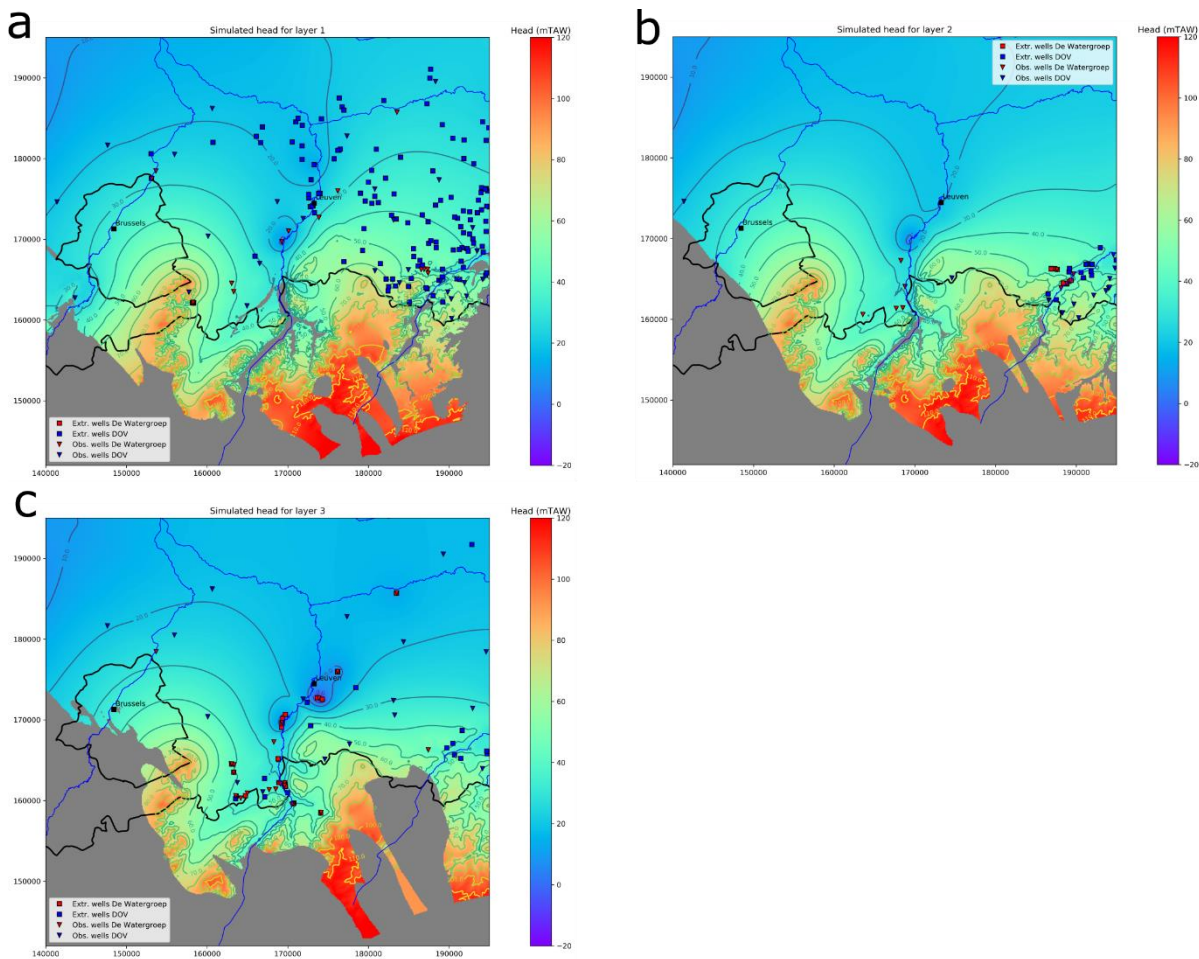


Figure 76: Map of simulated hydraulic heads for the 2018 SS model for: (a) Grandglise; (b) Lincent; and (c) the Cretaceous.

The scatterplot of simulated versus observed head and other diagnostic plots are shown in Figure 77. The model can reproduce the observed heads relatively well over the entire range of heads (-60 to +80 mTAW). A R^2 of 0.87 is obtained, a mean error (ME) of -1.43m, a mean absolute error (MAE) of 5.86m and a RMSE of 8.18m. However, still significant residuals are obtained for several observation wells. In Figure 78, the model residuals are visualized. In Grandglise, there is a strong overestimation of heads in the Vilvoorde area and in the northern part of the model area. In the Dijle valley, there is an underestimation. In the Cretaceous, a similar overestimation is visible in the Vilvoorde area, but also in the Leuven area and in the Dijle valley. The largest underestimation in the Cretaceous is for the sites of Cadol and Abdij. Due to the strong sensitivity of the model results to HK of the Cretaceous in this area, which is very low, a small change in HK can result in a difference of simulated heads of meters to tens of meters. In general, observations in extraction wells are also inherently more uncertain, due to effects like well losses and clogging. The overestimation in the Vilvoorde area and to the north of Leuven is related to historical extractions in these regions. As explained in section 3.3, the groundwater system is still recovering from over-extraction in these areas. As the system is not in equilibrium, a steady-state model will not be able to reproduce this. The underestimation of heads in Grandglise in the Dijle valley indicates that the resistance of the Lincent layer is underestimated in the model (this is improved in the transient model).

⁹ In reality, this effect is not so large. This is improved in the transient model.

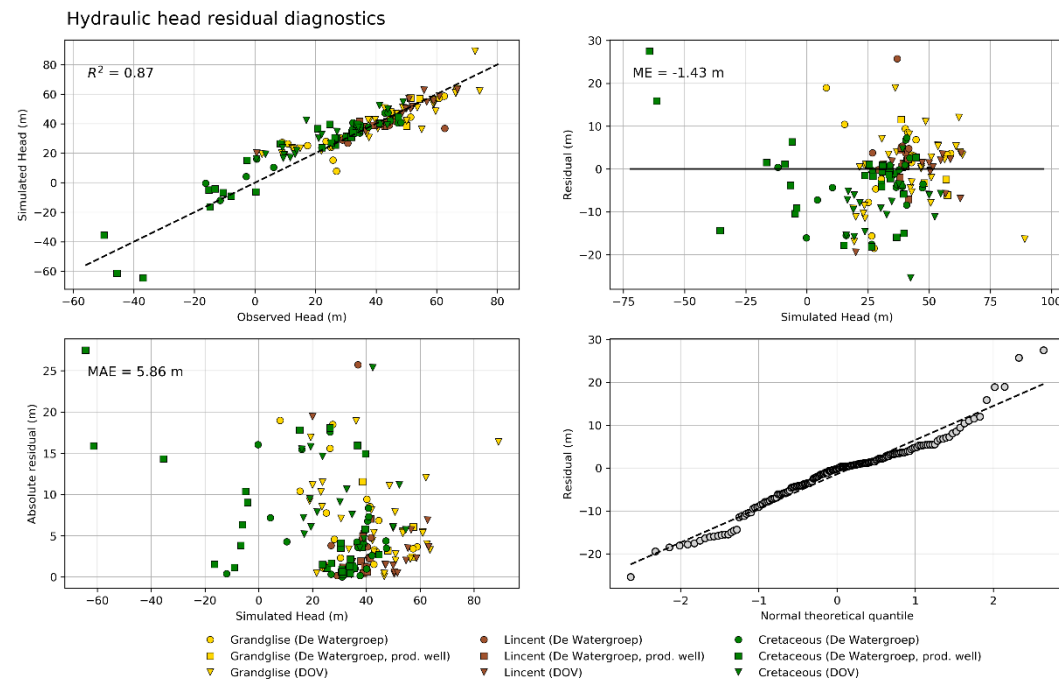


Figure 77: Overview of hydraulic head residual diagnostics plots for the 2018 SS model.

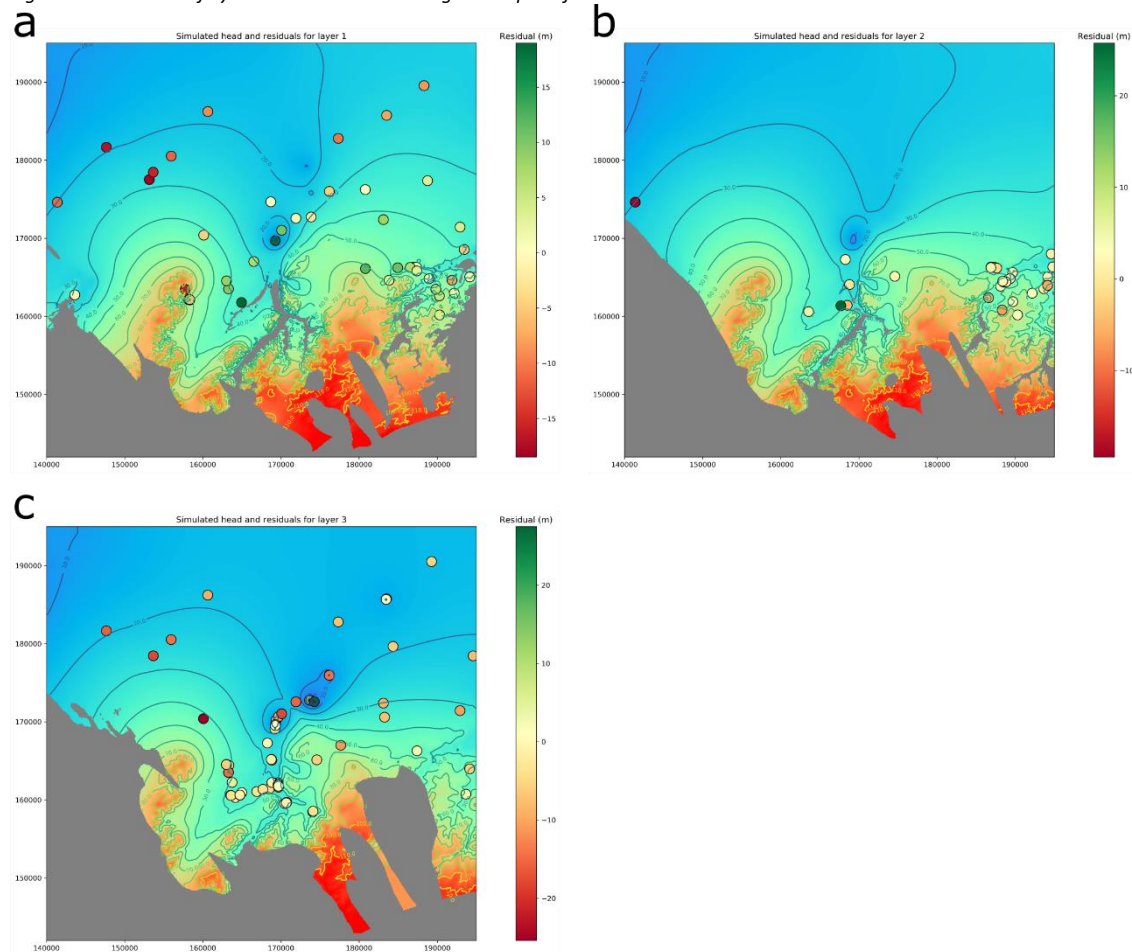


Figure 78: Map of hydraulic head residuals for the SS 2018 model for: (a) Grandglise; (b) Lincent; and (c) the Cretaceous.

4.6.2 Steady-state model 2000-2004

A transient model for the period 2004-2020 will be set up. However, accurate initial heads are needed as starting heads for this model. Therefore, a steady-state model is set up that is representative for the average conditions for the five years before the first timestep of the transient model, the period 2000-2004. This steady-state model is based on the steady-state model of 2018, but the input data and observations representative for the 2000-2004 period are used.

Initial heads

The initial heads for the 2000-2004 steady-state model are based on interpolation of average head observations for the 2000-2004 period from wells in and surrounding the study area. As there are limited observations available for layer 2 (Lincent), the observations of layer 1 and layer 2 are merged, and one interpolation of heads is used for both layers. In general, a lot fewer head observations are available for this period compared to 2018 (Figure 79).

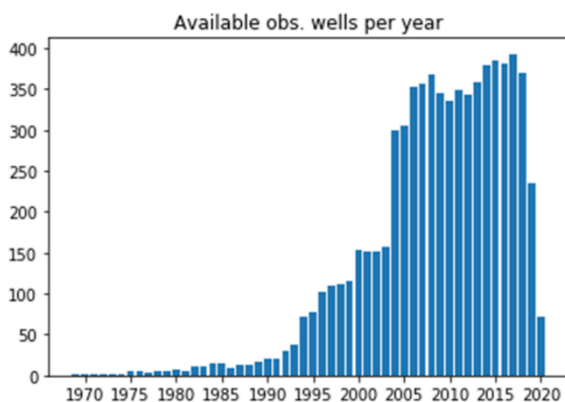


Figure 79: Overview of available observation well data in the Brabant Model area over time.

General-head boundary

West, north and east boundary

The GHB for the west, north and east boundary is set-up similar to the one for the 2018 steady-state model. The heads assigned to these boundaries are based on interpolation of nearby head observations. As only limited observations are available near these boundaries, the heads at different points along the boundaries are estimated based on nearby observations and observed trends in the hydraulic gradient. The heads along the west, north and east boundaries are plotted in Figure 80. For the west and north boundary, heads are estimated at a couple of points along the boundary, and linear interpolation is performed to estimate the heads between these points. For the east boundary, the same thing is done for the northern part, but for the southern part also interpolation of observed heads is used (as enough measurements were available), and for the part in the Walloon region, a correlation between head and topography is used. Note the effect of the topography in Figure 80c, which clearly shows the location of river valleys.

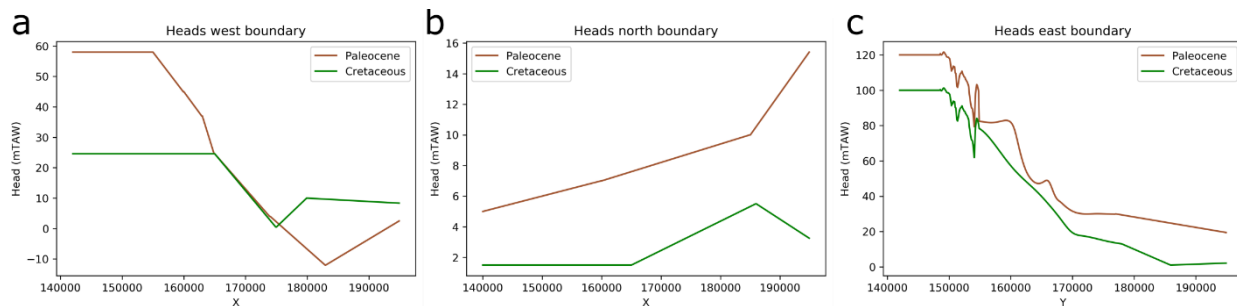


Figure 80: Specified heads used in the GHB package for the 2000-2004 SS model for: (a) the west boundary; (b) the north boundary; and (c) the east boundary.

Top boundary

For the confined zone, the Kortrijk zone, yearly average head observations from 907 wells in the layers above the Formation of Kortrijk are analysed. These observation wells mainly have filters in the Brussel Sands and the Quaternary deposits. Based on a linear regression of observed hydraulic head versus topography (Figure 81a), the hydraulic head is estimated in each cell of the Kortrijk zone. In the unconfined part of the model area, two zones are identified in which respectively the Brussels Sands and the Quaternary deposits are overlying the modelled layers. For the Brussels zone only a limited number of observations was available (24 observation wells), while for the Quaternary zone data from 90 observation wells is used. One regression of observed hydraulic head versus topography is derived for both the Brussels and Quaternary zone together (Figure 81b).

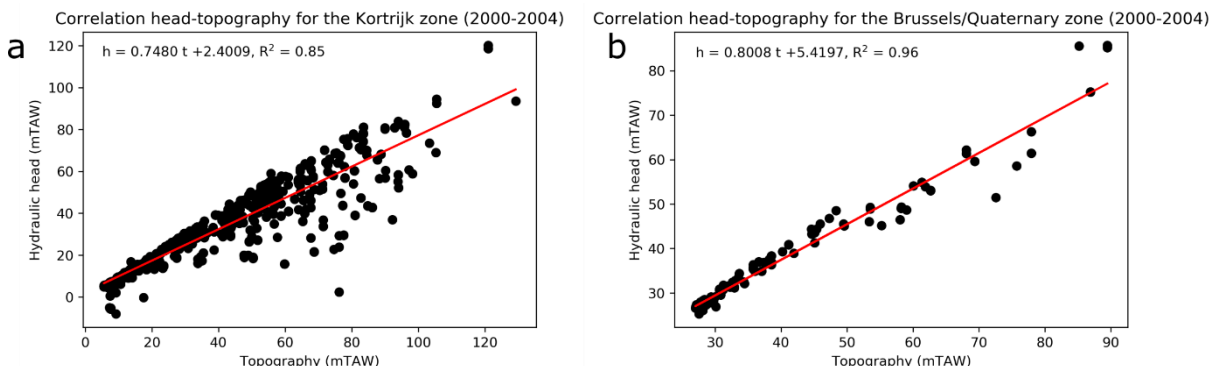


Figure 81: Correlation between observed hydraulic head and topography for the 2000-2004 SS model for: (a) the Kortrijk zone; and (b) the Brussels and Quaternary zone.

Based on these two regressions of hydraulic head versus topography, the hydraulic head in each cell of the model area is estimated (Figure 82). This head is used as a specified head in the general-head boundary package.

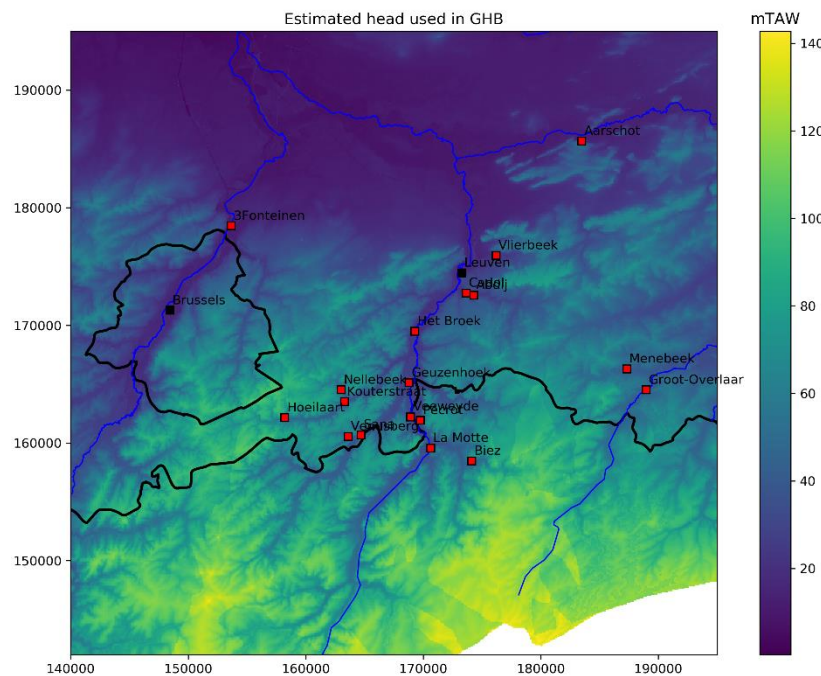


Figure 82: Map of the estimated hydraulic head based on the correlations between head and topography for the different zones for the 2000-2004 SS model.

Extraction wells

Extraction wells De Watergroep

The actual extraction rates averaged over the period 2000-2004 are used. An overview of all extraction wells and their extraction rates for the period 2000-2004 is shown in Table I. 12. In total, 30 extraction wells are modelled, 23 of which have a filter in the Cretaceous aquifer and 7 in the 'tuffeau' of Lincent. In this period, there was no extraction from Grandglise. The total extraction rate of these wells is 39,862 m³/d, of which 35,342 m³/d (89%) in the Cretaceous aquifer and 4520 m³/d (11%) in the 'tuffeau' of Lincent (Figure 83).

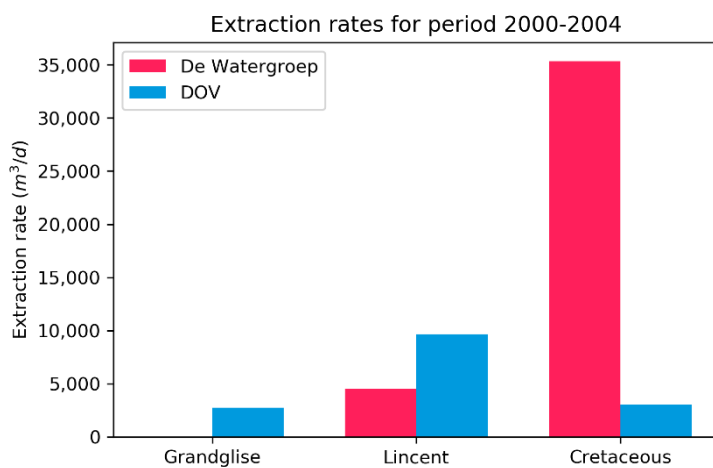


Figure 83: Overview of the extraction rates for the wells of De Watergroep and the DOV wells for the three model layers (average for the period 2000-2004).

The extraction wells in the Cretaceous are mainly situated in the Dijle valley (and valleys of its tributaries) and the Leuven area (Figure 84). The extraction wells in the ‘tuffeau’ of Lincent are situated in the Tienen area.

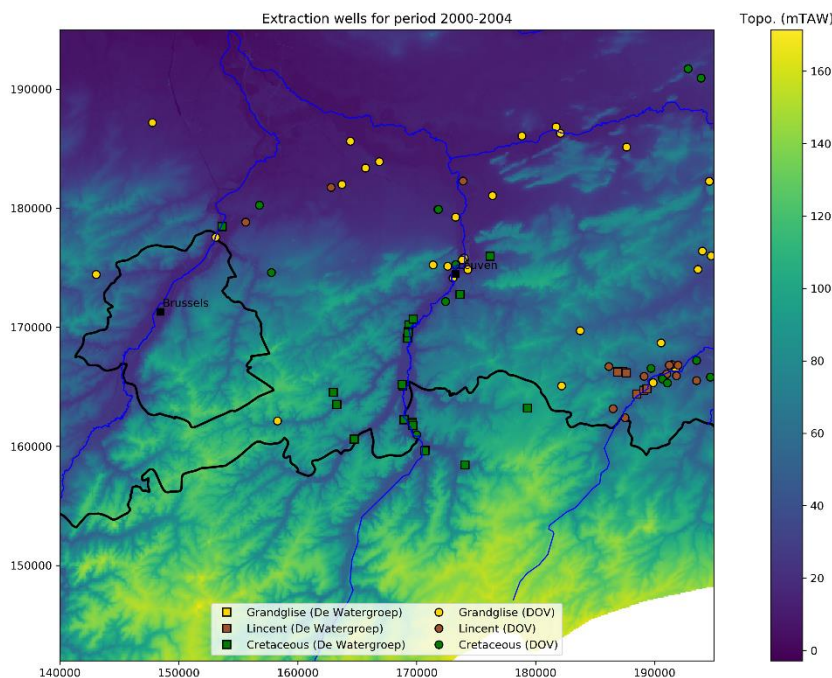


Figure 84: Overview of extraction wells of De Watergroep (squares) and DOV (circles) in the study area (year 2000-2004).

Extraction wells DOV

The extraction wells of DOV are modelled with the Well package. For most of the large extractions, reported extraction rates are made available by the VMM. For the other extractions, only information on the permits is available. In this case, initially 80% of the permitted rates are used as extraction rates in the model. Only wells with a permit $>10 \text{ m}^3/\text{d}$ are inserted in the model. An overview of all extraction wells and their extraction rates for 2000-2004 is shown in Table I. 13 and Table I. 14.

In total, 73 extraction wells are modelled, 45 of which have a filter in Grandglise, 15 in Lincent and 13 in the Cretaceous. The total extraction rate of these wells is $19,379 \text{ m}^3/\text{d}$, of which $3,531 \text{ m}^3/\text{d}$ (18%) in Grandglise, $12,088 \text{ m}^3/\text{d}$ (62%) in the ‘tuffeau’ of Lincent and $3,760 \text{ m}^3/\text{d}$ (19%) in the Cretaceous aquifer (Figure 83). For 19 of the largest wells actual extracted rates are available, for a total of $14,889 \text{ m}^3/\text{d}$. Most of the extraction comes from the Lincent layer ($11,095 \text{ m}^3/\text{d}$), mainly in the Tienen area (Figure 84). The extraction in Grandglise accounts for $2,907 \text{ m}^3/\text{d}$, mainly in the Leuven area. The extraction in the Cretaceous is limited, and accounts for $887 \text{ m}^3/\text{d}$. The wells for which only permits are available only account for $4,490 \text{ m}^3/\text{d}$, of which $624 \text{ m}^3/\text{d}$ in Grandglise, $993 \text{ m}^3/\text{d}$ in Lincent and $2,873 \text{ m}^3/\text{d}$ in the Cretaceous.

Observation wells

The observation wells are modelled with the HOB package. The annual average hydraulic head is used as observed head. In total, 124 observation wells are implemented of which 47 are extraction wells from De Watergroep, 27 are observation wells of De Watergroep and 50 are observation wells from DOV (Table I. 15). The distribution of the wells over the layers is as follows: 33 wells in Grandglise, 32 in Lincent and 59 in the Cretaceous. Note that several wells have filters spanning over multiple layers (Table I. 15). For these wells, an equivalent head is calculated based on a thickness-weighted average of simulated head in those layers. Most of the observations in the Cretaceous come from

extraction sites and observations wells close by (Figure 85). The observations in Lincent are mostly situated in the Tienen area, in the 'tuffeau' zone. Note that compared to the situation in 2018 (Figure 75), a lot less observation wells are available.

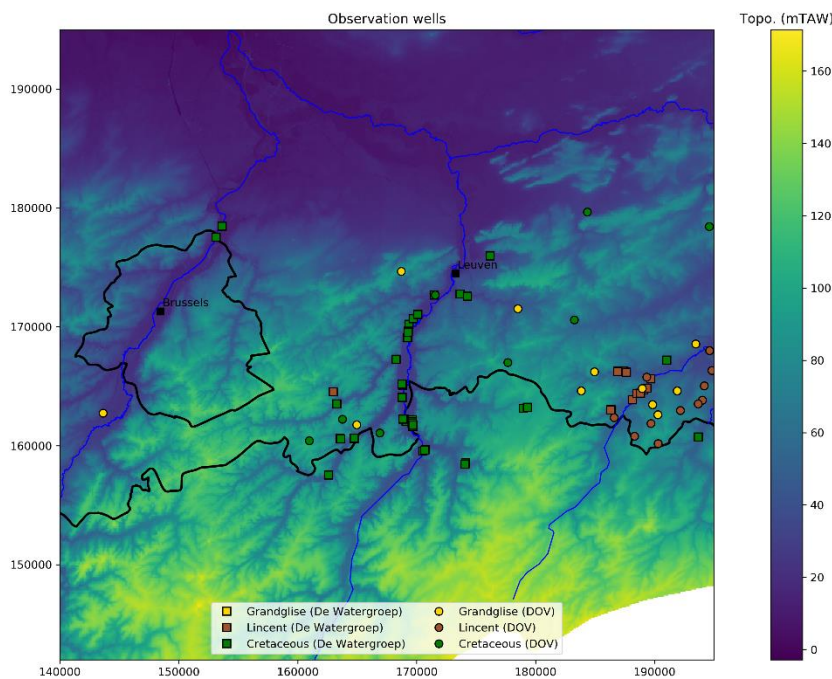


Figure 85: Overview of observation wells of De Watergroep and from DOV for the 2000-2004 SS model

Solver

The GMG solver is used with a maximum of 50 outer and 50 inner iterations, a head change and residual criterion for convergence of 1E-2, a relaxation parameter of 1 and a dampening parameter of 0.95. This resulted in a runtime of approx. 10 seconds.

Calibration

The simulated heads are visualized in Figure 86. Note the large effect of the extraction of Cargill France on the simulated heads in the Cretaceous. In the period 2000-2004, this site extracted at a rate of 804 m³/d. The effects of the extraction sites of De Watergroep near Leuven and Korbeek-Dijle Het Broek are also clearly visible. Also note the effect of the latter on the heads in the overlying layers of Lincent and Grandglise. The scatterplot of simulated versus observed head and other diagnostic plots are shown in Figure 87. The model can reproduce the observed heads relatively ok. A R² of 0.81 is obtained, a mean error (ME) of -2.59m, a mean absolute error (MAE) of 5.53m and a RMSE of 9.61m. However, still significant residuals are obtained for several observation wells, mainly in and near the extraction wells in the Leuven and Vilvoorde areas. Note the large residuals for the sites of Vlierbeek and Cadol.

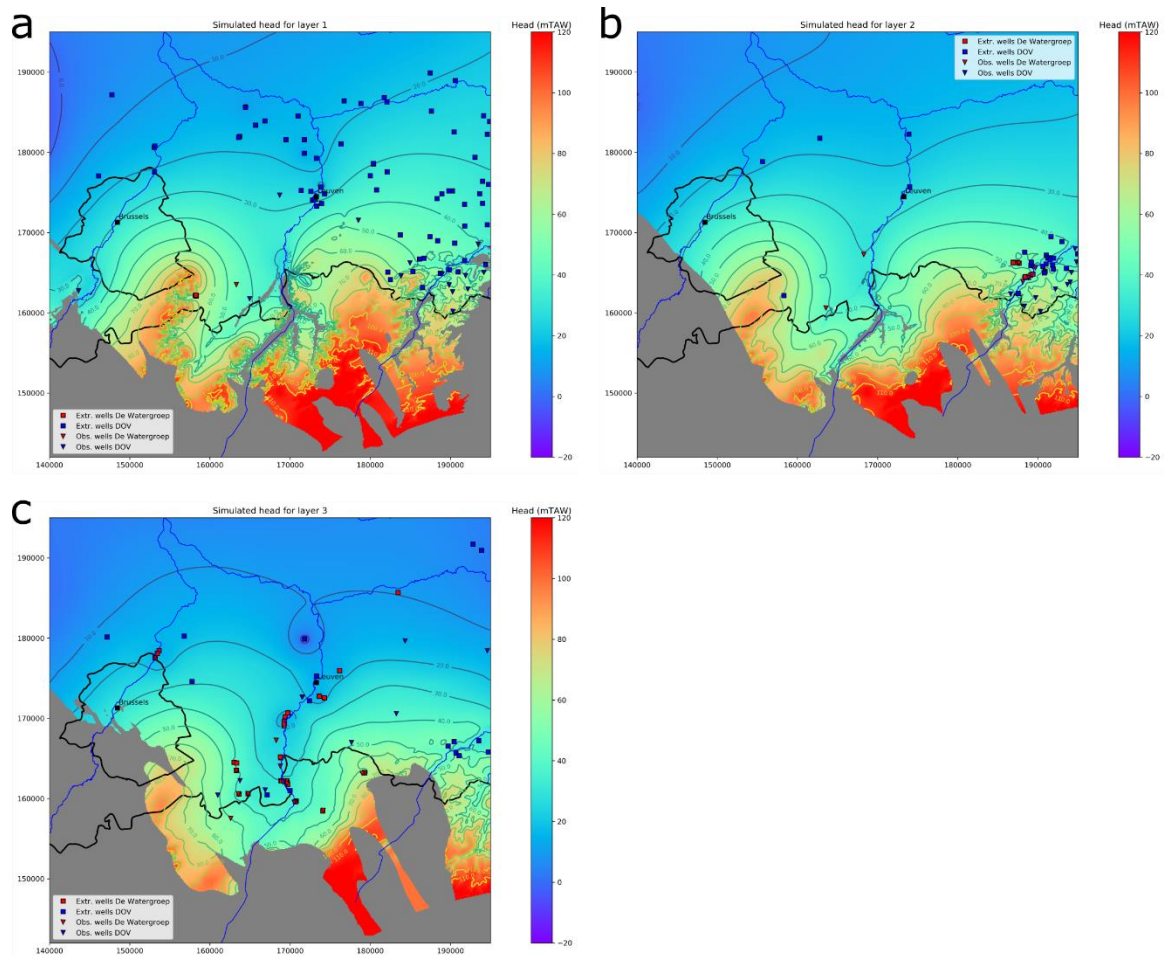


Figure 86: Map of simulated hydraulic heads for the 2000-2004 SS model for: (a) Grandgliste; (b) Lincent; and (c) the Cretaceous. Hydraulic head residual diagnostics

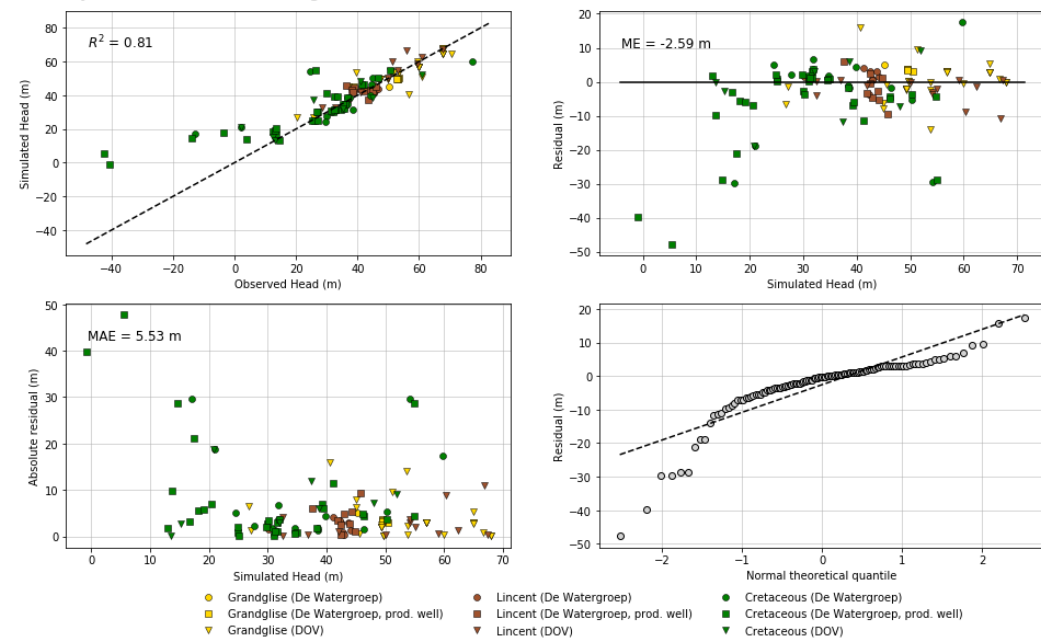


Figure 87: Overview of hydraulic head residual diagnostics plots for the 2000-2004 SS model.

In Figure 88 the model residuals are visualized. There is a strong overestimation of the heads in the Cretaceous in the Vilvoorde and Leuven areas. This overestimation can be up to several tens of meters and is significantly larger than seen for the 2018 SS model. These large residuals are related to historical extractions in these areas in the decades before the modelled period (see section 3.3). The hydraulic heads are recovering strongly over time in these areas. However, a steady-state model cannot capture this transient recovery.

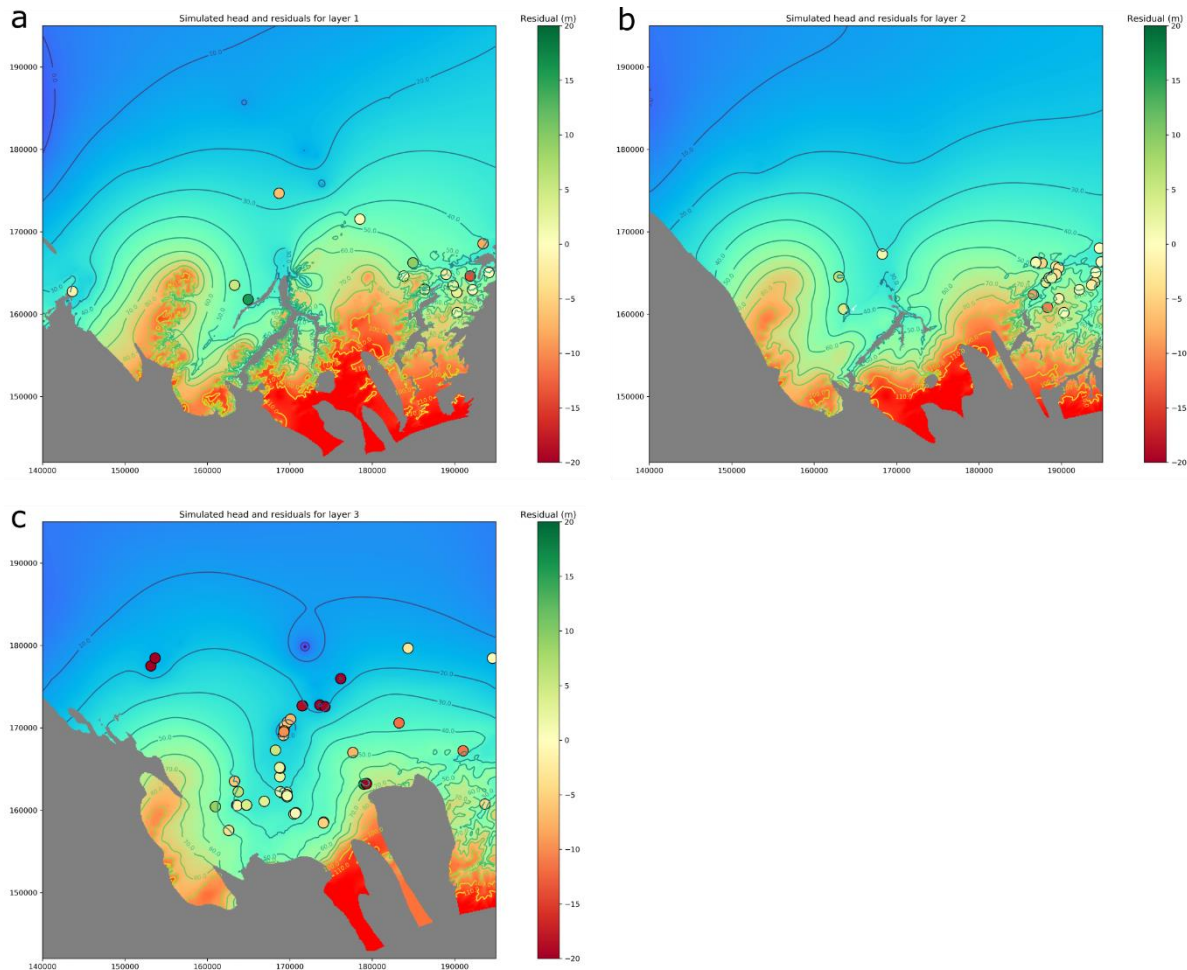


Figure 88: Map of hydraulic head residuals for the 2000-2004 SS model for: (a) Grandglaise; (b) Lincent; and (c) the Cretaceous.

4.7 Transient modelling

A transient model is set up for the period 2004-2020. The choice for the start in year 2004 is based on the availability of head observation data (Figure 79). Before 2004, not enough observations are available to accurately model the boundary conditions and to adequately calibrate the model. The transient model is largely based on the two iterations of the steady-state model. The different boundary conditions are expanded to be variable through time.

4.7.1 Initial heads

Initially, the simulated heads of the 2000-2004 steady-state model were used as initial heads for the transient model. However, as previously discussed, the steady-state model cannot accurately simulate the heads in the Vilvoorde and Leuven areas which are both recovering from historical extractions. Therefore, we use interpolated heads for the year 2004 as initial heads for the northern part (confined part) of the model area. As not many head observations are available for this period, some of the head time-series were extrapolated backwards in time based on observed trends. In the northern part of the model area, this interpolated field provides a better representation of the actual

heads than the steady-state model results. However, in the southern part not many head observations are available and due to the unconfined character and the strong variations in topography, interpolation of observed heads does not represent the actual heads accurately. In the southern part of the model area, the SS model for 2000-2004 performs reasonably well, and thus the simulated heads of this model are used as initial heads for the transient model. The initial head fields used in the transient model are shown in Figure 89. Note the relatively sharp boundary between the two regions. However, this is smoothed out in the first few time steps of the transient model and does not significantly influence model results in the later time steps.

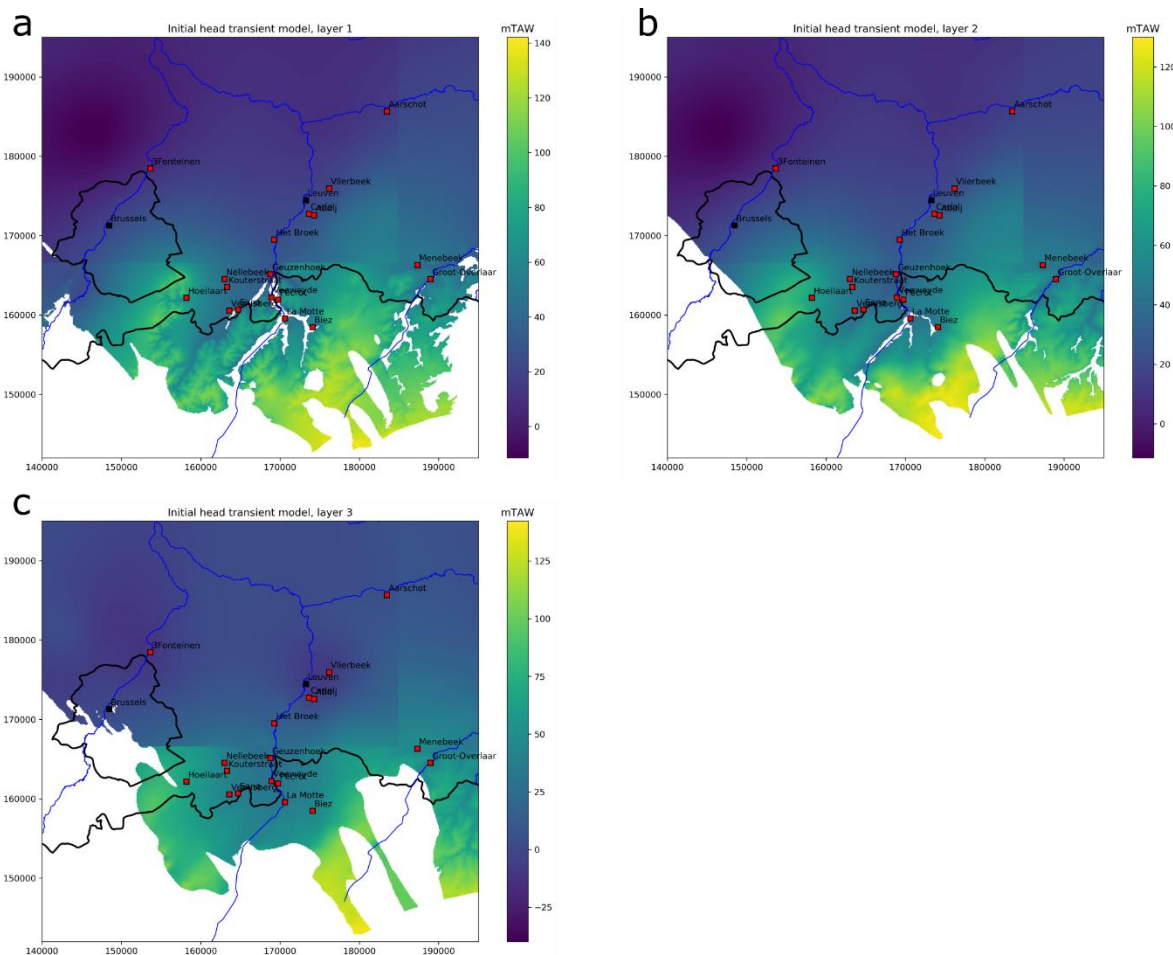


Figure 89: Initial heads used in the transient model, based on the results of the SS 2000-2004 model in the S and interpolation of observed heads in the N: (a) Grandgise; (b) Lincent; and (c) Cretaceous.

4.7.2 Boundary conditions

General-head boundary

The GHB for the west, north and east boundary is set-up similar to the one for the 2018 steady-state model. The heads assigned to these boundaries are based on interpolation of nearby head observations. As only limited observations are available near these boundaries, the heads at different points along the boundaries are estimated based on nearby observations and observed trends in the hydraulic gradient. The heads along the boundaries are estimated for four different moments in time: the years 2004, 2008, 2013 and 2018. The heads for the years between these four moments are estimated based on linear interpolation in time. As not enough observations are available

for 2019 and 2020, the heads for 2018 are used for these years. The heads along the west, north and east boundaries for the years 2004, 2008, 2013 and 2018 are plotted in Figure 90.

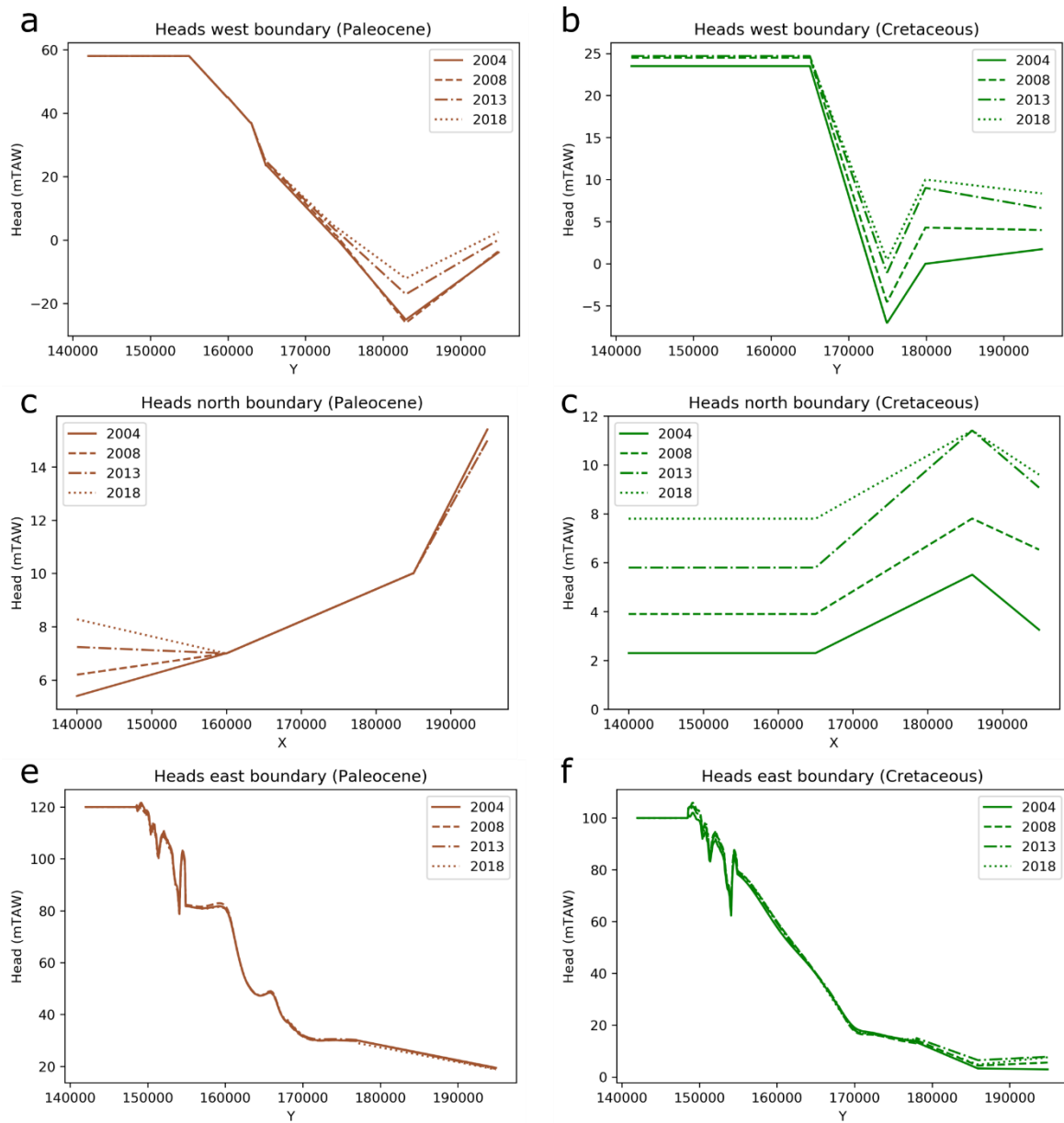


Figure 90: Specified heads for the GHB package through time for: (a) west boundary, Paleocene; (b) west boundary, Cretaceous; (c) north boundary, Paleocene; (d) north boundary, Cretaceous; (e) east boundary, Paleocene; and (f) east boundary, Cretaceous.

The largest changes through time are visible for the northern boundary and the northern part of the western boundary. For the west boundary, there is a significant increase of >10m in the head in the north for both the Paleocene (Figure 90a) and the Cretaceous (Figure 90b). For the north boundary, there is only an increase in the western part for the Paleocene, with an increase of a couple of meters (Figure 90c). For the Cretaceous, there is a significant increase over the entire northern boundary, with an increase of approx. 2m per 4 to 5 years (Figure 90d). At the eastern boundary, there is no significant change in time for the Paleocene (Figure 90e). For the Cretaceous, there is only an increase in the northern most part, with an increase of approx. 2m per 4 to 5 years (Figure 90f).

Top boundary

Similar to the steady-state models, a correlation between head and topography is derived for both the Kortrijk and the Brussels/Quaternary zones. For each modelled year, such a correlation is derived, and a resulting GHB head map is created. Due to limited data availability for the year 2020, the correlations and head map of 2019 is used for this year. The number of wells used for each year for each zone is shown in Table I. 16. Table I. 17 shows the statistics of the linear interpolation derived for the head versus topography for the two zones. Note the significant decrease in the slope for the Brussels & Quaternary zone from 2012 to 2013. This is caused by the fact that some observations at high topography only have data up until 2012. From 2013 onwards, no data is available, significantly affecting the linear regression. Plots of the correlation between head and topography for the years 2004, 2010, 2015 and 2018 are shown for respectively the Kortrijk zone and the Brussels & Quaternary zone in Figure I. 4 and Figure I. 5. The resulting GHB head maps are shown in Figure I. 6.

Extraction wells

An overview of the extraction rates for both the wells of De Watergroep and DOV for the 2004-2020 period is shown in Figure 91 and Table I. 18. Note that there is a general trend of decreasing total extraction in the area, which is mainly caused by a significant decrease in extraction of the DOV wells of about 60%. For the extraction wells of De Watergroep there is a slight increase in extraction rates. Note the small uptick in rates in the last few dry years (from 2018 onwards).

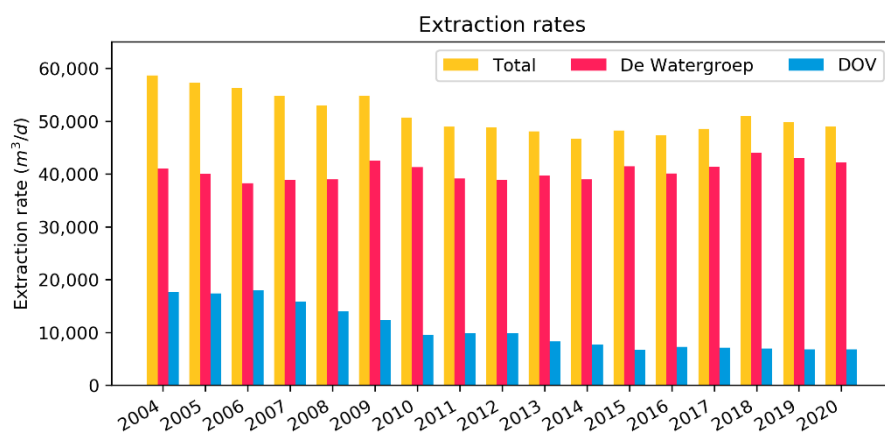


Figure 91: Overview of total extraction rates and extraction rates for respectively De Watergroep and DOV wells.

Extraction wells De Watergroep

The actual annual extraction rates for the period 2004 to 2020 are used. An overview of all extraction wells and their extraction rates for the period 2004-2020 is shown in Table I. 19. In total, 46 extraction wells are modelled, 33 of which have a filter in the Cretaceous aquifer, 9 in the 'tuffeau' of Lincent and 4 in Grandglise. The total extraction rates of these wells over the modelled period are relatively constant, with an average of 40,568 m³/d, a minimum of 38,288 m³/d in 2006 and a maximum of 43,984 m³/d in 2018 (Figure 92). The majority is extracted from the Cretaceous (average of 35,455 m³/d), followed by Lincent (average of 4,752 m³/d) and Grandglise (1,024 m³/d). Note a slight increase of the extraction rates in the Cretaceous in the last few, dry, years. The extraction site of Hoeilaart was taken over by De Watergroep in 2015. Before that, these wells were producing water for the Gemeentelijke Waterdienst Hoeilaart (and thus modelled as part of the DOV wells).

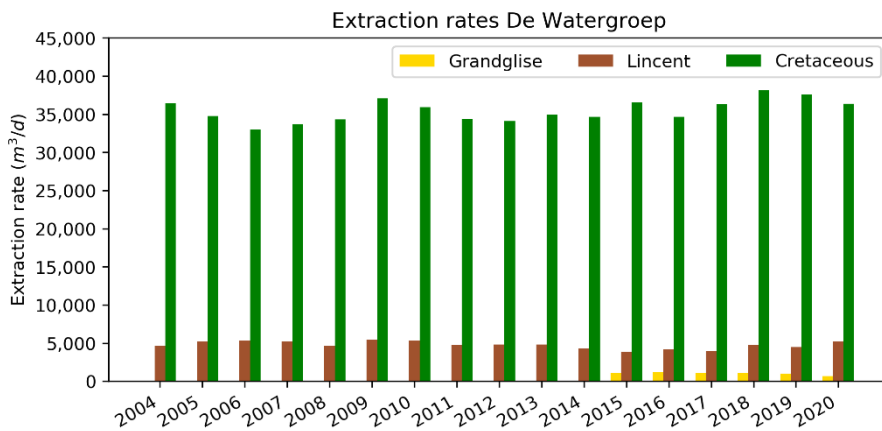


Figure 92: Overview of the extraction rates for the wells of De Watergroep for the three model layers.

The extraction wells in the Cretaceous are mainly situated in the Dijle valley (and valleys of its tributaries) and the Leuven area (Figure 64). The extraction wells in the ‘tuffeau’ of Lincent are situated in the Tienen area.

Extraction wells DOV

The extraction wells of DOV are modelled with the Well package. For most of the large extractions, reported extraction rates are made available by the VMM. For the other extractions, only information on the permits is available. In this case, initially 80% of the permitted rates are used as extraction rates in the model. Only wells with a permit $>10 \text{ m}^3/\text{d}$ are inserted in the model. An overview of all extraction wells and their extraction rates for 2004-2020 is shown in Table I. 20 and Table I. 21.

In total, 110 extraction wells are modelled, 71 of which have a filter in Grandglise, 21 in the ‘tuffeau’ of Lincent and 18 in Grandglise. For 23 of these wells, the actual reported extraction rates are available. The total extraction rates of the DOV wells over the modelled period are decreasing over time, with an average of $10,705 \text{ m}^3/\text{d}$, a minimum of $6,743 \text{ m}^3/\text{d}$ in 2015 and a maximum of $17,942 \text{ m}^3/\text{d}$ in 2006 (Figure 93). The majority is extracted from Lincent (average of $4,711 \text{ m}^3/\text{d}$), followed by Grandglise (average of $4,236 \text{ m}^3/\text{d}$) and the Cretaceous ($1,758 \text{ m}^3/\text{d}$). Note the strong decline of rates for the wells in Lincent and the Cretaceous, with declines of 70-80%.

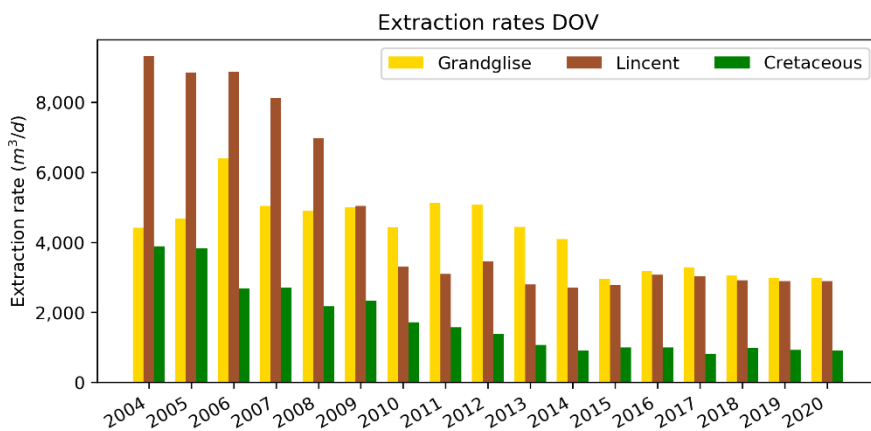


Figure 93: Overview of the extraction rates for the wells of DOV for the three model layers.

4.7.3 Observations

The observation wells are modelled with the HOB package. The annual average hydraulic head is used as observed head. In total, 191 observation wells are implemented, good for a total of 2526 head observation datapoints. Of these wells 54 are extraction wells from De Watergroep, 55 are observation wells of De Watergroep and 82 are observation wells from DOV (Table I. 22). The distribution of the wells over the layers is as follows: 65 wells in Grandglise (779 datapoints), 40 in Lincent (597 datapoints) and 87 in the Cretaceous (1150 datapoints). Note that several wells have filters spanning over multiple layers (Table I. 22). For these wells, an equivalent head is calculated based on a thickness-weighted average of simulated head in those layers. Most of the observations in the Cretaceous come from extraction sites and observations wells close by these sites (Figure 66). The observations in Lincent are mostly situated in the Tienen area, in the ‘tuffeau’ zone.

4.7.4 Hydrogeological parameters

The resulting hydraulic conductivities after calibration of the steady-state model of 2018 (see section 4.6.1) are used as initial conductivities for the transient model. For the hydraulic conductivity of the Cretaceous, the improved version obtained by performing kriging with the correlation HK-depth as secondary information is used (see 2.3.3). An extra correction is added for the northernmost parts of the model, where a minimum HK is assigned. From a certain depth onwards, HK doesn't seem to decrease significantly anymore. Two zones are identified: for the first zone where the Cretaceous is situated at a depth of more than -100 mTAW, a minimum HK of 0.25 m/d is assigned; where the Cretaceous is at a depth of less than -100 mTAW, a minimum HK of 0.55 m/d is used. Two different zones are used to get the best fit for the extraction site near Leuven (Vlierbeek, Cadol, Abdij) for which the simulated head is very sensitive to small changes in HK of the Cretaceous. The resulting HK field used for the Formation of Gulpen is visualized in Figure 94. The specific storage estimates from the pumping tests (see Section 2.3.1, Table 3) on the extraction wells of the Cretaceous vary between 2.5E-2 to 1.2E-6 m⁻¹, with most of the specific storage estimates being around 1E-4 m⁻¹. Initially, for all three layers, a specific storage of 1E-4 m⁻¹ is used.

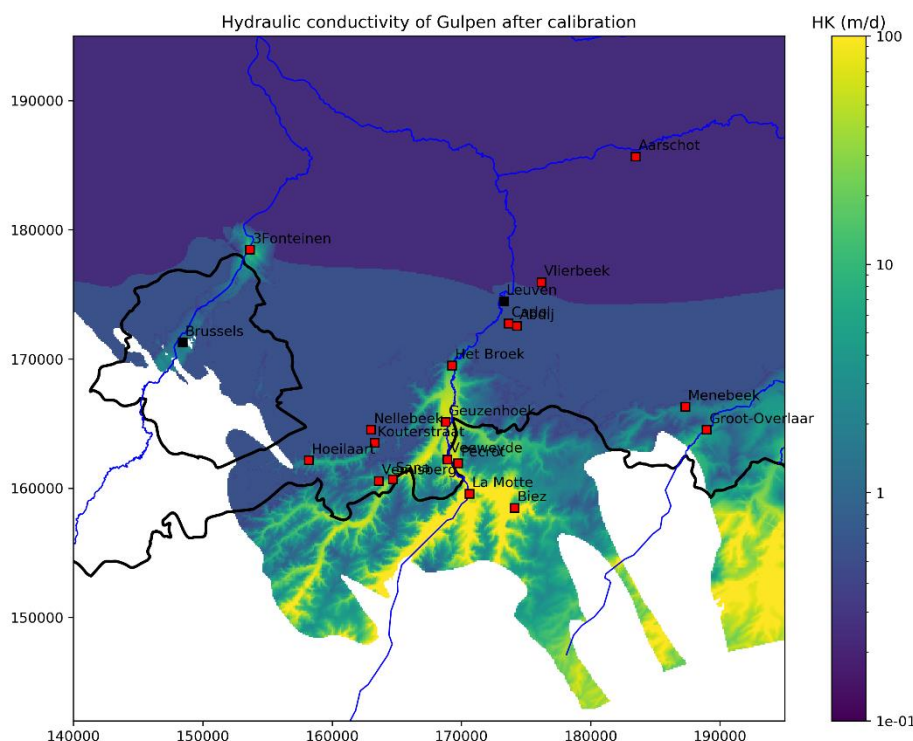


Figure 94: Spatially variable hydraulic conductivity used for the Formation of Gulpen after calibration.

4.7.5 Solver

The GMG solver is used with a maximum of 50 outer and 50 inner iterations, a head change and residual criterion for convergence of 1E-2, a relaxation parameter of 1 and a dampening parameter of 0.97. This results in a runtime of approx. 3 minutes 10 seconds¹⁰.

4.7.6 Results

Calibration

The simulated heads for the years 2004 and 2020 are visualized in Figure 95 and the years 2010 and 2015 in Figure I. 7. Note the effect of the historical extractions in 2004 in the Vilvoorde area (all three layers) and the Leuven area (Cretaceous). Compare this with the simulated heads for the 2000-2004 steady-state model (Figure 86) in which these depressions are not clearly visible. Another difference with the steady-state model is the more limited effect of the extraction of Het Broek on the overlying layers of Lincent and Grandglise.

When comparing the simulated heads for 2004 and 2020, the recovery of the historical extraction is clearly visible. Especially in Grandglise and Lincent, the historical extraction in the Vilvoorde area is not visible anymore in 2020. In the map of the simulated heads of 2020, the effect of the extraction in Het Broek is more clearly visible. In Figure 96 the difference in simulated head between the years 2004 and 2020 is shown for the Cretaceous and in Figure I. 8 for Grandglise and Lincent. This clearly shows the recovery from the historical extraction with an increase of head in the Cretaceous in the Vilvoorde area of up to 15m and up to 12m in the Leuven area. In Grandglise and Lincent, there is an increase of up to 10m in the Vilvoorde area and of a couple of meters in the Leuven area. Also note the decrease in hydraulic head in the southern, unconfined part of the Cretaceous. This difference in head is mainly related to inaccuracies in the head versus topography correlation used in the GHB boundary. As discussed previously, this is mainly caused by the absence of enough head observation at higher topography in the south.

The scatterplot of simulated versus observed head and other diagnostic plots are shown in Figure 97 and Figure 98. The model can reproduce the observed heads relatively well. There is a clear improvement in performance compared to the steady-state models. Considering all the stress periods, a R^2 of 0.94 is obtained, a mean error (ME) of -0.21m, a mean absolute error (MAE) of 3.70m, a RMSE of 5.16m and a PBIAS of 0.59. In Table I. 23 the model performance statistics for each year are shown. Model performance is similar for all time steps, with a slightly better performance in the first half of the modelled period. The last two timesteps (2019 and 2020) were added after calibration of the model and are used as validation. In this validation period, the model performed similarly to the period used for the calibration. A histogram of model residuals is shown in Figure 99. The residuals are normally distributed, with a mean of -0.21m and a standard deviation of 5.16m. 75% of residuals are smaller than 5m, and 94% of residuals are smaller than 10m. The distribution and spread of residuals are similar for all three layers.

¹⁰ Runtime can be reduced by approx. 50% by changing output control, e.g., not saving heads, not writing all package info to the listing file etc.

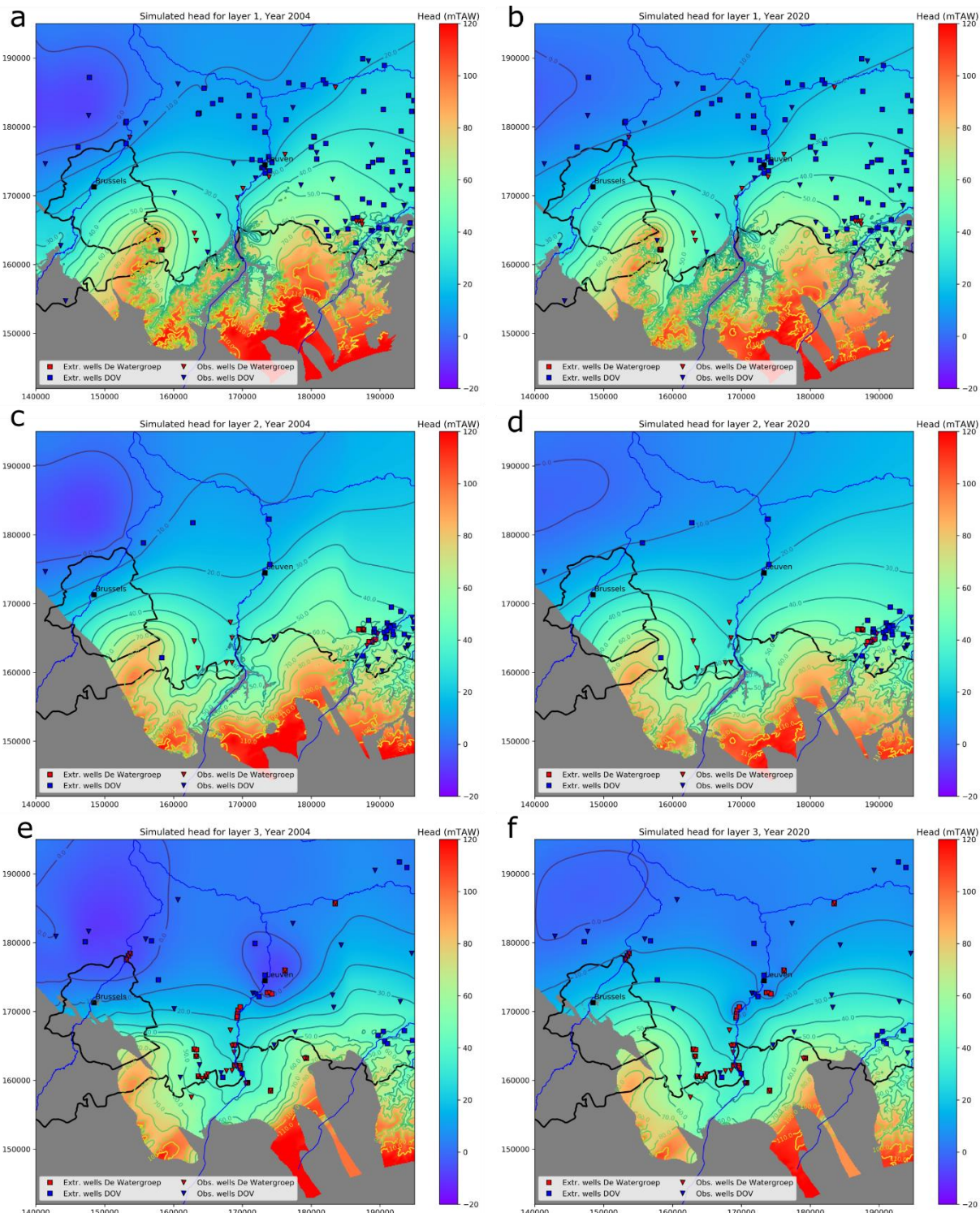


Figure 95: Simulated hydraulic heads for the year 2004 and 2020: (a) 2004, Grandglise; (b) 2020 Grandglise; (c) 2004, Lincent; (d) 2020, Lincent; (e) 2004, Cretaceous; and (f) 2020, Cretaceous.

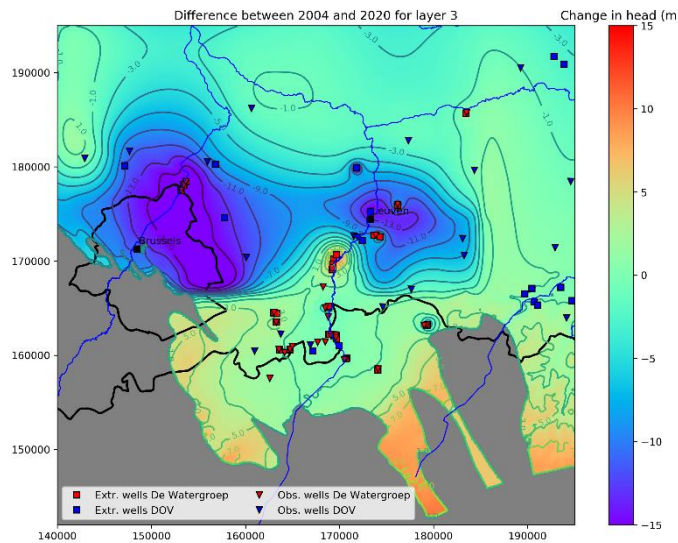


Figure 96: Difference in simulated head between the years 2004 and 2020 for the Cretaceous. (Blue is increase, red is decrease).

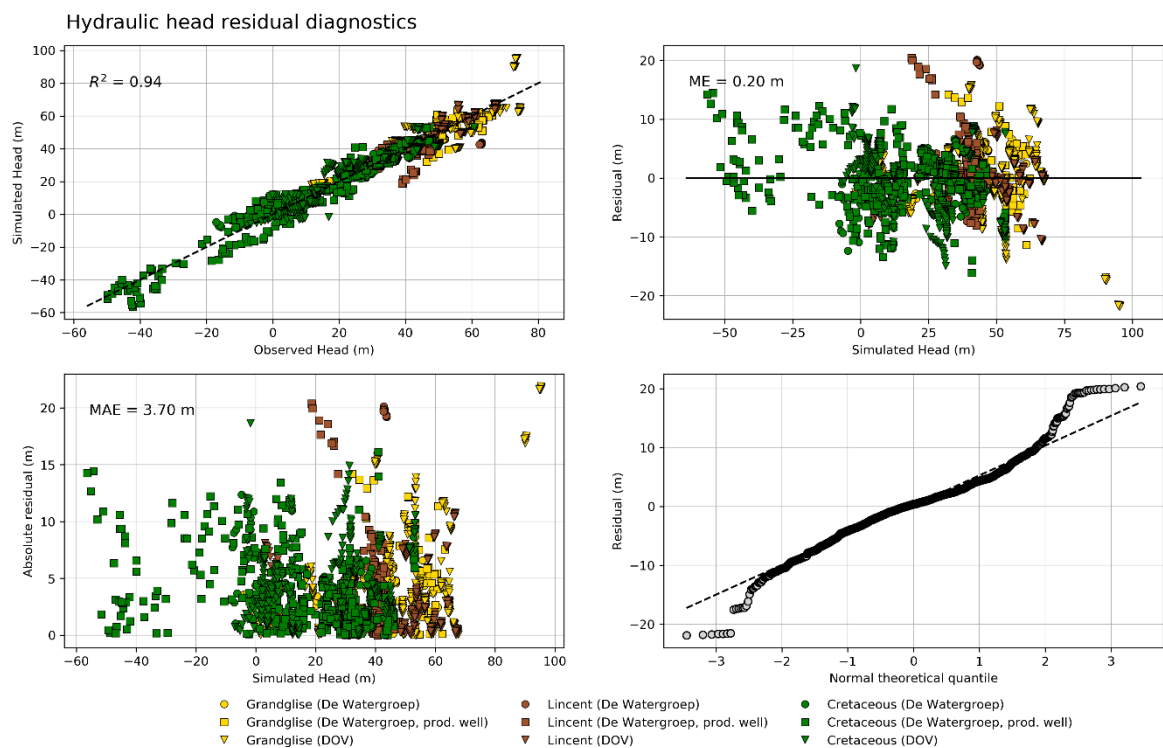


Figure 97: Overview of hydraulic head residual diagnostics plots for the transient model.

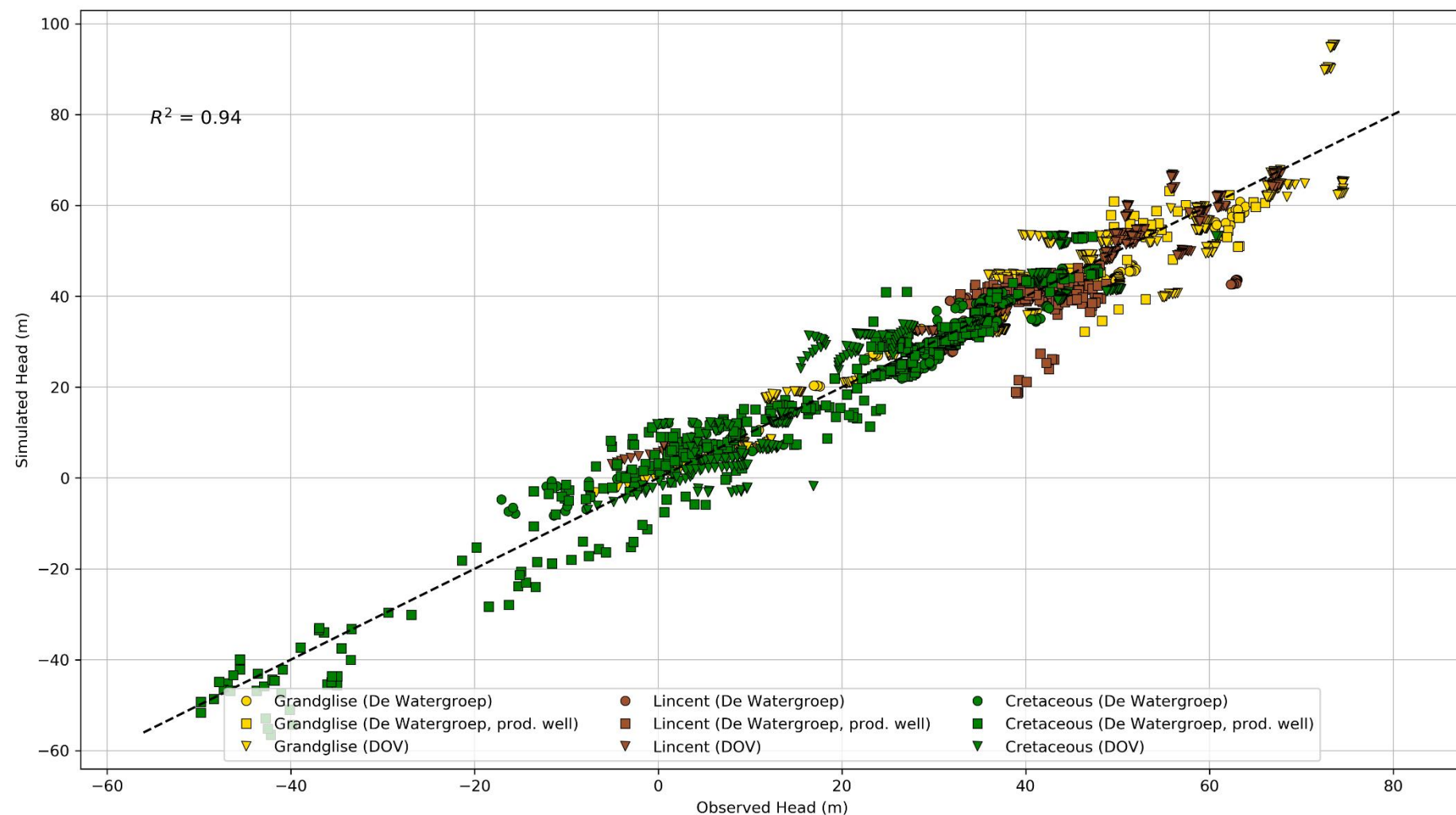


Figure 98: Scatterplot of simulated versus observed hydraulic head for the transient model.

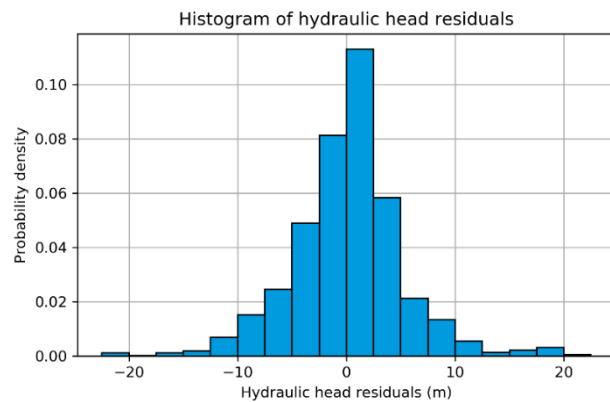


Figure 99: Histogram of hydraulic head residuals (observed heads minus simulated heads) for all stress periods.

The model performance only considering the observation wells and not the observations in the extraction wells, is similar to considering both (Figure I. 9). A R^2 of 0.92 is obtained, a mean error (ME) of 0.09m, a mean absolute error (MAE) of 3.79m, a RMSE of 5.26m and a PBIAS of 0.25.

The hydraulic head residuals for the year 2018 (most recent year with most observations) are plotted on a map in Figure 100. Similar maps for the years 2004 and 2010 are shown in Figure I. 10.

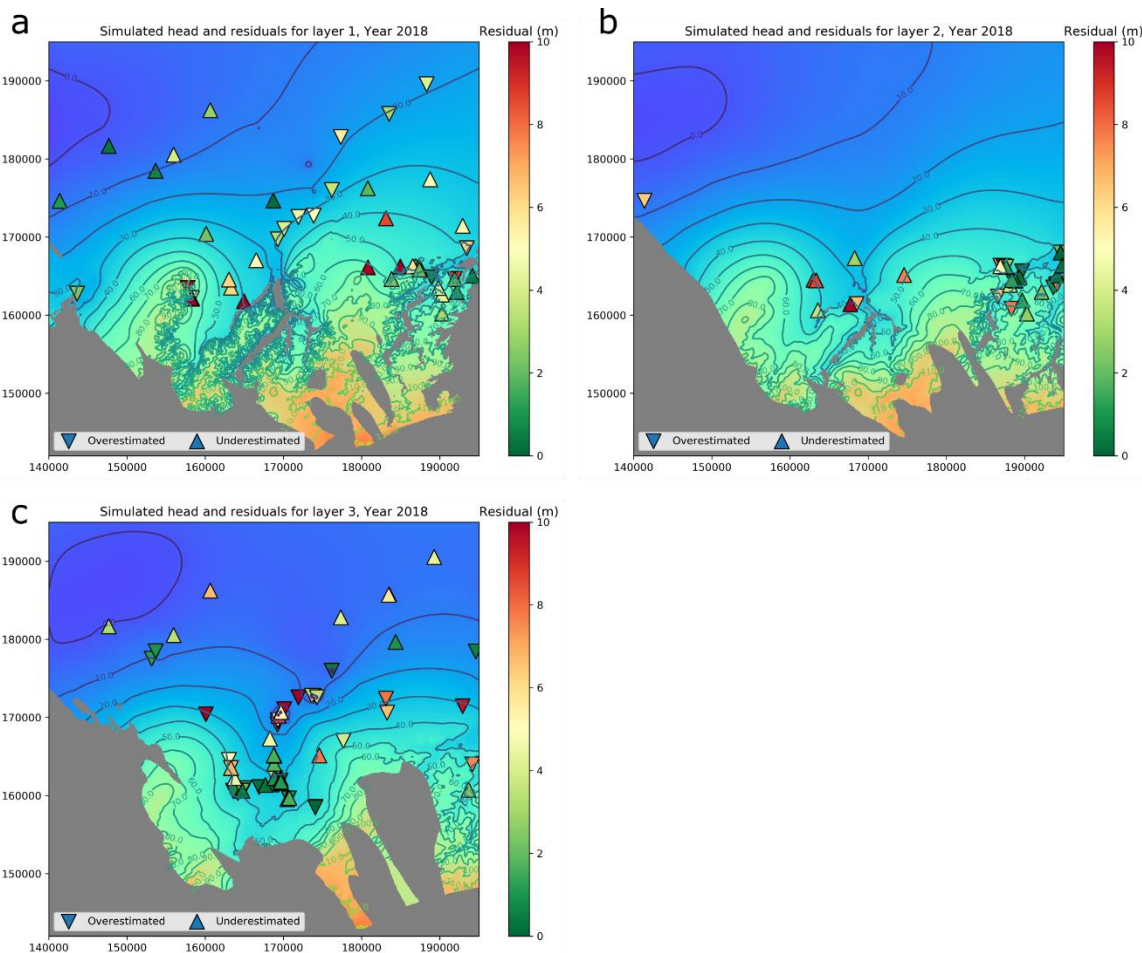


Figure 100: Model residuals for the year 2018 for: (a) Grandglise; (b) Lincent; and (c) the Cretaceous.

For Grandglise, the largest residuals are found for some wells near the Brusselian channel near Hoeilaart. The absence of the confining Formation of Kortrijk locally results in large head differences in this area, which are difficult to match. Some wells near the Tienen region also have relatively large residuals. In the rest of the model area, residuals are in general smaller than 5m.

In the Lincent layer, the largest residuals are found near the Nellebeek site, where there is a strong underestimation. At this site, water is extracted from the Lincent layer. Locally, the Lincent deposits have a larger transmissivity than in the rest of the model area due to the presence of fractures (see section 2.3.2). As not enough information on the reason and extent of this larger transmissivity is available, it was not possible to implement this in the model. Most of the observation well in the Lincent layer are in the 'tuffeau' of Lincent zone. In this area, residuals are in general relatively small.

For the Cretaceous, the largest residuals are situated near the extraction sites near Leuven and the site of Korbeek-Dijle Het Broek. Due to the low conductivities of the Cretaceous in this area, a small change in HK can already result in a significant change of the simulated heads. In the southern part of the Dijle valley, residuals are in general small, in the order of a couple of meters. The model seems to overestimate the head to the west and east of the Dijle valley, around Leuven. The performance of the model for the extraction sites of De Watergroep is discussed in more detail in the next section.

Parameter values after calibration

The resulting hydraulic conductivity values after calibration are summarized in Table 23. In general, the vertical conductivity is 10% of the horizontal conductivity. However, the Halen/Lincent sublayer is the exception. During the calibration, it became clear that the VK of this layer should be very low. This very low value can be explained by the strongly layered character of these deposits, with an alternation of silty to clayey layers. The clayey intercalations have a strong effect on the equivalent value of the VK. For the Lincent, the HK is based on a correlation between HK estimates from pumping tests and the depth of the deposits (Figure 67). The resulting spatially variable HK field is multiplied with a factor during the calibration. In the end, a factor of 2 gave the best fit. Similarly, the spatially variable field of HK of Gulpen (Figure 94) is multiplied with a factor during calibration. A factor of 0.7 gave the best results. This indicates that the HK estimates from the pumping tests might overestimate the actual HK. For the specific storage, a value of 2.5E-4 m⁻¹ for all three layers resulted in the best results. The storage parameters mainly affected the recovery in the zones with historical extractions. The final vertical hydraulic conductivities used to calculate the conductance in the GHB boundary at the top of the model were respectively 1E-5 m/d for the Kortrijk zone, 0.5 m/d for the Brussels zone and 5 m/d for the Quaternary zone.

Table 23: Resulting hydraulic conductivities after calibration of the transient model.

Parameter	HK (m/d)	VK (m/d)
Grandglise	3	0.3
Halen/Lincent	1	0.00005
Lincent zone	2*correlation	HK/10
Waterschei	0.00005	0.000005
Gelinden/Maaseik	0.001	0.00001
Orp	0.01	0.001
Gulpen	0.7*correlation	HK/10
Maastricht/Houthem	3	0.3

Extraction sites in the Cretaceous

In this section, the performance of the transient model in reproducing the heads at and near the extraction wells of De Watergroep in the Cretaceous is discussed in more detail.

Simulated and observed heads versus time for the sites near Leuven, **Vlierbeek**, **Cadol** and **Abdij**, are shown in Figure 102 and Figure 101. These extraction sites are situated in an area of the Cretaceous characterized by very low conductivities, which results in significant drawdowns of several tens of meters. The observed heads in the extraction wells (3007-001-F0, 3006-001-F0 and 3006-116-F0) are matched well. The sometimes-large changes due to changes in extraction rates are reproduced well by the model. The changes due to the initiation of extraction in Abdij are simulated well. The observation wells in the Cretaceous (3007-038-F3 and 3006-159-F2) overestimate the hydraulic heads. It seems that the areal extent of the drawdown is a bit larger than is simulated in the model. This might be related to the fact that only a small interval of a couple of meters in thickness is very permeable in this area, while the bottom part of the Cretaceous does not contribute to the flow in the wells at all. However, in the model, the Cretaceous is modelled as one layer with an equivalent conductivity.

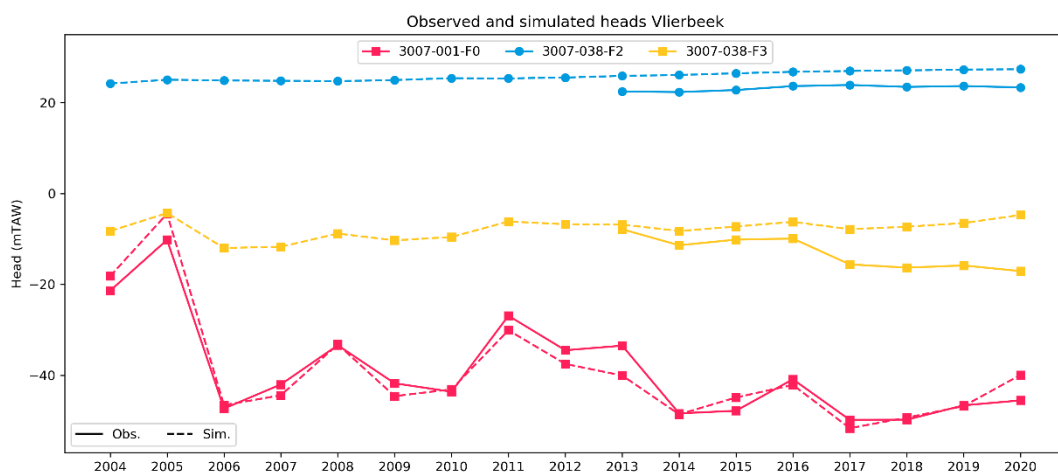


Figure 101: Observed and simulated heads versus time for the sites of Cadol and Abdij.

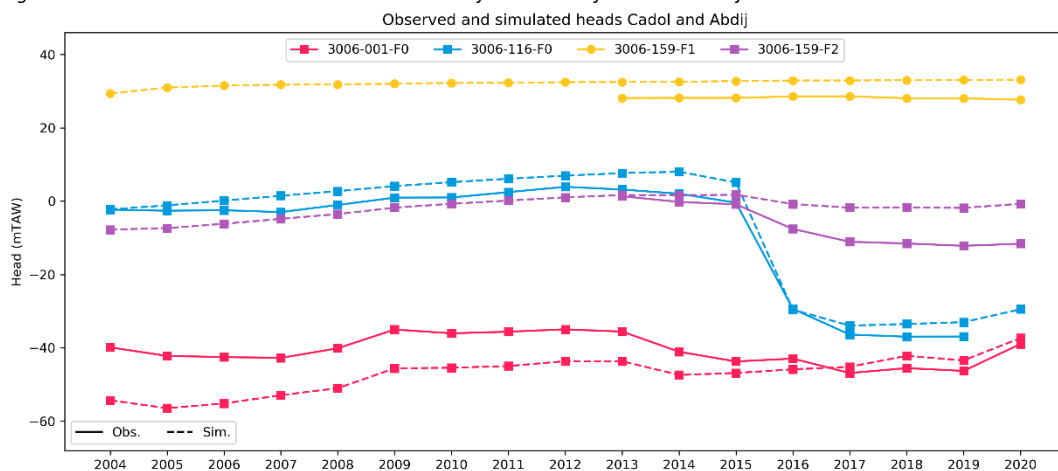


Figure 102: Observed and simulated heads versus time for the site of Vlierbeek.

Simulated and observed heads versus time for the **Korbeek-Dijle Het Broek** site are shown in Figure 104 and Figure 103. Wells 3008-001-F0, -002-F0, 003-F0, -005-F0 and -006-F0 are used as extraction wells since the beginning of the modelled period. Note the declining trend in heads over time in these extraction wells. The variations through time

related to changes in extraction can be reproduced reasonably well. Also note that the observed heads of these wells are in a smaller range than the simulated heads, which indicates a larger connectivity between the wells than simulated in the model. The lowest heads are simulated for the extraction wells in the north (-002-F0 and -003-F0) while higher heads are simulated for the extraction wells in the south (-001-F0, -005-F0 and -006-F0). This can be correlated with the hydraulic conductivities which are higher in the south than in the north. Note the overestimation of the heads in the observation well 3008-004-F0, which is probably due to similar reasons as explained for the observation wells in the Leuven area. The extraction wells 3008-063-F0 and -064-F0 were taken into production in 2020, as replacement of 3008-005-F0. The simulated head in the observation wells in Grandglise (3008-063-F3 and 3008-064-F3) is slightly overestimating the observed heads.

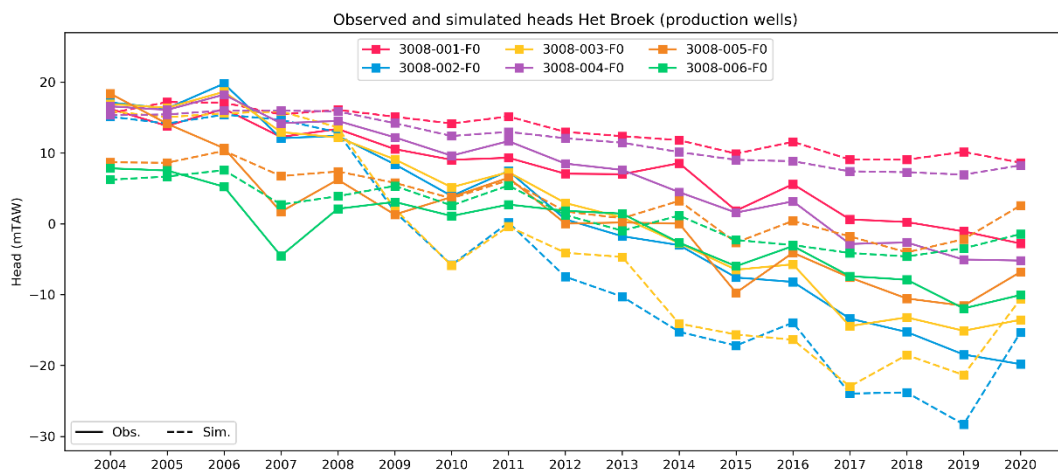


Figure 103: Observed and simulated heads versus time for the site of Het Broek (observation wells).

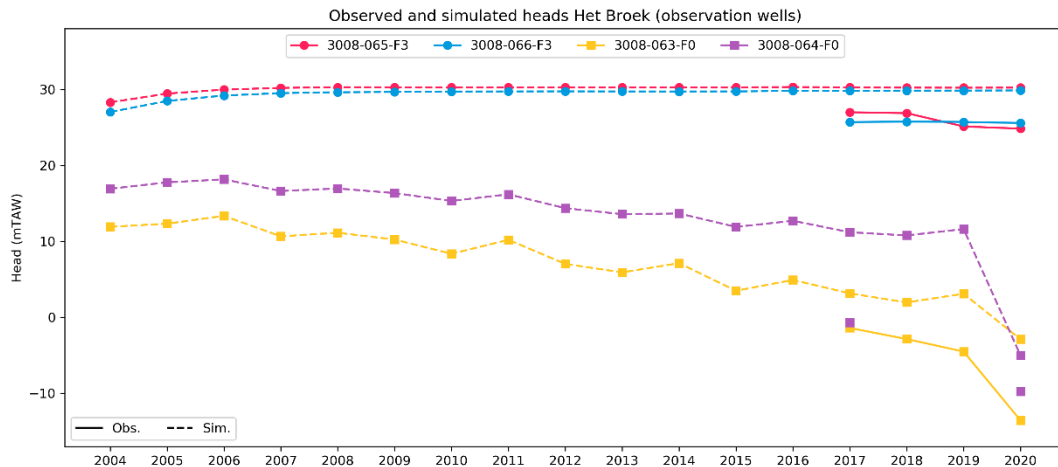


Figure 104: Observed and simulated heads versus time for the site of Het Broek (production wells).

Simulated and observed heads versus time for the sites of **Venusberg** and **Sana** are shown in Figure 105 and Figure 106. For **Venusberg**, water is produced from 3011-005-F0. Simulated heads match the variations in time due to extractions reasonably well. The simulated heads are slightly higher than observed heads for the production well and the nearby observation wells in the Cretaceous (3011-006-F2 and -007-F3). The head in Lincent (3011-007-F2) is slightly underestimated. For **Sana**, 3011-008-F0 is the main extraction well, with 3011-009-F0 being used as a backup. Simulated heads in -008-F0 are underestimating the observed heads with a couple of meters in the first part of the modelled period. For the second half of the modelled period, the correspondence is better. The simulated heads in the observation wells (3011-010-F1, -014-F1 and -023-F2) matches the observed heads well.

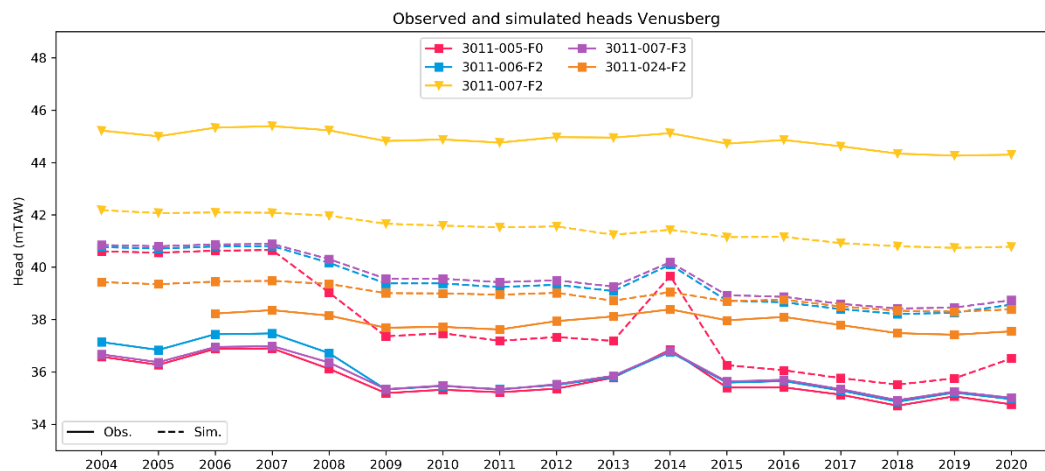


Figure 105: Observed and simulated heads versus time for the site of Venusberg.

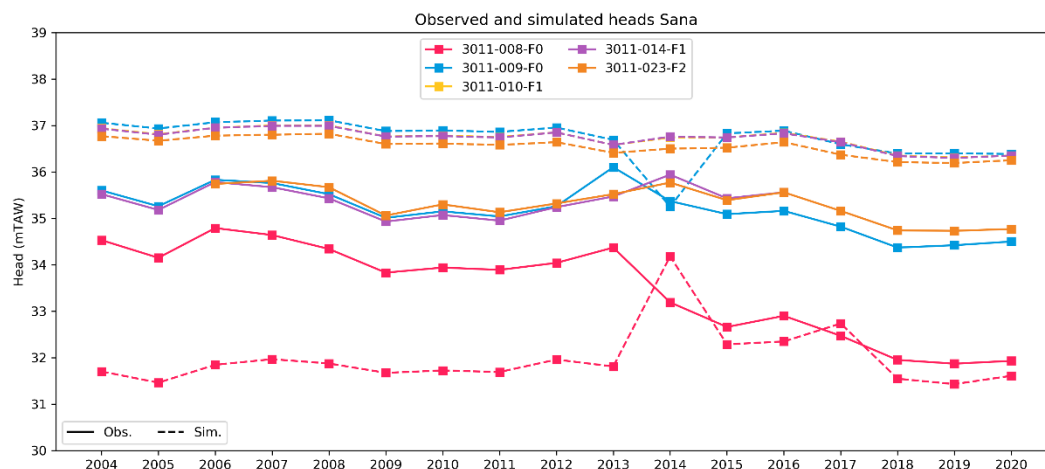


Figure 106: Observed and simulated heads versus time for the site of Sana.

Simulated and observed heads versus time for the site of **Nellebeek** are shown in Figure 107. This is arguably the area of the model with the worst performance. The flow measurements on the extraction wells indicate that most of the flow is coming from the filter in Lincent, while the Cretaceous contributes little to flow (see section 2.3.2). Nellebeek is also one of the outliers in the correlation between depth and conductivity (see section 2.3.3), as estimated conductivity is a lot lower than expected. A possible reason for this is the absence of the upper members of the Formation of Gulpen, including the permeable hardground interval, which in general have higher conductivities. Only the Member of Zeven Wegen is present, which is characterized by very low permeabilities. The pumping test result indicates that the Lincent deposits in this region are relatively permeable, more than expected. However, such an increased HK of Lincent is not implemented into the model due to not enough information on the reason and extent of this higher HK zone. The combination of a lower-than-expected HK of the Cretaceous and higher-than-expected HK in Lincent, results in the bad performance in the model. The extraction well 3010-006-F0 was used as a production well until 2013, 3010-017-F0 from 2014 until 2019 and 3010-018-F0 from 2019 onwards. The simulated heads for -006-F0 and -018-F0 are significantly lower (approx. 20m) than the observed heads. This is related to the underestimation of the HK of Lincent in this area in the model. The fit for -017-F0 is better. The head in the observation well 3010-016-F2 with filter in Grandglise is underestimated by a couple of meters.

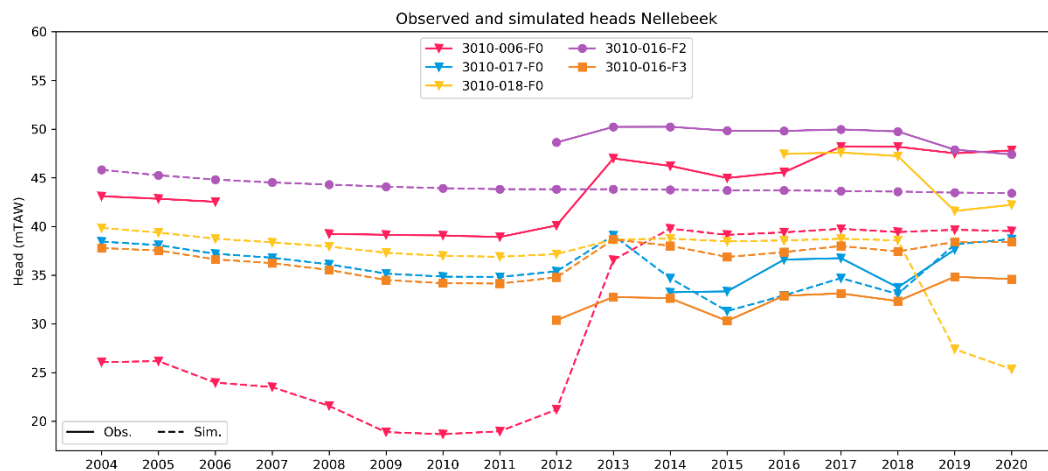


Figure 107: Observed and simulated heads versus time for the site of Nellebeek.

Simulated and observed heads versus time for the site of **Kouterstraat** are shown in Figure 108. 3010-001-F0 is the main production well, while 3010-002-F0 is used as a backup production well. Note that, like the extraction in **Het Broek**, the observed heads in these two wells are a lot closer than the simulated heads, indicating that the extraction cone in reality is less deep but wider than simulated in the model. The heads in **Grandglise** (3010-011-F1) are slightly underestimated.

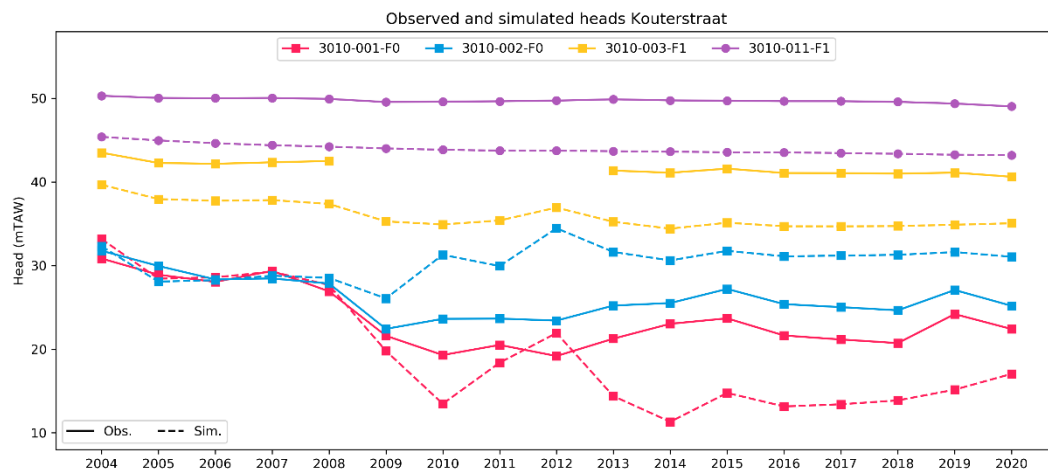


Figure 108: Observed and simulated heads versus time for the site of Kouterstraat.

Simulated and observed heads versus time for the site of **Veeweyde** are shown in Figure 109. The wells 3012-001-F0 and 3012-002-F0 are used as the main production wells. From 2019 onwards, 3012-002-F0 is replaced by 3012-059-F0 and in 2020 3012-003-F0 is taken into production. In general, the heads in the production wells are somewhat overestimated. For 3012-002-F0, the fluctuations of head through time due to changes in extraction rates are larger for the observed heads than simulated in the model. For 3012-001-F0, the fit is good, with exception of the decrease in 2019-2020 which is not visible in the simulated heads. This decrease might be related to a general increase of the total extraction rate in Veeweyde due to the addition of 3012-059-F0. Another possible reason is a decrease in recharge due to several dry years since 2018. The heads in the observation well 3012-004-F0 are reproduced well.

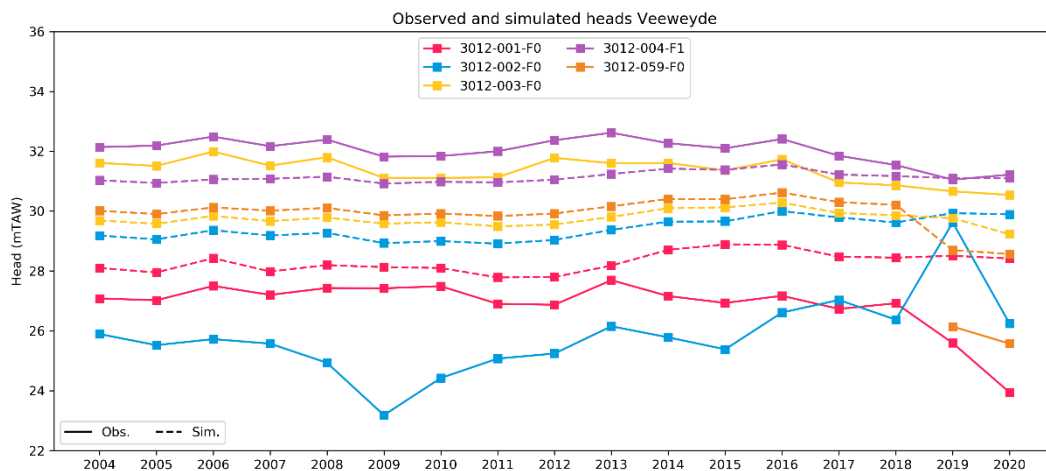


Figure 109: Observed and simulated heads versus time for the site of Veeweyde.

Simulated and observed heads versus time for the site of **Geuzenhoek** are shown in Figure 110. The wells 3012-007-F0 and -008-F0 are the production wells of this site. These wells have been temporarily shutdown since 2019 for maintenance. In general, the observed heads are reproduced adequately. Also note that the response of the shutdown is reproduced quite well. The heads in the observation wells in the Cretaceous (-009-F0 and 058-F3) are slightly underestimated, while the head in the observation well in Lincent (3012-058-F2) shows a good fit.

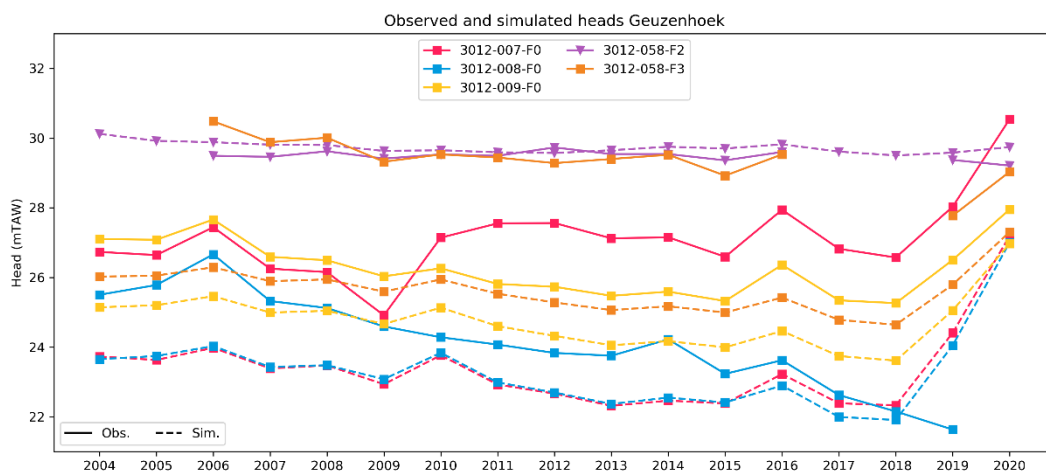


Figure 110: Observed and simulated heads versus time for the site of Geuzenhoek.

Simulated and observed heads versus time for the site of **Aarschot** are shown in Figure 111. The model reproduces the changes in head due to the initiation of the production well 3001-108-F0 relatively well. The absolute heads in the Cretaceous are underestimated, while the heads in Grandglise (3001-109-F3) are slightly overestimated. This might indicate a lower resistance of the Lincent layer in this area. Also note that similar to some of the previous sites, the effect of the extraction on the nearby observation well in the Cretaceous (3001-107-F1) is underestimated.

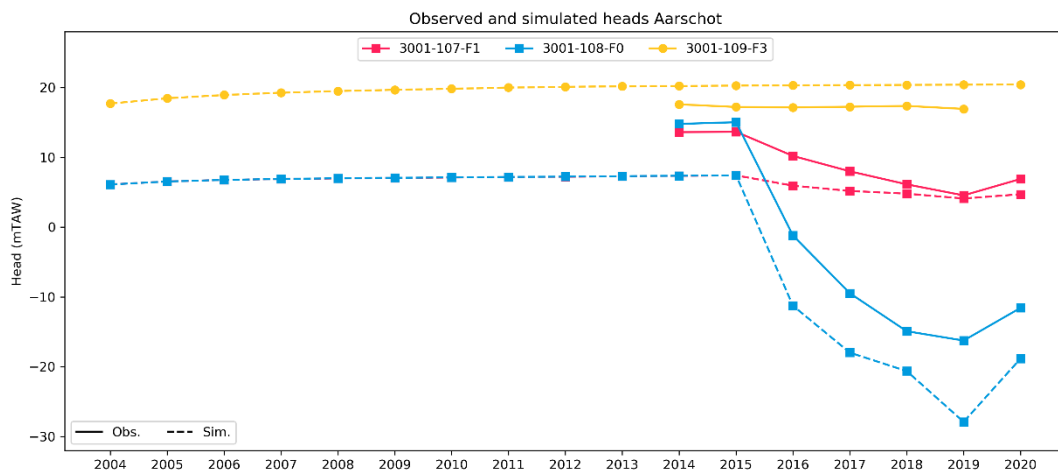


Figure 111: Observed and simulated heads versus time for the site of Aarschot.

Simulated and observed heads versus time for the site of **Pécrot** are shown in Figure 112. Wells 3012-014-F0, -015-F0 and -016-F0 are used as production wells. The temporal variations in head through time are reproduced reasonably well. In general, heads in the Cretaceous are slightly underestimated. Note that the observed heads are very similar for all wells, while in the model the range is slightly larger.

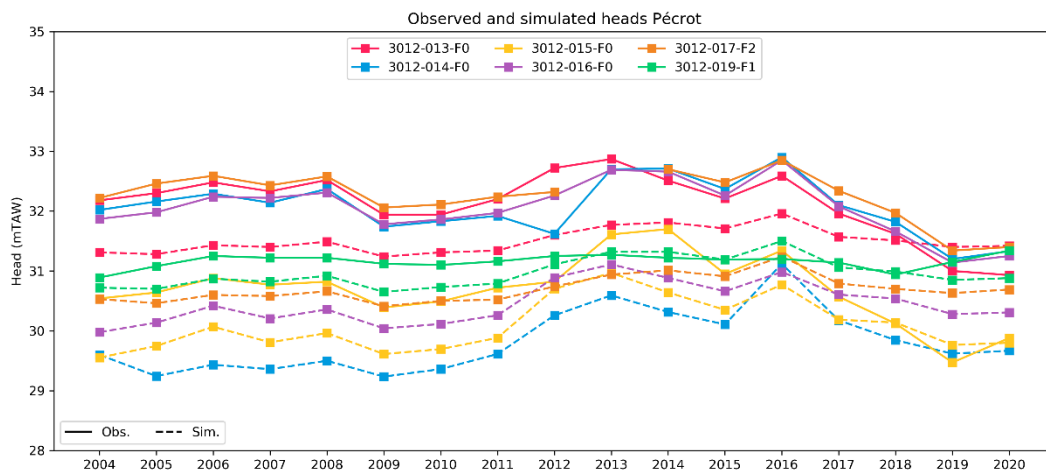


Figure 112: Observed and simulated heads versus time for the site of Pécrot.

Simulated and observed heads versus time for the site of **La Motte** are shown in Figure 113. Water is produced from extraction wells 3012-020-F0 and 3012-021-F0. The temporal variations in head through time due to changes in extraction are reproduced well. The head in extraction well 3012-020-F0 is slightly underestimated. The variations in the observation wells in the Cretaceous are larger in reality than those simulated in the model. The drop in observed heads visible for most of the wells since 2017 is not reproduced by the model. This decrease in head is possibly related to the dry last few years which impacts this site more due to its unconfined character.

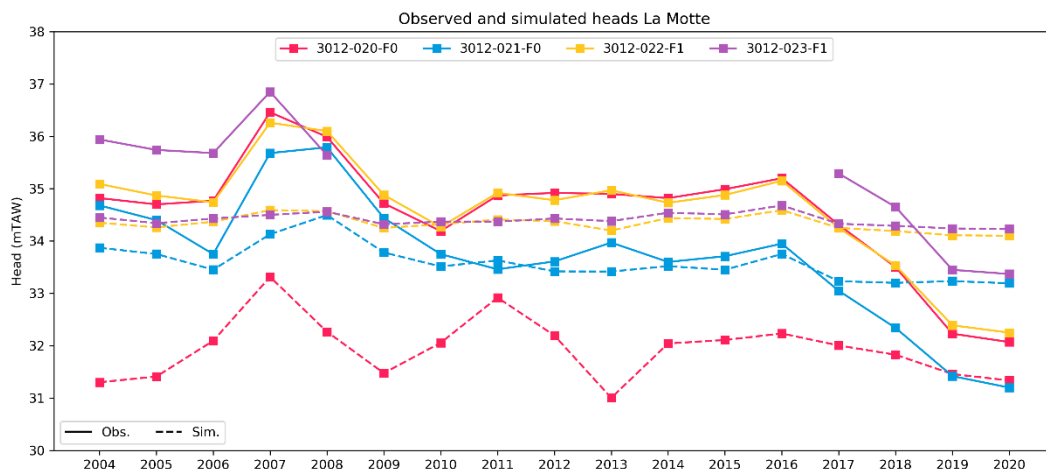


Figure 113: Observed and simulated heads versus time for the site of La Motte.

Simulated and observed heads versus time for the site of **Biez** are shown in Figure 114. Well 3020-001-F0 is the main production well of this site. In general, the heads in the Cretaceous are slightly over-estimated. The variations in time for the production well are larger for the observed heads than in simulated in the model, although the pattern match reasonably well.

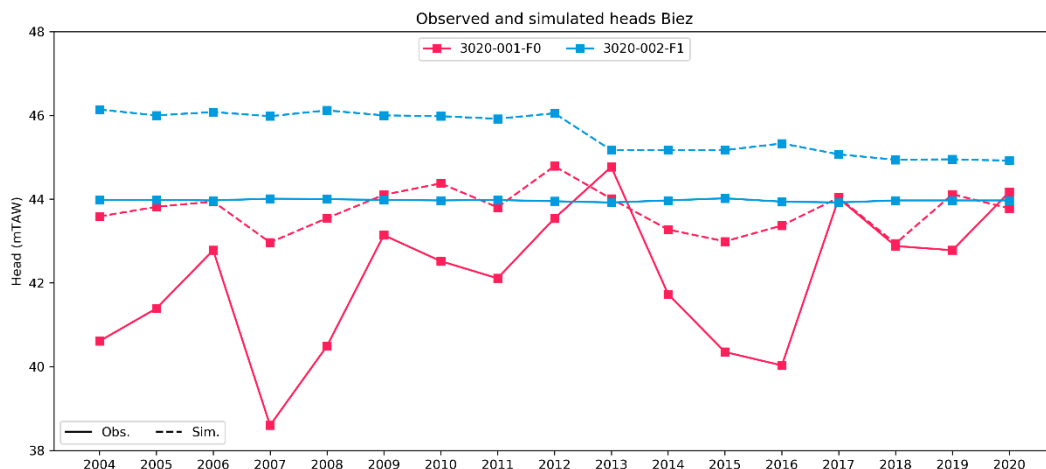


Figure 114: Observed and simulated heads versus time for the site of Biez.

Simulated and observed heads versus time for the site of **Vilvoorde** are shown in Figure 115. This site has been used to produce drinking water up until 2004. As discussed earlier, there is a strong lowering of the head in this area due to historical extractions. The model can reproduce the recovery of this extraction quite well, both in the Cretaceous and in Grandglise.

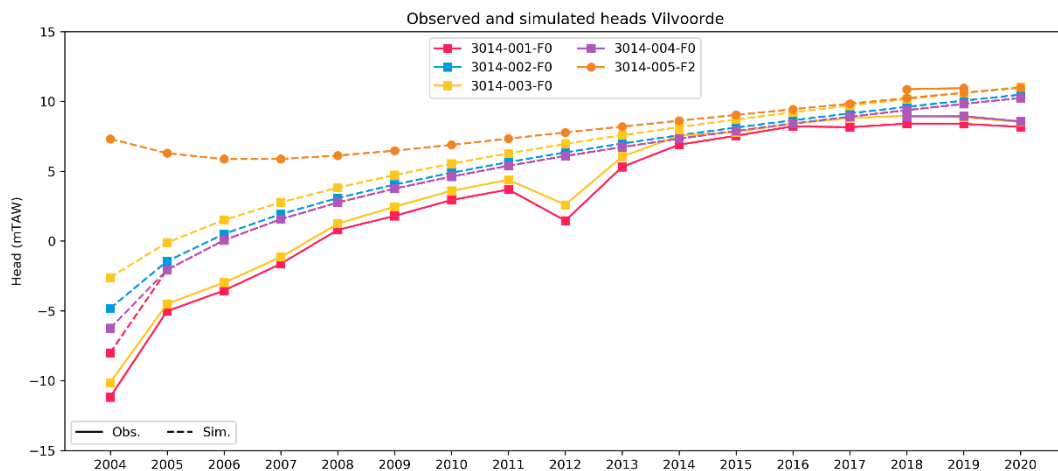


Figure 115: Observed and simulated heads versus time for the site of Vilvoorde.

The simulated and observed heads versus time plots for the extraction sites in Lincent (Menebeek and Groot-Overlaar) are shown in the Appendix in *Figure I. 11* to *Figure I. 14*. The plots for the site of Hoeilaart in Grandglise are shown in *Figure I. 15*.

4.7.7 Water Budget

In this section, the water budget of the transient model is analysed and discussed. The water budget for all stress periods is shown in *Figure 116* and *Table I. 24*. The outflow out of the model consists mainly of the extraction through the wells of De Watergroep (simulated with the MNW2 package). These extracted volumes are relatively constant in the modelled period (2004-2020) with an average volume of 40,568 m³/d. Smaller outflows are represented by other extractions (simulated with the WEL package) and by storage. The extracted volumes by wells other than those of De Watergroep have significantly decreased since the beginning of the modelled period. These volumes decreased more than 60%: from 17,609 m³/d to 6,785 m³/d. The total extracted volumes (wells of De Watergroep and other wells combined) have decreased by almost 17%: from 58,662 m³/d in 2004 to 48,972 m³/d in 2020. The water budget for the years 2004 and 2020 is shown in *Figure I. 16*.

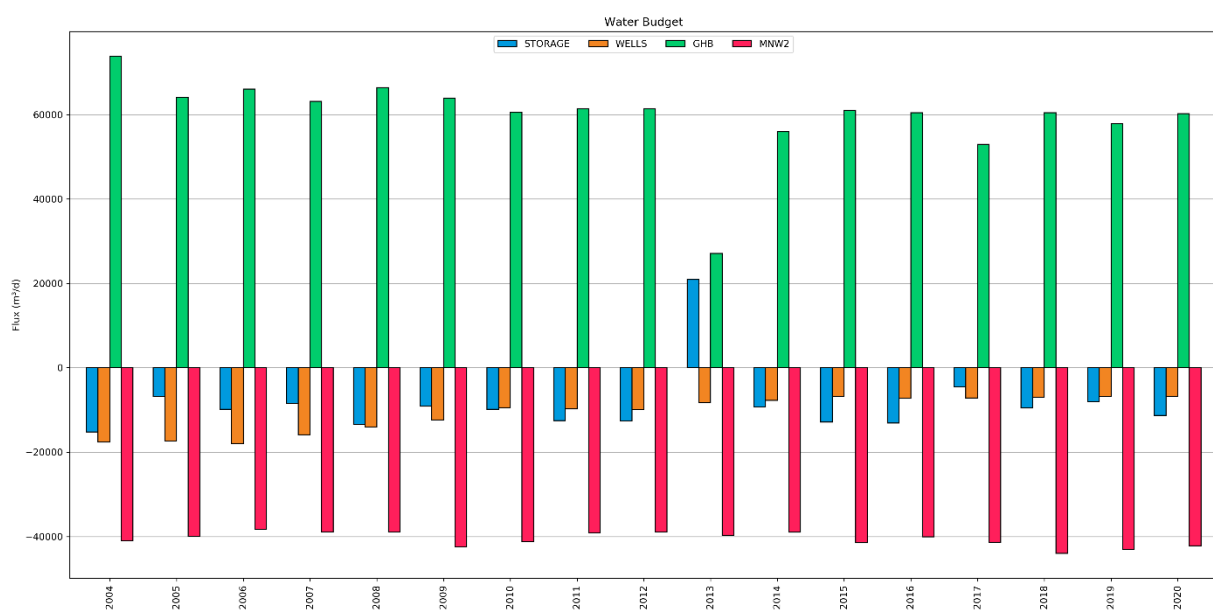


Figure 116: Water budget for the transient Brabant Model. Extraction wells of De Watergroep are modelled with the MNW2 package, other extraction wells with the WEL package. The GHB package is used for both the N, E & W boundaries, and the top boundary.

The inflow into the model consists of the inflow through all the boundaries modelled with the GHB package. This includes both the boundaries at the edge of the model in the north, west and east, as well as the top boundary. The latter consists of the inflow from the layers on top of the modelled layers in the unconfined part of the aquifer system and the leakage through the clay layer of the Formation of Kortrijk in the confined part of the aquifer system. The total inflow through all these GHB boundaries is relatively constant through time, with an average of 59,828 m³/d. The exception is the year 2013 which will be discussed later in this section.

The GHB flow in Figure 116 consists of many different components, including the boundaries at the edge of the model in the north, west and east (GHB_NORTH, GHB_WEST and GHB_EAST), as well as the top boundary. The latter consists of the inflow from the layers on top of the modelled layers in the unconfined part of the aquifer system (GHB_RECH) and the leakage through the clay layer of the Formation of Kortrijk in the confined part of the aquifer system (GHB_KORTRIJK). The water budget for the different GHB components is shown in Figure 117 and Table I. 25. The main inflow consists of the boundary in the east, while the main outflow is for the unconfined part of the aquifer. It might seem contra-intuitive that there is a net outflow in the unconfined area in the south, while this is presumed to be the main recharge area of the aquifer system. This is related to the fact that the GHB boundary in this unconfined part does not only simulate recharge coming into the modelled layers, but it is also used to simulate the discharge in the river valleys. The reason for the net negative flow for this unconfined area is that there is a large inflow into the model area through the east boundary in the south-eastern part of the model (Tienen area), but a large part of this flow discharges in the river valleys close-by. Mainly large discharges are observed in the Kleine Gete valley. The flows for the north and west boundary are small compared to those for the east boundary and the recharge zone. The leakage through the Kortrijk clay is also limited in size with an average inflow of 1,526 m³/d. The GHB water budget for the years 2004 and 2020 is shown in Figure I. 17.

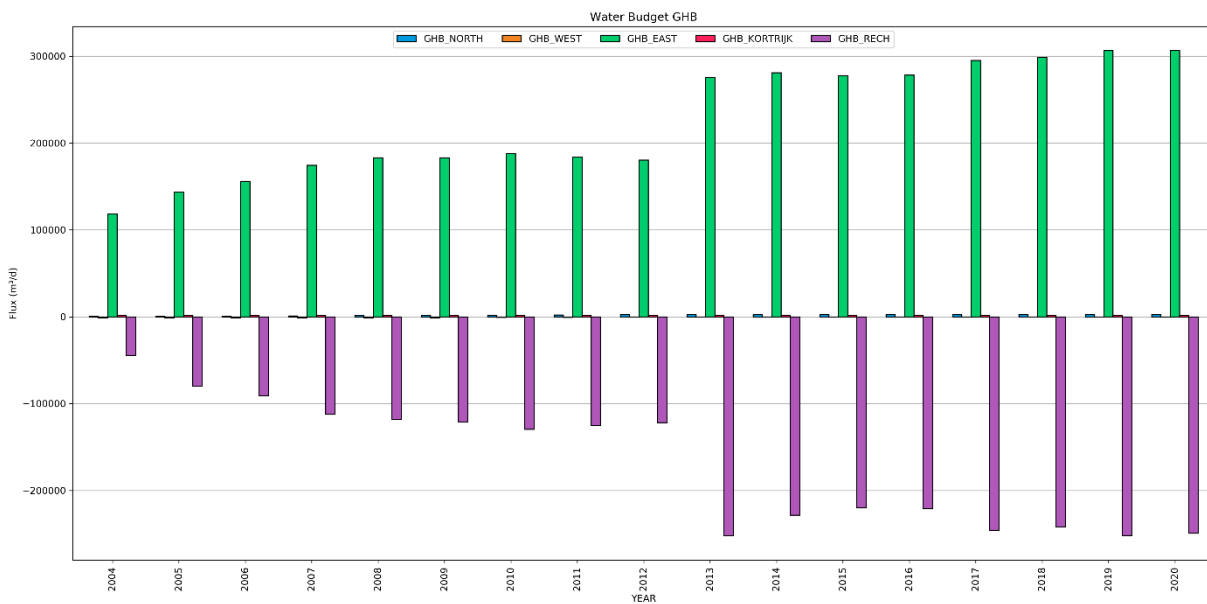


Figure 117: Water budget for the general-head boundaries used in the transient Brabant Model. The GHB package is used for both the N, E & W boundaries, and the top boundary.

The reason for the significant decrease in total GHB inflow (Figure 116) and respectively increase in inflow GHB_EAST and increase in outflow of GHB_RECH (Figure 117) is related to the conceptualization of the GHB boundary in the unconfined area. The hydraulic head specified in this boundary is derived based on a correlation between measured hydraulic heads and the topography. However, the number of heads measured at high elevations is limited. Furthermore, some of these wells at high elevation only have head data until the year 2012. From 2013 onwards, these wells are not taken into account for the correlation, resulting in a shift of the slope of the fit (Table I. 17). This

results in a decrease in head in the higher laying areas and thus a lower recharge in these areas. In the subsequent years, this is compensated by an increased inflow from the eastern boundary. With exception of the year 2013, the total inflow through the GHB boundary remains more or less constant.

4.8 Discussion

The transient Brabant Model is a quite complex model. The calibration results in a decent fit between observed and simulated heads, but the residuals can still be significantly high. This shows that even such a complex model in which lots of data and information is incorporated can still have difficulties simulating the actual situation. The confined character of the Cretaceous aquifer results in large drawdowns and slow evolution to equilibrium level. Combined with the fact that this is a complex geological area with limited data, relatively high residuals of several meters are to be expected. Furthermore, the Brabant model is a large-scale, regional model. It is difficult to find parameter values that result in a good fit in all areas of the model. This issue is of lesser importance for smaller-scale models, as the spatial variability in a smaller area is often much more limited. Moreover, depending on the objective of a certain modelling study, a resolution of 100x100m is relatively coarse. When a detailed analysis for a smaller area is needed, insights from smaller-scale models might give added value, in addition to the results from the large-scale regional model. The results of the regional model could for example be used as boundary conditions for higher-resolution smaller scale models.

There is a strong spatial variability of the hydrogeological properties of the different geological layers. This is obviously the case in the Cretaceous, with very low HK in the north and HKs of several order of magnitude higher in the south. The exact extent of the fracture zones in the south are not known, neither is the extent and permeability of the hardground interval in the north. The model results in the north are very sensitive to changes in the HK of the Cretaceous, with small changes resulting in head differences of meters to even >10m at the extraction sites near Leuven. Furthermore, the Cretaceous deposits are modelled as one layer in the Brabant Model, while in reality there are significant differences in lithology and permeability in the vertical direction. One layer with an equivalent HK does not react the same as two layers with distinct difference in HK, as is the case for the almost impermeable deposits for the Member of Zeven Wegen versus the permeable deposits linked to the hardground interval at the boundary between Zeven Wegen and Lixhe/Lanaye. This is possibly an explanation for the underestimation of the heads in observation wells close to the extraction sites in the Leuven area and for the fact that in e.g., Het Broek the heads in the different wells are closer together than the heads simulated in the model.

Another problem with the calibration of the heads in the Cretaceous is that most of the observations are from extraction wells. Inherently, the uncertainty on these heads is larger than for observation wells due to well losses, possible clogging of the filters, etc. As the simulated heads in the extraction wells are very sensitive to small changes in the model parameters, and the absolute changes in heads are significantly higher in the extraction wells compared to the observation wells, there is the danger that the calibration is focused too much on these extraction wells. One possibility is to assign smaller weights to the extraction wells so that they don't influence the model performance statistics as much as observation wells.

The spatial variability of the hydrogeological properties does not only play an important role for the Cretaceous, but also for the layers of Lincent and Grandglise. For both these layers, the available information is even more limited than for the Cretaceous. For Lincent, most of the available information is from the "tuffeau" zone in the Tienen area. Most of the borehole descriptions and head observation wells are located in this area. However, the exact extent of the "tuffeau" zone is unknown. In this zone, the high permeability of Lincent is a result of increased porosity due to the dissolution of silica combined with the presence of fractures. There seem to be significant lateral changes in the lithology of the Halen/Lincent deposits. In the "tuffeau" zone these deposits are more chalky to marly and often silicified, while in the rest of the Brabant area they are mostly described as clayey sand to silty, with intercalations of sandy clay, often lithified. There is a strong variability in the vertical direction with the alternation of more permeable

and less permeable intervals. The presence of these low permeable intervals results in a strong vertical resistance of this layer, which is clearly demonstrated by the fact that heads in Grandglise in general are not affected by variations in extraction rates in the Cretaceous. In the southern Dijle valley, where the Lincent deposits are closer to the surface, there are some indications that locally there might be fracture zones present (e.g., the water-bearing intervals in Lincent in the extraction wells of Nellebeek). However, the exact extent of these fracture zones is largely unknown. However, it seems that the deposits are much less fractured in this area than in the “tuffeau” zone.

The available information on the hydrogeological properties of Grandglise are even more limited. The extractions of companies to the north of Leuven indicate that permeabilities are decent, with HKs of approx. of 2-3 m/d. The pumping tests performed in the framework of the BSc. Thesis of Sarah Van den Keybus (2019) at the wells of Cadol, Vlierbeek, Campus and Ormendal resulted in HKs of 1.1-2.3 m/d. For the rest, only information is available for the extraction site of Hoeilaart, extracting from the sands of Grandglise. In the model, one homogeneous HK is used for the entire layer of Grandglise, while in reality possibly significant lateral variations in lithology can occur.

The presence and thickness of the confining clay layer of the Formation of Kortrijk also plays a very important role on the model results. This is demonstrated by the effect of the Brusselian channel (see section 1). The geological 3D model of Flanders does not represent the local absence of the Kortrijk clays in this area. Not taking this Brusselian channel into account would lead to an underestimation of the hydraulic heads of several tens of meters in this area. In other areas, the geological layers might also not be 100% accurate. This might mainly be the case in the river valleys in the south. Locally, the confining layers of either the Kortrijk Formation or the Member of Halen/Lincent might be locally eroded, while this is not represented in the geological model. This can significantly influence the simulated hydraulic heads in these areas. This was e.g., the case for the site of Overijse Sana: in reality the Cretaceous deposits are present directly underneath the Quaternary deposits, while in the geological model deposits of Halen/Lincent were present on top of the Cretaceous. In this case, we corrected this locally, but the same issue might arise in other areas.

Another issue is that the geological and hydrogeological data from the part of the Cretaceous in the Walloon region is very limited, while this is an important area for the recharge of both the Paleocene and Cretaceous aquifer systems. Furthermore, the use of the general-head boundary to represent the flow from the overlying layers that are not explicitly modelled in the southern part of the model is a simplification of reality. This GHB incorporates both the recharge reaching the modelled layers in the recharge areas as well as the discharge from these layers towards the rivers in the river valleys. The heads in the overlying layers are simulated using a correlation between head and topography. However, as discussed in the water budget in section 4.7.7, little data is available in the topographically higher areas in the southern part of the model, leading to possible inaccurate estimations of the head. The incorporation of more data from the Walloon region can improve the model performance in this area.

Finally, the historical extractions in the Leuven and Vilvoorde areas play an important role on the performance of the model in these areas. As discussed in section 3.3, little information is present on the causes and extent of these historical overexploitations. However, they must be explicitly taken into account in order to reproduce the evolution of hydraulic heads in these areas.

5 Scenario Analysis

The transient Brabant Model is used to simulate the effect of different extraction scenarios. For this, the model is extended until the year 2040. The new situation in the scenarios is modelled from the year 2021 onwards. This way, the effect of these extraction scenarios on the hydrogeological system in the future can be explored. The extraction rates for each extraction site used in the different scenarios are summarized in Table 24 and Figure 118.

5.1 Overview of scenarios

Scenario 1: Current/normal situation

In this scenario, the extraction rates for normal production are used. For most well sites the production rates of the year 2020 are used. However, due to the temporary shutdown of the Geuzenhoek site, the extraction rates for several other sites (mainly Veeweyde, Het Broek, Pécrot and La Motte) were temporarily increased to compensate for this. For these sites, the average rates over the last 5 years are used. Also, the new production wells at Het Broek are taken into account. The total extraction rate over all extraction sites for this scenario is approx. 13.7M m³/year.

Scenario 2: Maximal permitted situation

In this scenario, the maximal permitted extraction rates are used for all extraction sites. Two different sub scenarios are defined. In **Scenario 2a**, the extraction rates for Het Broek are limited to 2.5M m³/year. In **Scenario 2b**, the effective maximal permitted rate of 4.38M m³/year for Het Broek is used. Historical extraction rates and corresponding hydraulic head data indicate that the maximal permitted rate for Het Broek is too high for sustainable extraction at this site. For Scenario 2a, the total extraction rate is 32% higher than for Scenario 1, while for Scenario 2b this is 46% higher. The total extraction rate over all extraction sites for Scenario 2a and 2b is respectively 18.1M and 20.0M m³/year.

Scenario 3: Current/normal situation +10%

In this scenario, the boundaries of the current/normal situation are explored by adding 10% to the current extraction rates. For all extraction sites, 10% is added to the extraction rates used in Scenario 1. The total extraction rate over all extraction sites for this scenario is approx. 15.1M m³/year.

Scenario 4: Venusberg +100%/+300%

In this scenario, the planned increase in extraction rates for the Venusberg site is simulated. Two different sub scenarios are defined. In **Scenario 4a**, the extraction rate for Venusberg is increased with 100%. In **Scenario 4b**, the extraction rate is increased with 300%. For Scenario 4a, the total extraction rate is 3.4% higher than for Scenario 1, while for Scenario 4b this is 9.8% higher. The total extraction rate over all extraction sites for Scenario 4a and 4b is respectively 14.2M and 15.1M m³/year.

Scenario 5: no extraction De Watergroep in Cretaceous

In this scenario, the rates of all extraction sites of De Watergroep in the Cretaceous Aquifer are set to zero.

Table 24: Overview of extraction rates for each extraction site used in the different scenario, including the permitted rates, the rates for 2020 and the average rate over the last five years (2016-2020).

(in m ³ /year)	Permit	2020	2016-2020*	Scenario 1	Scenario 2a	Scenario 2b	Scenario 3	Scenario 4a	Scenario 4b
Total	20,015,800	13,267,852	13,869,193	13,755,953	18,135,800	20,015,800	15,131,549	14,225,066	15,101,066
Het Broek	4,380,000	3,000,531	2,566,820	2,500,000	2,500,000	4,380,000	2,750,000	2,504,901	2,504,901
Pécrot	3,285,000	2,079,499	1,755,314	1,755,314	3,285,000	3,285,000	1,930,846	1,755,314	1,755,314
La Motte	2,920,000	2,614,903	2,428,440	2,428,440	2,920,000	2,920,000	2,671,284	2,428,440	2,428,440
Veeweyde	2,372,500	2,545,806	1,952,360	1,952,360	2,372,500	2,372,500	2,147,596	1,952,360	1,952,360
Geuzenhoek	2,372,500	0	2,015,715	2,015,715	2,372,500	2,372,500	2,217,287	2,015,715	2,015,715
Sana	1,752,000	1,527,935	1,466,241	1,527,935	1,752,000	1,752,000	1,680,729	1,527,935	1,527,935
Biez	963,000	287,249	355,931	287,249	963,000	963,000	315,974	287,249	287,249
Venusberg	438,000	334,777	411,789	411,789	438,000	438,000	452,967	876,000	1,752,000
Aarschot	438,000	230,565	237,751	230,565	438,000	438,000	253,622	230,565	230,565
Cadol	262,800	170,413	192,317	170,413	262,800	262,800	187,454	170,413	170,413
Kouterstraat	262,800	138,136	149,179	138,136	262,800	262,800	151,950	138,136	138,136
Abdij	219,000	153,335	164,277	153,335	219,000	219,000	168,669	153,335	153,335
Vlierbeek	175,200	108,546	121,616	108,546	175,200	175,200	119,401	108,546	108,546
Nellebeek	175,000	76,157	51,443	76,157	175,000	175,000	83,773	76,157	76,157

*average rates for 2016-2020 with removal of outliers

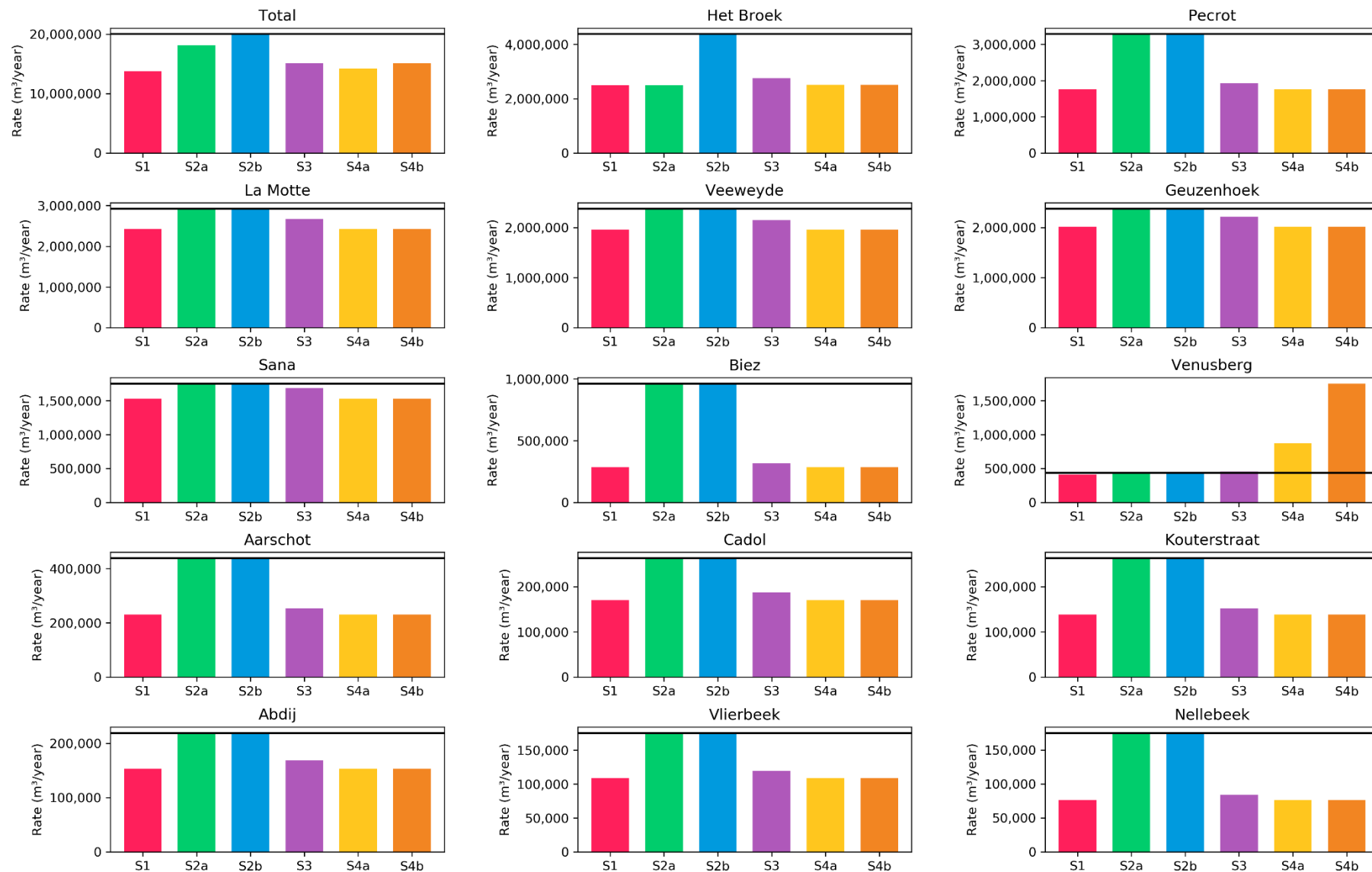


Figure 118: Overview of extraction rates for each extraction site used in the different scenarios. Black line is the permitted rate.

5.2 Scenario 1: Current/normal situation

In this scenario, the extraction rates for the current normal production are used. For most well sites, the production rates of the year 2020 are used. Due to the temporary shutdown of the Geuzenhoek site, the extraction rates for several sites (e.g., Veeweyde, Het Broek, Pécrot and La Motte) were increased to compensate for this. For these well sites, the average rate for the last five years was used. For the site of Venusberg, the extraction rate in 2020 was also temporarily lower than usual due to maintenance on the production well. Hence, also the average of the last five years was used. For the site of Het Broek, the new extraction wells 3008-063 and 3008-064 were taken into production in 2020, while the production in extraction well 3008-005 was phased out. To compensate for the temporary shutdown of Geuzenhoek, the total extraction rate at Het Broek was 3M m³/year in 2020. For the following years, a normalization to 2.5M m³/year is assumed. There is a slight shift in capacity from the wells in the north (3008-002 & 3008-003) towards the south (3008-063 & 3008-064).

The simulated head maps for the Cretaceous for the years 2020, 2030, and 2040 are shown in Figure 119. The simulated head maps for Grandglise and Lincent are added to the Appendix (Figure I. 18). To highlight the changes in head, difference maps are created for the situation in 2018 versus 2040 (Figure 120). The situation in 2018 is used to avoid the effect of the temporary shutdown of Geuzenhoek in 2019-2020 on these results. In general, we see two areas in which there is a significant increase in heads throughout time: the Vilvoorde & Leuven areas. This increase is the result of the recovery of the system from the historical extractions in the Vilvoorde area in both the Grandglise and Cretaceous aquifer and in the Leuven area in the Cretaceous aquifer (see section 3.3). For the rest, there are no clear significant increases or decreases in head in the model area. These results show that the model does not predict any clear decreasing head trends for the current situation.

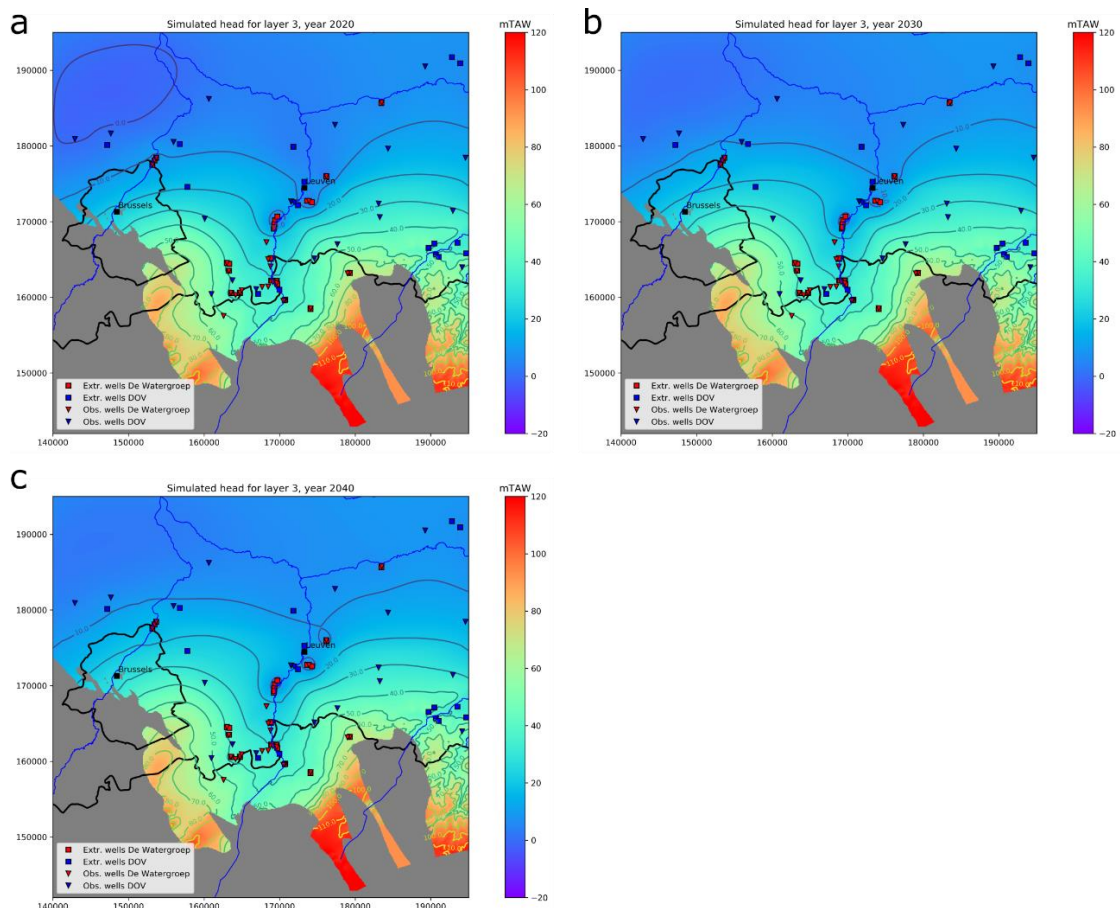


Figure 119: Simulated heads for the Cretaceous Aquifer for Scenario 1 for: (a) 2020; (b) 2030; and (c) 2040.

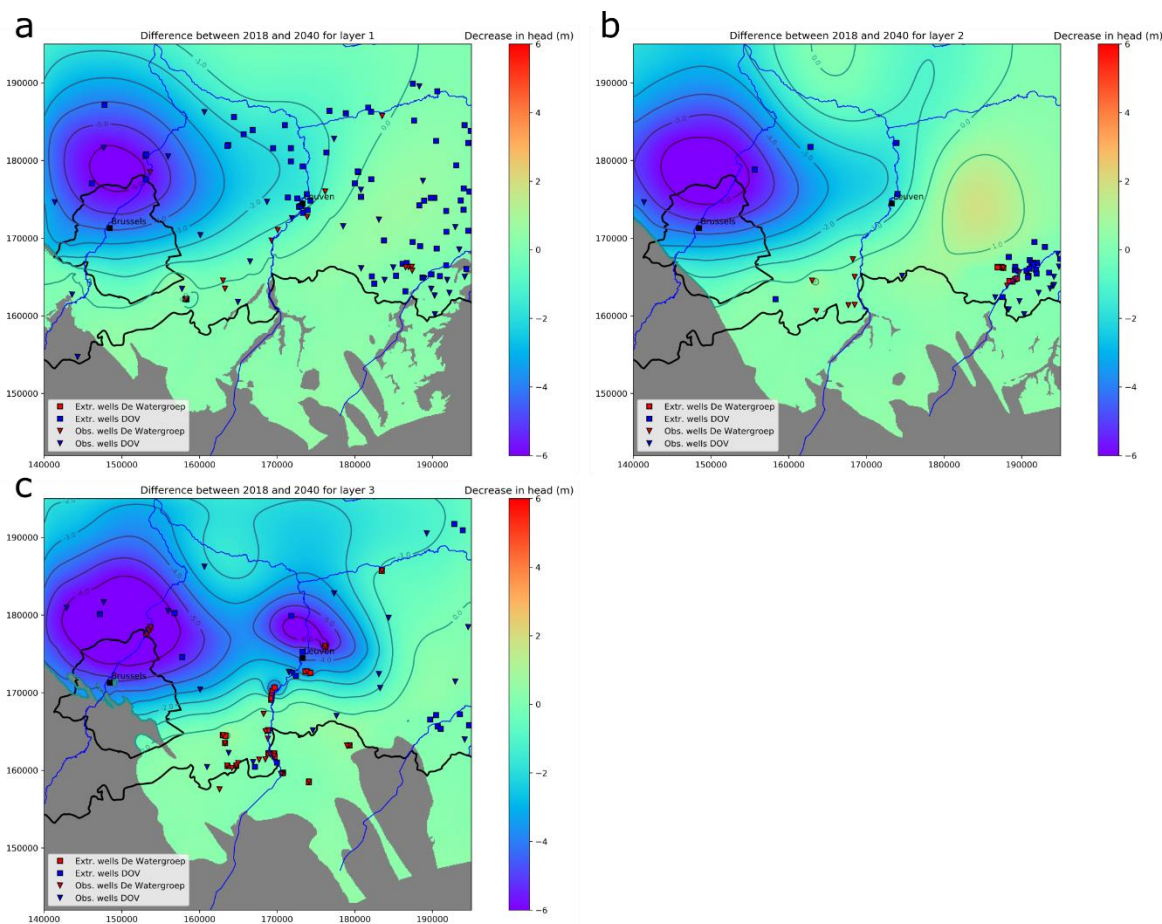


Figure 120: Difference in simulated heads for Scenario 1 between years 2018 and 2040 for: (a) Grandglaise; (b) Lincent; and (c) the Cretaceous.

Similar difference maps are created for the years 2010 versus 2040 (Figure I. 19). The effect of the recovery of the historical extractions is very clear. Furthermore, also a decrease of head in the southern, unconfined part of the modelled system is visible. This is related to a decrease in head in the overlying layers, which might be explained by the occurrence of several dry years in the late 2010s.

In the Appendix (Figure I. 20 and Figure I. 21), plots of the drawdown over time with respect to the situation in 2020 are shown for all the extraction sites in the Cretaceous. In general, these show that there are no clear decreasing trends simulated for the extraction sites in the Cretaceous. For some sites near Leuven, there is even an increase in head through time (up to 5m), which is related to the recovery of historical extractions in this area. Most of the changes from 2021 onwards can be explained by slight changes in extraction rates compared to the previous years. In general, equilibrium is reached relatively fast (couple of years at max). For Geuzenhoek, the effect of the temporary shutdown (2020) and restart of the production (2021) is clearly visible.

In Figure 121 the difference between the simulated head in the Cretaceous and the top of the Cretaceous is shown for the years 2020 and 2040. This difference indicates the 'potential' left for extraction, i.e., for the confined part of the aquifer, the head should not be lower than the top of the Cretaceous aquifer. Only for the extraction site of Biez the head in the Cretaceous is lower than the top of the Cretaceous. However, in this area the Cretaceous is unconfined, and thus this criterium is not valid. For one of the wells of La Motte (3012-020) the difference is lower than 5m. However, this well is also located in the unconfined part of the aquifer. For all other extraction wells, the difference is >5m. In Table 25 the difference between the simulated head and the top of the Cretaceous is shown for all the extraction wells. In Table I. 26 the change in head between the situation in 2020 and 2040 is shown for all extraction wells.

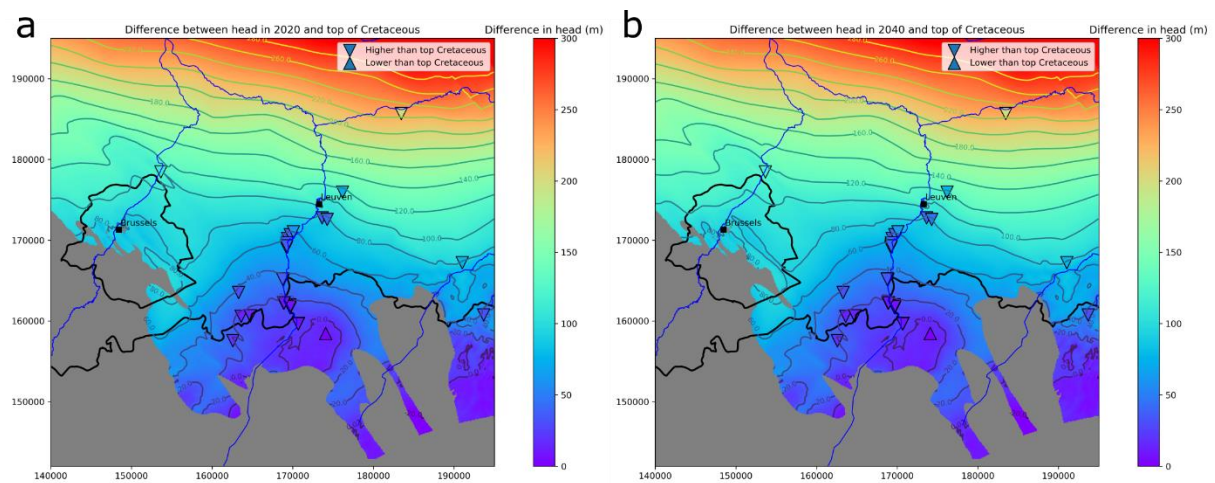


Figure 121: Difference in simulated heads for the Cretaceous in Scenario 1 and the top of the Cretaceous for: (a) the year 2020; and (b) the year 2040.

Table 25: Difference between head in Cretaceous and top of Cretaceous in the production wells in the Cretaceous for all scenarios.

Difference between head in Cretaceous and top of Cretaceous (in m)								
Well name	S1 (2020)	S1 (2040)	S2a (2040)	S2b (2040)	S3 (2040)	S4a (2040)	S4b (2040)	S5 (2040)
3001-108-F0	199.68	200.81	176.38	176.38	198.09	200.81	200.81	227.97
3006-001-F0	35.82	38.88	8.44	6.41	32.82	38.88	38.88	99.49
3006-116-F0	42.86	45.79	22.99	21.26	40.44	45.78	45.78	99.26
3007-001-F0	71.47	76.44	44.17	43.73	71.06	76.44	76.44	130.29
3008-001-F0	51.37	52.46	51.50	37.14	50.11	52.44	52.42	75.94
3008-002-F0	31.60	36.52	35.54	7.79	32.24	36.51	36.49	79.36
3008-003-F0	39.80	43.50	42.46	19.27	39.62	43.49	43.47	82.30
3008-004-F0	60.83	63.36	62.19	50.35	61.32	63.35	63.33	83.77
3008-005-F0	45.16	48.54	47.58	30.40	45.84	48.53	48.50	75.53
3008-006-F0	40.96	43.03	42.07	22.81	39.79	43.01	42.99	75.40
3008-063-F0	39.68	43.81	42.85	21.29	40.64	43.80	43.77	75.53
3008-064-F0	37.89	42.80	41.84	17.28	39.48	42.79	42.76	76.04
3010-001-F0	17.31	17.14	<u>-9.59</u>	<u>-10.03</u>	14.27	16.80	16.17	45.74
3010-002-F0	31.32	31.15	20.57	20.12	29.69	30.82	30.19	45.74
3011-005-F0	13.46	12.67	12.20	12.15	12.19	8.05	-0.66	17.52
3011-008-F0	9.19	9.12	8.03	7.96	8.41	8.97	8.70	16.21
3011-009-F0	14.64	14.56	14.31	14.23	14.38	14.43	14.17	16.35
3011-015-F0	20.77	20.68	20.57	20.54	20.63	20.40	19.88	21.25
3012-001-F0	8.21	8.60	8.02	7.72	8.30	8.59	8.59	11.56
3012-002-F0	9.42	9.52	9.20	8.95	9.35	9.52	9.51	11.22
3012-003-F0	9.02	9.22	8.77	8.48	8.99	9.22	9.21	11.56
3012-007-F0	35.49	30.39	28.99	25.93	29.27	30.38	30.35	41.56
3012-008-F0	36.54	31.42	30.00	26.83	30.28	31.40	31.38	42.82
3012-009-F0	36.51	33.07	31.94	28.75	32.09	33.05	33.02	42.82
3012-013-F0	9.75	9.78	9.46	9.41	9.73	9.78	9.78	10.30
3012-014-F0	9.60	9.87	8.56	8.46	9.71	9.87	9.87	11.48
3012-015-F0	7.27	7.47	6.21	6.15	7.30	7.47	7.47	9.17
3012-016-F0	7.92	8.03	7.09	7.04	7.89	8.03	8.02	9.41
3012-020-F0	<u>2.34</u>	<u>2.65</u>	<u>1.93</u>	<u>1.93</u>	<u>2.34</u>	<u>2.65</u>	<u>2.65</u>	5.83
3012-021-F0	7.29	7.31	7.15	7.15	7.19	7.31	7.31	8.48
3012-059-F0	8.09	8.50	7.96	7.71	8.23	8.50	8.49	11.22
3013-001-F0	77.48	77.48	77.48	77.48	77.48	77.48	77.48	77.48
3014-001-F0	112.46	118.25	118.23	118.19	118.24	118.25	118.25	118.34
3017-001-F0	32.42	32.42	32.42	32.42	32.42	32.42	32.42	32.42
3020-001-F0	<u>-6.81</u>	<u>-6.81</u>	<u>-9.53</u>	<u>-9.53</u>	<u>-6.93</u>	<u>-6.81</u>	<u>-6.81</u>	<u>-5.66</u>

5.3 Scenario 2: Maximal permitted situation

In this scenario, the maximal permitted extraction rates are used for all extraction sites. Two different sub scenarios are defined. In **Scenario 2a**, the extraction rates for Het Broek are limited to 2.5M m³/year. In **Scenario 2b**, the effective maximal permitted rate of 4.38M m³/year for Het Broek is used. Historical extraction rates and corresponding hydraulic head data indicate that the maximal permitted rate for Het Broek is too high for sustainable extraction at this site. For Scenario 2a, the total extraction rate is 32% higher than for Scenario 1, while for Scenario 2b this is 46% higher.

Scenario 2a: Maximal permitted rates + Het Broek at 2.5M m³/year

The simulated head maps for the Cretaceous for the years 2030 and 2040 are shown in Figure 122. The simulated head maps for Grandglise and Lincent are added to the Appendix (Figure I. 22). To highlight the changes in head, difference maps are created for the situation in 2040 for scenario 2a compared scenario 1 (Figure 123). These maps show the additional drawdown resulting from the increase in extraction rates to the maximal permitted rates. For the Cretaceous, the largest drawdowns are present in the Leuven area, due to the extractions in Vlierbeek, Cadol and Abdij. Drawdown is larger than 1 meter in an area with a diameter of 10km. Close to the extraction wells, drawdown is larger than 5m. Other areas with significant drawdown are the Nellebeek/Kouterstraat area and the Aarschot area. In the former, drawdown is larger than 1m in an area with 5km in diameter. The effects of the increased drawdown are visible in the entire confined part of the Dijle valley, with drawdown larger than 0.5m. In Aarschot, there is also drawdown of more than 1m in an area of approx. 5km. In the southern unconfined aquifer, no clear drawdown is visible. In Lincent, there is a clear drawdown due to the extraction site of Nellebeek (Figure I. 22). At this site, part of the water is produced from filters in the Member of Lincent. Furthermore, a limited drawdown is visible in the Leuven area, related to the extractions in the Cretaceous. In Grandglise, drawdown is limited except for the Nellebeek area where drawdown up to 1m is simulated (Figure I. 22).

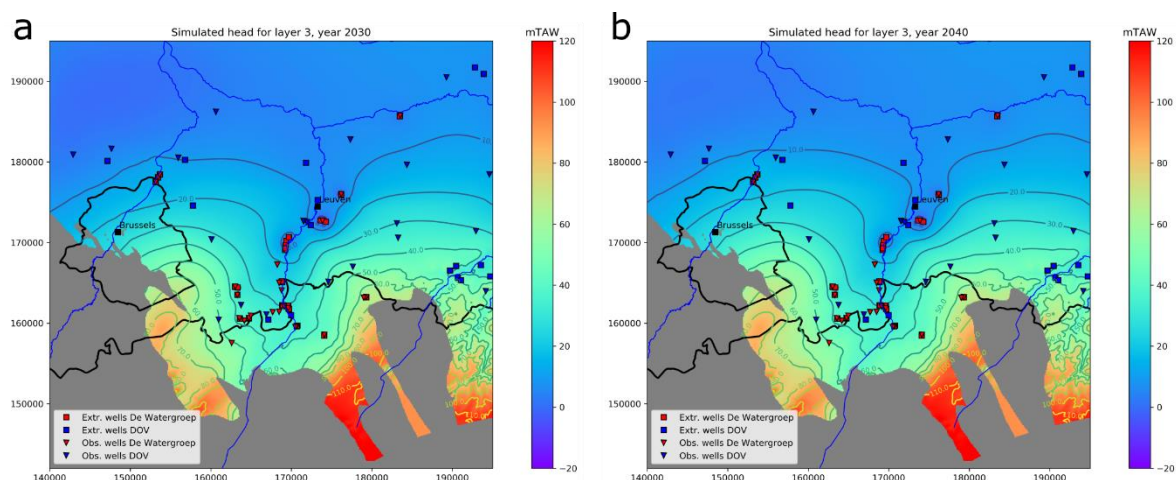


Figure 122: Simulated heads for the Cretaceous Aquifer for Scenario 2a for: (a) the year 2030; and (b) the year 2040.

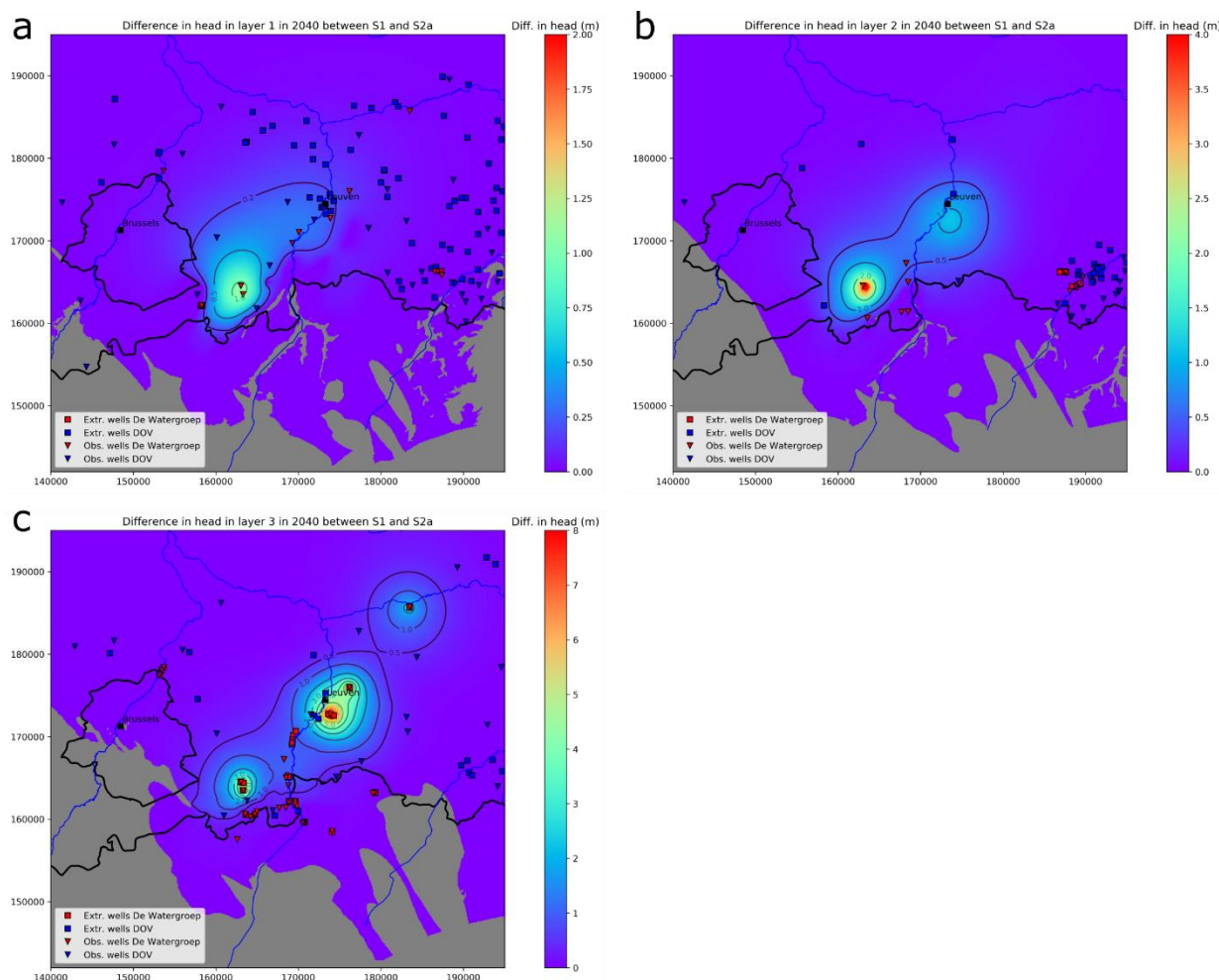


Figure 123: Difference in simulated head in the year 2040 between Scenario 1 and Scenario 2a for: (a) Grandgliste; (b) Lincent; (c) the Cretaceous.

In Figure 124 and Figure 125 the drawdown over time compared to the year 2020 for the different extraction sites is shown. Figure 124a shows the extraction sites with the largest simulated drawdowns in the wells, with a drawdown >25m for Vlierbeek, Cadol and Kouterstraat, and a drawdown >20m for Aarschot, Nellebeek and Abdij. The largest part of the drawdown takes part in the first year after the changes. For most of these wells, equilibrium is reached after 5 to 10 years. For the sites of Venusberg, Sana and Veeweyde the drawdown is limited (Figure 124b), with >1m drawdown for Venusberg and Sana, and 0.2m for Veeweyde. Equilibrium is reached after approx. 5 years for Sana and Veeweyde, and after 10 years for Venusberg. For the sites in the Walloon region, the drawdown is limited, and equilibrium state is reached after 1 to 2 years (Figure 124c). Simulated drawdown is >2.5m for Biez, around 1m for Pécrot and <0.5m for La Motte. For the site of Het Broek, first there is an increase in heads due to a lowering of the extraction rates compared to 2020 (3M vs 2.5 m³/year; Figure 125a). This results in an increase in head of up to 4m in the first years. In the next years, there is a slight decline in head, which is related to the increased extraction in the Cretaceous Aquifer as a whole. As the Geuzenhoek site was not in production in 2020, the resulting drawdown is relatively high (up to 7m), but it represents the total drawdown due to extraction at this site (Figure 125b). The change in head between the situation in 2020 and 2040 in the production wells in the Cretaceous is summarized in Table I. 26.

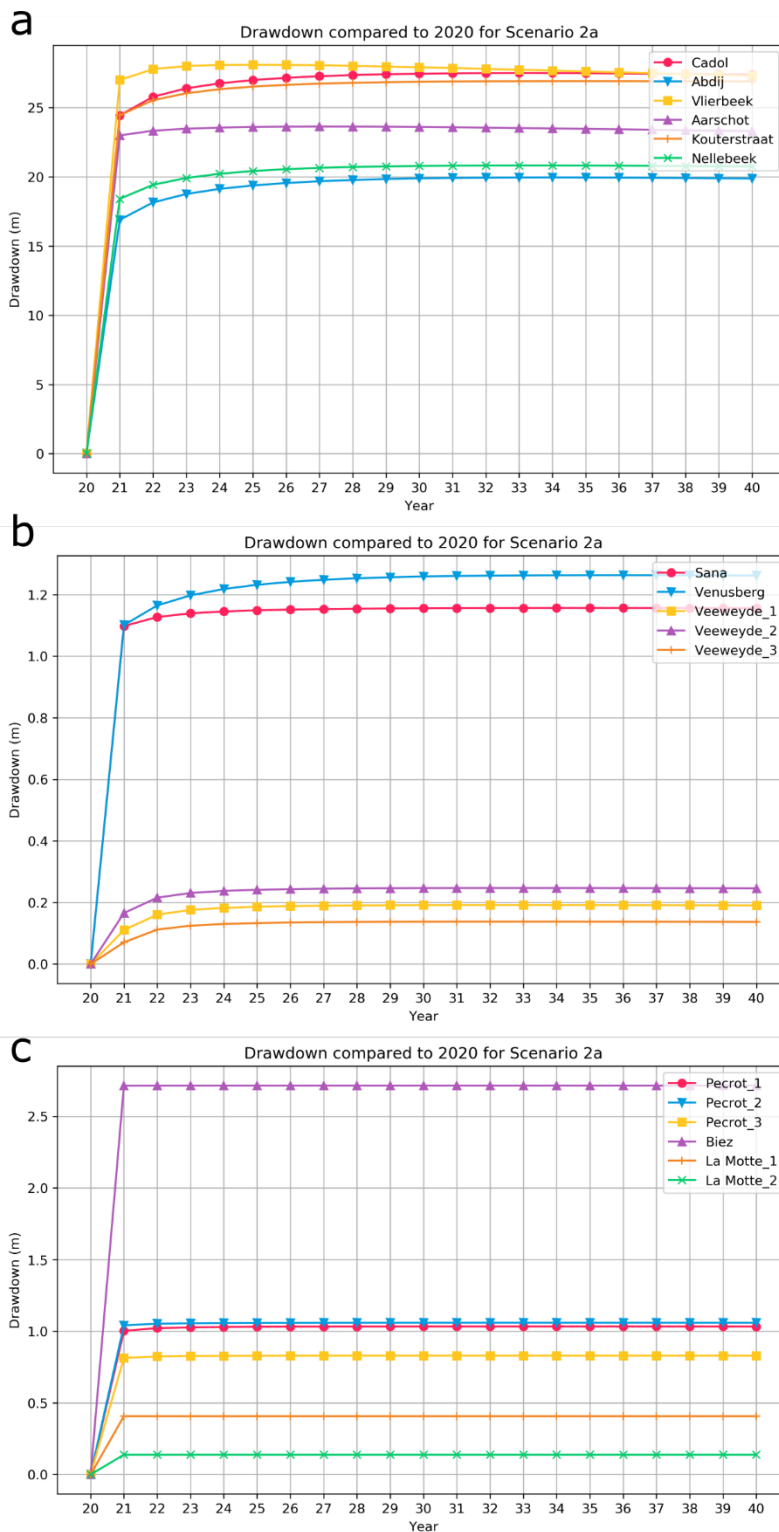


Figure 124: Drawdown over time compared to the heads in 2020 for Scenario 2a at the extraction wells of: (a) Cadol, Abdij, Vlierbeek, Aarschot, Kouterstraat and Nellebeek; (b) Sana, Venusberg and Veeweyde; and (c) Pécrot, Biez and La Motte.

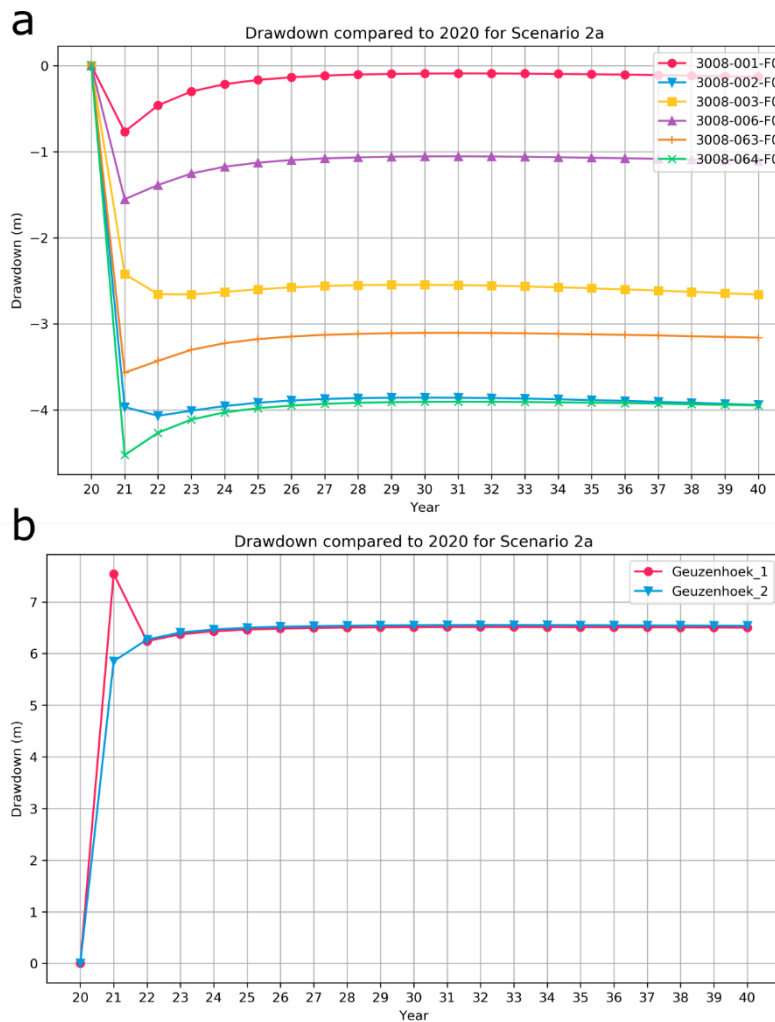


Figure 125: Drawdown over time compared to the heads in 2020 for Scenario 1 at the extraction wells of: (a) Het Broek; and (b) Geuzenhoek.

In Figure 126 the difference between the simulated head in the Cretaceous and the top of the Cretaceous is shown for the year 2040. Compared to Scenario 1, not only Biez but also Kouterstraat has a simulated head below the top of the Cretaceous. As the Cretaceous is confined in this area, this indicates that this situation is not sustainable. Note that the permitted extraction rates for Kouterstraat are almost twice as high as the effective rates in recent years. In this scenario, the extraction rates are thus doubled for this site, explaining the large effect on the drawdown. For one of the wells of La Motte (3012-020) the difference is lower than 5m. However, this well is located in the unconfined part of the aquifer. For all other extraction wells, the difference is >5m. In Table 25 the difference between the simulated head and the top of the Cretaceous is shown for all the extraction wells.

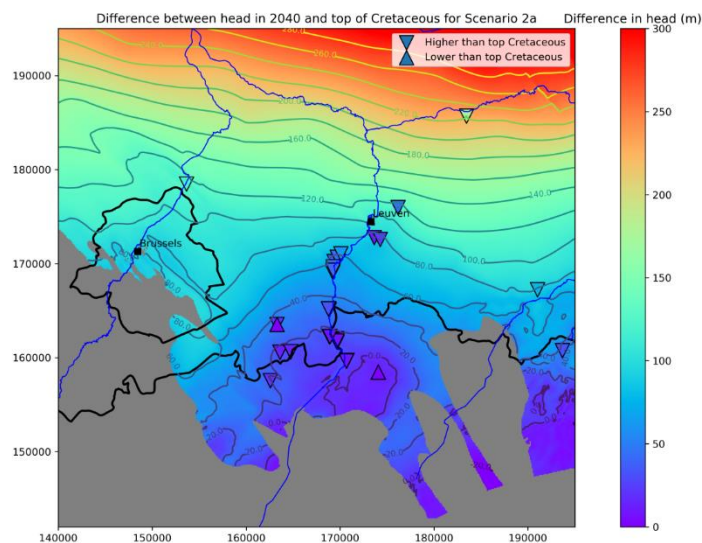


Figure 126: Difference in simulated heads in the Cretaceous and the top of the Cretaceous for Scenario 2a.

Scenario 2b: Maximal permitted rates + Het Broek at 4.38M m³/year

The simulated head maps for the Cretaceous for the years 2030 and 2040 are shown in Figure 127. The simulated head maps for Grandglise and Lincent are added to the Appendix (Figure I. 23). These maps clearly show a more significant effect of the extraction of Het Broek compared to Scenario 2a (Figure 122). This is more clearly visible in the difference maps for scenario 2b compared to scenario 1 for the head in the Cretaceous 2040 (Figure 128). A large area around Het Broek shows significant drawdowns of up to >10m. In an area of about 20km by 10km around Het Broek and the Leuven sites, there is more than 4m in drawdown. The effect on the southern extraction sites (Sana, Venusberg and the sites in the Walloon Region) is limited. The increased extraction of Het Broek also clearly affects the overlying layers (Lincent and Grandglise). In Lincent, drawdown up to 5m is visible near Het Broek (Figure I. 23). Furthermore, drawdown >1m is simulated for the entire area between Leuven and Overijse. In Grandglise, an increase in drawdown is visible, up to 2m around Het Broek and drawdown >0.5m in the area between Leuven and Overijse (Figure I. 23).

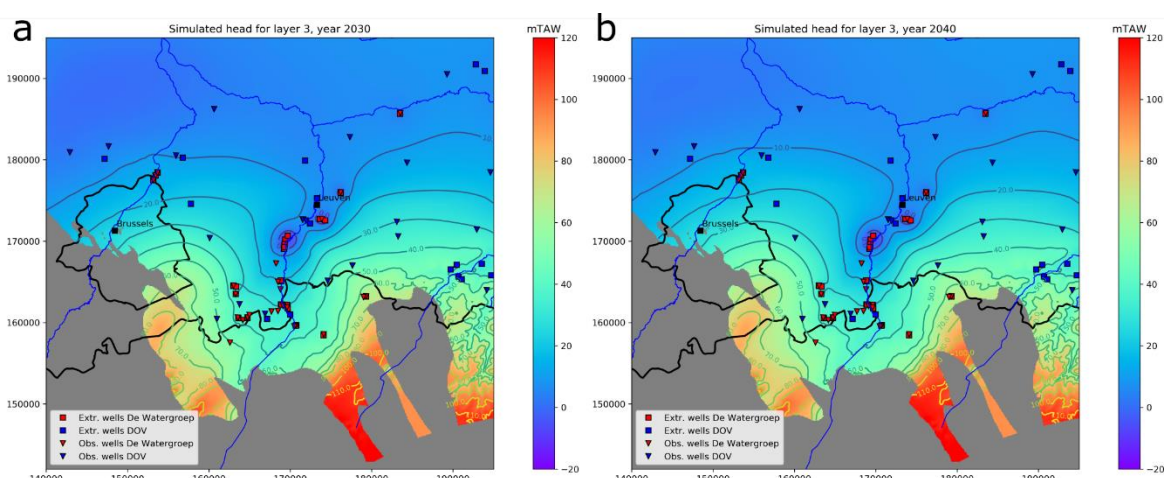


Figure 127: Simulated heads for the Cretaceous Aquifer for Scenario 2b for: (a) the year 2030; and (b) the year 2040.

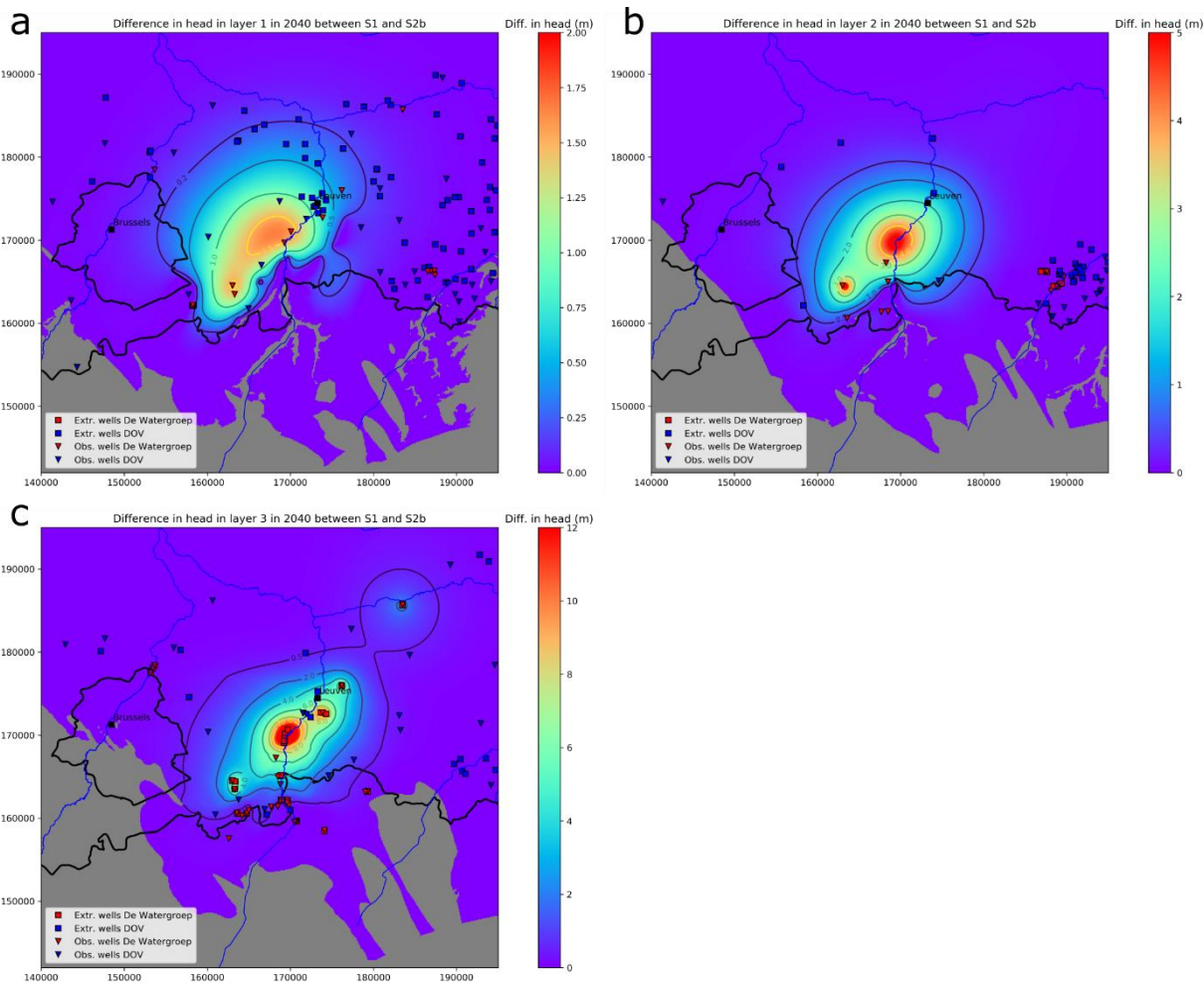


Figure 128: Difference in simulated head in the year 2040 between Scenario 1 and Scenario 2b for: (a) Grandglaise; (b) Lincent; (c) the Cretaceous.

In Figure 129 and Figure I. 24 the drawdown over time compared to the situation in 2020 is shown for the different extraction sites. For the sites near Leuven, there is an increase in drawdown compared to Scenario 2a of 0.5 (Vlierbeek) to 2m (Abdij and Cadol) (Figure 129a). For Kouterstraat and Nellebeek, the increase in drawdown is limited (<0.5m) and there is no difference for Aarschot. In Figure 129b the drawdown for the wells of Het Broek are shown. For these wells, drawdowns of 15 to 25m are simulated. It takes approx. 20 years to reach an equilibrium state. However, there is still a small decrease of approx. 1 cm per year for 2040 meaning equilibrium has not been reached completely yet. For the Geuzenhoek site, an additional drawdown of approx. 3m is simulated (Figure 129c). The most southern well sites (Sana, Venusberg, Veeweyde and the sites in the Walloon Region) are not significantly affected (see Figure I. 24 in the Appendix). The change in head between the situation in 2020 and 2040 in the production wells in the Cretaceous is summarized in Table I. 26.

In Figure 130 the difference between the simulated head in the Cretaceous and the top of the Cretaceous is shown for the year 2040. Similar to Scenario 2a, only Biez and Kouterstraat have heads below the top of the Cretaceous and for one well of La Motte the difference is lower than 5m. The difference with the top of the Cretaceous decreases significantly for the wells of Het Broek, with the lowest difference of 7.8m for 3008-002. This indicates that the head in the Cretaceous is dangerously close to the top of the Cretaceous in this area under these extraction conditions, and that extracting at these high permitted rates is not advised. In Table 25 the difference between the simulated head and the top of the Cretaceous is shown for all the extraction wells.

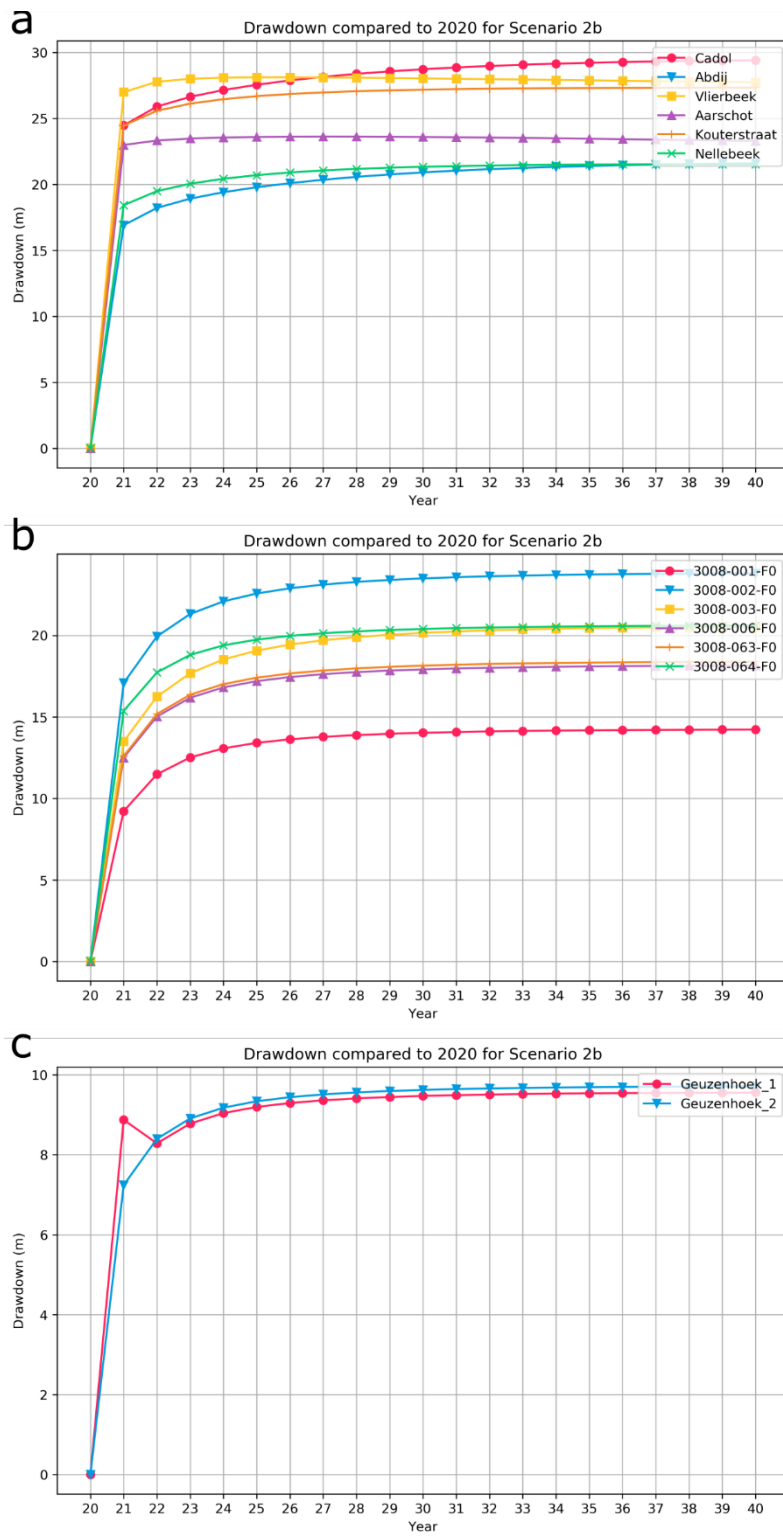


Figure 129: Drawdown over time compared to the heads in 2020 for Scenario 2b at the extraction wells of: (a) Cadol, Abdij, Vlierbeek, Aarschot, Kouterstraat and Nellebeek; (b) Het Broek; and (c) Geuzenhoek.

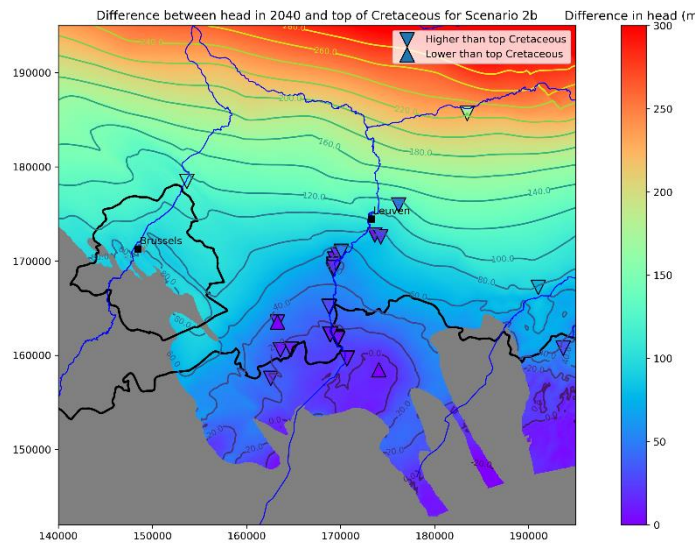


Figure 130: Difference in simulated heads in the Cretaceous and the top of the Cretaceous for Scenario 2b.

5.4 Scenario 3: Current/normal situation +10%

In this scenario, the boundaries of the current/normal situation are explored by adding 10% to the current extraction rates. For all extraction sites, 10% is added to the extraction rates used in Scenario 1.

The simulated head maps for the Cretaceous for the years 2030 and 2040 are shown in Figure 131. The simulated head maps for Grandglise and Lincent are added to the Appendix (Figure I. 25). To highlight the changes in head, difference maps are created for the situation in 2040 for scenario 3 compared scenario 1 (Figure 132). The main area in which a significant drawdown is simulated in the Cretaceous is the region of Het Broek. A 10% increase in rate for this site is quite significant due to the high total rates (from 2.5M m³/year to 2.75M m³/year). The area surrounding Het Broek and the sites of Cadol and Abdij shows drawdowns >1m. Except for some small regions around Vlierbeek and Kouterstraat/Nellebeek, the effect of a 10% increase is relatively limited. The drawdown in Grandglise and Lincent is limited, with respectively a drawdown of <0.5m and <1m in the region of Het Broek (Figure I. 25).

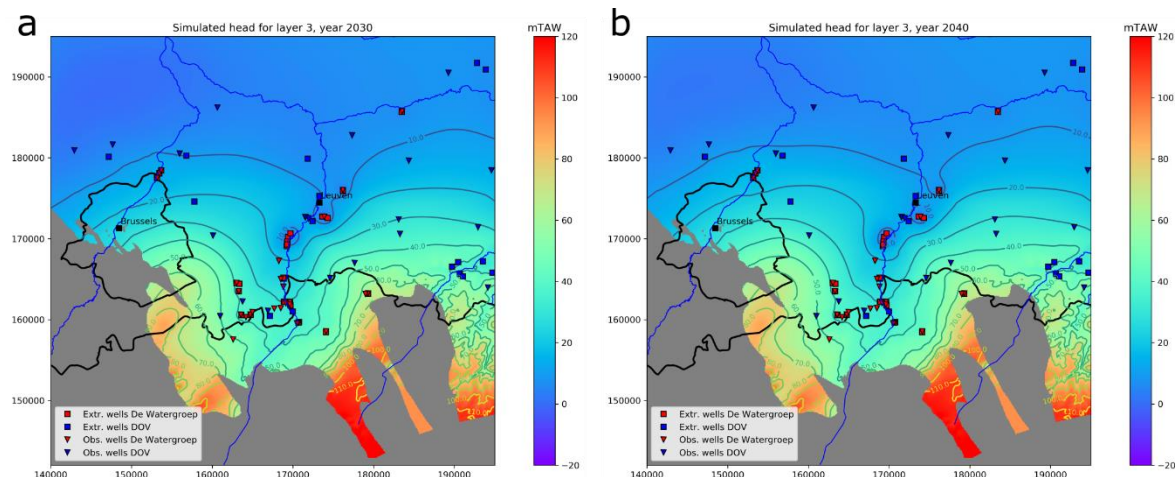


Figure 131: Simulated heads for the Cretaceous Aquifer for Scenario 3 for: (a) the year 2030; and (b) the year 2040.

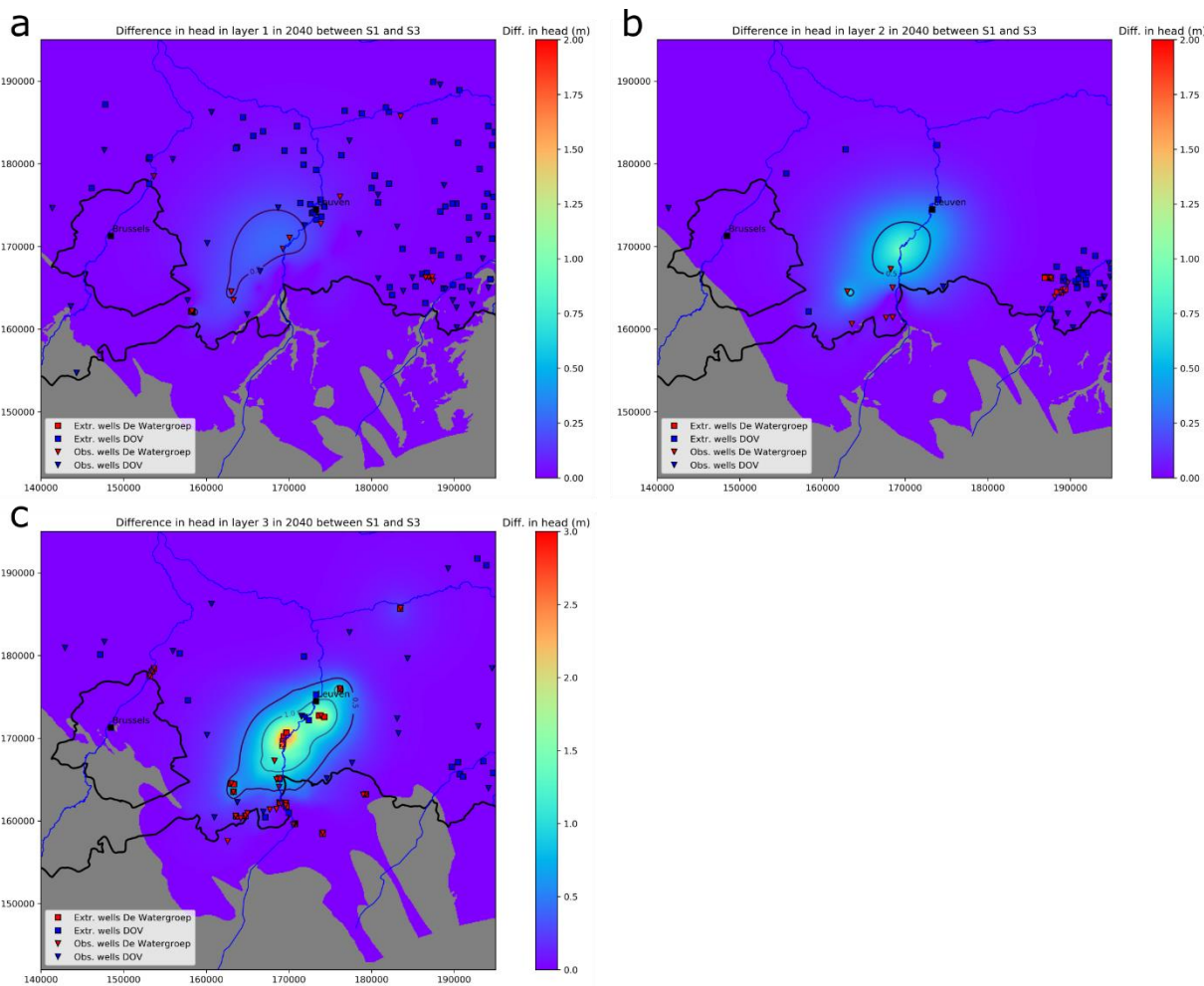


Figure 132: Difference in simulated head in the year 2040 between Scenario 1 and Scenario 3 for: (a) Grandglise; (b) Lincent; (c) the Cretaceous.

In Figure 133 and Figure 134 the simulated drawdown over time for the different extraction sites is shown. For the wells in the northern part of the study area (Aarschot, Vlierbeek, Cadol and Abdij) there is initially an increase in drawdown of 2-5m which then gradually decreases (Figure 133a). This decrease is related to the recovery of the head in the Cretaceous from historical extractions in the Leuven area. For Kouterstraat and Nellebeek the simulated drawdown is 2-3m (Figure 133a). For the sites of Sana and Venusberg, the drawdown is limited to 0.5 to 1.5m, while for Veeweyde there is a slight increase in head (Figure 133b). The latter can be explained by the temporarily higher extraction rates for Veeweyde in 2020 to compensate for the temporary shutdown of the Geuzenhoek site. For the sites in the Walloon Region there is a very slight increase or decrease in heads (Figure 133c). The drawdown for the wells of Het Broek are shown in Figure 134a. Wells 3008-001/003/006 show a decrease in head (<1.5m) while wells 3008-002/063/064 show an increase in head (<2.5m). These changes are related to the change in rate for each well with respect to the rate in 2020 which was a year with an exceptionally high rate and with some changes in the distribution among the different production wells. For the wells of Geuzenhoek, there is a drawdown of approx. 6m due to the activation of these wells after temporary shutdown of this site (Figure 134b). The change in head between the situation in 2020 and 2040 in the production wells in the Cretaceous is summarized in Table I. 26.

In Figure 135 the difference between the simulated head in the Cretaceous and the top of the Cretaceous is shown for the year 2040. Results are similar to Scenario 1 with only Biez having a head lower than the top of the Cretaceous, and La Motte having a difference <5m. However, both are wells in the unconfined part of the aquifer. In Table 25 the difference between the simulated head and the top of the Cretaceous is shown for all the extraction wells.

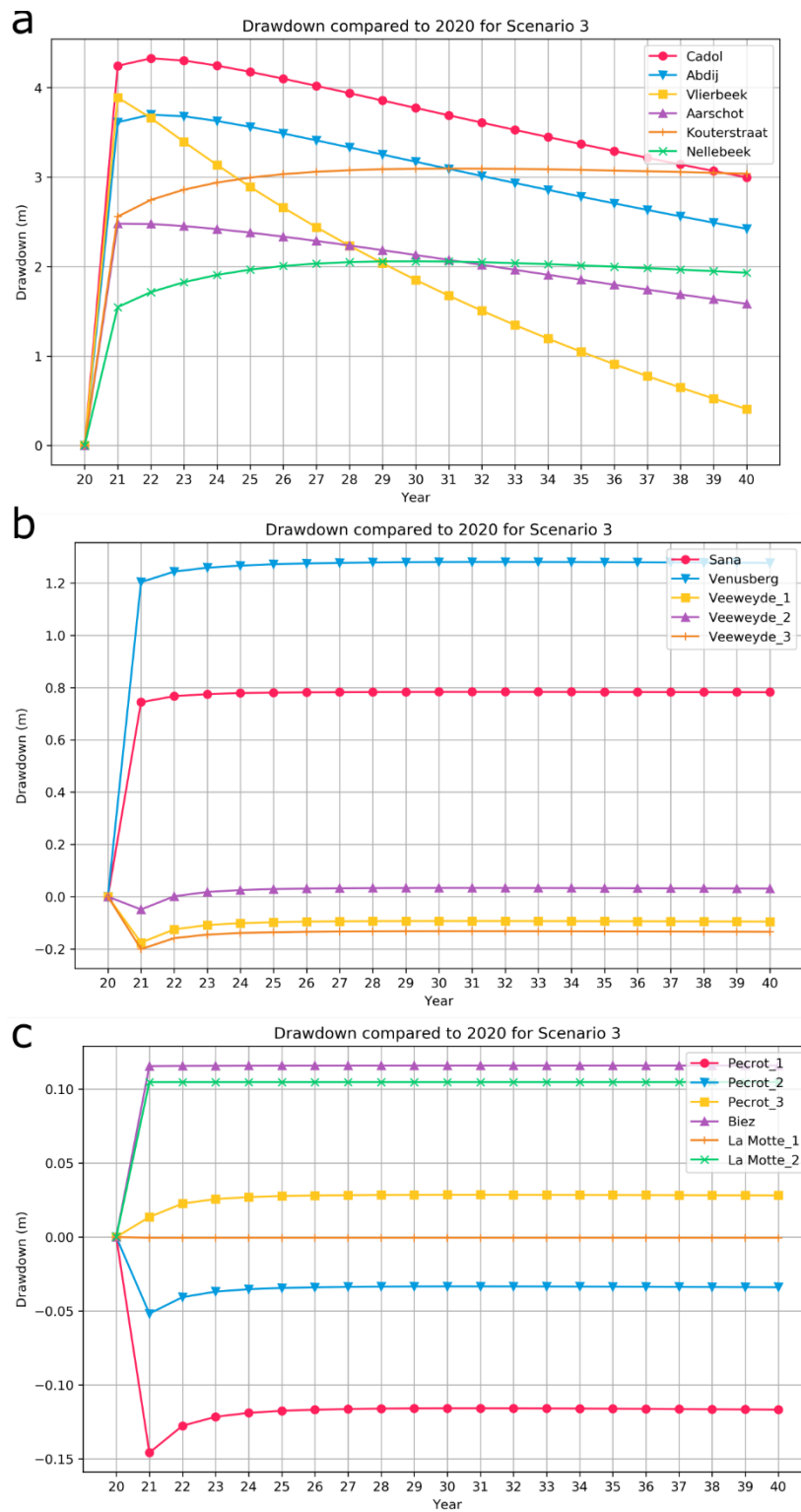


Figure 133: Drawdown over time compared to the heads in 2020 for Scenario 3 at the extraction wells of: (a) Cadol, Abdij, Vlierbeek, Aarschot, Kouterstraat and Nellebeek; (b) Sana, Venusberg and Veeweyde; and (c) Pécrot, Biez and La Motte

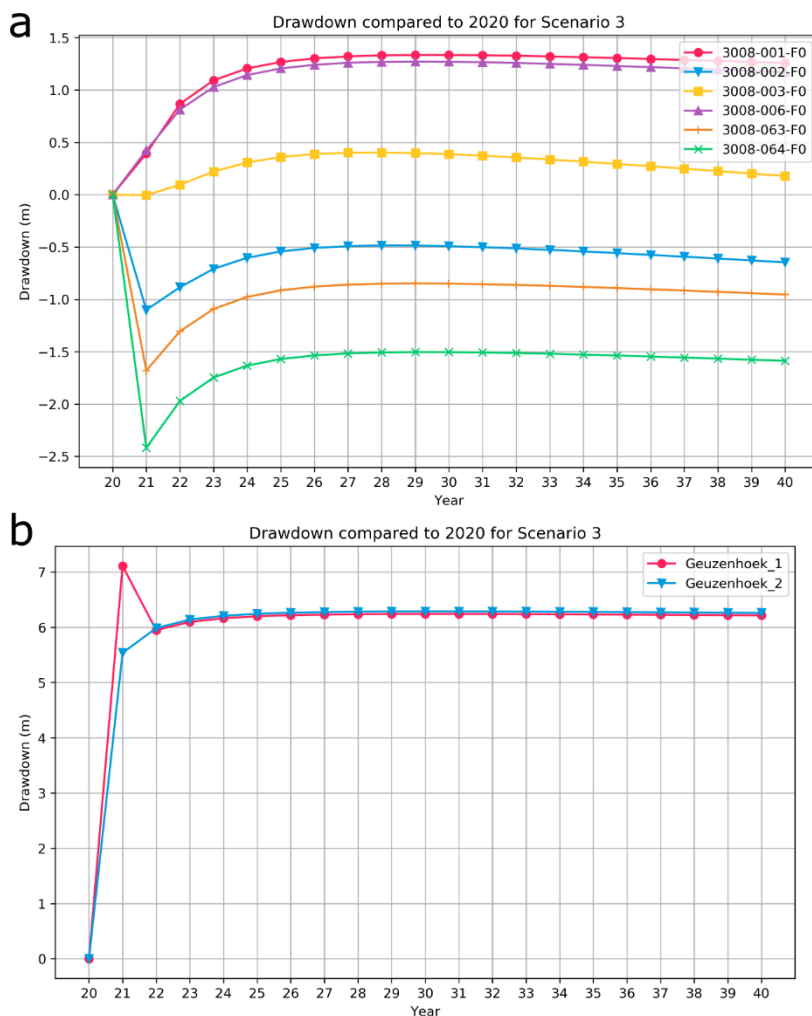


Figure 134: Drawdown over time compared to the heads in 2020 for Scenario 3 at the extraction wells of: (a) Het Broek; and (b) Geuzenhoek.

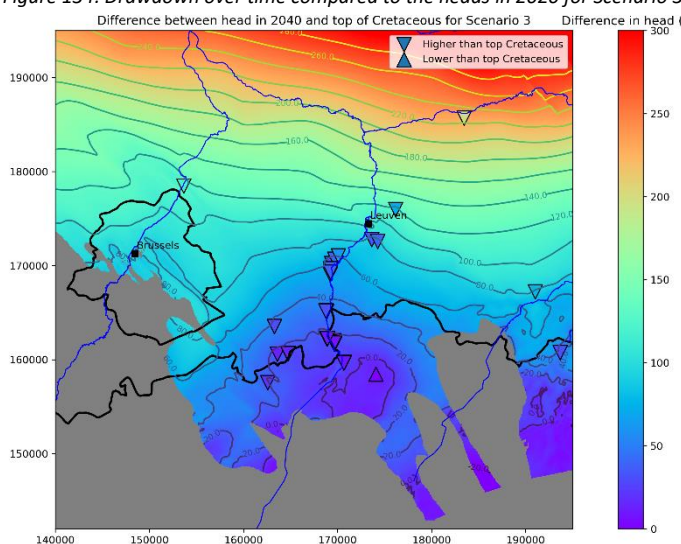


Figure 135: Difference in simulated heads in the Cretaceous and the top of the Cretaceous for Scenario 3.

5.5 Scenario 4: Venusberg +100%/+300%

In this scenario, the planned increase in extraction rates for the Venusberg site is simulated. Two different sub scenarios are defined. In **Scenario 4a**, the extraction rate for Venusberg is increased with 100%. In **Scenario 4b**, the extraction rate is increased with 300%. For Scenario 4a, the total extraction rate is 3.4% higher than for Scenario 1, while for Scenario 4b this is 9.8% higher. In the current permit, the extraction rate is 438,000 m³/year or 50 m³/hour. For Scenario 4a, the rate is 876,000 m³/year or 100 m³/hour and for Scenario 4b 1,752,000 m³/year or 200 m³/hour (Table 26).

Table 26: Overview of extraction rates of the Venusberg site for the current permit, Scenario 4a and Scenario 4b.

Yearly extraction rates (m ³ /y)	3011-005-F0	Total
Current permit	438,000	438,000
Scenario 4a	876,000	876,000
Scenario 4b	1,752,000	1,752,000

Scenario 4a: increase with 100%

An increase of 100% (50 m³/hour to 100 m³/hour) results in a drop in hydraulic head of 5.4 m in the production well 3011-005-F0 in the year 2030. The drop in head in the closest observation wells with filter in the Cretaceous is 2.32m for 3011-006-F2, 2.15m for 3011-007-F3 and 0.65m for 3011-024-F2 (Table 27). The head versus time plot for all production and observation wells near the Venusberg site is shown in Figure 136. A map of the simulated hydraulic heads for the Cretaceous in the year 2040 is shown in Figure I. 26.

Table 27: Overview of simulated heads in the wells of Venusberg in the year 2020, and in 2030 for respectively Scenario 4a and 4b. All values are in m.

Well	Layer	Scenario 4a		Scenario 4b	
		2020	2030	Δ	2030
3011-005-F0	Cretaceous	36.51	31.1	5.41	22.39
3011-006-F2	Cretaceous	38.57	36.25	2.32	32.56
3011-007-F2	Lincent	40.78	40.17	0.61	39.21
3011-007-F3	Cretaceous	38.74	36.59	2.15	33.16
3011-024-F2	Cretaceous	38.39	37.74	0.65	36.73

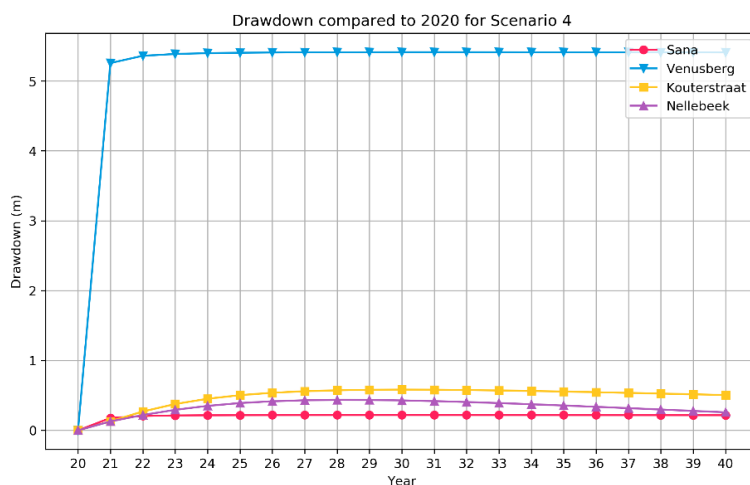


Figure 136: Drawdown over time compared to the heads in 2020 for Scenario 4a at the extraction wells of Venusberg, Sana, Kouterstraat and Nellebeek.

Difference maps for the situation in 2040 for scenario 4a compared to Scenario 1 are shown in Figure 137. In the Cretaceous, drawdown of >1m is simulated in an area of approx. 1.5km around the production well (Figure 137c). The drawdown is larger towards the west compared to the east. This is due to the absence of the Palaeocene deposits in the river valley in the east, resulting in a larger connectivity with the surface. The increase in extraction rate influences the three closest extraction sites in the Cretaceous: Sana, Kouterstraat and Nellebeek. The lowering of the hydraulic head at Kouterstraat is approx. 0.3m, and 0.2m for Nellebeek. The effect on Sana is approx. 0.2m. The effect on the overlying layers is limited (Figure 137ab), with drawdown in the Member of Grandglise being less than 0.4m. The drawdown in 3011-007-F2, with filter in the Member of Lincent, is 0.61m. The hydraulic head at the production well 3011-005-F0 is still 8.05m above the top of the Cretaceous (Figure I. 27).

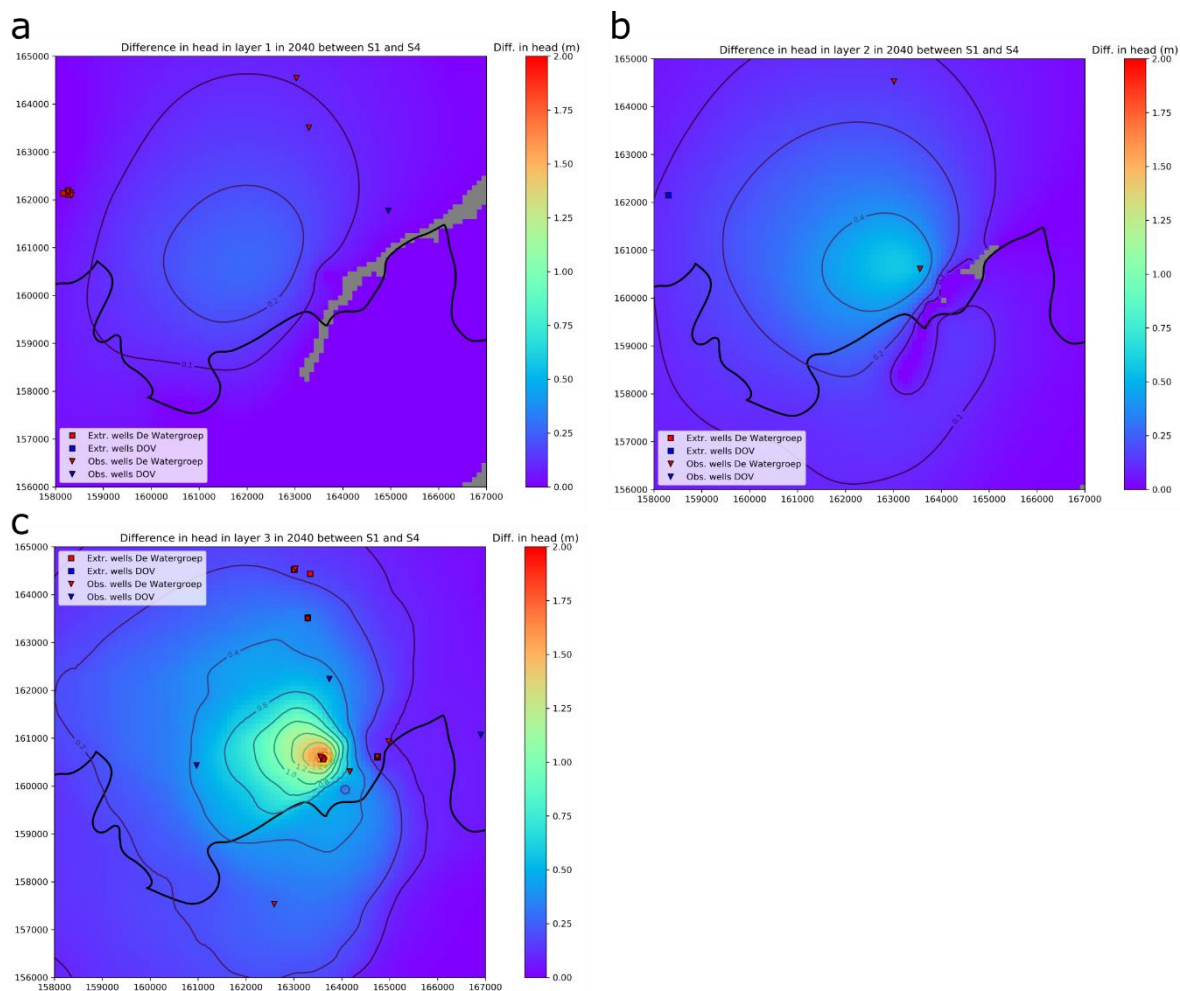


Figure 137: Difference in simulated head in the year 2040 between Scenario 1 and Scenario 4a for: (a) Grandglise; (b) Lincent; (c) the Cretaceous.

Scenario 4b: increase with 300%

An increase of 300% (50 m³/hour to 200 m³/hour) results in a drop in hydraulic head of 14.12 m in the production well 3011-005-F0 in the year 2030. The drop in head in the closest observation wells with filter in the Cretaceous is 6.01m for 3011-006-F2, 5.59m for 3011-007-F3 and 1.66m for 3011-024-F2 (Table 27 and Figure 138). A map of the simulated hydraulic heads for the Cretaceous in the year 2040 is shown in Figure I. 28.

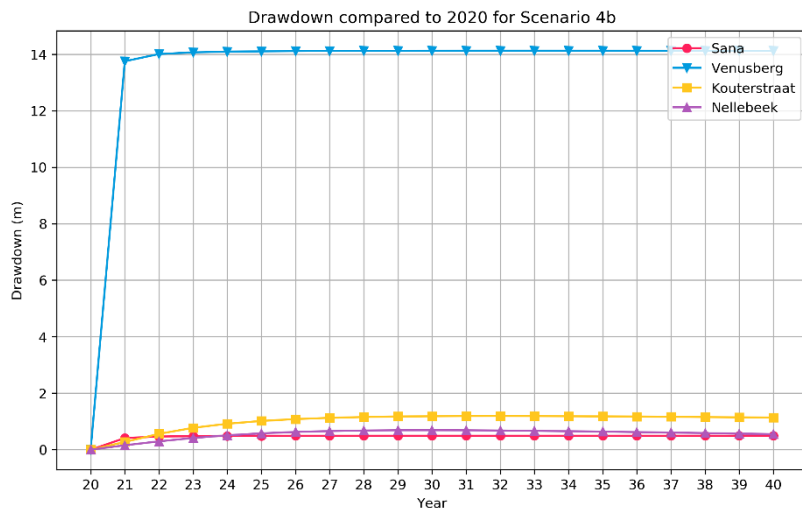


Figure 138: Drawdown over time compared to the heads in 2020 for Scenario 4b at the extraction wells of Venusberg, Sana, Kouterstraat and Nellebeek.

Difference maps for the situation in 2040 for Scenario 4b compared to Scenario 1 are shown in Figure 139. In the Cretaceous, drawdown of >1m is simulated in an area of approx. 5km around the production well (Figure 139c). The drawdown is larger towards the west compared to the east. This is due to the absence of the Paleocene deposits in the river valley in the east, resulting in a larger connectivity with the surface. The increase in extraction rate influences the three closest extraction sites in the Cretaceous: Sana, Kouterstraat and Nellebeek. The lowering of the hydraulic head at Kouterstraat is approx. 1.2m, and 0.8m for Nellebeek. The effect on Sana is approx. 0.5m. The effect on the overlying layers is larger than for Scenario 4a (Figure 139ab), with drawdown in the Member of Grandglise up to 1m. The drawdown in 3011-007-F2, with filter in the Member of Lincent, is 1.57m. The hydraulic head at production well 3011-005-F0 is 0.66m below the top of the Cretaceous (Figure I. 29).

Discussion

Based on the results of Scenario 4a, an increase of the extraction rates of Venusberg to 100 m³/h is feasible. The hydraulic heads in the Cretaceous are still higher than the top of the Cretaceous. The lowest heads above the top of the Cretaceous are present at the extraction well 3011-005-F0 in which the difference is still approx. 8m. The effect on the hydraulic heads in the Cretaceous is relatively limited, with a maximum extra drawdown of 5.4m at the extraction well and 2m at the closest observation wells 3011-006-F2 and 3011-007-F3 (at a respective distance of 30m and 70m from the extraction well). The effects on the overlying layers (Lincent and Grandglise) are minimal.

The increase to 200 m³/h has larger effects on both the heads in the Cretaceous as in the overlying layers. At the extraction well, the hydraulic head decreases with approx. 14m and is approx. 0.6m beneath the top of the Cretaceous. However, this drop beneath the top of the Cretaceous is very local. The drawdown at the closest observation wells 3011-006-F2 and 3011-007-F3 is approx. 6m, meaning that the heads are approx. 7m above the top of the Cretaceous. The effects on the overlying layers are significant, with drawdown of up to 1.5m in Lincent and 1m in Grandglise.

Recently, a pumping test with a rate of 200 m³/h was performed on the new extraction well 3011-025. The resulting drawdown in the extraction well was approx. 10m, which is about 4m less than the drawdown simulated in the model. In this case, the head in the Cretaceous was still approx. 3m higher than the top of the Cretaceous. The model seems to overestimate the drawdown compared to the actual drawdown. However, the drawdown of 14m predicted by the model is the drawdown in 2040 after continuous extraction at 200 m³/h, while the drawdown of the pumping test is only after pumping at this rate for a couple of days. Comparing the two drawdowns is thus not evident. The model might overestimate the drawdown and must thus be interpreted as a worst-case scenario. However, the difference between head and top of the Cretaceous of 3m in the pumping test does not provide much leeway. Continuous extraction at 200 m³/h might thus not be advisable.

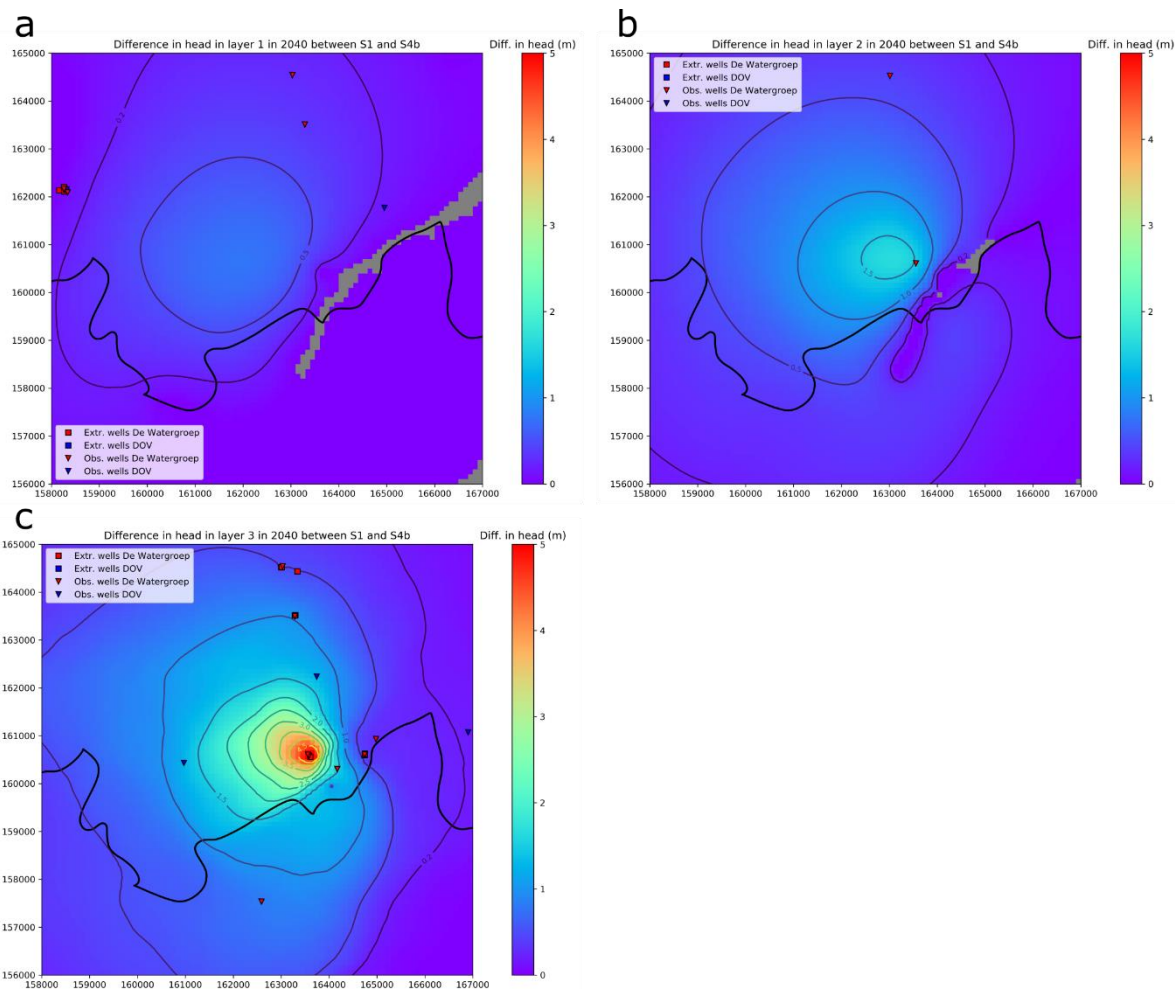


Figure 139: Difference in simulated head in the year 2040 between Scenario 1 and Scenario 4b for: (a) Grandglaise; (b) Lincent; (c) the Cretaceous.

5.6 Scenario 5: no extraction De Watergroep in the Cretaceous

In this scenario, the rates of all extraction sites of De Watergroep in the Cretaceous Aquifer are set to zero. This scenario shows how and how fast the aquifer recovers from the current extraction of De Watergroep. The simulated head maps for the Cretaceous for the years 2030 and 2040 are shown in Figure 140. Difference maps for the situation in 2040 for scenario 5 compared to Scenario 1 are shown in Figure 141. Note that positive values indicate a recovery of the hydraulic head (compared to a drawdown in the previous scenarios). These maps indicate indirectly what the effect is of current extraction on the head in the Cretaceous. The influence of the extractions (recovery >0.5m) is visible in the entire area between Aarschot, Leuven and the boundary Flanders-Wallonia. The recovery is

the largest in the area surrounding the Leuven wells (Vlierbeek, Cadol & Abdij) and the well site of Het Broek, with recovery of up to 20m. An area of 20 by 10km is characterized by recovery of more than 5m. Locally around the sites of Nellebeek and Kouterstraat the recovery is >5m. In the shallower parts of the aquifer, the recovery is limited to around 2m and even less for the sites in the unconfined part of the aquifer. There is also a significant effect on the heads in the Lincent layer in the area Leuven-Het Broek-Nellebeek/Kouterstraat with recovery up to 8m around Het Broek (Figure I. 30). The effect on the Grandgilde layer is more limited, with recovery of up to 3m in the area of Het Broek.

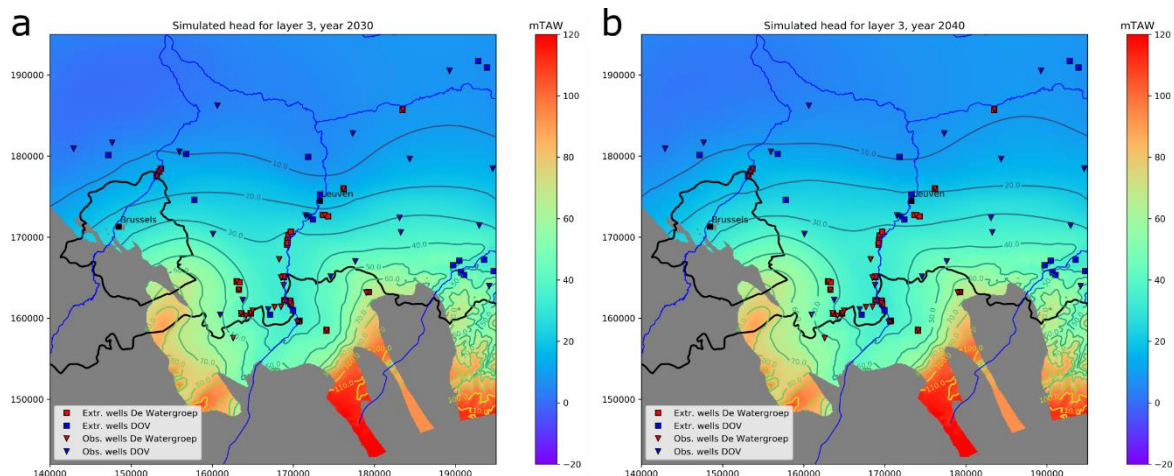


Figure 140: Simulated heads for the Cretaceous Aquifer for Scenario 5 for: (a) the year 2030; and (b) the year 2040.

In Figure 142 and Figure 143 the simulated recovery over time for the different extraction sites is shown. The recovery is the largest for the well sites near Leuven (Figure 142a), with recoveries of up to 55-65m. Note that the recovery in this area is slow and hasn't reached equilibrium yet in 2040. Full recovery is expected after three to four decades. The sites of Aarschot, Kouterstraat and Nellebeek show recovery of 20 to 30m (Figure 142a). For these wells, recovery is faster, and equilibrium is more or less reached in 2040. The well sites in the shallower parts of the aquifer show recoveries of around 3m (Veeweyde), 4m (Venusberg) and 7m (Sana) (Figure 142b). Note that recovery is faster and equilibrium state is reached after 5 to 10 years. The sites in the Walloon region show limited recovery of 1 to 3.5m (Figure 142c). Recovery is very fast, in a couple of years. The extraction wells of Het Broek show recoveries of 25 to 50m (Figure 143a), with largest recoveries for the wells in the north (3008-002/003) and smallest recoveries for the wells in the south (e.g., 3008-001). Recovery is slow, and equilibrium is not reached for most wells in 2040. Finally, the wells of Geuzenhoek show a recovery of >6m which is relatively slow. Equilibrium is not fully reached in 2040 (Figure 143b).

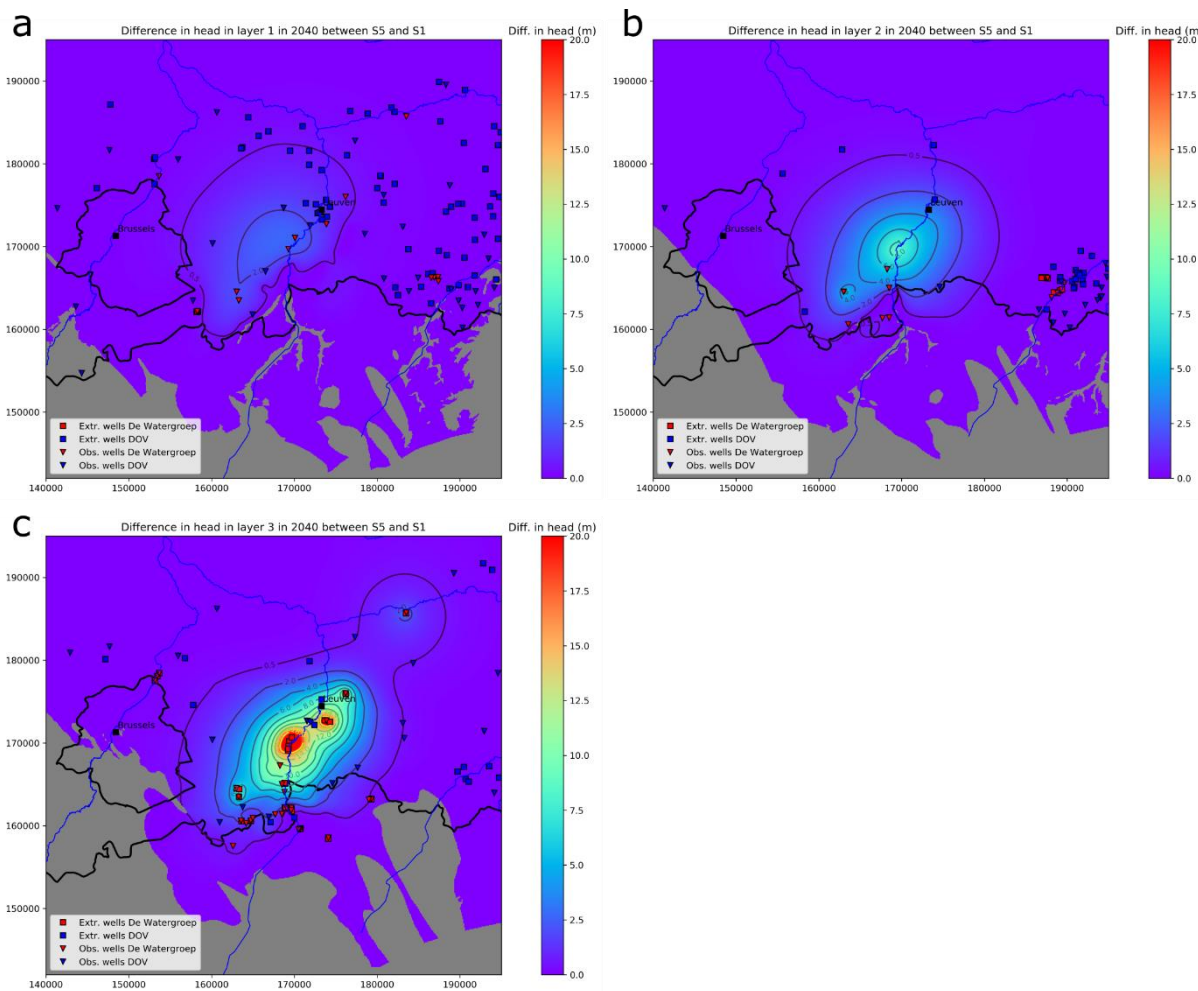


Figure 141: Difference in simulated head in the year 2040 between Scenario 1 and Scenario 4b for: (a) Grandglise; (b) Lincent; (c) the Cretaceous.

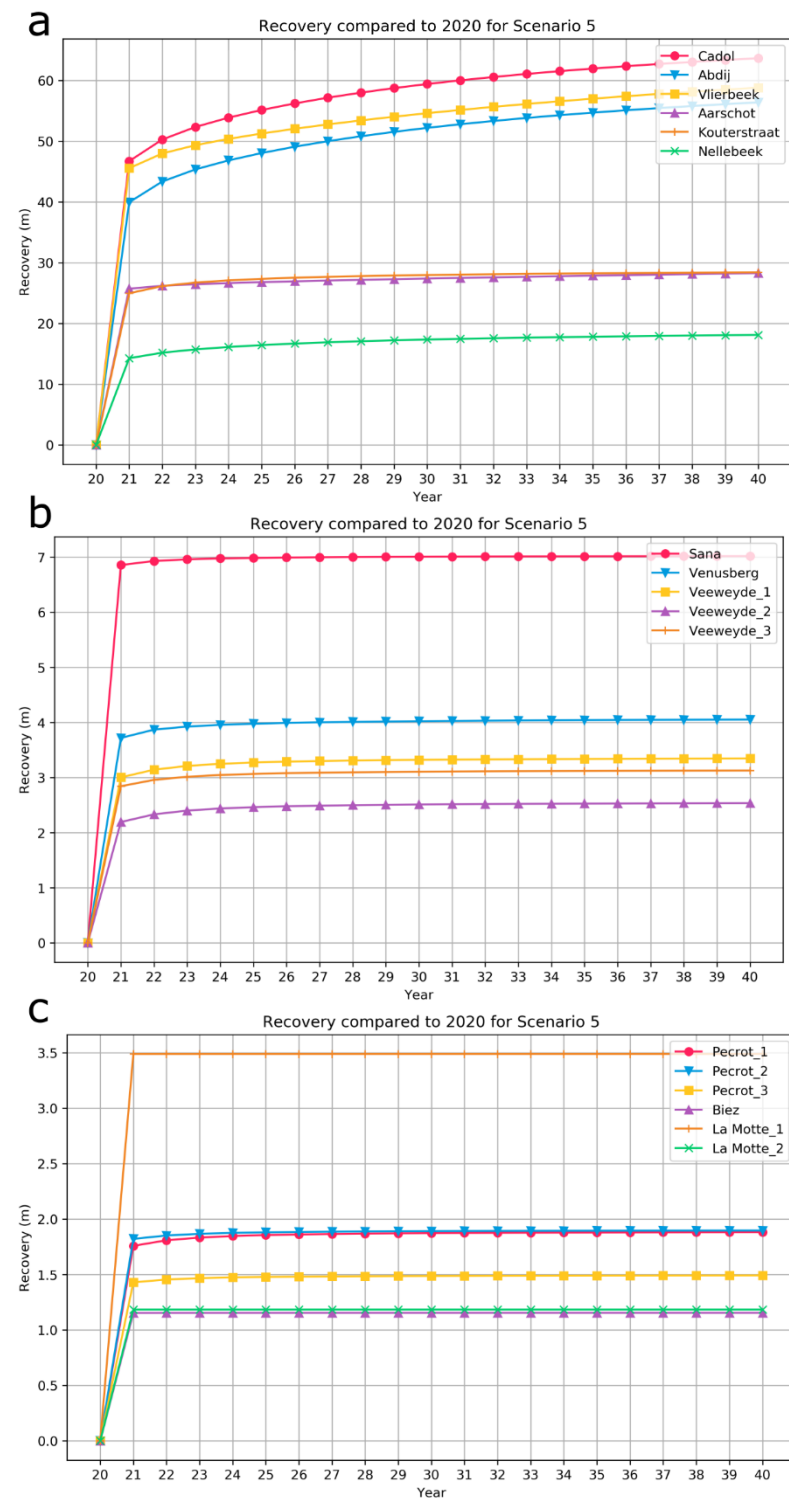


Figure 142: Drawdown over time compared to the heads in 2020 for Scenario 5 at the extraction wells of: (a) Cadol, Abdij, Vlierbeek, Aarschot, Kouterstraat and Nellebeek; (b) Sana, Venusberg and Veeweyde; and (c) Pécrot, Biez and La Motte.

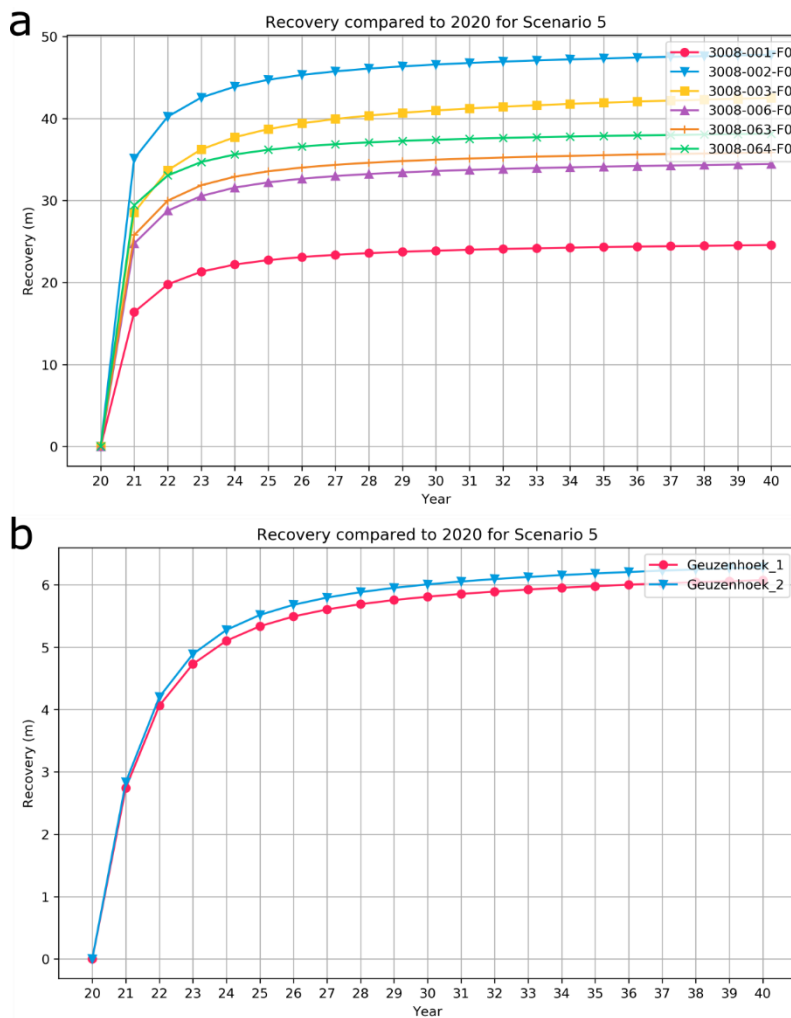


Figure 143: Drawdown over time compared to the heads in 2020 for Scenario 5 at the extraction wells of: (a) Het Broek; and (b) Geuzenhoek.

The difference between the simulated heads in the Cretaceous and the top of the Cretaceous is shown in Figure 144.

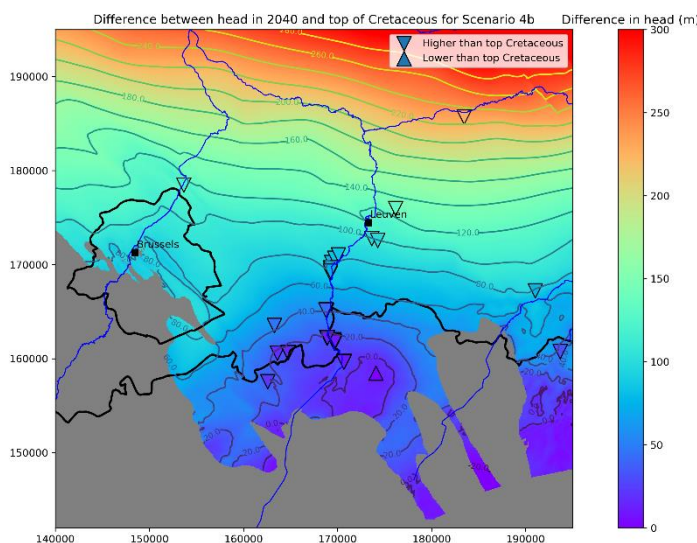


Figure 144: Difference in simulated heads in the Cretaceous and the top of the Cretaceous for Scenario 5.

6 Uncertainty Analysis

6.1 Integrated Bayesian Multi-model Uncertainty Estimation Framework (IBMUEF)

The reliability of model predictions is strongly influenced by uncertainties in model parameters (e.g., hydraulic conductivities and storage coefficients), model inputs (e.g., groundwater recharge, extraction rates, and initial and boundary conditions), and the structure of the conceptual model. The Integrated Bayesian Multi-model Uncertainty Estimation Framework (IBMUEF) of Mustafa et al. (2018, 2020) is used to quantify parameter and boundary conditions uncertainty (Figure 145). The framework is developed by coupling the MODFLOW model with the Differential Evolution Adaptive Metropolis (DREAM) algorithm (Vrugt, 2016) and by applying Bayesian combined model averaging (BCMA). This fully Bayesian approach can simultaneously quantify the uncertainty originating from the model conceptualization, the input data (boundary conditions), the parameter values, and measurement data. Input multipliers are introduced to quantify the uncertainty of the spatially distributed input data of the groundwater model. The heteroscedasticity of the groundwater heads is included by incorporating a novel generalized formal likelihood function. We refer the reader to Mustafa et al. (2018, 2020) for the details of the IBMUEF. Bayesian combined model averaging (BCMA) has not been applied in this study as alternative model conceptualizations have not been considered. The IBMUEF is applied to the Brabant Model to quantify the uncertainty associated with the model parameters and boundary conditions.

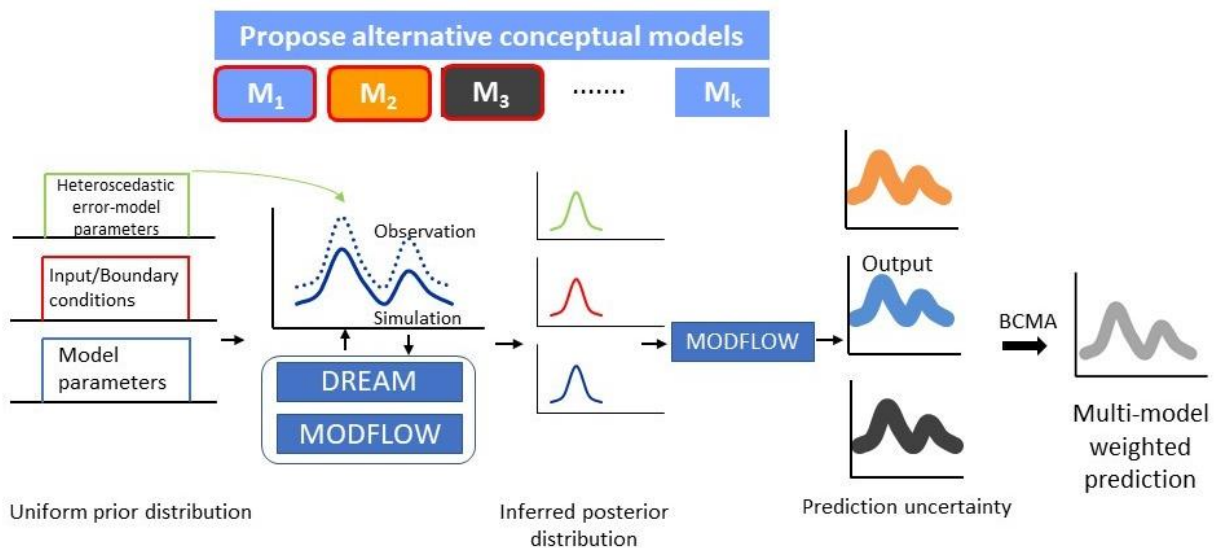


Figure 145: Integrated Bayesian Multi-model Uncertainty Estimation Framework (IBMUEF) (adapted from Mustafa et al., 2020).

6.2 Parameter and boundary condition uncertainty analysis

The following parameters of the MODFLOW model have been considered for uncertainty analysis: horizontal hydraulic conductivity (HK), vertical hydraulic conductivity (VK), and specific storage (SS). Three different parameters related to the general-head boundaries (GHB) are considered along with the model parameters for uncertainty analysis. We consider a uniform prior probability distribution within the hydrologically acceptable ranges (Table 28) for each parameter. Acceptable ranges for these hydrogeological parameters are defined based on literature values of sediment types. The selected parameters and their prior uncertainty bounds are presented in Table 28.

Table 28: Parameters of the MODFLOW model and boundary conditions used in the uncertainty analysis with their initial value and prior ranges.

Parameter		Initial	Ranges
hk_0	Horizontal hydraulic conductivity of layer 1 (Grandglise)	3 m/d	0.5 – 5 m/d
hk_Halen_Lincent	Horizontal hydraulic conductivity of layer 2 (Halen/Lincent)	1 m/d	0.5 – 5 m/d
vk_Halen_Lincent	Vertical hydraulic conductivity of layer 2 (Halen/Lincent)	5E-5 m/d	1E-06 – 0.01 m/d
hk_Waterschei	Horizontal hydraulic conductivity of layer 2 (Waterschei)	5E-5 m/d	1E-07 – 0.001 m/d
hk_Lincent	Horizontal hydraulic conductivity of layer 2 (Lincent Zone)	2 (Multiplier)	0.5 – 5
hk_Gulpen	Horizontal hydraulic conductivity of layer 3 (Gulpen)	0.7 (Multiplier)	0.25 – 1.5
K_0100	GHB vertical hydraulic conductivity of Quaternary Zone	5 m/d	0.1 – 10 m/d
K_0600	GHB vertical hydraulic conductivity of Brussels Zone	0.5 m/d	0.1 – 5 m/d
K_0900	GHB vertical hydraulic conductivity of Kortrijk Zone	1E-5 m/d	1E-07 – 1E-03 m/d
ss_0	Specific storage of Layer 1 (Grandglise)	2.5E-4 m ⁻¹	1E-05 – 1E-02 m ⁻¹
ss_1	Specific storage of Layer 2 (Halen/Lincent)	2.5E-4 m ⁻¹	1E-05 – 1E-02 m ⁻¹
ss_2	Specific storage of Layer 3 (Cretaceous)	2.5E-4 m ⁻¹	1E-05 – 1E-02 m ⁻¹

Model calibration and uncertainty analysis are performed simultaneously using the 12 parameters (Table 28). The observed annual average hydraulic head data of 191 observation wells (details in section 4.7.3) were used to calibrate 12 parameters. The last 2000 parameter sets of the posterior distribution after convergence are used for analysis.

The total uncertainty is calculated using the following equation:

$$H = H_{\text{sim}} + \varepsilon; \quad \varepsilon \sim N(0, \sigma^2), \quad \sigma = \text{constant} \quad (1)$$

Where H is the hydraulic head (m) adjusted for the total uncertainty quantification, H_{sim} is the simulated hydraulic head for the parameter and boundary conditions uncertainty, for the last 2000 parameter sets of the posterior distribution after convergence, ε is the total hydraulic head uncertainty, sampled from a normal distribution with mean zero and constant variance (σ^2), σ is the standard deviation of the residuals.

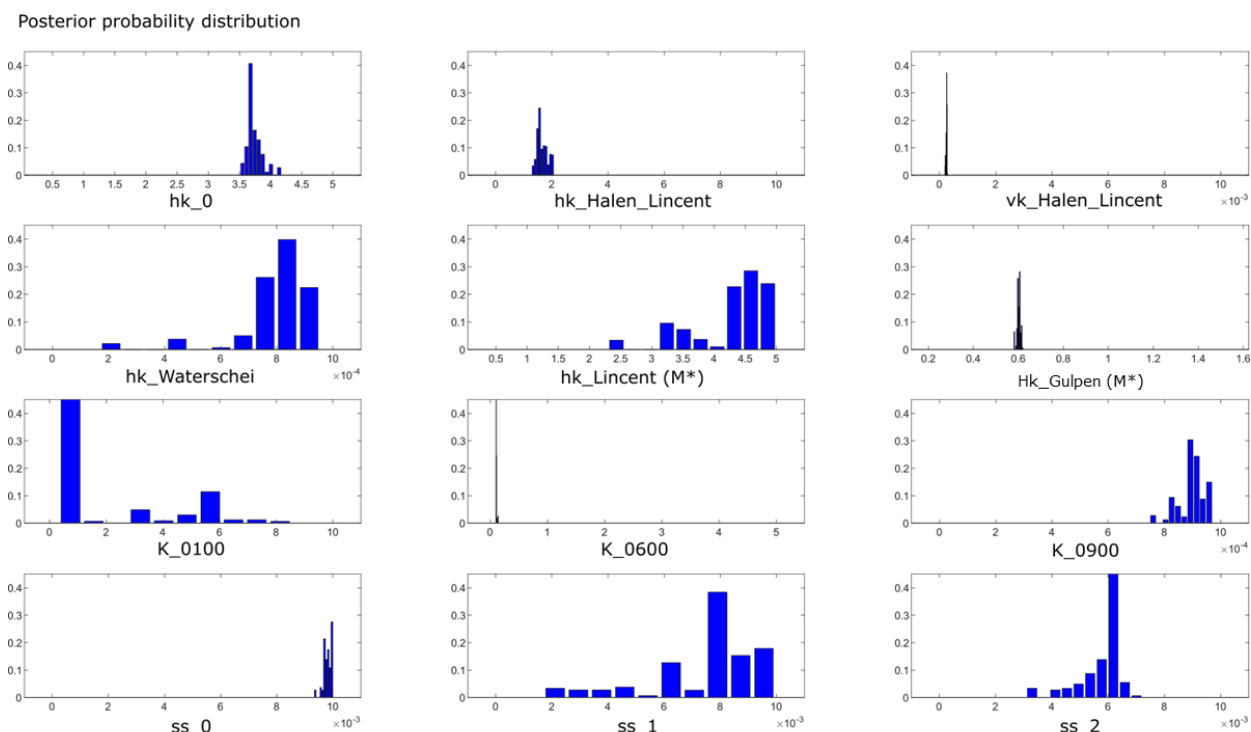
6.3 Threshold levels

It is important to define a sustainability criterion to avoid undesirable results due to increased abstraction. The definition of such criteria is also important for policy planning and decision support. The groundwater can be extracted only up to a certain threshold beyond which there are considerable adverse effects on environmental conditions. In this study, the threshold method is used to define the sustainability criterion. The top of the confined layer (the top of the Cretaceous) is used as a threshold for the confined part of the aquifer. For the unconfined part of the aquifer in the south, the top of the filter +1 m is used as a threshold.

6.4 Results

6.4.1 Parameter uncertainty

The posterior probability distribution of the model parameters and parameters of the boundary conditions is shown in Figure 146. It is observed that model parameters are well identified within their prior ranges. The distribution of most of the parameters is normally distributed. The specific storage of layers 1 and 2 are well-identified within their prior ranges but their distributions are not normally distributed. The distribution of 'GHB vertical hydraulic conductivity of Quaternary Zone (K_0100)' is bimodal, with a peak around 5 m/d and one for values <1 m/d. A possible reason for this is the heterogeneity of the Quaternary deposits. These include both fluvial deposits in the river valleys as eolian loess deposits at the surface. These two deposits can have different conductivities, resulting in a spatially variable K for the Quaternary zone. It is also observed that the posterior pdfs of most of the well-identified parameters cover only a very small part of their prior range. This indicates that available groundwater observations contain sufficient information to estimate most model parameters.



*M: Multiplier

Figure 146: The posterior probability distribution of the model parameters and parameters of the boundary conditions using 2000 samples generated after convergence. See Table 28 for a description of the parameters, their initial values and the parameter ranges.

6.4.2 Prediction uncertainty in simulated heads for different scenarios

The prediction uncertainty associated with model parameters and boundary conditions for respectively scenarios 1, 2a, 3, 4a, and 4b is shown in Figure 147 to Figure 151. It shows that the prediction uncertainty of the simulated head is varying from a couple of meters to around 10 meters. In general, there is no significant spatial variation in uncertainty across the model domain. However, the uncertainty increases towards the areas with lower observation density. The higher uncertainty around the Vilvoorde and Leuven areas might be because of the higher sensitivity of storage parameters related to historical extraction in those areas (see section 3.3). The maps of the prediction uncertainty should be considered along side with the simulated head map for the Cretaceous for the year 2040 shown in respectively Figure 119, Figure 122, Figure 131, Figure I. 26 and Figure I. 28. Although good prediction performances have been indicated both in calibration and validation, more attention should be paid during interpretation of the simulated heads located far away from the available groundwater observation wells. The map

of the available groundwater observation wells shows that there is a bias in the distribution of the observation wells with higher density around the Dijle valley and Tienen areas (Figure 66).

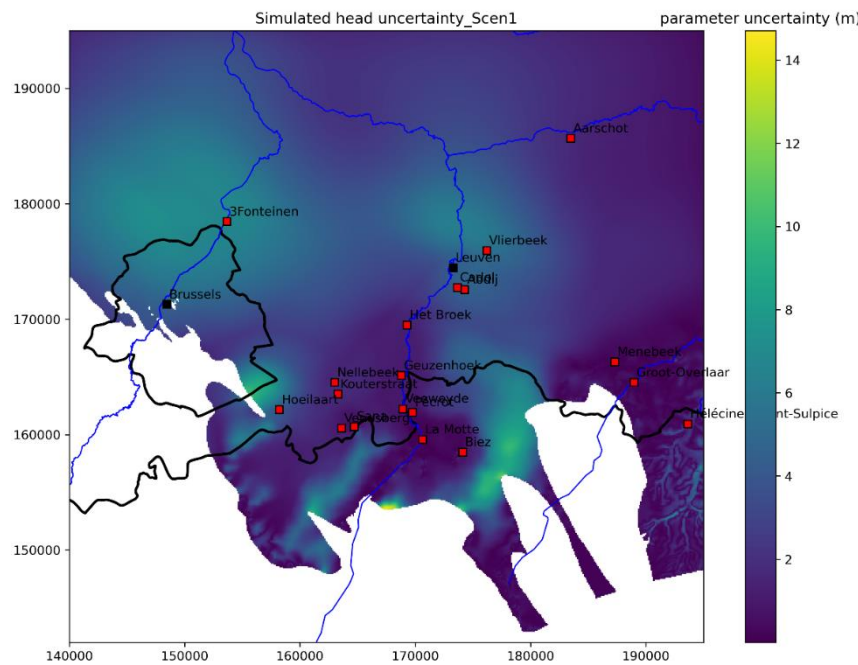


Figure 147: Prediction uncertainty associated with model parameters and boundary conditions for Scenario 1.

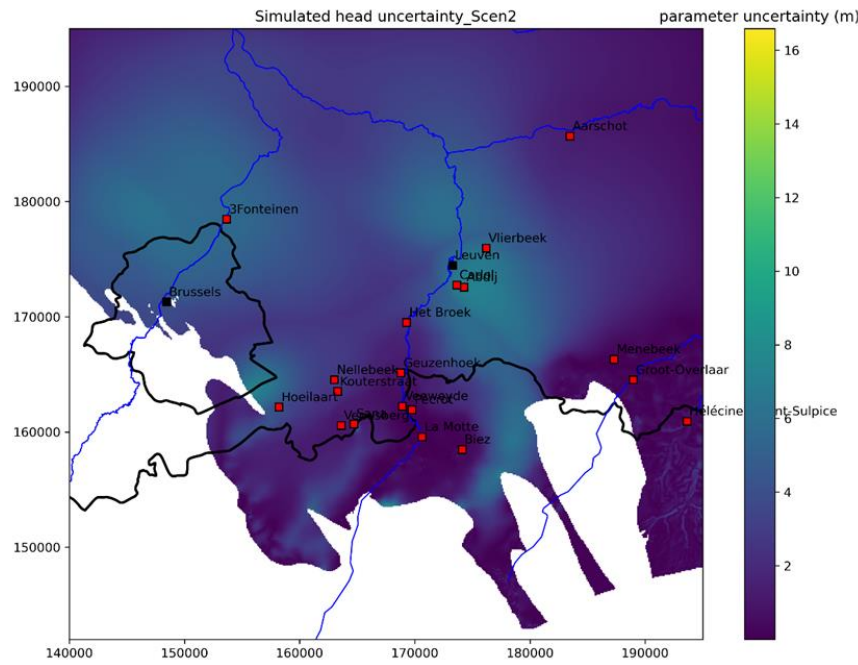


Figure 148: Prediction uncertainty associated with model parameters and boundary conditions for Scenario 2a.

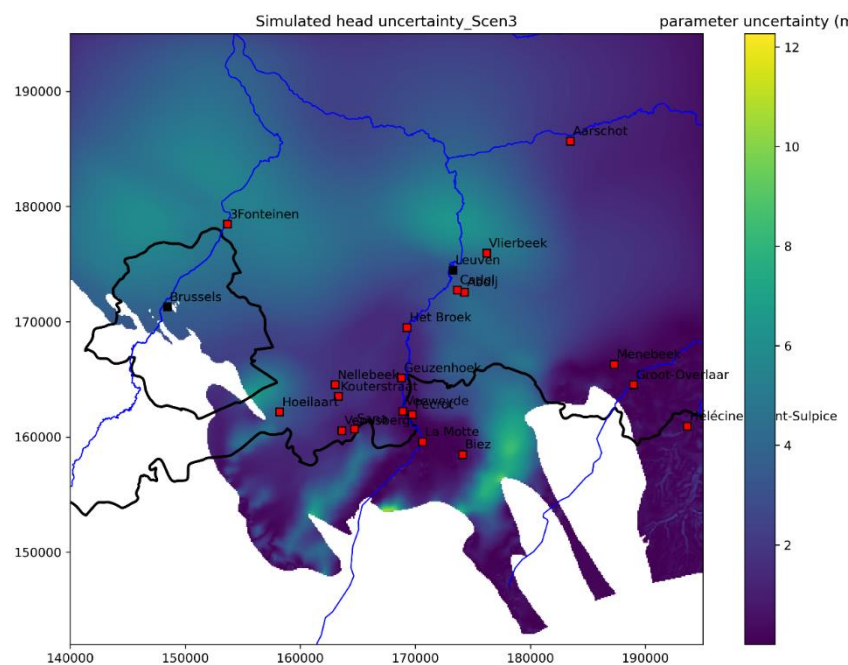


Figure 149: Prediction uncertainty associated with model parameters and boundary conditions for Scenario 3.

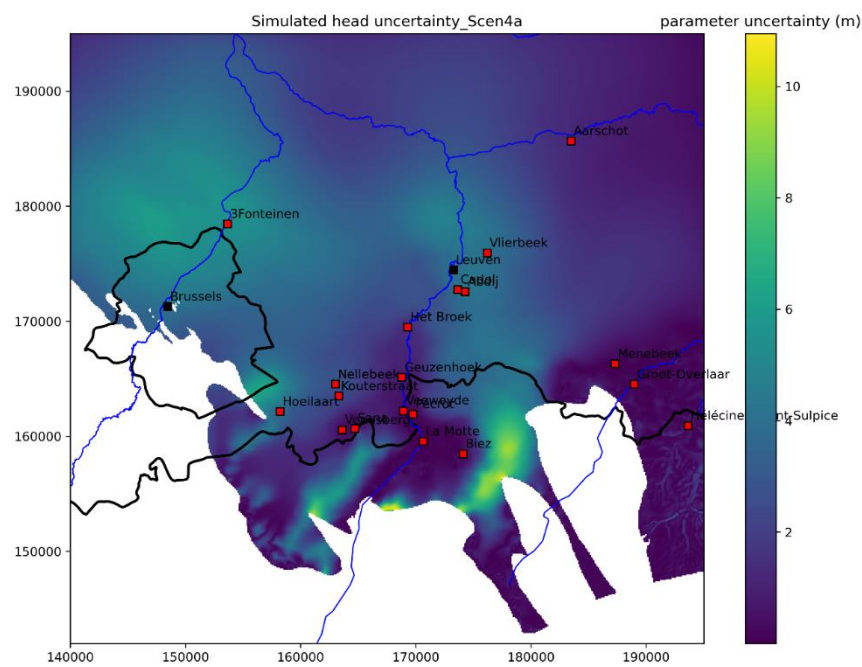


Figure 150: Prediction uncertainty associated with model parameters and boundary conditions for Scenario 4a.

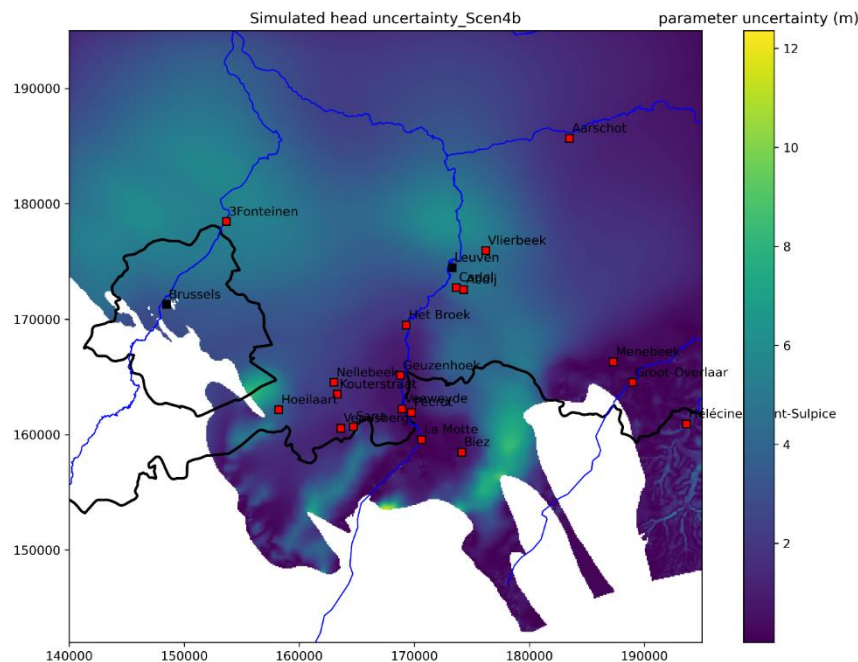


Figure 151: Prediction uncertainty associated with model parameters and boundary conditions for Scenario 4b.

6.4.3 Prediction uncertainty in simulated heads for selected extraction sites

Scenario 1: Current/normal situation

The prediction uncertainty in the simulated heads associated with model parameters and boundary conditions for Scenario 1 for a selection of extraction sites is shown in Figure 152. The total uncertainty in different extraction sites is varying from 0.85m to 5.97m and the parameter uncertainty (associated with model parameters and boundary conditions) is varying from 0.09 m to 5.76 m. The results also show that the simulated hydraulic is above the threshold level for all the extraction sites except for the site of Biez. For the more northern sites (e.g. Vlierbeek and Het Broek), the heads are several tens of meters higher than the top of the Cretaceous. More towards the south, in the unconfined part of the aquifer, this difference is smaller (approx. 10m). However, the effect of extraction on the heads in these areas is also a lot more limited. These results confirm that under the current extraction situation (Scenario 1) hydraulic heads will not go below the threshold in the next 20 years except for the site of Biez. However, the site of Biez is located in the unconfined part of the aquifer, in an area where the Cretaceous is karstified. The fact that the hydraulic head is below the top of the filter is not really an issue in these conditions.

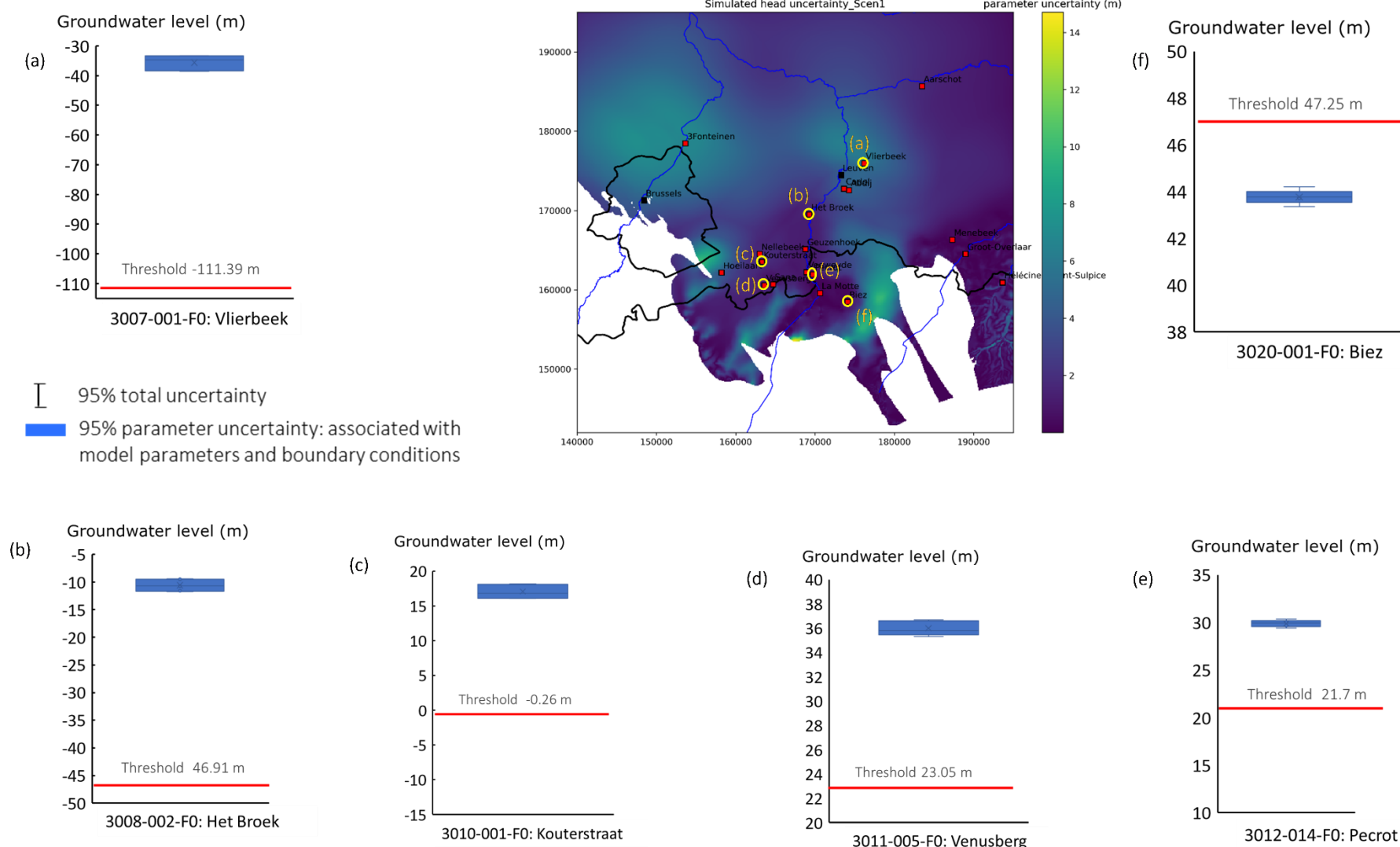


Figure 152: Prediction uncertainty in the simulated heads associated with model parameters and boundary conditions for the selected well sites for Scenario 1.

Scenario 2a: Maximal permitted rates + Het Broek at 2.5M m³/year

The prediction uncertainty in the simulated heads associated with model parameters and boundary conditions for Scenario 2a for a selection of extraction sites is shown in Figure 153. The total uncertainty at these extraction sites is varying from 0.5m to 5.4m and the parameter uncertainty (associated with model parameters and boundary conditions) is varying from 0.1m to 5.3m. The results show that the simulated hydraulic head is above the threshold level for all extraction sites except for the sites of Kouterstraat and Biez (the same reasoning is applicable as mentioned for Scenario 1, this is not really an issue in this case). The result is confirming that the hydraulic heads will not go below the threshold in the next 20 years except for the site of Kouterstraat if the groundwater extraction is continued at the maximal permitted extraction rates (Scenario 2a). At the site of Kouterstraat, the increased extraction (+90 %) will significantly decrease the hydraulic heads (by 26.5 m) compared to the current situation and will go below the threshold in the next 20 years. This can be explained by the fact that the hydraulic conductivity of the Cretaceous in this area is relatively low (see section 2.3) and that currently only approx. 50% of the permitted rates are used. Doubling of these rates will result in a strong drawdown due to the low hydraulic conductivity. Extraction at the permitted rates at the site of Kouterstraat is not sustainable on the long-term and is thus not recommended.

At the site of Vlierbeek, the increased extraction (+60 %) will significantly decrease the hydraulic head (by 33 m) compared to the current extraction situation. but will not decrease below the threshold in the next 20 years. Although the hydraulic head will not decrease below the threshold, the significant decrease in hydraulic head should be taken into account during decision making. One should consider the risk-reward ratio: the limited volumes extracted at this site have a relatively large effect on the drawdown (the same is true for Cadol and Abdij). The decrease in hydraulic heads at the site of Het Broek is not due to an increase in rates for this site¹¹, but due to increased extraction at the other sites in the vicinity. At the site of Pécrot, the hydraulic heads decrease only 1.5 m compared to the current situation, even though extraction is increased significantly high (+87%). This demonstrates the limited effect of extraction in the unconfined part of the aquifer in the south on the heads in this area.

Scenario 3: Current/normal situation +10%

The prediction uncertainty in the simulated heads associated with model parameters and boundary conditions for Scenario 3 for a selection of extraction sites is shown in Figure 154. The total uncertainty at these extraction sites is varying from 0.75m to 5.4m and the parameter uncertainty is varying from 0.1m to 5.25m. The results also show that the decrease in groundwater level due to increased extraction is also varying from 0.13m to 5.5m at different extraction sites. This indicates that the prediction uncertainty associated with model parameters is in the same magnitude as the impact of the extraction. The result also shows that groundwater level will not go below the threshold in the next 20 years for scenario 3. For the sites of Vlierbeek and Kouterstraat, the decrease in heads related to an increase in extraction is relatively large (respectively 5.5m and 3m). For the site of Het Broek, this decrease is also relatively large (4.3m). However, the absolute increase in rates is a lot higher (+250k m³/year for Het Broek versus +11k m³/year for Vlierbeek and 13k m³/year for Kouterstraat). For the more southern sites (Venusberg and Pécrot), the decrease in heads is more limited. This is related to the higher hydraulic conductivities in the south compared to the north.

¹¹ In Scenario 2a, a maximal rate of 2.5M m³/year is applied, while the actual permit is 4.38M m³/year. However, these permitted rates are too high as demonstrated in section 5.3. In 2020, the extracted rate at Het Broek was 3M m³/year, meaning there is a decrease in rates for this site in Scenario 2a.

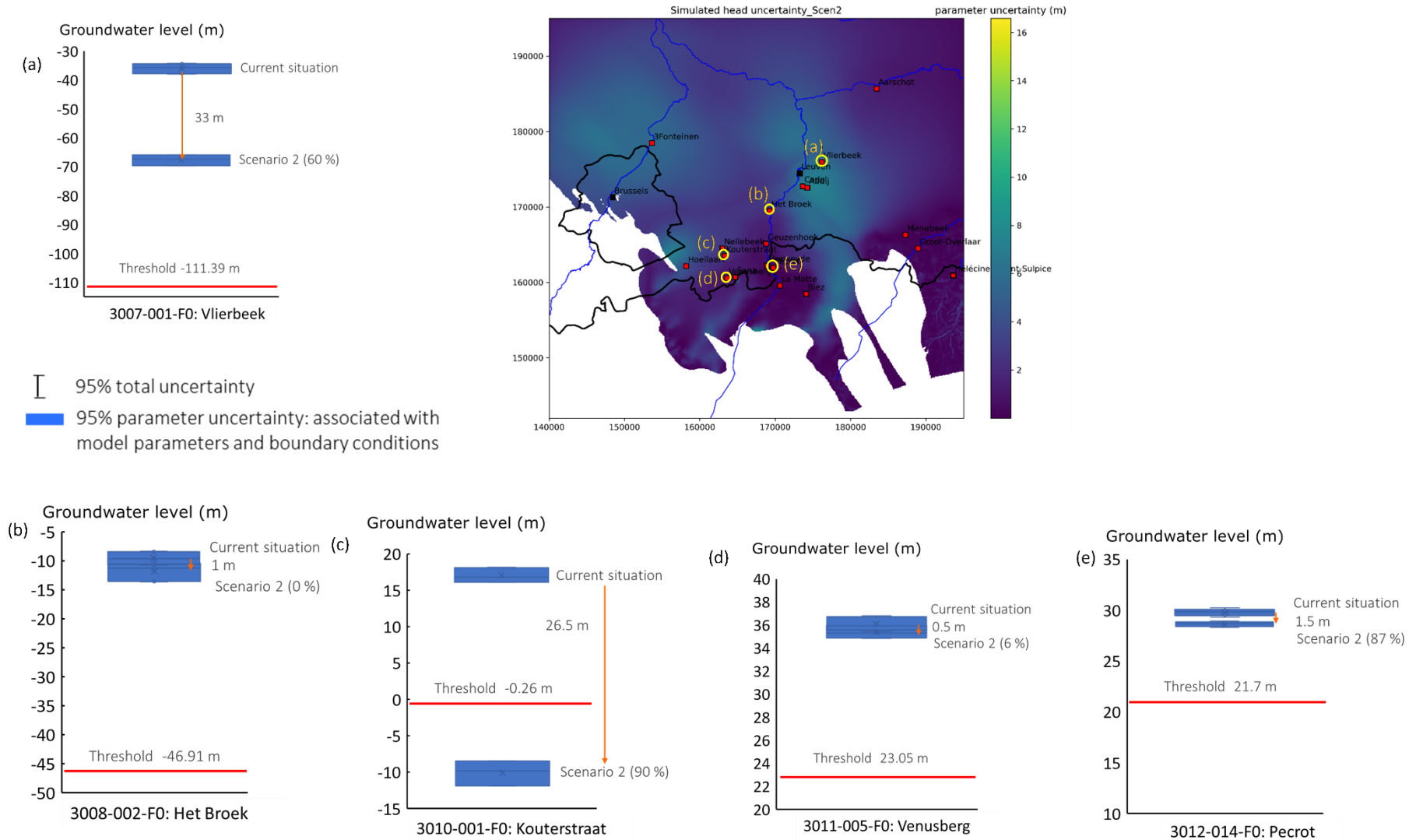


Figure 153: Prediction uncertainty in the simulated heads associated with model parameters and boundary conditions for the selected well sites for Scenario 2a.

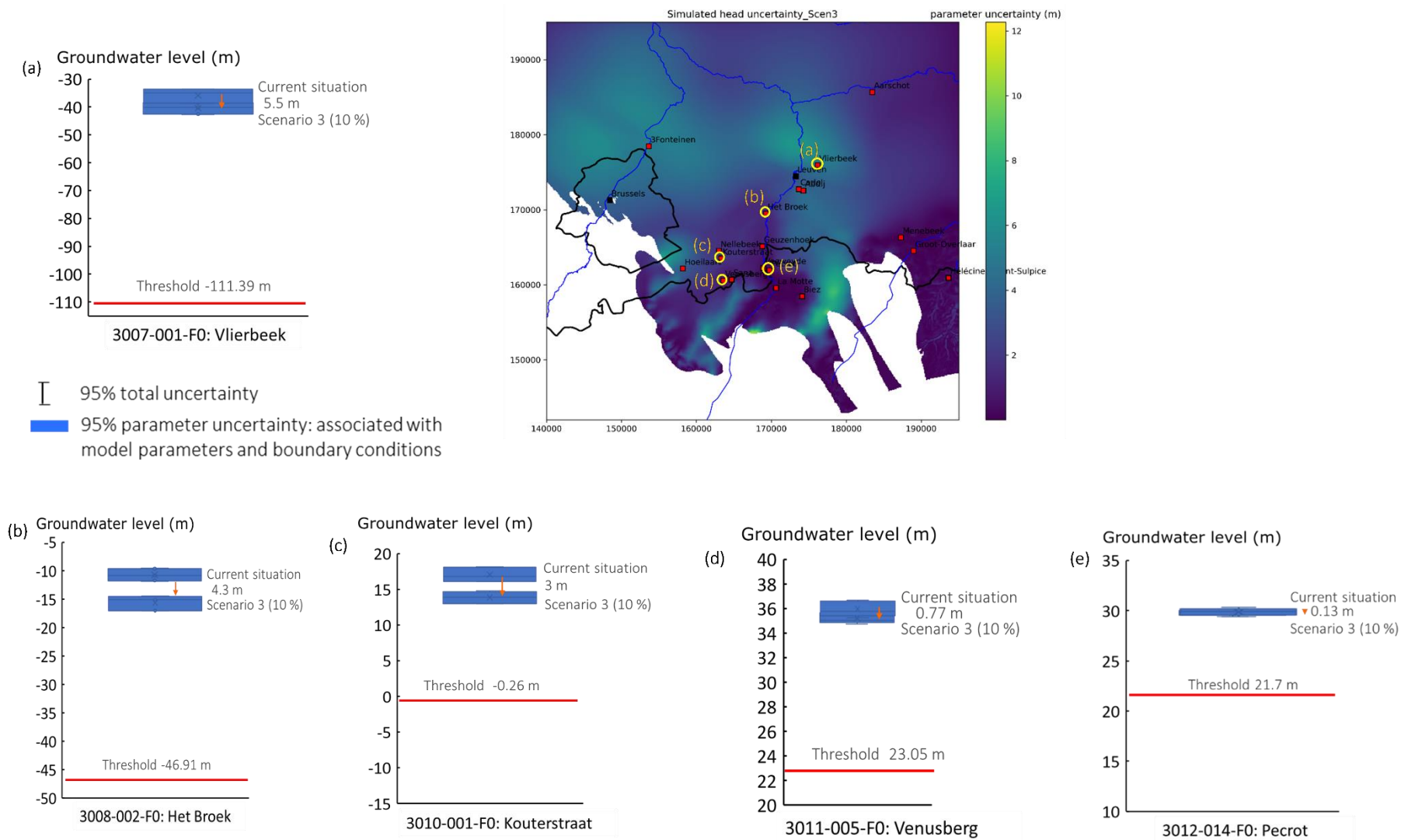


Figure 154: Prediction uncertainty in the simulated heads associated with model parameters and boundary conditions for the selected well sites for Scenario 3.

Scenario 4a: increase with 100%

The prediction uncertainty in the simulated heads associated with model parameters and boundary conditions for Scenario 4a for the sites around the Venusberg site is shown in Figure 155. The wells around the Venusberg site are selected as in Scenario 4a only the extraction rate for Venusberg is increased with 100%. The total uncertainty at the different extraction sites is varying from 0.92m to 7.27m and the parameter uncertainty from 0.1m to 7.25m. The results show that the decrease in hydraulic heads is varying from 0.21m to 5m at the different extraction sites. This indicates that the prediction uncertainty associated with model parameters is in the same magnitude as the impact of the extraction. The result also confirms that hydraulic heads will not go below the threshold in the next 20 years for Scenario 4a. At the site of Venusberg, the decrease in heads in the extraction well is 5m. There is still a difference of approx. 9m between the head in the well and the top of the Cretaceous. The uncertainty on the predictions is relatively small (1-2m). These results indicate that an increase in extraction rates of 100% at the site of Venusberg is feasible without endangering the sustainability on the long term.

Scenario 4b: increase with 300%

The prediction uncertainty in the simulated heads associated with model parameters and boundary conditions for Scenario 4b for the sites around the Venusberg site is shown in Figure 156. The total uncertainty at the nearby extraction sites is varying from 0.87m to 5.5 m and the parameter uncertainty is varying from 0.1m to 5.52m. The results show that the hydraulic head at the extraction well of Venusberg will go below the threshold. For the nearby sites, the heads do not go below the thresholds. At the Venusberg site, the large increase of extraction (+300%) results in a decrease of heads of approx. 14m, which is 1-2m below the top of the Cretaceous. This indicates that on the long-term, extraction at these high rates is not sustainable. However, as explained in Section 5.5 , a recent pumping test at these rates (+300%) indicated a decrease in heads of approx. 10m, which is approx. 2 meters above the threshold. In any case, the hydraulic heads will be close to the threshold, meaning that extra caution is advised while extraction at the +300% rates. It is not advised to extract at these rates continuously, but only in times when peak demands need to be met.

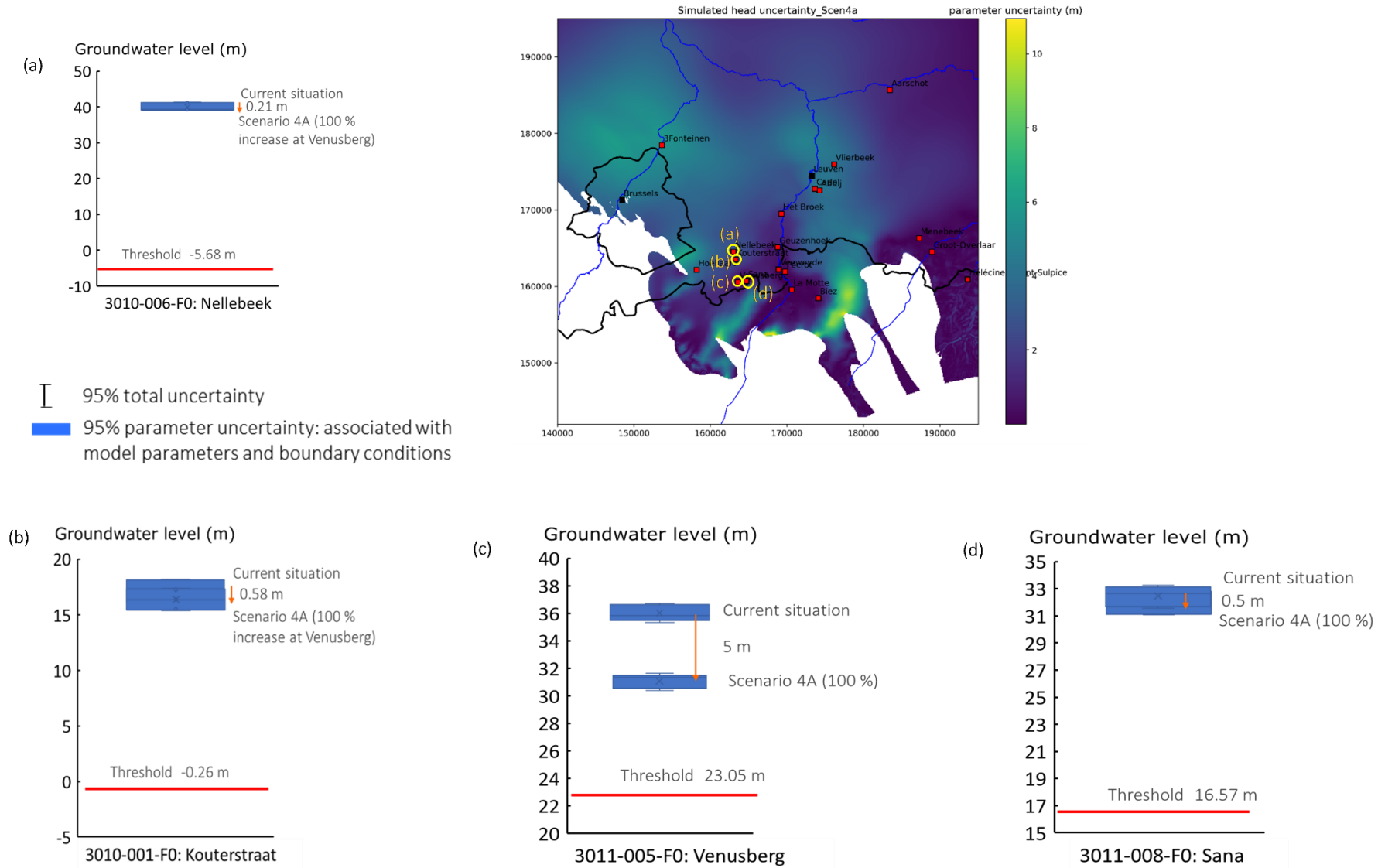
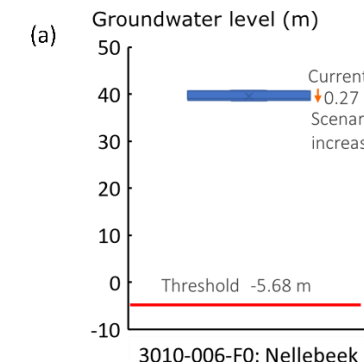


Figure 155: Prediction uncertainty in the simulated heads associated with model parameters and boundary conditions for the extraction sites around the Venusberg site for Scenario 4a.



- 95% total uncertainty
- 95% parameter uncertainty: associated with model parameters and boundary conditions

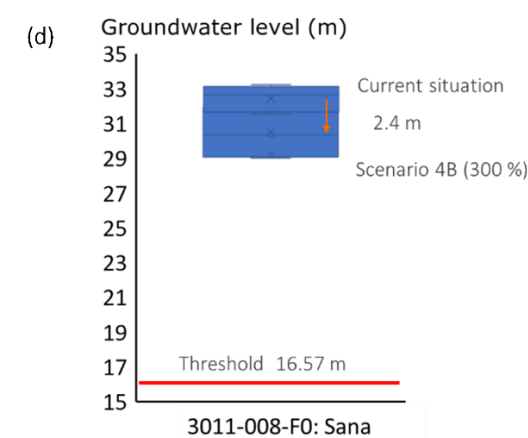
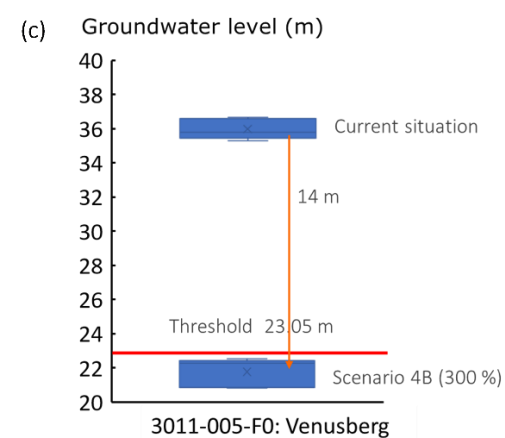
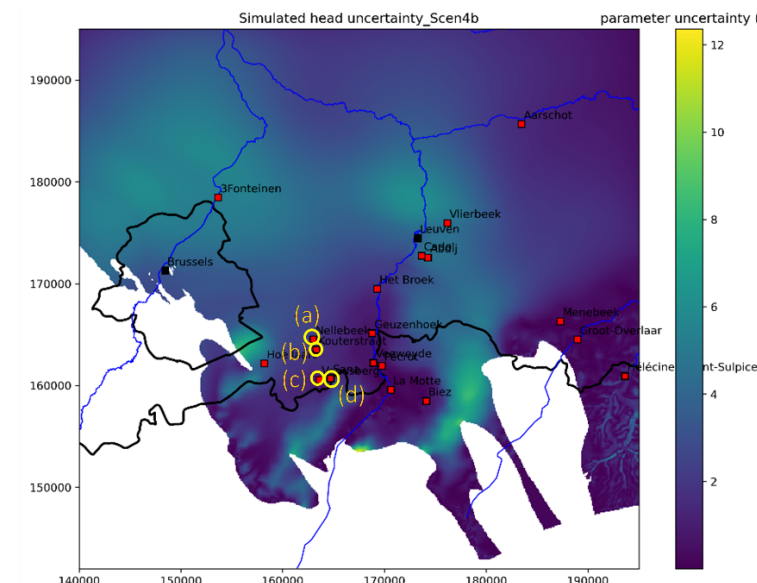
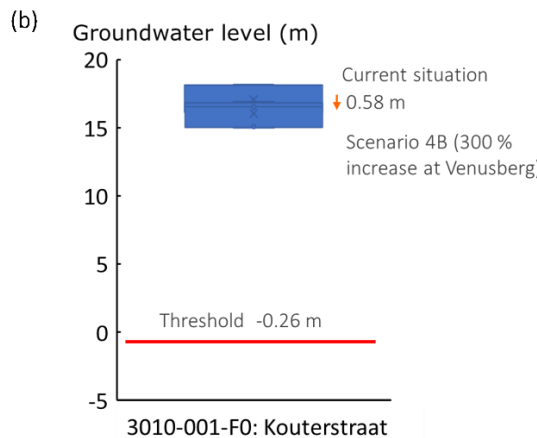


Figure 156: Prediction uncertainty in the simulated heads associated with model parameters and boundary conditions for the extraction sites around the Venusberg site for Scenario 4b.

6.4.4 Prediction uncertainty in simulated heads for all extraction sites

The prediction uncertainty in the simulated heads associated with model parameters and boundary conditions for all five scenarios are shown for all extraction wells separately in Figure 157, Figure 158, Figure 159, Figure I. 31 and Figure I. 32. The results show that the increased extraction will significantly decrease the hydraulic heads in the different scenarios but will not decrease below the threshold in the next 20 years except for the sites of Venusberg in Scenario 4b (Figure 158) and Kouterstraat in Scenario 2 (Figure 159).

For the site of Kouterstraat, the hydraulic heads will significantly decrease below the threshold only for Scenario 2 (i.e., extraction at maximal permitted rates) (Figure 159). However, for all other scenario's heads will not decrease below the threshold in the next 20 years. This indicates that the groundwater extraction at the maximal permitted rate is not sustainable at the Kouterstraat site. Extraction at current rates is, however, no problem.

For the site of Venusberg, the hydraulic heads will significantly decrease below the threshold only for Scenario 4b (i.e., extraction rate for Venusberg is increased with 300%) (Figure 158). However, for all other scenario's groundwater levels will not decrease below the threshold in the next 20 years. This indicates that an increase in the extraction rate for Venusberg with 100% is feasible, while an increase of 300% is not sustainable. Extracting at 300% continuously is therefore not advised but extracting at these higher rates for limited periods in times of high demand is possible.

Although the hydraulic heads will not decrease below the threshold, the significant decrease in heads for Scenario 2 (extraction at maximal permitted rates) should be considered during management decisions for the future for the sites near Leuven (Vlierbeek, Cadol and Abdij; Figure 157) and for the Nellebeek site (Figure 159).

As explained before, even though the threshold is reached at the site of Biez, this is not seen as a problem. This site is situated in the unconfined part of the aquifer which is characterized by karstification. The fact that the heads are below the top of the filter is not really an issue.

Note that in this study we did not take into account the effect of the extraction in the Cretaceous on the overlying shallow aquifers in the Quaternary and the Brussels sands. As these layers are not explicitly modelled, the heads in these layers are not simulated. For the sites in the unconfined part of the Cretaceous aquifer, the effects on the overlying layers should be further analysed on a case-by-case basis.

In summary, the prediction uncertainty (associated with model parameters and boundary conditions) at the extraction sites of De Watergroep in the Cretaceous are varying from 1m to 7.3m. The prediction uncertainty associated with model parameters and boundary conditions is in the same magnitude as the impact of the extraction for the different extraction scenarios. Policy planning and management strategies should be based on prediction results considering this uncertainty. Under the current situation, hydraulic heads at all extraction sites are above the threshold level. Increased extraction will significantly decrease the heads but in general, no decrease below the threshold is observed, except for scenarios 2a and 4b. Increased extraction at Kouterstraat (3010-001-F0) in scenario 2a (i.e., extraction at maximal permitted rates) and at Venusberg in scenario 4a (i.e., extraction rate for Venusberg is increased with 300%) will significantly decrease the hydraulic heads below the threshold.

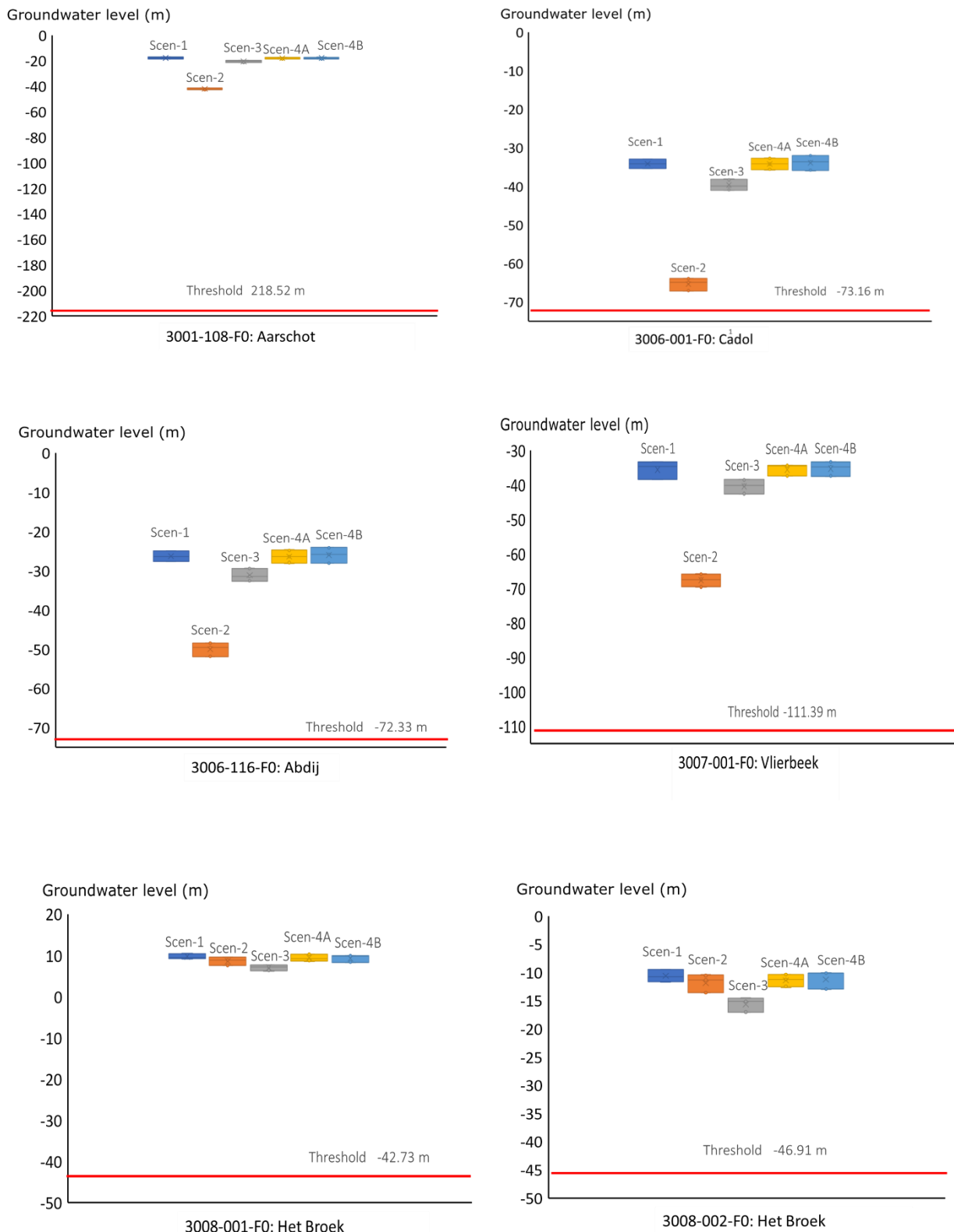


Figure 157: Prediction uncertainty in the simulated head associated with model parameters and boundary conditions for all five scenarios for the sites of Aarschot, Cadol, Abdij, Vlierbeek, and Het Broek.

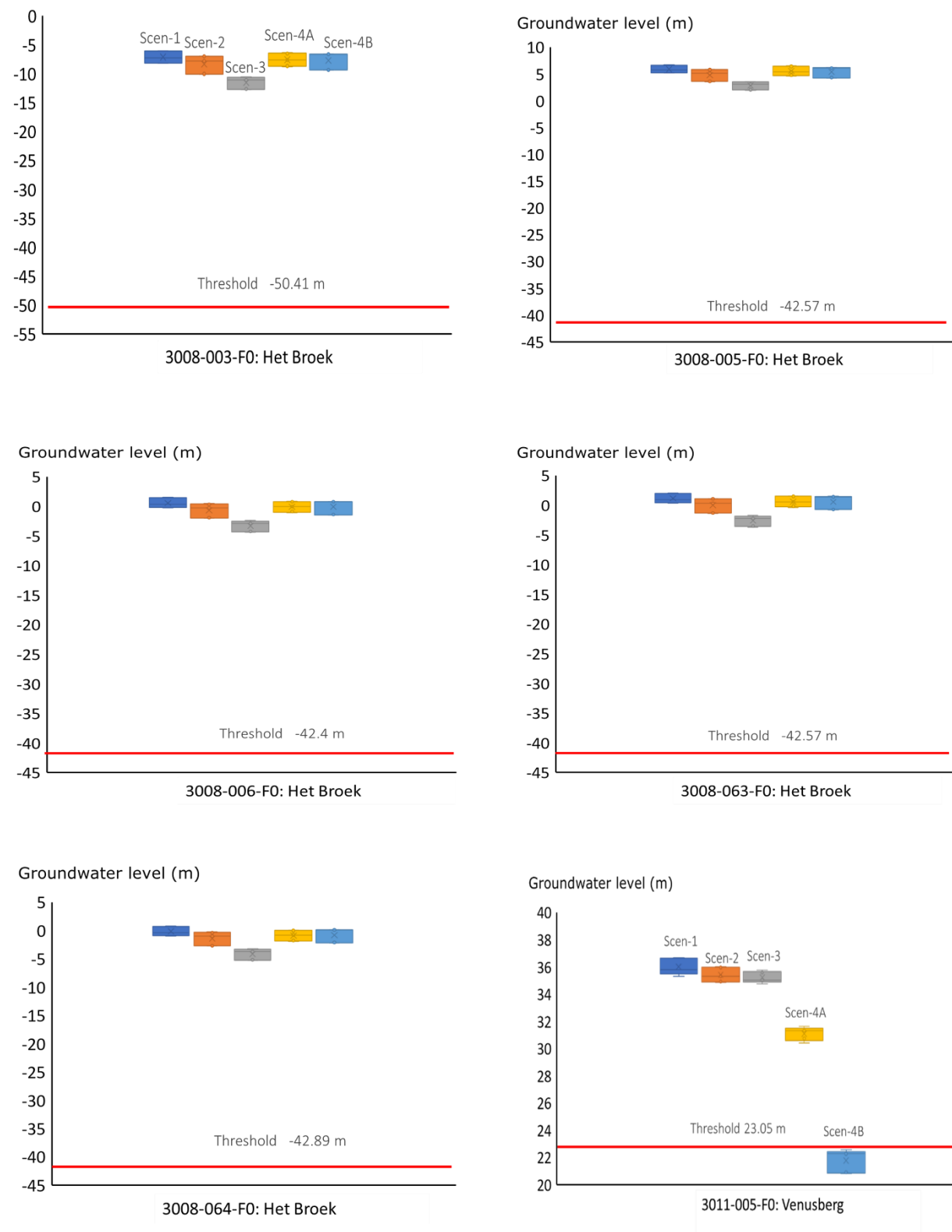


Figure 158: Prediction uncertainty in the simulated head associated with model parameters and boundary conditions for all five scenarios for the sites of Het Broek and Venusberg.

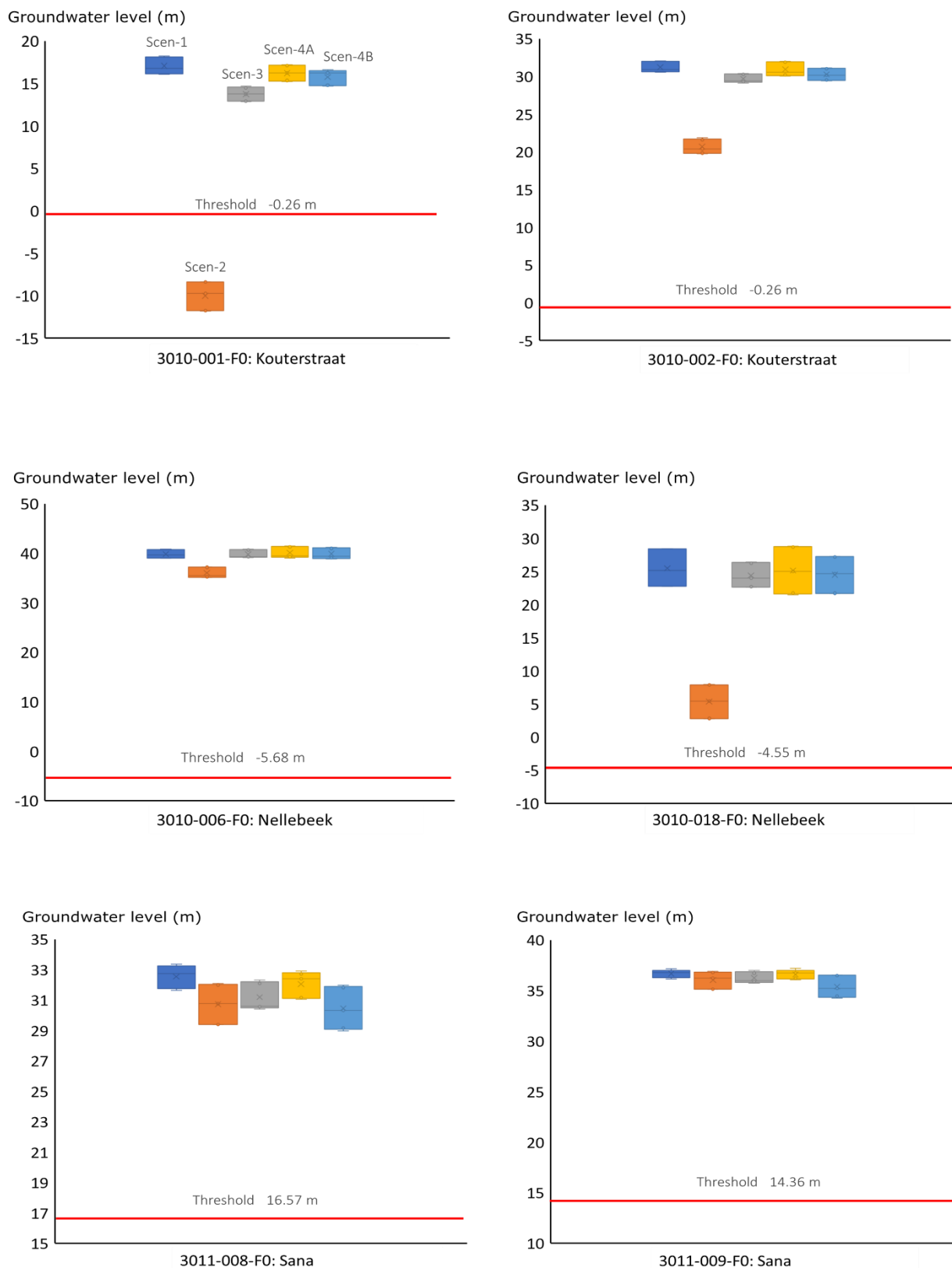


Figure 159: Prediction uncertainty in the simulated head associated with model parameters and boundary conditions for all five scenarios for the sites of Kouterstraat, Nellebeek and Sana.

7 Potential Maps

In this chapter, the potential for extraction in the Cretaceous is analysed. This is done by combining different spatially variable maps of factors that influence the extraction potential. The three factors that are considered are:

- The drawdown in a potential well with a given extraction rate
- The difference between the top of the Cretaceous and the hydraulic head in the Cretaceous in a potential well with a given extraction rate
- The depth of the Cretaceous (cost purposes)

For the first two factors, the effect of a synthetic well with an extraction rate of $600 \text{ m}^3/\text{d}$ is analysed. This synthetic well is implemented in the transient model that is extended until 2040. This well has a filter spanning across the entire Cretaceous aquifer, with a maximum filter length of 50m. The resulting heads in the year 2040 are analysed. The model is iteratively run by moving the position of this synthetic well on a grid of 2 by 2 km (see e.g., Figure I. 33). This way, the effect of this synthetic well can be analysed spatially. In total, the model is run 532 times (runtime approx. 30 hours). Note that the drawdown comprises other underlying factors like the transmissivity of the aquifer and the local hydraulic condition.

To better visualise the different spatially distributed maps, the results for the different factors are subdivided into potential classes which correspond with a very low, low, medium, and high extraction potential. By combining these three factors and assigning weights to each factor, a general map of the potential for the extraction in the Cretaceous is obtained. Note that the current extraction sites of De Watergroep are considered in the model. The potential map thus visualises the potential for additional extraction in the Cretaceous aquifer.

7.1 Drawdown

The effect of a synthetic well with $Q=600 \text{ m}^3/\text{d}$ on the hydraulic head in the extraction well is analysed. A point map of the simulated drawdown in the synthetic extraction well is shown in Figure I. 33. The drawdown point map is interpolated as to obtain a spatially distributed field of potential drawdown (Figure 160). Note the very large drawdowns in the north-western part of the model, with drawdown of $>50\text{m}$, with a maximum drawdown of 125m. This is caused by the very low hydraulic conductivities in this area. Furthermore, this area is especially vulnerable for over-exploitation since it is still recovering from historical extractions. Towards the north-eastern corner of the model, drawdown decreases significantly. This is caused by the presence of the Formation of Maastricht on top of the Formation of Gulpen in this area (which increases in thickness towards the north-east). The Formation of Maastricht is characterized by higher conductivities (approx. 3 m/d), resulting in a more limited drawdown. The area around Leuven has drawdowns of 40 to 80m. Drawdowns are low ($<20\text{m}$) in the Dijle valley in the south, in the Tienen area and in the unconfined part of aquifer in the Walloon Region. A more zoomed in version of this drawdown map is shown for respectively the Dijle valley and the Tienen area in Figure 161 and Figure 162.

The continuous drawdown map is subdivided into four discrete classes indicating the effect of drawdown on the potential for extraction. A drawdown of less than 5m is classified as high potential, between 5 and 20m medium potential, between 20 and 50m low potential and more than 50 very low potential. The resulting map is shown in Figure 163. This spatially distributed map gives a clear view of which areas are characterised by the lowest drawdown.

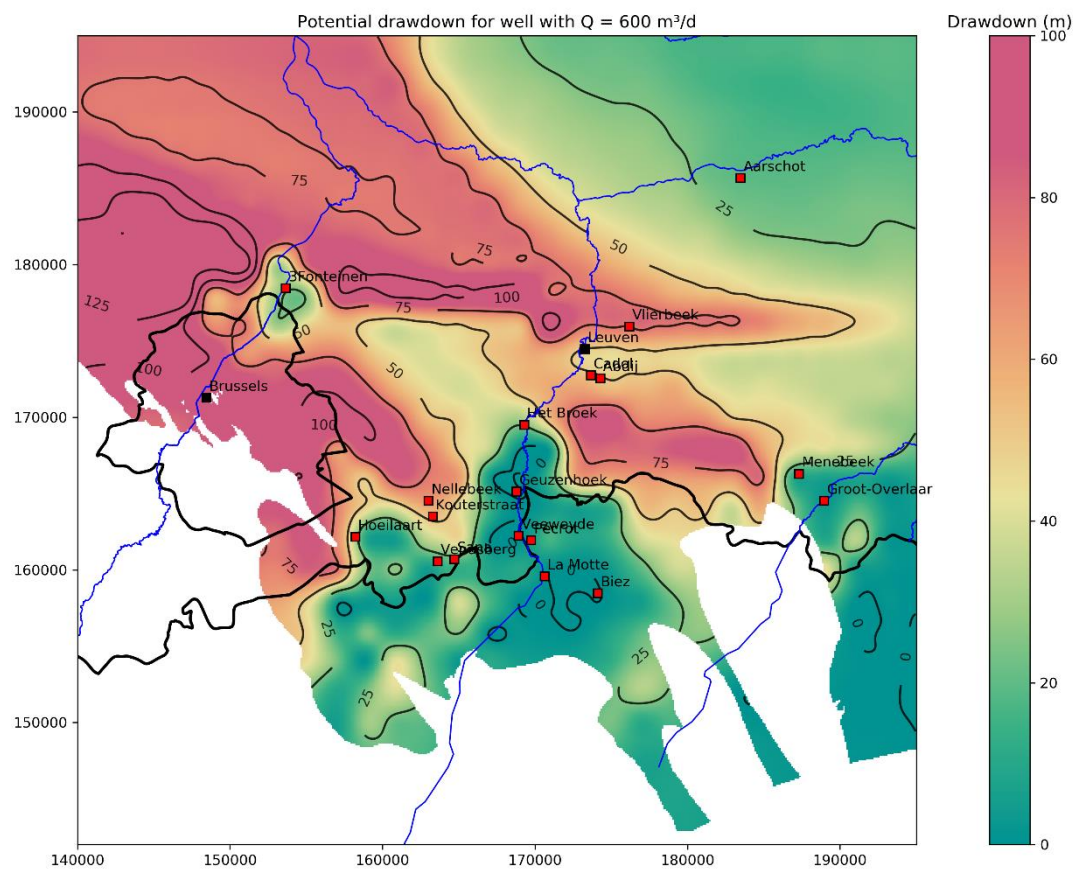


Figure 160: Continuous map of drawdown resulting from a synthetic extraction well with $Q=600\text{m}^3/\text{d}$.

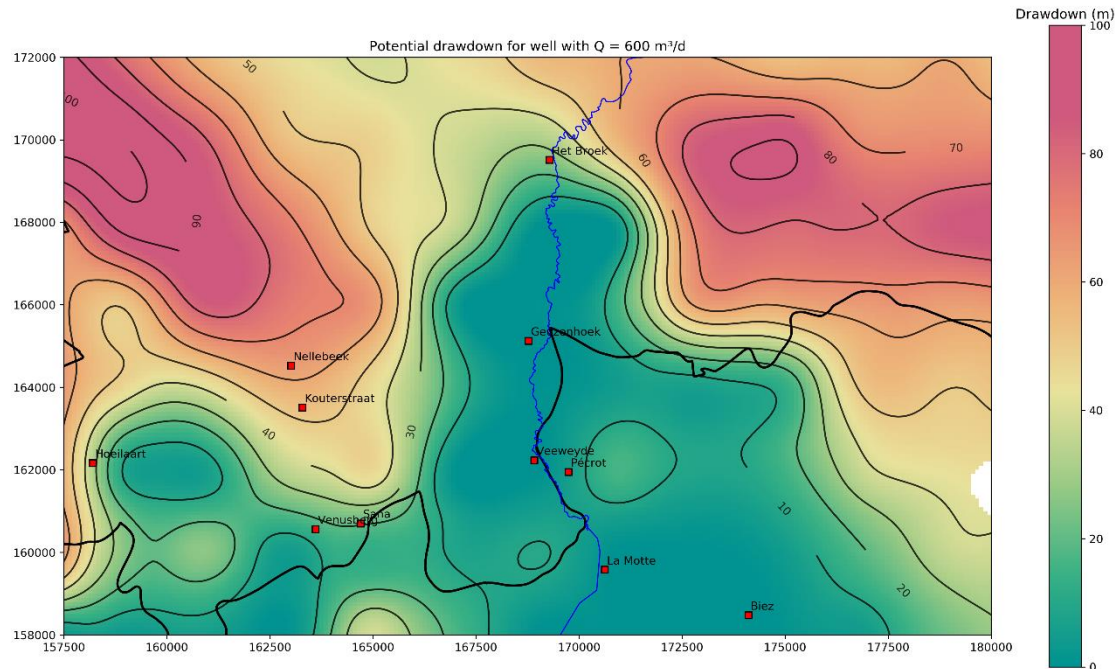


Figure 161: Zoom on the southern Dijle valley for the continuous map of drawdown resulting from a synthetic extraction well with $Q=600\text{m}^3/\text{d}$.

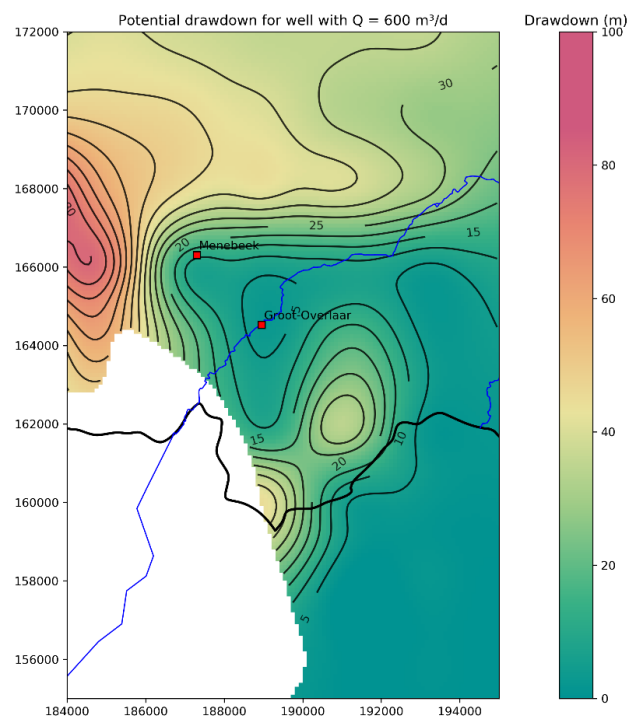


Figure 162: Zoom on the Tienen area for the continuous map drawdown resulting from a synthetic extraction well with $Q=600\text{m}^3/\text{d}$.

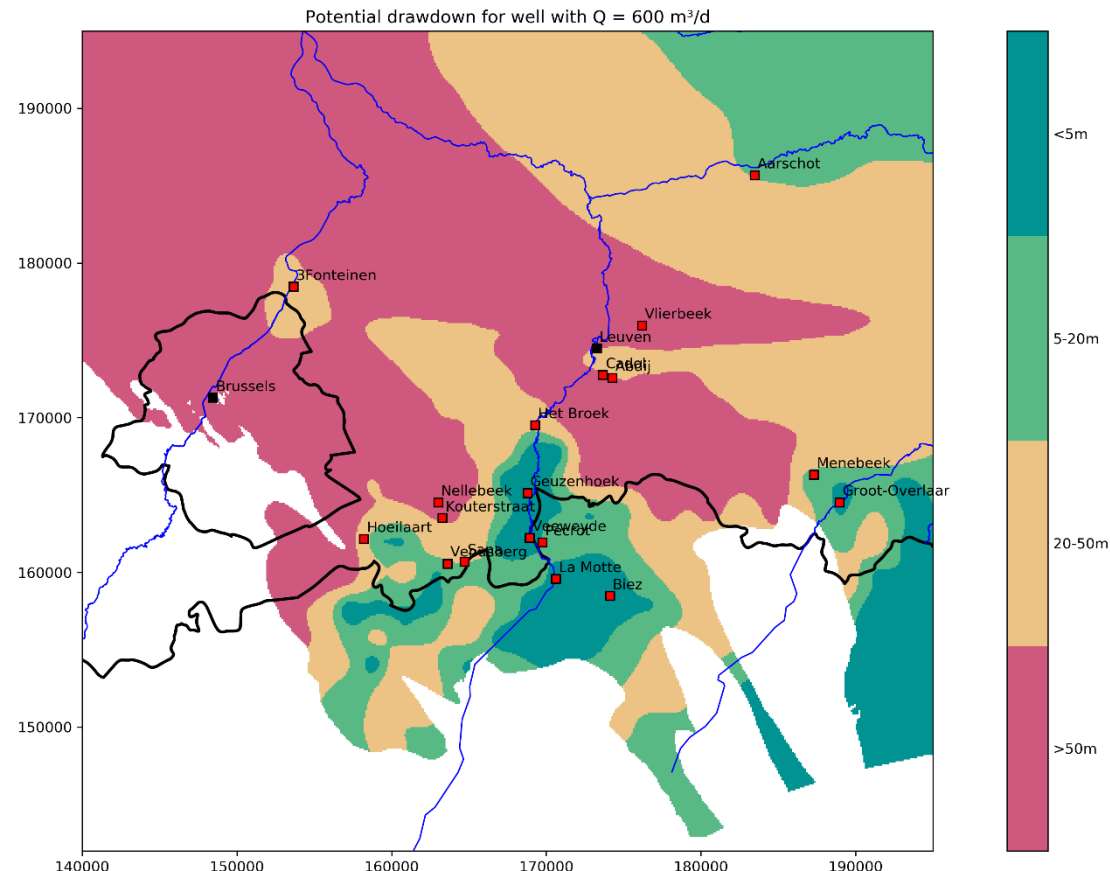


Figure 163: Discrete map of drawdown resulting from a synthetic extraction well with $Q=600\text{m}^3/\text{d}$.

7.2 Difference with top of the Cretaceous

The effect of a synthetic well with $Q=600 \text{ m}^3/\text{d}$ on the difference between the top of the Cretaceous and the hydraulic head in the synthetic extraction well is analysed. A point map of the difference between the two is shown in Figure 164. This difference point map is interpolated as to obtain a spatially distributed field of potential difference between the top of the Cretaceous and the head in the extraction well (Figure 164). In the northern part of the model area, there is still plenty of difference between the top of the Cretaceous and the simulated head. In this area, the Cretaceous is located very deep in the subsurface, and heads can be several hundreds of meters above the roof of the Cretaceous. From the west of the Vilvoorde area all the way up to the south-east of Brussels, heads can be close to or below the roof of the Cretaceous due to the very large drawdowns simulated in the synthetic well. In the Leuven area and around Het Broek, the difference is around 25-50m. This quite limited difference is due to the extractions already present in these areas, which already affect the heads quite strongly. In the southern part of the Dijle valley, heads are less than 20m above the roof of the Cretaceous. However, extraction in this area does not affect the hydraulic heads strongly. In the Tienen area, the head is still quite a lot higher than the top of the Cretaceous, up to 60m. In the southern part of the model area, in the unconfined part of the Cretaceous in the Walloon area, heads can be below the top of the Cretaceous. However, as the aquifer is unconfined in these parts, this is not so much an issue.

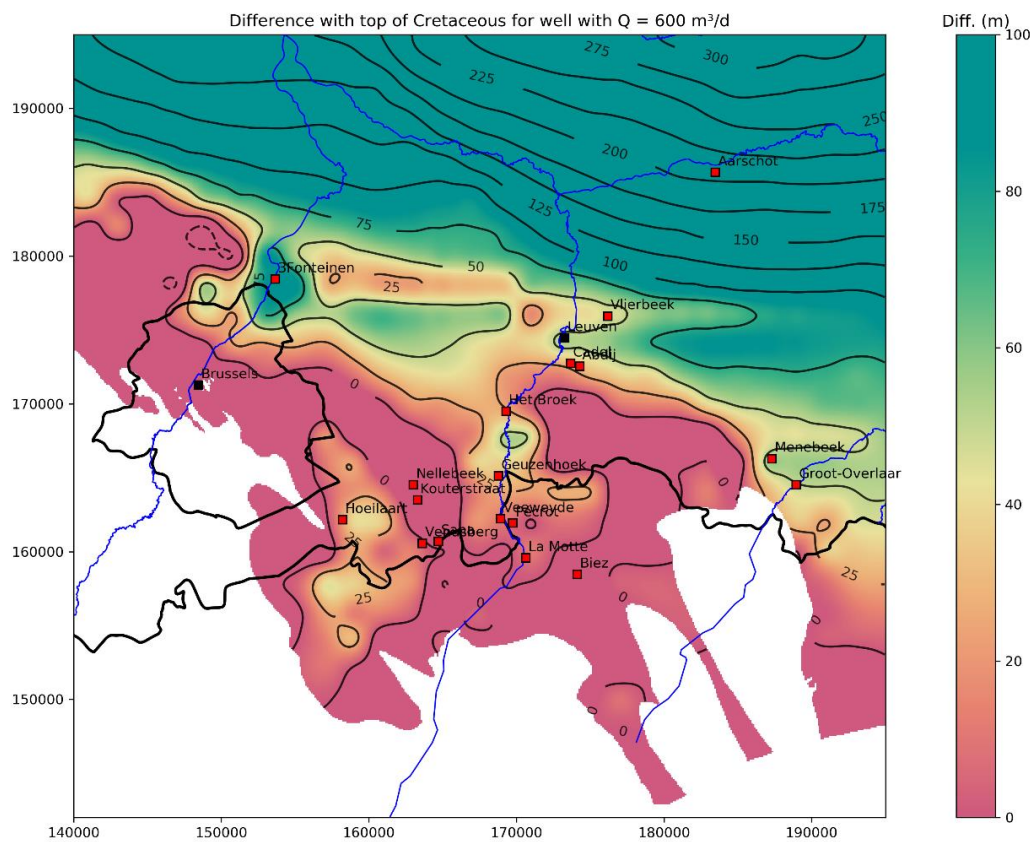


Figure 164: Continuous map of difference between top of Cretaceous and simulated head in a synthetic extraction well with $Q=600\text{m}^3/\text{d}$.

The continuous difference map is subdivided into four discrete potential classes indicating the effect of this difference on the potential for extraction. A difference of less than 0m is classified as very low potential, between 0 and 5m low potential, between 5 and 20m high potential and more than 50 very high potential. The resulting map is shown in Figure 165. One can argue that the unconfined parts of the aquifer can be assigned to the highest potential zone, as this criterion is much less of an issue here. The resulting map is shown in Figure 166.

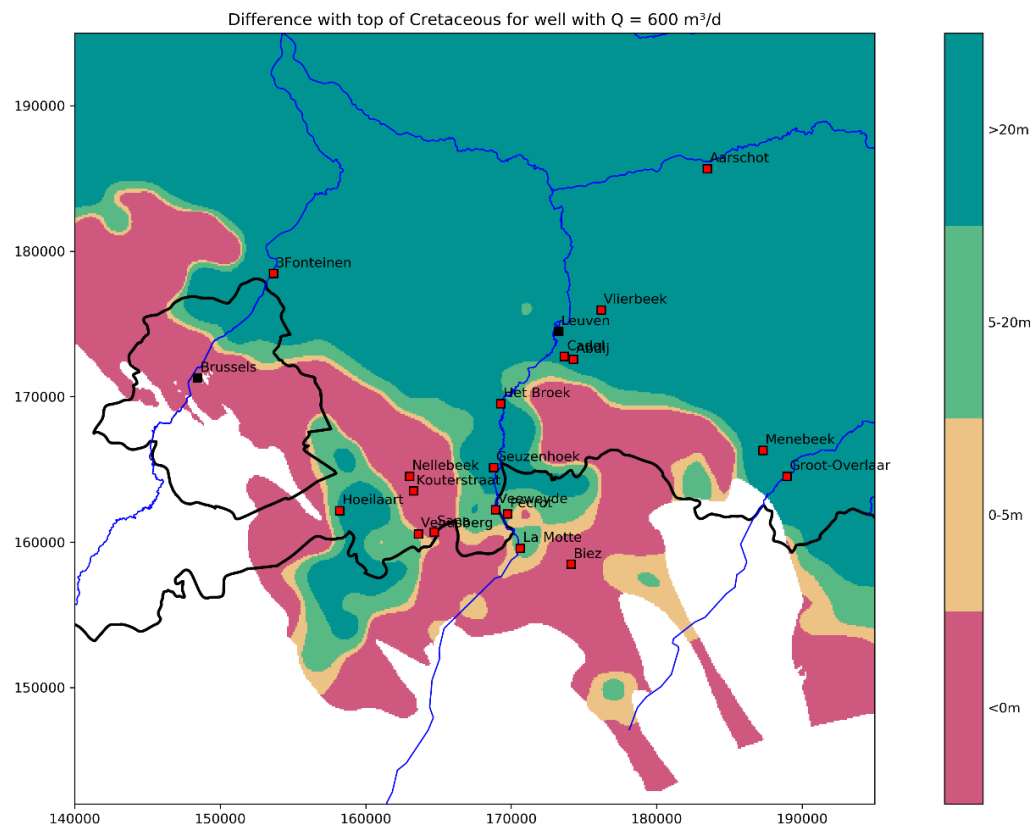


Figure 165: Discrete map of difference between top of Cretaceous and simulated head in a synthetic extraction well with $Q=600\text{m}^3/\text{d}$.
Difference with top of Cretaceous for well with $Q = 600 \text{ m}^3/\text{d}$

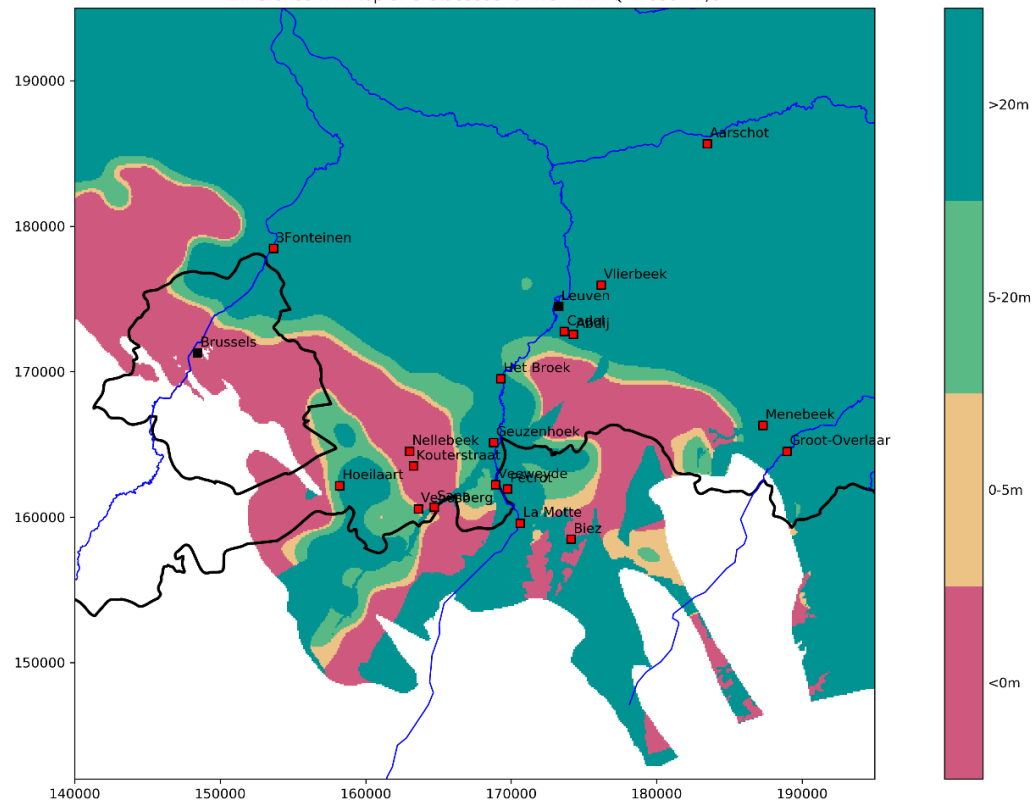


Figure 166: Discrete map of difference between top of Cretaceous and simulated head in a synthetic extraction well with $Q=600\text{m}^3/\text{d}$. Unconfined parts of the aquifer are assigned to the highest potential class.

7.3 Depth of the Cretaceous

The final criterion is the depth of the Cretaceous. The idea is that the deeper the Cretaceous is situated in the subsurface the more difficult and costly it is to drill boreholes, thus affecting the potential for extraction. A map of the depth of the top of the Cretaceous is shown in Figure 167. The Cretaceous dips towards the northeast, where it reaches a maximum depth of approx. 300m. In the Leuven area, the top of the Cretaceous is situated around 100 to 150m. Note the effect of the river valleys in the southern part of the model, causing the Cretaceous to be relatively close to the surface. In the southern part of the Dijle valley, the depth of the top of the Cretaceous is less than 50m.

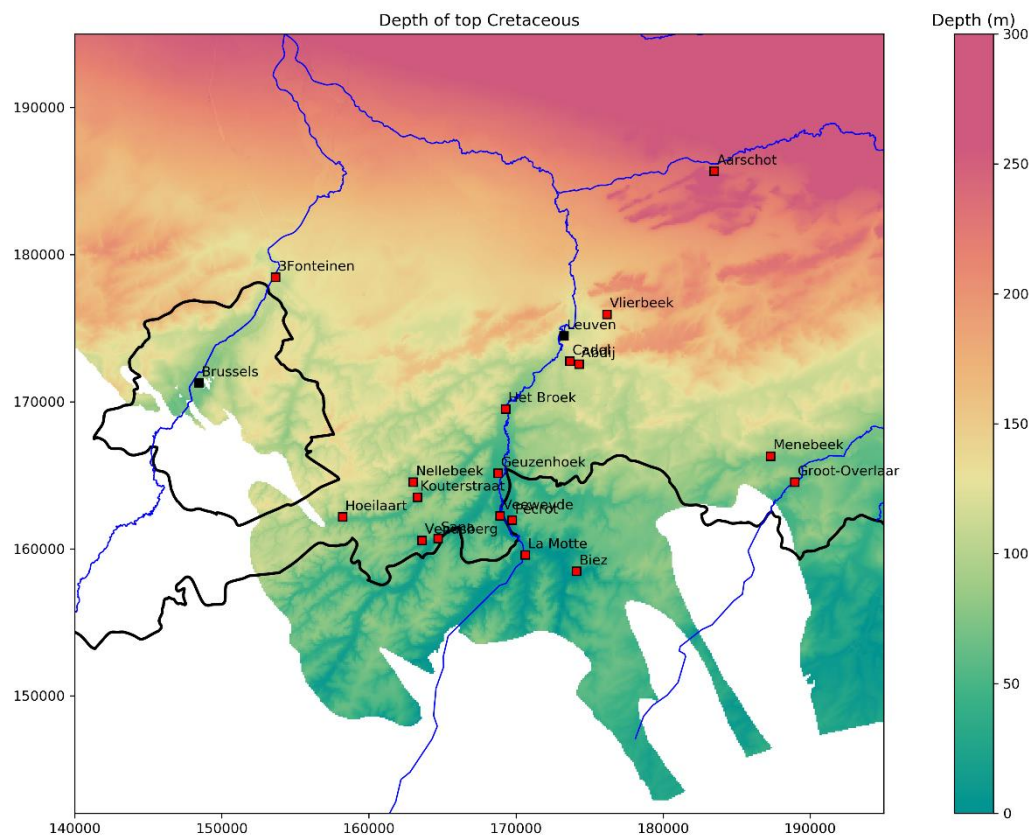


Figure 167: Continuous depth map of the top of the Cretaceous.

The continuous depth map is subdivided into four discrete classes indicating the effect of the depth on the potential for extraction. A depth of less than 25m is high potential, between 25 and 75m medium potential, between 75 and 150m low potential and more than 150m very low potential. The resulting map is shown in Figure 168.

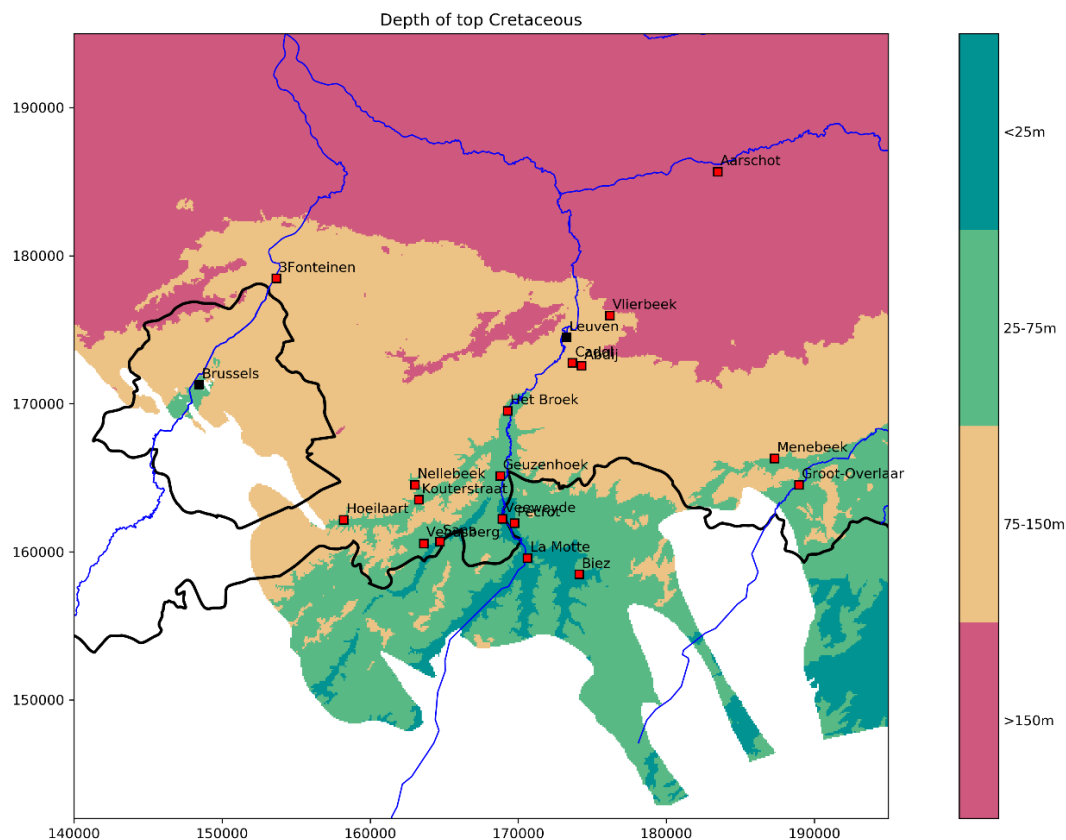


Figure 168: Discrete depth map of the top of the Cretaceous.

7.4 Potential for additional extraction in the Cretaceous

By combining the spatially distributed maps for the drawdown, difference with top of Cretaceous and depth of the Cretaceous, a combined map of the potential for additional extraction in the Cretaceous is created. This is done by assigning weights to each individual map. Furthermore, some hard rules are applied: when either the drawdown or the difference between top of Cretaceous and the hydraulic head is in the lowest potential class, the combined potential will automatically be classified as 'very low'. For the difference between the top of the Cretaceous and the hydraulic head, a correction is made for the unconfined areas of the model. When the aquifer is unconfined, the criterium of head not allowed to be lower than the top of the Cretaceous doesn't make as much sense as it does for the confined part. Therefore, the unconfined areas are assigned to the highest potential for the difference map. The weights are defined based on discussion and feedback with De Watergroep. The resulting potential map is shown in Figure 169, with weights of 60%, 10% and 30% for respectively the drawdown, the difference with the top of the Cretaceous and the depth of the Cretaceous. The areas classified as having high potential are the southern part of the Dijle valley (between the south of Het Broek up until Veeweyde and Pécrot), the unconfined part of the aquifer in the Walloon Region (region of La Motte) and in the south-east in the Walloon Region, but also some smaller patches near the Tienen area. These areas are characterized by high transmissivities and low depth of the Cretaceous. A larger part of the Tienen area is classified as medium potential. The north-eastern corner of the model area is also classified as medium potential, even though it is situated at large depths (>200m). The transmissivity is higher in this area due to the presence of the more permeable Formation of Maastricht. The Hoeilaart region is also characterized by medium potential. However, care must be taken in this area, as the more permeable upper Members of the Formation of Gulpen, including the important hardground interval, might not be present here (cfr. Nellebeek). The region around Leuven is classified as low to very low potential, due to its very low conductivities (and the already present extractions). The entire north-western part of the model area is classified as very low potential, due to the extremely low conductivities and large depths.

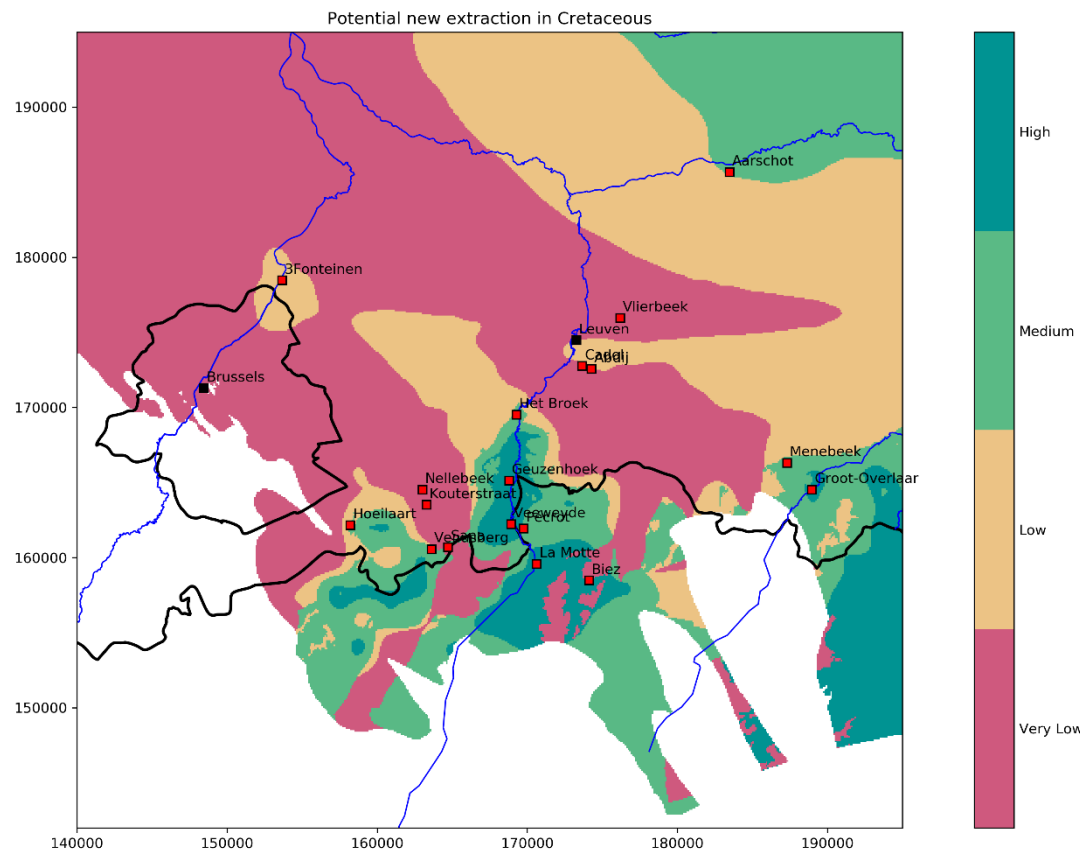


Figure 169: Potential map for new extraction in the Cretaceous with weighting of 60%, 10% and 30% for respectively the drawdown, difference with top of Cretaceous and depth of Cretaceous (including hard rules).

Maps resulting from other combinations of weights and hard rules are shown in Figure I. 35 and Figure I. 36.

8 Conclusions

8.1 Extractions and hydraulic heads

In Chapter 3, the evolution of extractions and hydraulic heads in the Brabant area are discussed in detail. The main extraction in this area is done by De Watergroep. Extracted rates increased from around 3.5M m³/year in the nineties to around 15M m³/year in recent years. The majority is extracted from the Cretaceous aquifer (12-14M m³/year), with some smaller volumes in the “tuffeau” zone of Lincent and in Grandglise. The extraction in the Cretaceous is mainly focused on the Dijle valley to the south of Leuven. The extracted volumes and the evolution of hydraulic head near the extraction site are discussed in detail. In general, hydraulic head fluctuations are caused by changes in extracted volumes at the extraction sites. In some areas, downward trends in head are present which can be linked to increased extraction rates at nearby sites (e.g., the site of Korbeek-Dijle Het Broek). In some extraction wells, a decrease in head in recent years is observed, which might be caused by well clogging or due to a decreased recharge in these last few dry years. The latter is mainly observed for the southernmost sites, which are located in or close to the unconfined part of the aquifer.

The extraction by other companies and organisations in the Brabant area decreased from 6M m³/year in the early 2000s to 2.5M m³/year in recent years. This decreasing trend is present for all three layers (Grandglise, Lincent and the Cretaceous). Most of the water is extracted from Grandglise and Lincent, while the extraction in the Cretaceous is very small. Extraction from the sands of Grandglise is mainly taking place in the Leuven area by Beneo Remy, Cargill and Inbev Leuven. In Lincent, extraction is located mostly in the “tuffeau” zone in the Tienen area, with the largest rates coming from Citrique, Affilips and Inbev Hoegaarden. In the Cretaceous, current extraction is very limited. In the past, there was mainly extraction in the Leuven area by Cargill and Inbev Leuven, but these extractions terminated at the end of the 2000s.

The evolution of the heads in the different regions of the Brabant area are discussed in detail. Near the west boundary, heads are recovering from historical extractions in both Grandglise and the Cretaceous. The historical drawdown is larger in the Cretaceous than in Grandglise. More towards the west, there is a strong historical drawdown in Grandglise, with recoveries of several tens of meters. In the Vilvoorde area, there is a similar trend of recovery of historical extraction, which is a couple of meters for Grandglise and up to 10m in the Cretaceous. These drawdowns are probably caused by historical extraction by the Vilvoorde Drie Fonteinen site and other extractions in the Cretaceous and the Basement in the industrial area around the former Renault site. In the north-eastern most side of the study area, heads are increasing in the Cretaceous (approx. 5-10m). This might be related to historical dewatering in the former mining areas more towards the east.

In the Leuven area, heads in the Cretaceous have been significantly decreasing (approx. 10m) in the period 1994-2002, after which they more or less recovered in the period 2003-2012. In recent years, a decreasing trend is visible again. These variations seem to be mainly related to changes in the extraction rates at the site of Korbeek-Dijle Het Broek, but there is also a contribution by the extraction of Inbev in the Cretaceous in Leuven in the late nineties, early 2000s. In the southern Dijle valley, changes in head are in general smaller. More towards the south, seasonal variations in the heads in both the Paleocene and Cretaceous aquifers are visible, around e.g., the sites of Geuzenhoek, Veeweyde and the sites in the Walloon Region. Near these southernmost sites, there is a slight decrease in heads in the last few years, which is related to a decrease in groundwater recharge due to the recent droughts.

8.2 Geology and hydrogeology

In Chapter 2, the geology and hydrogeology in the Brabant area is discussed in detail. First, the geology of the Cretaceous deposits in Flanders are analysed. Secondly, the hydrogeology of the Paleocene and Cretaceous aquifer systems in the Brabant area are discussed.

In the Brabant area, the Cretaceous and Paleocene aquifer systems are largely confined by the Ieperian aquitard, consisting of the clays of the Formation of Kortrijk. Most of the study area is confined by these clays, with exception of the south-east area around Tienen and in the south in the Walloon region. The Cretaceous deposits are present on top of the Palaeozoic basement (Brabant Massif). They are close to the surface in the south in the Walloon region but dip down towards the north where they quickly reach depths of several hundreds of meters. The thickness of these deposits varies from a couple of meters in the south, where they wedge out against the Brabant Massif, to more than 100m in the northeast. They are Campanian to Maastrichtian in age and consist mainly of the deposits of the Formations of Gulpen and Maastricht. The majority of the Cretaceous aquifer in this area is composed of the Formation of Gulpen, with the Member of Zeven Wegen accounting for the largest part of the thickness. The Zeven Wegen chalk is a fine-grained chalk, the typical "writing" chalk. On top of Zeven Wegen, a limited interval of deposits of the Members of Lixhe and Lanaye is present, respectively fine-grained chalk and fine calcarenites. In the Vilvoorde area, the Cretaceous consists of the Formation of Nevele, a lateral equivalent of the Formation of Gulpen. In the north-eastern corner of the study area, the coarser-grained calcarenites of the Formation of Maastricht are present, which dip strongly towards the north-east where they reach thicknesses of >80m.

On top of the Cretaceous, in the northeast of the study area, the deposits of the Formation of Heers are present which consist of the sands of Orp, the marls of Gelinden and the clayey marls of Maaseik. Together, these deposits can reach a thickness of up to 25m in the east. Next, the deposits of the Formation of Hannut are present, which are present everywhere in the study area and can reach thicknesses of 50 to 100m. In the north-east, the clays of Waterschei and Beselare are present. Next, the Member of Halen and Lincent is present, consisting of the silty deposits of Halen and the "tuffeau" of Lincent. The latter is present locally in the Tienen area and is a more chalky to marly deposit that is often silicified. Due to dissolution of silica, the porosity is strongly increased. In the Tienen area, these deposits are fractured, resulting in large permeabilities. The sands of Grandglise are present everywhere in the area, with an average thickness of approx. 20m. Locally in the east, the sandy deposits of Loksbergen and Dormaal are present. The clays of the Formation of Kortrijk are the main confining unit in the area, with a thickness of several tens of meters. The sands of Brussels are present on top of the Paleocene deposits in the areas where the Kortrijk clay is not present, mainly in the southern part of the area in the river valleys. Locally, Quaternary deposits are present on top of the Cretaceous and Paleocene aquifer systems, mainly in the river valleys and in the Tienen region in the southeast.

Combining pumping test data with flow and gamma-ray measurements

In section 2.3.2, information from pumping tests on the extraction wells of De Watergroep are combined with flow and geophysical measurements to analyse the reasons for the large variations in well yields in the Cretaceous aquifer.

The presence of an interval of a couple of meters in thickness associated with a hardground plays a crucial role for the well yields at the extraction wells in the Cretaceous. In the Leuven area, the permeability of this interval is relatively limited (around 2 m/d), but it significantly increases towards the south, with around 9 m/d for the northern wells of Het Broek and 60-140 m/d for the southern wells of Het Broek. The thickness also increases from north (2-3m) to south (5-6m). This hardground interval also plays an important role for the sites of Venusberg and Geuzenhoek. This hardground at the top of the Zeven Wegen chalk is characterized by branched glauconite-bearing bioturbations, at least partially cemented with phosphate cement. On top of the hardground, a phosphite horizon is observed, which indicates an important time hiatus between the Zeven Wegen chalk and the coarser deposits of Lixhe and Lanaye. The hardground probably corresponds with two hardgrounds more to the east in Limburg:

Bovenste Bos (Froidmont) and Wahlwiller (Lixhe). The lithological descriptions at Het Broek, Venusberg and Geuzenhoek indicate the presence of a phosphatic gravel, consisting of well-rounded (Het Broek) to badly rounded (Geuzenhoek) balls of 1-2cm in diameter of hard fine-grained phosphatic chalk. This phosphatic gravel might be the result of reworking or erosion and redeposition of chalk material. This interval associated with the hardground clearly has higher permeabilities in the south (Het Broek S, Venusberg, Geuzenhoek) than in the north (Het Broek N, Leuven area) indicating a stronger reworking or even karstification of this interval. In Biez, a similar interval with eroded coarse chalk with flint and a phosphate layer is identified, associated with a hardground (Vandenbergh & Gullentops, 2001).

The Zeven Wegen chalk is characterized by little to no flow contribution for the wells in the north (Leuven area, Het Broek, Nellebeek). This fine-grained chalk has a very low primary permeability, resulting in low well yields in the north. However, towards the south, at multiple sites (Venusberg, Sana, Veeweyde, the wells in the Walloon region) there is a significant contribution of flow all throughout the Zeven Wegen chalk. In some of the borehole descriptions, fracture zones in the Zeven Wegen chalk are observed. This corresponds well with the very high flows identified over the entire chalk interval at these sites. Most of the flow is concentrated at several relatively thin fracture zones. Due to these fracture zones, the well yields in these southern wells are very high. The site of Geuzenhoek is a bit of a transition between the area with fracture zones in the south, and the northern wells where the hardground interval plays the largest role.

The Members of Lixhe and Lanaye are present on top of the Zeven Wegen chalk at most of the sites (with exception of Nellebeek). In the northern site, these Members contribute a little to the total flow, more than the Zeven Wegen chalk, but all in all still a quite low contribution. At Aarschot, the coarser-grained and more permeable calcarenites of Maastricht are present on top of the Formation of Gulpen. Most of the flow comes from these Maastrichtian deposits, with a limited contribution from the top of Gulpen (Lixhe/Lanaye).

Spatial variability of the hydraulic conductivity of the Cretaceous

In section 2.3.3, a spatially distributed map of hydraulic conductivity of the Cretaceous is generated using a correlation between horizontal conductivity derived from pumping tests and the depth of the top of the Cretaceous deposits. This correlation between HK and depth of the Cretaceous includes both the effect of fractures and the presence and permeability of the hardground/phosphatic gravel interval. In the southern part of the area, where the Cretaceous deposits are close to the surface, the chalk is fractured, resulting in a strong increase of hydraulic conductivity. More towards the north, where the Cretaceous is deeper in the subsurface, these fractures are not observed, resulting in a much lower hydraulic conductivity. Superimposed on this, is the effect of an increase in permeability of the hardground/phosphatic gravel interval from the north towards the south. The combination of these two factors results in the correlation. Note that this correlation is only valid for the Formation of Gulpen. In the north-eastern part of the area the Formation of Maastricht is present. These deposits consist of coarser grained calcarenites with a higher primary permeability. Even when these deposits are present very deep in the subsurface, decent permeabilities are observed.

The sites of Nellebeek and Vilvoorde are exceptions to this correlation between HK and depth. At Nellebeek, estimated HK based on pumping tests is significantly lower than expected based on the correlation. This is caused by the absence of the hardground interval that provides the majority of the flow in the more northern wells. In the western site of the study area, from Nellebeek towards Brussels, the Cretaceous only consists of the Member of Zeven Wegen, while the overlying Members of Lixhe/Lanaye and thus also the hardground interval are absent. At the site of Vilvoorde, estimated HK is significantly higher than expected for the Cretaceous at such a large depth. Combined with the fact that the flow is spread over the entire filter (Nevele Formation), this indicates the presence of fractures in the Cretaceous in this area. This is the only area where fractures are observed at such a deep depth. A possible explanation for this is the fact that these deposits are closer to the axis of the Brabant Massif. The fractures might possibly be related to earlier phases of fracturing related to the upheaval of the Brabant Massif.

Using the correlation between depth and HK, a spatially distributed map of HK is generated. However, only using this correlation leads to significant differences between HK based on pumping tests and the HK estimated based on the correlation. For example, for the area of Het Broek, the different extraction wells show a strong variability in HK even though they are situated at the same depth. The map of HK is improved by performing kriging using the correlation HK-depth as secondary information. This way, the actual pumping test data is used as primary data, strongly affecting the HK field close to these pumping tests, while in areas far away from pumping test data, the HK field is purely based on the correlation depth-HK. This way, a much better match is obtained between the HK obtained by the pumping tests and the HK simulated using kriging with the correlation depth-HK as secondary data.

8.3 Groundwater modelling: the Brabant Model

In Chapter 4, groundwater models (MODFLOW) are set-up for the Brabant area. These models include the deposits of the Paleocene and Cretaceous aquifer systems, which are confined by the Ieperian Aquitard. First, a steady-state modelling approach is adapted to provide insights in the important parameters in the model area. Steady-state models are set-up for the year 2018 and for the period 2000-2004. The results of the latter are used as a start for a transient model for the period 2004-2020.

The Brabant Model comprises the deposits confined by the Ieperian Aquitard: the Paleocene and Cretaceous aquifer systems. Three layers are modelled. The first layer consists of the more permeable top of the Paleocene aquifer system, consisting mainly of the sands of Grandgîse. Layer 2 is the less permeable bottom part of the Paleocene aquifer system, consisting of clayey, silty to marly deposits of which the Halen/Lincent deposit is the most important one. Layer 3 consists of the Cretaceous aquifer system. The bottom boundary are the impermeable deposits of the Palaeozoic Basement, while the Ieperian clays are the confining unit at the top. The west, north and east boundaries are modelled as a General-Head Boundary, with a specified head at a certain distance outside the model area. The top boundary in the unconfined part of the area is modelled with a GHB boundary with specified heads based on a correlation between observed heads and topography. All the extraction wells of De Watergroep and of other companies and organisations are modelled with respectively the Multi-Node Well package and the Well package.

The transient model is calibrated for the period 2004-2018 and validated for 2019-2020. Performance in both periods is similar. The model can reproduce observed heads reasonably well over the entire range of heads from -50 to +80mTAW. An R^2 of 0.94 is obtained, a mean error (ME) of -0.21m, a mean absolute error (MAE) of 3.70m and a RMSE of 5.16m. In general, the evolution of heads at the extraction sites can be reproduced reasonably well. The effect of changes in extraction rate on the heads in the extraction wells are well reproduced. For the site of Het Broek, simulated heads in the extraction wells are in a smaller range than the observed heads, indicating a stronger connectivity between these well regions. In the area around Leuven, there is a slight underestimation of heads in the observation wells close to the extraction wells, indicating that the model underestimates the areal extent of the pumping cone in these areas.

The water budget shows that the outflow out of the model consists mainly of the extraction through the wells of De Watergroep with a more limited contribution by wells of other entities. The inflow into the model consists of the inflow through all the boundaries modelled with the GHB package. This includes both the boundaries at the edge of the model in the north, west and east, as well as the top boundary. The latter consists of the inflow from the layers on top of the modelled layers in the unconfined part of the aquifer system and the leakage through the clay layer of the Formation of Kortrijk in the confined part of the aquifer system. An import part of the inflow is through the eastern boundary in the south-east of the model area, but a large part of this flow discharges in river valleys in this area. In the southeast, the modelled layers are unconfined to semi-confined. This area is an important recharge area for the Cretaceous and Paleocene aquifer systems. The southern part of the study area in the Walloon region is also an important recharge area.

8.4 Scenario analysis

In Chapter 5, a scenario analysis is performed based on the transient model. The transient model is extended to 2040, and different extraction scenarios are calculated. The effects of an increase in extraction on the state of the aquifer are simulated and the sustainability of these extraction scenarios are analysed.

In Scenario 1 the current/normal extraction is simulated until 2040. The model does not predict any clear decreasing trends of head, indicating that the current extraction is sustainable on the long term. In the Vilvoorde and Leuven areas there is an increase in heads due to the recovery from historical extractions.

In Scenario 2, the maximal permitted scenarios are implemented. In Scenario 2a, a limited rate for Het Broek of 2.5M m³/year is applied because the current permit of 4.38M m³/year is unrealistically high. The largest effects in Scenario 2a are on the extractions around Leuven, the site of Aarschot and the sites of Nellebeek and Kouterstraat. These are mainly the areas with the lowest HKs in the Cretaceous. An increase in extraction rates results in significant additional drawdown in these areas. At the site of Nellebeek, there is also an effect on the heads in Lincent and Grandglise. The additional drawdown in the production wells near Leuven and Aarschot is 20 to 30m. Similar drawdowns are observed for Kouterstraat and Nellebeek. For these sites, equilibrium is reached after 5 to 10 years. The additional drawdown in the southern wells (Sana, Venusberg, Veeweyde and the sites in the Walloon Region) is limited to approx. 1m.

In Scenario 2b, the actual permitted rates for Het Broek of 4.38M m³/year are implemented. This results in a significantly larger effect than in Scenario 2a, with large drawdowns in the area around Het Broek. Additional drawdowns of more than 4m are observed in an area of 200km² around the site of Het Broek. In the production wells of Het Broek, an additional drawdown of 15 to 25m is simulated and it takes about 20 to reach a new equilibrium. The additional drawdown in the wells of Heverlee Cadol & Abdij is approx. 2m and 3m for Geuzenhoek. The heads in the extraction wells of Het Broek are still above the top of the Cretaceous, but the leeway is getting significantly smaller, with the smallest difference being 7.8m for 3008-002. This indicates that the head in the Cretaceous is getting dangerously close to the threshold and that extracting these very high permitted volumes is not advisable.

In Scenario 3, an increase of 10% compared to the normal situation is simulated. The areas surrounding the sites of Het Broek, Cadol and Abdij are characterized by drawdowns >1m. In the northern production wells, additional drawdowns of a couple of meters are simulated, while for the more southern wells the effect is limited.

In Scenario 4, the effect of an increase in extraction rates for the site of Venusberg is explored. In Scenario 4a, the current permit is doubled to 100 m³/h. This results in an additional drawdown of 5.4m in the production well and 2m in the closest observation wells. A drawdown of >1m is simulated in an area with radius 1.5km around the extraction well. There is a limited effect on the nearby extraction sites of Sana, Nellebeek and Kouterstraat.

In Scenario 4b, the extraction rate at Venusberg is increased to 200 m³/h. This results in an additional drawdown of 14m in the production well and 5-6m in the nearby observation wells. A drawdown of >1m is simulated for an area with radius 5km around the extraction well. The effect on the nearby extraction sites of Kouterstraat, Nellebeek and Sana is respectively 1.2, 0.8 and 0.5m. The hydraulic head at the extraction well is 0.6m below the top of the Cretaceous, indicating that this scenario is not sustainable. However, a recent pumping test on the new pumping well in Venusberg resulted in a drawdown of approx. 10m for a rate of 200 m³/h, indicating that the model might overestimate the drawdown. Comparing a pumping test of a couple of days with continuous extraction for 20 years as simulated in the model is, however, not evident. In the pumping test, the difference between head and the top of the Cretaceous was only 3m, indicating that there is not much room for error. Continuous extraction at 200 m³/h is thus not advised. Extraction at 100 m³/h is, however, feasible, as demonstrated in Scenario 4a.

In Scenario 5, all extraction from the wells of De Watergroep in the Cretaceous is terminated. This scenario shows the extent and the speed of recovery from the current extraction. The recovery is the largest for the area around Het

Broek and for the wells around Leuven. An area of 200km² is characterized by a recovery of more than 5m. In the shallower parts of the aquifer, the recovery is limited to approx. 2m and even less at the sites in the unconfined part. In the area of Het Broek, there is also a significant recovery of up to 8m in Lincent and up to 3m in Grandglise. The heads in the extraction wells recovered 55-65m for the sites in the Leuven area. Recovery is very slow, and heads are not fully recovered in 2040. Full recovery is expected after three of four decades. For the sites of Aarschot, Kouterstraat and Nellebeek, a recovery of 20-30m is simulated. Recovery is slightly faster, and equilibrium is reached in 2040. The extraction wells of Het Broek show recoveries of 25-50m, with the largest recoveries for the northern wells. Recovery is slow and is not fully reached in 2040. The recovery for the sites of Veeweyde, Venusberg and Sana is limited, and is respectively 3, 4 and 7m. Recovery is faster, and is reached after 5 to 10 years. For the wells in the Walloon Region, recovery is approx. 1-3m, is very fast, and heads are fully recovered in a couple of years.

8.5 Uncertainty analysis

In Chapter 6, an uncertainty analysis is performed on the groundwater model, quantifying the parameter uncertainty, and the total uncertainty. The Integrated Bayesian Multi-model Uncertainty Estimation Framework (IBMUEF) is applied, in which the DREAM algorithm for uncertainty analysis is coupled with MODFLOW. This uncertainty analysis is applied on the scenarios defined in Chapter 5, resulting in uncertainty estimates on the predictions in these scenarios.

In total, twelve parameters are included in the uncertainty analysis, including hydraulic conductivity and specific storage of the different layers as well as parameters related to the boundary conditions. The posterior probability distributions of the model parameters and boundary conditions show that the parameters are well identified within their prior ranges. The posterior distribution functions of most of the parameters cover only a very small part of their prior range, indicating that the hydraulic head observations contain sufficient information to estimate these model parameters.

The prediction uncertainty is quantified for the scenarios defined in Chapter 5. Spatially distributed maps of prediction uncertainty are created, demonstrating that the uncertainty varies from a couple of meters to around 10 meters. The uncertainty increases towards the areas with lower observation density. Furthermore, the areas affected by historical extractions show the largest uncertainties. This is probably related to the sensitivity of the model results in these zones to the specific storage, which locally strongly affects the recovery of the heads.

The prediction uncertainty on the model estimates in the extraction sites in five different scenarios is explored. The prediction uncertainty in these extraction wells vary from 1 to 7.3m. In general, the prediction uncertainty associated with the model parameters and boundary conditions are in the same magnitude as the impact of the extraction in the different scenarios. This indicates the importance of the inclusion of this prediction uncertainty in policy planning and management strategies of the extraction in the Cretaceous.

Under the current extraction conditions, the hydraulic heads at all extraction sites are above the defined thresholds. The threshold is defined as the top of the Cretaceous for the unconfined part and the top of the filter in the unconfined part of the aquifer. This demonstrates that the current extraction of De Watergroep in the Cretaceous is, in general, sustainable on the long term. Increased extraction explored in the scenarios will significantly decrease the heads but in general no decrease below the thresholds is observed. Exception to this is the increased extraction at the site of Kouterstraat in the maximal scenario (extraction at permitted rates) and at Venusberg for the +300% increase scenario for this site. In the northern wells in the Leuven area and at the sites of Kouterstraat and Nellebeek the increased extraction has a large effect on the heads. Even though in general the thresholds are not reached, these very large drawdowns should be avoided.

8.6 Potential maps

In Chapter 7, the potential for extraction in the Cretaceous is visualized by combining different factors, including the drawdown of a synthetic well, the difference between the head in the Cretaceous and the top of the Cretaceous, and the depth of the Cretaceous. By weighting these different factors and classifying the results in different potential classes, a clear view of the potential for additional extraction in the Cretaceous is obtained. These results can be used to optimize the distribution of the extraction rates in this aquifer.

The drawdown of a synthetic well is the smallest in the southern Dijle valley, in the area between the south of Het Broek and Pécrot. More towards the south, in the unconfined part of the aquifer around La Motte and Biez drawdown is very limited. The Tienen area is also characterized by relatively small drawdowns. In the north-eastern corner, the presence of the more permeable calcarenites of the Formation of Maastricht result in relatively limited drawdowns. Simulated drawdowns are the highest in the northwest and in the Leuven area, due to the low hydraulic conductivities and the presence of historical extractions.

The difference between the head in the synthetic well and the depth of the Cretaceous is very high in the northeast, where the Cretaceous deposits are present deep in the subsurface. From the west of the Vilvoorde area all the way up to the south-east of Brussels, heads can be close to or below the roof of the Cretaceous due to the large, simulated drawdowns. In the Leuven area and around Het Broek, the difference is around 25-50m. This quite limited difference is due to the extractions already present in these areas, which already affect the heads significantly. In the southern part of the Dijle valley, heads are less than 20m above the roof of the Cretaceous. However, extraction in this area does not affect the hydraulic heads strongly. In the Tienen area, the head is still quite a lot higher than the top of the Cretaceous, up to 60m.

The final criterion is the depth of the Cretaceous. The idea is that the deeper the Cretaceous is situated in the subsurface the more difficult and costly it is to drill boreholes, thus affecting the potential for extraction. The Cretaceous dips towards the northeast, where it reaches a maximum depth of approx. 300m. In the Leuven area, the top of the Cretaceous is situated around 100 to 150m. Note the effect of the river valleys in the southern part of the model, causing the Cretaceous to be relatively close to the surface. In the southern part of the Dijle valley, the depth of the top of the Cretaceous is less than 50m.

These three different factors are combined to generate a clear view of the potential for additional extraction in the Cretaceous. The areas classified as having high potential are the southern part of the Dijle valley (from the south of Het Broek up until Veeweyde and Pécrot), the unconfined part of the aquifer in the Walloon Region (region of La Motte) and in the south-east in the Walloon Region, but also some smaller patches near the Tienen area. These areas are characterized by high transmissivities and low depth of the Cretaceous. A larger part of the Tienen area is classified as medium potential. The north-eastern corner of the model area is also classified as medium potential, even though it is situated at very large depths. The transmissivity is higher in this area due to the presence of the more permeable Formation of Maastricht. The region around Leuven is classified as low to very low potential, due to its very low conductivities (and the already present extractions). The entire north-western part of the model area is classified as very low potential, due to the very low conductivities and large depths.

8.7 Limitations and directions for future research

The Brabant model is a complex, large-scale regional model. The model performance is decent for such a large-scale model of a geologically complex, confined aquifer system. However, locally, model residuals might still be relatively large. One should keep in mind that the aim of the Brabant model is to analyse the state of the aquifer system on a large-scale. The model can be used to make predictions for specific areas, but one should consider the coarse resolution of this model. Furthermore, it is difficult to find suitable parameter values that result in a good fit for the entire model area without over-parametrization of the model parameters. For smaller-scale models, this is less of an

issue, as spatial variability of the parameters is often much more limited. Smaller-scale local high-resolution models might be needed for more precise predictions in specific areas. The results of the Brabant Model can be used as a basis for such smaller-scale models, e.g., for the definition of the boundary conditions.

The uncertainty on the spatial variability of the hydrogeological properties of both the Cretaceous and Paleocene aquifer systems is large. Even though our understanding of the spatial variability in the Cretaceous is improved in this study, still significant uncertainty is present. The information we have on the spatial variability in the layers of Grandglise and Lincent is even more limited. Especially for Lincent, there is a strong lateral variability in lithology, but the exact extent of this variability is not known at this moment. Extra attention is needed to improve our understanding of these deposits so that they can be represented more accurately in groundwater models. The exact extent and thickness of the clays of the confining Ieperian aquitard can also be uncertain, especially in areas where river valleys are locally incised into this layer. This is exemplified by the Brusselian channel near Hoeilaart which has a strong effect on the heads in the Paleocene aquifer system. When this channel is not considered, heads in this area are underestimated significantly.

One of the main problems in the Cretaceous is that most of the available observation data is coming from extraction wells. The head measurements in these wells are inherently more uncertain than measurements in observation wells, due to the effect of well losses, clogging of the filter, etc. As the simulated heads in the extraction wells are very sensitive to small changes in the model parameters, and the absolute changes in heads are significantly higher in the extraction wells compared to the observation wells, the danger exists that the calibration is focused too much on these extraction wells. A possible improvement for future modelling studies is to use variable weighting of the different observations, so that smaller weights can be assigned to the more uncertain observations in the extraction wells. Furthermore, the calibration of the model is biased to those areas in which the most observation wells are present, mainly the areas in the vicinity of the extraction sites. A spatial declustering of the observation data might be able to produce more robust results.

In the Brabant Model, the groundwater recharge to the Paleocene and Cretaceous aquifer systems is not modelled explicitly. In the unconfined part of the aquifer, other deposits (Brussels sands and Quaternary) are present on top of the modelled layers which are not explicitly modelled. The conventional Recharge package cannot be used to represent the recharge from these overlying layers to the Paleocene and Cretaceous aquifer systems without explicitly modelling the overlying deposits and the rivers and drains present in these deposits. The latter would result in an increase in model complexity and runtime which would result in issues with the time-consuming uncertainty analysis. We used the general-head boundary to simulate the flow from these overlying deposits using head observations in these layers. The disadvantage of this approach is that one cannot easily implement scenarios of increased or decreased recharge. One can change the specified hydraulic heads in the GHB package, but a decrease in recharge cannot be linearly linked with a general decrease in head over an entire area. The effects will be different in the river valleys compared to the more topographically high areas. An option is to predict future hydraulic heads in the recharge area using time-series analysis. Time-series analysis can be used to find correlations between meteorological input, extraction, and groundwater heads. Using climate scenarios, time-series of meteorological input can be generated for different conditions (dry, wet, etc.) and resulting groundwater heads can be predicted. These predicted groundwater heads could be used as specified heads in the GHB to assess the influence of e.g., a future decrease in recharge on the aquifer system.

The geological and hydrogeological data on the Paleocene and Cretaceous aquifer systems in the part of the study area in Wallonia is very limited, while this area is the main recharge area for these aquifers. The lack of data on head observations in this part affect the reliability of the general-head boundary in this area used to simulate the flow from the overlying layers. Additional data should be collected in order to improve the model in this area.

An uncertainty analysis was performed, in which the parameter uncertainty was quantified. In general, the parameter uncertainty is quite small. The model structure uncertainty was not quantified, as we only made use of one

conceptual model. However, there are indications that the choice of the conceptual model has a large influence on the model results. To improve the uncertainty analysis in the future, an approach with multiple conceptual models is advised. Alternative conceptualizations of the boundary conditions (e.g., the recharge in the south) or of the vertical discretization (e.g., subdividing the Cretaceous in multiple layers) could be explored to get a better view of the total uncertainty on the model predictions.

In this project, we focused on the part of the Cretaceous aquifer in the Brabant area. However, the Cretaceous aquifer is also an important source of drinking water more towards the east, in the province of Limburg. De Watergroep produces drinking water from the Cretaceous from several extraction sites in this area. A similar approach as for the Brabant area could be applied to analyse the state of the Cretaceous aquifer in Limburg. Some of the lessons learnt in this project can be translated to the Limburg area. However, the issues with the Cretaceous in Limburg are not completely the same as those in Brabant. Large parts of the aquifer in Limburg are unconfined to semi-unconfined. In general, the spatial variability of permeabilities is less strong in Limburg. Very low permeabilities as observed in the northern part of the Brabant area are not observed in Limburg. This is related to the fact that the top part of the Cretaceous in Limburg generally consists of the more coarse-grained calcarenites of the Formation of Maastricht. The primary hydraulic conductivity of these sediments is in the order of 3 m/d. In the southern part of the Limburg area, the effect of fracture zones also play an important role. Moreover, several fault lines, related to the Ruhr Valley Graben, cross the area, resulting in a complex geological setting. Historical dewatering of the former mining areas might still have an influence on the heads in the deeper parts of the aquifer in the north.

8.8 Management conclusions

Based on the analyses in this study, several conclusions regarding the sustainable management of this aquifer for drinking water purposes can be made. The results of the groundwater modelling and scenario analysis indicate that the current exploitation of the Cretaceous by De Watergroep is sustainable for most extraction sites. Important note is that this is the case under current groundwater recharge conditions. The effect of a possible decrease in recharge has not been analysed in this study.

Current extraction

A clear distinction can be made between the sites in the northern and southern parts of the area. In the southern Dijle valley (Geuzenhoek, Veeweyde, Sana, Pécrot and La Motte), the effect of extraction on the hydraulic heads in the Cretaceous is limited. Exploitation at the current relatively high volumes is possible without causing long-term issues. An important sidenote for this is that the results of this study do not consider the effects of a possible decrease in recharge in the future. Long-term monitoring is needed to assess the influence of a possible decrease in recharge on the state of the aquifer in its southern unconfined to semi-confined part. For the site of Venusberg, the effect of an increase in permitted rates of +100% and +300% was analysed. The results show that an increase of +100% is feasible. An increase of +300% seems to be too high for continuous extraction, as the hydraulic heads in the Cretaceous are estimated to be close to or even slightly below the top of the Cretaceous.

For the extraction site of Kouterstraat, extraction at the current volumes is sustainable. However, current volumes are only approx. 50% of the permitted rates. The maximal scenario shows that extraction at the permitted volumes results in a decrease of the head below the top of the Cretaceous. Extraction at these high rates is thus not advised. The site of Nellebeek is a bit of special case, as most of the well yield comes from the deposits of Lincent. Extraction at this site has a large effect on the heads for low extraction volumes. Increased extraction in this area is not advised and even a phasing out or using it only as a backup should be considered.

The site of Korbeek-Dijle Het Broek is one of the most important extraction sites in the area, with a very high permitted rate of 4.38M m³/year. However, the maximal scenario demonstrates that these permitted rates are too high for sustainable extraction. At this site, there is a clear difference in the effect of extraction on the heads between

the more permeable southern part and the less permeable northern side. In the last decade, a decrease in head in the Cretaceous is observed for the wells in the north (and nearby wells more towards the north), which can be linked to the increased extraction in this northern area. The effect of extraction on the heads in the southern part is smaller. To prevent an ongoing decrease in heads, it might be best to minimize the rates at the northern wells. Extraction at the normal rates of the last few years of around 2.5M m³/year, with more focus on the southern wells, is sustainable.

For the extraction sites near Leuven (Cadol, Abdij and Vlierbeek), the extraction results in a drawdown of several tens of meters in the extraction wells. This is related to the very low hydraulic conductivities in this area. However, heads are still well above the top of the Cretaceous. An increase in extraction in this area will result in a significant additional drawdown at these wells and is thus not advised, as the additional volumes will be limited compared to the effect on the hydraulic heads in the area. Extraction at the current rates of about 50-60% of the permit seems to be sustainable, although the heads in nearby observation wells should be closely monitored to identify possible downwards trends. Extraction at the current rates at Aarschot is sustainable. No decreasing heads are identified, and recovery to pre-extraction levels is fast.

Future extraction

The results of this study can be used to find a suitable location for either additional extraction or for a better spatial optimization of the current extraction rates. When a new extraction well is considered, the geological context needs to be assessed rigorously. It is of utmost importance to perform well testing (pumping tests, geophysical measurements and flow measurements), as this provides the necessary information to assess the suitability and potential for extraction.

The importance of the hardground interval at the boundary between the Zeven Wegen chalk and the Members of Lixhe/Lanaye, associated with a very permeable phosphatic gravel, is demonstrated in this study. This is mainly important in the northern part of the study area (Geuzenhoek and northwards) in which the Cretaceous deposits are not fractured. As almost all flow in this area comes from this hardground interval, it is important to make sure the filter of the extraction wells is in connection with this highly permeable zone. The presence of this hardground interval can easily be identified with gamma-ray measurements. As the permeability and thickness of this interval decreases towards the north, the area north of Het Broek is not very suitable for potential new extraction. The area to the west of Nellebeek should be avoided, as the Members of Lixhe and Lanaye, and thus also the hardground interval, are not present on top of the Zeven Wegen chalk here. The area between Nellebeek and Vilvoorde is a bit of a blind spot, as not much information is present here. At Vilvoorde relatively high yields were observed, which are either related to the presence of fractures or of more permeable sandy intervals in the Nevele deposits. In the north-east of the study area, in the region of Aarschot, the presence of the more permeable calcarenites of the Formation of Maastricht results in a larger potential for extraction. Important here is to make sure the filter is present in these Maastrichtian deposits.

The potential map that was generated gives an overview of the areas which are most suited for additional extraction, considering the expected drawdown of extraction, the level of the hydraulic heads compared to the top of the aquifer and the depth of the aquifer. The most suitable areas are the southern Dijle valley from the south of Het Broek up until Veeweyde and Pécrot, the area between Veeweyde and Sana and the unconfined part of the aquifer in the Walloon Region around La Motte. In these parts, permeabilities are high, the effect on hydraulic heads is limited and the Cretaceous is close to the surface. The same is valid for the region of Tienen and to the south of Tienen in the Walloon Region. At this moment, the Cretaceous in this area is not used for the extraction of drinking water. At this moment, not much information is available on the hydrogeological properties of the Cretaceous in this area. Extra investigation is needed to analyse if this area is suitable for possible extraction in the future. The area to the northeast of Aarschot also has potential due to the relatively high permeabilities of the calcarenites of Maastricht. An issue here is the very large depth of the top of the Cretaceous (> 300m) which results in high drilling costs.

9 References

- AB Inbev (2012). Project-MER: Hervergunning en uitbreiding van de brouwerij. PR0594.
- CIW (2016). *Stroomgebiedbeheerplannen voor Schelde en Maas 2016-2021, Grondwatersysteemspecifiek deel Brulandkrijtsysteem*. Aalst. depotnummer: D/2016/6871/023 (<http://www.volvanwater.be/de-plannen>)
- Databank Ondergrond Vlaanderen (DOV). <https://dov.vlaanderen.be/>
- Deckers J, De Koninck R, Bos S, Broothaers M, Dirix K, Hambach L, Lagrou D, Lanckacker T, Matthijs J, Rombaut B, Van Baelen K and Van Haren T (2019). Geologisch (G3Dv3) en hydrogeologische (H3D) 3D-lagenmodel van Vlaanderen. VITO. 2018/RMA/R/1569.
- De Watergroep (1978). Overijse Kouterstraat.
- De Watergroep (1988). Technisch verslag: Korbeek-Dijle Het Broek.
- De Watergroep (1993). Technisch verslag: Verkenningsboringen in het Krijt (1993): Heverlee Abdij VB1, Heverlee Cadol VB2, Kessel-Lo Vlierbeek VB3.
- De Watergroep (2001). Technisch verslag: Waterwinning Overijse/Venusberg Krijt: Proefpomping op verkenningsboring 3011-005.
- De Watergroep (2004). Hydrogeologische studie: Overijse Sana-Tombeek.
- De Watergroep (2004b). Hydrogeologische studie: Sint-Agatha-Rode Veeweyde.
- De Watergroep (2010). Hydrogeologische studie: Grondwaterwinning in het Krijt te Heverlee Abdij.
- De Watergroep (2013). Technisch verslag: Aanleg van productieput 3010-017. Productieput in de Formatie van Hannut (Lid van Linent) en Gulpen.
- De Watergroep (2015). Hydrogeologische studie: Grondwaterwinning in het Krijt te Overijse Nellebeek Krijt.
- De Watergroep (2016). Technisch verslag: Aanleg van productieput 3010-018. Productieput in de Formatie van Hannut (Lid van Linent) en Gulpen.
- De Watergroep (2017). www.dewatergroep.be
- De Watergroep (2017b). Technisch verslag: Boren productieput 3008-063 en -064, boren peilput 3008-065 en -066.
- De Watergroep (2017c). Technisch verslag: Boren productieput 3012-059. Winning Sint-Agatha-Rode-Veeweyde.
- De Watergroep (2017d). Technisch rapport Vilvoorde 3014-004 en 005.
- De Watergroep (2017e). Technisch rapport Hoeilaart 3023-021 en 024.
- De Watergroep (2021). Grondwaterwinning Sint-Agatha-Rode Geuzenhoek: Hydrogeologische studie van de grondwaterwinning (Krijt).
- Diez T and Van Limbergen B (2014). Watervoerende lagen en grondwater in België: Tuffeau van Linent aquifer. Eds. Dassargues A and Walraevens K. Academia Press.
- Dusar M and Lagrou D (2007). Lithofacies and paleogeographic distribution of the latest Cretaceous deposits exposed in the Hinnisdael underground quarries in Vechmaal (Commune Heers, Belgian Limbourg). *Geologica Belgica* 10/3-4:176-181.
- Foster SSD and MacDonald AM (2014). *The 'water security' dialogue: why it needs to be better informed about groundwater*. *Hydrogeology Journal* 22 (7). 1489-1492. 10.1007/s10040-014-1157-6
- Hemker K and Randall J (2013). Modeling with MLU: applying the multilayer approach to aquifer test analysis. Tutorial. <http://www.microfem.com/download/mlu-tutorial.pdf>
- Hoedemaekers T (2016). Grondwaterstromingsmodel Krijt Aquifersysteem Midden Vlaams-Brabant. Hydrogeologische studie en scenarioberekeningen voor grondwaterwinning.
- Houthuys R (2011). A sedimentary model of the Brussels sands, Eocene, Belgium. *Geologica Belgica* 14/1-2:55-74.

- Lagrou D, Dreesen R and Dusar M (2005). Kartering en karakterisering (sedimentpetrografisch en petrofysisch) van de Krijtgesteenten in Vlaanderen. VITO. 2005/MAT/R/0216.
- Lagrou D, Dreesen R and Dusar M (2011). Update van rapport 2005/MAT/R/0216: Kartering en karakterisering (sedimentpetrografisch en petrofysisch) van de Krijtgesteenten in Vlaanderen. VITO.
- Lebbe (1999). Hydraulic Parameter Identification. Generalized Interpretation Method for Single and Multiple Pumping Tests.
- Matthijs J, Debacker T, Piessens K and Sintubin M (2005). Anomalous topography of the lower Palaeozoic basement in the Brussels Region, Belgium. *Geologica Belgica* 8/4:69-77.
- Mustafa SMT, Nossent J, Ghysels G and Huysmans M (2018). Estimation and impact assessment of input and parameter uncertainty in predicting groundwater flow with a fully distributed model. *Water Resources Research* 54(9):6585-6608.
- Mustafa SMT, Nossent J, Ghysels G and Huysmans M (2020). Integrated Bayesian-Multi-model approach to quantify input, parameter and conceptual model structure uncertainty in groundwater modelling. *Environmental Modelling & Software* 126. <https://doi.org/10.1016/j.envsoft.2020.104654>
- Slimani H, Louwye S, Dusar M and Lagrou D (2011). Connecting the Chalk Group of the Campine Basin to the dinoflagellate cyst biostratigraphy of the Campanian to Danian in borehole Meer (northern Belgium). *Netherlands Journal of Geosciences – Geologie en Mijnbouw* 90(2/3):129-164.
- Vandenberghen N and Gullentops (2001). Geologische kaart van België, kaartblad 32 Leuven.
- Vandenberghen N, Van Simaeys S, Steurbaut E, Jagt JWM and Felder PJ (2004). Stratigraphic architecture of the Upper Cretaceous and Cenozoic along the southern border of the North Sea Basin in Belgium. *Netherlands Journal of Geosciences - Geologie en Mijnbouw* 83(3):155-171.
- Van den Keybus (2019). Haalbaarheidsstudie voor een waterwinning in de Formatie van Hannut in de omgeving van Leuven. B.Sc. Thesis. KU Leuven.
- Van der Linden (2020). Groundwater modelling of a possible new public drinking water well field in an area around Leuven in the Formation of Hannut. M.Sc. Thesis, KU Leuven.
- Vrugt JA (2016). Markov chain Monte Carlo simulation using the DREAM software package: Theory, concepts, and MATLAB implementation. *Environmental Modelling & Software*, 75, 273–316.

I Appendix

I.1 Geology and hydrogeology

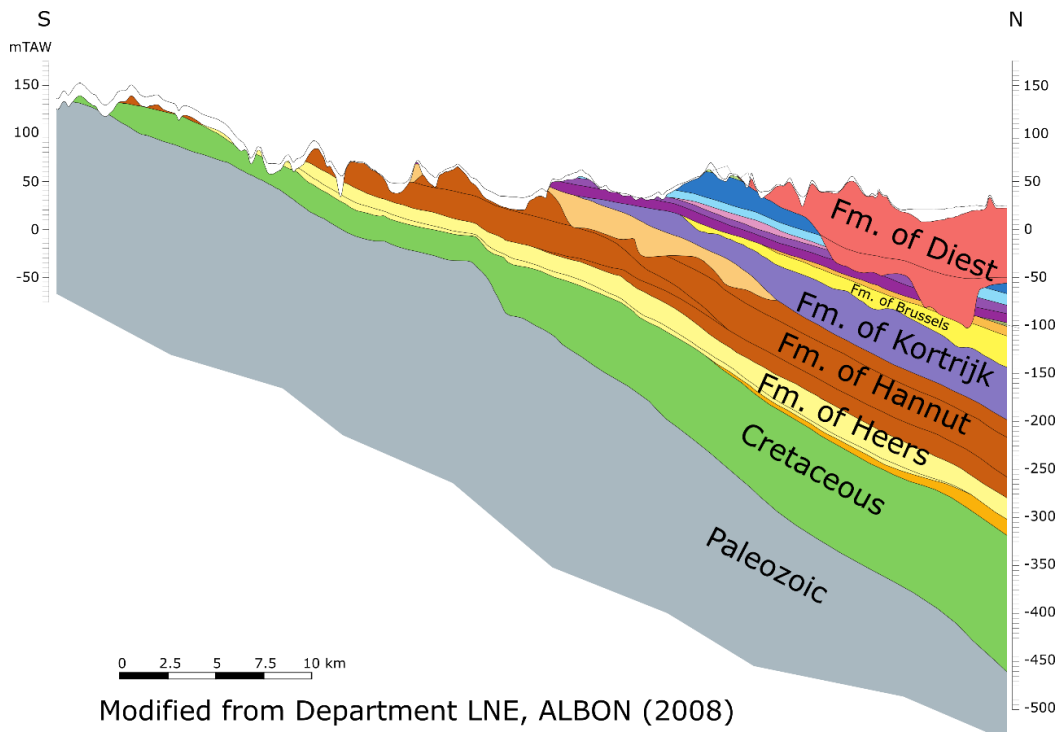


Figure I. 1: A north-south profile through the subsurface near the eastern boundary of the Brabant Model (modified from Department LNE, ALBON, 2008).

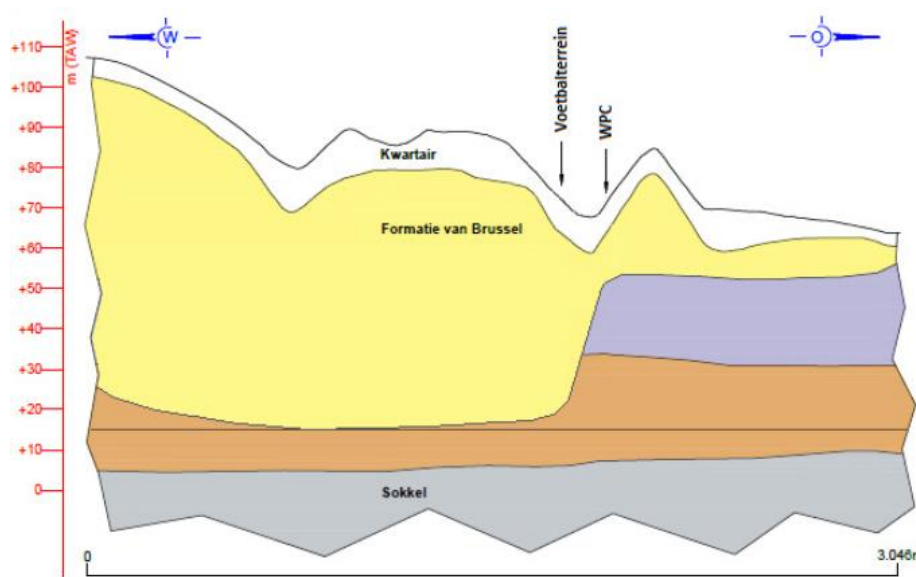


Figure I. 2: An east-west geological profile through the extraction site of Hoeilaart, indicating the local erosion of the Formation of Kortrijk by a channel filled with Brussel sands (De Watergroep, 2017e).

1.2 Extraction and hydraulic heads

Table I. 1: Overview of the actual yearly extraction rates (in m³/year) for all the extraction sites of De Watergroep in the Brabant area (Part 1).

Year	Total	Aarschot	Vlierbeek	Cadol	Abdij	Het Broek	Venusberg	Sana	Nellebeek	Kouterstraat
1990	3,490,690					202,440		1,783,460		143,120
1991	3,465,255					198,640		1,696,030		144,180
1992	3,427,105					164,900		1,723,035		134,410
1993	8,715,335			26,618		1,781,379		1,679,416	60,788	129,966
1994	10,786,712		58,099	200,579		2,810,952		1,401,706	104,806	98,400
1995	10,750,651		145,427	225,862		1,809,560		1,645,300	84,557	114,338
1996	11,596,059		134,349	236,000		2,576,836		1,654,689	105,990	124,764
1997	11,520,045		131,400	233,375		2,353,380		1,519,530	107,050	128,415
1998	16,364,205			126,490	217,270		2,516,660		1,320,515	112,935
1999	15,454,420			128,625	220,025		2,293,960		1,745,720	113,265
2000	15,622,335			125,885	200,985		2,315,740		1,769,940	114,750
2001	14,884,262			98,005	221,530		2,088,820		1,760,510	115,420
2002	12,710,397			103,971	216,201		1,490,017		1,721,366	111,246
2003	14,244,755			82,245	222,700		866,075		1,640,325	111,820
2004	14,917,040			30,310	210,470		1,427,894		1,633,217	109,742
2005	14,464,669			397	221,876		1,300,701		1,664,243	102,449
2006	13,853,033			106,703	221,104		1,290,699		1,595,829	113,226
2007	14,067,944			100,639	216,828		1,620,105		1,572,638	113,625
2008	14,115,305			75,181	213,967		1,526,723	172,485	1,599,165	123,880
2009	15,414,868			105,721	197,385		1,740,890	324,630	1,589,790	138,385
2010	15,052,770			103,335	201,380		2,017,615	306,725	1,578,995	137,625
2011	14,282,853			73,815	203,195		1,671,345	332,873	1,579,715	134,885
2012	14,204,326			94,845	201,175		2,117,165	323,013	1,532,265	121,119
2013	14,499,079			102,480	203,988		2,185,933	306,132	1,489,003	24,892
2014	14,225,192			124,468	220,721		2,206,549	51,899	1,500,957	31,061
2015	15,136,337			116,055	219,048	13,873	2,564,684	405,507	1,396,695	49,909
2016	14,625,599	168,623	110,697	207,884	159,328	2,334,773	429,640	1,432,192	40,535	157,092
2017	15,099,097	226,962	135,085	201,399	172,638	2,690,128	434,976	1,303,631	30,820	155,023
2018	16,054,116	249,118	129,559	188,518	169,425	2,648,843	446,318	1,536,880	39,831	151,853
2019	15,704,007	313,485	124,193	193,370	166,661	2,595,674	413,232	1,530,569	69,872	143,790
2020	15,398,272	230,565	108,546	170,413	153,335	3,000,531	334,777	1,527,935	76,157	138,136
Permit	20,454,000	438,000	175,200	262,800	219,000	4,380,000	438,000	1,752,000	175,200	262,800

Table I. 2: Overview of the actual yearly extraction rates (in m³/year) for all the extraction sites of De Watergroep in the Brabant area (Part 2).

Year	Total	Veeweyde	Geuzenhoek	Pécrot	La Motte	Biez	Vilvoorde	Groot-Overlaar	Menebeek	Hoeilaart
1990	3,490,690					882,330	479,340			
1991	3,465,255					862,000	564,405			
1992	3,427,105					922,680	482,080			
1993	8,715,335			2,535,628		967,150	519,880		1,014,510	
1994	10,786,712			1,970,437	1,978,550	799,082	388,207		975,894	
1995	10,750,651			2,279,970	2,255,498	907,974	340,730		941,435	
1996	11,596,059			2,195,536	2,179,675	892,652	550,780		944,788	
1997	11,520,045			2,047,605	1,960,410	855,890	489,785	815,225	877,980	
1998	16,364,205	2,187,910	2,119,500	2,201,715	2,271,440	916,055	444,990	1,037,145	796,685	
1999	15,454,420	1,679,750	2,073,955	1,927,810	2,537,435	773,125	429,700	717,210	727,860	
2000	15,622,335	2,001,250	2,145,200	2,101,985	2,248,085	889,325	302,000	599,625	757,700	
2001	14,884,262	2,202,830	2,158,260	1,895,405	1,912,930	739,710	37,530	646,495	935,167	
2002	12,710,397	2,056,996	1,959,382	1,484,485	1,324,465	486,895	140	847,665	857,147	
2003	14,244,755	2,057,037	2,014,150	1,711,623	2,860,405	440,965	259,710	983,630	920,840	
2004	14,917,040	2,057,065	1,923,325	2,386,347	2,542,590	668,436	131,195	779,170	921,574	
2005	14,464,669	2,111,017	1,896,358	2,153,821	2,421,014	568,545		952,821	945,529	
2006	13,853,033	1,858,760	1,833,612	1,929,140	2,291,964	555,379		973,277	962,221	
2007	14,067,944	2,138,696	1,996,363	2,228,518	1,282,034	797,047		912,094	975,064	
2008	14,115,305	2,067,265	1,979,370	2,115,581	1,755,457	676,219		762,483	927,599	
2009	15,414,868	2,059,210	2,075,980	2,222,345	2,343,855	490,410		1,042,310	925,935	
2010	15,052,770	2,112,650	1,690,610	2,191,340	2,209,380	411,075		938,945	996,300	
2011	14,282,853	2,247,930	2,069,285	1,894,455	1,643,400	549,725		741,625	998,750	
2012	14,204,326	2,246,080	2,081,615	1,058,165	2,250,515	316,735		797,235	955,150	
2013	14,499,079	2,051,326	2,172,728	909,595	2,847,470	289,217		862,803	900,769	
2014	14,225,192	1,839,630	2,115,112	1,523,206	2,377,224	492,734		690,706	882,700	
2015	15,136,337	1,702,004	2,048,830	1,776,371	2,337,666	570,179		581,858	823,773	381,643
2016	14,625,599	1,711,940	1,862,050	1,222,630	2,287,970	509,965		607,277	932,127	450,876
2017	15,099,097	1,644,385	2,056,710	1,617,084	2,321,332	256,895		649,458	788,191	414,380
2018	16,054,116	1,690,301	1,995,873	1,757,085	2,395,408	521,998		865,956	876,245	390,905
2019	15,704,007	2,169,366	1,170,559	2,100,274	2,522,586	203,549		1,064,236	561,110	361,481
2020	15,398,272	2,545,806	0	2,079,499	2,614,903	287,249		1,055,823	832,493	242,104
Permit	20,454,000	2,372,500	2,372,500	3,285,000	2,920,000	963,000	438,000	1,752,000	1,314,000	585,600

Table I. 3: Overview of all permitted extractions in m³/year in the Brabant area (Part 1: Q>7,500 m³/year)

Exploiter	Permit	X	Y	Layer	Commune	From	To	Active
CITRIQUE BELGE	800,000	191833	165935	Lincent	TIENEN	13/04/1994	17/06/2029	Yes
GEMEENTELIJKE WATERDIENST HOEILAART	650,000	158300	162150	Grandglise	HOEILAART	19/05/1998	07/11/2032	Yes
BNEO REMY (VROEGER REMY INDUSTRIES)	554,000	173270	179258	Grandglise	LEUVEN	17/07/1991	20/08/2023	Yes
INBEV BELGIUM (INTERBREW)	500,000	174000	175700	Grandglise	LEUVEN	15/02/1995	06/03/2033	Yes
CARGILL FRANCE SAS	410,000	171810	179895	Cretaceous	HERENT	10/02/1999	04/06/2013	No
INBEV BELGIUM (INTERBREW)	400,000	186509	163164	Grandglise	HOEGAARDEN	10/03/1993	20/10/2030	Yes
STAD TIENEN	365,000	193523	167225	Cretaceous	TIENEN	06/10/1977	08/02/2005	No
TIENSE SUIKERRAFFINADERIJ	351,000	190604	165816	Grandglise	TIENEN	14/10/1976	08/11/2019	No
KWONET	350,000	172794	174045	Grandglise	LEUVEN	04/10/2017	04/10/2037	Yes
CARGILL FRANCE SAS	320,000	171762	179895	Grandglise	HERENT	10/02/1999	24/10/2038	Yes
AFFILIPS	220,000	189110	165879	Lincent	TIENEN	17/02/1993	14/06/2026	Yes
TIENSE SUIKERRAFFINADERIJ	181,000	190658	165664	Cretaceous	TIENEN	09/10/1996	08/11/2019	No
INBEV BELGIUM (INTERBREW)	125,000	187516	162418	Lincent	HOEGAARDEN	03/03/1999	20/10/2030	Yes
BOORTMALT	100,000	164425	185625	Grandglise	BOORTMEERBEEK	13/04/1994	30/09/2006	No
INBEV BELGIUM (INTERBREW)	100,000	173269	175270	Cretaceous	LEUVEN	01/01/1993	01/01/2013	No
INBEV BELGIUM (INTERBREW)	100,000	173269	175270	Cretaceous	LEUVEN	15/02/1995	13/01/2004	No
ALUMETAL	87,600	157771	174600	Cretaceous	ZAVENTEM	14/03/1973	12/06/2005	No
ROBERT BOSCH PRODUKTIE	80,000	191456	166861	Lincent	TIENEN	04/12/1991	31/03/2024	Yes
ABDIJ DER NORBERTIJNEN VAN AVERBODE	62,000	192804	191725	Cretaceous	SCHERPENHEUVEL	05/02/1992	01/05/2032	Yes
STAD TIENEN	50,000	191027	167193	Lincent	TIENEN	30/01/2008	29/08/2013	No
BK	29,900	173829	175672	Grandglise	LEUVEN	04/03/2009	28/09/2010	No
VANKELECOM DAIRY YVES	29,500	188710	164940	Grandglise	TIENEN	14/01/2015	24/03/2030	Yes
SORTBAT NV	28,500	189160	166315	Lincent	TIENEN	12/07/2017	12/07/2037	Yes
BADRFAROUJ	27,000	153096	177566	Grandglise	VILVOORDE	29/03/2006	25/06/2013	No
DE VIJVERS	25,000	193891	190925	Cretaceous	SCHERPENHEUVEL	11/01/1972	19/08/2005	No
NATIONALE PLANTENTUIN VAN BELGIE	25,000	147181	180149	Cretaceous	MEISE	07/06/1978	02/12/2014	No
AVERMAETE MARC	25,000	194688	165815	Cretaceous	TIENEN	10/02/1999	23/01/2005	No
ANALU	24,000	155614	178836	Lincent	MACHELEN	07/08/1991	17/01/2005	No
KRIJGSMACHT MAJOR HOUSIAU	24,000	156780	180260	Cretaceous	VILVOORDE	22/06/1982	19/08/2005	No
INTER-BETON NV	22,500	191953	166829	Lincent	TIENEN	15/10/2000	18/08/2005	No
BROUWERIJ HAACHT	20,000	166856	183923	Grandglise	BOORTMEERBEEK	23/02/2000	16/03/2031	Yes
NATURELLO	18,660	165684	183387	Grandglise	KAMPENHOUT	17/09/2003	27/12/2009	No
STICHTING MARGUERITE-MARIE DELACROIX	15,000	189694	166550	Cretaceous	TIENEN	08/01/1992	15/01/2032	Yes
EXIDE AUTOMOTIVE	15,000	169980	160990	Cretaceous	HULDENBERG	02/02/2000	02/02/2020	No
GODTS BVBA	15,000	190885	165143	Lincent	TIENEN	25/11/2013	30/08/2026	Yes
REYNAERTS MARC & JAN	14,000	191232	166813	Lincent	TIENEN	08/07/2007	11/12/2022	Yes
COSTERMANS - OVERSTEYNS LV	11,800	188393	168990	Grandglise	TIENEN	22/09/2013	22/09/2033	Yes
VAN DOOREN PIETER	11,660	194596	182257	Grandglise	BEKKVOORT	05/10/2011	05/10/2031	Yes
CRISTAL MONOPOLE	10,800	182076	186290	Grandglise	AARSCHOT	17/07/1991	20/04/2010	No
TEXWORKS (ATOMIC)	10,750	178829	186082	Grandglise	BEGIJNENDIJK	08/10/2008	30/06/2010	No
IMMO BTR	10,000	162784	181760	Lincent	KAMPENHOUT	04/11/2001	07/06/2013	No
RUSTHUIS SINT JOZEF	10,000	187631	185144	Grandglise	AARSCHOT	22/03/1993	22/03/2013	No
STICHTING MARGUERITE-MARIE DELACROIX	10,000	193530	165540	Lincent	TIENEN	28/07/1993	28/07/2013	No
ATELIERS DE CONSTRUCTION E. MOLINET	9,855	189872	165356	Grandglise	TIENEN	19/04/1960	19/08/2005	No
VANELVEN LV	9,500	194131	184568	Grandglise	SCHERPENHEUVEL	17/02/2016	22/08/2032	Yes
SMETS KURT	9,500	182110	177586	Grandglise	HOLSBEEK	19/10/2011	19/10/2031	Yes
BENOIT MARC	9,000	194007	176411	Grandglise	KORTENAKEN	01/06/1997	01/06/2007	No
OSS	9,000	191065	165340	Cretaceous	TIENEN	30/08/2000	05/01/2014	No
SUEZ SITA VALOMAC	9,000	153048	180604	Grandglise	GRIMBERGEN	13/03/2013	21/03/2017	No
STAES LUC	8,690	188305	174241	Grandglise	GLABBEK	17/10/2004	16/10/2024	Yes
KBC BANK-GROEP	8,500	173143	174133	Grandglise	LEUVEN	27/11/2013	27/11/2033	Yes
DEPOTTER-VERBIEST LV	8,270	180784	175332	Grandglise	LUBBEEK	04/09/2013	23/04/2028	Yes
KBC BANK-GROEP	8,000	174290	174834	Grandglise	LEUVEN	29/06/1994	20/01/2013	No
RECOM NV	8,000	190793	164978	Lincent	TIENEN	22/06/2005	22/06/2008	No
PORKY FARM (VANDENDRIESSCHE GUY)	7,900	171756	181574	Grandglise	HAACHT	09/03/1997	23/03/2036	Yes
CAMPING SPARRENHOF	7,500	187476	189906	Grandglise	AARSCHOT	27/09/2006	16/09/2013	No
SIMONET PAUL	7,500	190527	168684	Grandglise	TIENEN	01/09/2004	01/09/2024	Yes
VAN DOORSLAER MARC	7,500	147779	187188	Grandglise	MEISE	21/06/1992	21/06/2012	No

Table I. 4: Overview of all permitted extractions in m³/year in the Brabant area (Part 2: Q<7,500 and >3,650 m³/year)

Exploiter	Permit	X	Y	Layer	Commune	From	To	Active
HENSKENS PASCAL	7,260	182178	165077	Grandglise	HOEGAARDEN	28/01/2000	28/01/2020	No
VAN ZURPELE GEERT	7,236	193056	179390	Grandglise	BEKKEVOORT	18/01/2017	18/01/2037	Yes
R.W.T / WILLEMS RUDDY	7,200	176732	186406	Grandglise	TREMOLO	07/05/2012	07/05/2032	Yes
VAN CRIEKINGEN BART	7,200	180410	178535	Grandglise	HOLSBECK	18/04/2012	18/04/2032	Yes
VANHELLEMONT FRUIT	7,200	190244	175204	Grandglise	GLABBEEK	24/01/2011	24/01/2021	Yes
NYS JOS & ELS	7,100	190456	182536	Grandglise	BEKKEVOORT	03/08/2011	03/08/2031	Yes
DPO BELGIUM	7,000	191620	169501	Lincent	TIENEN	12/03/2018	30/12/2099	Yes
FILOSOFISCH EN THEOLOGISCH COLLEGE	7,000	172410	172180	Cretaceous	LEUVEN	02/02/1994	18/10/2009	No
STROUVEN MARC	7,000	194758	175996	Grandglise	KORTENAKEN	24/03/2010	24/03/2030	Yes
COMMERS GUY	6,900	194899	183830	Grandglise	SCHERPENHEUVEL	31/03/2010	21/08/2018	No
VANSCHOUBROEK PETER - CRAENENBROEKHOF	6,900	191766	173519	Grandglise	GLABBEEK	27/03/2005	26/03/2025	Yes
VAN ESBROEK PAUL	6,600	181721	186827	Grandglise	AARSCHOT	09/01/1990	31/12/2009	No
VARKUM	6,600	186136	166708	Grandglise	TIENEN	04/08/2010	04/08/2030	Yes
LEUVENSE KATHOLIEKE SCHOLEN AAN DE DIJLE	6,539	173038	174150	Grandglise	LEUVEN	10/06/2010	10/06/2030	Yes
GODTS BVBA	6,500	191914	165452	Lincent	TIENEN	25/03/2015	25/03/2035	Yes
READY BETON /DDM BETON	6,500	176352	181053	Grandglise	ROTSELAAR	29/01/2003	28/01/2021	Yes
OVERSTEYN JOOST	6,300	190452	167107	Cretaceous	TIENEN	11/03/2012	11/03/2032	Yes
BAAZ JAN (FREDIMO)	6,000	191752	166513	Grandglise	TIENEN	09/05/1991	09/05/2011	No
VAN MEEUWEN	6,000	190614	188933	Grandglise	SCHERPENHEUVEL	27/07/2003	27/07/2005	No
ZILVERWIT WASSERIJ	6,000	173880	182281	Lincent	ROTSELAAR	15/04/1997	15/04/2017	No
AGROTECH BELGASIA NV /VERBIST E.E.G.	5,500	170996	184554	Grandglise	HAACHT	20/03/2013	20/03/2018	No
PACOLET KURT	5,500	192976	168870	Lincent	TIENEN	05/09/2011	05/09/2021	Yes
PEETERS DAVID	5,500	193633	174862	Grandglise	KORTENAKEN	05/10/1997	07/07/2007	No
FOX KRIS	5,200	185319	165155	Grandglise	HOEGAARDEN	23/05/2018	30/12/2099	Yes
BEULLEKENS RONNY	5,100	182499	164138	Grandglise	HOEGAARDEN	05/10/2005	05/10/2025	Yes
DEKREM MICHEL	5,000	163700	181999	Grandglise	KAMPENHOUT	10/05/1999	10/05/2009	No
JODOCO	5,000	191501	166597	Lincent	TIENEN	21/02/2018	30/12/2099	Yes
KABERG BVBA	5,000	187453	169498	Grandglise	TIENEN	23/04/2008	11/02/2024	Yes
KBIVB	5,000	191000	166080	Lincent	TIENEN	29/07/1993	29/07/2013	No
PROVINCIE VLAAMS BRABANT "DE WIJNPERS"	5,000	172591	175127	Grandglise	LEUVEN	05/09/1979	21/06/2005	No
RUSTOORD ROOSBEEK	5,000	183750	169710	Grandglise	BOUTERSEM	12/07/1993	12/07/2013	No
SITA REMEDIATION NV	5,000	153142	180797	Grandglise	GRIMBERGEN	24/01/2007	10/04/2016	No
STOCKX GUNTHER & GEORGES	5,000	188926	174838	Grandglise	GLABBEEK	09/11/2003	08/11/2023	Yes
VAN CRIEKINGEN BART	5,000	179998	177077	Grandglise	LUBBEEK	29/03/2006	29/03/2026	Yes
VLEMINCKX PAUL	5,000	171376	175252	Grandglise	HERENT	30/03/1993	30/03/2013	No
RENDERS MICHEL	4,800	194004	173659	Grandglise	KORTENAKEN	30/06/2010	30/06/2030	Yes
MINNART EDDY	4,600	194599	170971	Grandglise	LINTER	06/11/2013	29/01/2023	Yes
JONCKERS KAREL & RAF	4,500	194962	167348	Lincent	LINTER	03/02/2010	03/02/2030	Yes
NELISSEN	4,500	188326	167569	Lincent	TIENEN	04/01/1961	19/08/2005	No
OVERSTIJNS JOOST	4,250	191788	170822	Grandglise	GLABBEEK	16/08/1998	14/10/2006	No
MERCKX LUDO	4,053	186700	166800	Grandglise	TIENEN	27/06/2012	27/06/2032	Yes
ZUSTERS URSELINEN	4,015	169488	181585	Grandglise	HAACHT	05/12/1993	05/12/2013	No
WASSERIJ DE LELIE LEUVEN	4,000	173311	173282	Grandglise	LEUVEN	02/11/1994	11/08/2031	Yes
DENDOOVEN LUDO	4,000	189784	175192	Grandglise	GLABBEEK	10/09/2000	06/05/2007	No
GEMEENTE KAMPENHOUT	4,000	163570	181870	Grandglise	KAMPENHOUT	06/07/1992	06/07/2012	No
PATERS REDEMPTORISTEN	4,000	173916	173612	Grandglise	LEUVEN	06/10/1988	31/07/2005	No
SITA WASTE SEVICES DD MIX	4,000	190945	165104	Grandglise	TIENEN	26/02/2003	24/03/2015	No
WASSERIJ - DROOGKUIS WEMMEL	4,000	146120	177071	Grandglise	WEMMEL	27/08/1991	23/05/2007	No
DEPOTTER - LEMMENS	3,853	167126	160468	Cretaceous	HULDENBERG	02/08/2017	20/06/2027	Yes
AVERMAETE ETIENNE	3,650	194366	166034	Grandglise	TIENEN	01/07/1991	01/07/2011	No
VAN CRIEKINGEN BART	3,650	179998	177077	Grandglise	LUBBEEK	28/02/2000	28/03/2006	No
VAN CRIEKINGEN BART	3,650	180376	178609	Grandglise	HOLSBECK	05/07/1995	05/07/2015	No

Table I. 5: Overview of extraction rates for all other wells in the area (from DOV).

Year	Grandglise	Lincent	Cretaceous	Total
2004	1,609,452	3,400,842	1,417,218	6,427,512
2005	1,708,948	3,228,353	1,396,140	6,333,441
2006	2,331,785	3,234,443	982,676	6,548,904
2007	1,839,275	2,963,346	984,941	5,787,562
2008	1,786,570	2,545,050	794,155	5,125,775
2009	1,823,608	1,836,869	848,808	4,509,285
2010	1,617,022	1,208,033	626,241	3,451,296
2011	1,870,795	1,130,428	573,219	3,574,442
2012	1,850,195	1,261,074	505,520	3,616,789
2013	1,619,354	1,018,846	389,476	3,027,676
2014	1,495,130	988,584	332,540	2,816,254
2015	1,079,155	1,016,910	365,143	2,461,208
2016	1,159,366	1,122,957	363,763	2,646,086
2017	1,199,686	1,103,544	296,410	2,599,640
2018	1,113,763	1,065,109	361,226	2,540,098
2019	1,090,966	1,054,124	337,564	2,482,653
2020	1,089,973	1,054,124	332,451	2,476,548

Table I. 6: Overview of extraction rates for the largest DOV wells for period 2004-2012 (reported rates obtained from the VMM). Rates are in m³/year.

Exploiter	X	Y	Layer	2004	2005	2006	2007	2008	2009	2010	2011	2012
CITRIQUE BELGE	191833	165935	Lincent	3,114,966	2,955,153	2,971,778	2,705,633	2,339,299	1,558,451	925,121	850,391	1,007,061
INBEV (LEUVEN)	174000	175700	Grandglise	419,175	395,567	547,656	496,385	538,987	388,129	336,342	410,284	293,726
TIENSE SUIKERRAFFINADERIJ	190604	165816	Lincent	341,228	402,370	312,572	309,682	253,876	284,358	274,122	198,608	132,507
INBEV (HOEGAARDEN)	186509	163164	Grandglise	330,777	316,646	347,893	251,744	347,272	318,881	326,688	319,007	309,286
CARGILL FRANCE SAS (VROEGERE CARGILL MALT)	171810	179895	Cretaceous	293,575	221,130	221,130	250,834	171,319	168,793	0	0	0
TIENSE SUIKERRAFFINADERIJ	190658	165664	Cretaceous	247,145	247,145	247,145	218,722	247,145	274,193	236,332	259,333	252,319
GEMEENTELIJKE WATERDIENST HOEILAART	158300	162150	Grandglise	236,951	354,605	439,607	314,881	308,281	333,975	314,881	314,881	314,881
BENEOP REMY (VROEGER REMY INDUSTRIES)	173270	179258	Grandglise	183,696	179,653	206,744	286,875	218,915	406,143	217,911	351,853	436,823
CARGILL FRANCE SAS (VROEGERE CARGILL MALT)	171762	179895	Grandglise	162,688	207,856	530,581	228,206	107,599	101,800	148,833	187,617	221,135
INBEV (HOEGAARDEN)	187516	162418	Lincent	94,218	80,282	84,515	91,660	987	106,600	89,901	68,144	68,000
AFFILIIPS	189110	165879	Lincent	58,082	58,082	72,345	47,800	54,100	53,600	63,100	58,100	62,500
ROBERT BOSCH PRODUKTIE	191456	166861	Lincent	56,169	51,028	60,717	67,453	58,864	47,884	52,609	51,428	52,065
BOORTMALT	164425	185625	Grandglise	33,229	0	0	0	0	0	0	0	0
ANALU	155614	178836	Lincent	21,120	21,120	0	0	0	0	0	0	0
NATIONALE PLANTENTUIN VAN BELGIE	147181	180149	Cretaceous	16,590	16,590	16,590	16,590	16,590	16,590	16,590	16,590	16,590
BROUWERIJ HAACHT	166856	183923	Gr.	14,577	16,002	18,661	18,661	15,157	14,201	16,258	18,556	14,065
STICHTING MARGUERITE-MARIE DELACROIX	189694	166550	Cretaceous	11,529	11,529	11,529	14,396	11,529	11,529	11,529	10,812	10,508
DE VIJVERS	193891	190925	Cretaceous	8,988	0	0	0	0	0	0	0	0
ABDIJ DER NORBERTIJNEN VAN AVERBODE	192804	191725	Cretaceous	8,498	7,710	7,710	8,717	7,696	7,345	7,268	7,476	7,757
WASSERIJ DE LELIE LEUVEN	173311	173282	Grandglise	4,000	4,000	4,000	4,000	4,000	4,000	4,000	4,000	4,000
PORKY FARM (VANDENDRIESSCHE GUY)	171756	181574	Grandglise	3,800	3,800	3,800	3,800	3,800	3,800	6,500	6,500	6,500
STAD TIENEN	191027	167193	Lincent	0	0	0	0	33,000	17,134	23,302	43,965	13,048
VANELVEN LV	194131	184568	Grandglise	0	0	0	0	0	0	0	0	0
Total:				5,660,999	5,550,268	6,104,973	5,336,039	4,738,416	4,117,406	3,071,287	3,177,545	3,222,770

Table I. 7: Overview of extraction rates for the largest DOV wells for period 2013-2020 (reported rates obtained from the VMM). Rates are in m³/year.

Exploiter	X	Y	Layer	2013	2014	2015	2016	2017	2018	2019	2020
CITRIQUE BELGE	191833	165935	Lincent	766,984	771,994	786,033	886,501	879,307	818,164	818,164	818,164
INBEV (LEUVEN)	174000	175700	Grandglise	210,564	244,275	181,938	157,389	158,021	148,783	126,349	126,349
TIENSE SUIKERRAFFINADERIJ	190604	165816	Lincent	222,059	118,615	137,899	165,892	63,043	163,820	129,854	129,854
INBEV (HOEGAARDEN)	186509	163164	Grandglise	296,021	290,232	304,887	336,466	380,780	321,677	321,677	321,677
CARGILL FRANCE SAS (VROEGERE CARGILL MALT)	171810	179895	Cretaceous	0	0	0	0	0	0	0	0
TIENSE SUIKERRAFFINADERIJ	190658	165664	Cretaceous	85,666	132,174	169,336	144,402	178,674	142,157	153,349	153,349
GEMEENTELIJKE WATERDIENST HOEILAART	158300	162150	Grandglise	314,881	314,881	0	0	0	0	0	0
BENEOL REMY (VROEGER REMY INDUSTRIES)	173270	179258	Grandglise	335,048	308,742	290,347	328,375	313,970	315,296	315,296	315,296
CARGILL FRANCE SAS (VROEGERE CARGILL MALT)	171762	179895	Grandglise	164,566	69,882	12,237	48,379	55,599	46,524	46,524	46,524
INBEV (HOEGAARDEN)	187516	162418	Lincent	50,405	45,218	47,729	19,501	42,853	41,141	41,141	41,141
AFFILIIPS	189110	165879	Lincent	53,500	56,200	58,100	54,000	67,500	72,682	61,696	61,696
ROBERT BOSCH PRODUKTIE	191456	166861	Lincent	43,352	44,372	49,048	86,955	37,884	52,322	52,322	52,322
BOORTMALT	164425	185625	Grandglise	0	0	0	0	0	0	0	0
ANALU	155614	178836	Lincent	0	0	0	0	0	0	0	0
NATIONALE PLANTENTUIN VAN BELGIE	147181	180149	Cretaceous	16,590	16,590	0	0	0	0	0	0
BROUWERIJ HAACHT	166856	183923	Gr.	13,499	13,955	12,233	12,535	12,047	10,128	12,180	12,180
STICHTING MARGUERITE-MARIE DELACROIX	189694	166550	Cretaceous	10,812	10,812	10,759	11,920	10,062	10,618	9,730	10,618
DE VIJVERS	193891	190925	Cretaceous	0	0	0	0	0	0	0	0
ABDIJ DER NORBERTIJNEN VAN AVERBODE	192804	191725	Cretaceous	7,710	7,710	7,710	7,710	7,710	7,710	7,710	7,710
WASSERIJ DE LELIE LEUVEN	173311	173282	Grandglise	4,000	4,000	4,000	9,507	17,448	13,478	15,463	14,470
PORKY FARM (VANDENDRIESSCHE GUY)	171756	181574	Grandglise	6,500	6,500	6,500	11,222	8,059	9,641	9,641	9,641
STAD TIENEN	191027	167193	Lincent	12,205	0	0	0	0	0	0	0
VANELVEN LV	194131	184568	Grandglise	0	0	9,950	9,950	9,950	9,950	9,950	9,950
Total:				2,614,362	2,456,152	2,088,706	2,290,704	2,242,907	2,184,091	2,131,046	2,130,941

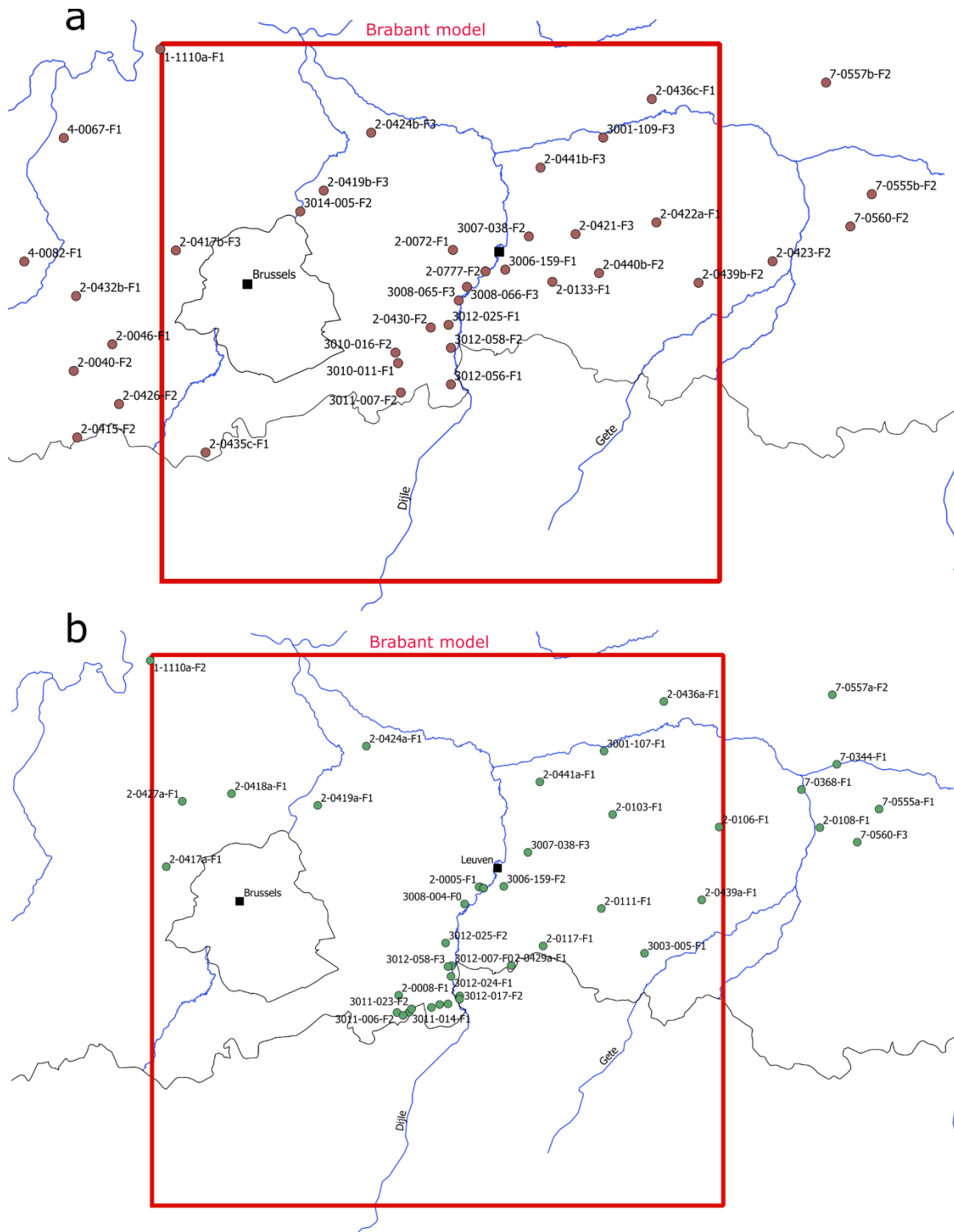


Figure I. 3 Overview of all observation wells used in the discussion of the hydraulic heads: (a) wells in the Paleocene aquifer system; (b) wells in the Cretaceous aquifer system.

I.3 Groundwater Modelling

Steady-state model for 2018

Table I. 8: Overview of all extraction wells of De Watergroep in the steady-state model for 2018 modelled with the MNW2 package. Q = extraction rate, negative values indicate extraction from the model.

Well name	X	Y	Layer	Q (m³/d)	Site
3001-108	183464	185677	3	-682.52	Aarschot
3003-002	186897	166310	2	-531.73	Menebeek
3003-003	187318	166293	2	-652.30	Menebeek
3003-004	187636	166182	2	-624.91	Menebeek
3003-016	188502	164399	2	-525.82	Groot-Overlaar
3003-017	189094	164694	2	-925.78	Groot-Overlaar
3003-018	189358	164835	2	-301.09	Groot-Overlaar
3003-028	188821	164404	2	-183.82	Groot-Overlaar
3003-029	186893	166240	2	-591.73	Menebeek
3003-041	188397	164498	2	-435.98	Groot-Overlaar
3006-001	173644	172757	3	-516.49	Cadol
3006-116	174276	172561	3	-464.18	Abdij
3007-001	176177	175954	3	-354.96	Vlierbeek
3008-001	169223	169076	3	-1997.63	Het Broek
3008-002	169373	170207	3	-847.25	Het Broek
3008-003	169696	170670	3	-819.36	Het Broek
3008-005	169298	169638	3	-1670.09	Het Broek
3008-006	169280	169513	3	-1922.78	Het Broek
3010-001	163296	163523	3	-415.98	Kouterstraat
3010-002	163288	163514	3	-0.06	Kouterstraat
3010-017	163013	164525	3	-109.13	Nellebeek
3011-005	163610	160562	3	-1222.79	Venusberg
3011-008	164745	160598	3	-4108.48	Sana
3011-009	164746	160626	3	-102.15	Sana
3012-001	168889	162233	3	-2998.42	Veeweyde
3012-002	168936	162225	3	-1632.54	Veeweyde
3012-007	168840	165086	3	-2447.66	Geuzenhoek
3012-008	168789	165194	3	-3020.48	Geuzenhoek
3012-014	169638	162007	3	-1779.78	Pécrot
3012-015	169627	161898	3	-1592.24	Pécrot
3012-016	169676	161752	3	-1441.92	Pécrot
3012-020	170744	159698	3	-4929.97	La Motte
3012-021	170679	159623	3	-1632.79	La Motte
3020-001	174072	158452	3	-1430.13	Biez
3023-005	158161	162137	1	-468.69	Hoeilaart

3023-006	158270	162109	1	-244.82	Hoeilaart
3023-007	158312	162153	1	-249.85	Hoeilaart
3023-008	158263	162200	1	-107.61	Hoeilaart

Table I. 9: Overview of all extraction wells from DOV in the steady-state model for 2018 modelled with the WEL package for which reported extraction rates are available. Q = extraction rate, negative values indicate extraction from the model.

Exploiter	X	Y	Layer	Q (m³/d)
CITRIQUE BELGE	191833	165935	2	-2241.5
INBEV BELGIUM (INTERBREW)	186509	163164	2	-881.3
BNEO REMY (VROEGER REMY INDUSTRIES)	173270	179258	1	-860.2
INBEV BELGIUM (INTERBREW)	174000	175700	1	-487.9
TIENSE SUIKERRAFFINADERIJ	190658	165664	3	-420.1
TIENSE SUIKERRAFFINADERIJ	190604	165816	2	-355.8
CARGILL FRANCE SAS (VROEGERE CARGILL MALT)	171762	179895	1	-192.1
AFFILIPS	189110	165879	2	-169.0
INBEV BELGIUM (INTERBREW)	144205	165350	1	-163.1
ROBERT BOSCH PRODUKTIE	191456	166861	2	-143.3
INBEV BELGIUM (INTERBREW)	187516	162418	2	-112.7
WASSERIJ DE LELIE LEUVEN	173311	173282	1	-36.9
BROUWERIJ HAACHT	166856	183923	1	-33.4
STICHTING MARGUERITE-MARIE DELACROIX	189694	166550	3	-29.9
PORKY FARM (VANDENDRIESSCHE GUY)	171752	181580	1	-26.4

Table I. 10: Overview of all extraction wells from DOV in the steady-state model for 2018 modelled with the WEL package for which only permitted rates are available. Q = extraction rate, negative values indicate extraction from the model. These extraction rates are the permitted rates multiplied with a factor 0.8.

Exploiter	X	Y	Layer	Q (m³/d)
VANKELECOM DAIRY YVES	188710	164940	1	-64.6
BK	173829	175672	1	-63.6
SORTBAT NV	189160	166315	2	-62.5
BADRFAROUJ	153096	177566	1	-59.2
INTER-BETON NV	191953	166829	2	-32.9
GODTS BVBA	190885	165143	2	-32.9
EXIDE AUTOMOTIVE	169980	160990	3	-32.9
REYNAERTS MARC & JAN	191232	166813	2	-30.7
ABDIJ DER NORBERTIJNEN VAN AVERBODE	192804	191725	3	-28.5
COSTERMANS - OVERSTEYNS LV	188393	168990	1	-25.8
VAN DOOREN PIETER	194596	182257	1	-25.5
SMETS KURT	182110	177586	1	-20.8
VANELVEN LV	194131	184568	1	-20.8
BENOIT MARC	194007	176411	1	-19.8
STAES LUC	188305	174241	1	-19.0
KBC BANK-GROEP	173143	174133	1	-18.6
DEPOTTER-VERBIEST LV	180784	175332	1	-18.2
SIMONET PAUL	190527	168684	1	-16.4
AVERMAETE MARC	194688	165815	3	-16.4
HENSKENS PASCAL	182178	165077	1	-15.9
VAN ZURPELE GEERT	193056	179390	1	-15.8
R.W.T / WILLEMS RUDDY	176732	186406	1	-15.8
VAN CRIEKINGEN BART	180410	178535	1	-15.8
VANHELLEMONT FRUIT	190244	175204	1	-15.8
NYS JOS & ELS	190456	182536	1	-15.6
STROUVEN MARC	194758	175996	1	-15.4
VANSCHOUWROEK PETER - CRAENENBROEKHOF	191766	173519	1	-15.1
COMMERS GUY	194899	183830	1	-15.1
VARKUM	186136	166708	1	-14.5
LEUVENSE KATHOLIEKE SCHOLEN AAN DE DIJLE	173038	174150	1	-14.3
READY BETON /DDM BETON	176352	181053	1	-14.2
GODTS BVBA	191914	165452	2	-14.2
OVERSTEYNS JOOST	190452	167107	3	-13.8
PEETERS DAVID	193633	174862	1	-12.1
PACOLET KURT	192976	168870	2	-12.1
AGROTECH BELGASIA NV /VERBIST E.E.G. SLACHTHUIS	170996	184554	1	-12.1
BEULLEKENS RONNY	182499	164138	1	-11.2

STOCKX GUNTHER & GEORGES	188926	174838	1	-11.0
VAN CRIEKINGEN BART	179998	177077	1	-11.0
PROVINCIE VLAAMS BRABANT "DE WIJNPERS"	172591	175127	1	-11.0
KABERG BVBA	187453	169498	1	-11.0
BAAZ JAN (FREDIMO)	191752	166513	1	-10.6
RENDERS MICHEL	194004	173659	1	-10.6
MINNART EDDY	194599	170971	1	-10.1
JONCKERS KAREL & RAF	194962	167348	2	-9.8
OVERSTIJNS JOOST	191788	170822	1	-9.3
MERCKX LUDO	186700	166800	1	-8.9
SITA WASTE SEVICES DD MIX	190945	165104	1	-8.8
DEPOTTER - LEMMENS	167126	160468	3	-8.5

Table I. 11: Overview of observations wells implemented in the 2018 SS model. Filter top, filter bot and head are in mTAW. L1,w, L2,w and L3,w are respectively the weights assigned to layer 1, 2 and 3 for the calculation of an equivalent head.

Well name	X	Y	Z	Layer	Filter top	Filter bot	Head	Group	L1, w	L2, w	L3, w
700-76-3-F3	143616.2	162751.2	26.01	1	8.01	7.01	25.07	DOV	1	0	0
2-0417a-F1	141375	174618	79.33	2, 3	-84.67	-86.67	0.59	DOV	0.0	0.514	0.486
2-0417b-F3	141379	174618	79.33	1	-58.67	-63.67	8.85	DOV	1	0	0
2-0418a-F1	147656	181650	52.37	3	-118.63	-123.63	3.48	DOV	0	0	1
2-0418b-F4	147660	181650	52.37	1	-93.63	-97.63	2.35	DOV	1	0	0
2-0419a-F1	155951	180524	18.63	3	-136.87	-142.87	9.09	DOV	0	0	1
2-0419b-F3	155955	180524	18.63	1	-90.37	-95.37	12.21	DOV	1	0	0
2-0008-F1	163743	162238	98.04	3	10.79	0.79	43.67	DOV	0	0	1
2-0012-F1	166900	161070	76.51	3	17.81	6.86	34.07	DOV	0	0	1
2-0072-F1	168699	174665	92.04	1	-34.96	-44.96	21.95	DOV	1	0	0
2-0111-F1	183254.1	170590.1	60.99	3	-96.51	-108.51	27.11	DOV	0	0	1
2-0117-F1	177651.4	166994.8	76.39	3	-27.61	-35.61	41.08	DOV	0	0	1
710-71-3-F3	164951.5	161768.6	88.79	1	46.79	45.79	55.06	DOV	1	0	0
2-0420a-F1	160078	170389	74.67	3	-49.83	-54.83	16.99	DOV	0	0	1
2-0420b-F2	160113.4	170398.4	74.67	1	-15.33	-17.33	37.83	DOV	1	0	0
2-0421-F3	180790	176231	74.9	1	-46.1	-52.1	34.72	DOV	1	0	0
2-0424a-F1	160635	186224	10.02	3	-199.98	-204.98	9.54	DOV	0	0	1
2-0424b-F3	160639	186224	10.02	1	-137.98	-142.98	9.67	DOV	1	0	0
2-0429a-F1	174586	165125	90.58	3	-7.42	-13.42	48.92	DOV	0	0	1
2-0429b-F2	174590	165125	90.58	2	5.08	-0.92	56.74	DOV	0	1	0
2-0430-F2	166516	167019	72.17	1	12.17	7.17	37.65	DOV	1	0	0
2-0431-F2	157749	163462	114.21	1	20.21	10.21	72.68	DOV	1	0	0
2-0438a-F1	180804	166112	95.1	1	46.1	44.1	74.18	DOV	1	0	0
2-0440a-F1	183106	172384	76.15	3	-88.85	-92.85	21.02	DOV	0	0	1
2-0440b-F2	183110	172384	76.15	1	0.15	-3.85	50.02	DOV	1	0	0
2-0441a-F1	177333	182788	20.11	3	-188.89	-192.89	9.35	DOV	0	0	1
2-0441b-F3	177337	182788	20.11	1	-107.89	-111.89	12.75	DOV	1	0	0
2-0777-F3	171911.1	172554.4	23.72	3	-67.28	-72.28	0.51	DOV	0	0	1
2-0777-F2	171911.1	172554.4	23.72	1	-13.28	-18.28	25.10	DOV	1	0	0
2-0103-F1	184343.3	179654.1	28.58	3	-165.42	-185.42	13.27	DOV	0	0	1
2-0106-F1	194594.8	178441.2	57.91	3	-139.09	-151.09	13.81	DOV	0	0	1
2-0113-F2	186589.7	162369.7	69.63	2	28.63	26.63	50.90	DOV	0	1	0
2-0124-F1	194611	168000	35.25	2	-17.25	-22.25	30.23	DOV	0	1	0
2-0123-F2	194610	168000	35.25	2	15.25	5.25	32.44	DOV	0	1	0
621-76-1-F2	190302	160182.8	75.8	1	63.8	62.8	66.51	DOV	1	0	0
621-76-1-F3	190302	160182.8	75.8	2	57.8	56.8	66.81	DOV	0	1	0
621-76-3-F2	194019.2	163846.7	62.47	2	49.47	48.47	50.02	DOV	0	1	0

621-76-3-F3	194019.2	163846.7	62.47	2	45.97	44.97	49.78	DOV	0	1	0
621-76-4-F3	193667.2	163532.2	62.65	2	48.05	47.05	52.03	DOV	0	1	0
622-71-11-F3	188318.7	160811	73.21	2	50.21	49.21	55.82	DOV	0	1	0
622-71-7-F2	183831.1	164618.3	76.24	1	61.74	61.24	66.85	DOV	1	0	0
622-71-7-F3	183831.1	164618.3	76.24	1	57.24	56.24	66.87	DOV	1	0	0
622-71-8-F3	184942.2	166222.5	69.76	1	53.76	52.76	59.60	DOV	1	0	0
622-76-2-F3	189693.9	161876.1	69.2	2	51.2	50.2	60.88	DOV	0	1	0
622-76-3-F2	190269.3	162620.2	74.46	1	63.96	62.96	66.37	DOV	1	0	0
622-76-3-F3	190269.3	162620.2	74.46	1	55.96	54.96	66.36	DOV	1	0	0
622-76-3-F4	190269.3	162620.2	74.46	1	50.96	49.96	66.23	DOV	1	0	0
622-76-4-F1	189823.6	163464.4	63.94	1	57.94	56.94	59.12	DOV	1	0	0
622-76-4-F2	189823.6	163464.4	63.94	1	53.94	52.94	59.05	DOV	1	0	0
622-76-4-F3	189823.6	163464.4	63.94	1	49.94	48.94	58.95	DOV	1	0	0
622-76-4-F4	189823.6	163464.4	63.94	1	45.94	44.94	58.84	DOV	1	0	0
622-76-6-F2	188955.9	164825.1	53.85	1	44.85	43.85	47.13	DOV	1	0	0
622-76-6-F3	188955.9	164825.1	53.85	1	39.85	38.85	47.09	DOV	1	0	0
622-76-6-F4	188955.9	164825.1	53.85	1	35.85	34.85	46.75	DOV	1	0	0
622-76-6-F1	188955.9	164825.1	53.85	1	47.85	46.85	47.13	DOV	1	0	0
623-76-17-F2	193447.3	168550.8	49.6	1	26.6	25.6	39.71	DOV	1	0	0
623-76-17-F3	193447.3	168550.8	49.6	1	23.6	22.6	37.41	DOV	1	0	0
623-76-2-F2	192173	162962.3	66.09	1	52.59	51.59	58.56	DOV	1	0	0
623-76-2-F3	192173	162962.3	66.09	2	49.09	48.09	58.94	DOV	0	1	0
623-76-4-F2	191895.9	164622.1	60.41	1	45.41	44.41	53.57	DOV	1	0	0
623-76-4-F3	191895.9	164622.1	60.41	1	41.91	40.91	48.80	DOV	1	0	0
623-76-4-F4	191895.9	164622.1	60.41	1, 2	37.41	36.41	42.76	DOV	0.845	0.155	0.0
623-76-5-F2	194159	165041.3	55.07	1	43.07	42.07	48.50	DOV	1	0	0
623-76-5-F3	194159	165041.3	55.07	2	40.57	39.47	48.59	DOV	0	1	0
623-76-8-F2	194811.8	166330.9	38.5	2	30.5	29.5	36.62	DOV	0	1	0
2-0422a-F1	188763	177376	72.56	1	-34.44	-36.44	36.80	DOV	1	0	0
2-0436a-F1	189271	190520	17.85	3	-291.15	-296.15	11.69	DOV	0	0	1
2-0437a-F1	194146	163971	57.8	2	36.9	34.9	51.35	DOV	0	1	0
2-0437a-F2	194146	163971	57.8	2	2.8	0.8	44.02	DOV	0	1	0
2-0437a-F3	194146	163971	57.8	3	-8.2	-13.2	43.87	DOV	0	0	1
2-0439a-F1	192918	171428	53.5	3	-74.5	-79.5	21.99	DOV	0	0	1
2-0439b-F2	192922	171428	53.5	1	8.5	6.5	40.60	DOV	1	0	0
2-0436c-F1	188312	189546	17.5	1	-171	-179	14.93	DOV	1	0	0
3020-001-F0	174072	158452	62.6	3	11.16	0.16	42.88	DW	0	0	1
3014-004-F0	153661.9	178449.2	13.31	3	-102.49	-131.69	8.93	DW	0	0	1
3008-063-F0	169297.7	169655.1	27.07	3	-44.23	-85.23	-2.86	DW	0	0	1

3010-018-F0	163340.5	164438.3	61.61	2, 3	8.61	-21.39	47.22	DW	0.0	0.024	0.976
3001-107-F1	183511	185746	13.8	3	-224.2	-239.2	6.12	DW	0	0	1
3003-001-F0	187630	166169	46.02	1, 2	23.02	-18.48	43.29	DW	0.033	0.967	0.0
3003-005-F1	187412	166283	49.25	2, 3	-1.25	-67.52	44.66	DW	0.0	0.49	0.51
3003-006-F1	187620.7	166189.5	46.13	1, 2	23.19	-21.81	43.23	DW	0.032	0.968	0.0
3003-015-F1	188824.7	164405.3	45.86	2	25.37	-0.13	44.02	DW	0	1	0
3003-021-F2	188121	163861	47.18	2	33.43	29.43	46.38	DW	0	1	0
3003-022-F2	189677.6	165613.3	44.23	1, 2	26.83	21.83	40.94	DW	0.269	0.731	0.0
3003-037-F2	186901.8	166280.6	48.58	1	28.58	23.58	46.25	DW	1	0	0
3003-038-F2	187334.8	166300.1	48.83	1	28.83	23.83	44.30	DW	1	0	0
3003-039-F2	186540.6	166265.1	54.98	1	34.48	29.48	51.43	DW	1	0	0
3003-040-F2	187390.8	165810.9	50.71	1	30.71	25.71	46.73	DW	1	0	0
3008-058-F2	171911.1	172554.4	23.72	1	-13.28	-18.28	25.07	DW	1	0	0
3008-058-F3	171911.1	172554.4	23.72	3	-67.28	-72.28	0.53	DW	0	0	1
3010-003-F1	163284.9	163496.8	51.79	2, 3	2.89	-15.61	41.01	DW	0.0	0.02	0.98
3010-006-F0	162999	164519	59.9	1, 2, 3	10.9	-21.11	48.18	DW	0.014	0.036	0.95
3010-011-F1	163289.6	163507.9	51.5	1	29.85	20.85	49.59	DW	1	0	0
3010-016-F2	163027.9	164541.8	59.28	1	19.28	14.28	49.75	DW	1	0	0
3010-016-F3	163027.9	164541.8	59.28	3	-8.72	-13.72	32.33	DW	0	0	1
3011-006-F2	163583.5	160580.9	50.42	3	18.42	10.42	34.86	DW	0	0	1
3011-007-F2	163555.4	160607.4	52.25	2	27.25	26.25	44.34	DW	0	1	0
3011-007-F3	163555.4	160607.4	52.25	3	17.25	7.25	34.92	DW	0	0	1
3011-023-F2	164979	160933	39.09	3	19.09	14.09	34.74	DW	0	0	1
3011-024-F2	164171	160305	42.34	3	22.34	17.34	37.48	DW	0	0	1
3012-004-F1	169109	162050	32.79	3	8.75	-1.25	31.54	DW	0	0	1
3012-017-F2	169628	162184	33.37	3	15.87	14.87	31.97	DW	0	0	1
3012-019-F1	169607	161869	32.03	3	20	-5	30.94	DW	0	0	1
3012-022-F1	170691	159619	36.95	3	25	2.5	33.53	DW	0	0	1
3012-023-F1	170501	159530	35.91	3	25	2.5	34.65	DW	0	0	1
3012-024-F1	168789	164064	30.4	2, 3	5.4	-2.4	28.90	DW	0.0	0.653	0.347
3012-025-F1	168265.4	167278.6	31.104	2	-4.594	-9.594	30.64	DW	0	1	0
3012-025-F2	168265.4	167278.6	31.104	2, 3	-20.59	-29.59	26.50	DW	0.0	0.155	0.845
3012-056-F1	168500	161410	50.48	2	25.48	23.48	32.41	DW	0	1	0
3012-056-F2	168500	161410	50.48	3	13.48	11.48	32.22	DW	0	0	1
3012-057-F2	167689	161354	88.07	2	30.07	28.07	62.62	DW	0	1	0
3012-057-F3	167689	161354	88.07	3	17	15	33.25	DW	0	0	1
3014-003-F0	153146.7	177509.8	13.86	1, 2, 3	-70.67	-114.64	8.97	DW	0.616	0.066	0.318
3020-002-F1	174109	158551	0	3	44.93	44.93	43.97	DW	0	0	1
3001-109-F3	183519.6	185738.2	14.29	1	-118.71	-123.71	17.35	DW	1	0	0

3014-005-F2	153646.8	178466.2	13.27	1	-73.73	-78.73	10.87	DW	1	0	0
3008-065-F3	169281.6	169688.4	27.35	1	-1.65	-5.65	26.87	DW	1	0	0
3008-066-F3	170086	171027.7	23.86	1	-9.14	-14.14	25.75	DW	1	0	0
3006-159-F1	173862.3	172721.2	24.89	1	-15.11	-20.11	28.07	DW	1	0	0
3006-159-F2	173862.3	172721.2	24.89	3	-74.11	-79.11	-11.53	DW	0	0	1
3007-038-F2	176188.8	175999.5	25.44	1	-39.57	-44.57	23.48	DW	1	0	0
3007-038-F3	176188.8	175999.5	25.44	3	-111.5	-115.5	-16.31	DW	0	0	1
3023-013-F1	158336.8	162091	64.87	1	34.75	32.75	62.44	DW	1	0	0
3023-014-F1	158263.5	162164.3	68.55	1	30.55	28.55	60.77	DW	1	0	0
3003-002-F0	186897	166310	50.32	1, 2	45.77	-22.48	34.51	DW_prod	0.487	0.513	0.0
3003-003-F0	187318	166293	48.76	1, 2	24.96	-16.84	39.32	DW_prod	0.061	0.939	0.0
3003-004-F0	187636.4	166181.8	46.25	2	18.18	-15.82	35.99	DW_prod	0	1	0
3003-016-F0	188502.1	164398.8	46.89	2	23.79	7.79	40.96	DW_prod	0	1	0
3003-017-F0	189094	164694	45.02	2	23.02	7.02	42.91	DW_prod	0	1	0
3003-018-F0	189357.8	164834.7	44.9	2	22.65	4.65	40.61	DW_prod	0	1	0
3003-028-F0	188821.1	164404.2	45.22	2	24.46	7.56	41.23	DW_prod	0	1	0
3003-029-F0	186893	166240	47.76	1, 2	27.76	-2.24	43.53	DW_prod	0.174	0.826	0.0
3003-041-F0	188396.8	164497.8	47.71	2	21.71	8.71	43.61	DW_prod	0	1	0
3006-001-F0	173644.1	172756.8	24.84	3	-73.71	-100.76	-45.53	DW_prod	0	0	1
3006-116-F0	174276	172561	28.5	3	-72.5	-101.5	-36.95	DW_prod	0	0	1
3007-001-F0	176177	175954	25.64	3	-116.36	-152.36	-49.79	DW_prod	0	0	1
3008-001-F0	169223	169076	27.77	2, 3	-39.68	-79.68	0.25	DW_prod	0.0	0.024	0.976
3008-002-F0	169373	170207	26.72	3	-47.78	-82.78	-15.27	DW_prod	0	0	1
3008-003-F0	169696	170670	25.74	2, 3	-49.26	-84.26	-13.21	DW_prod	0.0	0.007	0.993
3008-004-F0	170091	171033	24.01	2, 3	-51.99	-84.99	-2.63	DW_prod	0.0	0.004	0.996
3008-005-F0	169298.4	169638.5	27.136	2, 3	-40.36	-90.83	-10.54	DW_prod	0.0	0.011	0.989
3008-006-F0	169279.9	169512.8	27.13	2, 3	-37.87	-83.67	-7.89	DW_prod	0.0	0.027	0.973
3010-001-F0	163296.1	163523.4	51.74	3	-2.1	-15.1	20.73	DW_prod	0	0	1
3010-002-F0	163288	163514.2	51.56	2, 3	-0.24	-14.24	24.65	DW_prod	0.0	0.0	1.0
3011-005-F0	163610	160562	49.29	3	17.5	-18.5	34.71	DW_prod	0	0	1
3011-008-F0	164745	160598	39.47	3	15.57	-12.03	31.95	DW_prod	0	0	1
3011-009-F0	164746	160626	38.87	3	13.36	-9.14	34.37	DW_prod	0	0	1
3012-001-F0	168889	162233	33.86	3	12.86	-18.14	26.92	DW_prod	0	0	1
3012-002-F0	168936	162225	33.58	3	15.68	-14.82	26.37	DW_prod	0	0	1
3012-003-F0	168845	162230	37.73	3	14.13	-8.67	30.86	DW_prod	0	0	1
3012-007-F0	168840.1	165086	30.27	2, 3	-5.03	-42.03	26.57	DW_prod	0.0	0.121	0.879
3012-008-F0	168789	165194	29.35	3	-11.95	-42.65	22.15	DW_prod	0	0	1
3012-009-F0	168758	165170	29.02	3	-18.98	-47.98	25.26	DW_prod	0	0	1
3012-013-F0	169674	161619	33.23	3	16.98	-3.02	31.62	DW_prod	0	0	1

3012-014-F0	169638	162007	32.69	2, 3	20.7	-6.3	31.82	DW_prod	0.0	0.023	0.977
3012-015-F0	169627	161898	32.21	3	11.22	-10.78	30.12	DW_prod	0	0	1
3012-016-F0	169676	161752	32.65	3	17.06	-8.84	31.66	DW_prod	0	0	1
3012-020-F0	170744	159698	38.01	3	19.51	-0.64	33.50	DW_prod	0	0	1
3012-021-F0	170679	159623	37.1	3	20.8	6.8	32.34	DW_prod	0	0	1
3014-001-F0	153656.1	178455.1	12.08	3	-105.92	-128.62	8.41	DW_prod	0	0	1
3017-001-F0	193675	160731	50	3	12	-29.4	47.33	DW_prod	0	0	1
3023-005-F0	158161.1	162137.4	66.43	1	20.5	12.5	50.08	DW_prod	1	0	0
3023-006-F0	158269.6	162108.8	65.67	1	20.5	12.5	44.74	DW_prod	1	0	0
3023-008-F0	158262.7	162200.4	69.5	1	20.5	12.5	54.45	DW_prod	1	0	0
3023-024-F0	158311.9	162152.7	65.13	1	20.5	12.5	51.35	DW_prod	1	0	0
3001-108-F0	183464	185677	18.63	2, 3	-217.77	-257.77	-14.92	DW_prod	0.0	0.002	0.998
3010-017-F0	163013.5	164525.3	59.42	2, 3	6.91	-23.09	33.75	DW_prod	0.0	0.058	0.942

Steady-state model for 2000-2004

Table I. 12: Overview of all extraction wells of De Watergroep in the steady-state model for 2000-2004 modelled with the MNW2 package. Q = extraction rate, negative values indicate extraction from the model.

Well name	X	Y	Layer	Q (m³/d)	Site
3003-002	186897	166310	2	-708.30	Menebeek
3003-003	187318	166293	2	-767.17	Menebeek
3003-004	187636	166182	2	-832.34	Menebeek
3003-016	188502	164399	2	-659.93	Groot-Overlaar
3003-017	189094	164694	2	-1076.50	Groot-Overlaar
3003-018	189358	164835	2	-376.77	Groot-Overlaar
3003-029	186893	166240	2	-99.00	Menebeek
3006-001	173644	172757	3	-587.33	Cadol
3007-001	176177	175954	3	-241.32	Vlierbeek
3008-001	169223	169076	3	-1509.45	Het Broek
3008-002	169373	170207	3	-13.17	Het Broek
3008-003	169696	170670	3	-8.59	Het Broek
3008-005	169298	169638	3	-1123.91	Het Broek
3008-006	169280	169513	3	-1831.76	Het Broek
3010-001	163296	163523	3	-89.99	Kouterstraat
3010-002	163288	163514	3	-96.79	Kouterstraat
3010-006	162999	164519	3	-308.48	Nellebeek
3011-008	164745	160598	3	-4671.43	Sana
3012-001	168889	162233	3	-3485.69	Veeweyde
3012-002	168936	162225	3	-2199.34	Veeweyde
3012-007	168840	165086	3	-2845.77	Geuzenhoek
3012-008	168789	165194	3	-2743.44	Geuzenhoek
3012-014	169638	162007	3	-2264.64	Pécrot
3012-015	169627	161898	3	-1475.89	Pécrot
3012-016	169676	161752	3	-1508.70	Pécrot
3012-020	170744	159698	3	-4549.64	La Motte
3012-021	170679	159623	3	-1416.65	La Motte
3014-001	153656	178455	3	-400.32	Vilvoorde
3019-013	179303	163215	3	-202.50	Beauvechain
3020-001	174072	158452	3	-1767.30	Biez

Table I. 13: Overview of all extraction wells from DOV in the steady-state model for 2000-2004 modelled with the WEL package for which reported extraction rates are available. Q = extraction rate, negative values indicate extraction from the model.

Exploiter	X	Y	Layer	Q (m³/d)
CITRIQUE BELGE	191833	165935	2	-8741.7
INBEV BELGIUM (INTERBREW)	174000	175700	1	-1002.2
INBEV BELGIUM (INTERBREW)	186509	163164	2	-986.3
TIENSE SUIKERRAFFINADERIJ	190604	165816	2	-891.0
CARGILL FRANCE SAS (VROEGERE CARGILL MALT)	171810	179895	3	-804.3
GEMEENTELIJKE WATERDIENST HOEILAART	158300	162150	1	-620.3
CARGILL FRANCE SAS (VROEGERE CARGILL MALT)	171762	179895	1	-550.5
BENEON REMY (VROEGER REMY INDUSTRIES)	173270	179258	1	-369.9
INBEV BELGIUM (INTERBREW)	187516	162418	2	-265.4
BOORTMALT	164425	185625	1	-236.1
ROBERT BOSCH PRODUKTIE	191456	166861	2	-150.7
PURATOS	143054	174439	1	-80.7
ANALU	155614	178836	2	-60.1
BROUWERIJ HAACHT	166856	183923	1	-31.3
DE VIJVERS	193891	190925	3	-24.6
ABDIJ DER NORBERTIJNEN VAN AVERBODE	192804	191725	3	-23.3
AVERMAETE MARC	194688	165815	3	-20.5
MACHIELS	173976	175828	1	-16.5
ALUMETAL	157771	174600	3	-13.9

Table I. 14: Overview of all extraction wells from DOV in the steady-state model for 2000-2004 modelled with the WEL package for which only permitted rates are available. Q = extraction rate, negative values indicate extraction from the model. These extraction rates are the permitted rates multiplied with a factor 0.8.

Exploiter	X	Y	Layer	Q (m³/d)
TIENSE SUIKERRAFFINADERIJ	190658	165664	3	-1074.0
STAD TIENEN	193523	167225	3	-800.0
AFFILIPS	189110	165879	2	-642.6
INBEV BELGIUM (INTERBREW)	173269	175270	3	-219.2
STICHTING MARGUERITE-MARIE DELACROIX	189694	166550	3	-87.7
INTER-BETON NV	191953	166829	2	-52.7
KRIJGSMACHT MAJOOR HOUSIAU	156780	180260	3	-52.6
COVEE	165684	183387	1	-40.6
EXIDE AUTOMOTIVE	169980	160990	3	-32.3
CRISTAL MONOPOLE	182076	186290	1	-23.7
RUSTHUIS SINT JOZEF	187631	185144	1	-21.9
STICHTING MARGUERITE-MARIE DELACROIX	193530	165540	2	-21.9
ATELIERS DE CONSTRUCTION E. MOLINET	189872	165356	1	-21.6
BENOIT MARC	194007	176411	1	-19.7
BADRFAROUJ	153096	177566	1	-17.9

KBC BANK-GROEP	174290	174834	1	-17.5
OSS	191065	165340	3	-17.1
SIMONET PAUL	190527	168684	1	-16.4
VAN DOORSLAER MARC	147779	187188	1	-16.4
HENSKENS PASCAL	182178	165077	1	-15.7
FILOSOFISCH EN THEOLOGISCH COLLEGE	172410	172180	3	-15.3
REYNAERTS MARC & JAN	191232	166813	2	-15.0
VAN ESBROEK PAUL	181721	186827	1	-14.5
HOEVEN C.P.J.	186136	166708	2	-14.4
LEUVENSE KATHOLIEKE SCHOLEN AAN DE DIJLE	173038	174150	1	-14.2
SINT PIETERS COLLEGE	173038	174150	1	-14.2
IMMO BTR	162784	181760	2	-13.8
READY BETON /DDM BETON	176352	181053	1	-13.3
BAAZ JAN (FREDIMO)	191752	166513	1	-13.2
ZILVERWIT WASSERIJ	173880	182281	2	-13.2
TEXWORKS (ATOMIC)	178829	186082	1	-12.3
PEETERS DAVID	193633	174862	1	-12.1
VAN DOOREN PIETER	194596	182257	1	-12.1
BK	173829	175672	1	-11.4
DEKREM MICHEL	163700	181999	1	-11.0
KBIVB	191000	166080	2	-11.0
PROVINCIE VLAAMS BRABANT "DE WIJNPERS"	172591	175127	1	-11.0
RUSTOORD ROOSBEEK	183750	169710	1	-11.0
STROUVEN MARC	194758	175996	1	-11.0
VLEMINCKX PAUL	171376	175252	1	-11.0
VERSELE-LAGA	173829	175672	1	-10.6
NATURELLO	165684	183387	1	-10.5
NELISSEN	188326	167569	2	-9.9
OVERSTIJNS JOOST	191788	170822	1	-9.3
ZUSTERS URSELINEN	169488	181585	1	-8.8
GEMEENTE KAMPENHOUT	163570	181870	1	-8.8
PATERS REDEMPTORISTEN	173916	173612	1	-8.8
SITA WASTE SEVICES DD MIX	190945	165104	1	-8.8
WASSERIJ - DROOGKUIS WEMMEL	146120	177071	1	-8.8
WASSERIJ DE LELIE LEUVEN	173311	173282	1	-8.8
R.W.T / WILLEMS RUDDY	176732	186406	1	-8.3
BIERTOREN	162784	181760	1	-8.1
AVERMAETE ETIENNE	194366	166034	1	-8.0
VAN CRIEKINGEN BART	180376	178609	1	-8.0

Table I. 15: Overview of observations wells implemented in the 2000-2004 SS model. Filter top, filter bot and head are in mTAW. L1,w, L2,w and L3,w are respectively the weights assigned to layer 1, 2 and 3 for the calculation of an equivalent head.

Well name	X	Y	Z	Layers	Filter top	Filter bot	Head	Group	L1, w	L2, w	L3, w
700-76-3-F3	143616	162751	26.01	1	8.01	7.01	25.79	DOV	1	0	0
2-0005-F1	171549	172681	26.21	3	-67	-92.74	2.00	DOV	0	0	1
2-0007-F1	160970	160430	106.84	2,3	17.34	-28.66	61.00	DOV	0.0	0.014	0.986
2-0008-F1	163743	162238	98.04	3	10.79	0.79	44.71	DOV	0	0	1
2-0012-F1	166900	161070	76.51	3	17.81	6.86	35.08	DOV	0	0	1
2-0072-F1	168699	174665	92.04	1	-34.96	-44.96	20.30	DOV	1	0	0
2-0111-F1	183254	170590	60.99	3	-96.51	-108.51	25.64	DOV	0	0	1
2-0117-F1	177651	166995	76.39	3	-27.61	-35.61	40.86	DOV	0	0	1
2-0133-F1	178504	171525	45.61	1	0.61	-14.39	44.93	DOV	1	0	0
710-71-3-F3	164952	161769	88.79	1	46.79	45.79	56.54	DOV	1	0	0
2-0049-F1	189325	165770	46.19	2	1.19	-2.81	40.82	DOV	0	1	0
2-0103-F1	184343	179654	28.58	3	-165.42	-185.42	12.45	DOV	0	0	1
2-0106-F1	194595	178441	57.91	3	-139.09	-151.09	13.33	DOV	0	0	1
2-0113-F2	186590	162370	69.63	2	28.63	26.63	51.37	DOV	0	1	0
2-0124-F1	194611	168000	35.25	2	-17.25	-22.25	28.49	DOV	0	1	0
2-0123-F2	194610	168000	35.25	2	15.25	5.25	32.63	DOV	0	1	0
621-76-1-F2	190302	160183	75.8	1	63.8	62.8	67.57	DOV	1	0	0
621-76-1-F3	190302	160183	75.8	2	57.8	56.8	67.84	DOV	0	1	0
621-76-3-F2	194019	163847	62.47	2	49.47	48.47	51.01	DOV	0	1	0
621-76-3-F3	194019	163847	62.47	2	45.97	44.97	50.42	DOV	0	1	0
621-76-4-F3	193667	163532	62.65	2	48.05	47.05	52.92	DOV	0	1	0
622-71-11-F3	188319	160811	73.21	2	50.21	49.21	56.00	DOV	0	1	0
622-71-7-F2	183831	164618	76.24	1	61.74	61.24	67.72	DOV	1	0	0
622-71-7-F3	183831	164618	76.24	1	57.24	56.24	67.71	DOV	1	0	0
622-71-8-F3	184942	166222	69.76	1	53.76	52.76	60.77	DOV	1	0	0
622-76-2-F3	189694	161876	69.2	2	51.2	50.2	61.01	DOV	0	1	0
622-76-3-F1	190269	162620	74.46	1	68.96	67.96	70.40	DOV	1	0	0
622-76-3-F2	190269	162620	74.46	1	63.96	62.96	67.84	DOV	1	0	0
622-76-3-F3	190269	162620	74.46	1	55.96	54.96	67.82	DOV	1	0	0
622-76-3-F4	190269	162620	74.46	1	50.96	49.96	67.70	DOV	1	0	0
622-76-4-F1	189824	163464	63.94	1	57.94	56.94	59.99	DOV	1	0	0
622-76-4-F2	189824	163464	63.94	1	53.94	52.94	59.98	DOV	1	0	0
622-76-4-F3	189824	163464	63.94	1	49.94	48.94	59.89	DOV	1	0	0
622-76-4-F4	189824	163464	63.94	1	45.94	44.94	59.78	DOV	1	0	0
622-76-6-F2	188956	164825	53.85	1	44.85	43.85	47.24	DOV	1	0	0
622-76-6-F3	188956	164825	53.85	1	39.85	38.85	47.25	DOV	1	0	0
622-76-6-F4	188956	164825	53.85	1	35.85	34.85	46.81	DOV	1	0	0

622-76-6-F1	188956	164825	53.85	1	47.85	46.85	47.23	DOV	1	0	0
623-76-17-F2	193447	168551	49.6	1	26.6	25.6	38.68	DOV	1	0	0
623-76-17-F3	193447	168551	49.6	1	23.6	22.6	37.03	DOV	1	0	0
623-76-2-F2	192173	162962	66.09	1	52.59	51.59	59.47	DOV	1	0	0
623-76-2-F3	192173	162962	66.09	2	49.09	48.09	59.63	DOV	0	1	0
623-76-4-F2	191896	164622	60.41	1	45.41	44.41	53.57	DOV	1	0	0
623-76-4-F3	191896	164622	60.41	1	41.91	40.91	51.49	DOV	1	0	0
623-76-4-F4	191896	164622	60.41	1,2	37.41	36.41	39.66	DOV	0.845	0.155	0.0
623-76-5-F1	194159	165041	55.07	1	49.07	48.57	49.77	DOV	1	0	0
623-76-5-F2	194159	165041	55.07	1	43.07	42.07	49.76	DOV	1	0	0
623-76-5-F3	194159	165041	55.07	2	40.57	39.47	49.79	DOV	0	1	0
623-76-8-F1	194812	166331	38.5	1,2	32.5	31.5	37.61	DOV	0.17	0.83	0.0
623-76-8-F2	194812	166331	38.5	2	30.5	29.5	37.34	DOV	0	1	0
3003-001-F0	187630	166169	46.02	1,2	23.02	-18.48	43.64	DW	0.033	0.967	0.0
3003-005-F1	187412	166283	49.25	2,3	-1.25	-67.52	45.55	DW	0.0	0.595	0.405
3003-006-F1	187621	166190	46.13	1,2	23.19	-21.81	43.42	DW	0.032	0.968	0.0
3003-015-F1	188825	164405	45.86	2	25.37	-0.13	45.45	DW	0	1	0
3003-021-F2	188121	163861	47.18	2	33.43	29.43	46.74	DW	0	1	0
3003-022-F2	189678	165613	44.23	1,2	26.83	21.83	38.72	DW	0.269	0.731	0.0
3008-044-F1	171491	172669	25.18	3	-67	-92.22	2.12	DW	0	0	1
3010-003-F1	163285	163497	51.79	2,3	2.89	-15.61	44.16	DW	0.0	0.052	0.948
3010-011-F1	163290	163508	51.5	1	29.85	20.85	50.37	DW	1	0	0
3011-006-F2	163583	160581	50.42	3	18.42	10.42	37.28	DW	0	0	1
3011-007-F2	163555	160607	52.25	2	27.25	26.25	45.27	DW	0	1	0
3011-007-F3	163555	160607	52.25	3	17.25	7.25	36.80	DW	0	0	1
3011-010-F1	164754	160614	39.23	3	13.41	-0.59	38.54	DW	0	0	1
3011-014-F1	164742	160610	39.15	3	16.15	-8.85	35.60	DW	0	0	1
3011-017-F1	162590	157535	46.79	3	24.79	4.79	44.97	DW	0	0	1
3012-004-F1	169109	162050	32.79	3	8.75	-1.25	32.51	DW	0	0	1
3012-017-F2	169628	162184	33.37	3	15.87	14.87	32.59	DW	0	0	1
3012-019-F1	169607	161869	32.03	3	20	-5	31.53	DW	0	0	1
3012-022-F1	170691	159619	36.95	3	25	2.5	35.66	DW	0	0	1
3012-023-F1	170501	159530	35.91	3	25	2.5	36.52	DW	0	0	1
3012-024-F1	168789	164064	30.4	2,3	5.4	-2.4	30.01	DW	0.0	0.021	0.979
3012-025-F1	168265	167279	31.104	2	-4.594	-9.594	31.67	DW	0	1	0
3012-025-F2	168265	167279	31.104	2,3	-20.59	-29.59	29.56	DW	0.0	0.011	0.989
3014-003-F0	153147	177510	13.86	1,2,3	-70.67	-114.64	-12.72	DW	0.076	0.081	0.843
3019-012-F0	179310	163234	85.31	3	20.7	7.2	24.55	DW	0	0	1
3019-041-F0	178981	163150	85.75	2,3	22.91	7.91	77.23	DW	0.0	0.03	0.97

3020-002-F1	174109	158551	0	3	44.93	44.93	44.65	DW	0	0	1
3003-002-F0	186897	166310	50.32	1,2	45.77	-22.48	36.36	DW_prod	0.487	0.513	0.0
3003-003-F0	187318	166293	48.76	1,2	24.96	-16.84	38.85	DW_prod	0.061	0.939	0.0
3003-004-F0	187636	166182	46.25	2	18.18	-15.82	38.15	DW_prod	0	1	0
3003-009-F0	186324	163026	0	1	55.64	55.64	53.54	DW_prod	1	0	0
3003-010-F0	186370	163002	0	1	54.37	54.37	53.21	DW_prod	1	0	0
3003-011-F0	186383	163009	0	1	54.33	54.33	53.04	DW_prod	1	0	0
3003-012-F0	186359	162982	0	1	53.97	53.97	52.79	DW_prod	1	0	0
3003-013-F0	186306	163002	0	1,2	40.62	22.62	53.47	DW_prod	0.021	0.979	0.0
3003-016-F0	188502	164399	46.89	2	23.79	7.79	41.17	DW_prod	0	1	0
3003-017-F0	189094	164694	45.02	2	23.02	7.02	42.09	DW_prod	0	1	0
3003-018-F0	189358	164835	44.9	2	22.65	4.65	38.51	DW_prod	0	1	0
3003-028-F0	188821	164404	45.22	2	24.46	7.56	44.98	DW_prod	0	1	0
3003-029-F0	186893	166240	47.76	1,2	27.76	-2.24	46.01	DW_prod	0.174	0.826	0.0
3006-001-F0	173644	172757	24.84	3	-73.71	-100.76	-40.59	DW_prod	0	0	1
3006-116-F0	174276	172561	28.5	3	-72.5	-101.5	-3.70	DW_prod	0	0	1
3007-001-F0	176177	175954	25.64	3	-116.36	-152.36	-42.27	DW_prod	0	0	1
3008-001-F0	169223	169076	27.77	2,3	-39.68	-79.68	12.56	DW_prod	0.0	0.005	0.995
3008-002-F0	169373	170207	26.72	3	-47.78	-82.78	13.46	DW_prod	0	0	1
3008-003-F0	169696	170670	25.74	2,3	-49.26	-84.26	13.31	DW_prod	0.0	0.024	0.976
3008-004-F0	170091	171033	24.01	2,3	-51.99	-84.99	13.55	DW_prod	0.0	0.022	0.978
3008-005-F0	169298	169638	27.136	2,3	-40.36	-90.83	14.72	DW_prod	0.0	0.01	0.99
3008-006-F0	169280	169513	27.13	2,3	-37.87	-83.67	3.96	DW_prod	0.0	0.021	0.979
3010-001-F0	163296	163523	51.74	3	-2.1	-15.1	32.33	DW_prod	0	0	1
3010-002-F0	163288	163514	51.56	2,3	-0.24	-14.24	33.41	DW_prod	0.0	0.001	0.999
3010-006-F0	162999	164519	59.9	2,3	10.5	-21.11	43.46	DW_prod	0.0	0.656	0.344
3011-005-F0	163610	160562	49.29	3	17.5	-18.5	36.70	DW_prod	0	0	1
3011-008-F0	164745	160598	39.47	3	15.57	-12.03	34.58	DW_prod	0	0	1
3011-009-F0	164746	160626	38.87	3	13.36	-9.14	35.68	DW_prod	0	0	1
3011-015-F0	162580	157540	46.79	3	23.98	7.98	46.53	DW_prod	0	0	1
3012-001-F0	168889	162233	33.86	3	12.86	-18.14	27.16	DW_prod	0	0	1
3012-002-F0	168936	162225	33.58	3	15.68	-14.82	26.64	DW_prod	0	0	1
3012-003-F0	168845	162230	37.73	3	14.13	-8.67	31.99	DW_prod	0	0	1
3012-007-F0	168840	165086	30.27	2,3	-5.03	-42.03	25.96	DW_prod	0.0	0.002	0.998
3012-008-F0	168789	165194	29.35	3	-11.95	-42.65	25.16	DW_prod	0	0	1
3012-009-F0	168758	165170	29.02	3	-18.98	-47.98	26.91	DW_prod	0	0	1
3012-013-F0	169674	161619	33.23	3	16.98	-3.02	32.79	DW_prod	0	0	1
3012-014-F0	169638	162007	32.69	2,3	20.7	-6.3	32.39	DW_prod	0.0	0.0	1.0
3012-015-F0	169627	161898	32.21	3	11.22	-10.78	31.18	DW_prod	0	0	1

3012-016-F0	169676	161752	32.65	3	17.06	-8.84	32.34	DW_prod	0	0	1
3012-020-F0	170744	159698	38.01	3	19.51	-0.64	35.97	DW_prod	0	0	1
3012-021-F0	170679	159623	37.1	3	20.8	6.8	35.12	DW_prod	0	0	1
3013-001-F0	191027	167207	0	2,3	-29.77	-62.27	29.81	DW_prod	0.0	0.491	0.509
3014-001-F0	153656	178455	12.08	3	-105.92	-128.62	-14.02	DW_prod	0	0	1
3017-001-F0	193675	160731	50	3	12	-29.4	41.99	DW_prod	0	0	1
3019-013-F0	179303	163215	85.46	3	21.46	7.46	50.52	DW_prod	0	0	1
3019-014-F0	179308	163204	85.41	3	19.91	5.91	26.30	DW_prod	0	0	1
3020-001-F0	174072	158452	62.6	3	46.25	35.25	41.20	DW_prod	0	0	1

Transient model

Table I. 16: Overview of number of wells used for each zone to estimate the GHB head based on a head vs topography correlation for each year.

Number of wells				
Year	Total	Kortrijk	Brussels	Quaternary
2004	878	791	24	63
2005	905	820	24	61
2006	957	866	23	68
2007	954	862	23	69
2008	943	852	22	69
2009	937	847	22	68
2010	919	831	22	66
2011	910	823	22	65
2012	918	830	22	66
2013	925	842	19	64
2014	930	842	19	69
2015	917	838	17	62
2016	907	828	18	61
2017	941	860	19	62
2018	929	852	17	60
2019	922	846	15	61
2020	410	357	6	47

Table I. 17: Overview the slope, intercept and coefficient of determination for the head versus topography correlation for respectively the Kortrijk and Brussels & Quaternary zone.

Year	Kortrijk			Brussels + Quaternary		
	slope	intercept	R ²	slope	intercept	R ²
2004	0.74	2.20	0.84	0.80	5.14	0.96
2005	0.73	2.39	0.84	0.80	5.19	0.96
2006	0.72	2.54	0.84	0.80	5.30	0.95
2007	0.72	2.77	0.83	0.80	5.47	0.95
2008	0.72	2.88	0.82	0.80	5.48	0.95
2009	0.72	2.57	0.84	0.80	5.18	0.95
2010	0.72	2.81	0.84	0.79	5.45	0.95
2011	0.72	2.83	0.84	0.79	5.44	0.95
2012	0.72	3.03	0.84	0.79	5.59	0.95
2013	0.72	3.02	0.83	0.73	7.67	0.95
2014	0.71	3.03	0.83	0.73	8.00	0.95
2015	0.71	2.92	0.81	0.73	7.80	0.95
2016	0.72	3.02	0.82	0.73	8.04	0.95
2017	0.71	2.76	0.81	0.73	7.72	0.95
2018	0.70	3.00	0.80	0.73	7.66	0.95
2019	0.70	2.88	0.79	0.73	7.73	0.95
2020	0.64	3.74	0.72	0.73	7.88	0.89

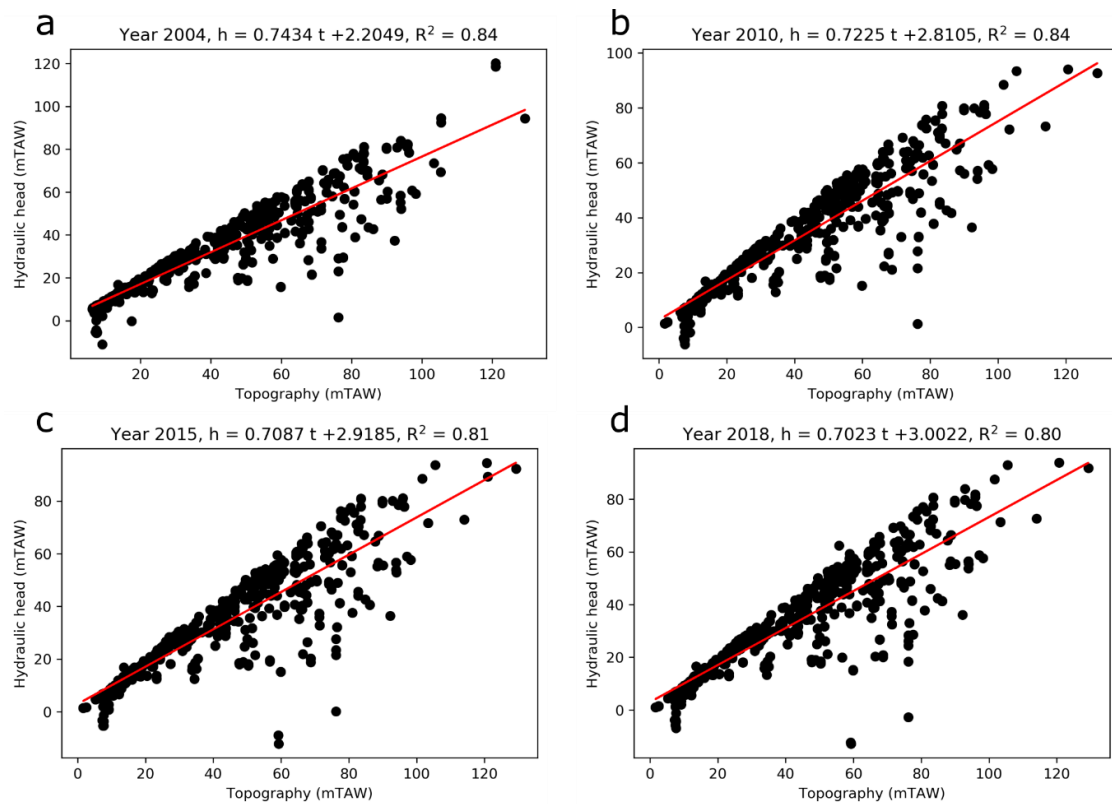


Figure I. 4: Correlations between head and topography for the Kortrijk zone for: (a) 2004; (b) 2010; (c) 2015; and (d) 2018.

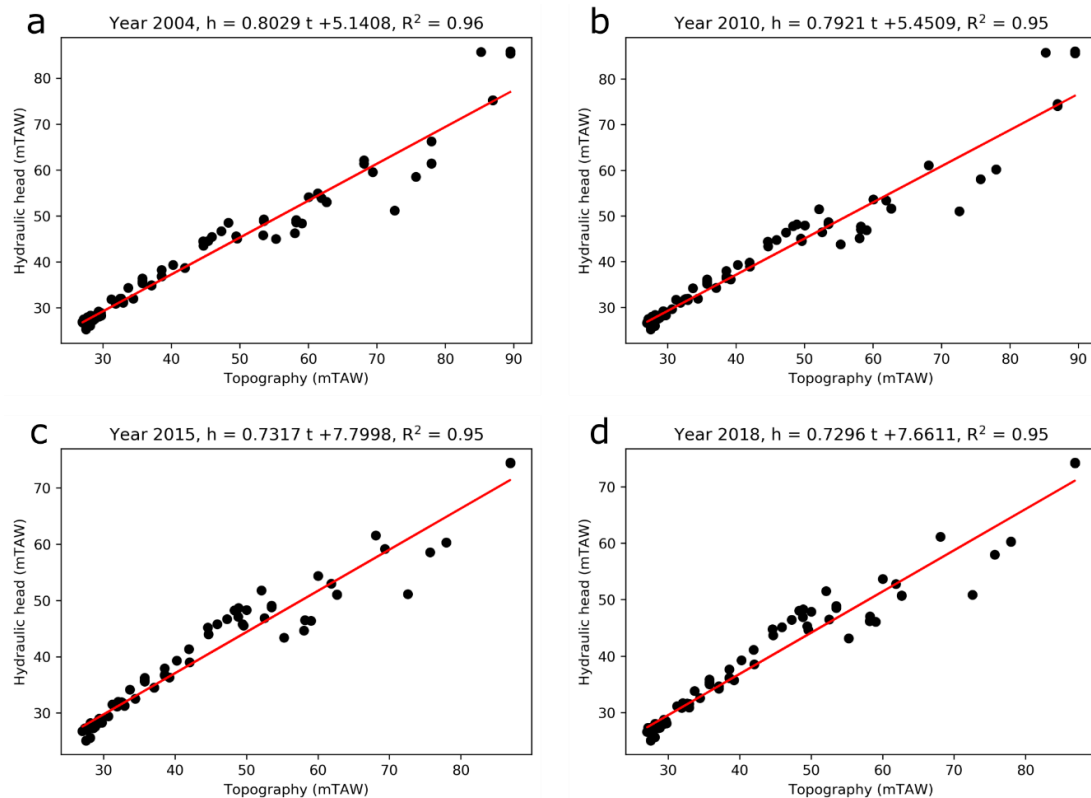


Figure I. 5: Correlations between head and topography for the Kortrijk zone for: (a) 2004; (b) 2010; (c) 2015; and (d) 2018.

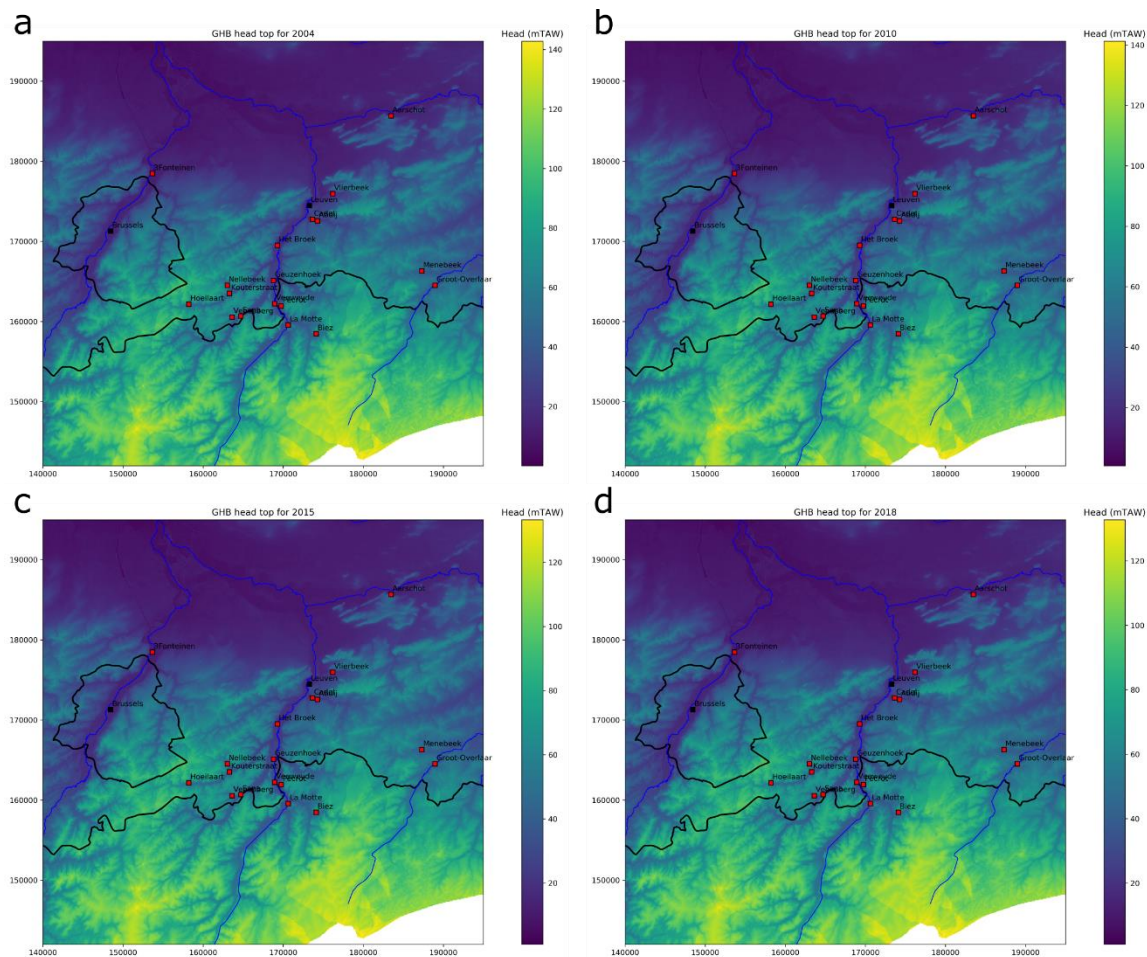


Figure I. 6: Estimated head for the GHB package based on head-topography correlation of the different zones for: (a) 2004; (b) 2010; (c) 2015; and (d) 2018.

Table I. 18: Overview of extraction rates for all wells and wells for De Watergroep and DOV (in m³/d).

Year	All wells	De Watergroep wells				DOV wells		
		Total	L1	L2	L3	Total	L1	L2
2004	58662	41053	0	4660	36393	17610	4409	9317
2005	57318	39966	0	5201	34765	17352	4682	8845
2006	56230	38288	0	5303	32985	17942	6388	8861
2007	54728	38871	0	5170	33701	15856	5039	8119
2008	52993	38950	0	4630	34320	14043	4895	6973
2009	54797	42443	0	5392	37050	12354	4996	5033
2010	50696	41240	0	5302	35938	9456	4430	3310
2011	48924	39131	0	4768	34363	9793	5125	3097
2012	48825	38916	0	4801	34115	9909	5069	3455
2013	48019	39724	0	4832	34892	8295	4437	2791
2014	46689	38973	0	4311	34662	7716	4096	2708
2015	48212	41469	1046	3851	36573	6743	2957	2786
2016	47320	40070	1235	4218	34617	7250	3176	3077
2017	48490	41367	1135	3939	36293	7122	3287	3023
2018	50943	43984	1071	4773	38140	6959	3051	2918
2019	49826	43025	990	4453	37581	6802	2989	2888
2020	48972	42187	663	5173	36350	6785	2986	2888

Table I. 19: Overview of all extraction wells of De Watergroep modelled with the MNW2 package. Columns 2004 to 2020 are the extraction rates in m³/d.

Well	X	Y	L	Site	2004	2005	2006	2007	2008	2009	2010	2011	2012	2013	2014	2015	2016	2017	2018	2019	2020
3001-108	183464	185677	3	Aarschot	0.0	0.0	0.0	0.0	0.0	0.0	0.0	0.0	0.0	0.0	0.0	-462.0	-621.8	-682.5	-858.9	-631.7	
3003-002	186897	166310	2	Menebeek	-373.5	0.0	-112.9	-564.4	-561.8	-573.9	-598.4	-681.9	-828.1	-612.3	-644.7	-402.6	-595.1	-671.0	-531.7	-74.4	-336.7
3003-003	187318	166293	2	Menebeek	-844.9	-819.3	-783.0	-861.0	-841.1	-849.3	-819.3	-748.0	-823.6	-802.5	-765.2	-716.9	-672.8	-740.1	-652.3	-366.4	-617.6
3003-004	187636	166182	2	Menebeek	-811.4	-811.1	-896.4	-756.6	-781.9	-754.9	-774.5	-692.3	-735.1	-829.1	-846.5	-758.8	-616.6	-654.5	-624.9	-511.6	-789.0
3003-016	188502	164399	2	Groot-Overlaar	-670.8	-796.8	-767.9	-686.7	-546.8	-785.5	-714.3	-563.3	-653.3	-656.4	-516.4	-343.1	-321.6	-348.8	-525.8	-44.0	-415.0
3003-017	189094	164694	2	Groot-Overlaar	-1089.7	-1355.9	-1310.7	-1084.5	-954.0	-1311.1	-1182.1	-933.9	-885.9	-1056.1	-618.6	-448.5	-554.5	-590.4	-925.8	-1232.3	-1037.1
3003-018	189358	164835	2	Groot-Overlaar	-374.2	-457.7	-451.0	-406.2	-324.2	-419.3	-371.8	-299.3	-367.6	-365.9	-263.6	-196.0	-197.0	-199.4	-301.1	-350.3	-274.8
3003-028	188821	164404	2	Groot-Overlaar	0.0	0.0	-136.9	-321.5	-264.0	-339.7	-304.2	-235.3	-277.5	-285.4	-246.2	-182.5	-182.9	-192.3	-183.8	-362.0	-368.0
3003-029	186893	166240	2	Menebeek	-495.0	-960.1	-843.9	-489.3	-356.5	-358.6	-537.3	-614.2	-230.1	-224.0	-162.0	-378.6	-669.2	-93.9	-591.7	-585.0	-537.5
3003-041	188397	164498	2	Groot-Overlaar	0.0	0.0	0.0	0.0	0.0	0.0	0.0	0.0	0.0	0.0	-247.5	-424.1	-407.7	-448.3	-436.0	-927.1	-797.7
3006-001	173644	172757	3	Cadol	-576.6	-607.9	-605.8	-594.0	-586.2	-540.8	-551.7	-556.7	-551.2	-558.9	-604.7	-600.1	-569.5	-551.8	-516.5	-529.8	-466.9
3006-116	174276	172561	3	Abdij	0.0	0.0	0.0	0.0	0.0	0.0	0.0	0.0	0.0	0.0	0.0	-38.0	-436.5	-473.0	-464.2	-456.6	-420.1
3007-001	176177	175954	3	Vlierbeek	-83.0	-1.1	-292.3	-275.7	-206.0	-289.6	-283.1	-202.2	-259.8	-280.8	-341.0	-318.0	-303.3	-370.1	-355.0	-340.3	-297.4
3008-001	169223	169076	3	Het Broek	-1425.6	-987.9	-1186.1	-1387.7	-1201.3	-1389.6	-1470.9	-1292.7	-1617.6	-1579.8	-1842.2	-2063.0	-1621.4	-2158.0	-1997.6	-1864.2	-1861.0
3008-002	169373	170207	3	Het Broek	0.0	-35.9	-17.5	-5.4	-55.7	-337.9	-499.0	-355.2	-526.1	-579.3	-706.0	-705.7	-620.5	-864.3	-847.2	-984.6	-624.8
3008-003	169696	170670	3	Het Broek	0.0	-25.4	-26.1	0.0	-71.4	-399.1	-601.4	-439.7	-517.4	-505.4	-790.5	-791.0	-821.0	-984.9	-819.4	-907.4	-587.0
3008-005	169298	169638	3	Het Broek	-904.0	-1031.6	-851.7	-1090.9	-1046.6	-1238.9	-1328.7	-1127.3	-1470.3	-1433.3	-1086.7	-1709.8	-1260.2	-1377.4	-1670.1	-1472.2	-146.1
3008-006	169280	169513	3	Het Broek	-1582.4	-1482.8	-1454.9	-1954.6	-1807.9	-1404.1	-1627.8	-1364.1	-1669.1	-1891.0	-1619.9	-1757.0	-2073.5	-1985.6	-1922.8	-1883.0	-1371.0
3008-063	169298	169655	3	Het Broek	0.0	0.0	0.0	0.0	0.0	0.0	0.0	0.0	0.0	0.0	0.0	0.0	0.0	0.0	0.0	0.0	-1247.3
3008-064	169259	169286	3	Het Broek	0.0	0.0	0.0	0.0	0.0	0.0	0.0	0.0	0.0	0.0	0.0	0.0	0.0	0.0	0.0	0.0	-2383.4
3010-001	163296	163523	3	Kouterstraat	-104.2	-159.9	-153.9	-143.2	-167.2	-284.7	-427.5	-329.7	-299.3	-415.9	-460.9	-406.0	-429.7	-424.7	-416.0	-393.5	-355.5
3010-002	163288	163514	3	Kouterstraat	-158.0	-185.0	-178.0	-169.9	-161.4	-148.3	-2.0	-59.0	0.0	-2.6	0.0	-0.1	-0.7	0.0	-0.1	-0.4	-22.9
3010-006	162999	164519	3	Nellebeek	-300.7	-280.7	-310.2	-311.3	-339.4	-379.1	-377.1	-369.5	-331.8	-68.2	0.0	0.0	0.0	0.0	0.0	0.0	0.0
3010-017	163013	164525	3	Nellebeek	0.0	0.0	0.0	0.0	0.0	0.0	0.0	0.0	0.0	-85.1	-136.7	-111.1	-84.4	-109.1	-12.6	0.0	
3010-018	163340	164438	3	Nellebeek	0.0	0.0	0.0	0.0	0.0	0.0	0.0	0.0	0.0	0.0	0.0	0.0	0.0	0.0	-178.8	-208.6	

3011-005	163610	160562	3	Venusberg	0.0	0.0	0.0	-472.6	-889.4	-840.3	-912.0	-885.0	-838.7	-142.2	-1111.0	-1177.1	-1191.7	-1222.8	-1132.1	-917.2	
3011-008	164745	160598	3	Sana	-4474.6	-4559.6	-4372.1	-4308.6	-4381.3	-4355.6	-4326.0	-4328.0	-4198.0	-4079.5	-2426.2	-3826.5	-3858.3	-3403.4	-4108.5	-4160.4	-4059.6
3011-009	164746	160626	3	Sana	0.0	0.0	0.0	0.0	0.0	0.0	0.0	0.0	0.0	-1686.0	0.0	-65.5	-168.2	-102.2	-32.9	-126.5	
3012-001	168889	162233	3	Veeweyde	-3351.8	-3436.6	-2986.7	-3558.3	-3354.1	-3073.5	-3231.8	-3606.8	-3708.5	-3433.5	-2944.0	-2617.5	-2984.0	-3081.5	-2998.4	-2651.1	-2580.3
3012-002	168936	162225	3	Veeweyde	-2283.9	-2347.0	-2105.8	-2301.1	-2309.7	-2568.1	-2556.2	-2551.9	-2445.1	-2186.6	-2096.1	-2045.5	-1706.2	-1423.6	-1632.5	-23.5	0.0
3012-003	168845	162230	3	Veeweyde	0.0	0.0	0.0	0.0	0.0	0.0	0.0	0.0	0.0	0.0	0.0	0.0	0.0	0.0	0.0	0.0	-912.2
3012-007	168840	165086	3	Geuzenhoek	-2645.7	-2638.4	-2514.0	-2723.9	-2679.8	-2901.5	-2352.6	-2836.1	-2842.7	-2982.9	-2933.3	-2813.8	-2329.2	-2545.5	-2447.7	-1409.4	0.0
3012-008	168789	165194	3	Geuzenhoek	-2623.7	-2557.1	-2509.6	-2745.6	-2743.1	-2786.2	-2279.2	-2833.2	-2860.4	-2969.8	-2861.5	-2799.5	-2772.3	-3089.3	-3020.5	-1797.6	0.0
3012-014	169638	162007	3	Pécrot	-2254.7	-2368.0	-2291.2	-2377.8	-2286.6	-2307.5	-2231.3	-1854.4	-1162.7	-940.1	-1512.4	-1689.5	-469.5	-1350.2	-1779.8	-2010.9	-1991.0
3012-015	169627	161898	3	Pécrot	-2163.7	-1789.6	-1509.7	-1885.0	-1783.7	-1939.2	-1929.4	-1696.4	-800.3	-684.2	-1273.5	-1569.5	-1363.6	-1638.2	-1592.2	-2022.3	-2002.3
3012-016	169676	161752	3	Pécrot	-2119.6	-1743.3	-1484.5	-1842.7	-1725.8	-1841.8	-1842.9	-1639.5	-936.2	-867.8	-1387.3	-1607.8	-1516.6	-1441.9	-1441.9	-1721.0	-1704.0
3012-020	170744	159698	3	La Motte	-6208.9	-5839.9	-4808.3	-2922.6	-4809.5	-5700.1	-4776.8	-3338.0	-4631.7	-6463.0	-4993.0	-4822.9	-4905.2	-4700.3	-4930.0	-5454.1	-5653.7
3012-021	170679	159623	3	La Motte	-757.1	-793.0	-1471.1	-589.9	0.0	-721.4	-1276.3	-1164.5	-1534.1	-1338.3	-1519.9	-1581.6	-1363.2	-1659.5	-1632.8	-1457.1	-1510.4
3012-059	168918	162218	3	Veeweyde	0.0	0.0	0.0	0.0	0.0	0.0	0.0	0.0	0.0	0.0	0.0	0.0	0.0	0.0	0.0	-3268.9	-3482.3
3014-001	153656	178455	3	Vilvoorde	-359.4	0.0	0.0	0.0	0.0	0.0	0.0	0.0	0.0	0.0	0.0	0.0	0.0	0.0	0.0	0.0	0.0
3019-013	179303	163215	3	Beauvechain	-184.0	-336.5	-334.3	-328.9	-277.9	-210.0	0.0	0.0	0.0	0.0	0.0	0.0	0.0	0.0	0.0	0.0	0.0
3020-001	174072	158452	3	Biez	-1831.3	-1557.7	-1521.6	-2183.7	-1852.7	-1343.6	-1126.2	-1506.1	-867.8	-792.4	-1350.0	-1562.1	-1397.2	-703.8	-1430.1	-557.7	-787.0
3023-005	158161	162137	1	Hoeilaart	0.0	0.0	0.0	0.0	0.0	0.0	0.0	0.0	0.0	0.0	0.0	-482.1	-570.1	-518.1	-468.7	-422.1	-263.3
3023-006	158270	162109	1	Hoeilaart	0.0	0.0	0.0	0.0	0.0	0.0	0.0	0.0	0.0	0.0	0.0	-280.2	-267.7	-258.0	-244.8	-242.4	-150.8
3023-007	158312	162153	1	Hoeilaart	0.0	0.0	0.0	0.0	0.0	0.0	0.0	0.0	0.0	0.0	0.0	-100.3	-232.8	-226.9	-249.9	-259.9	-234.4
3023-008	158263	162200	1	Hoeilaart	0.0	0.0	0.0	0.0	0.0	0.0	0.0	0.0	0.0	0.0	0.0	-183.0	-164.6	-132.2	-107.6	-66.0	-14.9
Total:					-41053	-39966	-38288	-38871	-38950	-42443	-41241	-39131	-38916	-39724	-38973	-41469	-40070	-41367	-43984	-43025	-42187

Table I. 20: Overview of all extraction wells from DOV in the period 2004-2020 modelled with the WEL package for which reported extraction rates are available. Columns 2004-2020 are extraction rates in m^3/d , negative values indicate extraction from the model.

Table I. 21: Overview of all extraction wells from DOV in the period 2004-2020 modelled with the WEL package for which only permitted rates are available. Columns 2004 tot 2020 are extraction rates in m^3/d , negative values indicate extraction from the model. These extraction rates are the permitted rates (not yet multiplied with a factor 0.8).

MERCKX LUDO	186700	166800	1	-4	-4	-4	-4	-4	-4	-4	-4	-4	-11	-11	-11	-11	-11	-11	-11	-11
ZUSTERS URSELINEN	169488	181585	1	-11	-11	-11	-11	-11	-11	-11	-11	-11	-11	-11	-11	-11	-11	-11	-11	-11
DENDOOVEN LUDO	189784	175192	1	-11	-11	-11	-11													
GEMEENTE KAMPENHOUT	163570	181870	1	-11	-11	-11	-11	-11	-11	-11	-11	-11	-11	-11	-11	-11	-11	-11	-11	-11
PATERS REDEMPTORISTEN	173916	173612	1	-11	-11															
SITA WASTE SEVICES DD MIX	190945	165104	1	-11	-11	-11	-11	-11	-11	-11	-11	-11	-11	-11	-11	-11	-11	-11	-11	-11
WASSERIJ - DROOGKUIS WEMMEL	146120	177071	1	-11	-11	-11	-11	-11	-11											
DEPOTTER - LEMMENS	167126	160468	3															-11	-11	-11
AVERMAETE ETIENNE	194366	166034	1	-10	-10	-10	-10	-10	-10	-10	-10	-10	-10	-10	-10	-10	-10	-10	-10	-10
VAN CRIEKINGEN BART	179998	177077	1	-10	-10	-10														
VAN CRIEKINGEN BART	180376	178609	1	-10	-10	-10	-10	-10	-10	-10	-10	-10	-10	-10	-10	-10	-10	-10	-10	-10
Total				-2625	-2682	-1520	-1546	-1327	-1342	-1301	-1359	-1349	-1415	-1233	-1276	-1217	-1222	-1219	-1204	-1184

Table I. 22: Overview of all observation wells used in the transient model. Columns 2004 to 2020 are the hydraulic heads for that year in mTAW.

Well name	X	Y	Z	L	Filter top	Filter bot	Group	2004	2005	2006	2007	2008	2009	2010	2011	2012	2013	2014	2015	2016	2017	2018	2019	2020		
700-76-3-F3	143616	162751	26.01	1	8.01	7.01	DOV	25.79	25.15	25.13	25.35	25.15	25.08	25.12	25.09	25.16	25.25	25.09	25.08	25.10	24.89	25.07				
2-0417a-F1	141375	174618	79.33	2, 3	-84.67	-86.67	DOV				-5.05	-4.48	-4.05	-3.70	-3.00	-2.13	-0.92	-0.06	0.53	1.07	1.06	0.59	0.62			
2-0417b-F3	141379	174618	79.33	1	-58.67	-63.67	DOV				5.13	5.49	5.81	6.16	6.65	7.23	7.62	7.92	8.31	8.64	8.85	8.72				
2-0418a-F1	147656	181650	52.37	3	-118.63	-123.63	DOV			-7.70	-6.64	-4.87	-3.58	-2.36	-1.38	-1.29	-0.66	0.49	1.32	2.36	2.96	3.48	3.72			
2-0418b-F4	147660	181650	52.37	1	-93.63	-97.63	DOV			-7.46	-6.74	-5.48	-4.38	-3.34	-2.34	-1.57	-1.24	-0.49	0.21	1.04	1.64	2.35	2.81			
2-0419a-F1	155951	180524	18.63	3	-136.87	-142.87	DOV			-1.75	0.08	1.99	3.49	4.58	5.46	5.42	6.09	7.49	8.15	8.72	8.90	9.09	9.13			
2-0419b-F3	155955	180524	18.63	1	-90.37	-95.37	DOV			9.47	9.67	10.09	10.40	10.70	10.79	10.90	11.07	11.36	11.55	11.84	12.00	12.21	12.26			
2-0427a-F1	142914	180915	67.66	3	-137.34	-142.34	DOV			4.32	5.53	4.31	5.44	7.97	9.04	8.49	9.01	9.62	9.68	16.89						
2-0435c-F1	144309	154699	122.60	1, 2, 3	50.60	46.60	DOV							72.59	72.80	72.97	73.00	72.97	72.88	73.11	72.86	72.84	72.56			
2-0005-F1	171549	172681	26.21	3	-67.00	-92.74	DOV	3.97	3.54	4.26	3.58	5.18	6.28	6.72												
2-0007-F1	160970	160430	106.84	2, 3	17.34	-28.66	DOV	60.99	60.68																	
2-0008-F1	163743	162238	98.04	3	10.79	0.79	DOV	44.65	43.95	44.30	44.38	44.38	43.69	43.66	43.75	43.81	44.02	44.13	44.01	44.03	43.89	43.67	43.50			
2-0012-F1	166900	161070	76.51	3	17.81	6.86	DOV	34.99	34.69	35.23	35.16	34.96	34.48	34.46	34.54	34.63	34.79	34.87	34.53	34.75	34.40	34.07	33.82			
2-0072-F1	168699	174665	92.04	1	-34.96	-44.96	DOV	20.47	20.55	20.60	20.35	20.26	20.53	20.87	20.83	20.75	20.94	21.15	21.50	21.98	22.12	21.95	21.84			
2-0111-F1	183254	170590	60.99	3	-96.51	-108.51	DOV	25.56	25.61	25.71	25.83	25.96	26.15	26.39	26.69	27.05	27.37	27.66	27.78	27.74	27.45	27.11	26.65			
2-0117-F1	177651	166995	76.39	3	-27.61	-35.61	DOV	41.35	41.36	41.48	41.48	41.47	41.60	41.73	41.86	42.16	42.33	42.34	42.19	42.01	41.60	41.08	40.65			
2-0133-F1	178504	171525	45.61	1	0.61	-14.39	DOV	44.94																		
710-71-3-F3	164952	161769	88.79	1	46.79	45.79	DOV	56.54	56.27	55.98	55.66	55.59						55.25	55.31	55.14	55.12	54.87	55.06			
2-0420a-F1	160078	170389	74.67	3	-49.83	-54.83	DOV			15.51	15.62	16.23	16.79	17.14	17.68	18.23	17.93	18.04	17.90	17.79	17.31	16.99	16.41			
2-0420b-F2	160113	170398	74.67	1	-15.33	-17.33	DOV			36.48	36.49	36.62	36.71	36.86	36.99	37.19	37.42	37.53	37.64	37.77	37.82	37.83	37.54			
2-0421-F3	180790	176231	74.90	1	-46.10	-52.10	DOV		34.91	34.98	34.69	34.66	34.72	34.76	34.73	34.78	34.72	34.55	34.63	34.89	34.96	34.72	34.63			
2-0424a-F1	160635	186224	10.02	3	-199.98	-204.98	DOV			2.98	3.47	4.08	4.75	5.46	6.17	6.92	7.46	8.01	8.50	8.97	9.29	9.54	9.73			
2-0424b-F3	160639	186224	10.02	1	-137.98	-142.98	DOV			9.29	9.39	9.31	9.19	9.25	9.19	9.19	9.11	9.14	9.17	9.41	9.54	9.67	9.72			
2-0429a-F1	174586	165125	90.58	3	-7.42	-13.42	DOV			50.37	50.32	50.16	50.00	49.95	49.92	49.99	50.08	49.76	49.50	49.45	49.25	48.92	48.74			
2-0429b-F2	174590	165125	90.58	2	5.08	-0.92	DOV			57.98	57.68	57.52	57.35	57.16	56.99	57.16	57.12	57.04	56.96	56.96	56.95	56.74	56.48			
2-0430-F2	166516	167019	72.17	1	12.17	7.17	DOV			37.66	37.73	37.72	37.60	37.64	37.65	37.74	37.76	37.79	37.71	37.81	37.69	37.65	37.59			
2-0431-F2	157749	163462	114.21	1	20.21	10.21	DOV			73.65	73.56	73.57	73.42	73.32	73.20	73.15	73.13	73.20	73.00	72.89	72.84	72.68	72.50			
2-0438a-F1	180804	166112	95.10	1	46.10	44.10	DOV			74.48	74.56	74.66	74.52	74.39	74.48	74.49	74.45	74.43	74.45	74.64	74.42	74.18	73.95			
2-0440a-F1	183106	172384	76.15	3	-88.85	-92.85	DOV			19.65	19.60	19.60	19.79	20.16	20.54	21.04	21.45	21.75	21.84	21.83	21.52	21.02	20.50			
2-0440b-F2	183110	172384	76.15	1	0.15	-3.85	DOV			50.09	50.18	50.27	50.15	50.12	50.20	50.26	50.26	50.14	50.16	50.33	50.16	50.02	49.84			
2-0441a-F1	177333	182788	20.11	3	-188.89	-192.89	DOV			4.59	4.70	4.82	5.15	5.66	6.43	7.28	8.06	8.59	9.04	9.36	9.39	9.35	9.03			
2-0441b-F3	177337	182788	20.11	1	-107.89	-111.89	DOV			12.33	11.98	11.85	11.99	12.23	12.16	11.87	11.65	11.73	12.19	12.80	12.84	12.75	12.43			
2-0777-F3	171911	172554	23.72	3	-67.28	-72.28	DOV										7.85	7.50	6.56	5.65	3.73	1.18	0.51	-0.14		
2-0777-F2	171911	172554	23.72	1	-13.28	-18.28	DOV										25.21	25.34	25.36	25.35	25.55	25.48	25.10	24.99		
2-0049-F1	189325	165770	46.19	2	1.19	-2.81	DOV																			
2-0103-F1	184343	179654	28.58	3	-165.42	-185.42	DOV	12.28	12.27	12.34	12.48	12.59	12.75	12.88	13.09	13.54	13.86	13.94	14.12	13.95	13.69	13.27	12.74			
2-0106-F1	194595	178441	57.91	3	-139.09	-151.09	DOV	13.41	13.46	13.63	13.82	14.20	14.37	14.26	14.60	15.11	15.05	15.12	15.16	14.83	14.39	13.81	13.41			
2-0113-F2	186590	162370	69.63	2	28.63	26.63	DOV	51.19	51.04	50.97	51.04	51.21	51.01	51.02	51.14	51.04	51.10	51.11	51.13	51.19	50.98	50.90	50.81			

2-0124-F1	194611	168000	35.25	2	-17.25	-22.25	DOV	28.27	28.27	28.28	28.69	29.49	29.82	30.28	30.35	30.70	29.95	31.18	30.44	30.62	30.11	30.23	29.94			
2-0123-F2	194610	168000	35.25	2	15.25	5.25	DOV	32.48	32.40	32.50	32.59	32.75	32.55	32.56	32.71	32.83	32.70	32.77	32.66	32.93	32.48	32.44	32.40			
621-76-1-F2	190302	160183	75.80	1	63.80	62.80	DOV	67.57	67.18	66.94	66.92	67.42	67.31	66.92	67.03	67.18	67.40	67.08	67.39	67.56	67.08	66.51				
621-76-1-F3	190302	160183	75.80	2	57.80	56.80	DOV	67.84	67.41	67.07	66.96	67.34	67.29	66.92	66.87	67.07	67.25	67.06	67.31	67.55	67.14	66.81				
621-76-3-F2	194019	163847	62.47	2	49.47	48.47	DOV	51.01	50.42	50.02	49.85	50.32	50.34	49.80	50.39	49.84	50.11	50.20	50.34	50.61	50.10	50.02				
621-76-3-F3	194019	163847	62.47	2	45.97	44.97	DOV	50.42	50.09	49.65	49.57	50.00	49.97	49.61	50.02	49.80	49.95	49.93	50.05	50.28	49.77	49.78				
621-76-4-F3	193667	163532	62.65	2	48.05	47.05	DOV	52.92	52.52	52.09	52.00	52.35	52.26	52.89	52.20	52.00	52.10	52.07	52.25	52.45	52.09	52.03				
622-71-11-F3	188319	160811	73.21	2	50.21	49.21	DOV	56.00	55.93	55.82	55.85	56.15	55.94	55.82	55.86	55.85	56.03	56.10	56.22	56.25	55.91	55.82				
622-71-7-F2	183831	164618	76.24	1	61.74	61.24	DOV	67.72	67.34	67.21	67.10	67.07	67.03	66.65	66.77	66.93	66.91	66.94	66.90	67.02	66.79	66.85				
622-71-7-F3	183831	164618	76.24	1	57.24	56.24	DOV	67.71	67.34	67.21	67.12	67.10	67.02	66.66	66.66	66.95	66.91	66.93	66.91	67.02	66.52	66.87				
622-71-8-F3	184942	166222	69.76	1	53.76	52.76	DOV	60.77	60.65	60.34	60.31	60.48	60.29	59.99	59.65	60.65	60.31	60.23	60.33	59.95	59.90	59.60				
622-76-2-F3	189694	161876	69.20	2	51.20	50.20	DOV	61.01	61.02	61.00	60.86	61.32	61.31	60.97	60.90	60.76	61.27	61.77	61.52	61.72	61.06	60.88				
622-76-3-F1	190269	162620	74.46	1	68.96	67.96	DOV	70.40	69.26	68.73	68.51	68.43											68.43			
622-76-3-F2	190269	162620	74.46	1	63.96	62.96	DOV	67.84	67.65	67.05	66.97	67.30	67.02	66.52	66.48	66.46	66.61	66.30	66.44	66.84	66.64	66.37				
622-76-3-F3	190269	162620	74.46	1	55.96	54.96	DOV	67.82	67.55	67.03	66.94	67.27	67.00	66.53	66.40	66.42	66.64	66.28	66.43	66.83	66.63	66.36				
622-76-3-F4	190269	162620	74.46	1	50.96	49.96	DOV	67.70	67.45	66.90	66.79	67.13	66.86	66.39	66.30	66.28	66.45	66.15	66.33	66.73	66.50	66.23				
622-76-4-F1	189824	163464	63.94	1	57.94	56.94	DOV	59.99	59.03	59.17	59.01	59.55	59.78	58.80	58.56	58.73	59.17	59.04	59.19	59.74	58.67	59.12				
622-76-4-F2	189824	163464	63.94	1	53.94	52.94	DOV	59.98	59.47	59.16	59.21	60.00	59.73	58.77	58.74	58.67	59.08	58.99	59.15	59.69	58.64	59.05				
622-76-4-F3	189824	163464	63.94	1	49.94	48.94	DOV	59.89	59.38	59.00	59.11	59.40	59.62	58.67	58.65	58.62	58.98	58.49	59.07	59.59	58.56	58.95				
622-76-4-F4	189824	163464	63.94	1	45.94	44.94	DOV	59.78	59.30	58.90	59.00	59.31	59.52	58.59	58.56	58.56	58.96	58.81	58.97	59.47	58.50	58.84				
622-76-6-F2	188956	164825	53.85	1	44.85	43.85	DOV	47.24	46.77	46.52	46.21	46.89	47.07	46.56	46.77	46.82	46.92	47.01	47.15	47.39	46.94	47.13				
622-76-6-F3	188956	164825	53.85	1	39.85	38.85	DOV	47.25	46.74	46.51	46.21	46.88	47.07	46.51	46.75	46.82	46.89	47.00	47.05	47.38	46.91	47.09				
622-76-6-F4	188956	164825	53.85	1	35.85	34.85	DOV	46.81	46.28	46.26	45.96	46.61	46.81	46.23	46.46	46.58	46.66	46.80	46.85	47.16	46.60	46.75				
622-76-6-F1	188956	164825	53.85	1	47.85	46.85	DOV	47.23	46.83			46.89						47.12	47.00	47.32		46.93	47.13			
623-76-17-F2	193447	168551	49.60	1	26.60	25.60	DOV	38.68	38.32	37.67	37.94	38.64	38.99	38.85	39.39	39.39	39.70	39.45	39.75	40.31	38.96	39.71				
623-76-17-F3	193447	168551	49.60	1	23.60	22.60	DOV	37.03	36.76	36.34	36.09	37.08	37.02	35.91	37.21	37.22	37.45	37.23	37.58	37.95	36.87	37.41				
623-76-2-F2	192173	162962	66.09	1	52.59	51.59	DOV	59.47	59.11	58.56	58.66	59.01	58.80	55.79	58.65	58.61	58.77	58.68	58.84	59.05	58.62	58.56				
623-76-2-F3	192173	162962	66.09	2	49.09	48.09	DOV	59.63	59.24	58.76	58.87	59.20	59.03	57.76	58.87	58.84	58.98	58.97	59.14	59.39	58.82	58.94				
623-76-4-F2	191896	164622	60.41	1	45.41	44.41	DOV	53.57	53.51	52.83	52.76	53.64	53.93	53.08	53.39	53.16	53.69	53.53	53.78	54.28	53.40	53.57				
623-76-4-F3	191896	164622	60.41	1	41.91	40.91	DOV	51.49	50.71	50.13	49.08	49.23	51.16	48.77	49.76	48.01	48.18	48.35	48.67	49.32	48.97	48.80				
623-76-4-F4	191896	164622	60.41	1,2	37.41	36.41	DOV	39.66	40.54	39.91	40.45	40.59	41.48	41.42	42.07	42.08	42.32	42.37	42.68	42.96	42.52	42.76				
623-76-5-F1	194159	165041	55.07	1	49.07	48.57	DOV	49.77	49.33			48.83	49.35	49.42		49.18		49.16	48.89	49.34	49.38	48.79				
623-76-5-F2	194159	165041	55.07	1	43.07	42.07	DOV	49.76	49.28	48.63	48.61	49.12	48.97	48.72	48.47	48.64	48.90	48.68	49.06	49.32	48.67	48.50				
623-76-5-F3	194159	165041	55.07	2	40.57	39.47	DOV	49.79	49.34	48.72	48.66	49.17	49.04	48.74	48.93	48.71	48.99	48.80	49.11	49.40	48.75	48.59				
623-76-8-F1	194812	166331	38.50	1,2	32.50	31.50	DOV	37.61	36.86	37.54	37.98	37.51		36.02	37.05	37.42	37.00	37.49	37.17	37.47	36.94	36.62				
623-76-8-F2	194812	166331	38.50	2	30.50	29.50	DOV	37.34	36.86	37.55	37.98	37.51		36.03	37.04	37.42	37.01	37.47	37.19	37.49	36.95	36.62				
2-0422a-F1	188763	177376	72.56	1	-34.44	-36.44	DOV		37.24	37.27	37.29	37.42	37.34	37.16	37.14	37.19	37.16	37.09	37.02	37.12	37.00	36.80	36.46			
2-0436a-F1	189271	190520	17.85	3	-291.15	-296.15	DOV				11.09	11.38	11.78	12.03	11.96	12.35	12.87	12.96	12.99	13.09	12.65	12.27	11.69	11.26		

2-0437a-F1	194146	163971	57.80	2	36.90	34.90	DOV			51.38	51.43	51.80	51.73	51.51	51.71	51.53	51.61	51.62	51.74	51.94	51.68	51.35	50.93						
2-0437a-F2	194146	163971	57.80	2	2.80	0.80	DOV			42.78	43.45	44.10	43.98	44.02	44.17	44.16	43.99	44.42	44.26	44.58	44.08	44.02	43.84						
2-0437a-F3	194146	163971	57.80	3	-8.20	-13.20	DOV			42.63	43.29	43.94	43.82	43.86	44.01	44.01	43.83	44.27	44.11	44.43	43.92	43.87	43.70						
2-0439a-F1	192918	171428	53.50	3	-74.50	-79.50	DOV			21.58	21.74	22.15	22.43	22.53	22.65	23.03	22.95	23.14	23.11	22.84	22.49	21.99	24.40						
2-0439b-F2	192922	171428	53.50	1	8.50	6.50	DOV			40.43	40.67	41.07	40.65	40.66	40.78	40.98	41.01	40.88	40.88	41.31	40.84	40.60	40.18						
2-0436c-F1	188312	189546	17.50	1	-171.00	-179.00	DOV							14.02	15.44	15.59	15.45	15.47	15.27	15.36	15.11	14.93	14.84						
3001-107-F1	183511	185746	13.80	3	-224.20	-239.20	DW													13.60	13.65	10.19	7.99	6.12	4.54	6.89			
3001-109-F3	183520	185738	14.29	1	-118.71	-123.71	DW													17.58	17.20	17.14	17.24	17.35	16.93				
3003-001-F0	187630	166169	46.02	1, 2	23.02	-18.48	DW	43.65	43.06	42.48	43.19	43.51	43.22	43.01	43.75	43.45	43.28	43.08	43.34	44.44	43.49	43.29	43.75	42.52					
3003-005-F1	187412	166283	49.25	2, 3	-1.25	-67.52	DW	44.71	44.23	43.91	43.76	44.74	44.30	44.34	44.72	44.54	44.77	44.87	45.17	45.66	45.06	44.66	46.17	44.55					
3003-006-F1	187621	166190	46.13	1, 2	23.19	-21.81	DW	43.58	42.98	42.38	43.10	43.43	43.08	42.91	43.59	43.36	43.20	43.23	43.26	44.39	43.43	43.23	44.15	42.41					
3003-015-F1	188825	164405	45.86	2	25.37	-0.13	DW	45.13	44.69	43.84	43.25	43.91	43.13	43.04	43.82	43.63	43.62	43.89	44.28	44.09	43.77	44.02	42.21	41.71					
3003-021-F2	188121	163861	47.18	2	33.43	29.43	DW	46.65	46.37	46.22	46.33	46.66	46.36	46.35	46.46	46.55	46.54	46.59	46.70	46.82	46.60	46.38	46.15	46.05					
3003-022-F2	189678	165613	44.23	1, 2	26.83	21.83	DW	38.49	38.02	37.57	38.11	38.70	39.10	39.68	40.42	40.62	40.82	40.97	41.16	41.42	41.00	40.94	40.84	40.90					
3003-037-F2	186902	166281	48.58	1	28.58	23.58	DW			46.99	47.23	47.85	47.63	46.61	46.82	47.27	47.95	47.74	47.30	47.92	47.77	46.25	47.62	46.37					
3003-038-F2	187335	166300	48.83	1	28.83	23.83	DW			43.80	44.21	45.00	44.49	44.55	44.89	44.54	44.53	44.46	44.62	45.58	44.70	44.30	45.80	44.21					
3003-039-F2	186541	166265	54.98	1	34.48	29.48	DW			51.35	51.47	51.64	51.53	51.29	51.32	51.47	51.66	51.66	51.73	51.99	51.81	51.43	51.47	51.25					
3003-040-F2	187391	165811	50.71	1	30.71	25.71	DW			45.91	46.76	47.07	46.69	46.55	46.83	47.03	46.94	46.94	47.07	47.66	46.93	46.73	46.67	46.27					
3006-159-F1	173862	172721	24.89	1	-15.11	-20.11	DW												28.14	28.17	28.17	28.59	28.62	28.07	28.05	27.68			
3006-159-F2	173862	172721	24.89	3	-74.11	-79.11	DW												1.35	-0.20	-0.86	-7.57	-11.08	-11.53	-12.18	-11.60			
3007-038-F2	176189	175999	25.44	1	-39.57	-44.57	DW												22.47	22.34	22.79	23.65	23.90	23.48	23.66	23.37			
3007-038-F3	176189	175999	25.44	3	-111.50	-115.50	DW												-7.86	-11.38	-10.14	-9.91	-15.59	-16.31	-15.83	-17.07			
3008-044-F1	171491	172669	25.18	3	-67.00	-92.22	DW	4.07	3.68	4.38	3.60	5.22	6.43	6.77					25.28	25.34	25.36	25.35	25.55	25.48	25.07	25.12	24.83		
3008-058-F2	171911	172554	23.72	1	-13.28	-18.28	DW												7.82	7.50	6.56	5.64	3.72	1.10	0.53	-0.07	4.23		
3008-058-F3	171911	172554	23.72	3	-67.28	-72.28	DW																26.98	26.87	25.12	24.83			
3008-065-F3	169282	169688	27.35	1	-1.65	-5.65	DW																25.69	25.75	25.71	25.57			
3008-066-F3	170086	171028	23.86	1	-9.14	-14.14	DW																						
3010-003-F1	163285	163497	51.79	2, 3	2.89	-15.61	DW	43.51	42.28	42.18	42.36	42.51							41.37	41.11	41.60	41.08	41.07	41.01	41.12	40.63			
3010-011-F1	163290	163508	51.50	1	29.85	20.85	DW	50.32	50.06	50.03	50.06	49.94	49.57	49.62	49.66	49.74	49.89	49.77	49.72	49.67	49.67	49.59	49.39	49.04					
3010-016-F2	163028	164542	59.28	1	19.28	14.28	DW												48.62	50.22	50.23	49.83	49.80	49.96	49.75	47.88	47.40		
3010-016-F3	163028	164542	59.28	3	-8.72	-13.72	DW												30.37	32.76	32.62	30.30	32.88	33.12	32.33	34.83	34.59		
3010-017-F0	163013	164525	59.42	2, 3	6.91	-23.09	DW													33.24	33.33	36.59	36.74	33.75	37.61				
3011-006-F2	163583	160581	50.42	3	18.42	10.42	DW	37.14	36.84	37.44	37.46	36.72	35.33	35.46	35.34	35.50	35.81	36.76	35.59	35.65	35.29	34.86	35.21	34.96					
3011-007-F2	163555	160607	52.25	2	27.25	26.25	DW	45.22	45.00	45.33	45.39	45.23	44.82	44.88	44.76	44.97	44.95	45.12	44.72	44.86	44.62	44.34	44.26	44.30					
3011-007-F3	163555	160607	52.25	3	17.25	7.25	DW	36.67	36.37	36.95	36.99	36.36	35.34	35.48	35.32	35.54	35.85	36.80	35.63	35.70	35.34	34.92	35.25	35.01					
3011-014-F1	164742	160610	39.15	3	16.15	-8.85	DW	35.52	35.18	35.78	35.67	35.43	34.93	35.07	34.95	35.24	35.47	35.94	35.43	35.56									
3011-017-F1	162590	157535	46.79	3	24.79	4.79	DW	44.06	43.79	45.74	46.21	46.48	46.09	46.13	45.97	46.42													
3011-023-F2	164979	160933	39.09	3	19.09	14.09	DW			35.74	35.81	35.67	35.06	35.30	35.13	35.32	35.52	35.77	35.39	35.56	35.16	34.74	34.73	34.77					
3011-024-F2	164171	160305	42.34	3	22.34	17.34	DW			38.23	38.36	38.15	37.69	37.72	37.62	37.94	38.12	38.39	37.97	38.10	37.79	37.48	37.42	37.55					
3012-004-F1	169109	162050	32.79	3	8.75	-1.25	DW	32.14	32.19	32.49	32.18	32.39	31.82	31.84	32.00	32.37	32.62	32.27	32.10	32.41	31.85	31.54	31.05	31.22					

3012-017-F2	169628	162184	33.37	3	15.87	14.87	DW	32.22	32.46	32.59	32.43	32.58	32.06	32.11	32.24	32.32		32.70	32.48	32.85	32.34	31.97	31.34	31.40	
3012-019-F1	169607	161869	32.03	3	20.00	-5.00	DW	30.89	31.09	31.25	31.22	31.22	31.12	31.10	31.16	31.25	31.27	31.22	31.19	31.21	31.14	30.94	31.15	31.34	
3012-022-F1	170691	159619	36.95	3	25.00	2.50	DW	35.09	34.87	34.74	36.26	36.10	34.88	34.27	34.92	34.78	34.97	34.73	34.88	35.15	34.25	33.53	32.39	32.25	
3012-023-F1	170501	159530	35.91	3	25.00	2.50	DW	35.94	35.74	35.68	36.85	35.64										35.29	34.65	33.45	33.37
3012-024-F1	168789	164064	30.40	2, 3	5.40	-2.40	DW	29.95	29.77	30.23	29.99	30.28	29.63	29.60	29.74	29.81	29.96	29.91	29.59	29.95	29.18	28.90	28.70	29.23	
3012-025-F1	168265	167279	31.10	2	-4.59	-9.59	DW	30.97	30.91	30.96	30.91	30.97	30.87	30.91	30.93	30.98	30.93	30.95	30.84	30.97	30.76	30.64	31.96	32.06	
3012-025-F2	168265	167279	31.10	2, 3	-20.59	-29.59	DW	28.93	29.00	29.77	28.75	28.94	28.17	28.27	28.31	28.05	27.87	28.08	27.35	27.88	26.78	26.50	25.95	25.70	
3012-056-F1	168500	161410	50.48	2	25.48	23.48	DW			33.55	33.45	33.61	33.00	32.95	33.05	33.29	33.39	33.22	33.16	33.38	32.72	32.41	31.71	31.74	
3012-056-F2	168500	161410	50.48	3	13.48	11.48	DW			33.26	33.13	33.33	32.69	32.66	32.78	33.00	33.19	33.01	32.94	33.24	32.54	32.22	31.49	31.51	
3012-057-F2	167689	161354	88.07	2	30.07	28.07	DW			63.05	62.93	62.92	62.92	62.79	62.80	62.84	62.88	62.87	62.74	62.75	62.91	62.62	62.45	62.33	
3012-057-F3	167689	161354	88.07	3	17.00	15.00	DW			34.39	34.27	34.33	33.80	33.87	33.88	34.06	34.18	34.19	33.85	34.19	33.61	33.25	32.92	33.15	
3012-058-F2	168496	165012	31.76	2	0.26	-1.74	DW			29.49	29.46	29.62	29.41	29.53	29.49	29.73	29.54	29.54	29.37	29.60			29.37	29.21	
3012-058-F3	168496	165012	31.76	3	-11.74	-16.74	DW			30.48	29.88	30.01	29.32	29.53	29.44	29.28	29.40	29.52	28.93	29.53			27.77	29.03	
3014-003-F0	153147	177510	13.86	1, 2, 3	-70.67	-114.64	DW	-10.14	-4.50	-2.98	-1.15	1.24	2.46	3.60	4.38	2.60	6.05	7.54	7.81	8.42	8.81	8.97	8.86	8.54	
3014-004-F0	153662	178449	13.31	3	-102.49	-131.69	DW															8.93	8.94	8.57	
3014-005-F2	153647	178466	13.27	1	-73.73	-78.73	DW															10.87	10.95		
3019-012-F0	179310	163234	85.31	3	20.70	7.20	DW	20.88	16.94	17.16	17.49	17.21	22.38	23.49	24.08	22.51									
3019-041-F0	178981	163150	85.75	2, 3	22.91	7.91	DW	77.19	47.91	48.00	47.69	51.76													
3020-002-F1	174109	158551	0.00	3	44.93	44.93	DW	43.98	43.98	43.97	44.01	44.00	43.98	43.97	43.98	43.95	43.92	43.97	44.02	43.94	43.92	43.97	43.97	43.97	
3023-013-F1	158337	162091	64.87	1	34.75	32.75	DW									63.32		62.44	63.77	62.85	62.65	62.47	62.44	63.05	63.88
3023-014-F1	158263	162164	68.55	1	30.55	28.55	DW									62.26		61.34	61.84	60.66	60.60	60.55	60.77	61.76	63.07
3001-108-F0	183464	185677	18.63	3	-218.60	-257.77	DW_prod												14.78	15.02	-1.20	-9.48	-14.92	-16.26	-11.58
3003-002-F0	186897	166310	50.32	1, 2	45.77	-22.48	DW_prod	43.26	48.02	45.69	42.15	42.19	42.20	41.29	40.41	35.85	38.29	36.05	39.42	36.50	34.45	34.51	42.71	38.08	
3003-003-F0	187318	166293	48.76	1, 2	24.96	-16.84	DW_prod	37.54	36.26	36.95	39.66	38.90	39.24	39.33	40.16	39.35	39.21	38.25	37.92	40.33	39.94	39.32	43.44	39.22	
3003-004-F0	187636	166182	46.25	2	18.18	-15.82	DW_prod	37.83	36.10	34.01	37.71	41.79	40.09	39.24	40.14				36.55	35.31	38.81	37.41	35.99	40.24	35.61
3003-016-F0	188502	164399	46.89	2	23.79	7.79	DW_prod	39.73	38.22	36.90	37.79	40.47	40.41	40.24	41.03	39.86	39.52	39.83	41.38	41.29	41.99	40.96	42.41	44.68	
3003-017-F0	189094	164694	45.02	2	23.02	7.02	DW_prod	41.17	39.58	39.93	41.83	41.90				41.82	42.54	42.48	42.73	43.09	43.56	43.65	42.91	41.83	41.45
3003-018-F0	189358	164835	44.90	2	22.65	4.65	DW_prod	37.40	36.05	35.29	36.38	37.77	36.39	35.87	37.88	39.30	39.44	40.65	40.54	42.90	42.75	40.61	40.32	37.70	
3003-028-F0	188821	164404	45.22	2	24.46	7.56	DW_prod	45.15	44.71	42.75	40.54	41.36	40.29	39.69	40.56	39.49	39.45	39.34	40.79	39.52	39.52	41.23	34.66	32.87	
3003-029-F0	186893	166240	47.76	1, 2	27.76	-2.24	DW_prod	45.65	43.45	43.17	45.94	46.64	45.76	44.18	43.28	46.89	47.24	47.82	45.52	47.23	48.76	43.53	46.13	44.24	
3003-041-F0	188397	164498	47.71	2	21.71	8.71	DW_prod									45.78	44.21	43.22	43.05	42.83	43.61	41.19	40.43		
3006-001-F0	173644	172757	24.84	3	-73.71	-100.76	DW_prod	-39.86	-42.20	-42.51	-42.74	-40.12	-35.00	-36.04	-35.59	-34.96	-35.56	-41.07	-43.71	-42.93	-46.87	-45.53	-46.29	-38.95	
3006-116-F0	174276	172561	28.50	3	-72.50	-101.50	DW_prod	-2.32	-2.58	-2.46	-2.97	-1.03	0.97	1.01	2.48	3.92	3.18	2.04	-0.41	-29.38	-36.38	-36.95	-36.91		
3007-001-F0	176177	175954	25.64	3	-116.36	-152.36	DW_prod	-21.38	-10.19	-47.32	-42.02	-33.39	-41.77	-43.62	-26.90	-34.49	-33.48	-48.39	-47.82	-40.89	-49.82	-49.79	-46.62	-45.53	
3008-001-F0	169223	169076	27.77	2, 3	-39.68	-79.68	DW_prod	16.23	13.82	16.23	12.26	13.39	10.55	9.04	9.32	7.07	7.01	8.56	1.86	5.60	0.63	0.25	-1.07	-2.78	
3008-002-F0	169373	170207	26.72	3	-47.78	-82.78	DW_prod	17.13	16.29	19.79	12.09	12.41	8.41	3.93	7.46	0.63	-1.76	-3.01	-7.58	-8.20	-13.38	-15.27	-18.45	-19.81	
3008-003-F0	169696	170670	25.74	2, 3	-49.26	-84.26	DW_prod	16.92	16.38	18.64	12.95	12.19	9.11	5.16	7.30	2.94	0.89	-2.73	-6.48	-5.72	-14.43	-13.21	-15.10	-13.55	
3008-004-F0	170091	171033	24.01	2, 3	-51.99	-84.99	DW_prod	16.59	16.08	18.24	14.20	14.53	12.21	9.62	11.67	8.50	7.62	4.47	1.58	3.17	-2.84	-2.63	-5.06	-5.18	
3008-005-F0	169298	169638	27.14	2, 3	-40.36	-90.83	DW_prod	18.38	14.13	10.67	1.70	6.23	1.31	3.78	6.50	0.04	0.18	0.04	-9.73	-4.08	-7.58	-10.54	-11.56	-6.80	
3008-006-F0	169280	169513	27.13	2, 3	-37.87	-83.67	DW_prod	7.83	7.53	5.24	-4.52	2.12	3.09	1.11	2.72	1.84	1.44	-2.66	-5.98	-3.14	-7.39	-7.89	-11.94	-10.05	

3008-063-F0	169298	169655	27.07	3	-44.23	-85.23	DW_prod														-1.40	-2.86	-4.51	-13.55		
3008-064-F0	169259	169286	25.68	2,3	-42.32	-76.32	DW_prod														-0.69			-9.76		
3010-001-F0	163296	163523	51.74	3	-2.10	-15.10	DW_prod	30.85	28.91	28.05	29.37	26.92	21.61	19.30	20.51	19.18	21.26	23.04	23.69	21.64	21.16	20.73	24.20	22.41		
3010-002-F0	163288	163514	51.56	2,3	-0.24	-14.24	DW_prod	31.78	29.96	28.35	28.46	27.86	22.43	23.63	23.66	23.42	25.22	25.52	27.21	25.39	25.03	24.65	27.08	25.19		
3010-006-F0	162999	164519	59.90	2,3	10.50	-21.11	DW_prod	43.10	42.84	42.53		39.23	39.14	39.07	38.91	40.10	46.98	46.21	44.97	45.56	48.20	48.18	47.51	47.80		
3010-018-F0	163340	164438	61.61	2,3	8.61	-21.39	DW_prod													47.44	47.59	47.22	41.58	42.22		
3011-005-F0	163610	160562	49.29	3	17.50	-18.50	DW_prod	36.58	36.27	36.88	36.90	36.12	35.19	35.32	35.22	35.36	35.78	36.85	35.40	35.41	35.13	34.71	35.07	34.76		
3011-008-F0	164745	160598	39.47	3	15.57	-12.03	DW_prod	34.53	34.15	34.79	34.64	34.34	33.83	33.94	33.89	34.04	34.37	33.19	32.66	32.90	32.47	31.95	31.87	31.93		
3011-009-F0	164746	160626	38.87	3	13.36	-9.14	DW_prod	35.60	35.26	35.83	35.76	35.52	35.01	35.15	35.04	35.26	36.10	35.37	35.09	35.16	34.82	34.37	34.42	34.50		
3011-015-F0	162580	157540	46.79	3	23.98	7.98	DW_prod	45.73	45.47	47.24		46.28	45.78	45.86	45.67	46.15										
3012-001-F0	168889	162233	33.86	3	12.86	-18.14	DW_prod	27.08	27.02	27.50	27.20	27.43	27.42	27.49	26.90	26.87	27.69	27.16	26.93	27.17	26.73	26.92	25.59	23.94		
3012-002-F0	168936	162225	33.58	3	15.68	-14.82	DW_prod	25.89	25.52	25.72	25.57	24.93	23.18	24.42	25.07	25.24	26.15	25.78	25.38	26.61	27.04	26.37	29.62	26.24		
3012-003-F0	168845	162230	37.73	3	14.13	-8.67	DW_prod	31.61	31.51	31.99	31.52	31.80	31.11	31.11	31.13	31.78	31.60	31.61	31.36	31.73	30.96	30.86	30.66	30.54		
3012-007-F0	168840	165086	30.27	2,3	-5.03	-42.03	DW_prod	26.73	26.64	27.44	26.25	26.15	24.91	27.14	27.55	27.56	27.12	27.15	26.59	27.94	26.82	26.57	28.03	30.54		
3012-008-F0	168789	165194	29.35	3	-11.95	-42.65	DW_prod	25.50	25.78	26.66	25.32	25.12	24.59	24.28	24.07	23.83	23.76	24.22	23.23	23.62	22.62	22.15	21.63			
3012-009-F0	168758	165170	29.02	3	-18.98	-47.98	DW_prod	27.10	27.08	27.66	26.59	26.49	26.04	26.26	25.81	25.73	25.47	25.59	25.32	26.36	25.34	25.26	26.50	27.95		
3012-013-F0	169674	161619	33.23	3	16.98	-3.02	DW_prod	32.18	32.30	32.48	32.33	32.52	31.94	31.94	32.20	32.72	32.87	32.51	32.21	32.59	31.96	31.62	31.01	30.93		
3012-014-F0	169638	162007	32.69	2,3	20.70	-6.30	DW_prod	32.02	32.16	32.29	32.14	32.37	31.74	31.83	31.92	31.62	32.70	32.71	32.37	32.90	32.10	31.82	31.20	31.33		
3012-015-F0	169627	161898	32.21	3	11.22	-10.78	DW_prod	30.54	30.64	30.88	30.77	30.82	30.39	30.49	30.72	30.82	31.61	31.70	30.95	31.34	30.57	30.12	29.47	29.88		
3012-016-F0	169676	161752	32.65	3	17.06	-8.84	DW_prod	31.87	31.98	32.24	32.22	32.31	31.79	31.86	31.97	32.26	32.69	32.66	32.27	32.85	32.08	31.66	31.14	31.25		
3012-020-F0	170744	159698	38.01	3	19.51	-0.64	DW_prod	34.82	34.70	34.77	36.46	35.99	34.72	34.20	34.87	34.92	34.90	34.82	34.99	35.20	34.31	33.50	32.23	32.07		
3012-021-F0	170679	159623	37.10	3	20.80	6.80	DW_prod	34.68	34.40	33.75	35.68	35.79	34.44	33.75	33.46	33.61	33.97	33.60	33.71	33.95	33.05	32.34	31.42	31.20		
3012-059-F0	168918	162218	33.81	3	15.51	-13.69	DW_prod																26.14	25.57		
3013-001-F0	191027	167207	0.00	2,3	-29.77	-62.27	DW_prod	27.06	24.77			42.59							39.15							
3014-001-F0	153656	178455	12.08	3	-105.92	-128.62	DW_prod	-11.18	-5.02	-3.55	-1.63	0.80	1.80	2.94	3.69	1.46	5.31	6.90	7.54	8.22	8.15	8.41	8.39	8.18		
3017-001-F0	193675	160731	50.00	3	12.00	-29.40	DW_prod	46.99	46.85	46.84		47.70	47.58	47.59	47.69	47.53	47.48	47.72	47.76	47.90	47.48	47.33	47.18	47.09		
3019-013-F0	179303	163215	85.46	3	21.46	7.46	DW_prod	46.22	14.55	15.05	15.23	19.23	43.57	48.10	50.90	47.83										
3019-014-F0	179308	163204	85.41	3	19.91	5.91	DW_prod	26.30	17.55	17.93	17.96	18.59	28.59	29.90	30.48	28.52										
3020-001-F0	174072	158452	62.60	3	46.25	35.25	DW_prod	40.61	41.39	42.78	38.60	40.49	43.14	42.52	42.11	43.54	44.77	41.73	40.35	40.04	44.02	42.88	42.78	44.17		
3023-005-F0	158161	162137	66.43	1	20.50	12.50	DW_prod									57.41		49.29	51.78	47.15	46.42	48.32	50.08	53.04	56.00	
3023-006-F0	158270	162109	65.67	1	20.50	12.50	DW_prod									43.62		63.23	63.10	48.14	43.07	43.91	44.74	47.44	51.25	
3023-007-F0	158312	162159	66.40	1	20.50	12.50	DW_prod									49.59		56.54	57.92	49.60	51.03					
3023-008-F0	158263	162200	69.50	1	20.50	12.50	DW_prod									55.65		64.77	66.02	55.39	53.08	54.73	54.45	58.27	62.14	
3023-012-F1	158160	162154	67.79	1	30.79	28.79	DW_prod									65.02		63.32	63.19	62.03	61.89					
3023-024-F0	158312	162153	65.13	1	20.50	12.50	DW_prod																53.59	51.35	52.77	54.22

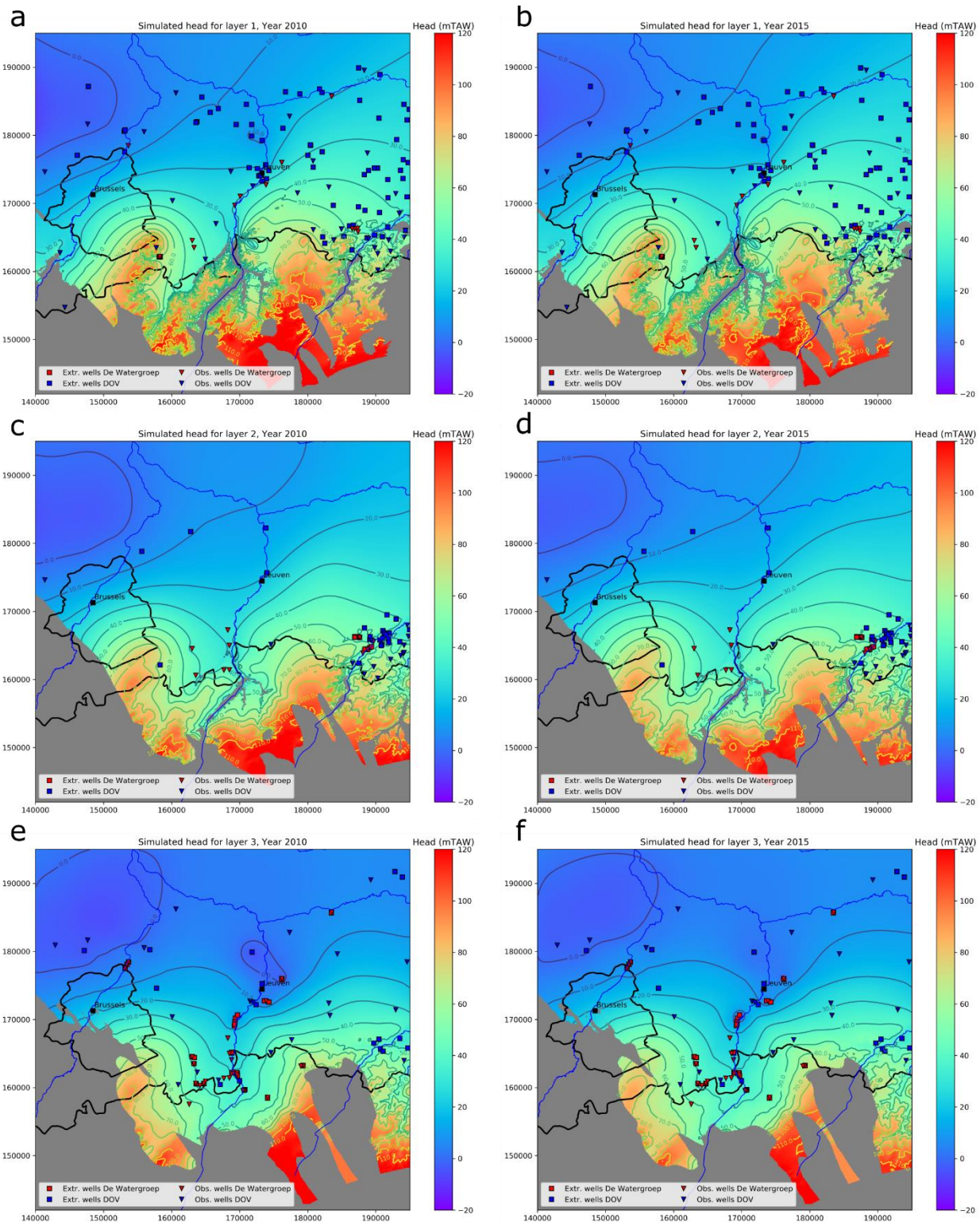


Figure I. 7: Simulated hydraulic heads for the year 2004 and 2020: (a) 2010, Grandglise; (b) 2015, Grandglise; (c) 2010, Lincent; (d) 2015, Lincent; (e) 2010, Cretaceous; and (f) 2015, Cretaceous.

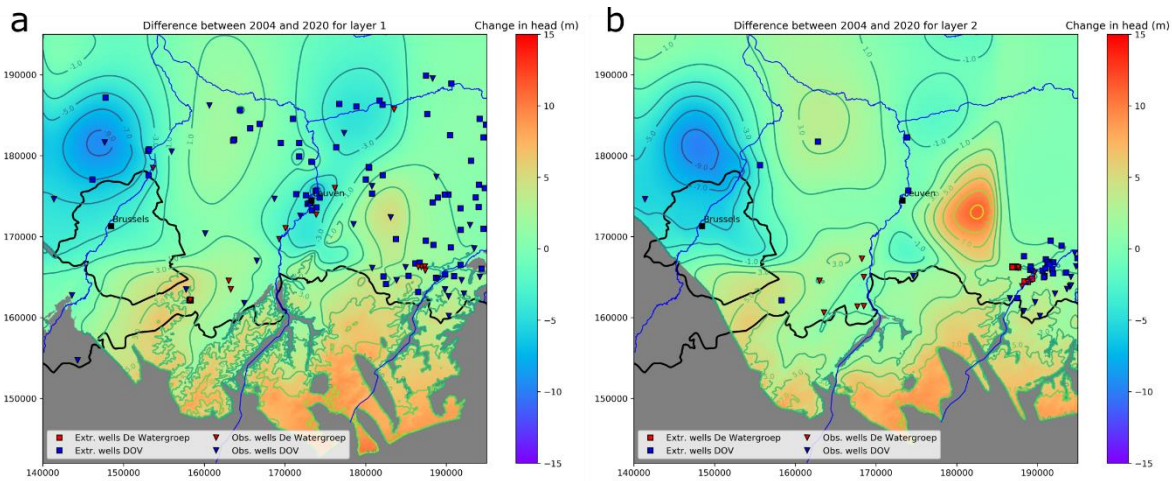


Figure I. 8: Difference in simulated head between the years 2004 and 2020 for: (a) Grandglaise; and (b) Lincent.

Table I. 23: Overview of model performance statistics for each modelled year for the transient model. n =# of wells; R^2 =coefficient of determination; RMSE=Root Mean Square Error; ME=Mean Error; MAE=Mean Absolute Error; PBIAS=% bias.

Year	n	R^2	RMSE	ME	MAE	PBIAS
2004	112	0.94	4.61	0.12	3.09	0.31
2005	113	0.94	4.65	-0.02	3.20	-0.05
2006	145	0.94	5.17	-0.01	3.51	-0.02
2007	144	0.94	5.01	-0.32	3.55	-0.90
2008	150	0.94	5.03	0.05	3.46	0.13
2009	142	0.94	5.11	-0.03	3.53	-0.09
2010	143	0.94	5.26	-0.12	3.63	-0.35
2011	150	0.93	5.21	0.00	3.64	0.00
2012	147	0.93	5.17	-0.10	3.69	-0.28
2013	160	0.94	5.07	0.90	3.81	2.53
2014	167	0.94	5.14	0.83	3.84	2.36
2015	166	0.94	5.07	0.65	3.84	1.87
2016	166	0.94	5.35	1.02	3.97	2.94
2017	168	0.94	5.37	0.40	3.99	1.18
2018	167	0.94	5.26	0.14	3.87	0.42
2019	137	0.93	5.69	-0.12	4.14	-0.42
2020	93	0.95	5.31	-0.68	3.80	-2.38
All	2470	0.94	5.16	0.21	3.70	0.59

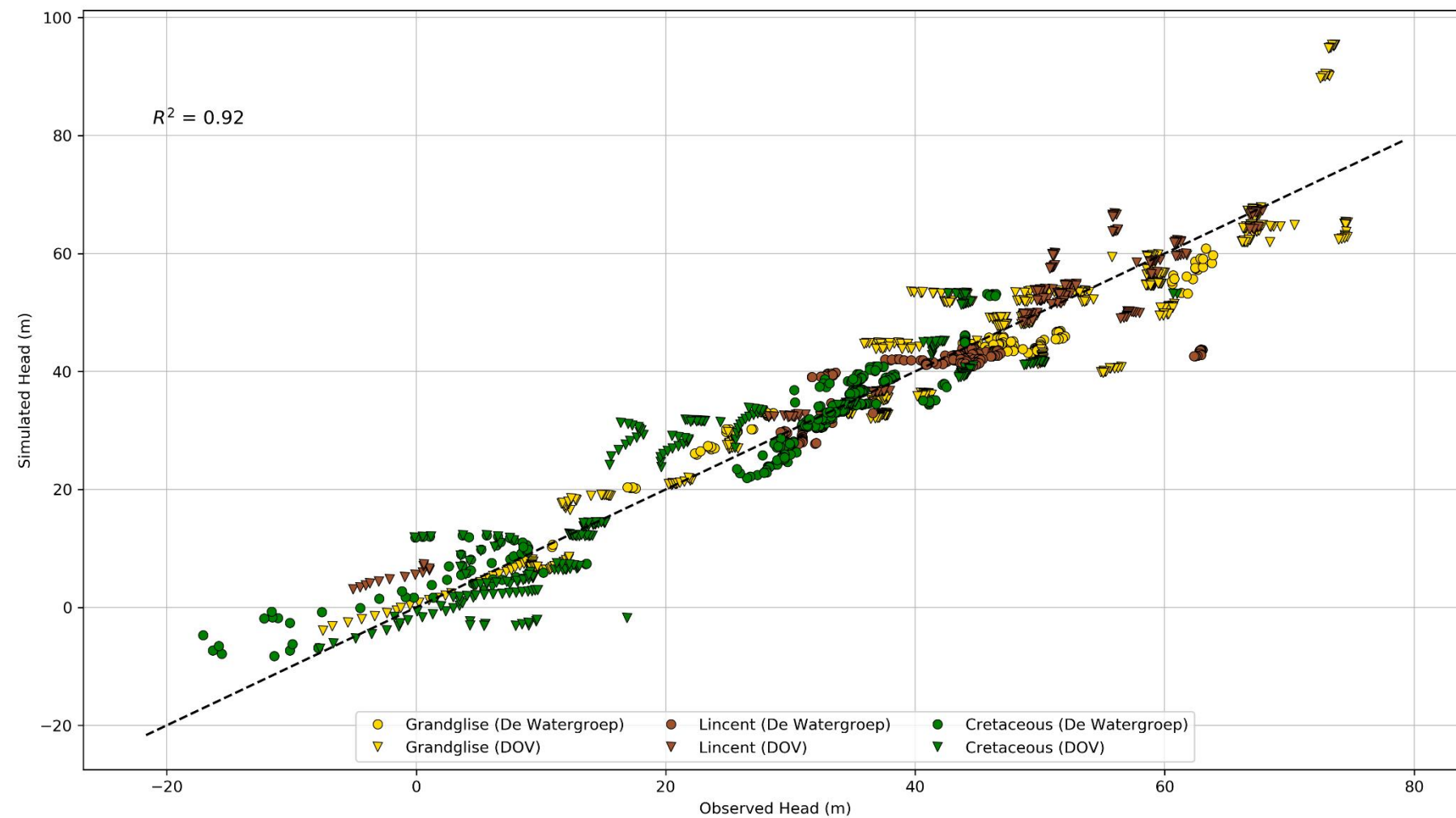


Figure I. 9: Scatterplot of simulated versus observed hydraulic heads without considering observations from extraction wells.

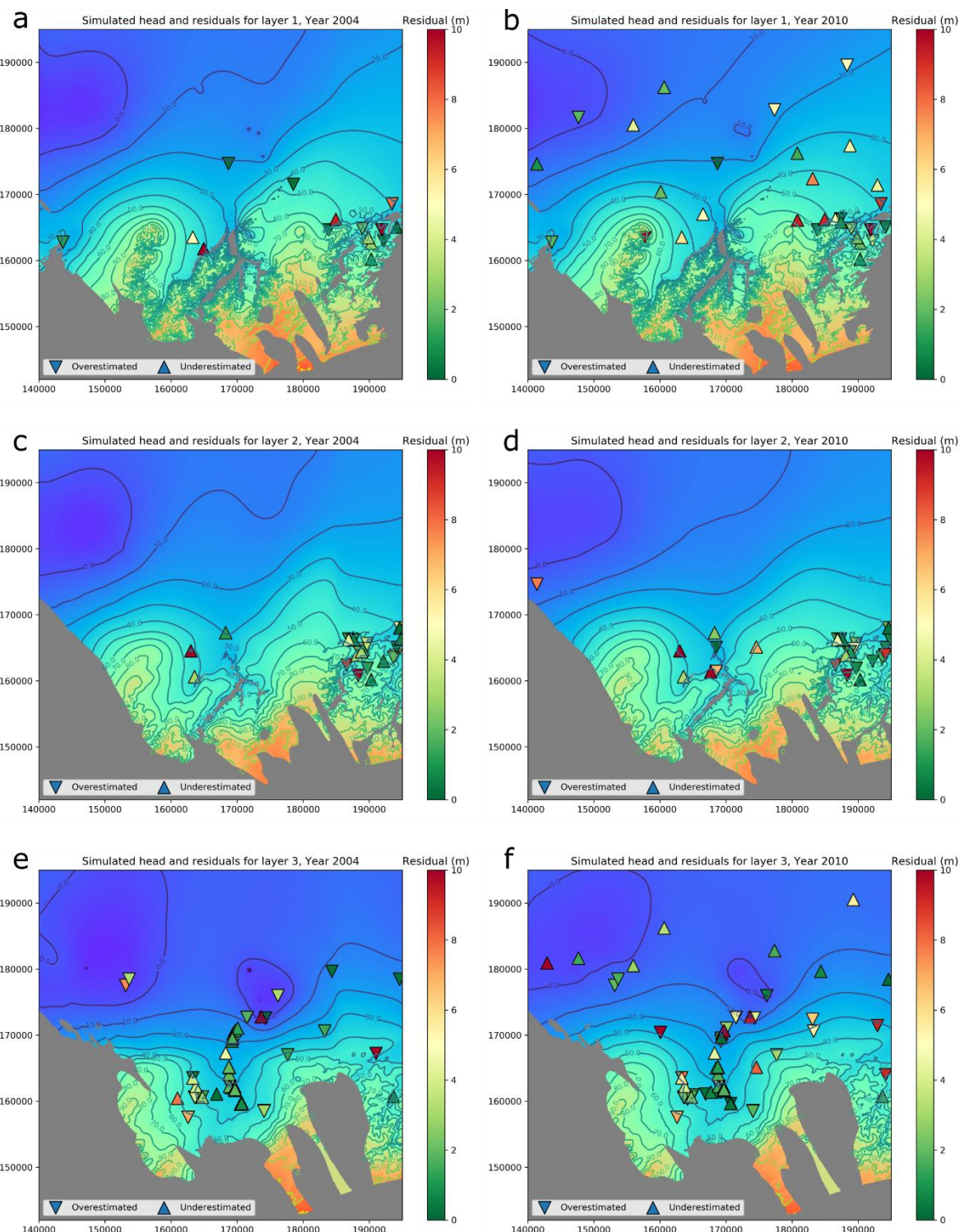


Figure I. 10: Model residuals for: (a) Grandglise, 2004; (b) Grandglise, 2010; (c) Lincent, 2004; (d) Lincent, 2010; (e) Cretaceous, 2004; and (f) Cretaceous, 2010.

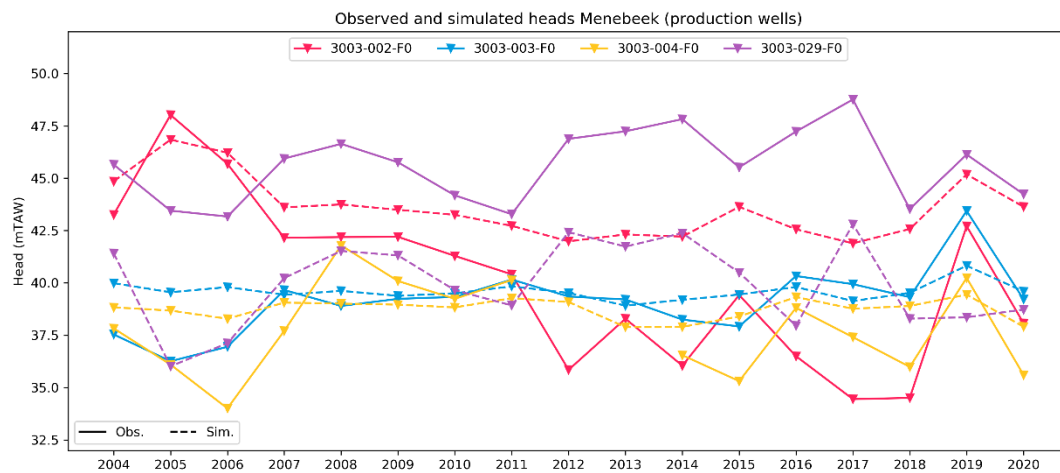


Figure I. 11: Observed and simulated heads versus time for the site of Menebeek (production wells).

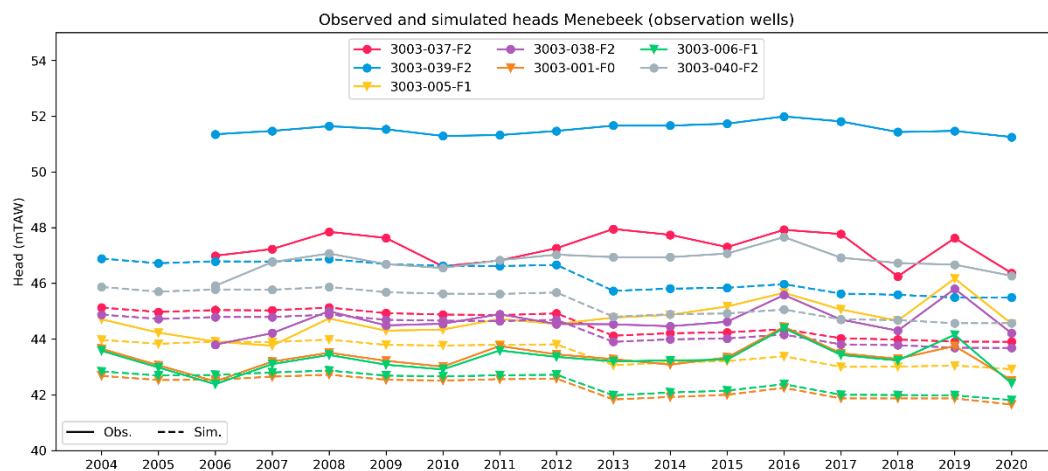


Figure I. 12: Observed and simulated heads versus time for the site of Menebeek (observation wells).

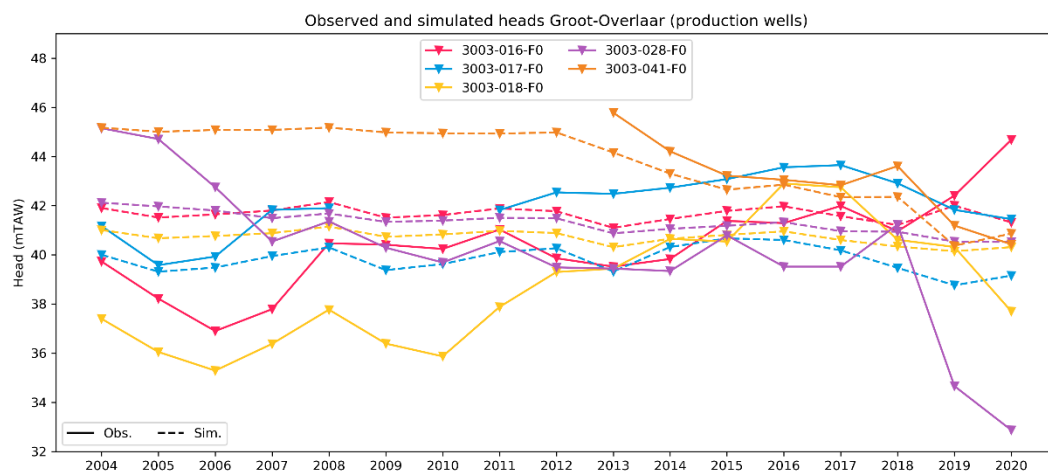


Figure I. 13: Observed and simulated heads versus time for the site of Groot-Overlaar (production wells).

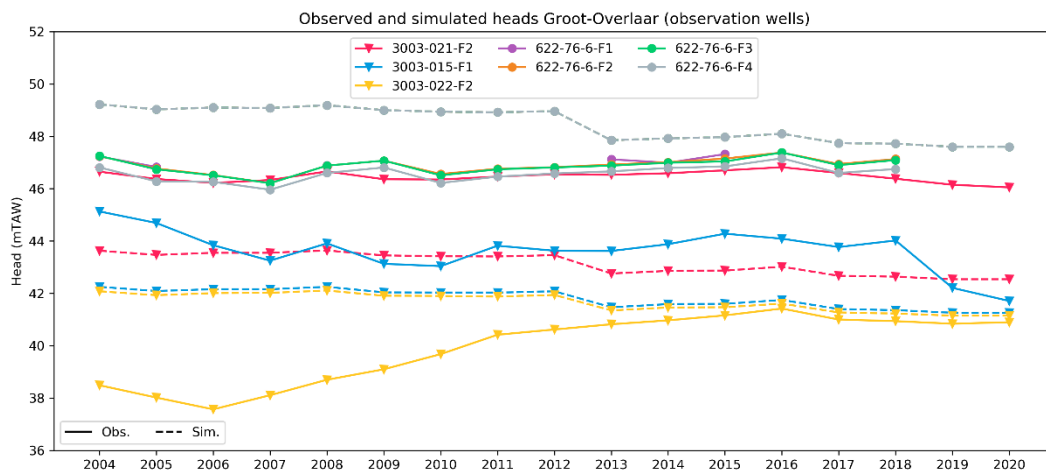


Figure I. 14: Observed and simulated heads versus time for the site of Groot-Overlaar (observation wells).

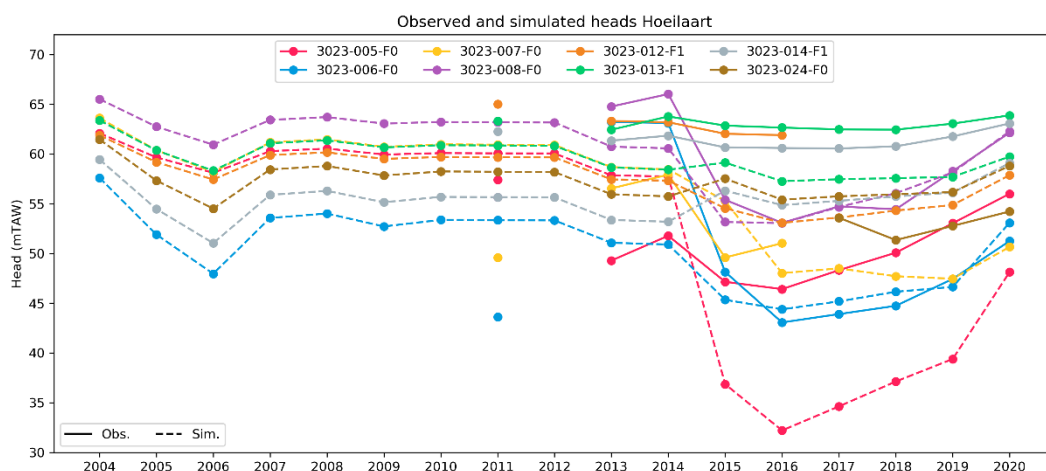


Figure I. 15: Observed and simulated heads versus time for the site of Hoeilaart.

Water Budget

Table I. 24: Overview of the fluxes in the water budget of the transient model for all stress periods.

Flow (in m ³ /d)	STORAGE	WELLS	HEAD	MNW2	TOTAL
2004	-15200	-17610	73861	-41053	-1
2005	-6790	-17352	64107	-39966	-1
2006	-9835	-17942	66064	-38288	0
2007	-8437	-15856	63165	-38871	0
2008	-13452	-14043	66443	-38950	-3
2009	-9143	-12354	63939	-42443	0
2010	-9811	-9456	60506	-41240	0
2011	-12491	-9793	61414	-39131	-1
2012	-12598	-9909	61422	-38916	-2
2013	20931	-8295	27084	-39724	-3
2014	-9271	-7716	55960	-38973	1
2015	-12869	-6743	61082	-41469	1
2016	-13131	-7250	60450	-40070	-1
2017	-4505	-7122	52994	-41367	-1
2018	-9542	-6959	60483	-43984	-2
2019	-8030	-6802	57855	-43025	-2
2020	-11281	-6785	60251	-42187	-3

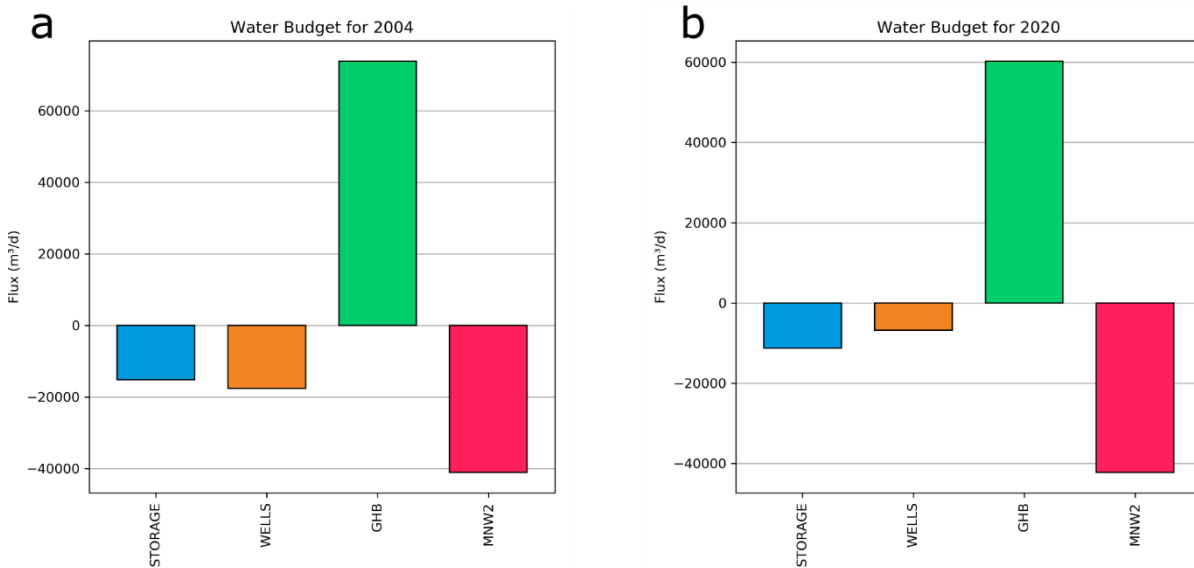


Figure I. 16: Water budget for: (a) the year 2004; and (b) the year 2020.

Table I. 25: Overview of the fluxes for the different components of the general-head boundary in the transient model.

Flow (in m ³ /d)	GHB_NORTH	GHB_WEST	GHB_EAST	GHB_KORTRIJK	GHB_RECH	GHB_TOTAL
2004	127	-1442	118075	1675	-44573	73862
2005	459	-1326	143467	1552	-80046	64107
2006	758	-1273	156101	1345	-90868	66063
2007	1034	-1240	174376	1385	-112392	63164
2008	1292	-1215	183169	1328	-118130	66444
2009	1537	-1058	183312	1377	-121227	63940
2010	1770	-924	187857	1500	-129697	60506
2011	1993	-798	184000	1494	-125275	61414
2012	2208	-681	180366	1435	-121907	61421
2013	2414	-573	275589	1777	-252123	27084
2014	2398	-543	281043	1734	-228672	55960
2015	2392	-505	277825	1615	-220246	61082
2016	2393	-471	278054	1778	-221304	60450
2017	2399	-425	295213	1580	-245774	52994
2018	2409	-384	298802	1503	-241847	60483
2019	2301	-438	306495	1437	-251941	57855
2020	2205	-484	306510	1427	-249407	60251

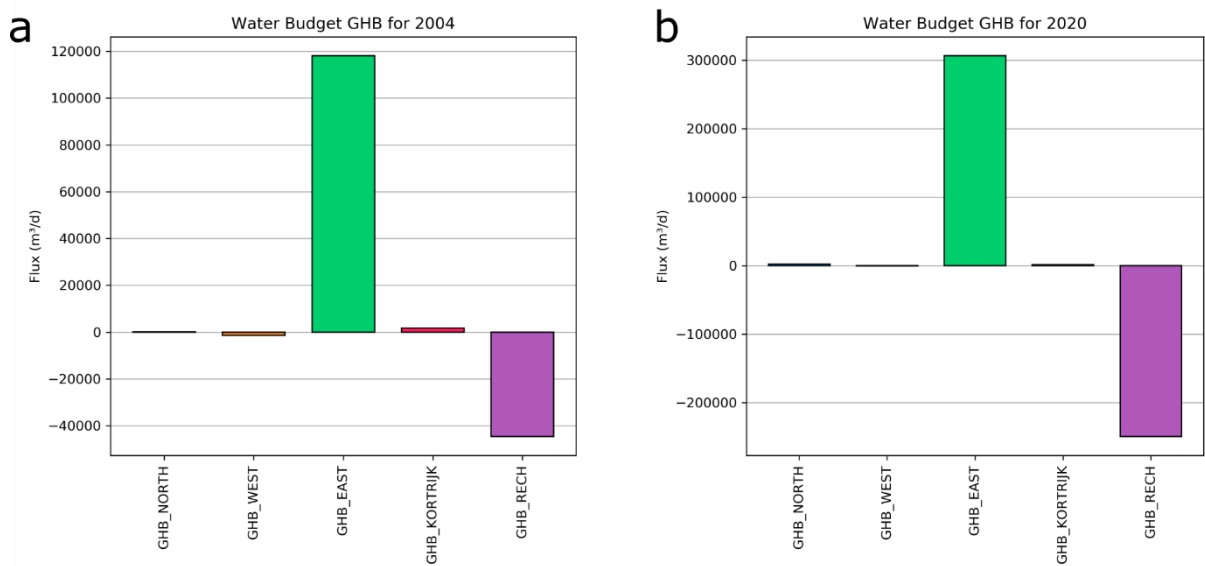


Figure I. 17: Water budget for the different components of general-head boundaries for: (a) the year 2004; and (b) the year 2020.

1.4 Scenario Analysis

Scenario 1

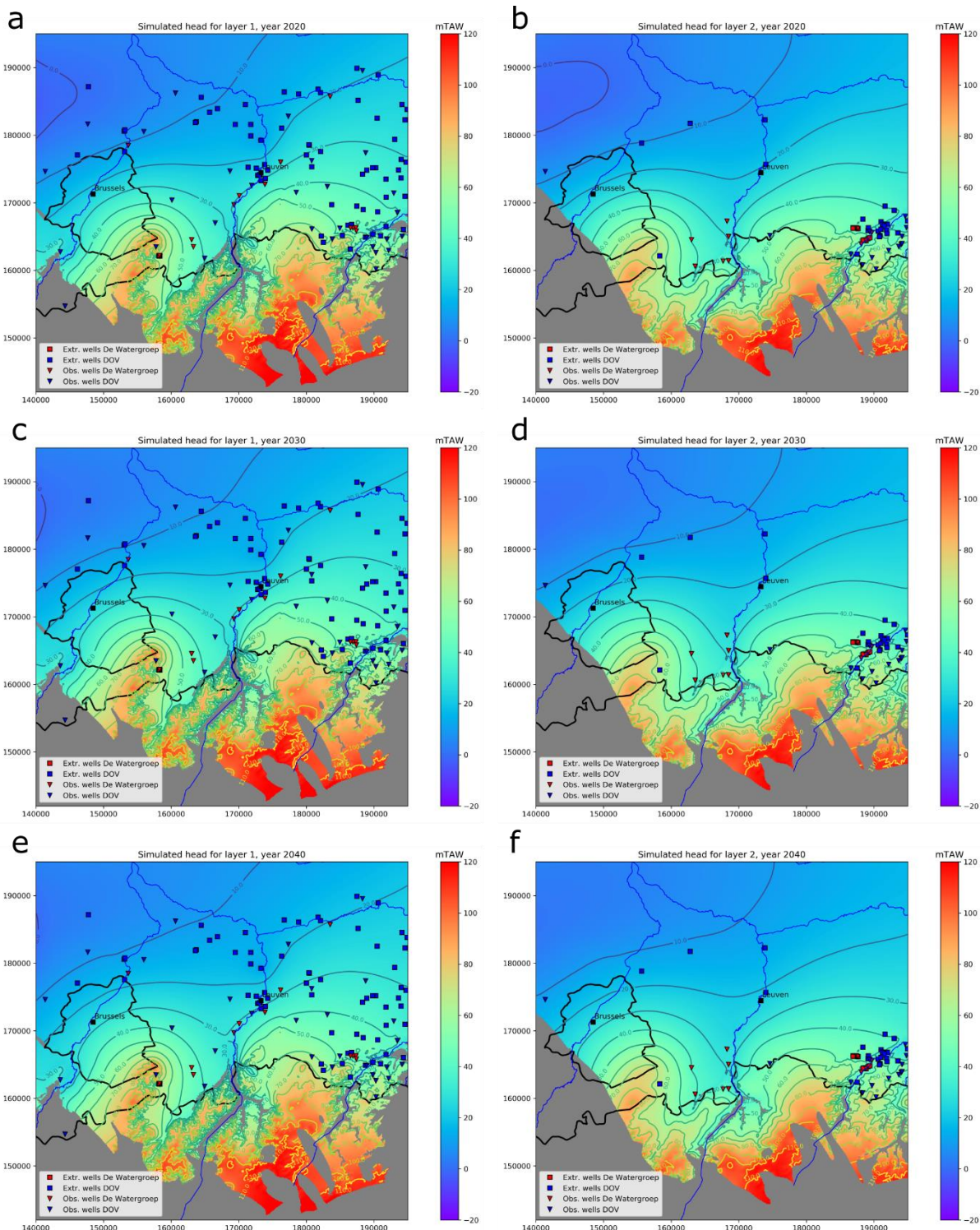


Figure I. 18: Simulated head maps for Scenario 1 for: (a) Grandglise, 2020; (b) Lincent, 2020; (c) Grandglise, 2030; (d) Lincent, 2030; (e) Grandglise, 2040; and (f) Lincent, 2040.

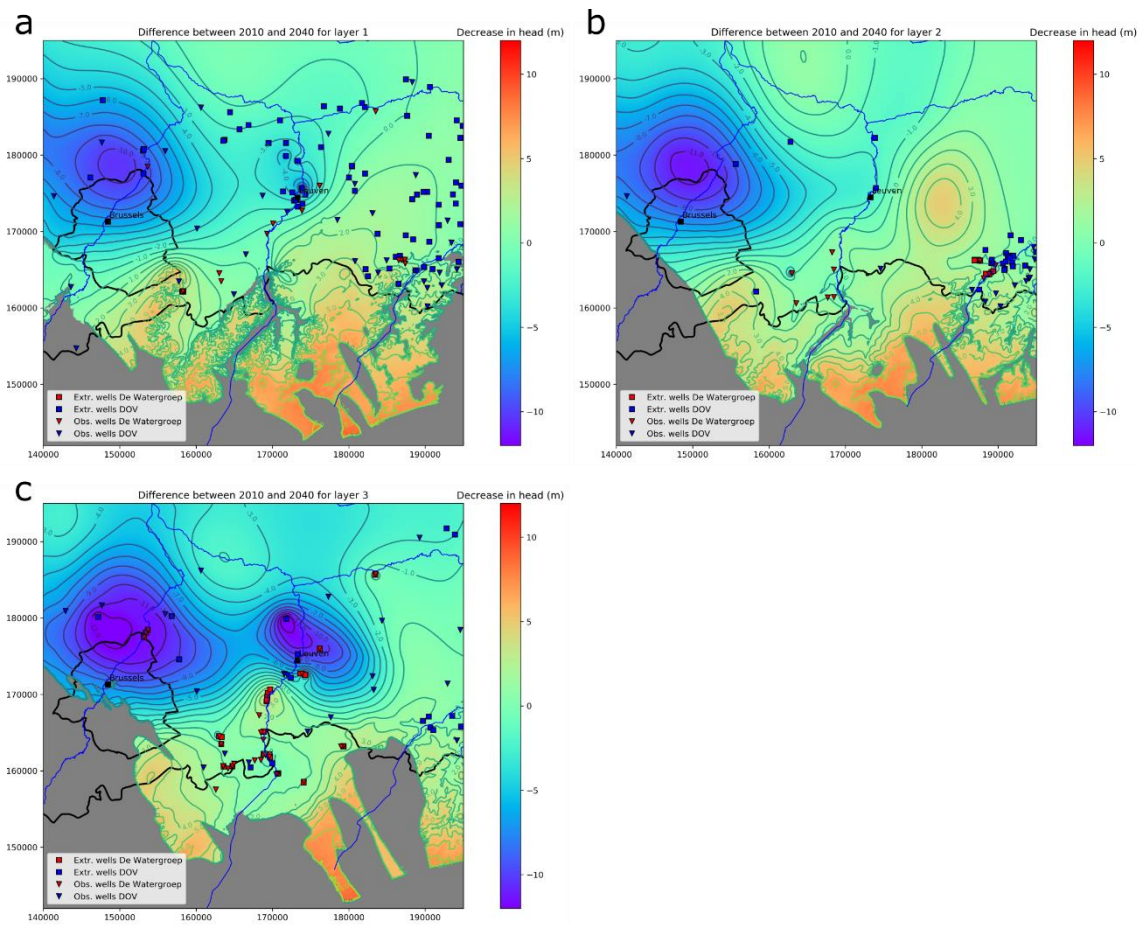


Figure I. 19: Difference in simulated heads for Scenario 1 between years 2010 and 2040 for: (a) Grandglise; (b) Lincent; and (c) the Cretaceous.

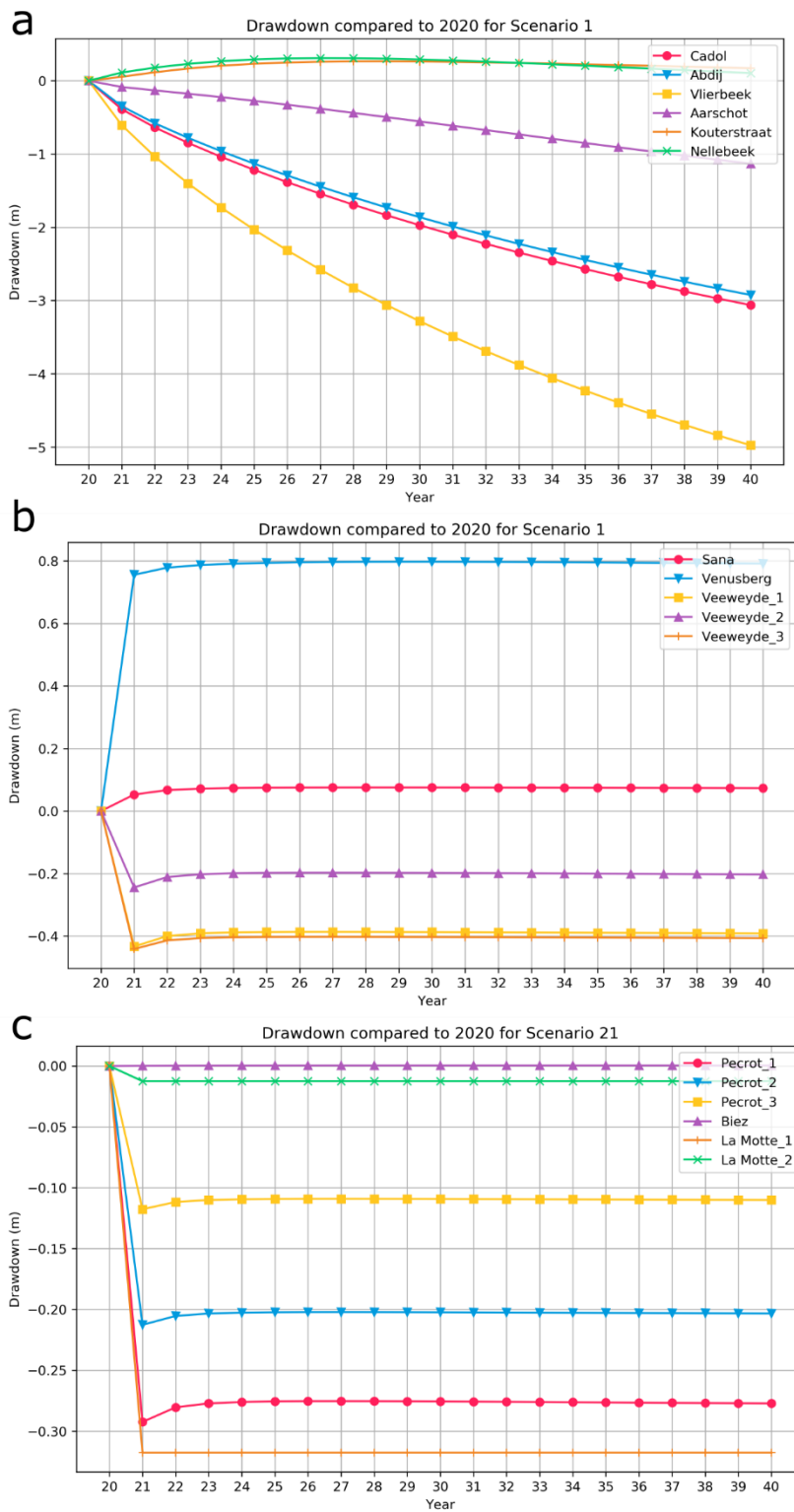


Figure I. 20: Drawdown over time compared to the heads in 2020 for Scenario 1 at the extraction wells of: (a) Cadol, Abdij, Vlierbeek, Aarschot, Kouterstraat and Nellebeek; (b) Sana, Venusberg and Veeweyde; and (c) Pécrot, Biez and La Motte.

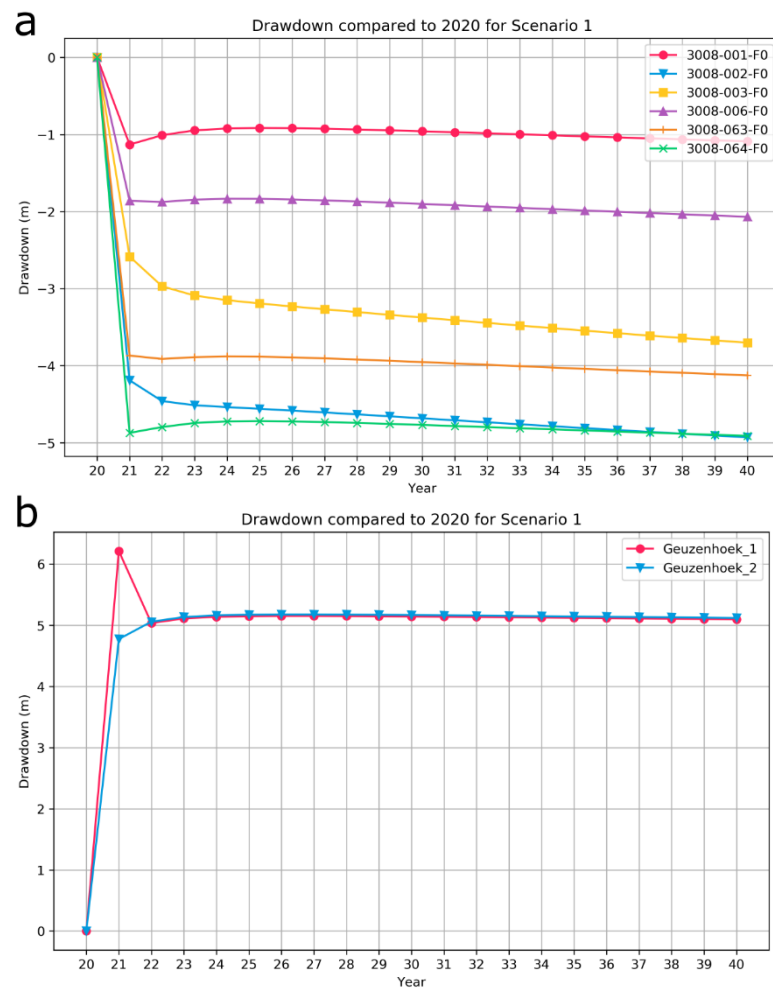


Figure I. 21: Drawdown over time compared to the heads in 2020 for Scenario 1 at the extraction wells of: (a) Het Broek; and (b) Geuzenhoek.

Table I. 26: Change in head between the situation in 2020 and 2040 in the production wells in the Cretaceous for all scenarios.

Well name	Head (m)		Change in head between the situation in 2020 and 2040 (in m)					
	S1 (2020)	S1 (2040)	S2a (2040)	S2b (2040)	S3 (2040)	S4a (2040)	S4b (2040)	S5 (2040)
3001-108-F0	-18.84	1.13	-23.30	-23.30	-1.58	1.13	1.13	28.29
3006-001-F0	-37.34	3.06	-27.38	-29.41	-3.00	3.06	3.06	63.67
3006-116-F0	-29.47	2.92	-19.88	-21.60	-2.42	2.92	2.92	56.40
3007-001-F0	-39.92	4.98	-27.30	-27.74	-0.41	4.98	4.97	58.82
3008-001-F0	8.64	1.09	0.13	-14.23	-1.26	1.08	1.05	24.57
3008-002-F0	-15.31	4.93	3.94	-23.81	0.65	4.92	4.89	47.77
3008-003-F0	-10.61	3.70	2.66	-20.53	-0.18	3.69	3.67	42.50
3008-004-F0	8.25	2.53	1.36	-10.48	0.49	2.52	2.50	22.94
3008-005-F0	2.59	3.38	2.42	-14.76	0.68	3.37	3.34	30.37
3008-006-F0	-1.44	2.07	1.11	-18.15	-1.17	2.06	2.03	34.45
3008-063-F0	-2.89	4.13	3.16	-18.39	0.95	4.11	4.09	35.85
3008-064-F0	-5.00	4.91	3.95	-20.61	1.59	4.90	4.87	38.14
3010-001-F0	17.05	-0.17	-26.89	-27.33	-3.04	-0.51	-1.14	28.44
3010-002-F0	31.06	-0.17	-10.75	-11.20	-1.64	-0.50	-1.14	14.42
3011-005-F0	36.51	-0.79	-1.26	-1.32	-1.28	-5.41	-14.12	4.05
3011-008-F0	31.61	-0.07	-1.16	-1.23	-0.78	-0.22	-0.49	7.02
3011-009-F0	36.38	-0.08	-0.33	-0.42	-0.26	-0.22	-0.48	1.70
3011-015-F0	51.15	-0.09	-0.20	-0.23	-0.14	-0.37	-0.89	0.48
3012-001-F0	28.42	0.39	-0.19	-0.48	0.10	0.39	0.38	3.35
3012-002-F0	29.89	0.10	-0.23	-0.47	-0.07	0.09	0.09	1.80
3012-003-F0	29.23	0.20	-0.25	-0.54	-0.03	0.20	0.19	2.54
3012-007-F0	27.19	-5.10	-6.50	-9.56	-6.22	-5.11	-5.14	6.07
3012-008-F0	27.00	-5.12	-6.54	-9.71	-6.26	-5.13	-5.16	6.28
3012-009-F0	26.97	-3.44	-4.57	-7.76	-4.42	-3.46	-3.49	6.31
3012-013-F0	31.42	0.03	-0.29	-0.34	-0.02	0.03	0.03	0.55
3012-014-F0	29.67	0.28	-1.03	-1.14	0.12	0.28	0.27	1.88
3012-015-F0	29.80	0.20	-1.06	-1.12	0.03	0.20	0.20	1.90
3012-016-F0	30.31	0.11	-0.83	-0.88	-0.03	0.11	0.11	1.49
3012-020-F0	31.34	0.32	-0.41	-0.41	0.00	0.32	0.32	3.49
3012-021-F0	33.19	0.01	-0.14	-0.14	-0.10	0.01	0.01	1.19
3012-059-F0	28.56	0.41	-0.14	-0.38	0.13	0.40	0.40	3.13
3013-001-F0	40.19	0.00	0.00	0.00	0.00	0.00	0.00	0.00
3014-001-F0	10.25	5.79	5.77	5.73	5.78	5.79	5.79	5.88
3017-001-F0	44.81	0.00	0.00	0.00	0.00	0.00	0.00	0.00
3020-001-F0	43.78	0.00	-2.71	-2.71	-0.12	0.00	0.00	1.15

Scenario 2a

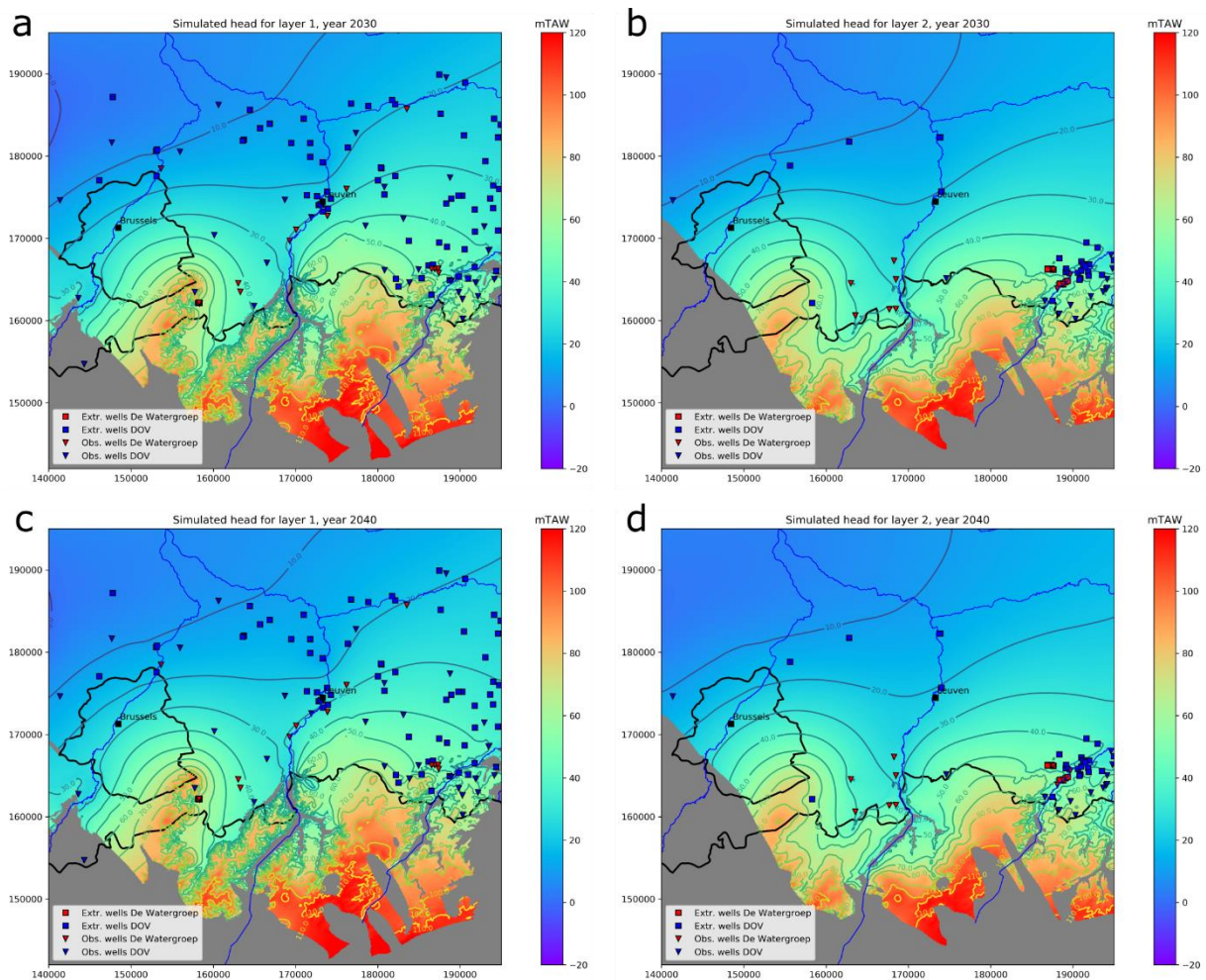


Figure I. 22: Simulated heads for Scenario 2a for: (a) Grandglise, 2030; (b) Lincent, 2030; (c) Grandglise, 2040; and (d) Lincent, 2040.

Scenario 2b

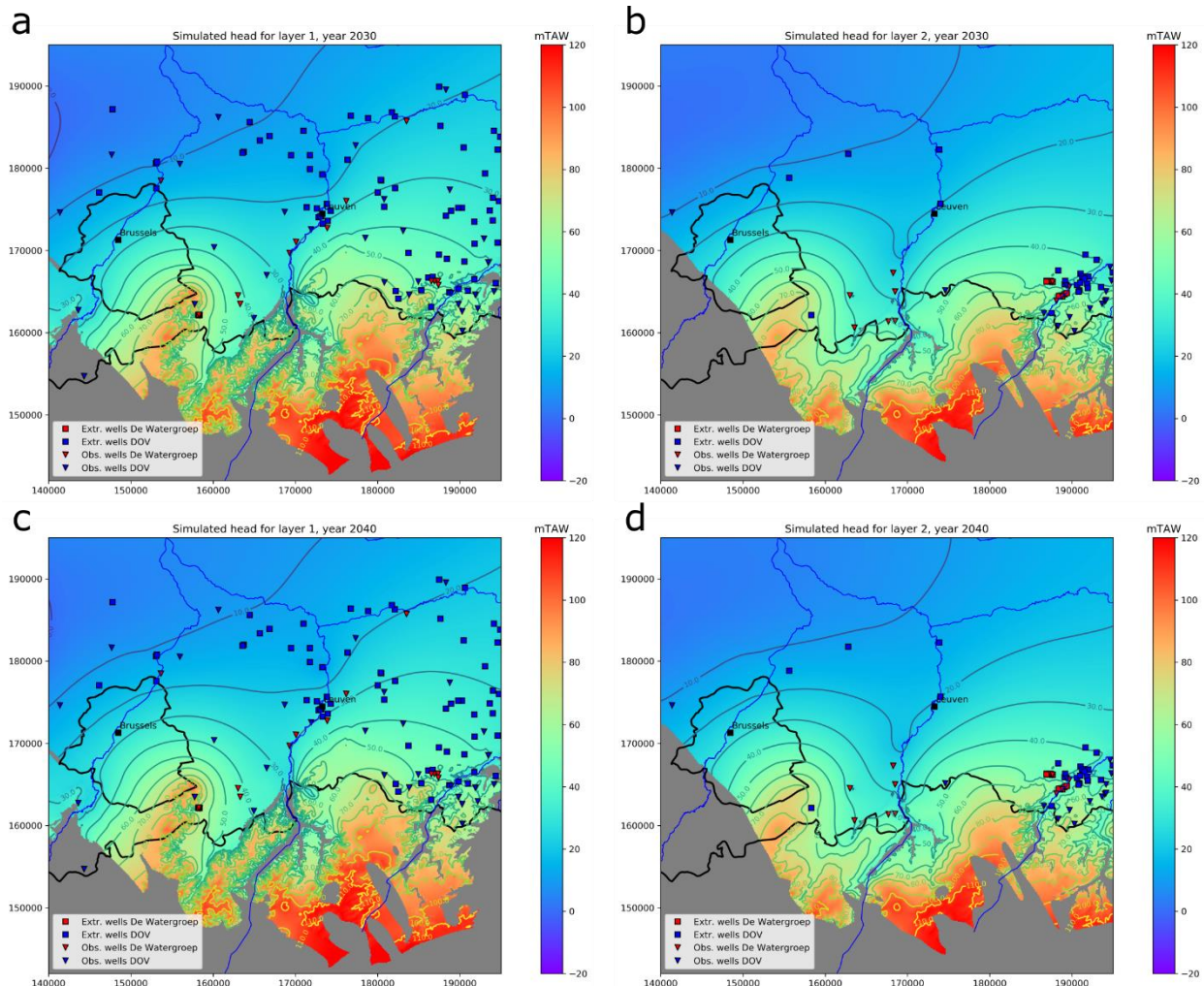


Figure I. 23: Simulated heads for Scenario 2b for: (a) Grandglise, 2030; (b) Lincent, 2030; (c) Grandglise, 2040; and (d) Lincent, 2040.

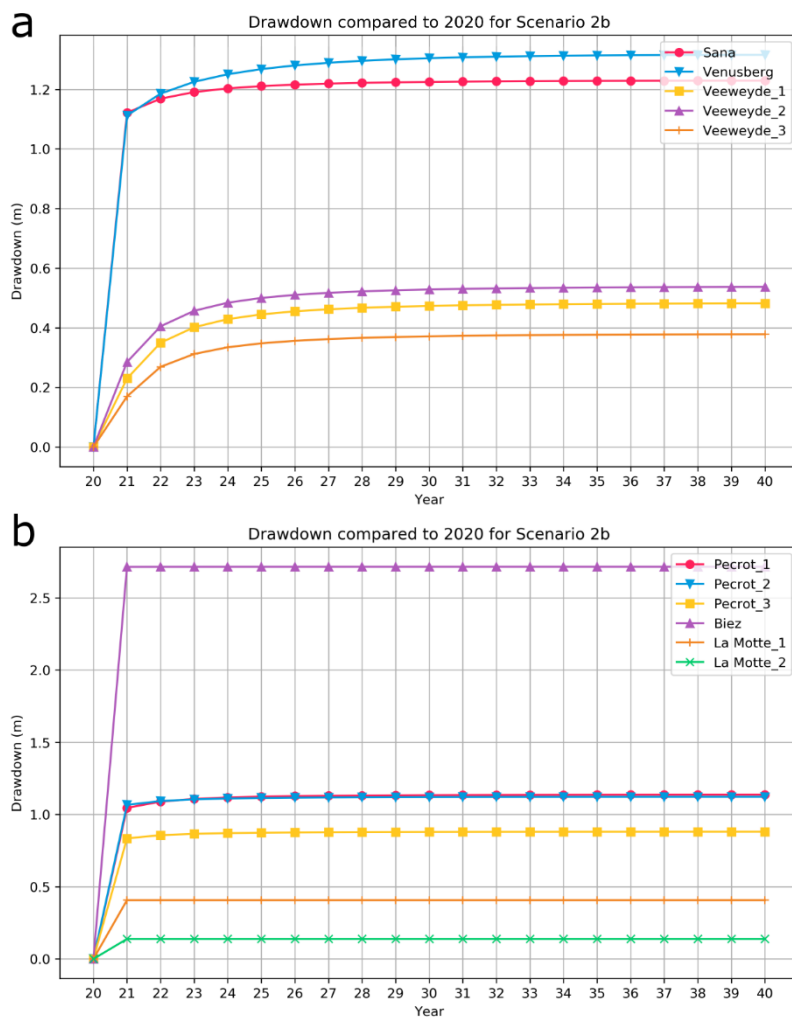


Figure I. 24: Drawdown over time compared to the heads in 2020 for Scenario 2b at the extraction wells of: (a) Sana, Venusberg and Veeweyde; and (b) Pécrot, Biez and La Motte.

Scenario 3

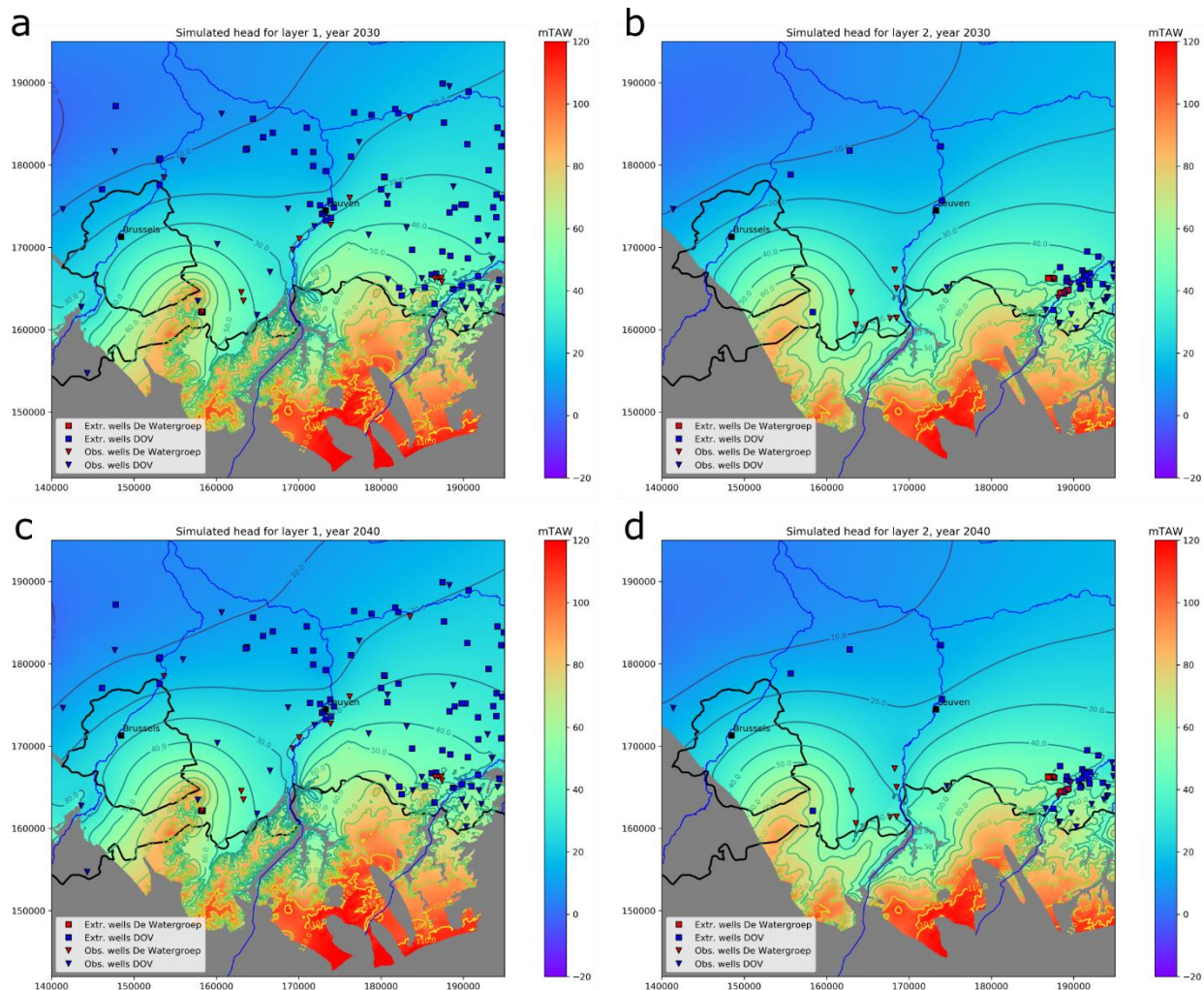


Figure I. 25: Simulated heads for Scenario 3 for: (a) Grandglise, 2030; (b) Lincent, 2030; (c) Grandglise, 2040; and (d) Lincent, 2040.

Scenario 4a

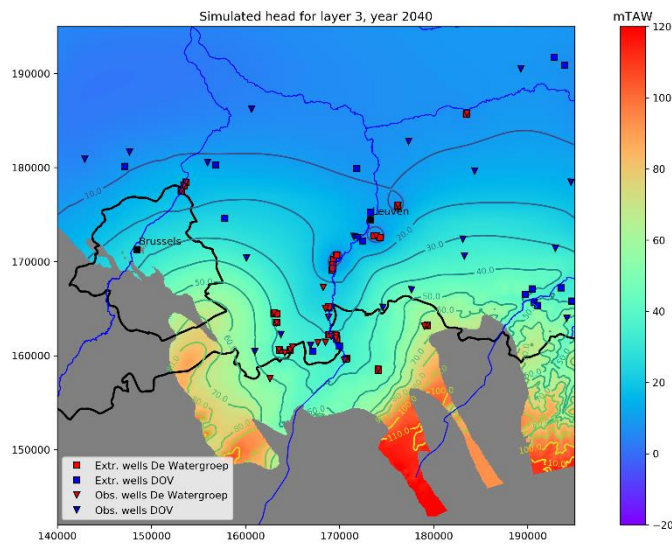


Figure I. 26: Simulated head map for the Cretaceous in the year 2040 for Scenario 4a.

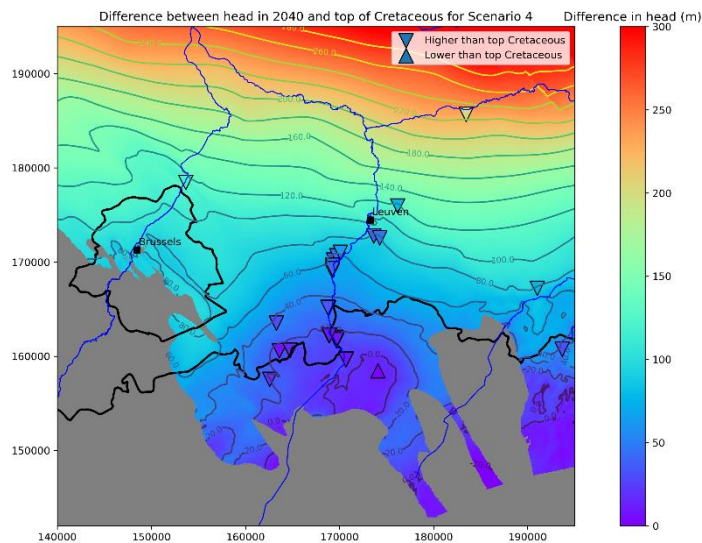


Figure I. 27: Difference in simulated heads in the Cretaceous and the top of the Cretaceous for Scenario 4a.

Scenario 4b

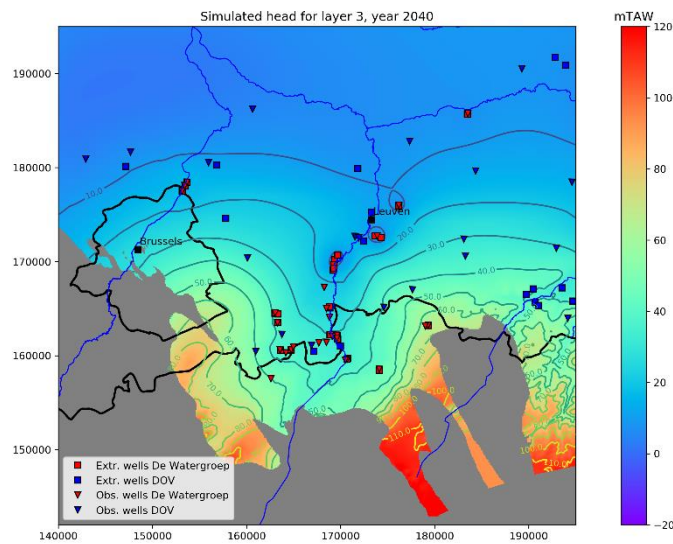


Figure I. 28: Simulated head map for the Cretaceous in the year 2040 for Scenario 4b.

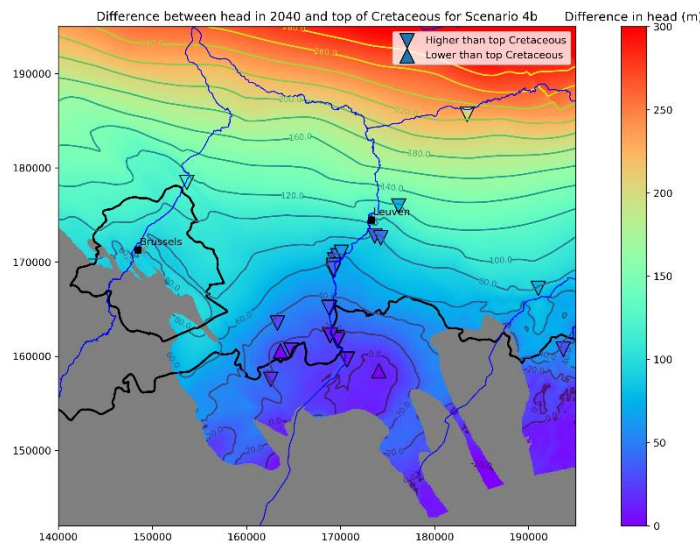


Figure I. 29: Difference in simulated heads in the Cretaceous and the top of the Cretaceous for Scenario 4b.

Scenario 5

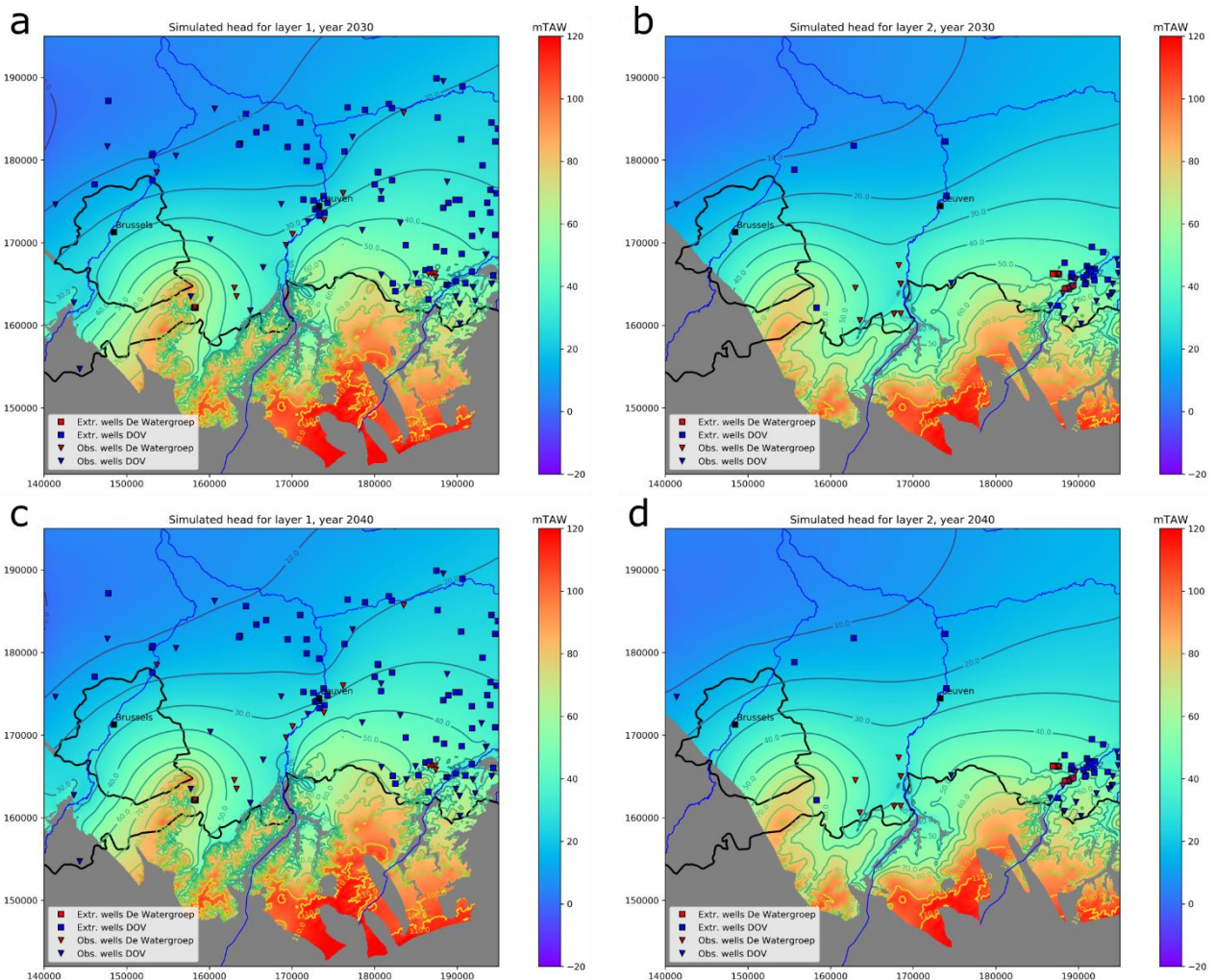


Figure I. 30: Simulated heads for Scenario 5 for: (a) Grandglise, 2030; (b) Lincent, 2030; (c) Grandglise, 2040; and (d) Lincent, 2040.

1.5 Uncertainty Analysis

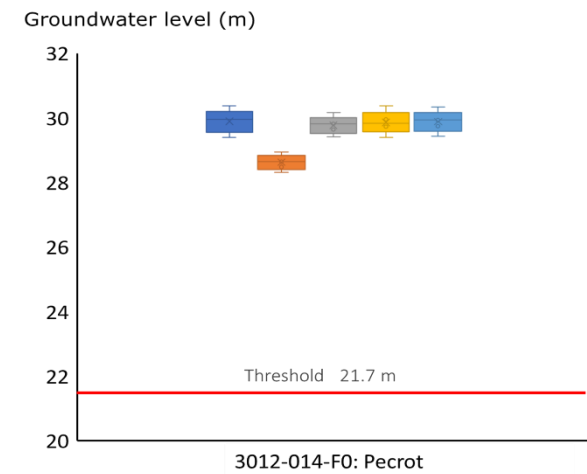
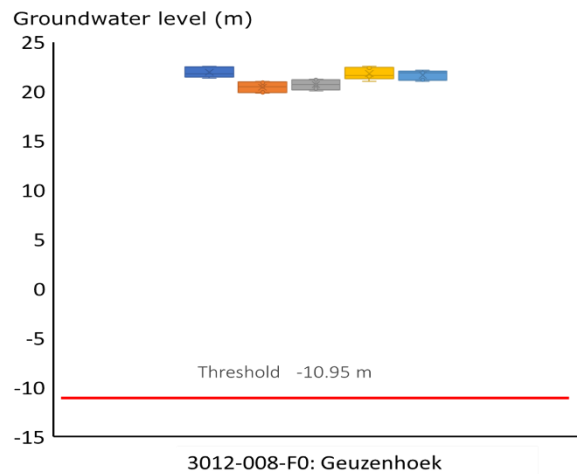
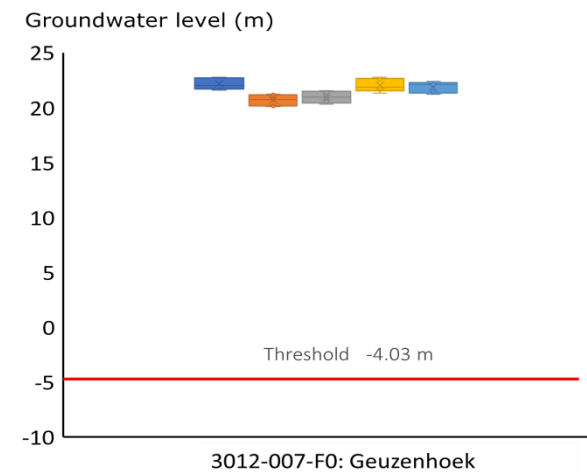
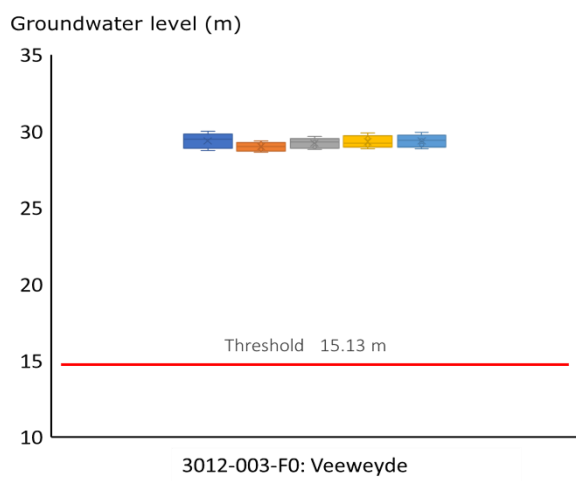
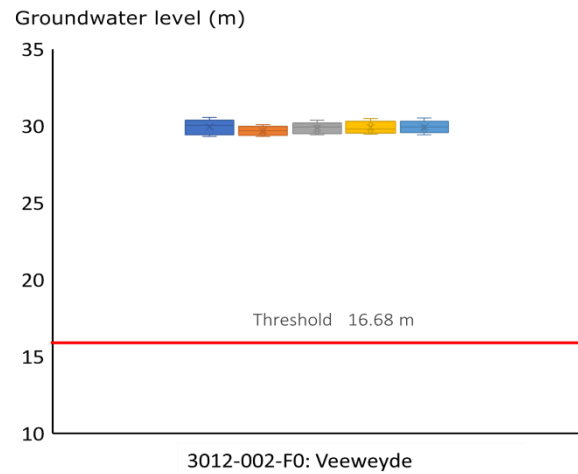
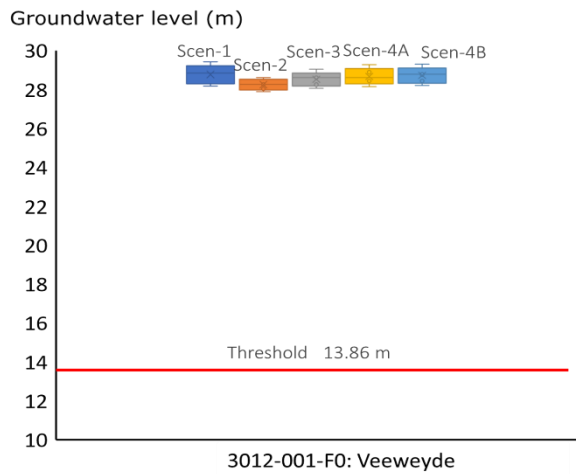


Figure I. 31: Prediction uncertainty in the simulated head associated with model parameters and boundary conditions for all five scenarios for the sites of Veeweyde, Geuzenhoek and Pécrot.

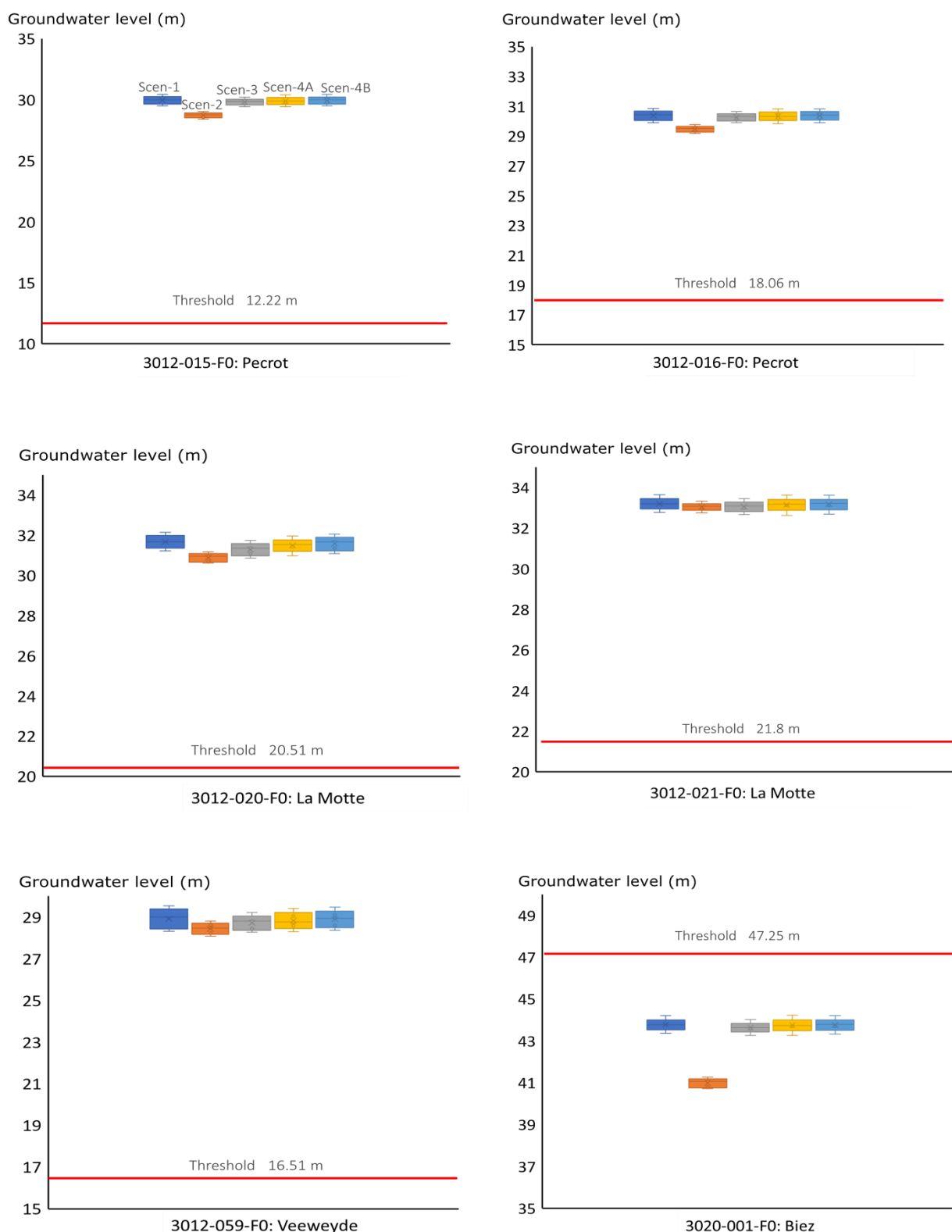


Figure I. 32: Prediction uncertainty in the simulated head associated with model parameters and boundary conditions for all five scenarios for the sites of Pécrot, La Motte, Veeweyde and Biez.

I.6 Potential Maps

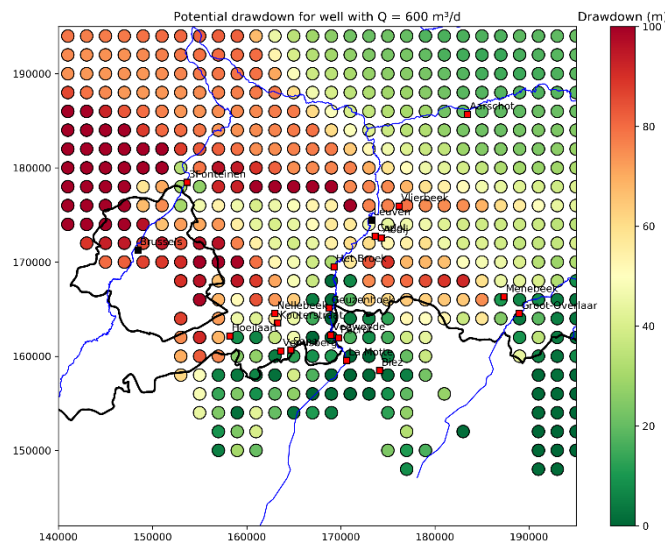


Figure I. 33: Potential drawdown for synthetic well with $Q=600 \text{ m}^3/\text{d}$.

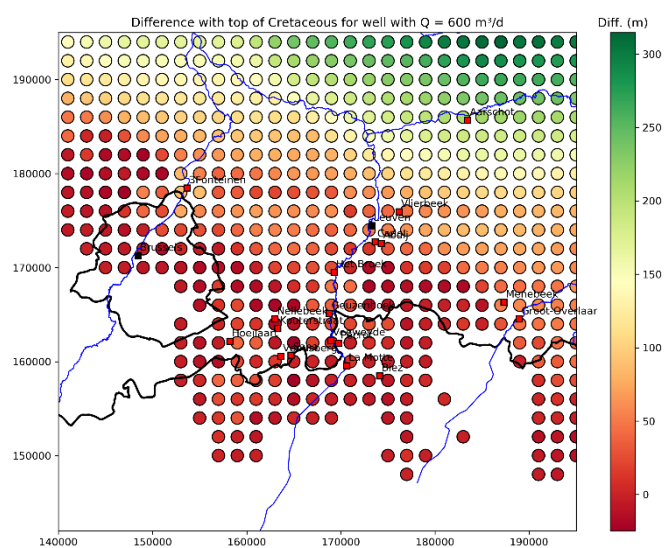


Figure I. 34: Difference between the top of the Cretaceous and simulated head in synthetic well with $Q=600 \text{ m}^3/\text{d}$.

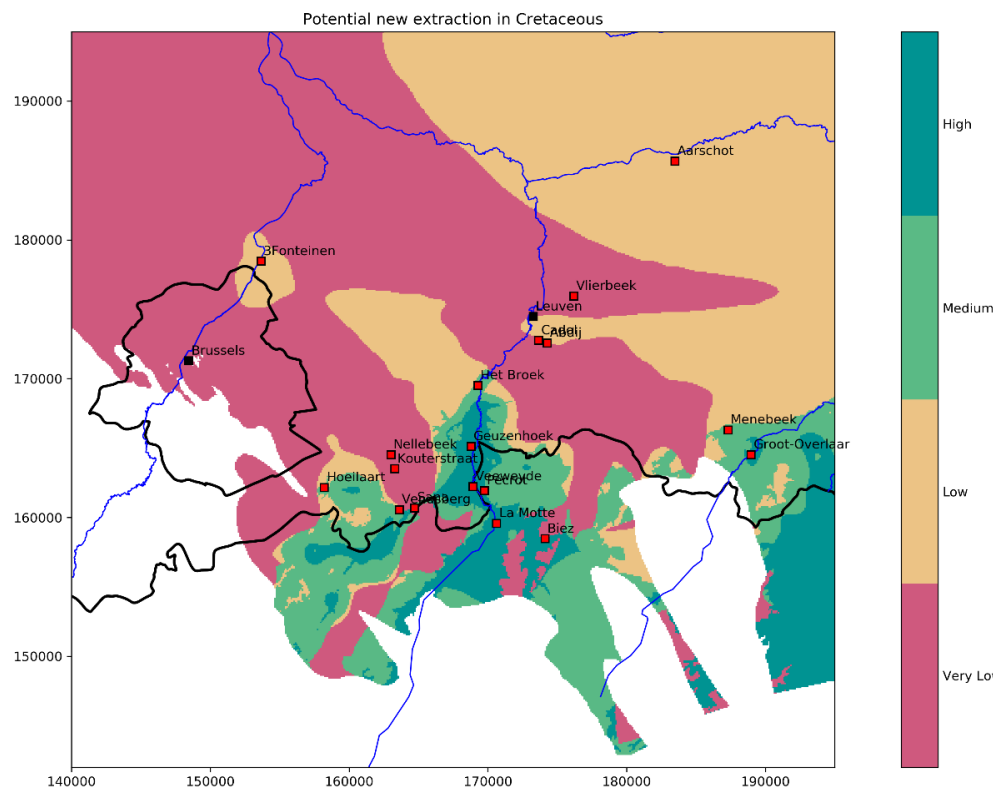


Figure I. 35: Potential map for new extraction in the Cretaceous with weighting of 50%, 10% and 40% for respectively the drawdown, difference with top of Cretaceous and depth of Cretaceous (including hard rules).

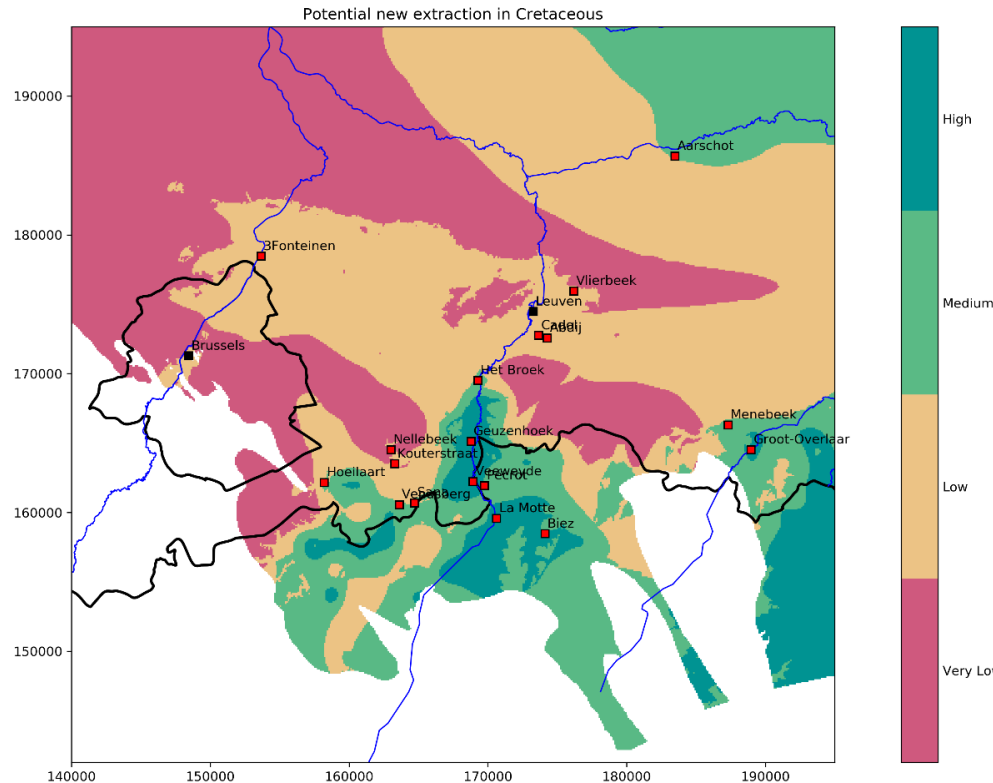


Figure I. 36: Potential map for new extraction in the Cretaceous with weighting of 60%, 10% and 30% for respectively the drawdown, difference with top of Cretaceous and depth of Cretaceous without hard rules.